NATIONAL UNIVERSITY OF IRELAND, GALWAY (NUIGalway)

SCHOOL OF CHEMISTRY

MARINE BIODISCOVERY GROUP

Ph.D. Thesis by

Paul O. Guillen Mena

CHEMICAL DIVERSITY OF ZOANTHARIANS FROM THE COAST OF ECUADOR IN THE TROPICAL EASTERN PACIFIC

Chemical diversity of Zoantharians from the Coast of Ecuador in the Tropical Eastern Pacific

By

Paul Orlando Guillen Mena

A thesis presented for the degree of

Doctor of Philosophy

School of Chemistry

National University of Ireland, Galway

Ireland

July 2019

CHEMICAL DIVERSITY OF ZOANTHARIANS FROM THE COAST OF ECUADOR IN THE TROPICAL EASTERN PACIFIC

A thesis submitted to the National University of Ireland as fulfilment of the requirement for the degree of

Doctor of Philosophy (Chemistry)

By

Paul Orlando Guillen Mena

School of Chemistry

National University of Ireland, Galway

Supervisor: Prof. Olivier P. Thomas

Co-supervisor: Dr. Jenny Rodriguez

Head of School: Dr. Patrick O'Leary

Submitted July 2019

DEDICACION

Para mis amados padres, Orlando y Martha

Por su incondicional apoyo, sacrificio y amor que me han brindado toda la vida. Gracias por su gran ejemplo de superación, constancia, y por ser los pilares fundamentales en mi vida.

Para mis hermanas Vannesa y Karina, a mi hermano Juanito, a mi adorado sobrino Juan Andres, mi cuñado Juan Carlos, a mis amados abuelitos Raquel, Gabriel, Juan y Maria.

Esta tesis se los dedico con todo el amor del mundo.

Paul

""It is not the strongest of the species that survives, nor the most intelligent that survives. It is the one that is most adaptable to change."

Charles Darwin

Abstract

This thesis describes the isolation and identification of marine natural products from five zoantharian species collected off the Marine Protected Area El Pelado located in Santa Elena, Ecuador. Ecuador is one of the countries with the greatest terrestrial and marine diversity in the world and relatively few studies have been performed in the marine ecosystem. The Galapagos Island has been considered a "hot spot" of biodiversity and most of these studies have been undertaken in the Archipelago. In 2015, a National Project entitled "**Characterization of the biodiversity of microorganisms and invertebrates from the Marine Protected Area El Pelado at the taxonomic, metabolomic and metagenomic level, and their applications for animal and human health**" was funded by the Secretary of Higher Education, Science and Technology (SENESCYT) with the aim of describing the existing marine biological and chemical diversity. Therefore, the first inspection of the biodiversity in the Marine Protected Area "El Pelado" (REMAPE) was focused on marine invertebrates. Among the invertebrates observed in this area, zoantharians were one of the most representative organisms with eight species belonging to four families; *Zoanthus* cf. *sociatus*, and *Zoanthus* cf. *pulchellus* from the family Zoanthidae, *Terrazoanthus patagonichus*, *Terrazoanthus* cf. *patagonichus* and *Terrazoantus* sp. from the family Hydrozoanthidae, *Parazoanthus darwini* and *Antipathozoanthus hickmani* from the family Parazoanthidae and *Palythoa* cf. *mutuki* belonging to the family Sphenopidae. Two species of the Parazoanthidae family; *P. darwini* and *A. hickmani* seems to be endemic of this ecoregion as there are no reports of the presence of these zoantharians in other marine ecosystems. Interestingly, no chemical studies have been reported from any of these species inhabiting the Ecuadorian coast including the Galapagos Islands. Therefore, this thesis was aimed to study for the first time the chemical diversity of: *Terrazoanthus patagonichus* (formerly known as *T. onoi*), *Antipathozoanthus hickmani*, *Parazoanthus darwini*, *Zoanthus* cf. *pulchellus* and *Terrazoanthus* cf. *patagonichus*.

A new family of 2-aminoimidazole alkaloids named terrazoanthines A-C were identified from *Terrazoanthus patagonichus*. Terrazoanthines A and B are characterized by the presence of the 2-aminoimidazole ring fused to a cyclohexane. Additionally, two zoanthoxanthin derivatives named zoamides E and F were isolated from the sister species *Terrazoanthus* cf. *patagonichus*. Then, four ecdysteroids derivatives named ecdysonelactones were obtained from *Antipathozoanthus hickmani*. These compounds feature a γ-lactone ring fused to ring A of the ecdysteroid skeleton. Further investigations on this organism led to the identification of four halogenated tyrosine derivatives named valdiviamides A-D and characterized by the presence of iodine and bromine atoms in the phenol ring. The bioactivity study revealed valdiviamide B to have moderate activity against the liver cancer cell line (HepG2) with an IC_{50} value of 7.8 μM. Additionally, two halogenated tyramine derivatives containing iodine and bromine atoms were identified from *Parazoanthus darwini*. The chemical

investigation of *Zoanthus* cf. *pulchellus* allowed the identification of two members of the bioactive family of zoanthamine alkaloids. These compounds revealed anti-inflammatory activity in microglia BV-2 cells used in neuroinflammatory studies with high inhibitory effects in reactive oxygen species (ROS) and nitric oxide (NO) generation.

Overall, the chemical studies of these zoantharians led to the identification of 24 secondary metabolites, from which 17 are new natural products. The presented results confirm this overlooked group of invertebrates as a rich source of diverse natural products with unique skeletons and diverse biological activities.

Declaration

I declare that all the work contained in this thesis is an original report of my research, has been composed by myself unless stated otherwise in the text, and it has not been submitted, in whole or in part, for any previous degree or professional qualification.

Paul O. Guillen Mena.

Acknowledgements

There are no words to explain how grateful I am for all the experiences I have lived during this incredible Ph.D. experience. After so many early mornings and late nights and all the hard work I put into my research work, I could finally say that my Ph.D. thesis is finished. Through this journey, there are a few people I would like to sincerely thank for their help and support.

First of all, I would like to thank GOD who has always guided me for the right path of life and provided me with the strength and good health to complete my research work. I would like to express my deepest and sincere gratitude to my supervisor and mentor Prof. Olivier P. Thomas for all his incredible support, patience, dedication, advices and guidance provided at all stages of my research work. I would not have had the passion and love for marine natural products that I have now if it wasn't for his motivation and outstanding expertise. I also would like to give a special thank my co-supervisor Dr. Jenny Rodriguez for all her support and for the opportunity given me to be part of the project to study the marine biodiversity of our beloved country Ecuador.

I would like to extend my gratitude to Ing. Andres, Dr. Stanislaus, Dr. Bonny, Dr. Wilfrido and Dr. Sofie for their unconditional support, to the biodiversity group, Bolivar, Cristobal, Gabriela, Cecilia, Eli, Marissa, to Leandro, Leda, Samira, Milton, Guillermo, Betsy, Ramiro, Adrian, Irma, Solanda, Cecibel, Nancy, Alexandra and to all the people at CENAIM for making me feel like home.

I would like to acknowledge the College of Science, National University of Ireland, Galway (NUIGalway) for the postgraduate scholarship provided for my Ph.D. studies. Thanks to the Marine Institute for the Networking & Travel Award for allowing me to attend to some international conferences during my studies.

A big thanks to my "Lab crew" the Marine Biodiscovery Ireland group; to Kevin for all the NMR classes and food challenges, we certainly shared a big love to chicken biryani, dough bro's pizza and burritos, to Daniel for always trying to keep the group together and organizing the hicking trips, to Hiren, Elliot, Perrine, Navdeep, Sam, Laurence, Kishor, Maria for all the incredible times we spent together and last but not least my dear friend and roommate Karla (best known as JUDAS) thanks for the all the good times and talks we had during our amazing time in Ireland. Thank you, guys for being my family in Galway for the past years. For certain, one of my proudest moments during this journey was given by my fourth-year student Shauna. Thanks for making me feel so proud and I hope I have contributed to her with a bit of the passion and motivation for this amazing field of natural products.

I would also like to thank to all the staff of the School of Chemistry (NUIGalway) and the external collaborators that contributed to this research:

Gregory Genta-Jouve for his collaboration with the ECD analysis.

Prof. Luis Botana and Fernando Reyes for their collaboration with the bioassays.

Dr. Roisin Doohan for her help with the acquisition of the spectra on the 500 and 600 NMR.

To my friends from the Chemistry Society (An Cumann Ceimice) and to all my fellow chemistry postgraduates for all the activities carried out in the benefit of our School.

I would like to extend my sincere gratitude to my viva examiners, Dr. Erica Burnell and Dr. Antonio H. Daranas for reviewing my thesis.

Finally, a special thanks to my beloved family for their love, motivation and their constant support from day one, I would not be achieving this dream if it wasn't for them and to all my friends (including the gym rats from Cuenca, Montañita and Kingfisher) for all the chats and encourage I have gotten all this time.

From the bottom of my heart

Thank you

Table of Contents

List of Figures

List of Tables

List of Abbreviations

ADME   Absorption, Distribution, Metabolism and Excretion

COSY ^1H-^1H COrrelation SpectroscopY

DAD   Diode Array Detector

DHA   Docosahexaenoic acid

DNA   DeoxyriboNucleic Acid

DSP   Diahrretic shellfish poisoning

ECD   Electronic Circular Dichroism

ELSD   Evaporative Light Scattering Detector

ENSO   El Niño Southern Oscillation

EPA   Eicosapentaenoic acid

EPMR   Evolutionary Programming for Molecular Replacement

GIAO   Gauge-Independent Atomic Orbital

GNPS   Global Natural Products Social Molecular Networking

GPS   Global Positioning System

gHMBC   gradient Heteronuclear Multiple-Bond Correlation

HPLC   High Performance Liquid Chromatography

HRESIMS   High-Resolution ElectroSpray Ionization Mass Spectrometry

gHSQC   gradient Heteronuclear Single-Quantum Correlation

HTS   High Throughput Screening

IC_{50} 50% Inhibitory concentration

LC-MS   Liquid Chromatography-Mass Spectrometry

LD_{50} Lethal dose

LECs   Lymphatic endothelial cells

MMAE   Monomethyl auristatin E

MNPs   Marine Natural Products

MS   Mass Spectrometry

NMR   Nuclear Magnetic Resonance

NOESY   Nuclear Overhauser Enhancement SpectroscopY

ppm   parts per millon

PUFAs   Polyunsaturated fatty acids

ROESY   Rotating frame nuclear Overhauser Effect SpectroscopY

ROS   Reactive Oxygen Species

ROVs	Remotely Operated Vehicles
RSV	Respiratory syncytial virus
SAR	Structure-Activity Relationship
SCUBA	Self-Contained Underwater Breathing Apparatus
SPE	Solid Phase Extraction
TEP	Tropical Eastern Pacific
TFA	TriFluoroacetic Acid
TMS	TetraMethylSilane
TNPs	Terrestrial Natural Products
UV	Ultraviolet
VLC	*Vacuum* Liquid Chromatography

1 Introduction

1.1 The marine environment as a rich source of bio and chemo diversity

The ocean represents about 70% of the earth's surface and is inhabited by more than 2.2 million of marine species from which only 9% have been reported, becoming the ecosystem with the largest biodiversity in the world and according to the World Register of Marine Species (WORMS), there are 233,260 accepted marine species [1, 2]. Furthermore, the first international census aimed to determine the diversity, abundance and distribution of marine life from intertidal to deep sea zones was carried out between 2000 and 2010 [3]. The results of the census revealed that at least 50 to 90 % of marine species are still unknown to science. In Addition, the marine microbial diversity could reach hundreds of millions of species, and according to the ocean exploration genome project in 2003, more than 1.2 million of new genes and the double of protein sequences were added in the NIH's GenBank [3]. Moreover, the marine environment also contributes to a wide range of unique chemical diversity with complex scaffolds [4]. Marine organisms, especially those living in benthic areas, have developed mechanisms to tolerate the extreme sea conditions such as strong currents and sediments, nutrient availability, light, temperature, pressure and predators to ensure their survival through their capacity to biosynthesize different secondary metabolites [5-8]. These secondary metabolites also known as "Marine Natural Products" (MNPs) play diverse ecological roles such as mechanism of chemical defense, interspecies signaling to find mates or to surpass competitors for substrate or food, fouling prevention and are also involved on the benthic and pelagic community structure of an ecosystem [5, 6]. The first studies on MNPs was focused on organisms that could be easily collected from shallow waters (less than 50 m) which yielded several compounds with unique structural features. Later, with the advancements of collection methods like Self-Contained Underwater Breathing Apparatus (SCUBA) in 1970s to the use of Remotely Operated Vehicles (ROVs) in 1990s, allowed the accessibility to a great diversity of samples such as sponges, algae, ascidians, octocorals, tunicates, other invertebrates and cyanobacteria from 0 to 10,898 m depth [9]. These advances in sampling collection has allowed the discovery of new species associated with unique chemical scaffolds, different from those found on terrestrial organisms [9, 10]. The originality of these natural products increased the interest of researchers to unveil the chemical treasures hidden in the sea. Therefore, Leal *et al*., suggest an adequate and organize sampling collection system which consist in the following: **a**) to explore remote geographical ecosystems and **b**) to investigate organisms that have been overlooked [11]. The mentioned system will enhance the opportunities of uncovering new species of organisms with unprecedented chemical archetypes. Although, most of the marine natural products are

continuously being reported from known sources and previously studied ecoregions, more efforts should be made to expand the biological and chemical exploration to other untapped ecosystems which can be located through the Global Positioning System (GPS).

1.2 Marine Natural Products (MNPs) as source of drugs

The marine environment is the source of bioactive substances that have been used in folk medicine for centuries. Some of the first reports are from 1600 BC by the Chinese and Japanese culture who used seaweed rich in iodine to treat thyroid problems [12]. In Ireland for example, the red alga *Chondrus crispus* and *Mastocarpus stellatus* were used to treat cold, sore throats, tuberculosis and if boiled with milk or water was used for kidney problems and burns. In addition, another red alga *Porphyra umbilicalis* prepared as a juice was used to treat cancer, particularly breast cancer, and it was also used in the Aran Islands to relieve indigestion [13]. The beginning of the marine natural products era as a source of new drugs started with the isolation of two nucleosides, spongothymidine or Ara-T (**1**) and spongouridine or Ara-U (**2**) from the Caribbean sponge *Tectitethya crypta* (formerly known as *Cryptotethya crypta*) [14]. Chemical modification of the sugar moieties led to the discovery of synthetic analogues; arabinosyl cytosine (Ara-C or Cytarabine) (**3**) and Ara-A or Vidarabine (**4**) (Figure 1). Cytarabine **3** (Cytosar-U$^{®}$) was first approved by the FDA in 1969 and used in the treatment of acute nonlymphoblastic, chronic myelocytic and meningeal leukemia and non-Hodgkin's lymphoma. It suppresses the synthesis of deoxyribonucleic acid (DNA) by specifically acting in the synthesis phase (S phase) of the cell cycle [15]. Vidarabine **4** (Vira-A$^{®}$) approved in 1976, was used for its antiviral activity against herpes simplex and herpes zoster. Subsequent phosphorylation of **4** produced the active form triphosphate ara-ATP which inhibits the viral DNA polymerase preventing DNA synthesis [10, 16]. Recent studies suggest a bacterial origin of the two nucleosides [17].
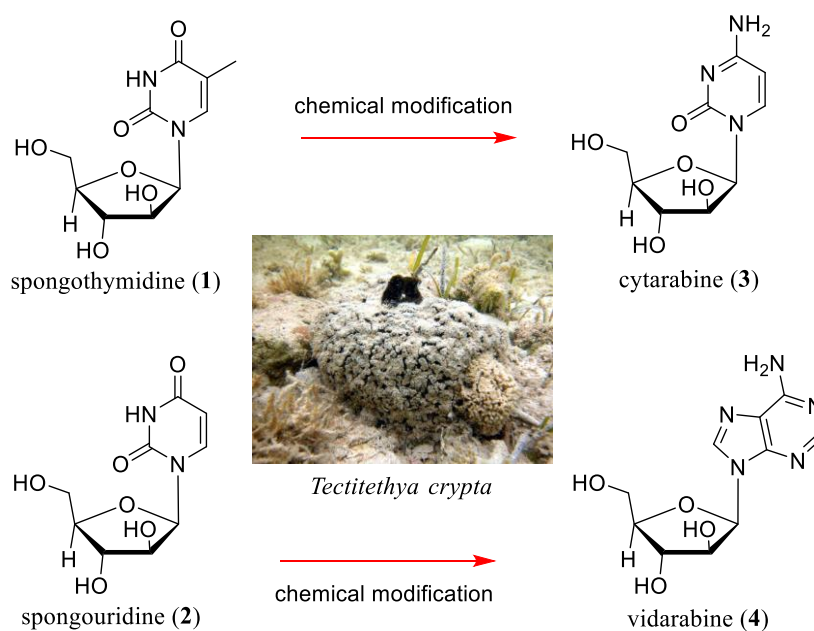
Figure 1 Structures of spongothymidine (**1**) and spongouridine (**2**) from the sponge *Tectitethya crypta*, and their synthetic analogues cytarabine (**3**) and vidarabine (**4**).

A toxic peptide ω-conotoxin MVIIA (**5**) (Figure 2) was first isolated from the Pacific fish-hunting snail *Conus Magnus* [16]. Its synthetic and structurally similar analogue ziconotide (Prialt®), was approved by the FDA in 2004 to treat severe and chronic pain in patients who reached intolerance to other pain medications. It is comprised of 25 amino acid residues with three disulphide bonds and it acts as a high specific N-type voltage-sensitive calcium channel blocker, becoming the first marine peptide of its class to be marketed [17].
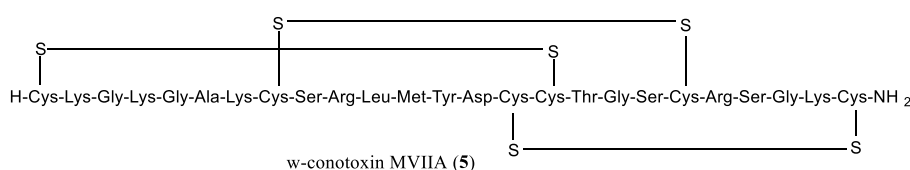
Figure 2 Peptide sequence of the ω-conotoxin MVIIA (**5**) isolated from the marine snail *Conus magnus*.

Lovaza®, is a mixture of ethyl esters ω-3 polyunsaturated fatty acids, primary composed by eicosapentaenoic acid (EPA) (**6**) and docosahexaenoic acid (DHA) (**7**) isolated from different fish (Figure 3) [10]. It was approved by the FDA in 2004 for the treatment of hypertriglyceridemia. It helps to reduce serum tryglicerides and VLDL-cholesterol levels and the risk of coronary atherosclerosis and cardiovascular diseases. There is no conclusive information of its mechanism of action, but it seems to inhibit acyl-CoA:1,2-diacylglycerol acyltransferase which increases mitochondrial and peroxisomal β-oxidation in the liver reducing lipogenesis and increasing the plasma lipoprotein lipase activity.

Additionally, a combination of *ω*-3 polyunsaturated acids under the name Epanova® were approved by the FDA in 2013 for the same indications as Lovaza® [17].

Figure 3 Structures of the ω-3 polyunsaturated acids eicopentaenoic acid (**6**) and docosahexaenoic acid (**7**) isolated from fish.

Ecteinascidin 743 (**8**) known as Yondelis®, is a potent anticancer compound isolated from the Caribbean tunicate *Ecteinascidia turbinata* [16]. The structure of **8** was elucidated 30 years after its isolation and the semi-synthesis of this product was achieved through fermentation of the bacteria *Pseudomona fluorescens* to obtain its precursor cyanosafracin B (**8a**) (Figure 4) [17]. It is used in the treatment of advance or soft tissue sarcomas and in combinatorial treatment with pegylated liposomal doxorubicil (Doxil®) against ovarian cancer. It binds to the minor groove of the DNA affecting different transcription factors and therefore, preventing cell division. It was first approved in Europe in 2007 and by the FDA in 2015 as a secondary line therapy for the treatment of metastatic liposarcoma. Additionally, an ecteinascidin derivative Zepsyre® (lurbinectedin) (**9**) has been granted by the FDA as Orphan Drug in 2018 for the treatment of small cell lung cancer (SCLC). Both anticancer compounds **8** and **9** have been developed by PharmaMar [18].
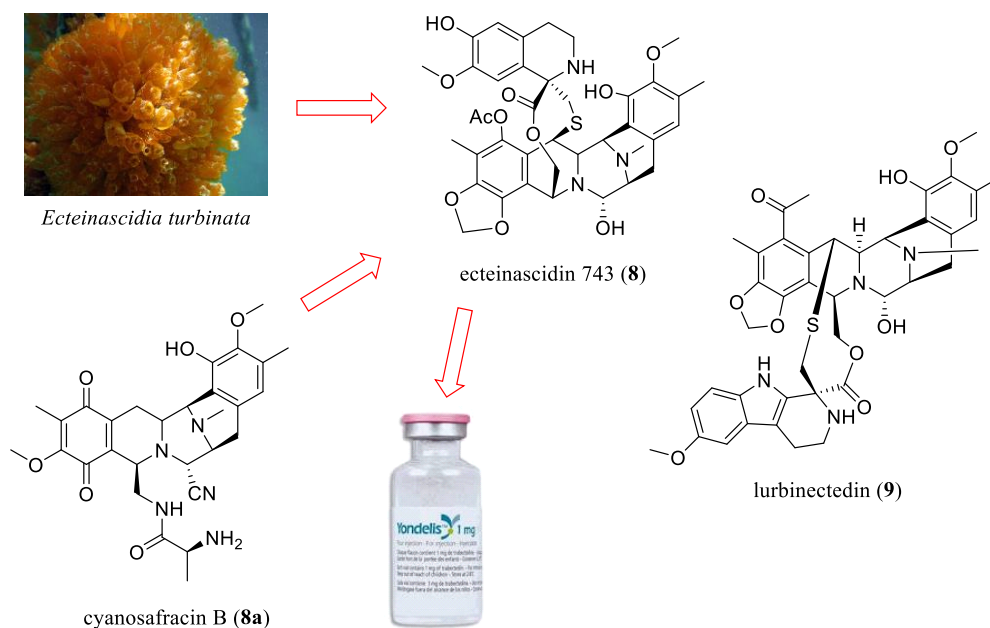
Figure 4 Structure of ecteinascidin 743 (**8**) isolated from the tunicate *Ecteinascidia turbinata*, its precursor cyanosafracin B (**8a**) and the ecteinascidin derivative lurbinectedin (**9**).

The potent cytotoxic compound halichondrin B (**10**) (Figure 5), was isolated in 1986 from the marine sponge *Halichondria okadai* and it inspired the synthesis of the simplified analogue eribulin mesylate (**11**) (Halaven®) [16, 19]. It inhibits microtubule polymerization causing disruption in the microtubule instability. It was approved by the FDA in 2010 for the treatment of breast cancer.

halichondrin B (**10**)

Halichondria okadai

eribulin mesilate (**11**)
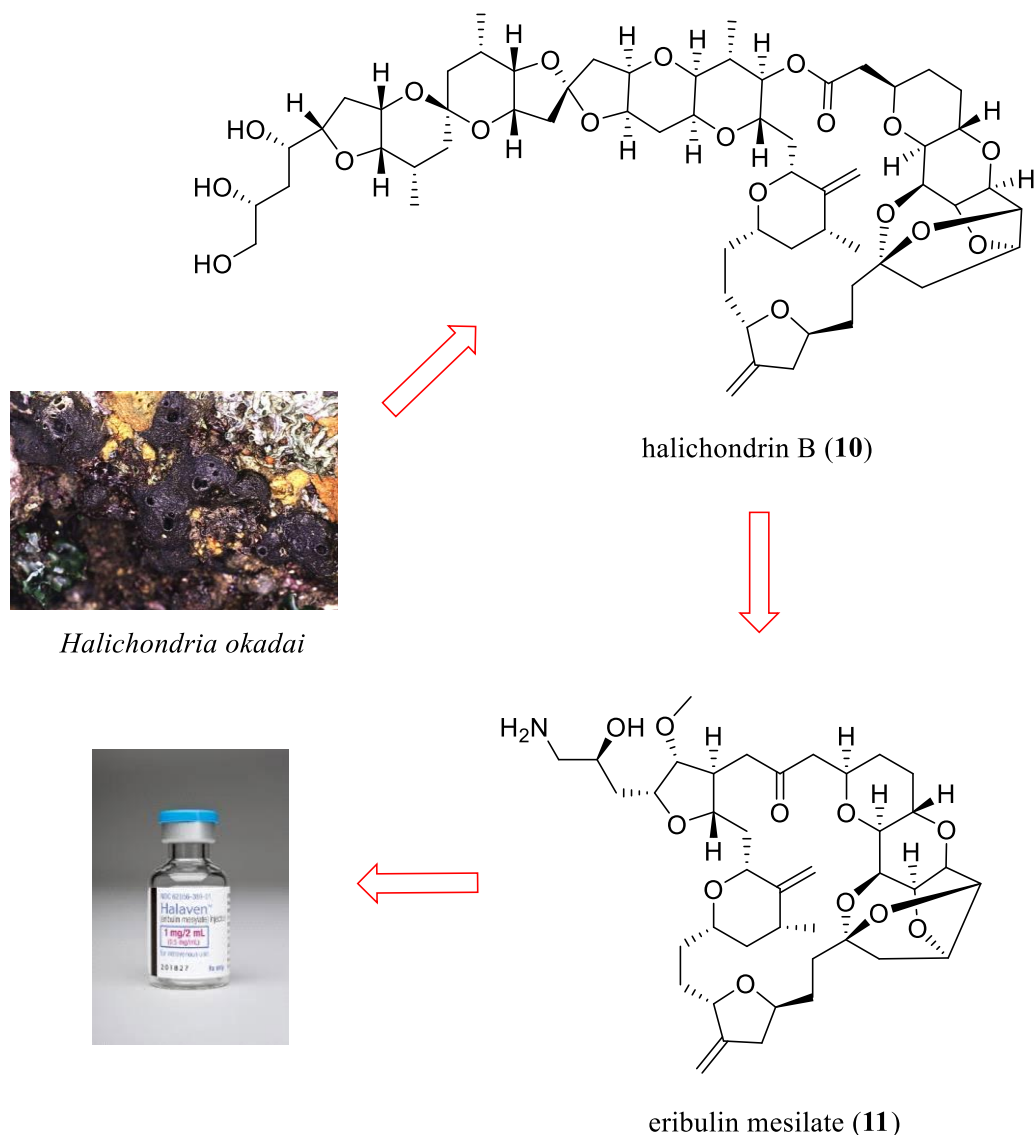
Figure 5 Structures of halichondrin B (**10**) isolated from the marine sponge *Halichondria okadai* and the synthetic analogue eribulin mesilate (**11**).

Dolastatin 10 (**12**), a potent cytotoxic compound was first isolated from the sea hare *Dolabella auricularia*. Its synthetic analogue monomethyl auristatin E (MMAE) was conjugated with an antibody (chimeric human-murine IgG1) to obtain the antibody-drug conjugated brentuximab-vedotin (**13**) (Figure 6) [16]. The specific binding of the antibody to tumor cells expressing the tumor necrosis factor receptor CD30, allows the drug to get into the cell, releasing MMAE causing microtubule disruption

and apoptosis. It was approved as Adcetris® by the FDA in 2011 and later in 2015 in Europe. It is used in the treatment against Hodgkin lymphoma [17].

Dolabella auricularia

dolastatin 10 (**12**)

antibody

brentuximab vedotin (**13**)
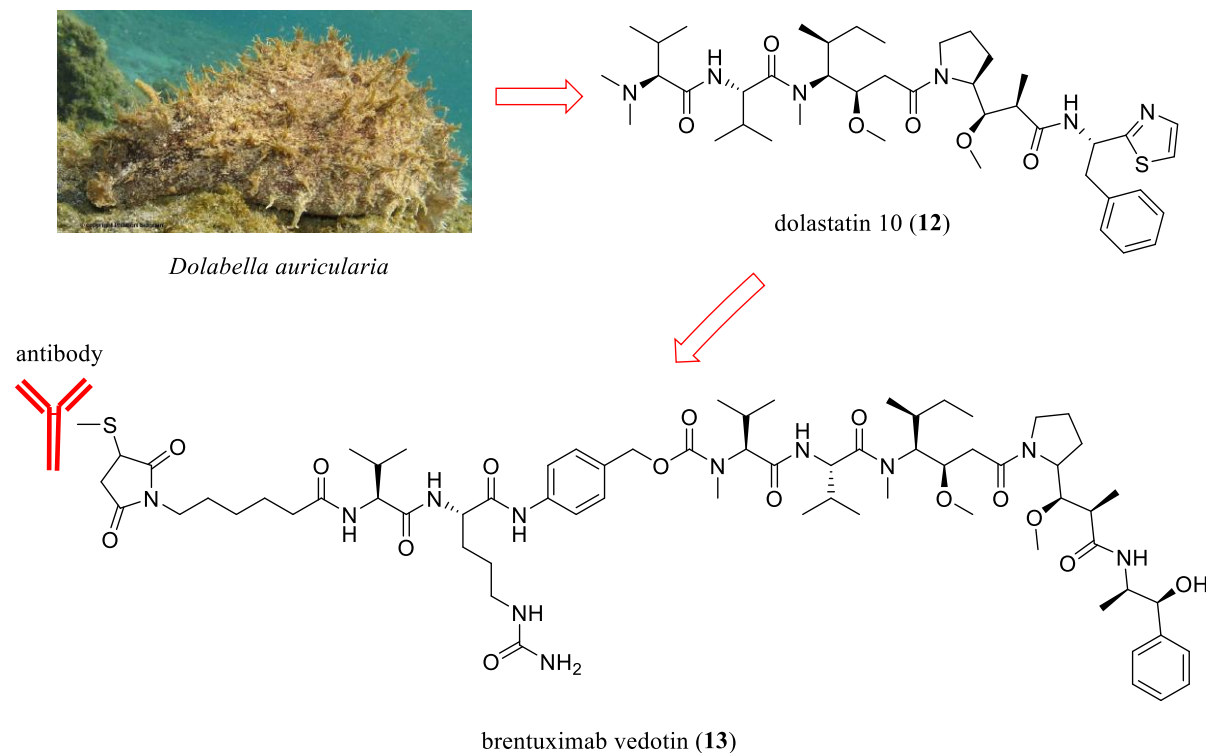
Figure 6 Structure of dolastatin 10 (**12**) isolated from the sea hare *Dolabella auricularia* and the antibody-drug conjugated brentuximab vedotin (**13**).

The most recent marine derived drug plitidepsin (**14**) (Figure 7), isolated from the ascidian *Aplidium albicans* was approved by the Australian Regulatory Agency (TGA) in 2018 under the name Aplidin® for the treatment of relapsed/refractory multiple myeloma in combination with dexamethasone [16, 20]. It specifically binds to the elongation factor 1-alpha 2 (eEF1A2) causing cell-cycle arrest, growth inhibition and induce apoptosis. Aplidin® was developed by PharmaMar and will be marketed by the biopharmaceutical company Specialised Therapeutics Asia Pte, Ltd [21].

Aplidium albicans
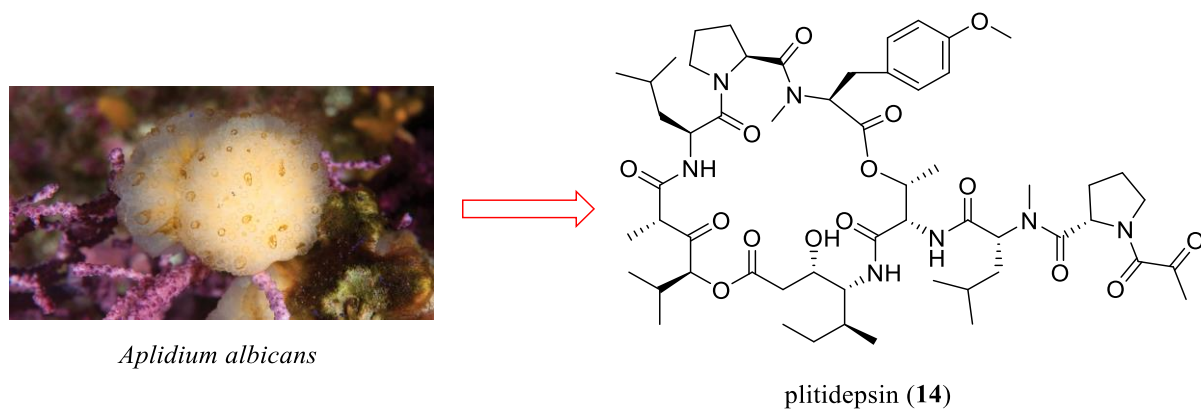
plitidepsin (**14**)

Figure 7 Structure of plitidepsin (**14**) isolated from the ascidian *Aplidium albicans*.

Chapter 1   Introduction

Up to date, more than 33,000 natural products have been isolated from marine organisms (Marinlit) and each year more than 1000 new compounds are reported in the annual review of Marine Natural Products [22, 23]. Table 1 shows the current natural products on phase III clinical trials.

Table 1 Marine derived drugs in phase III clinical trials

Compound Name	Commercial name	Marine Organism	Chemical class	Activity
Pinabulin (NPI-2358)	N/A	Fungus	Diketopiperazine	Antitumoral
Tetrodotoxin	Halneuron™	Pufferfish	Guanidinium alkaloid	Pain
Lurbinectedin (PM01183)	N/A	Tunicate	Alkaloid	Antitumoral
Depatuximab mafodotin (ABT-414)	N/A	Mollusk/ cyanobacterium	ADC (MMAF)	Antitumoral
Polatuzumab vedotin (DCDS-4501A)	N/A	Mollusk/ Cyanobacterium	ADC (MMAE)	Antitumoral
Marizomib (Salinosporamide A) NPI-0052	N/A	Bacterium	β-lactone-γ-lactam	Antitumoral

According to the National Cancer Institute, around 1% of marine samples have shown anticancer activity in the preclinical cytotoxicity screening comparing to 0.1 % of terrestrial tested samples [3]. More than 50% of the current marketed drugs are natural products (NPs) or NPs derivatives that have been chemically modified to enhance the selectivity and efficacy of the parent natural product [24]. Some studies aiming to determine the differences between successful drug leads with MNPs has been achieved by experimental and computational analysis of their physicochemical and structural features to potentially determine drug-like compounds [25, 26]. Additionally, Hou and co-workers compared the physicochemical and structural properties between MNPs and terrestrial natural products (TNPs) (Table 2), revealing that MNPs (78%) are slightly more drug-like compounds than TNPs (76%) and solubility was considered as one of the most important factors which is directly associated to the ADME (Absorption, Distribution, Metabolism and Excretion) properties of a pharmaceutical compound.

Table 2 Differences of relevant physicochemical properties between Marine Natural Products (MNPs) and Terrestrial Natural Products (TNPs) [24].

Physicochemical Properties	MNPs	TNPs	Outcome of MNPs
Molecular Size	Larger	shorter	Difficult cell permeation and intestinal absorption
Molecular solubility	Hydrophobic	Hydrophilic	Less solubility Reduce success rate for bioactivity
Elemental composition	Except O and F, all other atoms are higher including N, Br, S, I	Higher in O, F, Cl	Less N, Halogen and S than synthetic compounds. Diverse biosynthetic pathways for MNPs.
Number of molecular bonds, chains and rings	Higher rotatable, stereo bonds and chains. Higher 8 to 10 membered rings	Higher aromatic bonds and rings. Higher 4 to 7 membered rings	Increase flexibility and effective for chemical reactions
Difference of fragments and scaffolds	Higher	Lower	Diverse biosynthetic pathways

1.3   **Other applications of Marine Natural Products**

Despite their pharmacological properties, MNPs have also been used as nutraceuticals, cosmetics, anti-foulants, biofuels and as agrochemical agents [8, 27]. For example, nereistoxin (**15**), first isolated from the polychaeta worm *Lumbriconereis heteropoda* in 1934, is used as a precursor in the synthesis of cartap (**16**), a highly effective insecticide applied in different cultivations like orange, rice and sugarcane to control plague [28]. Okadaic acid (**17**) isolated from the dinoflagellate *Prorocentrum lima* and responsible for diahrretic shellfish poisoning (DSP) is being used as a tool to study the regulatory mechanisms of protein phosphorilation in cellular processes [29]. The UV protectants mycosporine-like amino acids (MAAs) such as asterina-330 (**18**) isolated from the sea star *Asterina pectinifera* and its analogues have been considered as potential active ingredients in the development of sun screening products (Figure 8) [30]. These compounds are characterized by their high UV-absorption (UV-A and UV-B), photostability, resistance to abiotic stress and as natural antioxidant capable of inhibiting the generation of reactive oxygen species (ROS) [30-32]. These metabolites have also been reported from terrestrial and marine organisms including red algae, zooxanthellae scleractinia corals, cyanobacteria and zoantharians. The distribution of MAAs in the cytoplasm of the organisms and their superficial localization reinforce their UV protective role [33].

The bioluminescent calcium indicator protein aequorin isolated from the jellyfish *Aequorea victoria* is used to measure intracellular Ca^{2+} [34]. The anti-freeze glycoproteins isolated from fishes inhabiting the polar oceans are being studied to preserve tissues to be transplanted, to enhance fish production in cold environments, to increase the life-shelf of frozen food and to improve heat resistance dyes [35]. Additionally, several species of marine macro and micro algae have been used in the cosmetic industry due to the presence of compounds such as phlorotannins, sulfated polysaccharides, tyrosine inhibitors, pigments, ω-3 fatty acids, vitamins A, B, C, E and essential amino acids [36]. Phlorotannins and sulfated polysaccharides are the most promising compounds in the development of cosmetic products from marine sources. For example, the extracts from species of the micro algae *Arthospira* are used to repair early skin aging and prevent stria formation while the extracts of *Chlorella vulgaris* are used to support tissue regeneration through the stimulation of collagen synthesis in the skin [37]. Both species are commonly used in commercial skin care products.

Within the food industry, species of microalgae and cyanobacteria such as *Chlorella vulgaris*, *Spirulina*, *Haematococcus pluvialis* or *Dunaliella salina* are commonly used due to their rich bioactive natural products composition including amino acids, proteins, peptides, lipids, fatty acids (especially polyunsaturated fatty acids or PUFAs), β-carotenes and phycocyanobilins [38]. In recent years, several researchers have been focused on biofuel production from species of microalgae due to their fast growth and high oil content. Some species like *Chlorella zofingiensis*, *Chlorella protothecoids* and *Schizochytrium limacinum* can accumulate more than 50% oil of dry biomass becoming an excellent

source for producing biodiesel [39]. Several studies for screening high-lipid content species and methodologies to improve lipid production are currently undertaken [40, 41].

Lumbriconereis heteropoda

nereistoxin (**15**)

Cartap (**16**)

Okadaic acid (**17**)
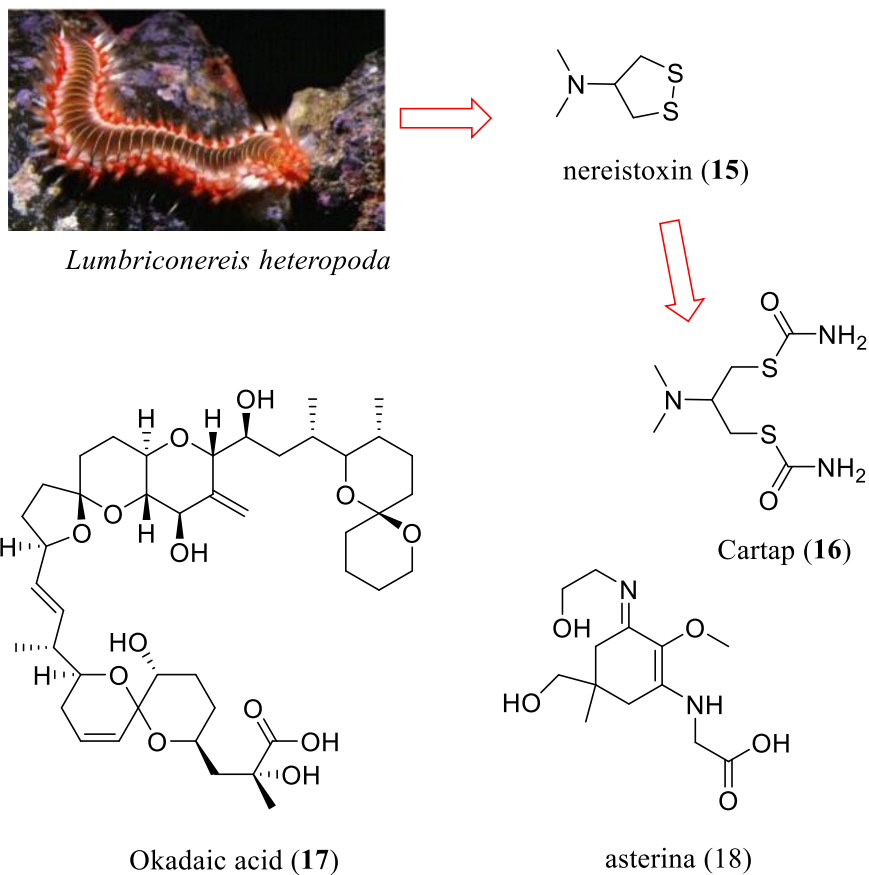
asterina (18)

Figure 8 Structures of nereistoxin (**15**), cartap (**16**), okadaic acid (**17**) and asterina (**18**).

1.4 **Marine Biodiversity from the Tropical Eastern Pacific (TEP)**

1.4.1 **The Tropical Eastern Pacific**

The Tropical Eastern Pacific (TEP) (Figure 9) is one of the 30 marine ecoregions extended from the south of Baja California peninsula to the north of Peru including Revillagigedo, Cocos, Clipperton and the Galapagos Islands [42]. Several authors have attempted to divide the TEP into biogeographic provinces based on the different taxa distribution. For example, Briggs *et al*., classified the TEP into three provinces with coral reefs included; Mexican province (Gulf of California to Tehuantepec), Panamanian province (El Salvador to Ecuador) and the Galapagos Islands. A classification based on decapod crustacean distribution by Boschi divided the TEP into two provinces; the Panamic and the Galapagos Archipelago while Robertson and Cramer based on fish distribution classified the TEP into three provinces; two coastal areas and the oceanic islands [42]. Additionally, Spalding *et al*., divided the TEP in eleven ecoregions including Revillagigedos, Clipperton, Mexican Tropical Pacific, Chiapas-Nicaragua, Nicoya, Cocos Islands, Panama Bight, Guayaquil, Northern, Eastern and Western Galapagos Islands [43, 44]. There are 32 Marine Protected Areas in the TEP, five of them are UNESCO World Heritage Sites including Gulf of California Islands (Mexico), Coiba National Park (Panama), Cocos Islands (Costa Rica), Malpelo Fauna and Flora Sanctuary (Colombia) and Galapagos Islands (Ecuador) [45].
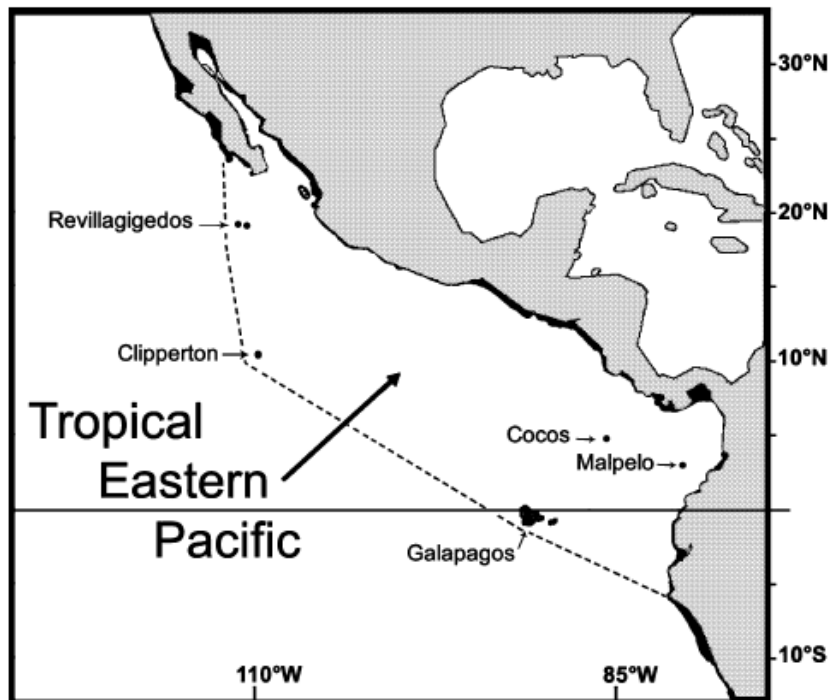
Figure 9 The Tropical Eastern Pacific ecoregion.   [46]

Additionally, the TEP is characterized by different ecosystems including sandy beaches, high cliffs, mangrove forests, alluvial or deltas plains, estuaries, lagoons, rocky coasts and reefs [47]. This ecoregion is also influenced by two natural currents; the Humboldt current characterized by cold water, high-salinity and high-nutrient availability with a massive upwelling system, and the Panama current with the warm surface layer and low-salinity concentration. The periodically occurrence of the El Niño Southern Oscillation (ENSO) characterized by a fluctuation of the sea layer temperature (warm water current) and the air pressure of the overlying atmosphere, has caused variation of the community composition and affluence of plankton affecting greatly the climatic and oceanographic conditions [48]. These currents are shaping the distribution of marine organisms and influencing the variability of salinity, temperature and nutrient concentration. For example, the ENSO which occurs every four to nine years, caused a massive coral bleaching by the loss of their associated zooxanthellae leading to coral death during the events in 1982-1983 and 1997-1998. In fact, the 82-83 ENSO event which lasted from 10-20 months depending on the location, caused 70 to 90% of zooxanthellate coral death in Costa Rica, Panama and Colombia, and more than 95% mortality was observed in the Galapagos Islands. Coral mortality occurred from 1 to 20 m depth and few species such as *Pocillopora* survived at 2-3 m [49]. The presence of very few coral reefs and coral development in the TEP has been limited by the regular impact of the ENSO, however, not all the regions in the TEP have experienced the negative effects of reduced coral communities by coral bleaching [50].

1.4.2 Marine Biodiversity in the Tropical Eastern Pacific

The first expeditions aiming to describe the marine biodiversity in the TEP started in the late 1700s through the coasts of Panama, Colombia, Costa Rica, Ecuador and Peru. Since then, several studies have been carried out to increase the knowledge of the different organisms inhabiting this ecoregion. In 1835, during one of the most important explorations, the voyage of Charles Darwin to the Galapagos Islands, the absence of coral reefs in the TEP was first noticed [45]. However, in 1870 Verril described the presence of several species of corals in Panama and the Gulf of California [51, 52]. In 1904, an organized study of the biological species of the TEP was accomplished by the Eastern Pacific expedition of the U.S National Museum of Natural History on the U.S Fish Commission Steamer Albatross [45]. During this expedition, several biological species and zooplankton were collected through the coast of Panama, Colombia and Ecuador. Other important expeditions that contributed to the description of the rich marine biodiversity of the TEP includes: The Saint George expedition in 1927 to the Gorgona Islands, the Allan Hancock cruises from 1931 to 1941 with the vessels Velero III and IV and the Askoy expedition in 1941 [53]. The results of those studies revealed a high level of endemism across the countries in the TEP. It has been reported that only the Gulf of California contains 852 endemic species followed by the Galapagos Islands with 565 endemic ones [42]. Additionally, 70% of fish in the TEP, 41% of ahermatypic corals in the Galapagos Islands and 29% of sponges in Mexico are also endemic.

Nevertheless, the numbers of endemic species could be higher because of the lack of marine studies in other locations within this ecoregion. Cortez *et al*., compiled the information of the distribution of marine organisms reported by different authors across the TEP [42]. Earlier studies on coral reefs in the TEP was pursued by local scientist in Mexico, Costa Rica, Panama and Colombia, and in the last few years researchers from Ecuador and Chile started to pay attention and characterize the marine biodiversity in those territories. Glynn *et al*., has strongly contributed with updated reports of the biodiversity of marine organisms inhabiting the TEP [45].

It was noted that the scleractinian corals in the TEP are strongly related to those of the Indo-Pacific except for the stony coral *Porites lobata* which is different from the Indo-Pacific population, suggesting its development on local larval sources instead of gene distribution across the Eastern Pacific Barrier [54]. The Eastern Pacific scleractinian corals were characterized as: **a**) small in size, **b**) highly dispersed, **c**) lack of reef flats or algal ridges, **d**) shallow development (<10 m depth), **e**) thin skeleton and **f**) composed by few species in comparison to those of the Indo-Pacific and Caribbean reefs [45]. The lack of taxonomist in some countries of the TEP has limited the identification of endemic species. Therefore, it is necessary to promote collaborations with local and international universities and research institutes to fully characterize the marine biodiversity and protect those species in danger. The global warming and uncontrolled fisheries are becoming the main factors for the extinction of local species. Mate *et al*., reported a photographic guide of the most representative marine organisms in the TEP and the respective locations where those samples were found [55]. Members of the phylum Phaeophyta, Chlorophyta, Porifera, Cnidaria, Nemertea, Annelida, Mollusca, Arthropoda, Echinodermata and Craniata were included in the study. Among them, the phylum Cnidaria was the most abundant with 53 species. An updated inventory of the biodiversity of marine invertebrates of each country within the TEP is required to protect the local species from invasive ones. One example is the presence of the snowflake coral *Carijoa riisei* which has been reported in the coast of Colombia, Mexico and Ecuador. It has been observed overgrowing several species of octocorals such as *Muricea*, *Pacifigorgia* and *Leptogorgia*, and some of these are native species from the TEP [56, 57]. The identification of potential invasive species will help local authorities to establish policies and protocols to protect the local marine biodiversity from becoming extinct.

1.4.3 Marine Biodiversity of the Ecuadorian coast

The Ecuadorian coast (4,403 km) is comprised by two areas; the continental coast and the Galapagos Archipelago and it is located within the Tropical Easter Pacific, one of the most biodiverse and overlooked ecoregion in the world [58]. The continental coast has been subdivided in two marine systems; the intertidal system characterized by mud, sandy rocky beaches and mangroves, while the subtidal system is characterized by soft bottom, rock bottom, grave bottom and coral reef bottom. Additionally, the continental coast and the Archipelago are influenced by different oceanic conditions;

the warm and low salinity water from the Panama current (north) and the cold and high salinity water of the Humboldt current (Peru Oceanic Current) from the south. The zone between these two currents is called the equatorial undercurrent (Crumwell Current) and it is characterized by a strong thermal and salinity gradient which goes through considerable seasonal variations. (Figure 10) [59].

Figure 10 Currents affecting the Ecuadorian coast [59].

The diversity of ecosystems, the oceanographic conditions, coast morphology and the geographic location of Ecuador has contributed to the vast marine biodiversity existing in this area [60]. The study of the marine biodiversity in the Ecuadorian coast started at the Galapagos Islands back in 1835 with the exploration of Charles Darwin in the Voyage of the Beagle. In fact, Darwin's discoveries in the Archipelago inspired different scientist to continue exploring the rich biodiversity of the Islands. The Galapagos is one of the most studied marine ecoresystems in the world. It has been reported the presence of 3089 invertebrates, 447 fish and 565 species of these species are endemic [42]. Additionally, 316 species of macroalgae, 38 species of sponges, 12 species of octocorals, 23 species of hermatypic corals and 872 species of reef-associated molluscs have been reported from the Galapagos. Despite the diversity of marine organisms in the Islands, studies on coral species was given more attention because of the negative impact caused by ENSO. In the early 1970's, the study of octocorals started by the pioneer work of Gerard Wellington, a volunteer at the Charles Darwin Station located in Santa Cruz Islands, Galapagos [45]. His research was focused on coral composition, biotic interactions and reef structure. However, el Niño event in 1982-1983 destroyed up to 99% of shallow corals in combination with the bio erosion activity caused by several species of bioeroders like sea urchins of the genus *Eucidaris, lithophagine* bivalve molluscs, etc. Except from shallow water corals which experienced

higher surface temperatures, coral communities populating below 14 m survived the 1982-83 ENSO event due to the cooler temperature and reduced light exposure. For example, two free-living corals *Diaseris distorta* and *Psammocora stellate* were observed on the north coast of Floreana Island after the strong oceanic phenomenon [45, 49]. Further monitoring showed the recovery of 22 reported reef-building corals dominated by two genera; *Pocillopora* and *Pavona* after both 82-83 and 97-98 ENSO events. However, neither of both corals were endemic to the Galapagos Islands. On the contrary, 29% of 43 species of ahermatypic corals are shallow-water endemic to the Islands [59].

On the other hand, studies of the marine biodiversity in the continental area of Ecuador started in the late 60's focusing on marine species of commercial value including fish, mollusks and crustaceans. Some of these studies have been reported from Esmeraldas, Gulf of Guayaquil, Santa Elena, Manta bay and Machalilla National Park [58]. Later, those studies were expanded to species of non-commercial value such as diatoms, phytoplankton, benthic mollusks, benthic polychaetas, pteropods and other organisms [58]. The number of non-commercial value species could have increased since those species were reported from a few sampling locations while the number of species of commercial value could have been reduced because of the uncontrolled exploitation. In 2011, Cruz investigated the benthonic macro-fauna of Manta bay reporting the presence of 41 species belonging to six different phyla [61]. The phylum Mollusk was the most representative with 31 species while the other 10 species where distributed among the phylum Coelenterate, Platyhelmynthes, Arthropod, Sipuncula and Echinodermata.

Machalilla National Park established in 1970, is another important spot which inhabits a great diversity of marine organisms. The first investigations in this area started in 1975 by Glynn and Wellington who reported the presence of seven species of zooxanthellate corals, being species of *Pocillopora* the most dominant in the zone [45]. However, during a coastal survey in 1991, it was observed that most corals were dead and eroded with great affluence of the sea urchin *Diadema mexicanum*. The massive coral dead was the consequence of the 82-83 ENSO event as occurred in the Galapagos Islands. Further investigation of the diversity of corals and octocorals at Machalilla National Park revealed the presence of 50 species including 19 scleractin corals, 29 octocorals and two black corals which were reported as *Myriophates panamensis* and *Antipathes galapagensis* [62]. The presence of *Myriopathes panamensis* has been reported from the shallow waters of Panama Bay (9-17 m depth), Galapagos Islands and Machalilla National Park in Ecuador, while *Antipathes galapagensis* was first reported from the Galapagos Islands and later throughout the coast from the Gulf of California to Ecuador at different depths between 3 to 76 m and from shallow waters in Costa Rica [63]. Additionally, two new species of octocorals, *Eugorgia ahorcadensis* sp. nov., and *Leptogorgia mariarosae* sp. nov., were described from this marine protected area [64].

The Marine Reserve EL Pelado (REMAPE) (Figure 11) is an important protected area located at the Peninsula of Santa Elena, Ecuador comprised by an islet and a coastal marine zone. In 2015, the first project aimed to characterize the biodiversity of microorganisms and marine invertebrates from the REMAPE at the taxonomic, metabolomic and metagenomic level and their application in animal and human health was funded by the Ecuadorian Government through the Secretary of Higher Education, Science and Technology (SENESCYT). This project was also the first one that attempted to investigate the chemical diversity from marine microorganisms and invertebrates inhabiting the Ecuadorian coast, representing the first step in the development of the field of marine natural products in the country.
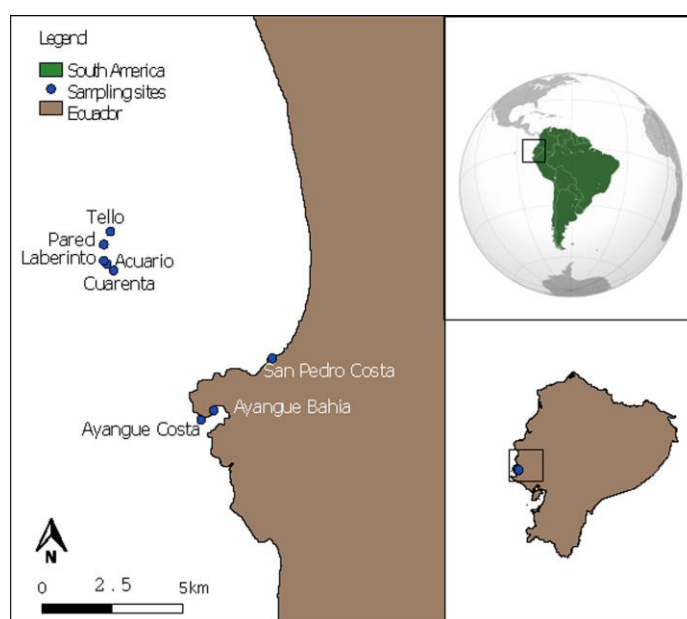
Figure 11 Location of the Marine Protected Area El Pelado [65].

Rodriguez and co-workers reported a quantitative assessment of the Alcyonacea community describing the presence of seventeen species from the families Plexauridae (8), Gorgoniidea (8) and Clavularidae (1) [66]. The monitoring of this marine reserve together with previous studies reported from the Galapagos Islands and Machalilla National Park confirm octocorals as the most representative and zoantharians as the second most representative group of marine invertebrates inhabiting the Ecuadorian Marine ecosystem [63, 67]. During this project, Thomas and co-workers assessed the biodiversity of zoantharians from this maritime area reporting the presence of six species of zoantharians [65]. The diversity of zoantharians fom the Ecuadorian coast will be disscussed below.

1.5   Zoantharians and their chemical diversity

1.5.1 General

Zoantharians (Cnidaria, Anthozoa, Hexacorallia, Zoantharia) are sessile invertebrates commonly found from shallow to deep-sea environments throughout the Indo-Pacific and Atlantic Ocean [68]. These sessile invertebrates are characterized by their color, soft bodied polyps with two rows of tentacles, one siphomoglyph and nematocysts. Most of these animals are commonly found in colonies, but species of the genus *Sphenopus* have been reported as solitary zoantharian [69]. Zoantharians are divided in two suborders, Brachycnemina and Macrocnemina (Table 3). Members of the Brachycnemina suborder are characterized by the presence of planktonic microalgae while they are absent in the suborder Macrocnemina [70]. The taxonomy identification of zoantharians at species level is still a difficult task to accomplish due to different factors affecting their morphological analysis, their intraspecific variation and the limited availability of accurate morphological markers [71]. Recent studies have suggested that substrate specificity is an important character being used for their taxonomical classification as a complement to the genetic and morphological analysis [68]. Some zoantharians have been found overgrowing other organisms. For example, species belonging to the genus *Hydrozoanthus* are associated with hydrozoans; members of the genus *Antipathozoanthus* are associated with Antipatharians; the genera *Kualamanamana*, *Zibrowius*, *Hurlizoanthus*, *Kauluzoanthus*, *Corallizoanthus* and *Bullagummizoanthus* are often associated with deep-sea octocorals, species of the genus *Parazoanthus* are associated with hydrozoans, sponges and octocorals, species of the genus *Savalia* are often associated with octocorals and species of the genera *Umimayanthus* and *Bergia* are associated with sponges [68, 72, 73]. However, the association between zoantharians and their host is not always symbiotic and some studies have reported zoantharians to be a threat for reef environments [74].

Despite several reports of zoantharians from the Indo-Pacific and Caribbean regions, new species are still being described from all the oceans [75]. Kise *et al*., reported three new species of the genus *Antipathozoanthus* identified as *A. obscurus*, *A. remengesaui* and *A. cavernus* from the Red Sea, the Maldives, Palau and Southern Japan [76]. While very few studies of zoantharians diversity have been carried out in ecoregions like the TEP, new genera and species are being described from this area. Reimer *et al*., reported a new genus and some new species of zoantharians from the Galapagos Islands, indicating the great potential of discovering species that are still unknown to science [77].

Table 3 Taxonomy classification of the order Zoantharia [2].

Order	Suborder	Family	Genus	Species
Zoantharia	Brachycnemina	Neozoanthidae	*Neozoanthus*	3
		Sphenopidae	*Palythoa*	132
			Sphenopus	4
			Protopalythoa	5
		Zoanthidae	*Acrozoanthus*	1
			Isaurus	14
			Zoanthus	43
	Macrocnemina	Epizoanthidae	*Epizoanthus*	105
			Thoracactis	1
			Paleozoanthus	1
			Sidisia	5
			Thoracactus	1
		Hydrozoanthidae	*Aenigmanthus*	1
			Hydrozoanthus	4
			Terrazoanthus	5
		Microzoanthidae	*Microzoanthus*	2
		Nanozoanthidae	*Nanozoanthus*	1
		Parazoanthidae	*Antipathozoanthus*	5
			Bergia	3
			Bullagummizoanthus	1
			Corallizoanthus	1
			Hurlizoanthus	2
			Isozoanthus	20
			Kauluzoanthus	1
			Kulamanamana	1
			Mesozoanthus	2
			Parazoanthus	22
			Savalia	2
			Umimayanthus	4
			Zibrowius	3

Order	Suborder	Family	Genus	Species
Zoantharia	Macrocnemina	Gerardidae	taxon under investigation	
		Hawaidae		
		Parasitozoanthidae		
		Primnozoanthidae		

1.5.2   Zoantharians in the Tropical Eastern Pacific and the Ecuadorian coast

The diversity of zoantharians in the TEP has been only little documented. One of the first descriptions of zoantharian species in the TEP was undertaken in 1869 by Verril *et al*., who reported the presence of *Epizoanthus elongatus* from Peru and Panama, *Epizoanthus humilis* from Panama and *Epizoanthus crassus* from El Salvador [78]. In the 1960, Cutress and Pequegnat compiled the information on the diversity of zoantharians in the TEP [79]. The reported species corresponded to the following; *Epizoanthus californicum, E. humile, E. gabrieli, E. patagonichus, Palythoa complanate, P. ignota, P. insignis, P. pazi, P. praelonga, P. rickettsi, Parazoanthus elongatus, P. fuegiensis, Zoanthus confertus, Z. danae, Z. depressum*, and *Z. nitidum*. Since then, there has been amendments in the taxonomic identification of some species. Even though, Fautin *et al*., observed the presence of zoantharians in the Galapagos Islands in 2007, it was not included in his report of sea anemones [80]. Later in 2008, Reimer *et al*., reported for the first time the presence of zoantharians in the Galapagos Islands [67]. Eight species of zoantharians present in shallow water (<35 m) were collected for analysis, seven of them corresponded to the genera *Zoanthus, Parazoanthus* and *Palythoa*, while one specie belonged to an undescribed genus. The known species were reported as: *Zoanthus* cf. *sansibaricus, Zoanthus* cf. *vietnamensis/kuroshio, Palythoa* cf. *mutuki, Palythoa* cf. *tuberculosa*, and three undescribed species of *Parazoanthus* sp. [67, 81]. Further studies of the diversity of zoantharians in the Galapagos allowed the identification of two new species; *Terrazoanthus patagonichus* (previously known as *T. onoi*) and *T. sinnigeri*, corresponding to the new genus *Terrazoanthus*, and two other new species belonging to the Parazoanthidae family; *Antipathozoanthus hickmani* and *Parazoanthus darwini* [77]. A non-parasitic association has been observed between *P. darwini* and some yellow-orange sponges, however, most of the time *P. darwini* is found over rocky substrate. Later, during the study of black corals at Machalilla National Park, the presence of two parasitic zoanthids *Antipathozoanthus hickmani* and *Terrazoanthus patagonichus* were reported growing over the black corals *Antipathes galapagensis* and *Myriopathes panamensis* respectively [63]. The parasitic behavior of *T. patagonichus* has been observed from the Gulf of California to the Galapagos Islands from 3 to 76 m depth. Additionally, the presence of *Zoanthus* cf. *vietnamiensis* in the coast of Ecuador, Galapagos Islands, Panama and the Central-Indo Pacific was reported by Mate *et al*., in 2016 [55]. Recently, within the National project aimed to characterize the

biodiversity of marine invertebrates from the Marine Protected Area el Pelado (REMAPE), eight species of zoantharians were identified. These species include *A. hickmani* (**a**), *P. darwini* (**b**), *T.* cf. *patagonichus* (**c**), *Terrazoanthus patagonichus* (**d**), *Terrazoanthus* sp. (**e**), *Zoanthus* cf. *pulchellus* (**f**), *Z.* cf. *sociatus* (**g**) and *Palythoa* cf. *mutuki* (**h**) (Figure 12). There are still other locations across the continental coast of Ecuador that remain untapped to investigate the biodiversity of zoantharians and other invertebrates.
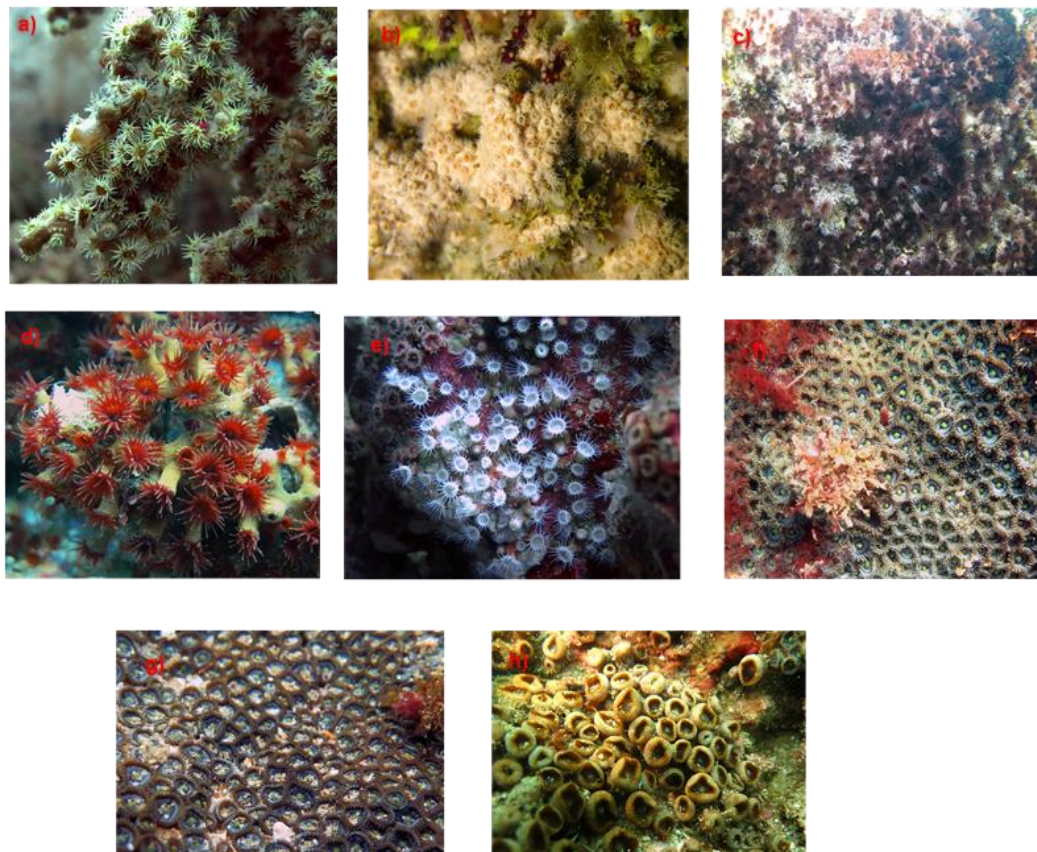
Figure 12 Zoantharian species identified from the Marine Protected Area El Pelado (REMAPE). (© Karla Jaramillo).

1.6 **Aims of the Thesis**

The aim of this thesis was to study the chemical diversity of the most representative species of zoantharians inhabiting the Marine Protected Area "El Pelado" located at the Peninsula of Santa Elena, Ecuador, and their potential applications in animal and human health. The specific objectives of this study were the following:

- ✓ To develop the most efficient method for isolation of natural products from the selected samples.
- ✓ To elucidate the structures of the isolated metabolites using 1D and 2D NMR spectrum and HRESIMS data.
- ✓ To assess the biological activity of the isolated compounds.

I   Chemical diversity of zoantharians - beyond their use as ornamental aquatic animals! (Submitted to NPR)

Paul O. Guillen,[a,b,†] **Karla B. Jaramillo** [b,c,†,] **Grégory Genta-Jouve**[d] **and Olivier P. Thomas** [*a]

I.I   Natural Products Isolated from Zoantharians

Zoantharians are the source of a rich diversity of metabolites with unique chemical scaffold, however, chemical studies of most species of this group has been overlooked. Herein, a description of the natural products isolated from zoantharians is presented. This information will be organized according to both suborders. This part of the thesis has been submitted in a review of the Chemical diversity of zoantharians to Natural Products Reports.

I.I.I   Suborder Brachycnemina

Four main families of natural products have been described from species of this sub-order: sterols, ecdysteroids, palytoxins and zoanthamines. The description of fatty acids is excluded of this study as it was difficult to properly retrieve this information.

I.I.I.I   Sterols

***Palythoa*:** The first chemical investigation of a *Palythoa* species was published by Bergmann *et al*. in 1951 on the Caribbean *Palythoa mammilosa* and it was focused on the sterol composition of this species. As the physicochemical properties of the main sterol showed differences from previously reported sterols, it was named palysterol. Comparison of its optical rotation with the sponge sterol haliclonasterol indicated that palysterol would be a C-24 ethyl sterol whereas haliclonasterol is the C-24 methyl analogue, but the authors mentioned it might should be a mixture [82]. Later, Gupta and Scheuer analyzed the sterol fraction of *Palythoa* sp. from Tahiti and *Palythoa tuberculosa* from the Marshall islands by Gas Liquid Chromatography indicating similar sterol composition of *P. tuberculosa* to the previously reported palysterol of *P. mammilosa* [83]. The sterols from *P. tuberculosa* were identified as cholesterol (**19**), brassicasterol (**20**), 22,23-dihydrobrassicasterol (**21**), gorgosterol (**22**), campesterol (**23**) and *β*-sitosterol (**24**) (Figure 13). Chalinasterol (**25**) was reported as the unique sterol from *Palythoa* sp. The identification of the sterols was deduced by comparison of the IR and NMR data to those acetate derivatives and standards. Quinn *et al*. analyzed the sterol composition of eight Hawaiian zoantharians including four species of *Palythoa* as a preliminary taxonomic assessment [84]. Methylenecholesterol (**25**), also named chalinasterol, was the only sterol found in *P. toxica,* like in *Palythoa* sp. from Tahiti reported by Gupta and Scheuer [83], while the sterol mixture of *P. tuberculosa*, *P. psammophilia* and *P. vestitus* (previously known as *Zoanthus vestitus*) showed similar sterol composition. The analysis of the sterol composition of *Palythoa* sp. collected from Okinawa- Japan revealed the presence of cholesta-5,22(*E*)-dien-3*β*-ol (**26**), along with **19**, **20**, **21**, **22**, **25** and traces of 23,24-dimethylcholesta-5,22(*E*)-dien-3*β*-ol (**27**) (Figure 13) [85]. The sterol **27**, commonly found in octocorals is considered an intermediate into the biosynthesis of gorgosterol (**22**). Three species of *Palythoa* were later collected from different sites of the Brazilian coast and studied for their sterol
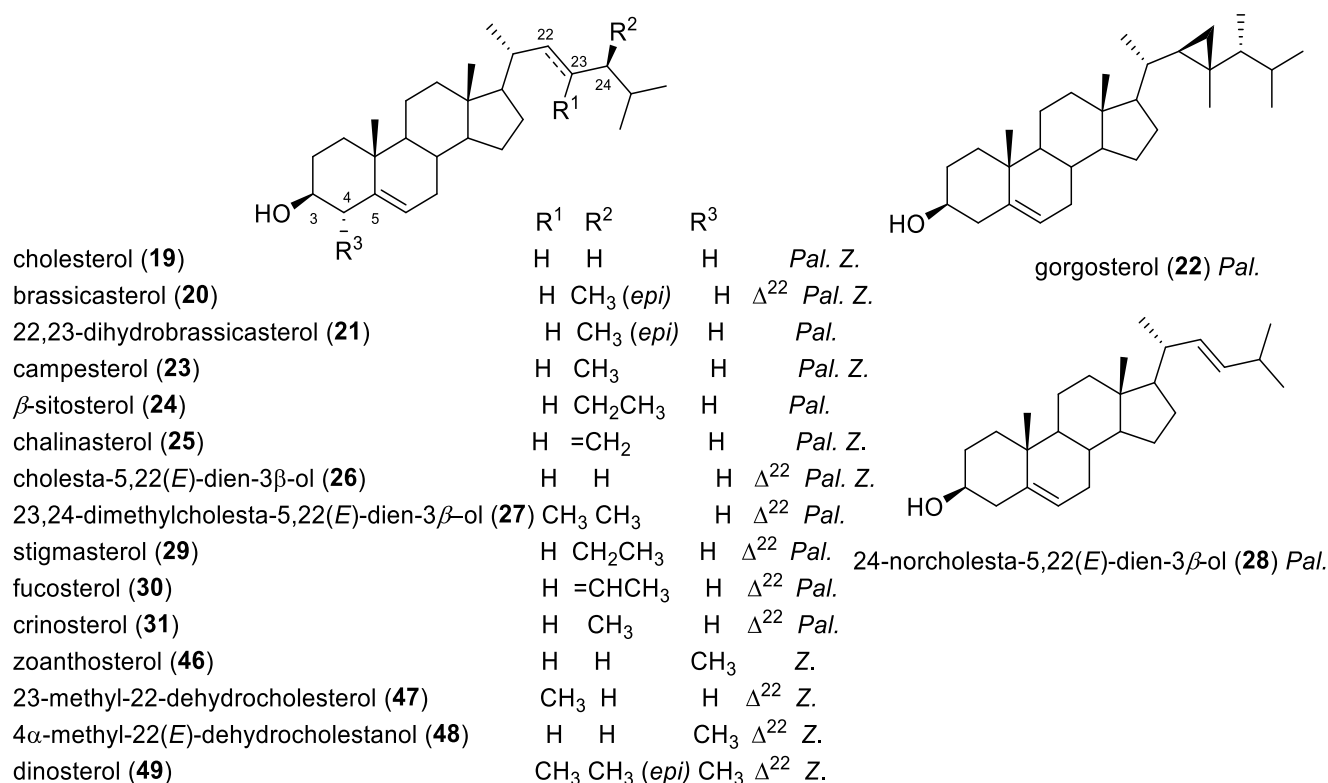
composition [86]. Analysis of the male and sterile colonies of *P. caribaeorum* revealed the presence of the same sterol composition as *P. mammilosa* previously reported by Gupta and Scheuer [83]. Analysis of the female or hermaphrodite colonies of *P. caribaeorum* showed higher concentration of **22** than male colonies. However, no significant variability with location or sex was evidenced except for one sample CF-72. The sterol mixture of both *Palythoa* sp. from Tahiti and CF-72 showed high concentration of **20** and small amount of **21**. Interestingly, the zooxanthella isolated from CF-72 had the same sterol composition as its host and doubled the concentration of **22**. The sterol composition of *P. variabilis* showed similar sterol composition to *P. tuberculosa* reported by Gupta *et al.*, except for the higher concentration of **21** and low concentration of **22**. The major sterols of CF-72 were identified as **19**, **20**, **21**, **22**. Sterols **25**, **26** and 24-norcholesta-5,22(*E*)-dien-3β-ol (**28**) were also identified but in lower amounts [87]. In 1986, the sterol composition of *P. dartevellei*, *P. monodi*, *P. senegalensis* and *P. variabilis* collected off the coast of Senegal was similar to those *Palythoa* species reported by Gupta *et al.*, Kanazawa *et al.*, and Kelecom *et al* [88]. The study of the sterol composition of *Palythoa senegambiensis* by the same group revealed the presence of **19**, **20**, **23**, **24** but also stigmasterol (**29**), fucosterol (**30**) and crinosterol (**31**) (Figure 13) [89]. The sterols were identified by comparison of their retention times in GLC with those of standard sterols. After an absence of work on zoantharian sterol for about 25 years, the chemical study of *P. tuberculosa* from the Red Sea allowed the identification of seven sterols oxidized at position C-1 and named palysterol A-F (**32-37**) and 24-methylenecholest-5-en-1α,3β,11α-triol (**38**) (Figure 13) [90]. The structures were elucidated from NMR and MS data. Compound **32** exhibited cytotoxic activity against breast adenocarcinoma (MCF-7) and human colon adenocarcinoma (HT-29) with an IC$_{50}$ values of 170 and 178 µM respectively and no activity on human cervical carcinoma (HeLa) and the non-cancerous human cell line (KMST-6). Compound **37** displayed selective antitumoral activity against MCF-7, HT-29, KMST-6 and HeLa with an IC$_{50}$ values of 82, 122, 126 and 128 µM respectively. Finally, two unusual ergostane-type sterols (24*R*)-7α-hydroperoxy-ergost-5-en-3β-ol (**39**) and (24*R*)-6β-carboxyl-(8→6)-abeoergostan-3β,5β-diol (**40**) were identified along with 7α-hydroxycampesterol (**41**), 5α,8α-*epi*-dioxycampesterol (**42**), 24(*R*)-ergost-7-en-3β,5α,6β-triol (**43**), cholest-4-en-3-one (**44**) and cholesta-3,5-dien-7-one (**45**) by GC-MS analysis of the hexane fraction of *P. caribaeorum* and *P. variabilis* collected from the coast of Brazil (Figure 13) [91]. Compound **40** exhibited moderated cytotoxic activity against human colorectal tumor cell line (HCT-116) with and IC$_{50}$ values of 50 and 4µM after 24 and 72 h respectively.

Zoanthus: In 1951, Bergmann and co-workers reported chalinasterol (**25**) as the major sterol present in *Zoanthus proteus* [82]. The characterization of the sterol was deduced by melting point and comparison with a standard. Cholesterol (**19**), brassicasterol (**20**), campesterol (**23**) and chalinasterol (**25**) were reported from *Zoanthus confertus* (now identified as *Z. pacificus*) collected around Coconut Island - Thailand by Gupta and Scheuer in 1968 (Figure 13) [83]. The characterization of these sterols was deduced based on their spectroscopy data, MS and by comparison of the GLC retention time with those

of standards. A new sterol zoanthosterol (**46**) was isolated from the Brazilian zoantharian *Zoanthus sociatus* along with **19** and **25** [92]. These sterols were isolated as their acetate derivatives and their structures deduced from NMR data and comparison with known analogues. Previous studies of the sterol composition of dinoflagellates isolated from the Jamaican *Zoanthus sociatus* revealed the presence of several 4α-methyl-5α-stanols suggesting **46** is in fact produced by the associated algae. Additionally, a local variation in the sterol composition has been observed since the sterol composition of *Z. sociatus* from Brazil contain mostly sterols with $\Delta^{24\,(28)}$ double bond while those sterols are absent in the associated algae isolated from the Jamaica *Z. sociatus*. Similar variations were reported from the symbionts associated to species of *Palythoa* [93]. Further analysis of the sterol composition of *Zoanthus* sp. from the coast of Brazil led to the identification of the sterol **26** together with **19, 20, 24** and **25** identified as their acetate salts. C-28 sterols were reported as the major components in species of the genus *Zoanthus* [94]. The study of the sterol composition of the dinoflagellate isolated from *Zoanthus sociatus* allowed the identification of **26**, 23-methyl-22-dehydrocholesterol (**47**), 4α-methyl-22*E*-dehydrocholestanol (**48**) and dinosterol (**49**) [95]. Their identification was based on interpretation of their NMR and MS data.

	R^1	R^2	R^3	
cholesterol (**19**)	H	H	H	*Pal. Z.*
brassicasterol (**20**)	H	CH₃ (*epi)*	H	Δ^{22} *Pal. Z.*
22,23-dihydrobrassicasterol (**21**)	H	CH₃ (*epi)*	H	*Pal.*
campesterol (**23**)	H	CH₃	H	*Pal. Z.*
β-sitosterol (**24**)	H	CH₂CH₃	H	*Pal.*
chalinasterol (**25**)	H	=CH₂	H	*Pal. Z.*
cholesta-5,22(*E*)-dien-3β-ol (**26**)	H	H	H	Δ^{22} *Pal. Z.*
23,24-dimethylcholesta-5,22(*E*)-dien-3*β*–ol (**27**)	CH₃	CH₃	H	Δ^{22} *Pal.*
stigmasterol (**29**)	H	CH₂CH₃	H	Δ^{22} *Pal.*
fucosterol (**30**)	H	=CHCH₃	H	Δ^{22} *Pal.*
crinosterol (**31**)	H	CH₃	H	Δ^{22} *Pal.*
zoanthosterol (**46**)	H	H	CH₃	*Z.*
23-methyl-22-dehydrocholesterol (**47**)	CH₃	H	H	Δ^{22} *Z.*
4α-methyl-22(*E*)-dehydrocholestanol (**48**)	H	H	CH₃	Δ^{22} *Z.*
dinosterol (**49**)	CH₃	CH₃ (*epi)*	CH₃	Δ^{22} *Z.*

gorgosterol (**22**) *Pal.*

24-norcholesta-5,22(*E*)-dien-3*β*-ol (**28**) *Pal.*

	R¹	R²	
palysterol A (**32**)	Ac	OH	*Pal.*
palysterol B (**33**)	Ac	=O	*Pal.*
palysterol C (**34**)	H	H	Δ²² *Pal.*
palysterol D (**35**)	Ac	H	Δ²² *Pal.*
palysterol E (**36**)	Ac	OAc	Δ²² *Pal.*
palysterol F (**37**)	Ac	=O	Δ²² *Pal.*
24-methylenecholest-5-en-1α,3β,11α-triol (**38**)	H	H	*Pal.*

	R
(24*R*)-7α-hydroperoxyergost-5-en-3β-ol (**39**)	OH *Pal.*
7α-hydroxycampesterol (**41**)	H *Pal.*

(24*R*)-6β-carboxyl-(8→6)-abeoergostan-3β,5β-diol (**40**) *Pal.*

5α,8α-*epi*-dioxycampesterol (**42**) *Pal.*

cholest-4-en-3-one (**44**) *Pal.*

(24*R*)-ergost-7-en-3β,5α,6β-triol (**43**) *Pal.*

cholesta-3,5-dien-7-one (**45**) *Pal.*

Figure 13 Structures of sterols from species of the suborder Brachycnemina. From *Palythoa* (Pal.), *Zoanthus* (Z.).

I.I.I.II Palytoxin analogues

The first reports of the toxicity exhibited by a *Palythoa* sp. dates back to 1961 when Ciereszko and co-workers experienced the toxicity of *Palythoa caribaeorum* immediately after crashing the dried material with sore throats, chills and fever [96]. Later, the same group reported the high toxicity of *Palythoa mammillosa* and *Palythoa grandis*. Palytoxin (**50**), known as one of the most potent natural and non-proteinaceous toxin for humans, was first isolated by Moore and Sheuer in 1971 from the Hawaiian zoanthid *Palythoa toxica* [97]. This species was previously known by the Hawaiian native population as "limu-makeo-Hana" which means deadly seaweed of Hana. The lethal dose (LD_{50}) exhibited by palytoxin was measured as 0.1 µg/kg by intravenous injection and 0.4 µg/kg by intraperitoneal injection
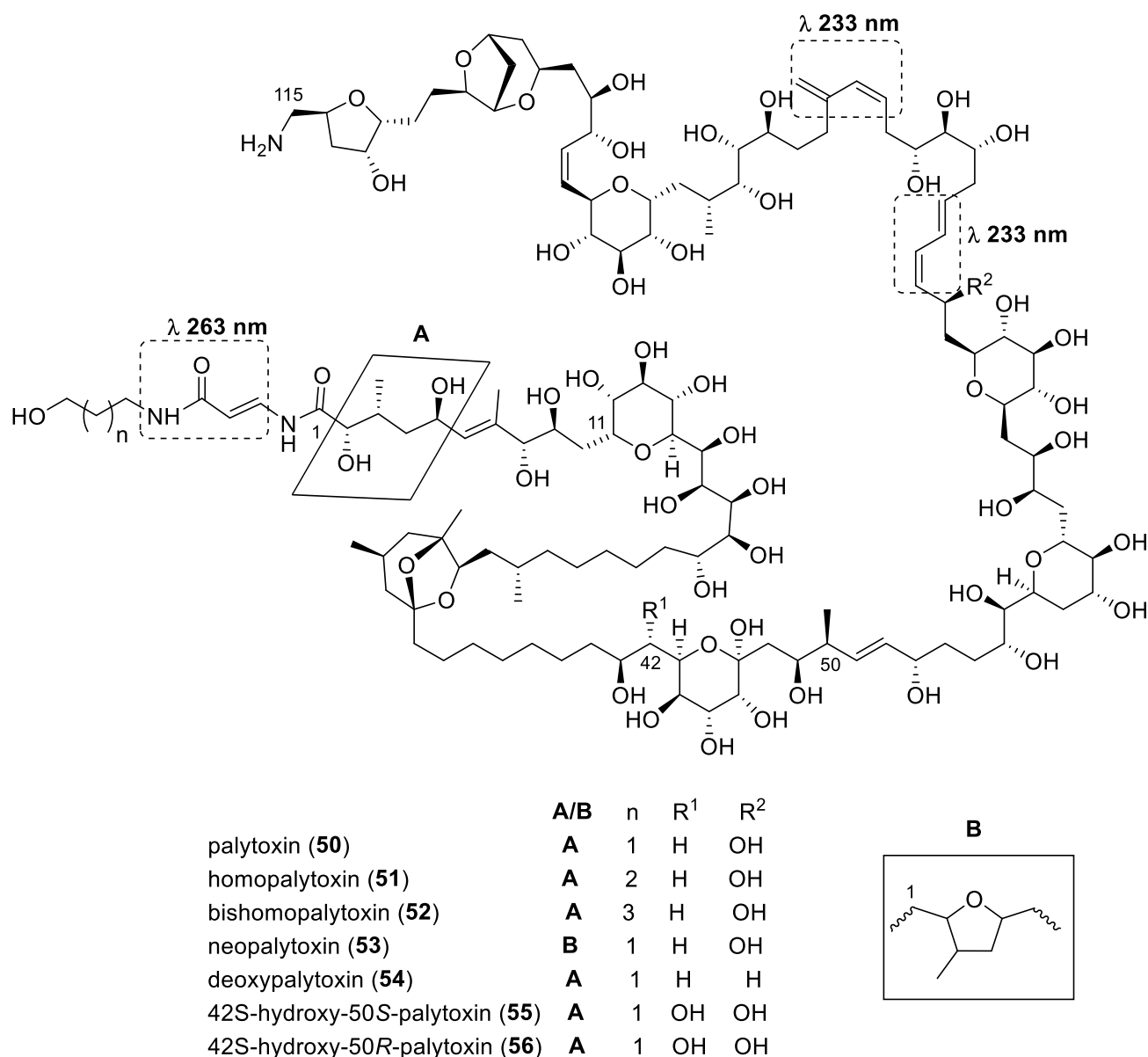
in mice. Based on NMR and combustion data, the molecular weight of the toxin was estimated to be about 3,300 Da [97-99]. It was described to be stable in water but a quick decomposition was observed under acidic or alkaline conditions leading to a reduction of its toxicity [100, 101]. The structure and stereochemistry of palytoxin (**50**) were elucidated a decade after the first report in 1981 by the work of two independent research groups led by Moore and Uemura (Figure 14) [102, 103]. Several groups worked on the stereochemistry of the different segments of the toxin [102-110]. Palytoxin (**50**) contains both hydrophilic and lipophilic moieties distributed among 129 aliphatic carbon atoms, 40 secondary hydroxyl groups, 64 chiral centers, 2 amides and 6 olefinic bonds with maximum UV absorbance at λ 233 and 263 nm [103, 105]. The total synthesis of palytoxin was accomplished by Kishi's group after several years of attempts [111, 112].

The presence of palytoxin has been reported from several species of *Palythoa* such as *P. toxica*, *P. tuberculosa*, *P. vestitus*, *P. caribaeorum*, *P.* aff. *margaritae*, *P. canariensis*, *P. heliodiscus*, and *P.* aff. *clavata*/*sakurajimensis* [84, 97-99, 113-118]. The concentration of palytoxin (**50**) in *Palythoa* aff. *clavata*/*sakurajimensis* is one of the highest reported in the literature with 2.22 mg/g of wet sample followed by *Palythoa heliodiscus* reported by Deeds *et al.*, with a concentration of 1 mg/g wet sample and deoxypalytoxin (**54**) was found at 3.51 mg/g wet sample [119]. Even though, the presence of the toxin was thought to be exclusive to the genus *Palythoa*, it was reported from *Zoanthus solanderi* and *Z. sociatus* from Colombia, *Zoanthus* sp. from Hawaii. *Z. pulchellus* from Netherlands and *Parazoanthus* sp. from Germany [84, 120, 121]. Additionally, this toxin has also been reported from other organisms such as the red algae *Chondria armata*, from various species of xanthid crabs from the Philippines, the warty crab *Eriphia verrucosa*, the trigger fish *Melichtys vidua*, the flathead mullet *Mugil cephalus*, the sea anemone *Radianthus macrodactylus*, the sea urchin *Paracentrotus lividus*, the rock shell *Stramonita haemastoma*, and from the marine cyanobacteria of the genus *Trichodesmium* [122-126]. Palytoxin analogues; homopalytoxin (**51**), bishomopalytoxin (**52**), neopalytoxin (**53**) and deoxypalytoxin (**54**) were reported from *P. tuberculosa* collected in Okinawa (Figure 14) [98]. Two palytoxin epimers; 42*S*-hydroxy-50*S*-palytoxin (**55**) and 42*S*-hydroxy-50*R*-palytoxin (**56**) were isolated from the Hawaiian zoantharians *P. toxica* and *P. tuberculosa* respectively [116, 127]. Compounds **50** and **55** were evaluated against skeletal myotubes revealing an increased of Ca^{2+} at 6 nM. The increase of Ca^{2+} could have occurred through either an induced activation of voltage calcium channels or by activation of the Na^+/Ca^{2+} exchanger [116]. These compounds also displayed cytotoxic activity against human skin keratinocytes (HaCaT cells) with an EC_{50} values of 2.7×10^{-11} M for **50**, 9.3×10^{-10} M for **55** and 1.0×10^{-10} M for **56** [127]. Rossi *et al.*, reported a new analogue named palytoxin b from a reference standard purchased to Wako chemicals GmbH (Neuss, Germany) [99]. The toxin was only identified through LC-ESI-ToF-MS analysis in positive mode by comparison of the fragmentation patterns to those of **50**. Compounds **50** and **54** were reported for the first time from the cyanobacteria *Trichodesmium* spp. collected in New Caledonia [126]. These toxins were identified through two

biological methods including mouse bioassay, neuroblastoma cell-based assay and LC-MS/MS analysis. Fraga *et al.* reported for the first time the presence of **50** and **56** from the Atlantic coral *Palythoa canariensis* [128]. The identification of the toxins was achieved through UPLC-IT-ToF-MS and by comparison of the fragmentation patterns to those of the standard palytoxin. In 2018, the presence of **50** was reported at a high concentration of 2.22 mg/g wet sample from *Palythoa* aff. *clavata*/*sakurajimensis* collected maintained in an aquarium in Indonesia [118]. A potent *in vitro* cytotoxicity was exhibited against A549 (lung carcinoma), Hs683 (glioma), U373n (glioma), 9L (gliosarcoma) and B16F10 (melanoma) with IC_{50} values of 0.67, 0.58, 0.56, 0.39 and 0.44 pM respectively. Palytoxin acts through the Na^+, K^+ ATPase of cell membranes turning the pump into an ion channel producing an Na^+ influx, K^+ efflux, therefore causing a membrane depolarization leading cells to apoptosis [129-131]. Additionally, a slight permeability of Ca^{2+} was observed when palytoxin binds the Na^+/K^+ pump and the palytoxin-Ca^{2+} complex was determined through NMR and molecular modelling analysis [132]. Dermal, ocular and respiratory problems have also been caused by direct exposure to some species of zoantharians being sold in home aquariums as these species are commonly used for ornamental purposes [119, 133]. Palytoxin (**50**) displayed inhibition on human immunodeficiency virus producing cells (MOLT-4/HIVHTLV-IIIB cells) at 2.0 pg/mL [134]. An increasing bioactivity was observed when a combination of a TPA-type tumour promoter (teleocidin) with a non-TPA type tumour promoter (palytoxin) was used. The increase of bioactivity was suggested to be due to the production of prostaglandin E_2. Additionally, Valverde *et al.*, reported the inhibition of human intestinal cell proliferation (Caco-2) by **50** with an IC_{50} value of 0.1 nM [135]. A potent activity against head and neck cancer cell lines was observed for **50** with a LD_{50} values between 1.5 to 3.5 ng/mL [136]. Also, compound **50** killed tumour cells in mice with a LD_{50} values between 68 to 83 ng/kg, with no tumour regression observed in control animals [135].

λ 233 nm

λ 233 nm

λ 263 nm

	A/B	n	R^1	R^2
palytoxin (**50**)	A	1	H	OH
homopalytoxin (**51**)	A	2	H	OH
bishomopalytoxin (**52**)	A	3	H	OH
neopalytoxin (**53**)	B	1	H	OH
deoxypalytoxin (**54**)	A	1	H	H
42S-hydroxy-50S-palytoxin (**55**)	A	1	OH	OH
42S-hydroxy-50R-palytoxin (**56**)	A	1	OH	OH

Figure 14 Structures of palytoxin analogues from species of *Palythoa.*

I.I.I.III   Ecdysteroids

Highly hydroxylated steroids featuring a conjugated ketone at C-6 and named ecdysteroids have been found in most of the species of both genera *Palythoa* and *Zoanthus.*

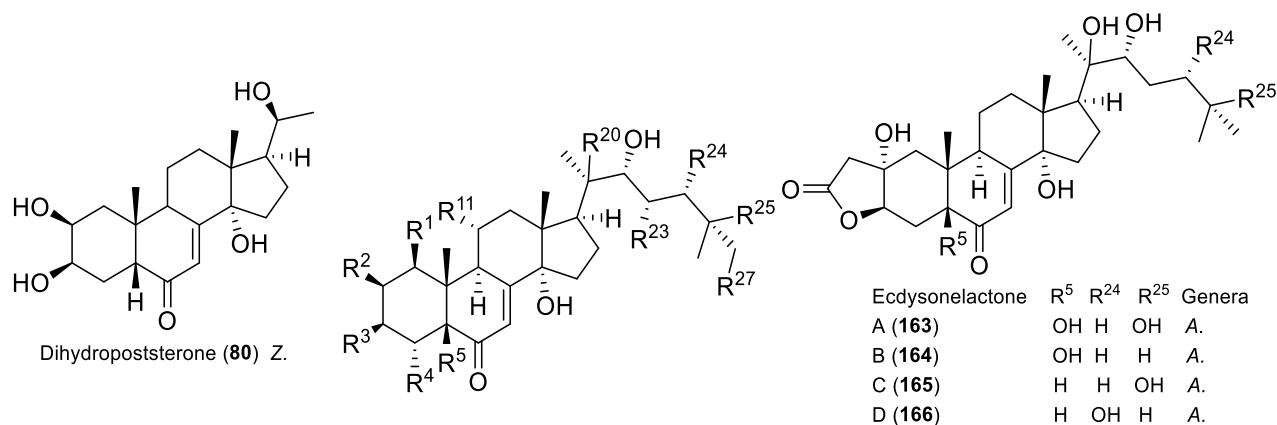**Palythoa:** The chemical study of an unidentified *Palythoa* sp. from Vietnam allowed the identification of the first ecdysteroid members: 20-hydroxyecdysone (**57**), 2-*O*-acetyl-20-hydroxyecdysone (**58**) and 3-*O*-acetyl-20-hydroxyecdysone (**59**) (Figure 15) [137]. These ecdysteroids were also reported from the Brazilian zoantharians *Palythoa variabilis* and *P. caribaeorum* and from the Taiwanese *P. tuberculosa*

[91, 138]. Palythoalone A (**60**), palythoalone B (**61**), makisterone B (**62**) and inokosterone (**63**) with a hydroxyl group at C-27, were reported from *Palythoa australiae* collected off the coast of Okinawa [139]. The structures were characterized based on NMR data and the absolute configuration was deduced using electronic circular dichroism (ECD) data after chemical derivatization. The anti-dengue guided activity of the ethanolic extract of the Vietnamese *Palythoa mutuki* let to the isolation of **57**, **58**, **59** along with palythone A (**64**), 3-deoxy-20-hydroxyecdysone (**65**), 24-*epi*-makisterone A (**66**), 2-deoxyecdysterone (**67**) and *α*-ecdysone (**68**) (Figure 15) [140].

Zoanthus: The oxytocic activity of the methanolic fraction of *Zoanthus* sp. collected off the coast of Goat, India, let to the isolation of 2-deoxyecdysterone (**67**) [141]. Compound **67** showed oxytocic activity in the oxytocin and $PGF_{2\alpha}$ assays at concentration of 50, 100 and 200 µg/mL. The new ecdysteroid zoanthusterone (**69**) was isolated along with the known ponasterone A (**70**), viticosterone E (**71**), integristerone A 25-acetate (**72**), ajugasterone C (**73**), dacryhainansterone (**74**), **57**, **58**, **63**, **67** and **68** from an unidentified specie of *Zoanthus* sp., collected off the coast of Samae-sarn, Thailand [142]. Analysis of the anti-dengue virus activity of the ethanolic extract from *Zoanthus* spp. collected off the coast of Taiwan allowed the identification of a new ecdysteroids zoanthone A (**75**) together with dehydromakisterone A (**76**), pterosterone (**77**), *epi*-inokosterone (**78**), turkesterone (**79**), dihydropoststerone (**80**), **57**, **59**, **63**, **67** and **68** [143]. Compounds **75** and **77** exhibited activity against dengue virus with an EC_{50} values of 19.61 and 10.05 µM respectively. Additionally, compound **75** displayed activity against three different dengue virus serotypes with an EC_{50} values of 15.70 µM for DENV-1, 9.48 µM for DENV-3 and 12.15 µM for DENV-4.

Dihydropoststerone (**80**) *Z.*

Ecdysonelactone	R^5	R^{24}	R^{25}	Genera
A (**163**)	OH	H	OH	*A.*
B (**164**)	OH	H	H	*A.*
C (**165**)	H	H	OH	*A.*
D (**166**)	H	OH	H	*A.*

	R^1	R^2	R^3	R^4	R^5	R^{11}	R^{20}	R^{23}	R^{24}	R^{25}	R^{27}	Genera
20-hydroxyecdysone (**57**)	H	OH	OH	H	H	H	OH	H	H	OH	H	*Pal. Z. Par. S.*
2-*O*-acetyl-20-hydroxyecdysone (**58**)	H	OAc	OH	H	H	H	OH	H	H	OH	H	*Pal. Z. Par.*
3-*O*-acetyl-20-hydroxyecdysone (**59**)	H	OH	OAc	H	H	H	OH	H	H	OH	H	*Pal. Z. Par.*
Palythoalone A (**60**)	H	OH	OH	H	OH	H	OH	H	CH_3	H	OH	*Pal.*
Palythoalone B (**61**)	H	OH	OH	H	OH	H	OH	H	H	H	OH	*Pal.*
Makisterone B (**62**)	H	OH	OH	H	H	H	OH	H	CH_3	H	OH	*Pal.*
Inokosterone (**63**)	H	OH	OH	H	H	H	OH	H	H	H (R)	OH	*Pal. Z.*
Palythone A (**64**)	H	H	H	OH	H	H	OH	H	H	OH	H	*Pal.*
3-deoxy-20-hydroxyecdysone (**65**)	H	OH	H	H	H	H	OH	H	H	OH	H	*Pal.*
24-*epi*-makisterone A (**66**)	H	OH	OH	H	H	H	OH	H	CH_3	OH	H	*Pal.*
2-deoxyecdysterone (**67**)	H	H	OH	H	H	H	OH	H	H	OH	H	*Pal. Z.*
α-ecdysone (**68**)	H	OH	OH	H	H	H	H	H	H	OH	H	*Pal. Z.*
Zoanthusterone (**69**)	OH	OH	OH	H	H	H	OH	H	H	H	H	*Z.*
Ponasterone A (**70**)	H	OH	OH	H	H	H	OH	H	H	H	H	*Z.*
Viticosterone E (**71**)	H	OH	OH	H	H	H	OH	H	H	OAc	H	*Z. Par.*
Integristerone A 25 acetate (**72**)	OH	OH	OH	H	H	H	OH	H	H	OAc	H	*Z.*
Ajugasterone C (**73**)	H	OH	OH	H	H	OH	OH	H	H	H	H	*Z. Par. S.*
Dacryhainansterone (**74**)	H	OH	OH	H	H	$\Delta^{10,11}$	OH	H	H	OH	H	*Z.*
Zoanthone A (**75**)	H	OH	OH	H	H	OH	OH	H	H	OAc	H	*Z.*
24(28)-dehydromakisterone A (**76**)	H	OH	OH	H	H	H	OH	H	$\Delta^{24,28}$	OH	H	*Z.*
Pterosterone (**77**)	H	OH	OH	H	H	H	OH	H	OH	H	H	*Z.*
25-*epi*-inokosterone (**78**)	H	OH	OH	H	H	H	OH	H	H	H (S)	OH	*Z.*
Turkesterone (**79**)	H	OH	OH	H	H	OH	OH	H	H	OH	H	*Z.*
4-dehydroecdysterone (**161**)	H	OH	OH	$\Delta^{4,5}$		H	OH	H	H	OH	H	*Par.*
Gerardiasterone (**162**)	H	OH	OH	H	H	H	OH	OH	H	OH	H	*S.*

Figure 15 Structures of ecdysteroids from species of zoantharians. *Palythoa* (Pal.), *Zoanthus* (Z.), *Parazoanthus* (Par.), *Savalia* (S.), *Antipathozoanthus* (A.).

31

I.I.I.IV Zoanthamine Alkaloids

A very original family of alkaloids called zoanthamines has been isolated only from the genus Zoanthus. A review on the chemistry and biological activities of these metabolites was published in 2008 [144]. Previously, another review was published on alkaloids found in zoantharians [145].

The first chemical investigation of a toxic *Zoanthus* species started in 1984 by Rao and co-workers when the spray ejected by colonies of an Indian species of *Zoanthus* caused prolonged eye irritation and pain [146]. Even though the zoantharian was first identified as *Zoanthus pacificus*, this species was thought to be endemic of the Caribbean and the authors decided to keep the name *Zoanthus* sp. They were able to isolate and characterize zoanthamine (**81**), the first member of a new family of alkaloids of unknown metabolic pathway and characterized by unique features of fused rings culminating in a rare azepane ring (Figure 16). The structure of **81** was elucidated by mass spectroscopy and NMR, and the relative configuration was deduced from crystallographic and X-ray diffraction analysis. Further chemical studies on the same species allowed the identification of zoanthenamine (**82**) and zoanthamide (**83**) [147]. These structures were elucidated by comparison of the ^{1}H and ^{13}C NMR signals to those of **81**. They both feature a γ-spirolactone ring at C-22. This new lactone ring is probably formed after opening of the unstable hemiaminal of **81**, leading to the enamine but also the spirolactone following cyclisation of the resulting carboxylic acid with the alcohol formed after oxidation of the methyl C-25. Compound **82** contains an additional hemiacetal that could be formed by addition of a primary alcohol at C-28 onto the ketone at C-20. While this ether ring is absent in **83**, opening of the second hemiaminal could lead to a terminal γ-lactone ring and an amide at C-7 after oxidative cleavage of the resulting enamine. The stereochemistry of these compounds was assumed to be the same as **81**, and the first biological studies on these alkaloids in mice revealed anti-inflammatory activity.

Later, the search for anti-inflammatory metabolites from a *Zoanthus* sp. collected off the Bay of Bengal, let to the isolation of 28-deoxyzoanthenamine (**84**) and 22-*epi*-28 deoxyzoanthenamine (**85**) (Figure 16) [148]. Compound **84** exhibited potent anti-inflammatory and analgesic activity. Zoanthaminone (**86**) together with **81** and **83** were isolated from *Zoanthus* sp. collected off the Arabian sea [149]. The structure of **86** was determined by X-ray diffraction, crystallographic and spectroscopic analysis. Recently, Li *et al*., reported the protective effect of **81** in Alzheimer's disease through differentiation of neural stem cells and reducing the miR-9 expression [150]. Norzoanthamine (**87**), oxyzoanthamine (**88**), norzoanthaminone (**89**), cyclozoanthamine (**90**), and epinorzoanthamine (**91**) were reported from an unidentified specie of *Zoanthus* collected off the Ayamaru coast of the Amami Islands – Japan (Figure 16) [151]. Compounds **87**, **89** and **91** are the first zoanthamines without the methyl at C-26. Zoanthamine (**81**) was proposed as a precursor of norzoanthamine (**87**) following oxidation of the methyl C-26 and decarboxylation. All five metabolites displayed cytotoxic activity against P388 murine

leukemia cells with an IC_{50} values of 24, 7.0, 1.0, 24 and 2.6 µg/mL respectively. One of the most promising bioactivities displayed by these alkaloids are against osteoporosis and a review on this potential activity was published in 2000 by Uemura and co-workers [152]. Compound **87** and its hydrochloride analogue showed inhibition of Interleukin 6 (IL-6) at 13 and 4.7 µg/mL respectively. The structure-activity relationship (SAR) of **87** indicated the C-15/C-16 double bond and the lactone ring plays an important role in the activity of the natural product [153]. The potent antiosteoporotic effect of norzoanthamine hydrochloride was confirmed by the *in vivo* assay in ovariectomized mice and by theoretical studies through molecular dynamics and docking investigations of zoanthamine analogues as matrix metalloproteinases-1 inhibitors [154, 155]. Additionally, Kinugawa *et al*., reported that **87** increases the production of collagen-hydroxyapatite composite, one of the major solid components of bone tissue by a non-specific binding to the polyvalent binding sites of collagen [156]. Therefore, the antiosteoporosis mode of action is suggested to be due to the collagen-norzoanthamine supramolecular association preventing collagen from a proteolytic cleavage. The protective function of **87** was further confirmed by Genji *et al*. They studied the distribution of norzoanthamine in *Zoanthus* sp., revealing a high concentration of the alkaloid in the epidermal tissue of the organism [157]. Tachibana and co-workers synthesized the bisaminal unit of norzoanthamine which exhibited similar collagen protection as the parent compound. The absence of the D ring led to the hydrolisis of the bisaminal inducing a decrease of the protective activity [158]. In 1998, epioxyzoanthamine (**92**), an isomer of **88** at C-19, was isolated from *Zoanthus* sp. collected off the Canary Islands [159]. An unusual deuterium exchange was observed in the presence of D_2O for the methylene signal at C-11 in **87** and **92** as previously reported for **81**. The deuterium exchange could originate from an equilibrium between the lactone and the enamine form in aqueous solution.

Later, zoanthenol (**93**), the first zoanthamine with an aromatized A ring, 3-hydroxynorzoanthamine (**94**), 30-hydroxynorzoanthamine (**95**), 11-hydroxynorzoanthamine (**96**), and 11-hydroxyzoanthamine (**97**) were reported from antoher *Zoanthus* sp. (Figure 16) [160]. No deuterium exchange at C-11 was observed for **96** and **97** suggesting that the first step in the enamine formation would be an elimination of H-11*β*. During the bioactivity study against human platelet aggregation, a strong inhibition of collagen, thrombin and arachidonic acid-induced aggregation was observed for compounds **87** and **97** both at 0.3, 0.5 and 1 mM [161]. The inhibitory effect caused by the zoanthamine analogues was suspected to be induced by the stimulation of calcium input into the cell, activation of protein kinase C or reduction of intracellular cyclic adenosine monophosphate levels. An important role is played by thromboxane A_2 (TXA$_2$) and phospholipase A_2 (PLA$_2$) when platelet aggregation is activated by arachidonic acid or collagen respectively. Additionally, compounds **94** and **95** selectively inhibited platelet aggregation induced by collagen at 0.3 and 1 mM while **93** was effective at 0.125, 0.5 and 1 mM [161]. Hirai *et al*., synthesized the ABC-ring and CDEFG-ring of **93** to study its SAR. The presence of the hydrochloride salt in the CEFG-ring is suggested to be the active pharmacophore to inhibit IL-6

production [162]. Furthermore, a pro-aggregan effect was observed for **87** at 1 mM and **88** between 0.125 to 1.5 mM. Interestingly, the bioactivity was enhanced in the presence of hydroxyl groups at C-3, C-11 or C-30 and the addition of a double bond at C-10/C-11 of the norzoanthamine skeleton [161].

Two structurally different zoanthamine analogues, zoaramine (**98**), and zoarenone (**99**) were isolated from an unidentified species of *Zoanthus* sp. collected off the coast of Punta del Hidalgo, Tenerife (Figure 16) [163]. Compound **98** is characterized by the absence of the N/C-10 bond and the presence of a C-7/C-24 bond. The relative configuration was assigned by ROESY experiment, coupling constant values and confirmed through Gauge-Independent Atomic Orbital (GIAO) NMR calculations using the density functional theory (DFT) analysis and the probabilistic DP4. Zoarenone (**99**) is closely related to **98** but the azepane ring has been lost. Additionally, the same research group reported three oxidized zoanthamine analogues; 2-hydroxy-11-ketonorzoanthamide B (**100**), norzoanthamide B (**101**) and 15-hydroxynorzoanthamine (**102**) from *Zoanthus* sp. (Figure 16) [164]. Kuroshine A (**103**) and kuroshine B (**104**) were then reported from the Taiwanese zoantharian *Zoanthus Kuroshio* [165]. Compound **103** is characterized by the presence of an ether bridge between C-10 and C-28, while **104** contains an eight membered lactone ring between C-24 to C-26. These compounds did not show any activity against human platelet aggregation, inflammatory nor cytotoxicity. Further studies on *Z. kuroshio* led to the identification of Kuroshines C-G (**105-109**), 3β-hydroxyzoanthenamide (**110**) and 7α-hydroxyzoanthenamide (**111**) (Figure 16) [166]. Kuroshines C-G contained the same ring system as **103** while **110** and **111** share the same ether bridge as zoanthenamine (**82**). These compounds were evaluated for their anti-inflammatory, antiviral, antimicrobial, antiosteoporosis and cytotoxic activity. Only compound **107** displayed weak toxicity against melanoma cell line B16 with an IC$_{50}$ value of 120 µM. Two halogenated zoanthamines analogues; 5α-iodozoanthenamine (**112**) and 11β-chloro-11-deoxykuroshine A (**113**) were isolated from *Z. kuroshio* along with 18-*epi*-kuroshine A (**114**), 7α-hydroxykuroshine E (**115**), 5α-methoxykuroshine E (**116**) and 18-*epi*-kuroshine E (**117**) [167]. Compounds **114** and **117** are the first zoanthamines with a *cis* A/B junction. The anti-inflammatory analysis revealed a significant activity of **112** at 10 µM. Finally, the first chemical study of *Zoanthus* cf. *pulchellus* collected off the coast of mainland Ecuador led to the isolation of 3-acetoxynorzoanthamine (**118**) and 3-acetoxyzoanthamine (**119**) together with the known **81**, **87** and **94** [168]. These compounds were evaluated for their antioxidant and anti-inflammatory activity in microglia BV-2 cell line. Compounds **87** and **118** displayed dose-dependent activity on Reactive Oxygen Species (ROS) while the other compounds exhibited inhibitory activities on ROS and Nitric Oxide generation (NO).
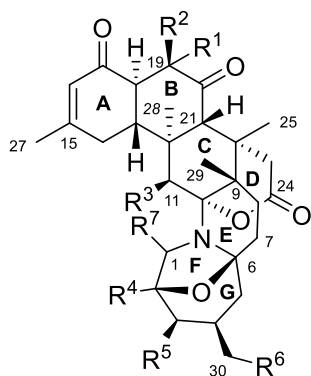
	R^1	R^2	R^3	R^4	R^5	R^6	R^7
Zoanthamine (**81**)	H	CH₃	H	H	H	H	H
Zoanthaminone (**86**)	H	CH₃	=O	H	H	H	H
Norzoanthamine (**87**)	H	H	H	H	H	H	H
Oxyzoanthamine (**88**)	H	CH₂OH	H	H	H	H	H
Norzoanthaminone (**89**)	H	H	=O	H	H	H	H
Epioxyzoanthamine (**92**)	CH₂OH	H	H	H	H	H	H
3-hydroxynorzoanthamine (**94**)	H	H	H	H	OH	H	H
30-hydroxynorzoanthamine (**95**)	H	H	H	H	H	OH	H
11-hydroxynorzoanthamine (**96**)	H	H	OH	H	H	H	H
11-hydroxyzoanthamine (**97**)	H	CH₃	OH	H	H	H	H
2-hydroxy-11-ketonorzoanthamide B (**100**)	H	H	=O	OH	H	H	=O
Norzoanthamide B (**101**)	H	H	H	H	H	H	=O
3-acetoxynorzoanthamine (**118**)	H	H	H	H	AcO	H	H
3-acetoxyzoanthamine (**119**)	H	CH₃	H	H	AcO	H	H

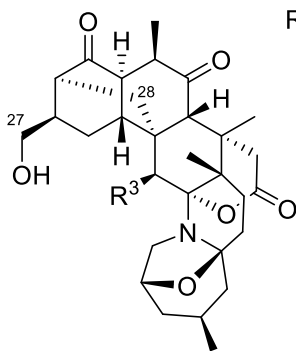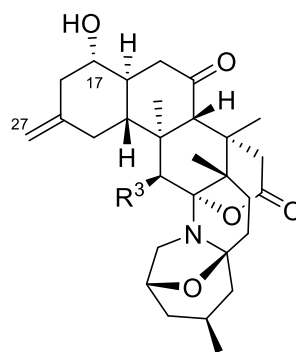|	R^1	R^2	R^3
Zoanthenamine (**82**)	H	H	H
3β-hydroxyzoanthenamide (**110**)	β-OH	H	H
7α-hydroxyzoanthenamide (**111**)	H	H	α-OH
5α-iodozoanthenamine (**112**)	H	α-I	H
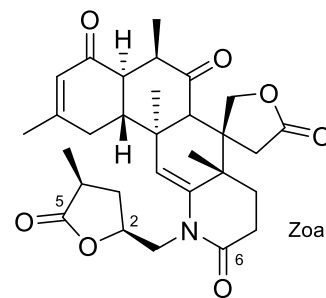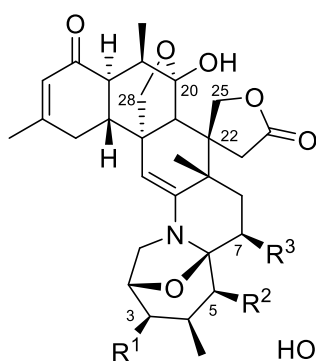
Zoanthamide (**83**)
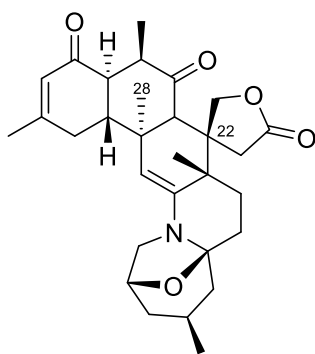
28-deoxyzoanthenamine (**84**)
22-*epi*-28-deoxyzoanthenamine (**85**)

cyclozoanthamine (**90**)

epinorzoanthamine (**91**)

zoanthenol (**93**)

zoaramine (**98**)

zoarenone (**99**)

15-hydroxynorzoanthamine (**102**)

	R^1	R^2	R^3	R^4	R^5	R^6
Kuroshine A (**103**)	OH	H	H	H	H	α-H
Kuroshine C (**105**)	OH	H	OH	H	H	α-H
Kuroshine D (**106**)	OH	H	H	OH	H	α-H
Kuroshine E (**107**)	=O	H	H	H	H	α-H
Kuroshine F (**108**)	=O	H	OH	H	H	α-H
Kuroshine G (**109**)	=O	OH	H	H	H	α-H
11β-chloro-11-deoxykuroshine A (**113**)	β-Cl	H	H	H	H	α-H
18-*epi*-kuroshine A (**114**)	OH	H	H	H	H	β-H
7α-hydroxykuroshine E (**115**)	=O	H	H	H	OH	α-H
5α-methoxykuroshine E (**116**)	=O	H	H	OCH$_3$	H	α-H
18-*epi*-kuroshine E (**117**)	=O	H	H	H	H	β-H

Kuroshine B (**104**)
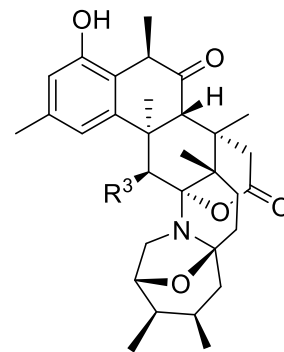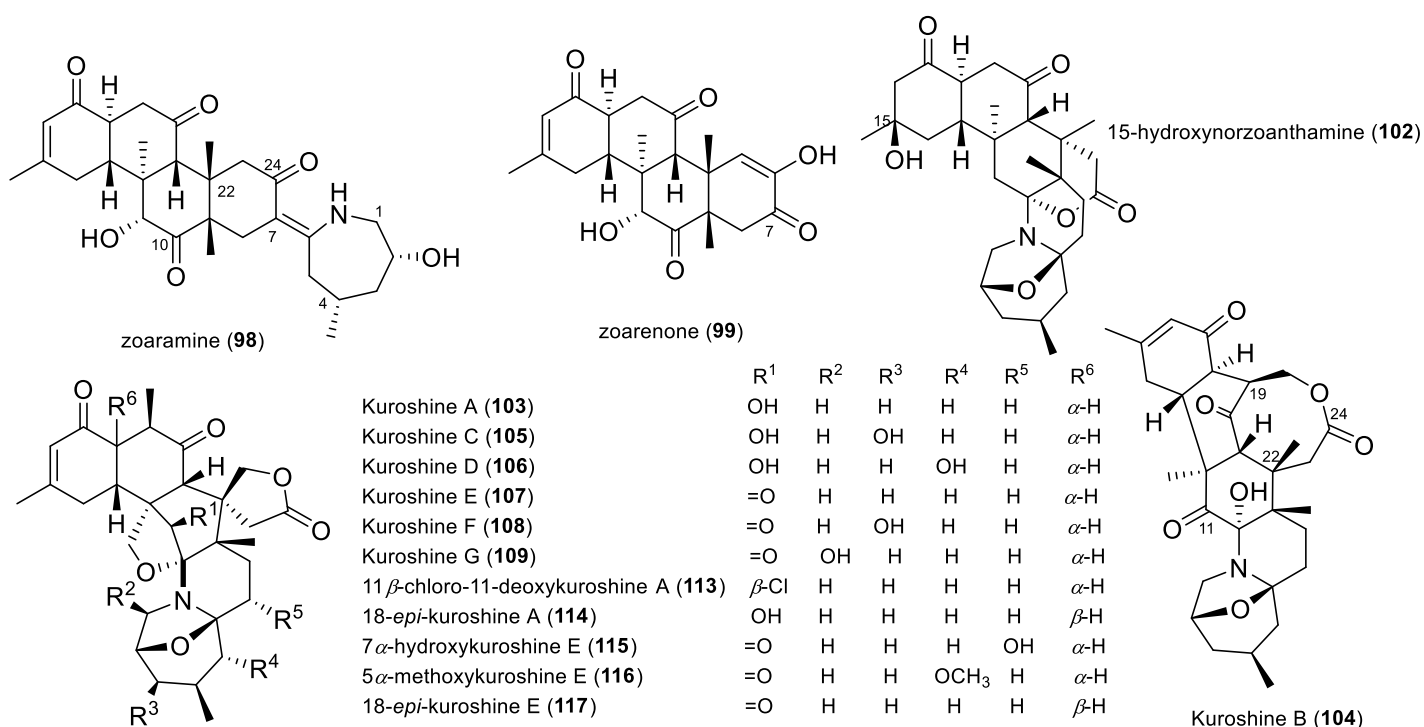
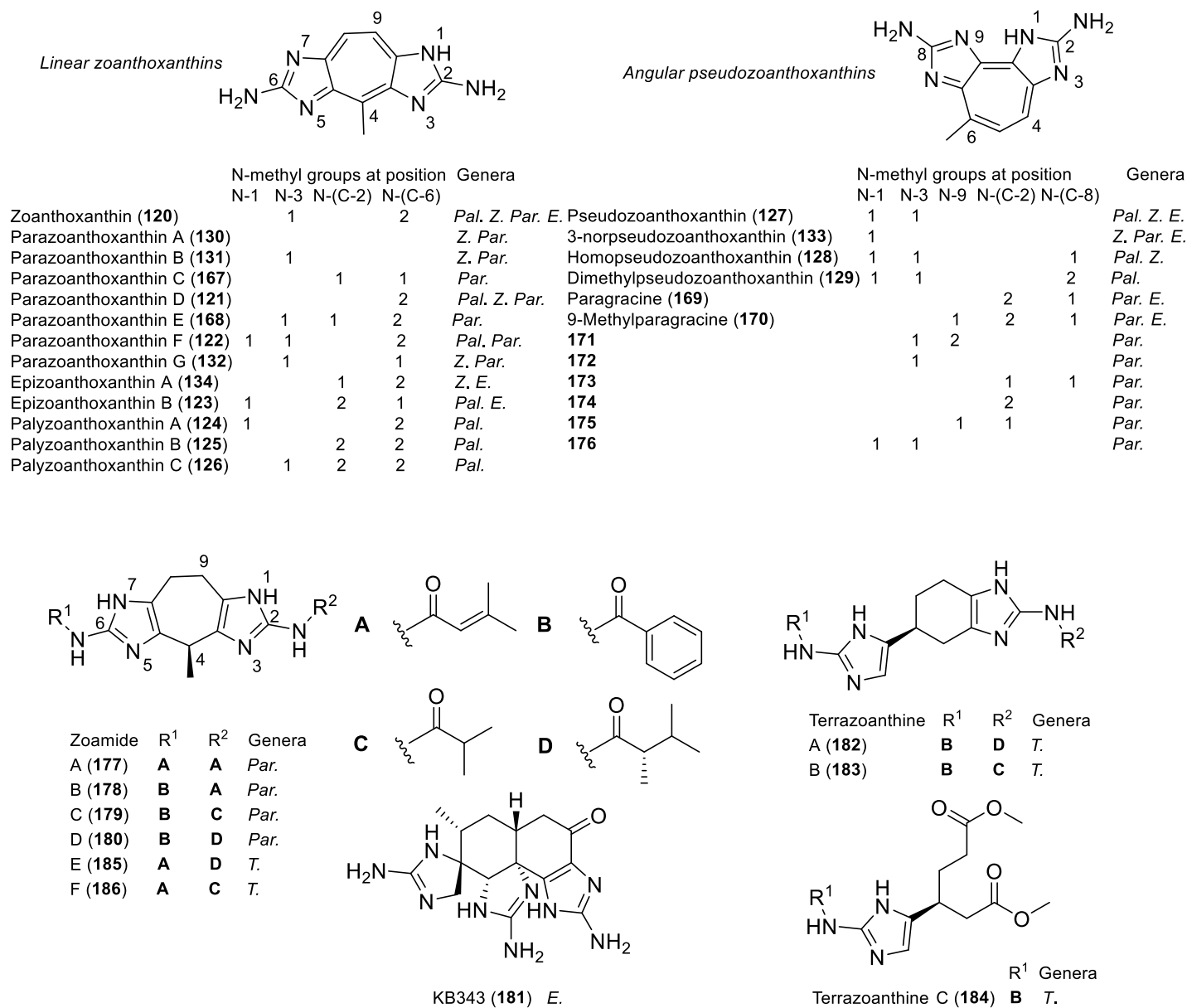**Figure 16** Structures of zoanthamine alkaloids from species of *Zoanthus*.

I.I.I.V   2-Aminoimidazole alkaloids

Other types of aromatic alkaloids containing 2-aminoimidazole rings are commnonly found in zoantharians.

Palythoa: During a survey of fluorescent bisguanidine aromatic alkaloids named zoanthoxanthins in different zoantharians, Cariello *et al.* reported the presence of zoanthoxanthin (**120**), parazoanthoxanthin D (**121**), parazoanthoxanthin F (**122**), epizoanthoxanthin B (**123**), palyzoanthoxanthin A-C (**124-126**), pseudozoanthoxanthin (**127**), homopseudozoanthoxanthin (**128**) and dimethylpseudozoanthoxanthin (**129**) in small amount from *Palythoa* sp. collected in Indonesia, *P. mammilosa* in the Caribbean and *P. tuberculosa* from the Marshall Islands (Figure 17) [169].

Zoanthus: *Zoanthus sociatus* from the Caribbean and *Z.* aff. *pacificus* were also screened for their content in pigment zoanthoxanthins [169]. The composition was different and for the *Zoanthus* species they found zoanthoxanthin (**120**), parazoanthoxanthin D (**121**), palyzoanthoxanthin A (**124**), pseudozoanthoxanthin (**127**), homopseudozoanthoxanthin (**128**), parazoanthoxanthin A (**130**), parazoanthoxanthin B (**131**), parazoanthoxanthin G (**132**), 3-norpseudozoanthoxanthin (**133**) and epizoanthoxanthin A (**134**) (Figure 17).

Linear zoanthoxanthins

Angular pseudozoanthoxanthins

Linear	N-1	N-3	N-(C-2)	N-(C-6)	Genera
Zoanthoxanthin (**120**)		1		2	*Pal. Z. Par. E.*
Parazoanthoxanthin A (**130**)					*Z. Par.*
Parazoanthoxanthin B (**131**)		1			*Z. Par.*
Parazoanthoxanthin C (**167**)			1	1	*Par.*
Parazoanthoxanthin D (**121**)				2	*Pal. Z. Par.*
Parazoanthoxanthin E (**168**)		1	1	2	*Par.*
Parazoanthoxanthin F (**122**)	1	1		2	*Pal. Par.*
Parazoanthoxanthin G (**132**)		1		1	*Z. Par.*
Epizoanthoxanthin A (**134**)			1	2	*Z. E.*
Epizoanthoxanthin B (**123**)	1		2	1	*Pal. E.*
Palyzoanthoxanthin A (**124**)	1			2	*Pal.*
Palyzoanthoxanthin B (**125**)			2	2	*Pal.*
Palyzoanthoxanthin C (**126**)		1	2	2	*Pal.*

(N-methyl groups at position — N-1, N-3, N-(C-2), N-(C-6))

Angular	N-1	N-3	N-9	N-(C-2)	N-(C-8)	Genera
Pseudozoanthoxanthin (**127**)	1	1				*Pal. Z. E.*
3-norpseudozoanthoxanthin (**133**)	1					*Z. Par. E.*
Homopseudozoanthoxanthin (**128**)	1	1			1	*Pal. Z.*
Dimethylpseudozoanthoxanthin (**129**)	1	1			2	*Pal.*
Paragracine (**169**)				2	1	*Par. E.*
9-Methylparagracine (**170**)			1	2	1	*Par. E.*
171			1	2		*Par.*
172			1			*Par.*
173				1	1	*Par.*
174				2		*Par.*
175			1	1		*Par.*
176	1	1				*Par.*

(N-methyl groups at position — N-1, N-3, N-9, N-(C-2), N-(C-8))

Zoamide	R^1	R^2	Genera
A (**177**)	**A**	**A**	*Par.*
B (**178**)	**B**	**A**	*Par.*
C (**179**)	**B**	**C**	*Par.*
D (**180**)	**B**	**D**	*Par.*
E (**185**)	**A**	**D**	*T.*
F (**186**)	**A**	**C**	*T.*

A **B** **C** **D**

Terrazoanthine	R^1	R^2	Genera
A (**182**)	**B**	**D**	*T.*
B (**183**)	**B**	**C**	*T.*

KB343 (**181**) *E.*

	R^1	Genera
Terrazoanthine C (**184**)	**B**	*T.*

Figure 17 Zoanthoxanthin derivatives from zoantharians. *Palythoa* (Pal.), *Zoanthus* (Z.), *Parazoanthus* (Par.), *Epizoanthus* (E.), *Terrazoanthus* (T.).

I.I.I.VI   Miscellaneous

Palythoa: In 1978, the water-soluble amino acid mycosporine-Gly (**135**) was isolated from *Palythoa tuberculosa* collected in Japan and converted into the stable methyl ester for its characterization by spectroscopy (Figure 18) [170]. An ultraviolet protective function was proposed in the organism because of its high UV absorbance at λ 310 nm. Palythine (**136**), palythinol (**137**), and palythene (**138**) were isolated from the same species and these compounds showed high UV absorption at λ 310, 332 and 360 nm respectively [171, 172]. Additional studies on UV-absorbing compounds from *P. tuberculosa* led to the isolation of pyrazine derivatives named palythazine (**139**) and isopalythazine (**140**), characterized by their spectroscopy data and chemical synthesis [173]. In 1982, two glycerol ethers named chimyl alcohol (**141**) and batyl alcohol (**142**) were identified along with a mixture of other glycerol derivatives from the ligroin fraction of *P. liscia* [174]. Two prostaglandins PGA$_2$ (**143**) and PGB$_2$ (**144**) were isolated in 2006 isolated from *P. kochii* collected off the coast of Okinawa, Japan [175]. The structures were established based on their NMR data and by comparison to those of the commercial PGA$_2$. Compound **143** displayed cytotoxic activity and neurite-extension inhibition (NGF-PC12 cell) with an IC$_{50}$ values of 70 and 20 µM respectively and the antitubulin polymerization activity at 100 µM. The PGA$_2$ bioactivity of **143** was comparable to the one of paclitaxel (Taxol) but **144** was found to be inactive. The chemical study of the Brazilian zoantharian *Protopalythoa variabilis* allowed the identification of two lipidic α-aminoacids 2-aminotriacontanoic acid (**145**) and 2-aminohentriacontanoic acid (**146**) for the first time from natural sources [176, 177]. The mixture of the two amino acids **145** and **146** exhibited potent cytotoxicity against human colon cancer (HCT-8), melanoma (MDA-MB-435), CNS glioblastoma (SF-295) and leukemia (HL-60) with an IC$_{50}$ values of 0.13, 0.05, 0.07 and 0.1 µg/mL respectively (Figure 18). In 2012, two unprecedented sulfonoceramides named palysulfonoceramide A (**147**) and palysulfonoceramide B (**148**) along with the known ceramides **149** and **150** were isolated from *Palythoa caribaeorum* and *Palythoa variabilis* collected off the coast of Brazil [178]. Remarkably, sulfonylated groups on ceramides have only been obtained through synthesis before. These ceramides were tested against human colon adenocarcinoma (HCT-116) cell line with no significant bioactivity. The DCM fraction exhibited high toxicity in the artemia lethality test with an LC$_{50}$ value of 52.10 µg/mL. All fractions showed low hemolytic and no antimicrobial activity at 100 µg/mL [179].

The anti-dengue apocarotenoid pigment peridin (**151**) was isolated from the Vietnamese *P. mutuki* (Figure 18) [140]. The pigment exhibited a potent antiviral activity against all sero-types of DENV 1-4 with an EC$_{50}$ values of 7.62, 4.50, 5.84 and 6.51 µM respectively. Additionally, **151** showed inhibition of DENV protease activity with an EC$_{50}$ value of 8.50 µM suggesting a potential anti-dengue virus candidate. Additional pyrazine derivatives named tuberazines A-C (**152-154**) were isolated along with **155**, tyramine, *N*-methylserotonin, phenethylamine, isobutylamine, isoamylamine, **156, 58** and **59** from

the Taiwanese zoantharian *P. tuberculosa* (Figure 18) [138]. The absolute configuration of **152** was assigned through ECD analysis and compound **154** exhibited anti-lymphangiogenic activity in human lymphatic endothelial cells (LECs) with an IC_{50} value of 33 µg/mL.

The variability of the metabolomic profiling using the MS/MS fragmentation pattern and the Global Molecular Networking Analysis (GNPS) was assessed on two species of zoantharians *P. caribaeorum* and *P. variabilis* collected from different locations of the coast of Brazil [180]. This new approach deepens our knowledge on the metabolome of marine invertebrates. The study revealed the presence of mycosporine-like aminoacids, ecdysteroids, phosphatidylcholine derivatives, indole diterpenes, sulphonoceramides and zoanthamine alkaloids. In 1982, the cytotoxic activity of the ethanolic extract of *Palythoa liscia* collected off the coast of Mauritius led to the isolation of three peptides named palystatins 1-3 [181]. Palystatins 1-3 were separated by gel permeation chromatography. Palystatin 1 which is suggested to be a sub-unit of palystatin 2-3, displayed cytotoxic activity against the murine PS *in vivo* system at a concentration of 0.3 mg/Kg. Additionally, the bioactivity guided purification of the methanolic extract of *P. liscia* allowed the isolation of four distinct peptides named palystatins A-D [182]. The molecular weights of palystatins A-D were determined by gel permeation and corresponded to 4500, 4000, 3300 and 3000 Da respectively. Palystatins A-D displayed cytotoxic activity against murine lymphocytic leukemia (P388-PS system) with ED_{50} values of 0.0023, 0.020, 0.0018 and 0.022 µg/mL respectively. The biological study on the sodium channel of the low molecular weight fraction of the Mexican zoantharian *P. caribaeorum* allowed the isolation and identification of a new toxic peptide containing 32 amino acid residues with a molecular weight of 3,648 Da [183]. It is characterized by an unusual V-shape α-helical structure with the presence of two cysteine residues and one disulphide bridge unlike other sea anemone toxins that commonly possess three to four disulphide bridges. Analysis of the transcriptome of the Brazilian *Protopalythoa variabilis* revealed the presence of several putative toxic-related peptides with neurotoxic, hemorrhagic and membrane-disrupting proteins activity [184]. These peptides are possible related to four neurotoxin families including turripeptide, ShK, three-finger toxin and a novel anthozoan neurotoxin-like peptide. Further analysis allowed the identification and synthesis of two peptides; one related to the ShK/Aurelin K^+-ion channel blocker ShK/Aurelin and the second one to the anthozoan neurotoxin family. Both peptides were synthesized by solid phase chemistry for *in vivo* bioassays in zebrafish. The LD_{50} value of the ShK/Aurelin-like peptide for zebrafish ranges from 15 to 20 µM and exhibited potent neurotoxic activity at 10 µM. The anthozoan neurotoxin-like peptide showed cytotoxic activity with a LD_{50} value of 3 - 30 µM.

The pharmacological study of the mucus of *P. caribaeorum* revealed the presence of four metalloproteases corresponding to 55, 63, 109 and 260 KDa [185]. The 109 and 260 KDa proteases were more sensitive to higher temperatures than the smaller ones. Further analysis revealed a hemagglutinating activity against all human erythrocyte types, an inhibition of platelet aggregation was observed at 2.3 µg, a pro-coagulant activity at 0.75 µg while higher concentration of the mucus between

1.5 to 6 µg displayed anticoagulant activity. Three kunitz-like peptides (PcKuz 1-3) were described based on the transcriptome sequencing from the Brazilian *P. caribaeorum* [186]. PcKuz3 is related to the known snake-type kunitz-like toxin comprising between 50 to 60 amino acids, six cysteine residues which could fold due to the presence of three disulfide bridges at C1-C6, C2-C4, and C3-C5. The protein-protein docking was analyzed *in silico* and zebra fish was used as model for the *in vivo* toxicity analysis. PcKuz3 showed high toxicity in zebra fish larvae with an IC_{50} value between 10 to 20 µM, and at 5µM the locomotion of the zebrafish was significantly reduced. Additionally, based on the similarity to dendrotoxins, it was suggested that PcKuz3 blocks the potassium ion channels, and therefore it can be considered as neurotoxin. The ShK-like peptide (PcShK3) characterized by the presence of the ShK domain containing three disulphide bridges, was identified from the transcriptome of *P. caribaeorum* through computational processing, structural phylogenetic analysis, model prediction and dynamic simulation of peptide-receptor interaction. PcShK3 exhibited cytotoxic activity with a LD_{50} value of 43.5 µM after 48h exposure [187].

The neurotoxic phospholipase A2-PLTX-Pcb1a was obtained from *P. caribaeorum* collected off the coast of Mexico [188]. It was isolated through cationic exchange column and size exclusion HPLC column. This enzyme belongs to the secreted PLA_2-type enzymes ($sPLA_2$) within the family of calcium dependent PLA_2 phospholipases. It contains 149 amino acid residues with a molecular weight of 16,617 Da. The enzyme is characterized by the absence of the calcium-binding site and the histidine active site as commonly found in other PLA_2 enzymes. Based on the low similarity with other $sPSA_2$, it is suggested to be a member of a new group of phospholipases A2 PLA_2. It displayed neurotoxic activity in the primary motor cortex in rats by intraventricular injection of A2-PLTX-Pcb1a with a concentration of 3.5 mg/mL. The peptide Pp V-shape α-helical peptide (PpVα) belonging to the sodium channel toxin type was isolated from *Protopalythoa variabilis* [189]. The peptide was synthesized by solid phase for the *in vivo* bioassays and it is characterized by the presence of two cysteine residues. The peptide-protein docking analysis and dynamic simulation revealed its capacity to block the sodium channel. The PpVα exhibited a LD_{50} value of 10.88 µM in zebrafish in the folded version and 21.23 µM in the linear one, and their locomotion was also disturbed at concentrations over 5.0 and 2.5 µM in the folded and linear form respectively. Additionally, the folded peptide showed higher protective activity against epileptic seizure at a concentration of 5 µM and at 10 µM it inhibited totally the epileptic seizures in zebrafish. Furthermore, both forms of the PpVα prevented neuronal death with concentrations higher than 1 µM in the 6-OHDA- induced cell death assay.

Zoanthus: The *α*-amino-*β*-phosphonopropionic acid (**157**) was identified from the aqueous-ethanolic extract of the Caribbean *Zoanthus sociatus* by Kittredge and Hughes in 1964 (Figure 18) [190]. The identification of the amino acid was based on comparison with the synthetic labelled analogue by paper chromatography, paper electrophoresis and ion-exchange chromatography. In 1997, hariamide (**158**), a sulphated sphingolipid, was isolated together with **159** from an unidentified species of *Zoanthus* sp.,
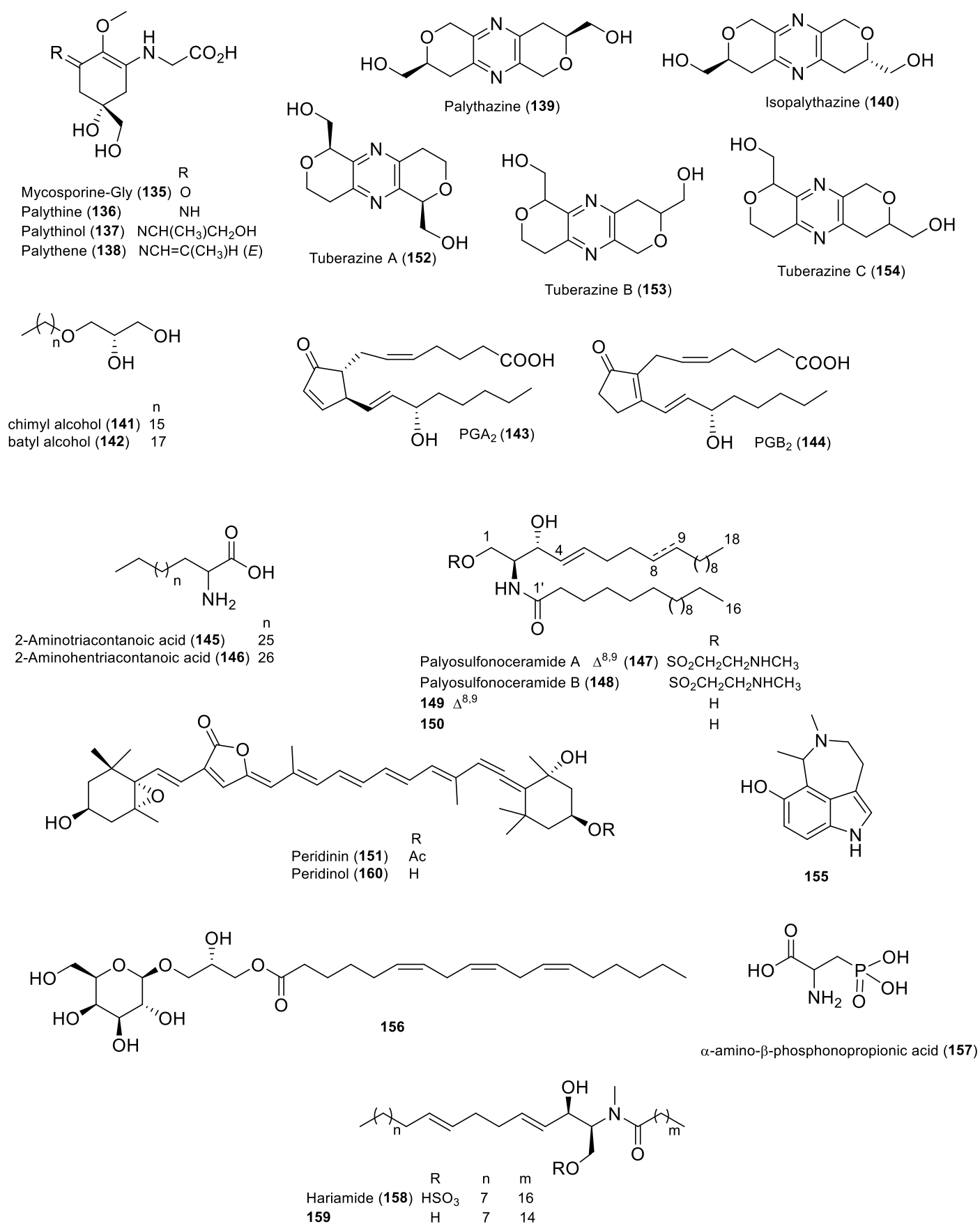
collected off the Indian coast [191]. The anti-spasmodic C_{37} carotenoid pigment peridinol (**160**) was isolated from a *Zoanthus* sp., collected off the coast of Goa, India [192]. Garcia *et al*., reported the inhibition of insulin secretion via Ca^{2+} channel in isolated rat pancreatic *β* cells of the crude extract and the low molecular weight fractions of *Zoanthus sociatus* collected in La Habana, Cuba [193]. The MS analysis revealed the presence of four major compounds with a molecular weight of 6397.7, 4179.1, 4874.7 and 2131.2 Da. The HPLC analysis showed similar retention times to those of insulin and *ω*-conotoxin GVIA, a potent inhibitor of neuronal N-type Ca^{2+} channels, suggesting similar structures with a difference of 3.8 to 6 kDa to *ω*-conotoxin GVIA. The *in vivo* toxicity in mice of the low molecular weight fraction from the Cuban *Z. sociatus* was assessed by Antunes *et al*., revealing a toxic effect with a LD_{50} value of 792 μg/Kg [194].

 Furthermore, the identification of cyanotoxin microcystin-LR (MC-LR) from this fraction was reported for the first time in *Z. sociatus* based on mass-matching against libraries of non-ribosomal peptide database (NORINE) and confirmed by HPLC/MS analysis [195]. Two florescent proteins; a yellow-like fluorescence protein (zFP538) and a green-like fluorescence protein (zFP506) were identified from *Zoanthus* sp. [196]. These fluorescent proteins exhibited a maximum absorption at *λ* 528 and 496 nm respectively, and both proteins contain 231 amino acid residues. A protective activity against solar radiation has been suggested for these proteins as ecological role in *Zoanthus*, especially for species inhabiting shallow tropical waters. The YFP zFP538 showed some potential applications for *in vivo* labelling since its fluorescence remained stable for four weeks. A red fluorescence protein zoan2RFP (AY059642) was reported from an unidentified species of *Zoanthus* sp., along with the previously reported GFP (zFP506) and YFP (zFP538) [197]. Here also, a photoprotective activity of the fluorescent proteins was suggested. Further studies on these fluorescence proteins demonstrated that the amino acid residues Tyr66 and Gly67 form the chromophore of GFP zFP506 while the amino acid Lys65 was the main responsible for the yellow fluorescence of zFP538, suggesting that the fluorescence emitted by both proteins are caused by two chemically different chromophores [198]. Consequently, the structure of the YFP zFP538 chromophore was determined through crystallography, MS and *via* molecular replacement with the evolutionary programming for molecular replacement (EPMR) method [199, 200]. The synthesis of the zFP538 chromophore was achieved by Lukyanove and his group in 2009 [201]. Pletneva *et al*., determined the RFP zRFP574 chromophore structure through crystallography studies and the three-dimensional structure of the zYFP538, zRFP574 and zGFP506 chromophores by X-ray analysis with a resolution of 1.8, 1.51 and 2.2 Å respectively [202, 203].

Mycosporine-Gly (**135**)   O
Palythine (**136**)   NH
Palythinol (**137**)   NCH(CH$_3$)CH$_2$OH
Palythene (**138**)   NCH=C(CH$_3$)H (*E*)

Palythazine (**139**)

Isopalythazine (**140**)

Tuberazine A (**152**)

Tuberazine B (**153**)

Tuberazine C (**154**)

chimyl alcohol (**141**)   15
batyl alcohol (**142**)   17

PGA$_2$ (**143**)

PGB$_2$ (**144**)

2-Aminotriacontanoic acid (**145**)   25
2-Aminohentriacontanoic acid (**146**)   26

Palyosulfonoceramide A $\Delta^{8,9}$ (**147**)   SO$_2$CH$_2$CH$_2$NHCH$_3$
Palyosulfonoceramide B (**148**)   SO$_2$CH$_2$CH$_2$NHCH$_3$
149 $\Delta^{8,9}$ H
150   H

Peridinin (**151**)   Ac
Peridinol (**160**)   H

155

156

α-amino-β-phosphonopropionic acid (**157**)

                 R   n   m
Hariamide (**158**)   HSO$_3$ 7   16
159   H   7   14

Figure 18 Structures of diverse compouds isolated from *Palythoa* and *Zoanthus* species

I.I.II Macrocnemina

This suborder contains many more genera than the suborder Brachycnemina, but only five of them have been chemically studied: *Savalia*, *Parazoanthus*, *Epizoanthus*, *Terrazoanthus* and *Antipathozoanthus*. Two families of natural products have been usually identified in species of these genera: ecdysteroids and zoanthoxanthins but other halogenated tyrosine derivatives are also present.

I.I.II.I   Ecdysteroids

Parazoanthus: In 1979, Fedorov *et al.*, reported for the first time the isolation of 20-hydroxyecdysone derivatives **57-69** from a *Palythoa* sp. but also a *Parazoanthus* sp., collected in the coast of Vietnam (Figure 15) [137]. The structures were deduced from their NMR and MS data and by comparison with those of previously reported analogues. The new 4-dehydroecdysterone (**161**) was isolated from the Australian *Parazoanthus* sp., together with the known 20-hydroxyecdysone (**57**) and ajugasterone C (**73**) (Figure 15) [204, 205]. The relative configuration of **161** was assigned through coupling constants analysis and nOe correlations. An *in vivo* feeding assay to test the protective role of ecdysteroids present in marine invertebrates was performed in the study. No protective role was observed with treatment up to 1% of ecdysteroids. This finding was further confirmed by a palability study carried out by Fenical and co-workers [205]. No antifungal activity was found in the tested metabolites. Recently during a deep chemical investigation of two morphotypes of *P. axinellae* in the Mediterranean Sea, the four ecdysteroids **57**, **58**, **59** and **71** were identified [206].

Savalia: In 1982, compound 20-hydroxyecdysone (**57**) was isolated as the major component of the Mediterranean zoantharian *Gerardia savaglia* (now *Savalia savaglia*) (Figure 15) [207]. The structure was deduced by NMR analyses and comparison with the commercially available ecdysterone. Consequently, gerardiasterone (**162**) and then ajugasterone C (**73**) were isolated from *S. savaglia* by Pietra's group [208, 209]. The structure of **162** was established through its spectroscopic data and by comparison to those of ecdysterone. This was the first ecdysteroid reported with four hydroxyl groups at the side chain having the new OH group at C-23. Tsubuki and co-workers synthesized gerardiasterone *via* a diastereoselective synthesis and the absolute configuration of the side chain was confirmed to be 20*R*, 22*R* and 23*S* [210, 211].

Antipathozoanthus: Only one chemical study has been published from a species of *Antipathozoanthus*. Ecdysonelactones A-D (**163-166**) were reported from the Tropical Eastern Pacific zoantharian *A. hickmani*, collected at the marine protected area El Pelado, Ecuador (Figure 15) [212]. Ecdysonelactones are characterized by the incorporation of a *γ*-lactone ring fused at the C-2/C-3 bond of ring A of the ecdysteroid skeleton. The structures were inferred from their NMR and HRESIMS data. The relative configuration was assigned through NOESY correlations, coupling constants analysis and

comparison of the NMR data to those of 4-dehydroecdysterone (**161**). These compounds did not display antimicrobial and cytotoxic activity.

I.I.II.II   2-Aminoimidazole Alkaloids

Parazoanthus: The first alkaloids isolated from a zoantharian are characterized by an unusual heteroaromatic system cyclohepta[1,2-d:4,5-d']diimidazole or cyclohepta[1,2-d:3,4-d']diimidazole. These alkaloids can be classified depending on their skeleton type; zoanthoxanthin (linear system) or pseudozoanthoxanthin (angular system). Within the zoanthoxanthin type, they are differentiated into *para* and *epi* zoanthoxanthins depending on the methylation pattern on the imidazole ring. The fluorescent pigment zoanthoxanthin (**120**), was first isolated in 1973 from the Mediterranean zoantharian *Parazoanthus* cfr. a*xinellae* (Figure 17) [213, 214]. The structure of this compound featuring a new heterocyclic system was determined by spectroscopy data, chemical derivatization and X-ray crystallographic of its chloro derivative. Compound **120** displayed a non-competitive inhibition of succinic oxidase activity of beef heart mitochondria with an IC_{50} value of 5.7 x 10^{-4} M [215]. Further chemical studies on the same *P. axinellae* led to the isolation of parazoanthoxanthines A-D (**130, 131, 167, 121**) (Figure 17) [216]. Only compounds **130** and **121** were fully characterized by comparison of spectroscopic data with those of **120**. The structures of **131** and **167** could not be fully elucidated due to the small amount of isolated material. Compound **130** inhibits DNA synthesis at 2.7 x 10^{-4} M and an electrostatic binding of **130** to the double-stranded DNA has been suggested as a mechanism of action [217]. Compound **130** also showed anticholinesterase activity with an inhibition constant values (Ki) of 19 and 26μM and inhibition of the nicotinic acetylcholine receptors [218, 219]. Screening of zoanthoxanthin alkaloids in zoantharians led to the detection of other parazoanthoxanthin derivatives E (**168**), F (**122**) and G (**132**) in *P. axinellae* (Figure 17) [169]. The histamine-like activity of the methanolic fractions of the Japanese zoanthid *Parazoanthus gracilis* allowed the isolation of a yellowish-green fluorescence compound paragracine (**169**) [220]. The structure of **169** was established based on its chemical reactivity, spectroscopy data and X-ray crystallography analysis of its dehydrobromide trihydrate derivative. Compound **169** exhibited a papaverine-like activity and a frequency-depended blocking action of the sodium channel [221]. In addition to **169**, six paragracine-related alkaloids, 9-methylparagracine (**170**), **171**, **172**, **173**, **174** and **127** were subsequently isolated from the Japanese *P. gracilis* (Figure 17) [222]. A papaverine-like activity was exhibited by these compounds. Earlier, and during the chemical study of a Hawaiian zoantharian *Parazoanthus* sp. collected at a depth of 350 m, the pseudozoanthoxanthin analogue **171** was also isolated by Scheuer and co-workers [223]. However, a following publication by the same group admitted an uncertainty in the taxonomy of the species that could also belong to the genus *Savalia* [224]. Further analysis of the chemical content of this species allowed the characterization of **171** and another pseudozoanthoxanthin derivative **175**. The inhibition of acetylcholinesterase was reported from the ethanolic extract of *Parazoanthus axinellae* from the Northern Adriatic Sea, leading to the isolation of **176**, even if the

position of the methyl on either C-4 or C-6 was not confirmed [225]. This fluorescence compound displayed similar activity *in vivo* as the extract in mice and crabs with an inhibition constant (Ki) of 4 µM. The components of the extract could also be cholinergic agonist on the nicotinic and muscarine receptors. The *in vivo* results on the rat phrenic nerve-diaphragm with the isolated compound suggested a possible binding to the acetylcholine receptor. Finally, a recent study of the same species led to the identification of **129** and **169** [206]. For the first time, non-fully aromatic zoamides A-D (**177-180**) were reported in 1997 from an unidentified black species of *Parazoanthus* sp. from the Philippines (Figure 17) [226]. They feature an unprecedent acylation on both terminal primary amines.

Epizoanthus: The first metabolites reported from a species of the genus *Epizoanthus* are four zoanthoxanthin derivatives; epizoanthoxanthin A (**134)**, epizoanthoxanthin B (**123)**, pseudozoanthoxanthin (**127**) and 3-norpseudozoanthoxanthin (**129**) isolated from the Mediterranean *Epizoanthus arenaceus* collected off the Bay of Naples (Figure 17) [227]. The structures of the compounds were established by comparison with those of zoanthoxanthine derivatives previously reported from *Parazoanthus axinellae*. In 1993, 9-mehtylparagracine (**170**) was isolated together with **120** and **169** from an undescribed species of *Epizoanthus* from Namena Islands, Fiji [228]. Compound **170** displayed cytotoxic activity against two human colon adenocarcinoma (HCT8 and HT29), human lung carcinoma (A549) and mouse lymphocytic leukemia (P-388) with an IC_{50} values of 1.61, 0.824, 2.38 and 1.77 µg/mL respectively. Recently, the bioactive-guided chemical study of the extract of *Epizoanthus illoricatus* collected in the Republic of Palau, allowed the isolation of KB343 (**181**), an unusual cyclic tris-guanidine alkaloid [229]. The relative configuration was deduced from NOESY correlations and the absolute configuration was established through ECD analysis. Compound **181** exhibited moderate toxicity against murine leukemia cell line (L1210), human tumor cell line (HeLa) and model neuronal cell line derived from human bone marrow (SH-SY5Y) with IC_{50} values between 2 and 5 µM.

Terrazoanthus: A new family of 2-aminoimidazole alkaloids named Terrazoanthines A-C (**182-184**) were isolated from the zoantharian *Terrazoanthus patagonichus* (formerly known as *T. onoi*) collected off the coast of mainland Ecuador (Figure 17) [230]. This was the first report on the chemical diversity of a species of *Terrazoanthus*. The alkaloids **182** and **183** feature a novel skeleton with a 2-aminoimidazole ring fused to a cyclohexene and they still contain the 2-aminoimidazoles of zoanthoxanthins. The acylation is like the one observed for zoamides. Two additional non-fully aromatized bisguanidine derivatives zoamide E-F (**185-186**) were isolated from *Terrazoanthus* cf. *patagonichus* collected in the same area of the Tropical Eastern Pacific [231]. They differ only from the acyls substituted on both primary amines and the absolute configuration at the central methyl was proposed based on ECD calculation.

I.I.II.III Halogenated tyrosine derivatives

Parazoanthus: A new class of halogenated tyrosine alkaloids named parazoanthines A-E (**187-191**) were reported from the Mediterranean zoanthid *Parazoanthus axinellae* (Figure 19) [232]. They feature a rare 3,5 disubstituted hydantoin skeleton. Even if the antitumoral and antimalarial assays did not reveal significant activity for these compounds, the Microtox® bioassay revealed that **189** displayed highest toxicity with an EC_{50} value of 1.64 µM. Later, parazoanthines F-J (**192-196**) were identified by MS/MS analysis of the crude extract of *P. axinellae* from which parazoanthines A-E were reported [233, 234]. The structures were deduced by comparison of the fragmentation pattern to those previously reported analogues and MS/MS spectra simulation of predicted compounds. The absolute configuration was assigned using an online UPLC/ECD system. Two simple brominated and iodinated tyramine derivatives **197** and **198** were identified from *Parazoanthus darwini* collected off the coast of Ecuador (Figure 19) [231].

Antipathozoanthus: Four halogenated dipeptides named valdiviamides A-D (**199-202**) were isolated from *A. hickmani* collected off the coast of Ecuador (Figure 19) [231]. These compounds feature bromine and iodine atoms in the *ortho* position of the phenol ring of a common tyrosine amino acid. The relative and absolute configuration were assigned by nOe correlations, comparison of the theoretical and experimental ECD data and DP4 calculations based on ^{13}C NMR chemical shifts. Compound **200** exhibited moderated cytotoxic activity against hepatocellular carcinoma cell line (HepG2) with an IC_{50} value of 7.8 µM.

Parazoanthine	R	R^1	R^2	*Par.*
A (**187**)	H	H	H	
B (**188**)	H	H	H	$\Delta^{5,6}$
C (**189**)	CH$_3$	H	H	$\Delta^{5,6}$
D (**190**)	CH$_3$	Br	H	
E (**191**)	CH$_3$	Br	H	$\Delta^{5,6}$
F (**192**)	CH$_3$	H	H	
G (**193**)	H	Br	H	
H (**194**)	H	Br	H	$\Delta^{5,6}$
I (**195**)	CH$_3$	Br	Br	
J (**196**)	CH$_3$	Br	Br	$\Delta^{5,6}$

	R	*Par.*
197	I	
198	Br	

Valdiviamide	R	*A.*
A (**199**)	Br	
B (**200**)	I	

Valdiviamide	R	*A.*
C (**201**)	Br	
D (**202**)	I	
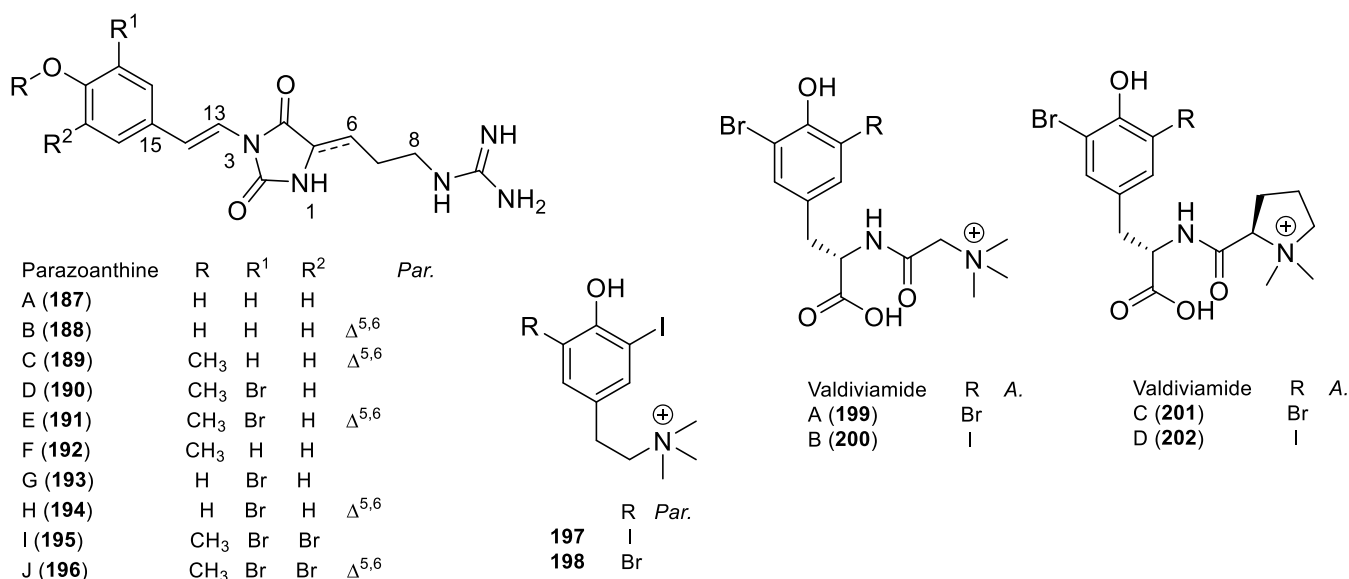
Figure 19 Halogenated tyrosine derivatives isolated from the genera *Parazoanthus* (Par.) and *Antipathozoanthus* (A.)

I.I.II.IV   Miscellaneous

A D-mannose-specific lectin was isolated by affinity chromatography from *S. savaglia* collected off the Bay of kotor, ex-Yugoslavia [235]. The lectin was identified to be a dimer composed of two similar subunits of approximately 15,819 Da each. The specificity of D-mannose was determined by electrophoretic, Scatchard blot analysis and by hemagglutination-inhibition studies. Additionally, the D-mannose-specific lectin exhibited a protective function of the H9 cells against human immunodeficiency virus type I (HIV-1; strain HTLV-IIIB) at a concentration of 0.2 µM [236].

2 Terrazoanthines, 2-aminoimidazole alkaloids from the Tropical Eastern Pacific Zoantharian *Terrazoanthus patagonichus (formerly known as T. onoi)*

Terrazoanthus patagonichus (© Karla B. Jaramillo)

Terrazoanthines, 2-Aminoimidazole Alkaloids from the Tropical Eastern Pacific Zoantharian *Terrazoanthus onoi*

Paul O. Guillen,[†,‡] Karla B. Jaramillo,[†,‡] Gregory Genta-Jouve,[§] Frederic Sinniger,[⊥] Jenny Rodriguez,*[,†] Olivier P. Thomas*[,§]

† Escuela Superior Politécnica del Litoral, ESPOL, Centro Nacional de Acuicultura e Investigaciones Marinas, CENAIM, Campus Gustavo Galindo Km 30.5 Vía Perimetral, P.O. Box 09-01-5863, Guayaquil, Ecuador.

‡ National University of Ireland Galway, School of Chemistry, Marine Biodiscovery, University Road, Galway, Ireland.

§ Université Paris Descartes, équipe C-TAC, COMETE UMR 8638 CNRS, 4 avenue de l'observatoire, 75006 Paris, France

⊥ University of the Ryukyus, Tropical Biosphere Research Center, 3422 Sesoko, 905-0227 Okinawa, Japan

Supporting Information Placeholder

ABSTRACT: The first chemical study of the common species *Terrazoanthus onoi* present off the coast of Ecuador led to the identification of a new family of 2-aminoimidazole alkaloids named terrazoanthines A-C (**1-3**). The homologues **1** and **2** feature an unprecedented 6-(imidazol-5-yl)benzo[d]imidazole. The acyl substitution pattern as well as complete configurational assignments were deduced from comparison between experimental and theoretical ^{13}C NMR and ECD data respectively. These compounds may represent key derivatives in the biosynthesis of zoanthoxanthins.

Zoantharians are a group of marine invertebrates (Cnidaria: Hexacorallia) widely distributed in all oceans and especially throughout the Indo-Pacific Oceans. While several studies have described their diversity around the western part of the Pacific, the Tropical Eastern part has been less investigated. The descriptions of zoantharians in this marine ecoregion were reported first from the Galapagos Islands but, overall, continental species have yet to be studied.[1,2] Interestingly, there is no chemical study reported on species of this group in this marine region so far. In the course of a national project setting up the basis for a first inventory of the bio- and chemo-diversity of the Ecuadorian maritime area, zoantharians were found to be largely present and distributed off the coasts of the Peninsula of Santa Elena. After a taxonomic assessment of the main species of this group we undertook the chemical study of one the most common zoantharian present in the marine protected area El Pelado, identified as *Terrazoanthus onoi* Reimer and Fujii, 2010.[1]

To date, the main natural products reported from zoantharians include ecdysteroids,[3-5] a large family of bioactive alkaloids named zoanthamines,[6,7] aromatic guanidine alkaloids,[8-10] and some hydantoin peptidic analogues.[11,12] The chemical study of *T. onoi* was conducted with two main objectives: i) to identify potential chemotaxonomic markers useful for the classification of zoantharians; and ii) to identify molecules with applications in animal and human health. Gratifyingly, the first insight into the chemical content of *T. onoi* led to the isolation and

structure elucidation of a new family of 2-aminoimidazole alkaloids named terrazoanthines A-C (**1-3**) (Figure 1). Compounds **1** and **2** feature an unprecedented 6-(imidazol-5-yl)benzo[d]imidazole skeleton. We report herein the isolation and structure elucidation of the three major and related metabolites produced by this species. A biosynthetic hypothesis is proposed to explain the formation of this unique skeleton. No significant antimicrobial or cytotoxic bioactivity was evidenced for these compounds through a first biological screening.
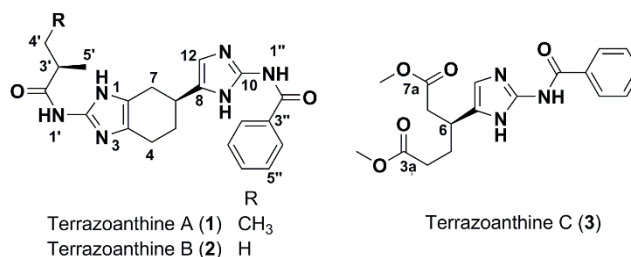
Figure 1. Structure of terrazoanthines A-C from *Terrazoanthus onoi*.

After an organic extraction of a freeze-dried sample of *T. onoi* the extract was submitted to a first fractionation process through reversed phase vacuum liquid chromatography. Because the methanolic fractions revealed interesting chemical profiles by UHPLC-DAD-ELSD

we undertook its purification by successive reversed phase HPLC.

The (+)-HRESIMS analysis of compound **1** revealed a major ion peak at *m/z* 407.2187 which was consistent with the molecular formula $C_{22}H_{27}N_6O_2$ [M+H]⁺ (Δ –0.7 ppm). A first inspection of the ¹H NMR spectrum evidenced a benzoyl moiety with signals at δ_H 8.07 (d, *J* = 8.0 Hz, 2H, H-4"), 7.58 (t, *J* = 8.0 Hz, 2H, H-5") and 7.69 (t, *J* = 8.0 Hz, 1H, H-6") together with a 2-methylbutyryl unit with methyl signals at δ_H 0.97 (t, 3H, *J* = 7.0 Hz, H-6'), 1.23 (d, *J* = 7.0 Hz, 3H, H-5') (Table 1). Both spin coupled systems were confirmed by the expected COSY correlations. The two carbonyls were placed on the basis of key HMBC correlations H-4"/C-2" and H-5'/C-2'. Even if the presence of a singlet at δ_H 7.04 (s, 1H, H-12) suggested a second aromatic ring no clear conclusion could be ascertained based on the ¹H NMR spectrum.

Table 1. ¹H NMR data for **1-3** at 600 MHz in CD₃OD: δ_H in ppm, multiplicity (*J* in Hz).

no.	1	2	3
H-N₁	8.40ᵃ	a	a
4	2.75, m	2.75, m	2.37, t (7.5)
5	2.36, br d (15.0)	2.36, br d (15.0)	2.03, m
	2.05, m	2.05, m	
6	3.31, m	3.31, m	3.33, m
7	3.09, dd (15.0, 3.5)	3.09, dd (15.0, 3.5)	2.78, m
	2.79, dd (15.0, 10.0)	2.79, dd (15.0, 10.0)	
H-N₉	a	a	a
12	7.04, s	7.04, s	7.03, s
H-N₁'	11.58ᵃ	a	a
3'	2.53, sext (7.0)	2.72, hept (7.0)	
4'	1.78, dquint (14.0, 7.0)	1.25, d (7.0)	
	1.56, dquint (14.0, 7.0)		
5'	1.23, d (7.0)	1.25, d (7.0)	
6'	0.97, t (7.0)		
H-N₁"	a	a	a
4"	8.07, d (8.0)	8.07, d (8.0)	8.03, d (8.0)
5"	7.58, t (8.0)	7.58, t (8.0)	7.58, t (8.0)
6"	7.69, t (8.0)	7.69, t (8.0)	7.69, t (8.0)
H₃CO-C-3a			3.64, s
H₃CO-C-7a			3.67, s

ᵃ In DMSO-d_6

The ¹³C NMR spectrum of **1** revealed six additional unsaturated carbons that could only be consistent with one or two additional aromatic rings. Because no clear HMBC correlation allowed connection of the first two SCS to these rings, we focused on the last SCS containing saturated carbons (Figure 2). The methylene at C-7 was COSY correlated to the methine at C-6 and then to two successive methylene at C-5 and C-4. HMBC correlations with the two terminal methylenes at C-7 and C-4 allowed closure of the cyclohexene ring through a tetrasubstituted double bond at δ_C 122.9 (C-7a) and 124.0 (C-3a). Additional H-6/C-8 and H-

6/C-12 HMBC correlations placed a trisubstituted double bond at C-6. Key information was obtained from a H-12/C-10 HMBC correlation that was only consistent with the presence of a 2-aminoimidazole connected at C-6. This proposition was confirmed by the observation of similar chemical shifts described for dimers of pyrrole 2-aminoimidazoles, a large family of metabolites produced by sponges of the Axinellida or Agelasida groups.[13]

Table 2. ¹³C NMR data for **1-3** at 125 MHz in CD₃OD: δ_C in ppm.

no.	1	2	3
2	139.4	139.4	
3a	124.0	124.0	175.0
4	20.6	20.5	32.1
5	28.6	28.6	30.0
6	32.0	32.0	33.6
7	26.5	26.5	39.3
7a	122.9	122.9	173.7
8	134.4	134.4	133.4
10	140.9	140.9	140.6
12	111.7	111.8	113.0
2'	177.3	177.8	
3'	43.7	36.5	
4'	24.2	19.3	
5'	27.9	19.3	
6'	11.9		
2"	167.5	167.5	167.5
3"	133.0	133.0	133.0
4"	129.3	129.3	129.2
5"	130.0	130.0	130.0
6"	134.6	134.6	134.6
H₃CO-C-3a			52.2
H₃CO-C-7a			52.3

The presence of a second 2-aminoimidazole ring fused to the cyclohexene was first inferred from the molecular formula of **1** which indicated the presence of 6 nitrogens. Even if no HMBC correlation was visible involving the quaternary carbon C-2, a clear signal at δ_C 139.4 was assigned to this last carbon.
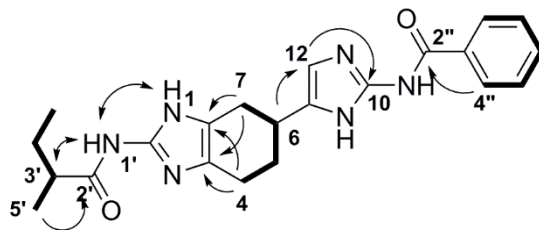
Figure 2. Key COSY (bold), HMBC (arrow from H to C) correlations for **1**. nOe correlations are indicated with double arrows.

The next issue to be addressed was the location of the two acyl groups around this bisguanidine core. We first recorded the NMR spectra of this compound in DMSO-d_6 to reveal the N-H of the alkaloid. Gratifyingly, four new singlets were observed in the deshielded region of the spectrum. Both H-1'/H-3' and H-1'/H-1 ROESY correlations unambiguously placed the 2-methylbutyryl on one of the two primary amines. This substitution pattern was

confirmed by the chemical shift at δ_H 8.40 (s, 1H, H-1') observed for the signal of this first secondary amide. Similar chemical shifts were indeed observed for pyrrole 2-aminoimidazole named nagelamides.[14] Because no HMBC was observed from all four H-N signals we compared the experimental and theoretical ^{13}C NMR chemical shifts of all possible substitution patterns. Choosing the location of the 2-methylbutyryl on one primary amine afforded two possible substitutions for the benzoyl on the other imidazole. Among the four possible substitution patterns, the most probable locations of the acyls are shown in Figure 1 with 100% confidence (see supporting information).[15] Confirmation was obtained when comparing the ^{13}C NMR chemical shifts of 1 with those of zoamide D.[8]

We next paid attention to the absolute configurations of 1. The experimental ECD spectrum revealed four successive Cotton Effects (Figure 3). Theoretical calculation of the ECD spectra of both enantiomers was performed using TDDFT. As depicted in figure 3, a good agreement was observed between experimental and theoretical spectra with the 6*S* absolute configuration.
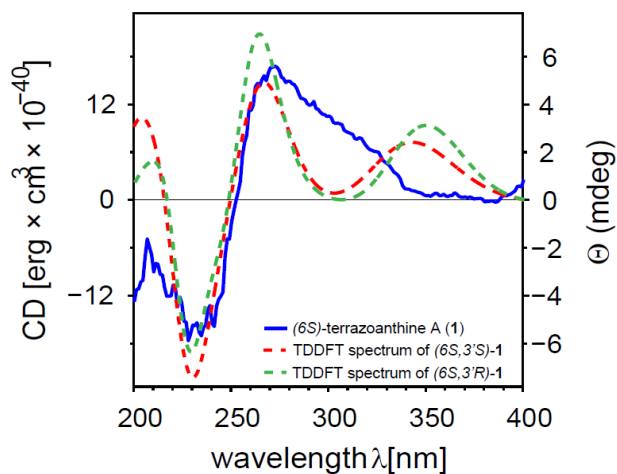
Figure 3. Comparison between the experimental (line) and theoretical (dashed) ECD spectra of two diastereoisomers of 1 at C-3'.

Because the ECD spectra for the diastereoisomers 6*S*,3'*R* and 6*S*,3'*S* did not allow the determination of the absolute configuration at C-3' (figure 3), the use of the DP4 probability was also required for the determination of the relative configuration of compound **1**. As shown in figure 4, the relative configuration was established as 6*S*,3'*R* with 81.8% of confidence (dia a).
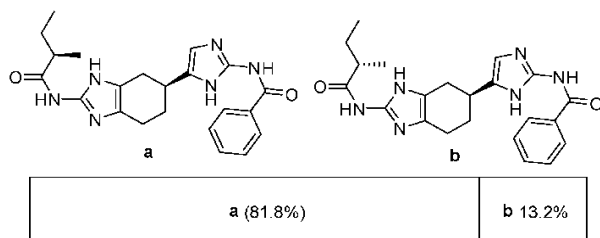
Figure 4. DP4 probabilities of ^{13}C NMR data for both diastereo-isomers of 1.

The (+)-HRESIMS analysis of compound 2 revealed a major ion peak at m/z 393.2043 which was consistent with the molecular formula $C_{21}H_{24}N_6O_2$ [M+H]+ (Δ 2.3 ppm). This

molecular formula was consistent with the loss of a methylene unit comparing to **1**. The ^{1}H NMR spectrum showed a different pattern for the methyls. Unlike **1** with two methyl signals, only one methyl signal of integration 6 was observed in the case of **2**. We then concluded that the 2-methylbutyryl substituent of the benzimidazole ring was replaced by an isobutyryl in **2** (Table 1). We assumed the same *S* absolute configuration at C-6 for **2**.

The (+)-HRESIMS analysis of compound **3** revealed a major ion peak at m/z 360.1556 consistent with the molecular formula $C_{18}H_{22}N_3O_6$ [M+H]+ (Δ 0.2 ppm). This molecular formula suggested the absence of one of the two 2-aminoimidazole rings. The ^{1}H NMR spectrum confirmed the presence of the benzoyl while the butyryl signals were absent. New signals corresponding to methoxy groups suggested the presence of two methyl ester functions. They were confirmed by H3-7/C-7a and H3-4/C-3a HMBC correlations. The remaining imidazole ring was still located at C-6 after COSY, HSQC and HMBC interpretation.

Guanidine alkaloids are common in the marine environment and especially in marine invertebrates like sponges.[16] Their biosynthesis is still subject of controversy due to the difficulty to perform feeding experiments or to isolate the biosynthetic genes of these compounds. The presence of two 2-aminoimidazole units in terrazoanthines A and B is an important feature these compounds share with other marine natural products. They are clearly related to a large family of fluorescent alkaloids named zoanthoxanthins also present in several zoantharians. It is important here to underline the pioneering work of Cariello *et al.* who were the first to propose a C5N3 unit like arginine as a precursor of zoanthoxanthins.[10] This hypothesis was later supported by some successful biomimetic syntheses from the group of Büchi.[17,18] Two decades later the group of Horne was inspired by this hypothesis to conduct other straightforward approaches towards the syntheses of these pigments.[19,20] In their work they also proposed an alkylation at C-4 of 2-aminoimidazole derived from arginine as a possible step towards the production of C2-2-aminoimidazole key precursors. The structures of terrazoanthines are of high biosynthetic interest as they can be seen as a clue towards the hypothesis of a C5N3 precursor. Indeed, we can propose a dimerization process of a key intermediate 4-vinylimidazol-2-amine through a Diels Alder type [4+2] cycloaddition. The key intermediate may originate from arginine after an oxidation at the β position of the arginine. Interestingly, the same type of oxidation but with homoarginine was proposed in the biosynthesis of pyrrole 2-aminoimidazole alkaloids.[13] While the existence of a natural Diels-Alderase was still a matter of debate until recently, a report gave some conclusive evidence of its occurrence.[21] The feasibility of this reaction was confirmed by Hartree-Fock theoretical calculations (see SI).

Scheme 1. Proposed biosynthetic pathway for terrazoanthines **1** and **2**, zoanthoxanthins and pseudozoanthoxanthins.
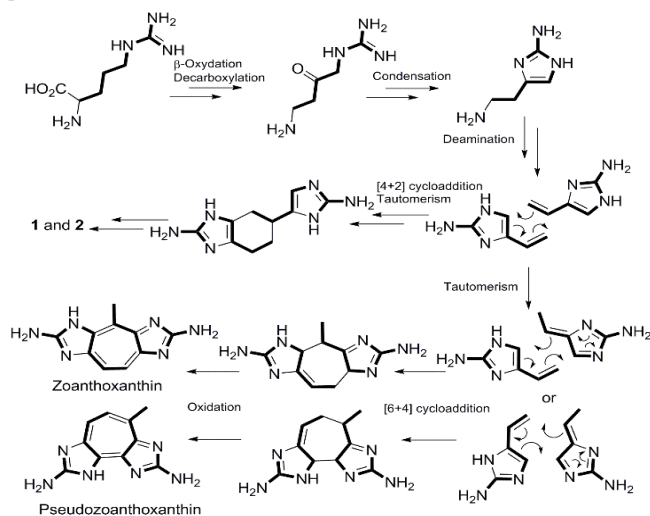
As proposed earlier by the group of Büchi, the key 2-amino-4-vinylimidazole is in a tautomeric equilibrium with a di-azafulvene analogue.[17, 18] This fulvene derivative can undergo a [6+4] cycloaddition with the non-isomerized tautomer form leading to the seven-membered ring after subsequent oxidation and aromatization. These unusual high order cycloadditions are of clear biosynthetic interests as, according to the regioselectivity of the reaction, they can lead to both zoanthoxanthins and pseudozoanthoxanthins. For compound **3**, we could suggest a hydrolysis of both imines present in the benzimidazole ring leading to the loss of the guanidine and the formation of a cyclohexa-1,2-dione. This dione derivative would lead to the corresponding dicarboxylic acid after an oxidative cleavage. Methylation of these carboxylic acids could occur either naturally or during the extraction process.

From a biological point of view these three compounds were tested for their antimicrobial activities but also for their cytotoxicity against the human liver cancer cell line Heg2 but they were found inactive. The search for bioactivity will be extended towards the inhibition of Acetylcholine Esterase as some zoanthoxanthin derivatives have shown promising results for these targets.[22]

The first chemical study undertaken on a common marine invertebrate present in the coastal area of Ecuador has been extremely positive. The zoantharian *Terrazoanthus onoi* provided a new family of natural products named terrazoanthines. Terrazoanthines A and B feature a unique bis 2-aminoimidazole attached around a central cyclohexene. The benzoyl substituted on one primary amine seems to be a common feature of this novel family of natural product. These results show good promise in the use of metabolomics for the classification of zoantharians as guanidine alkaloids and ecdysteroids appear as common to most species of this group.

ASSOCIATED CONTENT

Supporting Information. Description of the species, General Experimental Procedures, HRMS and ^{1}H, ^{13}C, COSY, HSQC and HMBC NOESY NMR data for **1-3**. Computational methods and biological assays. This material is available free of charge via the Internet at http://pubs.acs.org.

AUTHOR INFORMATION

Corresponding Authors

jenrodri@espol.edu.ec (J.Rodriguez);
olivier.thomas@nuigal-way.ie (O.Thomas)
+353(0)91493563.

Author Contributions

The manuscript was written through contributions of all authors. / All authors have given approval to the final version of the manuscript.

REFERENCES

1. Reimer, J. D.; Fujii, T., Four new species and one new genus of zoanthids (Cnidaria, Hexacorallia) from the Galápagos Islands. ZooKeys 2010, 1-36.
2. Reimer, J. D.; Sinniger, F.; Hickman, C. P., Zoanthid diversity (Anthozoa: Hexacorallia) in the Galapagos Islands: a molecular examination. Coral Reefs 2008, 641-654.
3. Searle, P. A.; Molinski, T. F., 4-Dehydroecdysterone, a new ecdysteroid from the zoanthid Parazoanthus sp. J. Nat. Prod. 1995, 58, 264-8.
4. Guerriero, A.; Traldi, P.; Pietra, F., Gerardiasterone, a new ecdysteroid with a 20,22,23,25-tetrahydroxylated side chain from the Mediterranean zoanthid Gerardia savaglia. J. Chem. Soc., Chem. Commun. 1986, 40-1.
5. Suksamrarn, A.; Jankam, A.; Tarnchompoo, B.; Putchakarn, S., Ecdysteroids from a Zoanthus sp. J. Nat. Prod. 2002, 65, 1194-1197.
6. Behenna, D. C.; Stockdill, J. L.; Stoltz, B. M., The Biology and Chemistry of the Zoanthamine Alkaloids. Angew. Chem. Int. Ed. 2008, 47, 2365-2386.
7. Rao, C. B.; Anjaneyula, A. S. R.; Sarma, N. S.; Venkatateswarlu, Y.; Rosser, R. M.; Faulkner, D. J.; Chen, M. H. M.; Clardy, J., Zoanthamine; a novel alkaloid from a marine zoanthid. J. Am. Chem. Soc. 1984, 106, 7983-4.
8. D'Ambrosio, M.; Roussis, V.; Fenical, W., Zoamides A-D: new marine zoanthoxanthin class alkaloids from an encrusting Philippine Parazoanthus sp. Tetrahedron Lett. 1997, 38, 717-720.
9. Cariello, L.; Crescenzi, S.; Prota, G.; Capasso, S.; Giordano, F.; Mazzarella, L., Zoanthoxanthin, a natural 1,3,5,7-tetraazacyclopent[f]azulene from Parazoanthus axinellae. Tetrahedron 1974, 30, 3281-7.

10. Cariello, L.; Crescenzi, S.; Prota, G.; Zanetti, L., New zoanthoxanthins from the Mediterranean zoanthid Parazoanthus axinellae. Experientia 1974, 30, 849-850.

11. Audoin, C.; Cocandeau, V.; Thomas, O. P.; Bruschini, A.; Holderith, S.; Genta-Jouve, G., Metabolome consistency: additional parazoanthines from the Mediterranean zoanthid Parazoanthus axinellae. Metabolites 2014, 4, 421-432, 12 pp.

12. Cachet, N.; Genta-Jouve, G.; Ivanisevic, J.; Chevaldonne, P.; Sinniger, F.; Culioli, G.; Perez, T.; Thomas, O. P., Metabolomic profiling reveals deep chemical divergence between two morphotypes of the zoanthid Parazoanthus axinellae. Sci. Rep. 2015, 5, 8282.

13. Genta-Jouve, G.; Cachet, N.; Holderith, S.; Oberhänsli, F.; Teyssié, J.-L.; Jeffree, R.; Al Mourabit, A.; Thomas, O. P., New Insight into Marine Alkaloid Metabolic Pathways: Revisiting Oroidin Biosynthesis. ChemBioChem 2011, 12, 2298-2301.

14. Endo, T.; Tsuda, M.; Okada, T.; Mitsuhashi, S.; Shima, H.; Kikuchi, K.; Mikami, Y.; Fromont, J.; Kobayashi, J. i., Nagelamides A–H, New Dimeric Bromopyrrole Alkaloids from Marine Sponge Agelas Species. J. Nat. Prod. 2004, 67, 1262-1267.

15. Smith, S. G.; Goodman, J. M., Assigning Stereochemistry to Single Diastereoisomers by GIAO NMR Calculation: The DP4 Probability. J. Am. Chem. Soc. 2010, 132, 12946-12959.

16. Berlinck, R. G. S.; Romminger, S., The chemistry and biology of guanidine natural products. Nat. Prod. Rep. 2016, 33, 456-490.

17. Braun, M.; Büchi, G.; Bushey, D. F., Synthesis of parazoanthoxanthins and pseudozoanthoxanthins. J. Am. Chem. Soc. 1978, 100, 4208-13.

18. Braun, M.; Büchi, G. H., The synthesis of zoanthoxanthins. J. Am. Chem. Soc. 1976, 98, 3049-50.

19. Xu, Y.-z.; Yakushijin, K.; Horne, D. A., Oxidative Dimerization of 2-Aminoimidazoles by Molecular Bromine. Synthesis of Parazoanthoxanthin A. J. Org. Chem. 1996, 61, 9569-9571.

20. Xu, Y.; Yakushijin, K.; Horne, D. A., Biomimetic transformations of 2-aminoimidazole into zoanthoxanthins: exposing a potential biogenic missing link. Tetrahedron Lett. 1992, 33, 4385-8.

21. Byrne, M. J.; Lees, N. R.; Han, L.-C.; van der Kamp, M. W.; Mulholland, A. J.; Stach, J. E. M.; Willis, C. L.; Race, P. R., The Catalytic Mechanism of a Natural Diels–Alderase Revealed in Molecular Detail. J. Am. Chem. Soc. 2016, 138, 6095-6098.

22. Turk, T.; Maček, P.; Šuput, D., Inhibition of acetylcholinesterase by a pseudozoanthoxanthin-like compound isolated from the zoanthid Parazoanthus axinellae (O. Schmidt). Toxicon 1995, 33, 133-142.

3 Zoanthamine alkaloids from the Zoantharian *Zoanthus* cf. *pulchellus* and Their Effects in Neuroinflammation

Zoanthus cf. *pulchellus* (© Karla B. Jaramillo)

Article

Zoanthamine Alkaloids from the Zoantharian Zoanthus cf. pulchellus and Their Effects in Neuroinflammation

Paul O. Guillen [1,2], Sandra Gegunde [3], Karla B. Jaramillo [1,4], Amparo Alfonso [3], Kevin Calabro [2], Eva Alonso [3], Jenny Rodriguez [1], Luis M. Botana [3,*] and Olivier P. Thomas [2,*]

[1] ESPOL Escuela Superior Politécnica del Litoral, ESPOL, Centro Nacional de Acuacultura e Investigaciones Marinas, Campus Gustavo Galindo km. 30.5 vía Perimetral, P.O. Box 09-01-5863, Guayaquil, Ecuador.; P.GUILLENMENA1@nuigalway.ie (P.O.G.); K.JARAMILLOAGUILAR1@nuigalway.ie (K.B.J.); jenrodri@espol.edu.ec (J.R.)

[2] Marine Biodiscovery, School of Chemistry and Ryan Institute, National University of Ireland Galway (NUI Galway), University Road, H91 TK33 Galway, Ireland; kevin.calabro@nuigalway.ie

[3] Departamento de Farmacología, Facultad de Veterinaria, Universidade de Santiago de Compostela, 27002 Lugo, Spain; sandra.gegunde@rai.usc.es (S.G.); amparo.alfonso@usc.es (A.A.); eva.alonso@usc.es (E.A.)

[4] Zoology, School of Natural Sciences and Ryan Institute, National University of Ireland Galway (NUI Galway), University Road, H91 TK33 Galway, Ireland

* Correspondence: luis.botana@usc.es (L.M.B.); Tel.: +34-982822233 (L.M.B.); olivier.thomas@nuigalway.ie (O.P.T.); Tel.: +353-91-493563 (O.P.T.)

Abstract: Two new zoanthamine alkaloids, namely 3-acetoxynorzoanthamine (**1**) and 3-acetoxyzoanthamine (**2**), have been isolated from the zoantharian *Zoanthus* cf. *pulchellus* collected off the coast of the Santa Elena Peninsula, Ecuador, together with three known derivatives: zoanthamine, norzoanthamine, and 3-hydroxynorzoanthamine. The chemical structures of **1** and **2** were determined by interpretation of their 1D and 2D NMR data and comparison with literature data. This is the first report of zoanthamine-type alkaloids from *Zoanthus* cf. *pulchellus* collected in the Tropical Eastern Pacific. The neuroinflammatory activity of all the isolated compounds was evaluated in microglia BV-2 cells and high inhibitory effects were observed in reactive oxygen species (ROS) and nitric oxide (NO) generation.

1. Introduction

Zoanthamines are a bioactive family of marine alkaloids featuring a unique chemical architecture of fused cycles culminating in an unusual azepane ring. They have been isolated essentially from marine zoantharians, particularly from the genus *Zoanthus*. The first alkaloid of this group was isolated in 1984 from an unidentified species of *Zoanthus*, collected off the coast of India by Faulkner et al. [1]. Following this first description, several studies on the chemical diversity of species of the genus *Zoanthus* have led to the discovery of additional zoanthamine-type alkaloids, including zoanthenamine, zoanthenamide [2], norzoanthamine, oxyzoanthamine, norzoanthaminone, cyclozoanthamine, epinorzoanthamine [3], zoanthaminone [4], zoaramine [5], kuroshines [6], epioxyzoanthamine [7], zoanthenol [8], hydroxylated zoanthamines and norzoanthamines [9], and two halogenated zoanthamines [10]. This interesting family of alkaloids has been structurally classified in two different groups based on the presence of a methyl at C-19 (Type I) or its absence (Type II), also called norzoanthamines [10]. Due to the structural complexity of these natural products, the first total

synthesis of norzoanthamine was accomplished by Miyashita et al. in 2004 [11], who also synthesized other analogues [12,13]. Other research groups are now addressing this synthetic challenge through alternative approaches [14–16]. Up to date, 38 zoanthamine-type alkaloids have been reported from zoantharian species essentially inhabiting the Central Indo-Pacific and these polycyclic alkaloids seem to be chemical markers of zoantharians from the genus *Zoanthus*. In addition, some members of this family have displayed a wide range of biological activities against P388 murine leukemia cells [3] as well as anti-osteoporosis, anti-inflammatory, and anti-bacterial activity, and have also been found to inhibit human platelet aggregation [9,17]. The most promising therapeutic application is associated with norzoanthamine in the treatment of osteoporosis, as it inhibits interleukin-6, a primary mediator of bone resorption. Furthermore, an interesting study by Tachibana et al. suggested that the principal function of norzoanthamine in *Zoanthus* sp. is collagen strengthening [18].

In our continuous investigation of the bio- and chemodiversity of marine invertebrates present in the understudied Marine Protected Area El Pelado, Santa Elena, Ecuador, located in the Tropical Eastern Pacific [19,20], we came across a massive substrate cover of the intertidal region by undescribed fluorescent green zoantharians. A first taxonomic assessment of these zoantharian species led to the identification of the main species as being closely related to *Zoanthus* cf. *pulchellus*, previously described in the Caribbean [21]. No chemical study of this species has been reported so far, and our first chemical screening by UHPLC-HRMS revealed unknown masses related to the zoanthamine family as major compounds of the extract. In this paper, we describe the isolation and structure elucidation of two new zoanthamine alkaloids, namely 3-acetoxynorzoanthamine (**1**) and 3-acetoxyzoanthamine (**2**) (Figure 1), along with the known zoanthamine [1], norzoanthamine [3], and 3-hydroxynorzoanthamine [8] from the Eastern Pacific zoantharian *Zoanthus* cf. *pulchellus*, as well as their biological activity in cellular pathways related to oxidative stress and neuroinflammation.

	R
3-Acetoxynorzoanthamine (**1**)	H
3-Acetoxyzoanthamine (**2**)	CH$_3$
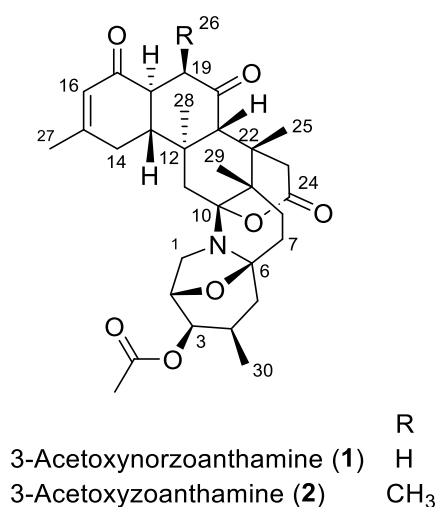
Figure 1. Structures of 3-acetoxynorzoanthamine (**1**) and 3-acetoxyzoanthamine (**2**), isolated from *Zoanthus* cf. *pulchellus*.

2. Results

Colonies of the zoantharian *Zoanthus* cf. *pulchellus* were collected by hand in the intertidal coast of San Pedro, Santa Elena, Ecuador. The sample was freeze-dried and extracted with a mixture of solvents CH$_3$OH:CH$_2$Cl$_2$ (*v/v*; 1:1). The extract was then fractionated through reversed-phase C18 Vacuum Liquid Chromatography (VLC) using a mixture of solvents of decreasing polarity. The aqueous methanolic fractions were analyzed by UPLC-DAD-ELSD, combined, and then subjected to semipreparative RP-HPLC using a C18 column to yield two new zoanthamine-type alkaloids: 3-

acetoxynorzoanthamine (**1**) and 3-acetoxyzoanthamine (**2**), along with the known zoanthamine [1], norzoanthamine [18], and 3-hydroxynorzoanthamine [8].

Compound **1** was obtained as a brown amorphous powder and (+)-HRESIMS analyses revealed a major molecular peak at *m/z* 540.2956 [M + H]⁺, consistent with the molecular formula $C_{31}H_{41}NO_7$ for the neutral molecule. A preliminary inspection of the ^1H and ^{13}C NMR data revealed characteristic signals of the zoanthamine family, as already speculated on the basis of the HRMS data: an olefinic proton at δ_H 5.90 (H-16) along with four methyl singlets at δ_H 0.97 (H-28), 0.99 (H-25), 1.15 (H-29), and 2.00 (H-27), and a methyl doublet at δ_H 0.87 (H-30) together with two ketone signals at δ_C 198.5 (C-17) and δ_C 209.0 (C-20), one ester signal at δ_C 172.3 (C-24), and two olefinic carbons at δ_C 125.6 (C-16) and 160.0 (C-15) (Table 1). The absence of a second doublet of a methyl present in zoanthamines was indicative of a loss of the methyl CH₃-26 at C-19; therefore, the compound belonged to the norzoanthamine-type. Unlike most studies on norzoanthamines, in order to make the NMR table more homogeneous, we decided to keep the numbering of the zoanthamines especially for the methyls 27, 28, 29, and 30. Comparing with analogues of this type, we observed the presence of an additional methyl singlet signal at δ_H 2.11 corresponding to an acetyl moiety (Table 1). The presence of the acetyl group on an oxygen at C-3 was evidenced by the deshielding of the signal corresponding to the methine H-3 with δ_H 4.62 and key H-3/C-1′ and H₃-2′/C-1′ HMBC correlations.

Table 1. ^1H and ^{13}C NMR data in ppm for compounds **1** and **2** in CDCl₃ (500 MHz for ^1H NMR and 125 MHz for ^{13}C NMR data).

	1		**2**	
No.	**δ_H, mult. (*J* in Hz)**	**δ_C**	**δ_H, mult. (*J* in Hz)**	**δ_C**
1	3.24, t (7.0) 3.19, d (7.0)	45.3	3.24, t (7.5) 3.20, d (7.0)	45.5
2	4.58, br d (6.5)	75.6	4.59, d (7.0)	75.7
3	4.62, br t (3.0)	72.5	4.63, t (3.0)	72.6
4	2.44, br sext (5.5)	26.0	2.43, br sext (6.0)	26.1
5	1.92, dd (12.0, 6.0) 1.36, t (12.5)	40.3	1.95, dd (12.5, 6.0) 1.37, t (13.0)	40.4
6	-	90.1	-	90.2
7	1.88, dd (12.5, 4.5) 1.80, dt (12.5, 3.5)	29.8	1.90, dd (12.5, 4.5) 1.80, dt (12.5, 3.5)	29.9
8	1.66, td (13.5, 3.5) 1.57, dt (13.5, 4.0)	23.7	1.67, td (14.0, 3.5) 1.57, dt (14.0, 4.0)	23.8
9	-	40.0	-	40.5
10	-	100.9	-	101.0
11	2.08, d (13.0) 1.94, d (13.0)	41.8	2.11, d (13.0) 1.93, d (13.0)	42.0
12	-	39.9	-	39.8
13	2.20, td (12.0, 4.5)	53.1	2.41, td (12.0, 4.5)	48.1
14	2.26, br s 2.24, br s	32.0	2.24, br s 2.22, br s	30.7
15	-	160.0	-	160.1
16	5.90, s	125.6	5.92, s	127.0
17	-	198.5	-	197.3
18	2.69, td (12.0, 6.5)	46.4	2.66, dd (12.5, 6.5)	48.2
19	2.62, dd (14.5, 6.5) 2.50, dd (14.5, 12.0)	42.4	3.02, dq (7.0, 6.5)	45.9
20	-	209.0	-	212.2
21	2.83, s	59.1	3.23, s	53.9
22	-	36.5	-	40.3
23	3.65, d (20.0) 2.36, d (20.0)	35.9	3.68, d (20.0) 2.37, d (20.0)	36.1
24	-	172.3	-	172.4
25	0.99, s	21.1	0.98, s	20.8
26	-	-	1.17, d (7.0)	13.9
27	2.00, s	24.4	2.01, s	24.6
28	0.97, s	18.5	0.99, s	18.5
29	1.15, s	18.4	1.21, s	18.4

30	0.87, d (7.0)	16.3	0.89, d (7.0)	16.4
Ac	-	171.2	-	171.4
	2.11, s	21.1	2.14, s	21.2

We then addressed the question of the relative configurations of the different chiral centers. To the best of our knowledge, this is the first occurrence of an acetoxy group at position C-3 for zoanthamines; however, other analogues oxygenated at this position have already been described. First, 3-hydroxynorzoanthamine was isolated from an undescribed species of *Zoanthus* from the Canary Islands in the Atlantic Ocean [8]. Later, kuroshines C and F as well as 3β-hydroxyzoanthenamide also possess an hydroxyl group at this position [6]. All these four derivatives were shown to have a hydroxyl group on the β-side of the polycyclic compound and this position was deduced from nOes between H-3 and other protons of the azepane ring. In our case, and because both H-3/H-4a and H-3/H-4b coupling constant values were not fully conclusive, we relied on the key H-3/H-1b nOe correlation to place H-3 on the opposite side of the bridged oxygen (α-side). Subsequently, the acetoxy group was located on the β-side like for the other four 3-hydroxylated analogues. The very low coupling constant values of H-3 with H-2 and H-4 were similar to those observed for all 3-hydroxylated compounds and in perfect agreement with this relative configuration. Additionally, a previous study by Uemura et al. assigned the absolute configuration of norzoanthamine as 2*R*, 4*S*, 6*S*, 9*S*, 10*R*, 12*R*, 13*R*, 18*S*, 21*S*, and 22*S* and suggest the same absolute configuration for all norzoanthamine-type alkaloids [22]. In our case, the positive specific rotation obtained for **1** was in accordance with that obtained for 3-hydroxyzoanthamine and therefore confirmed the same absolute configuration [8].

Compound **2** was isolated as an amorphous yellowish powder and the molecular formula $C_{32}H_{43}NO_7$ was deduced from HRESIMS revealing a major peak at *m/z* 554.3115 [M + H]$^+$; therefore, **2** is an homologue of **1**. A quick inspection of the ^{1}H NMR spectrum evidenced the presence of the acetoxy group at C-3 as in **1**. An additional methyl signal at δ_H 1.17 (d, *J* = 7.0 Hz, H$_3$-26) suggested that **2** is a member of the zoanthamine-type alkaloids. The presence of the methyl at C-19 was confirmed by the key H-19/C-26 and H$_3$-26/C-18/C-19 HMBC correlations. The β-position of the methyl 26 was then inferred from the coupling constant value $J_{H-18/H-19}$ of 6.0 Hz, reminiscent of an axial/equatorial coupling. Because H-18 is placed in an axial position, H-19 should be placed in an equatorial position; therefore, the methyl 26 occupies the corresponding axial β-position at C-19. The β-position of the acetoxy at C-3 was deduced from the same coupling constant values of H-3 as for **1,** and the absolute configuration was supposed to be the same as that of **1**, again because of similar positive specific rotations.

The compounds were tested for biological activity in the BV-2 microglia cell line, a cellular model often used in neuroinflammation studies. The first step was to determine the effect of compounds on cell viability. Five concentrations (from 0.001 to 10 μM) were investigated and after 24 h of incubation no effects on cell viability were observed, which suggested non-toxic compounds. Microglia-mediated inflammation is known to produce reactive oxygen species (ROS) and release nitric oxide (NO), and thus induce oxidative damage [23]. Therefore, zoanthamines were checked as modulators within these processes. BV-2 cells were activated with lipolysaccharide (LPS) to simulate neuroinflammatory conditions. As shown in Figure 2, when cells were pre-treated with the same concentrations of compounds for 1 h and then incubated for 24 h with LPS (500 ng/mL), a significant reduction in ROS production was observed. As expected, the stimulation of BV-2 cells with LPS significantly increased the ROS production, 50% (*p* < 0.001), while the compounds alone did not induce any effect. However, when cells were pre-treated with norzoanthamine and **1**, a dose-dependent inhibitory effect was observed, while 3-hydroxynorzoanthamine, zoanthamine, or **2** were effective at all concentrations tested, with **2** being the most potent ROS inhibitor. From these results, 0.1 and 1 μM were chosen to investigate the effect on NO release (Figure 3). Zoanthamine alkaloids alone did not produce any effect on NO production, while LPS treatment increased it by three times. In the presence of this family of compounds, NO release was significantly inhibited. The anti-inflammatory effect of zoanthamines was previously investigated in neutrophils [10]. From our results in the BV-2 cellular model, zoanthamine and derivatives show effective properties as protective drugs in neuroinflammation processes.
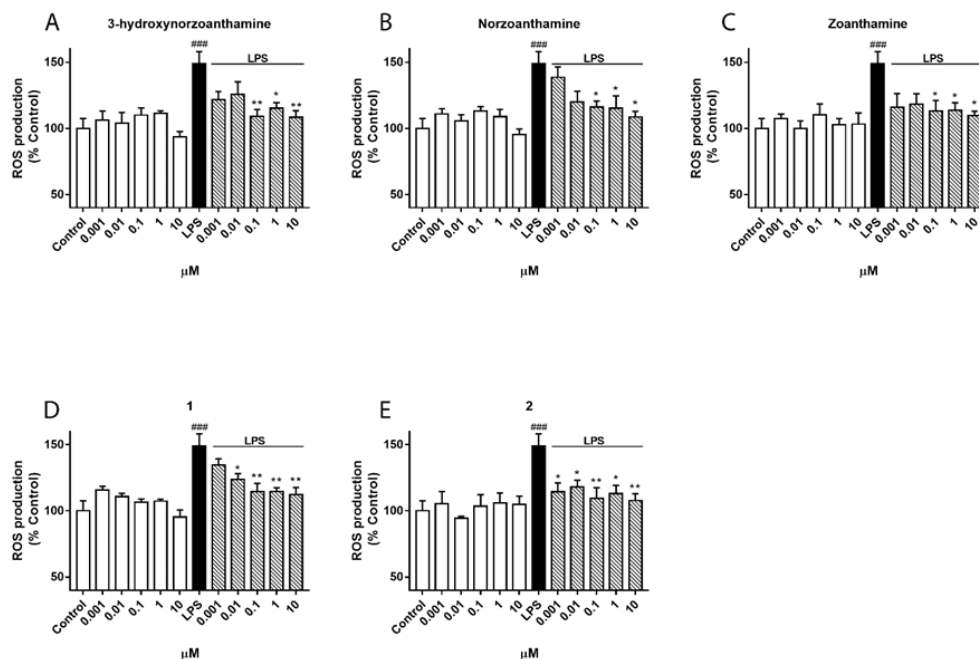
Figure 2. Effect of zoanthamines on intracellular reactive oxygen species (ROS) production in microglia BV-2 cell line. Cells were pre-treated with 3-hydroxynorzoanthamine (**A**), norzoanthamine (**B**), zoanthamine (**C**), **1** (**D**), and **2** (**E**) at different concentrations (0.001, 0.01, 0.1, 1, and 10 μM) 1 h and then stimulated with lipolysaccharide (LPS) (1 μg/mL) for 24 h. ROS production is presented as a percentage of cells control, being the result of mean fluorescence intensity ± SEM of three independent experiments. The values are shown as the difference between cells treated with LPS alone versus cells treated with zoanthamines in presence of LPS by ANOVA followed by *post hoc* Dunnett's test. * $p < 0.05$ and ** $p < 0.01$, and LPS-treated cells versus control cells ### $p < 0.001$.
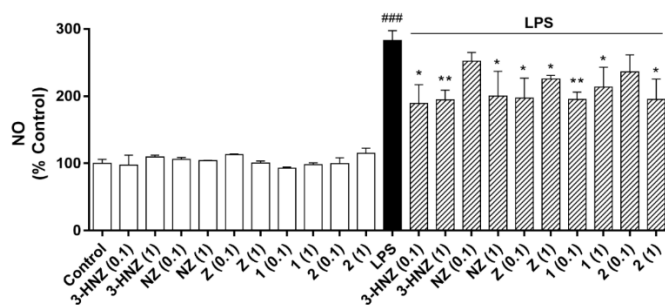
Figure 3. Effect of zoanthamines on nitric oxide (NO) production in BV-2 microglia cell line. Cells were pre-treated with 3-hydroxynorzoanthamine (3-HNZ), norzoanthamine (NZ), zoanthamine (Z), **1,** and **2** (0.1 or 1 μM) for 1 h and then stimulated with lipolysaccharide (LPS) (500 ng/mL) for 24 h. The values are presented in percentage of cells control, being the result of mean ± SEM of a minimum of three independent experiments. The cells treated only with LPS were compared to cells treated with compounds in presence of LPS by ANOVA followed by *post hoc* Dunnett's test. * $p < 0.05$ and ** $p < 0.01$, and LPS-treated cells versus control cells ### $p < 0.001$.

3. Discussion

The isolation of two 3-acetoxy derivatives of zoanthamine and norzoanthamine in *Zoanthus* cf. *pulchellus* strengthens the hypothesis that zoanthamines are markers of the genus *Zoanthus*. However, another species identified as *Zoanthus* cf. *sociatus* was found in the same area and did not present any zoanthamine derivatives [21]. Nevertheless, even if these compounds should not be considered as

taxonomic markers of the genus *Zoanthus*, they are clear and characteristic features of some species of *Zoanthus* and could facilitate a more precise classification of this group.

Interestingly, we first ran the NMR analyses of **1** in a different solvent, CD₃OD, and observed clear changes for the signals surrounding the nitrogen atom. Especially, the signals corresponding to H-11 disappeared. This observation reinforced the conclusions on zoanthamine analogues reached by the group of Norte [8]. In a highly polar and protic solvent, the opening of the lactone ring would give rise to an iminium ion at C-11 in equilibrium with its enamine base that can be trapped by exchangeable deuterium atoms provided by the protic deuterated solvent. This behavior signals the high reactivity of this family of compounds at this particular position.

Because these compounds were isolated after a purification step involving acetic acid in the eluent of the HPLC, we wanted to ascertain the presence of these compounds in the collected specimen. For this purpose, we inspected the chemical profiles obtained before any contact with acetic acid and were able to observe the masses corresponding to the new compounds **1** and **2**. These analyses rule out the possibility of a transformation during the purification process.

Finally, the activity observed for all compounds highlights the potential of zoanthamine derivatives as new ROS and NO modulators in neuronal processes, and we will continue our efforts in the study of their mode of action in neuroinflammatory related diseases.

4. Materials and Methods

4.1. General Experimental Procedures

Optical rotation measurements were obtained at the sodium D line (589.3 nm) with a 10-cm cell at 20 °C on a UniPol L1000 polarimeter (Schmidt + Haensch, Berlin, Germany). The UV measurements were obtained on a Cary 300 UV-Visible spectrophotometer (Agilent, Santa-Clara, CA, USA). NMR spectra were recorded on an Inova 500 MHz spectrometer (500 and 125 MHz for ¹H and ¹³C, respectively) (Varian, Palo Alto, CA, USA), and signals were referenced in ppm to the residual solvent signals (CDCl₃, at δ_H 7.26 and δ_C 77.16 ppm). HRESIMS data were obtained with a UHPLC-qTOF 6540 mass spectrometer (Agilent, Santa Clara, CA, USA). Purification was carried out on a HPLC equipped with a PU4087 pump (JASCO, Tokyo, Japan) and a UV4070 UV/Vis detector (JASCO, UV, Japan).

4.2. Biological Material

Specimens of *Zoanthus* cf. *pulchellus* were collected by hand on rocks of the shoreline of San Pedro located in the Santa Elena Peninsula, Ecuador. A sample with a voucher 161125SP-01 is stored at CENAIM-ESPOL (San Pedro, Santa Elena, Ecuador). This species has been previously identified using morphological and molecular data [21].

4.3. Extraction and Isolation

The freeze-dried sample of *Z.* cf. *pulchellus* (200 g) was extracted with a mixture of solvents DCM/MeOH (1:1) three times (500 mL) at room temperature. The collected extract was concentrated under reduced pressure to obtain the extract (10 g). The extract was subjected to C18 reversed-phase VLC (LiChroprep® (Merck KGaA, Darmstadt, Germany) RP-18, 40–63 μm, 1:25 ratio for the weight of C18 used, funnel of 10 cm × 10 cm) using a mixture of solvents of decreasing polarity (1) H₂O; (2) H₂O/MeOH (1:1); (3) H₂O/MeOH (1:3); (4) MeOH; (5) MeOH/DCM (3:1); (6) MeOH/DCM (1:1); and (7) DCM using 500 mL of each solvent. The aqueous-methanolic fraction F3 was purified by reversed-phase HPLC (Ultra AQ C18, 10 × 250 mm, 5 μm) using an isocratic method CH₃CN:H₂O:Acetic acid (30:70:0.1) as a mobile phase with a flow rate of 3 mL/min with detection at λ 254 nm for 20 min yielding compound **1** (52.7 mg) and the known compounds norzoanthamine (6.3 mg) [3] and zoanthamine (6.6

mg) [1] . The methanolic fraction F4 was purified by reversed-phase HPLC (Ultra AQ C18, 10×250 mm, 5 μm) using the following mobile phases: (A) CH_3CN/Acetic acid 0.1%; (B) H_2O/Acetic acid 0.1%; starting with an isocratic 0–25 min with A 22, B 78; linear gradient for 25–30 min until A 100; then isocratic for 30–60 min at a flow rate of 3 mL/min with UV detection at λ 254 nm to yield compounds **2** (12.3 mg) and the known 3-hydroxynorzoanthamine (2.7 mg) [8].

4.4. 3-Acetoxynorzoanthamine (**1**)

Amorphous yellow powder; $[\alpha]_D^{20}$ +10 (*c* 0.45, CH_3OH); UV (CH_3OH) λ_{max} (log ε) 237 (4.1) nm; ^1H NMR and ^{13}C NMR data see Table 1; HRESIMS (+) *m/z* [M + H]$^+$ 540.2956 (calc. for $C_{31}H_{42}NO_7$ 540.2956Δ + 0.0 ppm) (Spectra in the Supplementary Materials).

4.5. 3-Acetoxyzoanthamine (**2**)

Amorphous yellowish powder; $[\alpha]_D^{20}$ + 6.7 (*c* 0.12, CH_3OH); UV (CH_3OH) λ_{max} (log ε) 238 (4.0) nm; ^1H NMR and ^{13}C NMR data see Table 1; HRESIMS (+) *m/z* [M + H]$^+$ 554.3115 (calc. for $C_{32}H_{44}NO_7$ 554.3112Δ + 0.5 ppm) (Spectra in the Supplementary Materials).

4.6. Biological Assays

4.6.1. Cell Culture

The microglia BV-2 cell line was obtained from InterLab Cell Line Collection (ICLC) (Genova, Italy), number ATL03001. Cells were maintained in Roswell Park Memorial Institute Medium (RPMI) supplemented with 10% fetal bovine serum (FBS), penicillin (100 U/mL), and 100 μg/mL streptomycin at 37 °C in a humidified atmosphere of 5% CO_2 and 95% air. Cells were dissociated twice a week using 0.05% trypsin/EDTA.

4.6.2. Cell Viability

The 3-(4,5-dimethyl thiazol-2-yl)-2,5-diphenyl tetrazolium bromide (MTT) assay was used to analyzed cell viability as previously described [24]. Briefly, the microglia BV-2 cell line was grown in a 96-well plate at a density of 4×10^4 cells per well. Cells were exposed to different compounds concentration (0.001, 0.01, 0.1, 1 and 10 μM) for 24 h. Then, cells were rinsed and incubated with MTT (500 μg/mL) diluted in a saline buffer for 1 h at 37 °C. The resulting formazan crystals were dissolved with 5% sodium dodecyl sulfate, (SDS) and the absorbance values were obtained using a spectrophotometer plate reader (595 nm). Saponin was used for cellular death control and its absorbance was substrate from the other data.

4.6.3. Measurement of Intracellular ROS Production

The intracellular ROS levels in microglia activation were performed using 7′,2′-dichlorofluorescein diacetate (DCFH-DA), as previously described [25]. Cells were pre-treated with different compounds concentration (0.001, 0.01, 0.1, 1, and 10 μM) 1 h prior to the stimulation with LPS (500 ng/mL) for 24 h. Afterwards, cells were rinsed twice with saline solution and incubated 1 h at 37 °C with 20 μM DCFH-DA. Then, cells were washed and kept in saline solution for 30 min at 37 °C. Intracellular production of ROS was measured by fluorescence detection of dichlorofluorescein (DCF) as the oxidized product of DCFH-DA on a spectrophotometer plate reader (495 nm excitation and 527 nm emission).

4.6.4. NO Determination

The NO concentration in the culture media was established by measuring nitrite formed by the oxidation of NO, using the Griess reagent kit, according to manufacturer instructions. The detection limit of this method is 1 μM. Briefly, microglia cells were seeded in a 12-well plate at a density of 1×10^6 cells per well and pre-incubated with compounds (0.1 and 1 μM) for 1 h and then stimulated with LPS (500 ng/mL) for 24 h. Thereafter, the following were mixed in a microplate: 150 μL of cells supernatant, 130 μL of deionized water, and 20 μL of Griess Reagent, which was incubated for 30 min at room temperature. The absorbance was measured on a spectrophotometer plate reader at a wavelength of 548 nm.

4.6.5. Statistical Analysis

Results were expressed as mean ± SEM of a minimum of three experiments, repeated twice or three times. Comparisons were performed using Student's *t*-test or one-way ANOVA with Dunnett's *post hoc* analysis. *p* values <0.05 were considered statistically significant.

References

1. Rao, C.B.; Anjaneyula, A.S.R.; Sarma, S.S.; Venkatateswarlu, Y.; Chen, M.; Clardy, J.; Rosser, R.; Faulkner, J. Zoanthamine: A novel alkaloid from a marine zoanthid. *J. Am. Chem. Soc.* **1984**, *106*, 7984–7985, doi:10.1021/ja00337a062.
2. Rao, C.B.; Anjaneyulu, A.S.R.; Sarma, N.S.; Venkateswarlu, Y.; Rosser, R.M.; Faulkner, J. Alkaloids from a marine zoanthid. *J. Org. Chem.* **1985**, *50*, 3757–3760, doi:10.1021/jo00220a016.
3. Fukuzawa, S.; Hayashi, Y.; Uemura, D.; Nagatsu, A.; Yamada, K.; Ijuin, Y. The isolation and structures of five new alkaloids, norzoanthamine, oxyzoanthamine, norzoanthamine, cyclozoanthamine and epinorzoanthamine. *Heterocycl. Commun.* **1995**, *1*, 207–214, doi:10.1515/HC.1995.1.2-3.207.

4. Atta-ur-Rahman; Alvi, K.A.; Abbas, S.A.; Choudhary, M.I.; Clardy, J. Zoanthaminone, a new alkaloid from a marine zoanthid. *Tetrahedron Lett.* **1989**, *30*, 6825–6828, doi:10.1016/S0040-4039(01)93362-3.

5. Cen-Pacheco, F.; Norte, M.; Fernández, J.J.; Daranas, A.H. Zoaramine, a zoanthamine-like alkaloid with a new skeleton. *Org. Lett.* **2014**, *16*, 2880–2883, doi:10.1021/ol500860v.

6. Cheng, Y.-B.; Lo, I.-W.; Shyur, L.-F.; Yang, C.-C.; Hsu, Y.-M.; Su, J.-H.; Lu, M.-C.; Chiou, S.-F.; Lan, C.-C.; Wu, Y.-C.; et al. New alkaloids from Formosan zoanthid *Zoanthus kuroshio*. *Tetrahedron* **2015**, *71*, 8001–8006, doi:10.1016/j.tet.2015.09.023.

7. Daranas, A.H.; Fernández, J.J.; Gavin, J.A.; Norte, M. Epioxyzoanthamine, a new zoanthamine-type alkaloid and the unusual deuterium exchange in this series. *Tetrahedron* **1998**, *54*, 7891–7896, doi:10.1016/S0040-4020(98)00423-2.

8. Daranas, A.H.; Fernandez, J.J.; Gavin, J.A.; Norte, M. New alkaloids from a marine zoanthid. *Tetrahedron* **1999**, *55*, 5539–5546, doi:10.1016/s0040-4020(99)00198-2.

9. Behenna, D.C.; Stockdill, J.L.; Stoltz, B.M. The biology and chemistry of the zoanthamine alkaloids. *Angew. Chem. Int. Ed.* **2008**, *47*, 2365–2386, doi:10.1002/anie.200703172.

10. Hsu, Y.-M.; Chang, F.-R.; Lo, I.W.; Lai, K.-H.; El-Shazly, M.; Wu, T.-Y.; Du, Y.-C.; Hwang, T.-L.; Cheng, Y.-B.; Wu, Y.-C. Zoanthamine-type alkaloids from the zoanthid *Zoanthus kuroshio* collected in Taiwan and their effects on inflammation. *J. Nat. Prod.* **2016**, *79*, 2674–2680, doi:10.1021/acs.jnatprod.6b00625.

11. Miyashita, M.; Sasaki, M.; Hattori, I.; Sakai, M.; Tanino, K. Total synthesis of norzoanthamine. *Science* **2004**, *305*, 495–499, doi:10.1126/science.1098851.

12. Takahashi, Y.; Yoshimura, F.; Tanino, K.; Miyashita, M. Total synthesis of zoanthenol. *Angew. Chem. Int. Ed.* **2009**, *48*, 8905–8908, doi:10.1002/anie.200904537.

13. Yoshimura, F.; Sasaki, M.; Hattori, I.; Komatsu, K.; Sakai, M.; Tanino, K.; Miyashita, M. Synthetic studies of the zoanthamine alkaloids: The total syntheses of norzoanthamine and zoanthamine. *Chem. Eur. J.* **2009**, *15*, 6626–6644, doi:10.1002/chem.200900310.

14. Yoshimura, F.; Tanino, K.; Miyashita, M. Total synthesis of zoanthamine alkaloids. *Acc. Chem. Res.* **2012**, *45*, 746–755, doi:10.1021/ar200267a.

15. Fischer, D.; Nguyen, T.X.; Trzoss, L.; Dakanali, M.; Theodorakis, E.A. Intramolecular cyclization strategies toward the synthesis of zoanthamine alkaloids. *Tetrahedron Lett.* **2011**, *52*, 4920–4923, doi:10.1016/j.tetlet.2011.07.054.

16. Nakajima, T.; Yamashita, D.; Suzuki, K.; Nakazaki, A.; Suzuki, T.; Kobayashi, S. Different modes of cyclization in zoanthamine alkaloid system, bisaminal versus spiroketal formation. *Org. Lett.* **2011**, *13*, 2980–2983, doi:10.1021/ol200486c.

17. Villar, R.M.; Gil-Longo, J.; Daranas, A.H.; Souto, M.L.; Fernández, J.J.; Peixinho, S.; Barral, M.A.; Santafé, G.; Rodríguez, J.; Jiménez, C. Evaluation of the effect of several zoanthamine-type alkaloids on the aggregation of human platelets. *Biorg. Med. Chem.* **2003**, *11*, 2301–2306, doi:10.1016/S0968-0896(03)00107-X.

18. Genji, T.; Fukuzawa, S.; Tachibana, K. Distribution and possible function of the marine alkaloid, norzoanthamine, in the zoanthid *Zoanthus* sp. using MALDI imaging mass spectrometry. *Mar. Biotechnol.* **2010**, 81–87, doi:10.1007/s10126-009-9202-5.

19. Guillen, P.O.; Calabro, K.; Jaramillo, K.B.; Dominguez, C.; Genta-Jouve, G.; Rodriguez, J.; Thomas, O.P. Ecdysonelactones, ecdysteroids from the Tropical Eastern Pacific zoantharian *Antipathozoanthus hickmani*. *Mar. Drugs* **2018**, *16*, 58, doi:10.3390/md16020058.

20. Guillen, P.O.; Jaramillo, K.B.; Genta-Jouve, G.; Sinniger, F.; Rodriguez, J.; Thomas, O.P. Terrazoanthines, 2-aminoimidazole alkaloids from the Tropical Eastern Pacific zoantharian *Terrazoanthus onoi*. *Org. Lett.* **2017**, *19*, 1558–1561, doi:10.1021/acs.orglett.7b00369.

21. Jaramillo, K.B.; Reverter, M.; Guillen, P.O.; McCormack, G.; Rodriguez, J.; Sinniger, F.; Thomas, O.P. Assessing the zoantharian diversity of the Tropical Eastern Pacific through an integrative approach. *Sci. Rep.* **2018**, *8*, 7138, doi:10.1038/s41598-018-25086-4.

22. Kuramoto, M.; Hayashi, K.; Fujitani, Y.; Yamaguchi, K.; Tsuji, T.; Yamada, K.; Ijuin, Y.; Uemura, D. Absolute configuration of norzoanthamine, a promising candidate for an osteoporotic drug. *Tetrahedron Lett.* **1997**, *38*, 5683–5686, doi:10.1016/S0040-4039(97)01238-0.

23. Dumont, M.; Beal, M.F. Neuroprotective strategies involving ROS in Alzheimer disease. *Free Radic. Biol. Med.* **2011**, *51*, 1014–1026, doi:10.1016/j.freeradbiomed.2010.11.026.

24. Sanchez, J.A.; Alfonso, A.; Leiros, M.; Alonso, E.; Rateb, M.E.; Jaspars, M.; Houssen, W.E.; Ebel, R.; Tabudravu, J.; Botana, L.M. Identification of *Spongionella* compounds as cyclosporine A mimics. *Pharmacol. Res.* **2016**, *107*, 407–414, doi:10.1016/j.phrs.2016.03.029.

25. Leiros, M.; Alonso, E.; Rateb, M.E.; Houssen, W.E.; Ebel, R.; Jaspars, M.; Alfonso, A.; Botana, L.M. Gracilins: Spongionella-derived promising compounds for Alzheimer disease. *Neuropharmacology* **2015**, *93*, 285–293, doi:10.1016/j.neuropharm.2015.02.015.

4 Ecdysonelactones, Ecdysteroids from the Tropical Eastern Pacific Zoantharian *Antipathozoanthus hickmani*

Antipathozoanthus hickmani (© Karla B. Jaramillo)

Article

Ecdysonelactones, Ecdysteroids from the Tropical Eastern Pacific Zoantharian *Antipathozoanthus hickmani*

Paul O. Guillen [1,2]**, Kevin Calabro** [2]**, Karla B. Jaramillo** [1,3]**, Cristobal Dominguez** [1]**, Grégory Genta-Jouve** [4]**, Jenny Rodriguez** [1,]***and Olivier P. Thomas** [2,]*

[1]   Escuela Superior Politécnica del Litoral, ESPOL, Centro Nacional de Acuacultura e Investigaciones Marinas, CENAIM, Campus Gustavo Galindo km. 30.5 vía Perimetral, P.O. Box 09-01-5863, Guayaquil Ecuador; P.GUILLENMENA1@nuigalway.ie (P.O.G.); K.JARAMILLOAGUILAR1@nuigalway.ie (K.B.J.); cdoming@espol.edu.ec (C.D.)

[2]   Marine Biodiscovery Laboratory, School of Chemistry and Ryan Institute, National University of Ireland, Galway (NUI Galway), University Road, H91 TK33 Galway, Ireland; kevin.calabro@nuigalway.ie (KC)

[3]   School of Zoology and Ryan Institute, National University of Ireland Galway, University Road, H91 TK33 Galway, Ireland

[4]   Laboratoire de Chimie-Toxicologie Analytique et Cellulaire (C-TAC) UMR CNRS 8638 COMETE, Université Paris Descartes, 4 avenue de l'observatoire, 75006 Paris, France; gregory.genta-jouve@parisdescartes.fr

*   Correspondance: jenrodri@espol.edu.ec (J.R.); olivier.thomas@nuigalway.ie Tel.: ++353 (0)91493563 (O.P.T.)

Abstract: Despite a large occurrence, especially over the Pacific Ocean, the chemical diversity of marine invertebrates belonging to the order Zoantharia is largely underexplored. For the two species of the genus *Antipathozoanthus* no chemical study has been reported so far. The first chemical investigation of *Antipathozoanthus hickmani* collected at the Marine Protected Area "El Pelado", Santa Elena, Ecuador, led to the isolation of four new ecdysteroid derivatives named ecdysonelactones. The structures of ecdysonelactones A–D (**1–4**) were determined based on their spectroscopy data, including 1D and 2D NMR and HRMS. The four compounds of this family of ecdysteroids feature an unprecedented γ-lactone fused at the C-2/C-3 position of ring A. These derivatives exhibited neither antimicrobial nor cytotoxic activities.

Keywords: ecdysteroids; ecdysonelactones; γ-lactone; Zoantharia; relative configuration; Cnidaria

1. Introduction

Zoantharians (Cnidaria:Anthozoa:Hexacorallia) are sessile marine invertebrates widely distributed in all oceans, and they can represent a high substrate cover in some shallow tropical coral reefs and deep sea environments [1,2]. While marine sponges have been deeply studied in the search for bioactive chemical entities, zoantharians are also known to biosynthesize a wide array of natural products with unique structural features and interesting bioactivity, such as zoanthamines [3-5]. Other families of natural products have also been isolated from different species of zoantharians, such as alkaloids [3,6-8] including zoanthoxanthins [9,10] and parazoanthines [11] isolated from the Mediterranean zoantharian *Parazoanthus axinellae*, prostaglandins such as PGA₂ [12], fatty acids or palytoxin [13,14], one of the most toxic compounds, as well as ecdysteroids [15,16].

Studies on the diversity of marine invertebrates present off the Ecuadorian coast have shown that zoantharians are one of the most representative marine invertebrates inhabiting this maritime area [17-19]. The first records of zoantharian species in this maritime ecoregion were from the Galapagos Islands, where four new species and one new genus, *Terrazoanthus*, have been described. Within the

context of a national project aiming at the description of the biological and chemical diversity of marine invertebrates from the marine protected area El Pelado of the Peninsula of Santa Elena, Ecuador, we noticed the presence of several species of zoantharians, representing a high substrate cover. The first inspection of the chemical diversity of one zoantharian of this ecoregion named *Terrazoanthus patagonichus* (formerly known as *T. onoi*) was very promising and revealed a new family of 2-aminoimidazole alkaloids named terrazoanthines [20]. A second species, commonly found in this area, was identified as *Antipathozoanthus hickmani*. The genus *Antipathozoanthus* belongs to the family Parazoanthidae and is composed by only two species so far: *A. macaronesicus* and *A. hickmani*, which are only found to be associated with black corals [21,22]. *Antipathozoanthus hickmani* was first recorded in the Tropical Eastern Pacific around the Galapagos Islands and later in Machalilla National Park, Ecuador, where this species was found as an epibiont of the antipatharian *Antiphates galapagensis* [17,19]. Interestingly, no studies on the chemical diversity of both species have been recorded so far, and we therefore decided to undertake the first chemical investigation of *A. hickmani*.

Herein, we report the isolation and structure elucidation of a new family of ecdysteroids named ecdysonelactones A–D (**1–4**), featuring for the first time a five-membered ring lactone moiety fused at the C-2 and C-3 positions of ring A (Figure 1). Three known compounds, including a lysine derivative first isolated from the marine sponge *Axinyssa terpnis* [237] and two ecdysteroids 20-hydroxyecdysone [16] and polypodine B [24,25], were also isolated from this zoantharian.

Ecdysonelactone	R^1	R^2	R^3
A (**1**)	OH	H	OH
B (**2**)	OH	H	H
C (**3**)	H	H	OH
D (**4**)	H	OH	H
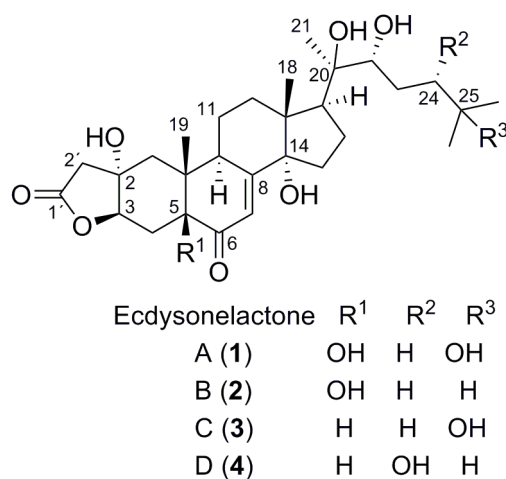
Figure 1. Structures of ecdysonelactones A–D (**1–4**) from *Antipathozoanthus hickmani*.

2. Results and Discussion

The frozen organism was first lyophilized, and the freeze-dried material was extracted with a mixture of solvents CH_3OH/CH_2Cl_2 (*v/v*; 1:1) under sonication. The extract was first subjected to fractionation through reversed phase C18 Vacuum Liquid Chromatography (VLC) with solvents of decreasing polarity from H_2O to CH_3OH, until CH_2Cl_2 was reached. The methanolic fractions disclosed some interesting chemical profiles by UHPLC-DAD-ELSD and they were subjected to semipreparative Reversed Phase (RP) HPLC using a C18 column, yielding pure compounds ecdysonelactones A–D (**1–4**) along with the known compounds 20-hydroxyecdysone, polypodine B, and a lysine derivative.

Compound **1** was isolated as a white powder and (+)-HRESIMS analysis revealed a major peak at *m/z* 537.3070 [M + H]$^+$, consistent with the molecular formula $C_{29}H_{44}O_9$. The fragmentation pattern of the molecule indicated the loss of at least three molecules of water, suggesting the presence of three highly reactive alcohols in the molecule. NMR data were recorded in CD_3OD even if most of the literature data are reported in C_5D_5N. Indeed, compounds were perfectly soluble in CD_3OD with only rare overlaps of the signals with residual peaks of the solvents that did not prevent the structure elucidation of the compounds. The ^1H NMR, ^{13}C NMR, and HSQC analyses revealed one ester function,

one α,β-unsaturated ketone, five oxygenated quaternary carbons, two oxygenated methines, three quaternary carbons, and five characteristic steroidal methyl signals. The ecdysteroid family was inferred from the signal at δ_H 5.88 (d, J = 2.5 Hz, 1H, H-7), corresponding to a trisubstituted olefinic proton. The H-7/C-5, C-9, and C-14 HMBC correlations confirmed the 7-en-6-one tetracyclic ring system and therefore the ecdysteroid family. Compared with other usual ecdysteroids found in zoantharians such as ecdysone, **1** lacked the oxymethine in position C-2, while the ^{1}H NMR spectrum revealed a clear AB system at δ_H 2.74 (d, J = 17.0 Hz, H-2′a) and δ_H 2.56 (d, J = 17.0 Hz, H-2′b) (Table 1). The structure elucidation started with HMBC correlations from H$_3$-19, allowing the assignment of the signals at C-1. Analysis of the HMBC spectrum revealed key H-2′/C-1, C-2, C-3 correlations showing that this methylene was directly linked to the A ring at C-2. The presence of a tertiary alcohol at C-2 was further proposed based on the signal at δ_C 74.2 (qC, C-2). Moreover, the HMBC spectrum revealed another key H-2′/C-1′ correlation with C-1′ corresponding to an ester function. Despite the lack of any other correlation with the latter carbonyl group, closure into a lactone at C-3 was suggested by the deshielding of the proton and carbon signals at the C-3 position of the A ring. This assumption was in accordance with the molecular formula of **1**. The presence of a hydroxy group at C-5 was then evidenced by HMBC correlations starting from H$_3$-19, especially with another oxygenated quaternary carbon at δ_C 77.8 (qC, C-5). This oxidation pattern at C-5 is commonly found in ecdysteroids but more rarely in those isolated from zoantharians [139]. Focusing now on the side-chain of the steroid, the presence of a tertiary alcohol at C-20 and a secondary alcohol at C-22 was confirmed by key H$_3$-21/C-22 and C-20 HMBC correlations. Finally, the presence of two terminal methyls and a tertiary alcohol at C-25 was demonstrated by additional key H$_3$-26/C-24, C-25 and H$_3$-27/C-24, C-25 HMBC correlations and a complete set of COSY correlations starting from H-22.

Table 1. NMR spectroscopic data for ecdysonelactones A–D (**1–4**) in CD$_3$OD (600 MHz for ^{1}H NMR data and 150 MHz for ^{13}C NMR data).

No.	1		2		3		4	
	δ_H, Mult. (J in Hz)	δ_C	δ_H, Mult. (J in Hz)	δ_C	δ_H, Mult. (J in Hz)	δ_C	δ_H, Mult. (J in Hz)	δ_C
1a	1.87, d (15.0)	38.4	1.85, d (15.0)	38.4	2.11, m	41.9	2.13, m	41.9
1b	1.71, d (15.0)		1.70, d (15.0)		1.09, d (15.0)		1.10, d (15.0)	
2	-	74.2	-	74.2	-	74.0	-	74.0
3	4.50, br d (4.5)	82.5	4.49, br d (4.5)	82.5	4.40, br s	82.0	4.40, br s	82.1
4a	2.35, dd (16.0, 4.5)	31.9	2.35, m	31.9	2.13, m	25.1	2.11, m	25.8
4b	1.91, m		1.92, m		1.93, m		1.93, m	
5	-	77.8	-	77.8	2.10, m	52.1	2.11, m	52.1
6	-	203.9	-	203.9	-	205.3	-	203.7
7	5.88, d (2.5)	120.1	5.86, d (2.5)	120.1	5.83, d (2.0)	121.6	5.83, d (2.0)	121.6
8	-	169.2		169.2	-	169.3	-	169.2
9	3.91, m	39.2	3.90, m	39.2	3.80, ddd (11.5, 6.5, 2.0)	35.7	3.80, br dd (11.5, 6.5)	35.7
10	-	42.4	-	42.4	-	37.0	-	37.0
11a	1.93, m	22.3	1.92, m	22.3	1.93, m	21.4	1.93, m	21.4
11b	1.68, m		1.68, m		1.65, m		1.64, m	
12a	2.14, td (13.0, 4.5)	32.5	2.12, td (13.0, 4.5)	32.6	2.15, m	32.5	2.14, m	32.5

12b	1.83, td (13.0, 4.5)		1.81, m		1.84, m		1.84, dd (13.5, 3.5)	
13	-	48.7	-	48.6	-	48.8	-	48.7
14	-	84.9	-	84.9	-	85.1	-	85.0
15a	1.97	31.9	1.94, m	31.9	1.98, m	31.9	1.93, m	31.9
15b	1.59, t (10.0)		1.59, m		1.59, t (10.0)		1.61, m	
16a	1.98, m	21.5	1.97, m	21.5	1.98, m	21.5	1.99, m	21.5
16b	1.73, m		1.69, m		1.73, m		1.71, m	
17	2.39, m	50.4	2.35, m	50.4	2.39, t (8.6)	50.5	2.34, m	50.4
18	0.90, s	18.1	0.88, s	18.1	0.89, s	18.1	0.89, s	18.1
19	0.86, s	16.7	0.85, s	16.7	0.93, s	24.1	0.93, s	24.1
20	-	77.9	-	77.9	-	77.9	-	77.8
21	1.19, s	21.0	1.16, s	21.0	1.19, s	21.0	1.21, s	20.9
22	3.32, m	78.4	3.33, m	78.0	3.33, m	78.4	3.59, m	77.6
23a	1.67, m	27.3	1.56, m	30.5	1.66, m	27.3	1.71, m	35.7
23b	1.28, m		1.21, m		1.28, m		1.34, m	
24a	1.80, m	42.4	1.46, m	37.7	1.80, td (12.5, 4.5)	42.4	3.59, m	77.5
24b	1.42, td (12.5, 4.5)		1.22, m		1.43, td (12.5, 4.5)			
25		71.3	1.56, m	29.2		71.3	1.69, m	34.1
26	1.19, s	28.9	0.91, d (6.5)	23.4	1.19, s	28.9	0.95, d (7.0)	19.4
27	1.20, s	29.7	0.90, d (6.5)	22.8	1.20, s	29.7	0.91, d (7.0)	17.0
1′		176.3		176.2		176.1		176.0
2′a	2.74, d (17.0)	47.5	2.72, d (17.0)	47.5	2.71, d (16.5)	47.1	2.70, d (16.5)	47.4
2′b	2.56, d (17.0)		2.56, d (17.0)		2.50, d (16.5)		2.49, d (16.5)	

For the relative configuration of the side-chain, the ^{1}H and ^{13}C NMR chemical shifts of the signals from C-20 until C-27 for **1** were absolutely identical to those of 4-dehydroecdysterone reported by the group of Molinski, especially the signals and coupling constants [27]. For this compound, NMR data were also recorded in CD_3OD, which allows a clean comparison, and the structure of the side-chain is therefore identical to the 17S^*, 20R^*, 22R^* relative configurations for this part of the molecule. The *trans* C/D junction corresponding to 13R^*, 14S^* was also confirmed by the comparison of NMR signals with the same compound (Figure 1).

The relative configuration of the gamma lactone ring fused on the A ring then had to be assessed. First, the signal H-3 appeared as a doublet with $^3J_{H3-H4}$ 4.5 Hz, which was only consistent with a chair conformation for ring A where the methyl H_3-19 is placed in an equatorial position, like that already found for ecdysteroids of this type [28]. The oxygen at C-3 must then be β orientated and of the 3R^*configuration. Indeed, for a α orientation of the oxygen at C-3, the proton H-3 would be placed in an axial position with a coupling constant of at least 10 Hz (See Supplementary Materials). For the relative configuration at the quaternary carbon C-2, we relied on the nOes between the different protons of the bicycle. The epimer with a *cis*-junction between the lactone and ring A was in accordance with the observed nOes and the distances measured (Figure 2), especially for the nOes H-9/H-4a, H_3-19/H-1a, H-2′b/H-1a, and H-1b and H-3/H-2′a. All NMR data are therefore in agreement with this

conformation of the 2S^*, 3R^*, 5S^*, 9R^*, 10R^* epimer. Another confirmation came from the comparison between the chemical shifts of the four possible stereoisomers at C-2 and C-3 as well as literature data of non ecdysteroid analogues [29]. We did not investigate the absolute configuration of this molecule as, for all ecdysteroids described so far, all have the usual β orientation for the methyls H$_3$-18 and H$_3$-19 and therefore we propose the same absolute configuration as determined for all compounds of this large family.
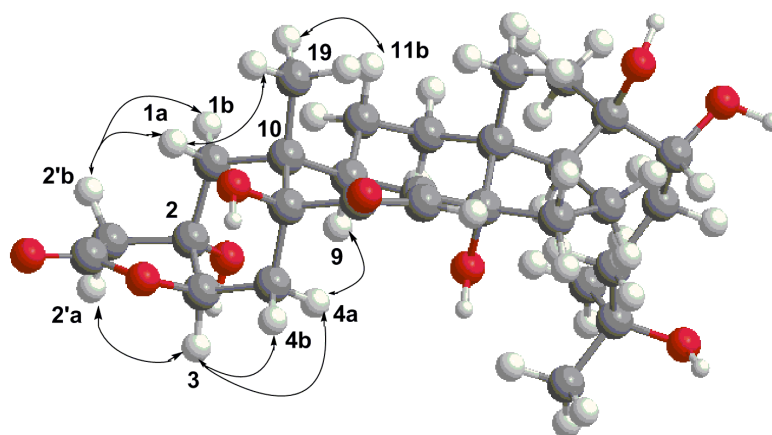
Figure 2. Minimum energy conformer for the *cis* epimer of **1**, where nOes are shown with arrows.

Compound **2** was isolated as a white powder and its (+)-HRESIMS analysis suggested the molecular formula C$_{29}$H$_{44}$O$_8$ with *m/z* 521.3104 [M + H]$^+$. The fragmentation pattern evidenced the loss of three water molecules, and **2** was therefore thought to be a deoxygenated analogue of **1**. The ^{13}C NMR spectrum of **2** indicated the presence of only six saturated and oxygenated carbons with a lack of one oxygenated quaternary carbon compared to **1**. The absence of the tertiary alcohol at C-25 was evidenced in the ^{1}H NMR spectrum where the three singlets at δ_H 1.19 (6H, H$_3$-21, H$_3$-26) and 1.20 (3H, H$_3$-27) in **1** were replaced by one remaining singlet at δ_H 1.19 (3H, H$_3$-21) and two diastereotopic methyls with doublets at δ_H 0.90 (3H, H$_3$-26) and 0.91 (3H, H$_3$-27). The COSY spectrum confirmed the scalar coupling of these signals with a methine at C-25. Apart from these changes, all other signals in the ^{1}H and ^{13}C NMR spectra were like those of **1**, and we thus concluded that **2** is the C-25 deoxy analogue of **1**. The similarities between the ^{1}H and ^{13}C NMR data of **1** and **2** for C-20, C-21, and C-22 confirmed the same relative configuration at C-20 and C-22.

Compound **3** was isolated as a white powder and the molecular formula C$_{29}$H$_{44}$O$_8$ was determined by (+)-HRESIMS with *m/z* 521.3107 [M + H]$^+$. This compound is an isomer of **2**. The side-chain of **3** was found to be identical to that of **1**, as the same pattern was observed for the ^{1}H NMR signals of the side-chain methyls. Therefore, and unlike **2**, **3** contains a tertiary alcohol at C-25. Because the molecular formula was found to be identical to that of **2**, we expected the loss of an oxygen in the polycyclic core. The absence of an oxygen was located at position C-5 due to the appearance of a new signal in the HSQC spectrum at δ_H 2.10 (m, 1H, H-5) and δ_C 52.1 (CH, C-5). Deoxygenation at this position is particularly common in ecdysteroids, especially in 20-hydroxyecdysone analogues already found in the zoantharian *Parazoanthus axinellae*, for example [238]. The location of this methine at C-5 was easily confirmed by a key H$_3$-19/C-5 HMBC correlation. Due to the overlap of the ^{1}H NMR signal H-5 with other signals, it was impossible to use nOe or coupling constant to assess the relative configuration at C-5. Gratifyingly, the presence of the same key H-4a/H-9 nOe as that found in **1** allowed us to conclude that the same *cis* junction existed between rings A and B. Indeed, this nOe would not be consistent with a *trans* decaline configuration between rings A and B. This assumption was further confirmed by very similar chemical shifts between the corresponding signals of **3** and those of analogues in the literature [27]. A *cis* junction between rings A and B seems to be a common feature of most ecdysteroids, an epimerization likely occurring because of the presence of the ketone at C-6. Identical chemical shifts in

^{1}H and ^{13}C NMR signals with those of **1** indicated the same relative configurations for the side-chain. Compound **3** is therefore the deoxy analogue of **1** at C-5.

Compound **4** was isolated as a white powder and its molecular formula $C_{29}H_{45}O_8$ was determined by HRESIMS with *m/z* 521.3104 [M + H]+. This compound is therefore a third isomer of **2** and **3**. While the signals corresponding to the polycyclic part of the ecdysteroid were identical to those of **3**, major differences occurred for the signals of the side-chain. Indeed, like in **1** and **3**, the tertiary alcohol was not present at C-25 because the methyls H3-26 and H3-27 appeared as two diastereotopic methyls, as they did in **2**. The HSQC spectrum revealed changes for H-22 and another oxygenated methine overlapping with H-22 at δ_H 3.59 (m, 2H, H-22, and H-24). Based on key H3-21/C-22 and H3-26 and 27/C-24 HMBC correlations, we concluded that a hydroxylation occurred at C-24. To establish the relative configuration of the hydroxyl at C-24, we relied on literature data for pterosterone and its related epimer at C-24, even if those data were recorded in pyridine-*d5* [28]. Comparison of the ^{13}C NMR data of the signals corresponding to the side-chain of **1** recorded in CD3OD with those of abutasterone containing the same side-chain but recorded in C_5D_5N showed a maximum difference of 1.5 ppm [31]. While chemical shifts of δ_C 76.7 (C-22) and 77.5 (C-24) were observed in C_5D_5N for pterosterone with a 24*S* configuration, values of δ_C 73.4 (C-22) and 73.5 (C-24) were recorded for its epimer at C-24, 24-epipterosterone (24*R*) in the same solvent [28,32]. In the case of compound **4**, both carbons resonate at δ_C 77.6 (C-22) and 77.5 (C-24) in CD3OD, in total accordance with the values obtained for pterosterone. Because the change of solvent does not seem to strongly affect the chemical shifts of the ^{13}C NMR signals, we assumed the same 24*S* configuration as pterosterone for compound **4**.

Ecdysteroids are known to be a widespread family of natural products produced by plants and arthropods, where they are known to play the role of molting hormones for arthropods, for example [33,34]. They are also widely found in some marine invertebrates and may be considered as chemomarkers of zoantharians, even if their ecological role is not known in this case. The first chemical investigation of a species of the genus *Antipathozoanthus* led to the discovery of a new family of ecdysteroids featuring an unprecedented γ-lactone ring fused between the positions C-2/C-3 of the A ring. The presence of a lactone ring in ecdysteroids has been found in compounds like cyasterone [35], ajugalactone [36], or even the very rare C-29 ecdysteroid named reptanslactone [37] with five- and six-membered ring lactones only present on the side chain. The formation of the five-membered ring lactone between the C-2 and C-3 positions of ring A in ecdysonelactones can be explained by the presence of very reactive secondary alcohols at C-2 and C-3 [38,39]. To explain the formation of the lactones, ecdysteroids from zoantharians seem to be prone to acetylation at position OH-2 or OH-3. Acetylation at OH-3 would lead to an acetylated product at this position that could undergo a cyclization into a γ-lactone on a ketone at C-2 (Scheme 1). Oxidation at positions C-2 or C-3 have already been observed [40], and such a nucleophilic addition of a methyl ester on an adjacent ketone was demonstrated synthetically in strongly basic conditions with a derivative of taxol [41]. An enzyme could catalyze the addition reaction in the case of this natural product and impose the observed stereochemistry. The presence of this enzyme seems restricted to the species *A. hickmani* among all studied zoantharians and other living organisms of the terrestrial world. Interestingly, only the *cis* fused product was formed through cyclization with the A ring, giving rise to the OH-2 on the α side of the polycyclic ring.
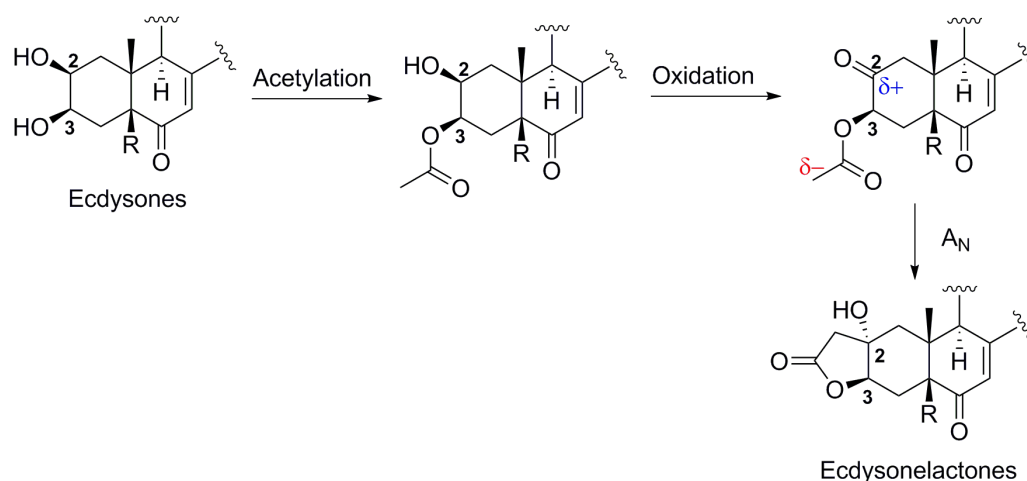
Scheme 1. Proposed biosynthetic conversion of ecdysones into ecdysonelactones.

Ecdysonelactones A–D (**1–4**) were tested for antibacterial activity against Gram-positive (Methicillin-resistant *Staphylococcus aureus* MRSA, *Staphylococcus aureus*) and Gram-negative bacteria (*Acinetobacter baumannii*, *Escherichia coli*, *Klebsiella pneumoniae*); antifungal activity against *Candida albicans*; and cytotoxicity against MCF-7 breast cancer, A2058 melanoma, HT-29 colon cancer, A549 lung cancer, and HepG2 hepatic cancer cell lines [42]. Despite the new lactone function fused on the A ring of the ecdysteroid, ecdysonelactones, like other ecdysteroids, did not exhibit significant antimicrobial or cytotoxic activities.

3. Materials and Methods

3.1. General Experimental Procedures

UV measurements were obtained by the extraction of the Diode Array Detector (DAD) signal of the Ultra-High Pressure Liquid Chromatography (UHPLC) Dionex Ultimate 3000 (Thermo Scientific, Waltham, MA, USA). Optical rotation measurements were obtained at the sodium D line (589.3 nm) with a 10-cm cell at 20 °C on a UniPol L1000 polarimeter (Schmidt + Haensch, Berlin, Germany). NMR spectra were acquired on an Agilent 600 MHz spectrometer equipped with a cryoprobe with pulse field gradient, and signals were referenced in ppm to the residual solvent signals (CD$_3$OD, at δ_H 3.31 and δ_C 49.0). HRESIMS data were obtained with a UHR-qTOF Agilent 6540 mass spectrometer. Purification was carried out on a JASCO HPLC equipped with a PU4087 pump and a UV4070 UV/Vis detector.

3.2. Biological Material

The specimen identified as *Antipathozoanthus hickmani* (73 g dry weight) was collected by SCUBA at 24 m at the Marine Protected Area El Pelado (La Pared) of the Peninsula of Santa Elena, Ecuador. A voucher (150924EP01-02) of the sample is held at CENAIM-ESPOL (San Pedro, Santa Elena, Ecuador) (See Supplementary Materials).

3.3. Extraction and Isolation

The freeze-dried sample (73.8 g) was extracted at room temperature with a mixture of solvents DCM/MeOH (1:1) three times (500 mL); each time with sonication and gravity filtration. The organic solvent was removed under pressure to obtain an extract (4.7 g). The extract was subjected to C18 reversed phase vacuum liquid chromatography (LiChroprep® RP-18, 40–63 μm) using a mixture of solvents of decreasing polarity (1). H$_2$O, (2). H$_2$O/MeOH (1:1), (3). H$_2$O/MeOH (1:3), (4). MeOH, (5).

MeOH/DCM (3:1), (6). MeOH/DCM (1:1), and (7). DCM (using 500 mL of each solvent). Fractions 3 and 4 were purified by semi-preparative RP-HPLC with a C18 column (Restek, 10 × 250 mm, 5 μm), using the following elution steps with A CH$_3$CN/acetic Acid 0.1%, B H$_2$O/acetic acid 0.1% as mobile phases; isocratic for 0–20 min with A 22, B 78; linear gradient for 20–35 min until A 60, B 40; then isocratic for 35–45 min at a flow rate of 3.5 mL/min and UV detection at λ 254 nm for 50 min of acquisition time. These purifications yielded pure compounds; ecdysonelactone A (**1**, 0.9 mg), B (**2**, 1 mg), C (**3**, 0.7 mg), and D (**4**, 3 mg), and three known compounds; a lysine derivative (14.9 mg) [237], 20-hydroxyecdysone (1.3 mg) [239], and polypodine B (2.2 mg) [240].

3.4. Compound Characterization

3.4.1. Ecdysonelactone A

1: White, amorphous solid; $[\alpha]_D^{20}$ + 22 (*c* 0.1, CH$_3$OH); UV (DAD) λ_{max} 248 nm; ^{1}H NMR and ^{13}C NMR data see Table 1; HRESIMS (+) *m/z* 537.3070 [M + H]$^+$ (537.3058 calcd. for C$_{29}$H$_{45}$O$_9$, Δ +2.2 ppm) and fragments 519.2963 [M + H–H$_2$O]$^+$ (519.2952 calcd. for C$_{29}$H$_{43}$O$_8$); 501.2853 [M + H–2H$_2$O]$^+$ (501.2847 calcd. for C$_{29}$H$_{41}$O$_7$); 483.2749 [M + H–3H$_2$O]$^+$ (483.2741 calcd. for C$_{29}$H$_{39}$O$_6$).

3.4.2. Ecdysonelactone B

2: White amorphous solid; $[\alpha]_D^{20}$ + 24 (*c* 0.1, CH$_3$OH); UV (DAD) λ_{max} 246 nm; ^{1}H NMR and ^{13}C NMR data see Table 1; HRESIMS (+) *m/z* 521.3104 [M + H–H$_2$O]$^+$ (521.3109 calcd. for C$_{29}$H$_{45}$O$_8$ Δ −0.96 ppm) and fragments 503.3001 [M + H–2H$_2$O]$^+$ (503.3003 calcd. for C$_{29}$H$_{43}$O$_7$); 485.2884 [M + H–3H$_2$O]$^+$ (485.2898 calcd. for C$_{29}$H$_{41}$O$_6$); 467.2776 [M + H]$^+$ (467.2792 calcd. for C$_{29}$H$_{39}$O$_5$).

3.4.3. Ecdysonelactone C

3: White, amorphous powder; $[\alpha]_D^{20}$ +30 (*c* 0.1, CH$_3$OH); UV (DAD) λ_{max} 248 nm; ^{1}H NMR and ^{13}C NMR data see Table 1; HRESIMS (+) *m/z* [M + H–H$_2$O]$^+$ 521.3107 (521.3109 calcd. for C$_{29}$H$_{45}$O$_8$ Δ −0.38 ppm) and fragments 503.3006 [M + H–2H$_2$O]$^+$ (503.3003 calcd. for C$_{29}$H$_{43}$O$_7$); 485.2894 [M + H–3H$_2$O]$^+$ (485.2898 calcd. for C$_{29}$H$_{41}$O$_6$); 467.2787 [M + H]$^+$ (467.2792 calcd. for C$_{29}$H$_{39}$O$_5$).

3.4.4. Ecdysonelactone D

4: White, amorphous powder; $[\alpha]_D^{20}$ +29 (*c* 0.1, CH$_3$OH); UV (DAD) λ_{max} 240 nm; ^{1}H NMR and ^{13}C NMR data, see Table 1; HRESIMS (+) *m/z* 521.3104 [M + H–H$_2$O]$^+$ (521.3109 calcd. for C$_{29}$H$_{45}$O$_8$ Δ −0.96 ppm) and fragments 503.2993 [M + H–2H$_2$O]$^+$ (503.3003 calcd. for C$_{29}$H$_{43}$O$_7$); 485.2885 [M + H–3H$_2$O]$^+$ (485.2898 calcd. for C$_{29}$H$_{41}$O$_6$); 467.2868 [M + H]$^+$ (467.2792 calcd. for C$_{29}$H$_{39}$O$_5$).

3.5. Computational Analyses

The most stable conformer for the four diastereoisomers of **1** were generated using the MMFF94 force field (MarvinView, version 6.2.2, calculation module developed by ChemAxon, Budapest Hungary) and the geometry described in Ohta et al. as the initial input [28] The $^3J_{H,H}$ couplings were predicted using MSpin (Mestrelab Research, Santiago de Compostela, Spain) for each diasteroisomer.

4. Conclusions

Ecdysonelactones A–D (**1–4**), isolated from the Tropical Eastern Pacific zoantharian *A. hickmani*, are new members of the ecdysteroid family of natural products as they feature an unprecedented γ-

lactone fused at C-2 and C-3 of ring A. To our knowledge, this is the first report of ecdysteroids containing a five-membered lactone fused to ring A. The fusion of the lactone moiety to ring A could originate from a cyclization of the 3-*O* acetate onto a ketone at C-2.

References

1. Burnett, W.J.; Benzie, J.A.H.; Beardmore, J.A.; Ryland, J.S. Zoanthids (Anthozoa, Hexacorallia) from the Great Barrier Reef and Torres Strait, Australia: Systematics, evolution and a key to species. *Coral Reefs* **1997**, *16*, 55–68.
2. Reimer, J.D.; Foord, C.; Irei, Y. Species Diversity of Shallow Water Zoanthids (Cnidaria: Anthozoa: Hexacorallia) in Florida. *J. Mar. Biol.* **2012**, *2012*, 856079, doi:10.1155/2012/856079.
3. Behenna, D.C.; Stockdill, J.; Stoltz, B.M. The Biology and Chemistry of the Zoanthamine Alkaloids. *Angew. Chem. Int. Ed.* **2008**, *47*, 2365–2386.
4. Rao, C.B.; Anjaneyula, A.S.R.; Sarma, S.S.; Venkatateswarlu, Y.; Chen, M.; Clardy, J.; Rosser, R.; Faulkner, J. Zoanthamine: A Novel Alkaloid from a Marine Zoanthid. *J. Am. Chem. Soc.* **1984**, *106*, 7983–7984.
5. Fukuzawa, S.; Hayashi, Y.; Uemura, D. The Isolation and Structures of Five New Alkaloids, Norzoanthamine, Oxyzoanthamine, Norzoanthamine, Cyclozoanthamine and Epinorzoanthamine. *Heterocycl. Commun.* **1995**, *1*, 207–214.
6. Cen-Pacheco, F.; Martín, M.N.; Fernández, J.J.; Daranas, A.H. New Oxidized Zoanthamines from a Canary Islands *Zoanthus* sp. *Mar. Drugs* **2014**, *12*, 5188–5196.
7. Cheng, Y.-B.; Lo, I.-W.; Shyur, L.-F.; Yang, C.-C.; Hsu, Y.-M.; Su, J.-H.; Lu, M.-C.; Chiou, S.-F.; Lan, C.-C.; Wu, Y.-C.; et al. New alkaloids from Formosan zoanthid *Zoanthus kuroshio*. *Tetrahedron* **2015**, *71*, 8601–8606.
8. Rosser, R.M.; Faulkner, D.J. Alkaloids from a Marine Zoanthid. *J. Org. Chem.* **1985**, *50*, 3757–3760.
9. Cariello, L.; Crescenzi, S.; Prota, G.; Giordano, F.; Mazzarella, L. Zoanthoxanthin, a Heteroaromatic Base from *Parazoanthus* cfr. *axinellae* (Zoantharia): Structure Confirmation by X-Ray Crystallography. *J. Chem. Soc. Chem. Commun.* **1973**, 99–100, doi:10.1039/C39730000099.

10. D'Ambrosio, M.; Roussis, V.; Fenical, W. Zoamides A-D: New Marine Zoanthoxanthin Class Alkaloids from an Encrusting Philippine *Parazoanthus* sp. *Tetrahedron Lett.* **1997**, *38*, 717–720.

11. Cachet, N.; Genta-Jouve, G.; Regalado, E.L.; Mokrini, R.; Amade, P.; Culioli, G.; Thomas, O.P. Parazoanthines A-E, Hydantoin Alkaloids from the Mediterranean Sea Anemone *Parazoanthus axinellae*. *J. Nat. Prod.* **2009**, *72*, 1612–1615.

12. Rocha, C.D. Bioactive compounds from Zoanthids (Cnidaria:Anthozoa): A brief review with emphasis on alkaloids. *Int. Res. J. Biochem. Bioinform.* **2013**, *3*, 1–6.

13. Deeds, J.R.; Handy, S.M.; White, K.D.; Reimer, J.D. Palytoxin Found in *Palythoa* sp. Zoanthids (Anthozoa, Hexacorallia) Sold in the Home Aquarium Trade. *PLoS ONE* **2011**, *6*, e18235.

14. Babu, U.V.; Bhandari, S.P.S.; Garg, H.S. Hariamide, a Novel Sulfated Sphingolipid from a *Zoanthus* sp. of the Indian Coast. *J. Nat. Prod.* **1997**, *60*, 1307–1309.

15. Kelecom, A. Zoanthosterol, a New Sterol from the Zoanthid *Zoanthus sociatus* (Hexacorallia, Zoanthidea). *Bull. Soc. Chim. Belg.* **1981**, *90*, 971–976.

16. Suksamrarn, A.; Jankam, A.; Tarnchompoo, B.; Putchakarn, S. Ecdysteroids from a *Zoanthus* sp. *J. Nat. Prod.* **2002**, *65*, 1194–1197.

17. Bo, M.; Lavorato, A.; Camillo, C.G.D.; Poliseno, A.; Baquero, A.; Bavestrello, G.; Irei, Y.; Reimer, J.D. Black Coral Assemblages from Machalilla National Park (Ecuador). *Pac. Sci.* **2012**, *66*, 63–81.

18. Reimer, J.D.; Sinniger, F.; Hickman, C.P., Jr. Zoanthid diversity (Anthozoa: Hexacorallia) in the Galapagos Islands: A molecular examination. *Coral Reefs* **2008**, *27*, 641–654.

19. Reimer, J.D.; Fujii, T. Four new species and one new genus of zoanthids (Cnidaria, Hexacorallia) from the Galápagos Islands. *ZooKeys* **2010**, *42*, 1–36.

20. Guillen, P.O.; Jaramillo, K.B.; Genta-Jouve, G.; Sinniger, F.; Rodriguez, J.; Thomas, O.P. Terrazoanthines, 2-Aminoimidazole Alkaloids from the Tropical Eastern Pacific Zoantharian Terrazoanthus onoi. *Org. Lett.* **2017**, *19*, 1558–1561.

21. Low, M.E.Y.; Sinniger, F.; Reimer, J.D. The order Zoantharia Rafinesque, 1815 (Cnidaria, Anthozoa: Hexacorallia): Supraspecific classification and nomenclature. *ZooKeys* **2016**, *641*, 1–80.

22. Sinniger, F.; Reimer, J.D.; Pawlowski, J. The Parazoanthidae (Hexacorallia: Zoantharia) DNA taxonomy: Description of two new genera. *Mar. Biodivers.* **2009**, *40*, 57–70.

23. Li, C.-J.; Schmitz, F.J.; Kelly-Borges, M. A New Lysine Derivative and New 3-Bromopyrrole Carboxylic Acid Derivative from Two Marine Sponges. *J. Nat. Prod.* **1998**, *61*, 387–389.

24. Bathory, M.; Toth, I.; Szendrei, K.; Reisch, J. Ecdysteroids in *Spinacia oleracea* and *Chenopodium bonus-henricus*. *Phytochemistry* **1982**, *21*, 236–238.

25. Jizba, J.; Herout, V.; Sorm, F. Polypodine B/A novel ecdysone-like substances from plant material. *Tetrahedron Lett.* **1967**, *8*, 5139–5143.

26. Shigemori, H.; Sato, Y.; Kagata, T.; Kobayashi, J.I. Palythoalones A and B, New Ecdysteroids from the Marine Zoanthid Palythoa australiae. *J. Nat. Prod.* **1999**, *62*, 372–374.

27. Searle, P.A.; Molinski, T.F. 4-Dehydroecdysterone, a New Ecdysteroid from the *Zoanthid Parazoanthus* sp. *J. Nat. Prod.* **1995**, *58*, 264–268.

28. Ohta, S.; Guo, J.-R.; Hiraga, Y.; Suga, T. 24-Epi-pterosterone: A novel phytoecdysone from the roots of Athyrium yokoscense. *Phytochemistry* **1996**, *41*, 745–747.

29. Chappell, G.S. Stereochemistry of some .DELTA.1-butenolide syntheses. *J. Org. Chem.* **1973**, *38*, 240–245.

30. Cachet, N.; Genta-Jouve, G.; Ivanisevic, J.; Chevaldonne, P.; Sinniger, F.; Culioli, G.; Perez, T.; Thomas, O.P. Metabolomic profiling reveals deep chemical divergence between two morphotypes of the zoanthid Parazoanthus axinellae. *Sci. Rep.* **2015**, *5*, 8282, doi:10.1038/srep08282.

31. Pinheiro, M.L.B.; Filho, W.W.; Da Rocha, A.I.; Porter, B.; Wenkertt, E. Abutasterone, an ecdyone from abuta velutina. *Phytochemistry* **1983**, *22*, 2320–2321.

32. Blunt, J.W.; Lane, G.A.; Munro, M.H.G.; Russell, G.B. The Absolute Configuration at C24 of the Ecdysteroids Dacrysterone, Pterosterone and Ponasterone C. *Aust. J. Chem.* **1979**, *32*, 779–782.

33. Dinan, L. *Studies in Natural Products Chemistry: Bioactive Natural Products (Part J)*; Atta-Ur_Rahman, Ed.; Elsevier B.V: Amsterdam, The Netherlands, 2003; Volume 29.

34. Dinan, L. Phytoecdysteroids: Biological aspects. *Phytochemistry* **2001**, *57*, 325–339.

35. Okuzumi, K.; Hara, N.; Uekusa, H.; Fujimoto, Y. Structure elucidation of cyasterone stereoisomers isolated from *Cyathula officinalis*. *Org. Biomol. Chem.* **2005**, *3*, 1227–1232.

36. Nakanishi, K.; Koreeda, M.; Goto, M. Insect hormones. XX. Ajugalactone, an insect-molting inhibitor, as tested by the Chilo dipping method. *J. Am. Chem. Soc.* **1970**, *92*, 7512–7513.

37. Ványolós, A.; Simon, A.; Tóth, G.; Polgár, L.; Kele, Z.; Ilku, A.; Mátyus, P.; Báthori, M. C-29 Ecdysteroids from *Ajuga reptans var. reptans*. *J. Nat. Prod.* **2009**, *72*, 929–932.

38. Riddiford, L.M. *Biosynthesis, Metabolism and Mode of Action of Invertebrates Hormones*; Hoffman, J.A., Porchet, M., Eds.; Springer: Berlin/Heidelberg, Germany; New York, NY, USA, 1984.

39. Báthori, M.; Girault, J.P.; Kalasz, H.; Mathé, I.; Dinan, L.N.; Lafont, R. Complex Phytoecdysteroid Cocktail of Silene otites (Caryophyllaceae). *Arch. Insect Biochem. Physiol.* **1999**, *41*, 1–8.

40. Calcagno, M.P.; Camps, F.; Coll, J.; Melé, E.; Sánchez-Baeza, F. New phytoecdysteroids from roots of Ajuga reptans varieties. *Tetrahedron* **1996**, *52*, 10137–10146.

41. Gao, F.; Yang, Z.-K.; Chen, Q.-H.; Chen, X.-G.; Wang, F.-P. A novel D-ring modified taxoid: Synthesis and biological evaluation of a [gamma]-lactone analogue of docetaxel. *Org. Biomol. Chem.* **2012**, *10*, 361–366.

42. Audoin, C.; Bonhomme, D.; Ivanisevic, J.; de la Cruz, M.; Cautain, B.; Monteiro, M.C.; Reyes, F.; Rios, L.; Perez, T.; Thomas, O.P. Balibalosides, an original family of glycosylated sesterterpenes produced by the Mediterranean sponge Oscarella balibaloi. *Mar. Drugs* **2013**, *11*, 1477–1489.

5   Halogenated Tyrosine Derivatives from the Tropical Eastern Pacific Zoantharians *Antipathozoanthus hickmani* and *Parazoanthus darwini*

Parazoanthus darwini (© Karla B. Jaramillo)

Halogenated Tyrosine Derivatives from the Tropical Eastern Pacific Zoantharians *Antipathozoanthus hickmani* and *Parazoanthus darwini.*

Paul O. Guillen, [†,‡] *Karla B. Jaramillo,*[†,§] *Laurence Jennings,*[‡] *Grégory Genta-Jouve,* [⊥,‖] *Mercedes de la Cruz,*[∇] *Bastien Cautain,*[∇] *Fernando Reyes,*[∇] *Jenny Rodríguez,*[†] *Olivier P. Thomas*[*,‡]

† ESPOL Escuela Superior Politécnica del Litoral, ESPOL, Centro Nacional de Acuacultura e Investigaciones Marinas, Campus Gustavo Galindo km. 30.5 vía Perimetral, P.O.Box 09-01-5863, Guayaquil, Ecuador.

‡ Marine Biodiscovery, School of Chemistry and Ryan Institute, National University of Ireland Galway (NUI Galway), University Road, H91 TK33 Galway, Ireland.

§ Zoology, School of Natural Sciences and Ryan Institute, National University of Ireland Galway (NUI Galway), University Road, H91 TK33 Galway, Ireland.

⊥ Équipe C-TAC, UMR CNRS 8038 CiTCoM – Université Paris Descartes, 4 Avenue de l'Observatoire, 75006 Paris, France

‖ Unité Molécules de Communication et Adaptation des Micro-organismes (UMR 7245), Sorbonne Universités, Muséum National d'Histoire Naturelle, CNRS, Paris, France

∇ Fundación MEDINA, Centro de Excelencia en Investigación de Medicamentos Innovadores en Andalucía, Avda. del Conocimiento 34, Parque Tecnológico de Ciencias de la Salud, E-18016, Armilla, Granada, Spain.

ABSTRACT: In the search for bioactive marine natural products from zoantharians of the Tropical Eastern Pacific, four new tyrosine dipeptides named valdiviamides A-D (**1-4**) were isolated from *Antipathozoanthus hickmani* and two new tyramine derivatives **5** and **6** from *Parazoanthus darwini*. The phenols of all six tyrosine derivatives are substituted by bromine and/or iodine atoms at the ortho positions of the hydroxyl. The planar structures of these aromatic alkaloids were elucidated from 1D and 2D NMR experiments in combination with HRESIMS data and the absolute configurations of **1-4** were deduced from comparison between experimental and calculated electronic circular dichroism (ECD) spectra. As halogenated tyrosine derivatives could represent chemotaxonomic markers of these genera, we decided to undertake the first chemical investigation of another species *Terrazoanthus* cf. *patagonichus*. As expected, no halogenated metabolite was evidenced in the species, but we report herein the identification of two new zoanthoxanthin derivatives named zoamides E (**7**) and F (**8**) from this species. Antimicrobial and cytotoxicity bioassays revealed that valdiviamide B (**2**) displayed moderate cytotoxicity against the HepG2 cell line with an IC_{50} value of 7.8 μM.

The structures of marine natural products are usually characterized by a higher occurrence of halogen atoms than their terrestrial counterparts. Within the marine environment, most of the marine invertebrates but especially algae and sponges are sources of halogenated secondary metabolites.[1-5] By far, the most common halogen in marine natural products is bromine.[6, 7] The incorporation of halogens into natural products is catalyzed by enzymes such as vanadium-dependent haloperoxidases which have been reported mainly from algae, sponges or bacteria.[2, 6-11] Among the different halogenated structural units reported from marine organisms, bromotyrosine derivatives are the most common and mainly found in marine sponges of the order Verongida,[12-14] but also some species of ascidians.[15-18] Interestingly, a wide range of biological activities including antibacterial, anticancer, antiparasitic, antiplasmodial, anti-inflammatory and antifouling have been reported for halogenated tyrosine derivatives.[18-22]

Zoantharians are sessile invertebrates inhabiting diverse marine environments like coral reefs, shallow waters and, deep seas around the world. They are known to produce a number of interesting metabolites including zoanthamine alkaloids,[23, 24] fluorescent pigments like zoanthoxanthins,[25, 26] ecdysteroids,[27, 28] and some halogenated metabolites. The first halogenated natural product from zoantharians was the fatty acid 6-bromo-5,9-eicosadienoic acid isolated from *Palythoa caribaeorum* in 1995.[29] Later, two monobrominated tyrosine derivatives named parazoanthines D and E were reported in 2009 from the Mediterranean zoantharian *Parazoanthus axinellae*.[30] Additionally, two mono and two dibrominated parazoanthines G-J were reported in 2014 from the same species.[31] In another context, two halogenated zoanthamine alkaloids; 5α-iodozoanthenamine and 11β-chloro-11-deoxykuroshine A were isolated from *Zoanthus kuroshio* collected off the coast of Taiwan.[32] Despite the great diversity of natural products isolated from zoantharians, most of the chemical studies are reported from species collected in the Central Indo-Pacific, while only a few studies have been undertaken from species inhabiting the Tropical Eastern Pacific.[33-35]

During a dereplication process on zoantharians from the Ecuadorian coast,[36] the UPLC-HRMS analyses of both species *Antipathozoanthus hickmani* and *Parazoanthus darwini* revealed the presence of some metabolites with unreported masses and isotopic patterns characteristic of mono and

dibrominated compounds. The first chemical study of *A. hickmani* revealed ecdysteroids derivatives named ecdysonelactones A-D as the major compounds of the methanolic fraction.[34] As no chemical studies from *P. darwini* have been reported so far, we decided to undertake a deeper chemical study of *A. hickmani* and the first one on *P. darwini* collected off the Marine Protected Area El Pelado, Santa Elena, Ecuador.

In this study, we describe the isolation and structure elucidation of four new halogenated tyrosine dipeptides named valdiviamides A-D (1-4) from *A. hickmani* and two halogenated tyramine derivatives 5 and 6 from *P. darwini* (Figure 1). These compounds were isolated as TFA salts as they contain an ammonium ion and they are characterized by the presence of bromine and iodine atoms around the phenol. Because halogenated tyrosine derivatives could serve as chemotaxonomic markers for these two genera of the family Parazoanthidae, we decided to perform the first chemical study of a non-studied species of this area *Terrazoanthus* cf. *patagonichus*, belonging to the family Hydrozoanthidae. In agreement with this hypothesis, no halogenated derivative was obtained from this species of the genus *Terrazoanthus* but two new zoanthoxanthin derivatives named zoamides E-F (7-8) were isolated as neutral molecules.
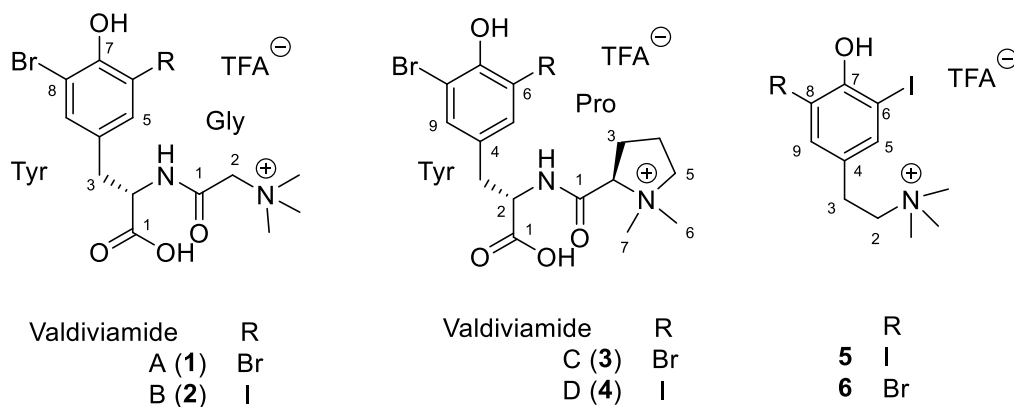
Figure 1. Structures of valdiviamides A-D (1-4) from *Antipathozoanthus hickmani* and tyramine derivatives 5 and 6 from *Parazoanthus darwini*

RESULTS AND DISCUSSION

The freeze-dried samples of *A. hickmani* (68 g) and *P. darwini* (54 g) were extracted with a mixture of CH_2Cl_2/MeOH (1:1) under ultrasonication. The extracts (2.60 g and 2.10 g, respectively) were fractionated by RP-C18 vacuum liquid chromatography with mixtures of solvents of decreasing polarity from H_2O to MeOH to CH_2Cl_2. The hydromethanolic fractions containing the halogenated derivatives were purified by semi-preparative RP-C18 HPLC yielding pure compounds **1** – **6** as their TFA salts.

From *A. hickmani*, compound **1** was purified as a yellow, amorphous solid. The (+)-HRESIMS analysis revealed an isotopic cluster of ions [M]$^+$ at *m/z* 436, 438 and 440 in the ratio 1:2:1 consistent with the presence of two bromine atoms and the molecular formula $C_{14}H_{19}Br_2N_2O_4$. A first inspection of the ^{1}H NMR data revealed a singlet at δ_H 7.39 (s, H$_2$-5/9) suggesting the presence of a symmetric *ortho*/*ortho*/*para* tetrasubstituted aromatic ring. Additionally, the ^{1}H NMR, COSY and HSQC spectra evidenced a ABX spin system with three signals at δ_H 4.72 (dd, *J* = 9.5, 5.0 Hz, Tyr-H-2), δ_H 3.21 (dd, *J* = 14.5, 5.0 Hz, Tyr-H-3a), δ_H 2.88 (dd, *J* = 14.5, 9.5 Hz, Tyr-H-3b), and another AB system at δ_H 4.09 (d, *J* = 15.0 Hz, Gly-H-2a) and δ_H 4.00 (d, *J* = 15.0 Hz, Gly-H-2b). The deshielded singlet integrating for nine protons at δ_H 3.25 was assigned to the three methyls of a quaternary ammonium ion. The ^{13}C NMR spectrum disclosed signals corresponding to six non-protonated carbons: one carboxylic acid carbon at δ_C 173.4 (Tyr-C-1), one amide carbonyl group at δ_C 164.5 (Gly-C-1), one aromatic signal at

δ_C 132.3 (Tyr-C-4), an oxygenated aromatic carbon signal at δ_C 151.3 (Tyr-C-7) and the brominated

aromatic signal at δ_C 112.1 (C-6/8). The *ortho* position of the two bromine atoms and the *meta* position

of the aromatic protons with respect to the hydroxy group were supported by key Tyr-H_2-3/C-5, Tyr-

H-5/C-6 and C-7 HMBC correlations (Figure 2). The Tyr-H_2-3/Tyr-H-2 coupled system together with

the key Tyr-H-2/C-1, C-4 HMBC correlations secured the structure of the tyrosine moiety. For the other

part of the molecule, key Gly-H_2-2/C-1 and $(CH_3)_3N$ HMBC correlations confirmed the trimethylated

glycine subunit. Finally, the key Tyr-H-2/Gly-C-1 HMBC correlation allowed the connection between

both amino acids.
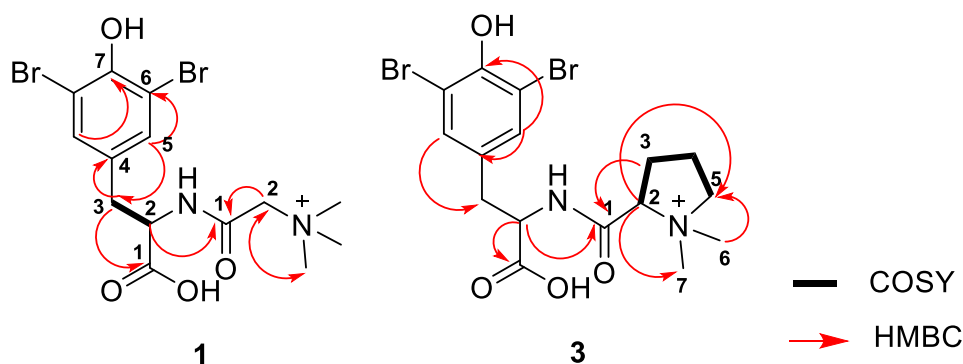
Figure 2. Key COSY and HMBC (H to C) correlations of **1** and **3**.

Table 1. ^{1}H and ^{13}C NMR Data for Valdiviamides A-D (1-4) in CD$_3$OD (500 MHz for ^{1}H NMR and 125 MHz for ^{13}C NMR data).

Position	1 δ_C, type	1 δ_H, mult. (*J* in Hz)	2 δ_H, mult. (*J* in Hz)	3 δ_C type	3 δ_H, mult. (*J* in Hz)	4 δ_H, mult. (*J* in Hz)
Tyrosine						
1	173.4, C	-	-	173.7, C	-	-
2	54.7, CH	4.72, dd (9.5, 5.0)	4.72, dd (9.5, 5.0)	54.8, CH	4.72, dd (10.5, 5.0)	4.72, dd (10.5, 5.0)
3a	36.6, CH$_2$	3.21, dd (14.5, 5.0)	3.20, dd (14.5, 5.0)	36.5, CH$_2$	3.27, dd (14.0, 5.0)	3.19, dd (14.0, 5.0)
3b		2.88, dd (14.5, 9.5)	2.86, dd (14.5, 9.5)		2.91, dd (14.0, 10.5)	2.89, dd (14.0, 10.5)
4	132.3, C	-	-	132.9, C	-	-
5	134.0, CH	7.39, s	7.61, d (2.0)	134.1, CH	7.41, s	7.62, s
6	112.1, C	-	-	112.1, C	-	-
7	151.3, C	-	-	151.3, C	-	-
8	112.1, C	-	-	112.1, C	-	-
9	134.0, C	7.39, s	7.41, d (2.0)	134.1, CH	7.41, s	7.43, s
Glycine						
1	164.5, C	-	-			
2a	65.6, CH$_2$	4.09, d (15.0)	4.09, d (15.0)			
2b		4.00, d (15.0)	4.01, d (15.0)			
N(Me)$_3$	54.8, CH$_3$	3.25, s	3.25, s			
Proline						
1				166.4, C	-	-
2				75.7, CH	4.10, t (8.0)	4.08, t (8.0)
3a				26.6, CH$_2$	2.51, dddd (14.5, 9.0, 8.0, 5.0)	2.55, m
3b					2.38, ddt (14.5, 8.0, 6.5)	2.38, m
4a				21.3, CH$_2$	2.28, m	2.28, m
4b					2.24, m	2.24, m
5a				67.8, CH$_2$	3.78, ddd (11.5, 8.5, 6.0)	3.77, ddd (11.5, 8.5, 6.0)
5b					3.57, ddd (11.5, 8.5, 7.5)	3.61, ddd (11.5, 8.5, 7.5)
6				48.2, CH$_3$	2.95, s	2.94, s
7				53.1, CH$_3$	3.11, s	3.10, s

With the planar structure of the dipeptide in hand, the absolute configuration of the tyrosine stereogenic center was assigned by comparison of experimental and predicted ECD spectra. After conformational analysis and geometry optimization, the ECD spectra of the two enantiomers of **1** were calculated using time-dependent density functional theory (TDDFT) with the B3LYP/6-311+G (d,p)//B3LYP/6-31G(d) level of theory. The calculated ECD spectrum of the 2*S* enantiomer matched the experimental spectrum of **1** confirming the presence of a L-tyrosine derived residue (Figure 3).
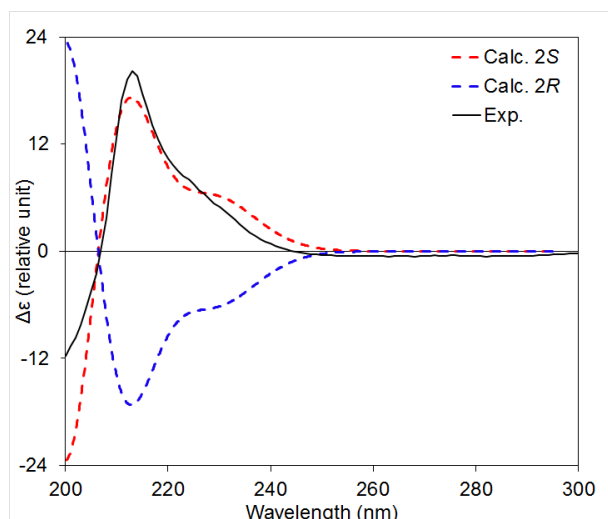
Figure 3. Comparison of the calculated ECD spectra of the two enantiomers of **1** at Tyr-C-2, with the experimental ECD spectrum.

Valdiviamide B (**2)** was isolated as an amorphous white solid. Its HRESIMS spectrum revealed an isotopic cluster of ions at *m/z* 484 and 486 $[M]^+$ in a ratio of 1:1, consistent with the presence of one bromine atom and the molecular formula $C_{14}H_{19}BrIN_2O_4$. The analysis of the ^1H NMR spectrum revealed similar signals to those of compound **1** except for the presence of two doublets in the aromatic regions at δ_H 7.60 (d, *J* = 1.5 Hz, H-5) and δ_H 7.41 (d, *J* = 1.5 Hz, H-9) indicative of a loss of symmetry around the aromatic ring. The replacement of one bromine in **1** by one iodine atom in **2** in the molecular formula suggested a similar change on the phenol ring. Despite a small amount of pure compound **2** preventing the acquisition of interpretable ^{13}C and 2D NMR spectra and based on the MS data and the significant increased chemical shift of the aromatic proton at δ_H 7.60 in comparison to those of **1**, we are confident to assigned **2** as the iodo analogue of **1**. The absolute configuration at C-2 was assigned as *S* due to a similar positive Cotton effect at 219 nm in the ECD spectrum of **2** compared to that of **1**. Valdiviamide C (**3**) was isolated as a colorless, amorphous solid and the molecular formula $C_{16}H_{21}Br_2N_2O_4$ was determined by HRESIMS with an isotopic cluster of ions at *m/z* 462, 464 and 466 $[M]^+$ in the ratio 1:2:1 indicative of the presence of two bromine atoms. Analysis of the ^1H NMR spectrum of **3** revealed similar tyrosine signals to those of **1** with a singlet at δ_H 7.41 (s, Tyr-H-5/9) and a deshielded methine at δ_H 4.72 (dd, *J* = 10.5, 5.0 Hz, Tyr-H-2), indicating the presence of the same

dibromotyrosine moiety in **1**. The ^{1}H NMR and COSY spectra of **3** differed from those of **1** with the presence of an additional spin-coupled system replacing the AB system of the glycine moiety in **1**. This spin coupled system include resonances associated with a methine at δ_H 4.10 (H-2) and three methylene groups at δ_H 2.51 (H-3a), δ_H 2.38 (H-3b), δ_H 2.27 (H$_2$-4), and δ_H 3.78 (H-5a), δ_H 3.57 (H-5b). The methyl singlet integrating for nine in **1** was also replaced by two singlets at δ_H 3.11 (s, H$_3$-7) and δ_H 2.95 (s, H$_3$-6) corresponding to non-equivalent *N*-methyl groups. These data combined with the key Pro-H$_3$-6/C-5, Pro-H-2/C-7 and Pro-H$_2$-3/C-1 HMBC correlations suggest the presence of a *N*,*N*-dimethyl proline subunit (Figure 2). Finally, the connection between the two subunits was confirmed by the key Tyr-H-2/Pro-C-1 HMBC correlation.

First, we assumed an *S* absolute configuration for the tyrosine residue due to a positive Cotton effect at 220 nm similar to those found for **1** and **2**. For the relative configuration between the two residues, comparisons between the experimental and theoretical ECD spectra of *S*, *S* and *S*, *R* diastereoisomers were not conclusive and therefore we decided to proceed with a DP4 probability calculations.[241] Even though the purification was performed with TFA in the eluent, the conformational analyses were undertaken on both possible ionic forms: first the zwitterion and then the ammonium ion with TFA$^-$ as a counter anion. After a conformational analysis using a 1.5 kcal/mol energy threshold, four conformers were obtained for both the *S*, *S* and the *S*, *R* diastereoisomers. ^{13}C NMR chemical shifts were calculated using the B3LYP/6-31g(d)//MPW1PW91/6-311+g(2d) level. For both ionic forms, the *S*, *R* diastereoisomer was predicted as the most probable structure with 100% DP4 probability (See Supplementary Information). Despite possible influences of the solvent and concentration on the chemical shifts of ionic molecules, we were quite confident on this assignment as the prediction was totally in favor of one of the two diasteroisomers. However, this unexpected result led us to inspect the NOESY spectrum of **3** and the distances between the atoms of the lowest energy conformers. On the most stable conformer of the diastereoisomers (2*S*)-Pro and (2*R*)-Pro, the distances between Tyr-H-5/9 and the methyls on the proline nitrogen were calculated as 2.9 and 3.8 Å respectively. These observations came as a confirmation of the *S*, *R* diastereoisomer as no nOe was observed between these two signals in the experimental spectrum of **3**.

Valdiviamide D (**4**) was isolated as a colorless amorphous powder. The HRESIMS data exhibited an isotopic cluster of ions at *m/z* 510 and 512 [M]$^+$ in a 1:1 ratio, consistent with the presence of one bromine atom and a molecular formula of $C_{16}H_{21}BrIN_2O_4$. Analysis of the ^{1}H NMR spectrum of **4** revealed similar signals to those of compound **3** (Table 1), except for the replacement of the aromatic singlet in **3** by two doublets at δ_H 7.61 (1H, d, *J* = 2.0 Hz) and δ_H 7.43 (1H, d, *J* = 2.0 Hz). This was indicative of the substitution of one bromine for an iodine around the phenol ring in **4** similar to that observed for **2**.

From *Parazoanthus darwini*, compound **5** was isolated as a colorless powder and its HRESIMS spectrum revealed a major molecular ion peak at *m/z* 431.9349 [M]$^+$ consistent with the molecular formula of $C_{11}H_{16}I_2NO$. A first inspection of the ^{1}H NMR spectrum revealed a deshielded aromatic singlet integrated for two protons at δ_H 7.74 (2H, s, H-5/9) and these signals were HMBC correlated to C-6/8 at δ_C 85.5 revealing an unusual shielding for the aromatic non-protonated carbon (Table 1). These chemical shifts were in accordance with the data obtained for the iodinated compounds **2** and **4** therefore suggesting two iodine atoms on the aromatic ring. Furthermore, the deshielded signal at δ_C 156.3 (C-7) confirmed the occurrence of a hydroxyl group at C-7 and was confirmed by a key H-5/C-7 HMBC correlation. The ^{1}H NMR and HSQC spectra also evidenced a AA′BB′ system with signals at δ_H 3.50 (H$_2$-2) and δ_H 3.00 (H$_2$-3). The remaining methyl singlet integrating for nine protons at δ_H 3.18 (9H, s) was assigned to a $N(CH_3)_3$ group. Altogether, these data suggest that compound **5** is a halogenated tyramine derivative. Key H$_2$-3/C-2, C-4, C-5, $N(CH_3)_3$/C-2 and H$_2$-2/C-3, C-4 HMBC correlations allowed the establishment of the structure of **5** as 2-(4-hydroxy-3,5-diiodophenyl)-*N,N,N*-trimethylethanaminium. This new natural product has a similar structure to that of iodocionin.[20]

Compound **6** was isolated as a pale-yellow solid. The HRESIMS data revealed an isotopic cluster of ions at *m/z* 383 and 385 [M]$^+$ in a ratio of 1:1 suggesting the presence of one bromine atom, and it was consistent with the molecular formula $C_{11}H_{16}BrINO$, differing from **5** by the replacement of one iodine with one bromine atom. This was confirmed by the loss of symmetry of the phenol with two aromatic doublets at δ_H 7.71 (d, *J* = 2.0 Hz) and 7.51 (d, *J* = 2.0 Hz) and the shift of C-8 carbon signal at δ_C 110.6.

Therefore, the structure of **6** was assigned as 2-(4-hydroxy-3-bromo-5-iodophenyl)-*N*,*N*,*N*-trimethylethanaminium.

Valdiviamides A-D (**1-4**) isolated from the zoantharian *Antipathozoanthus hickmani* are bromotyrosine derivatives obtained by condensation between the amine group of the tyrosine to the carboxylic acid group of the glycine for valdiviamide A-B (**1-2**) and to the carboxylic acid group of proline for valdiviamides C-D (**3-4**). The name valdiviamide is given as a tribute to the Valdivia culture, one of the oldest settled cultures in Ecuador and South America and still present in the area of the sample collection. Interestingly, the absolute configuration for compound **3** is proposed to be L-Tyr, D-Pro. Even though the presence of the D-Pro was unexpected, there are several reports of this enantiomer in natural products and especially in the presence of a betaine proline.[38] We anticipate that the epimerization from *S* to *R* configuration at the α position of the proline would be favored by the presence of the positive charge on the nitrogen when doubly substituted. Indeed, the strong withdrawing effect of the ammonium group would increase the acidity of the proton α.

All six metabolites are characterized by the presence of halogens like bromine and/or the less common iodine in the *ortho*-positions of the phenol. These results raise the question of the use of simple bromotyrosine derivatives as chemical markers of zoantharians from the family Parazoanthidae, containing the genera *Parazoanthus* and *Antipathozoanthus*. This assumption has to be confirmed, as for instance, only one morphotype of the Mediterranean *P. axinellae* contains the bromotyrosine parazoanthines.[242] However, this proposition is consistent with all the chemical studies we undertook on tropical eastern Pacific zoantharians. As we recently collected an undescribed species of zoantharian named *Terrazoanthus* cf. *patagonichus* from this area, we wanted to verify if it contained any halogenated tyrosine derivatives. Even though the dereplication process did not suggest the presence of such halogenated natural products, we decided to identify its major metabolites due to the presence of unidentified masses. We were finally able to characterize two new acylated zoanthoxanthin derivatives named zoamides E (**7**) and F (**8**).
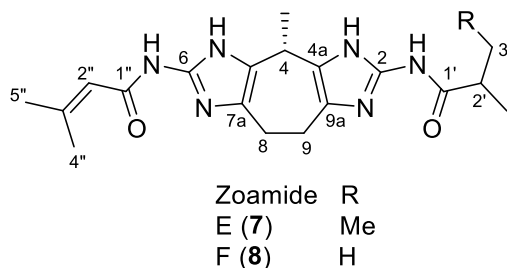
Zoamide   R
E (**7**)   Me
F (**8**)   H

Zoamide E (**7**) was isolated as a colorless powder and the (+)- HRESIMS analysis revealed a major peak at *m/z* 385.2369 [M+H]$^+$, consistent with the molecular formula of $C_{20}H_{29}N_6O_2$. A first inspection of the ^{1}H NMR spectrum revealed an olefinic proton signal at δ_H 5.94 (septet, *J* = 1.0 Hz, H-2″), two methines at δ_H 4.30 (q, *J* = 7.0 Hz, H-4) and δ_H 2.56 (sextet, *J* = 7.0 Hz, H-2′), three methylenes at δ_H 3.05 (m, H$_2$-8/H$_2$-9), δ_H 1.78 (dquint, *J* = 15.0, 7.0 Hz, H-3′a) and δ_H 1.55 (dquint, *J* = 15.0, 7.0 Hz, H-3′b) and five methyls at δ_H 2.30 (d, *J* = 1.0 Hz, H$_3$-5″), δ_H 2.01 (d, *J* = 1.0 Hz, H$_3$-4″), δ_H 1.59 (d, *J* = 7.0 Hz, C$\underline{H}_3$-C-4), δ_H 1.23 (d, *J* = 7.0 Hz, H-5′) and δ_H 0.97 (t, *J* = 7.5 Hz, H-4′). The 1D NMR data were in good agreement with zoanthoxathin derivatives already reported.[242] However, additional signals were evident in the 1D NMR spectra for saturated protons/carbons. Comparing with data reported for terrazoanthines isolated recently from *Terrazoanthus patagonichus* (ex *T. onoi*) we could quickly assign a 2-methylbutanoyl substituent on the primary amine of a terminal guanidine.[33] A second acyl substituent was identified as 3-methyl-2-butenoyl and placed on the second primary amine. Similar acylated zoanthoxathin derivatives were already reported from a *Parazoanthus* sp. and named zoamides A-D.[40] The only difference between our compound and those reported previously is the nature of one acyl substituent. For the absolute configuration we decided to work on compound **8** as it contains only one stereogenic center.

Zoamide F (**8**) was isolated as a white colorless powder and the (+)-HRESIMS analysis revealed a major peak at *m/z* 371.2214 [M+H]$^+$, consistent with the molecular formula of $C_{19}H_{26}N_6O_2$ and therefore **8** is a nor derivative of **7**. Analysis of the ^{1}H NMR spectrum revealed similar signals to those of **7** with the difference of the loss of one methylene signal in **8**. The COSY spectrum allowed us to locate this loss on one acyl group replacing the 2-methylbutanoyl in **7** by an isobutanoyl in **8**. To assign the absolute configuration at the unique C-4 stereogenic center of the two zoamides we used ECD analysis of **8**. The

calculation of the ECD spectrum was not straightforward due to the slight difference between both sides of the chiral center. The ECD and UV spectra calculated at the commonly used B3LYP/6-31G(d) level did not match with experimental UV and did not allow a definitive assignment of the chirality. Therefore, to confidently assign the absolute configuration of **8**, the ECD was predicted with different combinations of reported functions and basis sets with a higher computational power.[41] Spectra calculated using ωB97X-D/6-311+G(d,p)//B3LYP/6-31G(d,p) and cam-B3LYP/def2-TZVP//B3P86/aug-cc-pVDZ had successful matches with the experimental UV and ECD allowing us to confidently assign the C-4 stereogenic center in an *R* configuration (Figure 4). This highlights the need for TDDFT calculations to be performed with multiple functional/basis set combinations to conclusively identify the chirality of complex molecules. The structures of zoamide E and F were finally confirmed by a direct comparison of their ^{13}C NMR data to those of zoamides A-D isolated from a dark black unidentified specie of *Parazoanthus*.[40] The MS and NMR data supported unambiguously the structures of these new zoanthoxanthin derivatives (See Supporting Information).

This specie of *Terrazoanthus* cf. *patagonichus* is morphologically related to the previously studied *Terrazoanthus patagonichus* from which some other acylated zoanthoxanthin analogues named terrazoanthines were isolated.[33] Based on the similarity of these bisguanidinylated alkaloids, acylation seems restricted to species of the genus *Terrazoanthus*. Therefore, as there was no clear taxonomic description of the zoantharian from which zoamides A-D were isolated, we propose that the organism reported as *Parazoanthus* sp. could be a species of *Terrazoanthus*. Furthermore, the absence of halogenated compounds in *Terrazoanthus* species strengthens the hypothesis of halogenated tyrosine derivatives as a common feature of the genera *Antipathozoanthus* and *Parazoanthus*.

Compounds **1-8** were subjected to antimicrobial activity testing against a panel of Gram-positive (methicillin sensitive and methicillin resistant *Staphylococcus aureus*) and Gram-negative bacteria (*Escherichia coli*, *Klebsiella pneumoniae*, *Acinetobacter baumannii*, and *Pseudomonas aeruginosa*), and yeast (*Candida albicans*). None of the compounds displayed antimicrobial activity against any of the pathogenic strains at the highest concentration tested (128μg/mL). Compounds **1-3** and **5-8** were additionally evaluated as cytotoxic agents against three human tumor cell lines, namely HepG2 (liver),

A549 (colon) and MIA PaCa-2 (pancreas). Regarding their cytotoxic activity, only compound **2** displayed moderate activity against the HepG2 cell line, with an IC_{50} value of 7.8 μM.

EXPERIMENTAL SECTION

General Experimental Procedures. Optical rotations, UV and ECD data were obtained on Chirascan V100 (Applied Photophysics). IR data was obtained on a Perkin-Elmer FT-IR spectrometer, spectrum 100. NMR experiments were performed on a 500 MHz spectrometer (Varian) or a 600 MHz spectrometer (Agilent) for compounds **2** and **4** and signals were referenced in ppm to the residual solvent signals (CD$_3$OD, at δ_H 3.31 and δ_C 49.0). HRESIMS data were obtained with an Agilent UHR-qTOF 6540 mass spectrometer. HPLC purification was carried out on a JASCO HPLC equipped with a PU4087 pump and a UV4070 UV/Vis detector.

Animal material. Samples of *Antipathozoanthus hickmani*, *Parazoanthus darwini* and *Terrazoanthus* cf. *patagonichus* were collected by SCUBA at 24 m depth at the Marine Protected Area El Pelado (Santa Elena, Ecuador). Vouchers of the samples with codes 150924EP01-02 (*A. hickmani*), 150820EP01-05 (*P. darwini*) and 170416EP02-01 (*Terrazoanthus* cf. *patagonichus*) are held at the Centro Nacional de Acuicultura e Investigaciones Marinas CENAIM-ESPOL (San Pedro, Santa Elena, Ecuador) (Supporting Information).

Extraction and Isolation. The freeze-dried samples of *A. hickmani* (68 g), *P. darwini* (54 g) and *Terrazoanthus* cf. *patagonichus* (8 g) were extracted with a mixture of solvents MeOH/CH$_2$Cl$_2$ (1:1) three times (500 mL) at room temperature. The solvents were removed under pressure to obtain an organic extract of *A. hickmani* (2.60 g), *P. darwini* (2.10 g) and *Terrazoanthus* cf. *patagonichus* (0.308 g). Each extract was then subjected to RP-C18 vacuum liquid chromatography (VLC) (LiChroprep RP-18, 40-63 μm) using a mixture of solvents of decreasing polarity (1) H$_2$O; (2) H$_2$O/MeOH (1:1); (3) H$_2$O/MeOH (1:3); (4) MeOH; (5) MeOH/ CH$_2$Cl$_2$ (3:1); (6) MeOH/ CH$_2$Cl$_2$ (1:1); and (7) CH$_2$Cl$_2$ using 500mL of each solvent. The mobile phases used for HPLC purification of the three samples were: (A) H$_2$O/TFA 0.1%; (B) CH$_3$CN:TFA 0.1%. The aqueous-methanolic fractions F2 and F3 of *A. hickmani* were combined and purified by semi-preparative RP-HPLC with a C18 column (SymmetryPrep, 7.8 x

300 mm, 7 μm), using an isocratic method for 0-5 min with 95% A, 5% B; then a linear gradient from 5 to 20 min until 65% A, 35% B; then isocratic for 10 min at a flow rate of 3 mL/min and UV detection at λ 210 nm for 30 min leading to pure compounds valdiviamide A (**1**) (14.8 mg), valdiviamide B (**2**) (0.2 mg), valdiviamide C (**3**) (1.8 mg) and valdiviamide D (**4**) (0.2 mg).

The aqueous-methanolic fraction F3 of *P. darwini* was purified by semi-preparative RP-HPLC with a C-18 column (SymmetryPrep, 7.8 x 300 mm, 7 μm), using an isocratic method for 0-8 min with 92% A, 8% B; then a linear gradient from 8 to 25 min with 60% A, 40% B; then isocratic for 5 min at a flow rate of 3 mL/min and UV detection at λ 210 for 30 min to obtain compounds **5** (3.8 mg) and **6** (0.9 mg).

The aqueous-methanolic fractions F3 and F4 of *Terrazoanthus* cf. *patagonichus* were combined and purified by semi-preparative RP-HPLC using a C-18 column (SymmetryPrep™, 7.8 x 300 mm, 7μm), starting with an isocratic method 0-15 min with 80% A, 20% B; linear gradient for 16-30 min until 60% A, 40% B; then isocratic for 30-45 min at a flow rate of 3.5 mL/min with UV detection at λ 254 nm to yield zoamide E (**7**) (1.5 mg), zoamide F (**8**) (2.4 mg) and the known zoamide D (6.4 mg).

Valdiviamide A (**1**): amorphous yellow solid; $[\alpha]^{20}_{D}$ + 13 (*c* 0.01, CH_3CN); UV (CH_3CN) λ_{max} (log ε) 290 (3.72), 224 (4.34), 207 (4.92) nm; ECD (*c* 2.28 x 10^{-5} M, CH_3CN) λ_{max} (Δ ε) 298 (-0.32), 224 (+10.74), 212 (+26.7) nm; ^1H NMR and ^{13}C NMR data, Table 1; HRESIMS *m/z* 436.9723 [M]$^+$ (calcd for $C_{14}H_{19}Br_2N_2O_4$, 436.9706, Δ +3.8 ppm).

Valdiviamide B (**2**): amorphous white solid; $[\alpha]^{20}_{D}$ +13 (*c* 0.01, CH_3CN); UV (CH_3CN) λ_{max} (log ε) 273 (3.66), 230 (4.29) nm; ECD (*c* 2.06 x 10^{-5} M, CH_3CN) λ_{max} (Δ ε) 295 (-0.46), 255 (-1.39), 219 (+4.78), 208 (-1.06) nm; ^1H NMR data, Table 1; HRESIMS *m/z* 484.9566 [M]$^+$ (calcd for $C_{14}H_{19}BrIN_2O_4$, 484.9567, Δ -2.0 ppm).

Valdiviamide C (**3**): amorphous pale yellow; $[\alpha]^{20}_{D}$ + 12.4 (*c* 0.01, ACN); UV (ACN) λ_{max} (log ε) 290 (3.56), 224 (4.14), 207 (4.62) nm; ECD (*c* 2.15 x 10^{-5} M, ACN) λ_{max} (Δε) 277 (-0.89), 251 (-2.61), 225 (+5.19), 214 (+10.5) nm; ^1H NMR and ^{13}C NMR data, Table 1; HRESIMS *m/z* 462.9879 [M]$^+$ (calcd. for $C_{16}H_{21}Br_2N_2O_4$, 462.9863, Δ +3.4 ppm).

Valdiviamide D (**4**): amorphous white solid; $[\alpha]^{20}{}_D$ +12 (*c* 0.01, CH_3CN); UV (CH_3CN) λ_{max} (log ε) 293 (2.94), 261 (3.23), 241 (3.45), 212 (3.86) nm; ECD (*c* 1.95 x 10^{-4} M, CH_3CN) $\lambda_{max\,(\Delta\varepsilon)}$ 285 (-0.15), 251 (-0.86), 220 (+1.61), 212 (+0.59) nm; ^{1}H NMR data, Table 1; HRESIMS *m/z* 510.9749 [M]$^+$ (calcd for $C_{16}H_{21}BrIN_2O_4$, 510.9724, Δ +4.6 ppm).

2-(4-Hydroxy-3,5-diiodophenyl)-*N,N,N*-trimethylethan-1-aminium 5: amorphous white solid; UV (DAD, MeOH) λ_{max} 210 nm; ^{1}H NMR (CD_3OD, 500 MHz) δ 7.74 (2H, s, H-5/H-9), δ 3.50 (2H, AA′BB′, *J* = 9.0, 5.0 Hz, H_2-2), δ 3.18 (9H, s, N(CH$_3$)$_3$), δ 3.00 (2H, AA′BB′, *J* = 9.0, 5.0 Hz, H_2-3); ^{13}C NMR (CD_3OD, 125 MHz) δ 156.3 (C-7), δ 141.1 (C-5/C-9), δ 132.4 (C-4), δ 85.5 (C-6/C-8), δ 68.0 (C-2), δ 53.6 (N(CH$_3$)$_3$), δ 28.1 (C-3); HRESIMS*m/z* 431.9334 [M]$^+$ (calcd for $C_{11}H_{16}I_2NO$, 431.9316, Δ +4.1 ppm).

2-(4-Hydroxy-3-bromo-5-iodophenyl)-*N,N,N*-trimethylethan-1-aminium 6: amorphous white solid; UV (DAD, MeOH) λ_{max} 210 nm; ^{1}H NMR (CD_3OD, 500 MHz) δ 7.71 (1H, d, *J* = 2.0 Hz, H-5), δ 7.51 (1H, d, *J* = 2.0 Hz, H-9), δ 3.51 (2H, AA′BB′, *J* = 9.0, 5.0 Hz, H_2-2), δ 3.19 (9H, s, N(CH$_3$)$_3$), δ 3.02 (2H, AA′BB′, *J* = 9.0, 5.0 Hz, H_2-3); ^{13}C NMR (CD_3OD, 125 MHz) δ 153.9 (C-7), δ 140.3 (C-5), δ 134.7 (C-9), δ 131.6 (C-4), δ 110.6 (C-8), δ 86.7 (C-6), δ 68.0 (C-2), δ 53.6 (N(CH$_3$)$_3$), δ 28.3 (C-3); HRESIMS *m/z* 383.9467 [M]$^+$ (calcd for $C_{11}H_{16}BrINO$, 383.9454, Δ +3.3 ppm).

Zoamide E (7): $[\alpha]^{20}{}_D$ – 20 (*c* 0.001, CH_3OH); UV (ACN) λ_{max} (log ε) 294 (4.15), 265 (4.28), 236 (4.18), 213 (4.09) nm; ECD (*c* 2.15 x 10^{-5} M, ACN) $\lambda_{max\,(\Delta\varepsilon)}$ 318 (-1.55), 303 (-9.40), 258 (-58.99), 211 (-29.02) nm; ^{1}H NMR (CD_3OD, 500 MHz) δ 5.94 (1H, septet, *J* = 1.2 Hz, H-2″), 4.30 (1H, q, *J* = 7.0 Hz, H-4), 3.05 (4H, m, H_2-8-9), 2.56 (1H, sext, *J* = 7.0 Hz, H-2′), 2.30 (3H, d, *J* = 1.0 Hz, H_3-5″), 2.01 (3H, d, *J* = 1.1 Hz, H_3-4″), 1.78 (1H, dq, *J* = 15.0, 7.5 Hz, H-3′a), 1.59 (3H, d, *J* = 7.0 Hz, H-4(CH$_3$)), 1.55 (1H, dq, *J* =15.0, 7.5 Hz, H-3′b), 1.23 (3H, d, *J* = 7.0 Hz, H_3-5′), 0.97 (3H, t, *J* = 7.5 Hz, H_3-4′); ^{13}C NMR (CD_3OD, 125 MHz) δ 177.3 (C-1′), 165.6 (C-1″), 161.8 (C-3″), 139.4 (C-6), 138.7 (C-2), 125.5 (C-4a), 125.2 (C-3a), 124.7 (C-7a), 124.5 (C-9a), 116.7 (C-2″), 43.6 (C-2′), 29.3 (C-4), 27.9 (C-

4″), 27.8 (C-3′), 23.4 (C-4(CH$_3$)), 22.7 (C-8-9), 20.7 (C-5″), 17.1 (C-5′), 11.8 (C-4′); HRESIMS m/z 385.2358 [M+H]$^+$ (calcd. for C$_{20}$H$_{29}$N$_6$O$_2$, 385.2347, Δ +2.8 ppm).

Zoamide F (8): [α]^{20}$_D$ - 4 (c 0.005, CH$_3$OH); UV (CH$_3$CN) λ_{max} (log ε) 374 (1.25), 266 (2.49), 230 (2.36), 212 (2.28) nm; ECD (c 1.35 x 10^{-3} M, CH$_3$CN) $\lambda_{max\,(\Delta\varepsilon)}$ 293 (-0.01), 268 (-0.05),215 (+0.04) nm; ^{1}H NMR (CD$_3$OD, 125 MHz) δ 5.94 (1H, septet, J = 1.2 Hz, H-2″), 4.31 (1H, q, J = 7.0 Hz, H-4), 3.06 (4H, m, H$_2$-8-9), 2.75 (1H, septet, J = 7.0 Hz, H-2′), 2.30 (3H, d, J = 1.0 Hz, H$_3$-5″), 2.01 (3H, d, J = 1.0 Hz, H$_3$-4″), 1.59 (3H, d, J = 7.0 Hz, H-4(CH$_3$)), 1.25 (6H, d, J = 7.0 Hz, H$_3$-3′-4′); ^{13}C NMR (CD$_3$OD, 125 MHz) δ 177.8 (C-1′), 165.6 (C-1″), 161.8 (C-3″), 139.4 (C-6), 138.9 (C-2), 124.7 (C-7a, C-9a), 125.2 (C-3a, C-4a), 116.7 (C-2″), 36.5 (C-2′), 29.3 (C-4), 27.8 (C-4″), 23.4 (C-4(CH$_3$)), 22.7 (C-8-9), 20.7 (C-5″), 19.2 (C-3′-4′); HRESIMS m/z 371.2202 [M+H]$^+$ (calcd for C$_{19}$H$_{26}$N$_6$O$_2$, 371.2190, Δ + 3.2 ppm).

Computational Methods. The methods used for the calculation of ECD spectra are as described previously.[42] The conformational analysis of each compound was performed with Schrodinger MacroModel 2018 as described by Willoughby et al.[43] Using density functional theory (DFT), at the w, the conformers were optimized using Gaussian 16. At the same time, the zero-point energy, electronic transition and rational strength of all conformers were calculated.[44] The ECD spectra were calculated using Gaussian 16 at the B3LYP/6-311+G(d) level, and spectra were produced and corrected with the UV spectra using the freely available software SpecDis 1.7.[45] NMR properties were predicted at the B3LYP/6-31g(d)// MPW1PW91/6-311+g(2d) level on the four most stable confirmers (conformational analysis performed using the GMMX module implemented in Gaussian 16). DP4 probabilities were calculated using an in-house implementation of the Goodman original script.

Bioactivity Tests. The antimicrobial activity of compounds 1-8 was tested against a panel of human pathogens including Gram-positive (*S. aureus* ATCC29213 (MSSA), and *S. aureus* MB5393 (MRSA)) and Gram-negative bacteria (*E. coli* ATCC25922, *K. pneumoniae* ATCC700603, *P. aeruginosa* PAO1, and *A. baumannii* MB5973), and a yeast (*C. albicans* ATCC64124), following previously described methodologies.[46,47] Cytotoxic activities of compounds **1-3** and **5-8** against the human-derived cell lines

A549 (lung carcinoma), HepG2 (hepatocellular carcinoma), and MIA PaCa-2 (pancreatic carcinoma) were determined as previously reported.[48]

ASSOCIATED CONTENT

Supporting Information.

The Supporting Information is available free of charge on the ACS Publications website at DOI:

Biological description of the species; UV, ECD, NMR, MS data of compounds **1-8** together with the IR spectrum of **1** and computational analyses for compounds **3** and **8**.

AUTHOR INFORMATION

Corresponding Author

*Tel.: +353-(0)91493563. E-mail: olivier.thomas@nuigalway.ie

Author Contributions

The manuscript was written through contributions of all authors. All authors have given approval to the final version of the manuscript.

Notes

The authors declare no competing financial interest.

REFERENCES
(1)   Dembitsky, V. M. *Russ. J. Bioorganic. Chem.* **2002,** 28, 170-182.
(2)   Gschwend, P. M.; Macfarlane, J. K.; Newman, K. A. *Science* **1985,** 227, 1033.
(3)   Nongmaithem, B. D.; Mouatt, P.; Smith, J.; Rudd, D.; Russell, M.; Sullivan, C.; Benkendorff, K. *Sci. Rep.* **2017,** 7, 17404.
(4)   Rocha, J.; Peixe, L.; Gomes, N. C. M.; Calado, R. *Mar. Drugs.* **2011,** 9, 1860-1886.
(5)   Fielman, K. T.; Woodin, S. A.; Walla, M. D.; Lincoln, D. E. *Mar. Ecol. Prog. Ser.* **1999,** 181, 1-12.
(6)   Fenical, W., Natural Halogenated Organics. In *Elsevier Oceanography Series*, Duursma, E. K.; Dawson, R., Eds. Elsevier: 1981; Vol. 31, Chapter 12, pp 375-393.
(7)   Pauletti, P. M.; Cintra, L. S.; Braguine, C. G.; da Silva Filho, A. A.; Silva, M. L. A. e.; Cunha, W. R.; Januário, A. H. *Mar. Drugs.* **2010,** 8, 1526-1549.
(8)   Sillen, L. G. *Science* **1967,** 156, 1189-1197.
(9)   Butler, A.; Walker, J. V. *Chem. Rev.* **1993,** 93, 1937-1944.
(10)   Fournier, J.-B.; Rebuffet, E.; Delage, L.; Grijol, R.; Meslet-Cladière, L.; Rzonca, J.; Potin, P.; Michel, G.; Czjzek, M.; Leblanc, C. *Appl. Environ. Microbiol.* **2014,** 80, 7561-7573.
(11)   Agarwal, V.; Miles, Z. D.; Winter, J. M.; Eustáquio, A. S.; El Gamal, A. A.; Moore, B. S. *Chem. Rev.* **2017,** 117, 5619-5674.
(12)   Makarieva, T. N.; Stonik, V. A.; Alcolado, P.; Elyakov, Y. B. *Comp. Biochem. Physiol. B.* **1981,** 68, 481-484.
(13)   Lira, N. S.; Montes, R. C.; Tavares, J. F.; da Silva, M. S.; da Cunha, E. V. L.; de Athayde-Filho, P. F.; Rodrigues, L. C.; da Silva Dias, C.; Barbosa-Filho, J. M. *Mar. Drugs.* **2011,** 9, 2316-2368.
(14)   Niemann, H.; Marmann, A.; Lin, W.; Proksch, P. *Nat. Prod. Commun.* **2015,** 10, 219-231.
(15)   Yin, S.; Cullinane, C.; Carroll, A. R.; Quinn, R. J.; Davis, R. A. *Tetrahedron Lett.* **2010,** 51, 3403-3405.
(16)   McDonald, L. A.; Christopher Swersey, J.; Ireland, C. M.; Carroll, A. R.; Coll, J. C.; Bowden, B. F.; Fairchild, C. R.; Cornell, L. *Tetrahedron.* **1995,** 51, 5237-5244.
(17)   Rao, M. R.; Faulkner, D. J. *J. Nat. Prod.* **2004,** 67, 1064-1066.
(18)   Won, H. T.; Kim, C.-K.; Lee, S.-H.; Rho, J. B.; Lee, K. S.; Oh, D.-C.; Oh, K.-B.; Shin, J. *Mar. Drugs.* **2015,** 13, 3836-3848.
(19)   Carroll, A.; Bowden, B.; Coll, J. *Aust. J. Chem.* **1993,** 46, 825-832.
(20)   Aiello, A.; Fattorusso, E.; Imperatore, C.; Menna, M.; Müller, W. E. G. *Mar. Drugs.* **2010,** 8, 285-291.
(21)   Pettit, G. R.; Butler, M. S.; Williams, M. D.; Filiatrault, M. J.; Pettit, R. K. *J. Nat. Prod.* **1996,** 59, 927-934.
(22)   Galeano, E.; Thomas, O. P.; Robledo, S.; Munoz, D.; Martinez, A. *Mar. Drugs.* **2011,** 9, 1902-1913.
(23)   Fukuzawa, S.; Hayashi, Y.; Uemura, D.; Nagatsu, A.; Yamada, K.; Ijuin, Y. *Heterocyclic. Commun.* **1995,** 1, 207-214.
(24)   Rao, C. B.; Anjaneyula, A. S. R.; Sarma, N. S.; Venkatateswarlu, Y.; Rosser, R. M.; Faulkner, D. J.; Chen, M. H. M.; Clardy, J. *J. Am. Chem. Soc.* **1984,** 106, 7983-7984.
(25)   Komoda, Y.; Kaneko, S.; Yamamoto, M.; Ishikawa, M.; Itai, A.; Iitaka, Y. *Chem. Pharm. Bull.* **1975,** 23, 2464-2465.
(26)   Cariello, L.; Crescenzi, S.; Prota, G.; Giordano, F.; Mazzarella, L. *J. Chem. Soc., Chem. Commun.* **1973**, 99-100.
(27)   Suksamrarn, A.; Jankam, A.; Tarnchompoo, B.; Putchakarn, S. *J. Nat. Prod.* **2002,** 65, 1194-1197.
(28)   Sturaro, A.; Guerriero, A.; De Clauser, R.; Pietra, F. *Experientia* **1982,** 38, 1184-1185.
(29)   Carballeira, N. M.; Reyes, M. *J. Nat. Prod.* **1995,** 58, 1689-1694.
(30)   Cachet, N.; Genta-Jouve, G.; Regalado, E. L.; Mokrini, R.; Amade, P.; Culioli, G.; Thomas, O. P. *J. Nat. Prod.* **2009,** 72, 1612-1615.
(31)   Audoin, C.; Cocandeau, V.; Thomas, O. P.; Bruschini, A.; Holderith, S.; Genta-Jouve, G. *Metabolites* **2014,** 4, 421-432, 12 pp.

(32)   Hsu, Y.-M.; Chang, F.-R.; Lo, I. W.; Lai, K.-H.; El-Shazly, M.; Wu, T.-Y.; Du, Y.-C.; Hwang, T.-L.; Cheng, Y.-B.; Wu, Y.-C. *J. Nat. Prod.* **2016,** 79, 2674-2680.

(33)   Guillen, P. O.; Jaramillo, K. B.; Genta-Jouve, G.; Sinniger, F.; Rodriguez, J.; Thomas, O. P. *Org. Lett.* **2017,** 19, 1558-1561.

(34)   Guillen, P. O.; Calabro, K.; Jaramillo, K. B.; Dominguez, C.; Genta-Jouve, G.; Rodriguez, J.; Thomas, O. P. *Mar. Drugs.* **2018,** 16, 58.

(35)   Guillen, P.; Gegunde, S.; Jaramillo, K.; Alfonso, A.; Calabro, K.; Alonso, E.; Rodriguez, J.; Botana, L.; Thomas, O. *Mar. Drugs.* **2018,** 16, 242.

(36)   Jaramillo, K. B.; Guillen, P. O.; Rodriguez, J.; McCormack, G.; Reverter, M.; Thomas, O. P.; Sinniger, F. *Sci. Rep.* **2018,** 8, 7138.

(37)   Smith, S. G.; Goodman, J. M. *J. Am. Chem. Soc.* **2010,** 132, 12946-12959.

(38)   Sakiyama, F.; Irreverre, F.; Friess, S. L.; Witkop, B. *J. Am. Chem. Soc.* **1964,** 86, 1842-1844.

(39)   Cachet, N.; Genta-Jouve, G.; Ivanisevic, J.; Chevaldonné, P.; Sinniger, F.; Culioli, G.; Pérez, T.; Thomas, O. P. *Sci. Rep.* **2015,** 5, 8282.

(40)   D'Ambrosio, M.; Roussis, V.; Fenical, W. *Tetrahedron Lett.* **1997,** 38, 717-720.

(41)   Pescitelli, G.; Bruhn, T. *Chirality* **2016,** 28, 466-474.

(42)   Robertson, L. P.; Duffy, S.; Wang, Y.; Wang, D.; Avery, V. M.; Carroll, A. R. *J. Nat. Prod.* **2017,** 80, 3211-3217.

(43)   Willoughby, P. H.; Jansma, M. J.; Hoye, T. R. *Nat. Prot.* **2014,** 9, 643.

(44)   Tomasi, J.; Mennucci, B.; Cammi, R. *Chem. Rev.* **2005,** 105, 2999-3094.

(45)   Bruhn, T.; Schaumlöffel, A.; Hemberger, Y.; Bringmann, G. *Chirality* **2013,** 25, 243-249.

(46)   Audoin, C.; Bonhomme, D.; Ivanisevic, J.; Cruz, D. M.; Cautain, B.; Monteiro, C. M.; Reyes, F.; Rios, L.; Perez, T.; Thomas, P. O. *Mar. Drugs.* **2013,** 11.

(47)   Braña, A. F.; Sarmiento-Vizcaíno, A.; Pérez-Victoria, I.; Otero, L.; Fernández, J.; Palacios, J. J.; Martín, J.; de la Cruz, M.; Díaz, C.; Vicente, F.; Reyes, F.; García, L. A.; Blanco, G. *J. Nat. Prod.* **2017,** 80, 569-573.

(48)   Cautain, B.; de Pedro, N.; Schulz, C.; Pascual, J.; da S. Sousa, T.; Martin, J.; Pérez-Victoria, I.; Asensio, F.; González, I.; Bills, G. F.; Reyes, F.; Genilloud, O.; Vicente, F. *Plos One* **2015,** 10, e0125221.

6 Discussion

The present study is the first description of the chemical diversity of zoantharians inhabiting the Tropical Eastern Pacific Coast of Ecuador, as part of the first National Project directed to characterize the bio and chemo diversity of marine invertebrates from the Marine Protected Area El Pelado (REMAPE). Different groups of invertebrates were observed such as octocorals, ahermatypic corals, sponges, ascidians and zoantharians. The latter ones were one of the most representative invertebrates inhabiting this area and no chemical investigation have been reported from these species. A total of eight organisms were identified and analyzed during this project and corresponded to the following: *Terrazoanthus patagonichus* (formerly known as *T. onoi*), *Terrazoanthus* cf. *patagonichus*, *Terrazoanthus* sp. (white), *Zoanthus* cf. *pulchellus*, *Zoanthus* cf. *sociatus*, *Antipathozoanthus hickmani*, *Parazoanthus darwini* and *Palythoa* cf. *mutuki*. The zoantharians *Zoanthus* cf. *sociatus*, *Terrazoanthus* sp., and *Palythoa* cf. *mutuki* were also investigated for their chemical diversity during this project. However, due to the limited amount of collected sample and the purified compounds, it was not possible to characterize the isolated metabolites.

6.1 Biological activities

6.1.1 *Terrazoanthus patagonichus* and *T.* cf. *patagonichus*

Terrazoanthines A-C (**182**-**184**) isolated from *T.* cf. *patagonichus*, are the first members of a new family of 2-aminoimidazole alkaloids featuring the 2-aminoimidazole ring fused to a cyclohexane as observed for terrazoanthines A-B (**182**-**183**). The fusion of 2-aminoimidazole to other rings have been observed in analogues such as agelamide J, agelamadin A and B featuring the 2-aminoimidazole ring fused to a cyclopentane [243]. Additionally, terrazoanthines are closely related to the zoanthoxanthin alkaloids isolated from zoantharian species. In fact, the study of *Terrazoanthus* cf. *patagonichus* let to the identification of two zoanthoxanthin derivatives zoamide E-F (**185**-**186**). The bioactivity results of these compounds will be discussed herein. The guanidine alkaloids have been isolated from several marine organisms such as marine algae, mollusks, ascidians but sponges have been the main source of these alkaloids. Most of the guanidine derivatives have shown activity as antibacterial, antiviral, anticancer, antiparasitic and enzymatic inhibitor agent among others. Several reviews of this family of alkaloids have been published highlighting the diversity of structures, their biological activity and chemical synthesis [244, 245]. The interest on these alkaloids for their potential as drug leads relies on the specific hydrogen/ionic interactions of the guanidinium cation with other functional groups which is enhanced by the strong basic

character of guanidine (pk$_a$=13.6) [246]. A subclass of the guanidine alkaloids includes the amino imidazole which have also been characterized by their potential pharmacological activities of the isolated natural products or through the synthesis of several derivatives. Some of the 2-aminoimidazole derivatives displayed selective adenosine receptor antagonist, antibacterial, different enzyme inhibitor, antifouling, biofilm inhibitor, and cytotoxic activities [247-249]. However, two of the most promising activities for this class of compounds are their antibiofilm and antifouling activity [250, 251]. The variation of the biological activity displayed by these alkaloids could be explained by the difference observed in their chemical structures. In fact, studies on the structure-activity relationships (SAR) of 2-aminoimidazole derivatives revealed an increasing or decreasing in the bioactivity when the structures have suffered some modifications [251]. In our study, terrazoanthines A-C were analyzed for their biological activity against Gram-positive (methicillin resistant *Staphylococcus aureus*, MRSA and MSSA) and Gram-negative (*Acinetobacter baumannii*, *Escherichia coli*, *Klebsiella pneumoniae* and *Pseudomonas aeruginosa*) bacteria, for their antifungal activity against *Aspergillus fumigatus*, and their cytotoxicity against human liver tumor cell line (HepG2). The limited amount of pure compounds impeded to test them in a wide range of bioassays. Despite the negative results for these compounds, there is a lot of potential for testing terrazoanthines as antifouling and antibiofilm agents and against other different bioactivities including cancer cell lines.

The zoanthoxanthin alkaloids and its analogues have shown papaverine-like activity, histamine-like activity, acetylcholinesterase (AChE) inhibition and parazoanthoxanthin A (**130**) have shown affinity to bind the nicotinic acetylcholine receptors (nAChR) through a competitive mechanism of action [145]. Also, a moderate antiviral activity against the Herpes simplex virus (HSV-1) was observed in a pseudozoanthoxanthin analogue isolated from the Sea gorgonian *Echinogorgia pseudossapo* [252]. In our study, zoamides E-F (**185-186**) were subjected to antimicrobial and cytotoxic activity against several cancer cell lines. These compounds did not displayed activity in any of the bioassays even at the highest concentration tested (128 µg/mL). Our results corroborate what has been reported in the literature up to date, none of the members of this family of alkaloids exhibits cytotoxic or antimicrobial activity. However, there is potential applications for these alkaloids as anticholinesterase inhibitors and further biological studies with zoamides E-F and terrazoanthines A-C should be carried out to find potential pharmaceutical or biotechnological applications.

6.1.2 *Zoanthus* cf. *pulchellus*

The zoanthamines are a very interesting family of alkaloids characterized by their unique structural framework and their wide range of biological activities. One of the most promising bioactivities reported is the antiosteoporotic activity exhibited by norzoanthamine and its hydrochloride analogue. It has been

observed that norzoanthamine prevents the osteoporosis symptoms in ovariectomized mice, commonly used as a model for postmenopausal osteoporosis in the pharmaceutical industry and also it suppresses interleukin-6 (IL-6) production which is a mediator of bone resorption caused by estrogen deficiency [74]. Kinugawa *et al*., studied the anti-osteoporotic mechanisms of action of norzoanthamine suggesting a non-specific binding to collagen. This association stabilizes its secondary structure enhancing bone formation. Norzoanthamine also prevent the proteolysis of elastin and bovine serum albumin by protecting the substrate from proteolytic cleavage rather than inhibiting protease activity [156]. Furthermore, Gengi *et al*., analyzed the distribution and the possible function of norzoanthamine. The results revealed a high concentration of the alkaloid in the epidermal tissue of *Zoanthus* sp., and suggested a possible collagen protective function in *Zoanthus* by increasing its resistance to external stresses such as UV irradiation [157]. Other bioactivities reported from zoanthamine alkaloids includes inhibition of inflammation induced by phorbol myristate acetate (PMA) in mouse ears, cytotoxic activity against murine leukemia cells (P388), antibacterial activity and inhibition of platelet aggregation caused by collagen, arachidonic acid and thrombin, which makes these alkaloids potential drug candidates in the treatment of cardiovascular diseases. In fact, Villar *et al*., evaluated the human platelet aggregation activity of ten zoanthamine alkaloids and one semi-synthetic analogue and their structure activity relationship. Their results showed a strong inhibition of platelet aggregation induced by thrombin, collagen and arachidonic acid for 11-hydroxyzoanthamine, and the synthetic norzoanthamine analogue. The structure activity relationship (SAR) revealed that small changes in the zoanthamine structure would enhance or diminish their biological activities [161]. The potential bioactivities displayed by these family of alkaloids has convinced scientist to continuously work on different mechanisms of action. During our study, we isolated two new zoanthamine analogues; 3-acetoxynorzoanthamine (**118**) and 3-acetoxyzoanthamine (**119**) along with the known norzoanthamine (**87**), zoanthamine (**81**) and 3-hydroxynorzoanthamine (**94**). We reported a new activity for these alkaloids as protective agents in neuroinflammatory processes using the BV2-microglia cell line commonly used as a model for neuroinflammatory studies. These alkaloids showed no-citotoxicity effect in the cell viability assay supporting their potential as a therapeutic agent. Even if compounds **81** and **118** exhibited a dose-dependent activity, the efficacy observed for **87**, **94** and **119** at the different concentration used from 0.001 to 10 µM, clearly demonstrate a potential application as antioxidant and neuroprotective agents. The diverse biological activities and diverse mechanisms of action reported for zoanthamine alkaloids certainly reveals a bright future as therapeutics.

6.1.3 *Zoanthus* **cf.** *sociatus*

Even though, no compounds were characterized from this species, there is a lot of potential for uncovering its chemical diversity and biological activities. The reported bioactivities includes the inhibition of insulin

secretion via Ca^{2+} channel exhibited by the crude extract of the low molecular weight fraction from the Cuban *Zoanthus sociatus* reported by Garcia *et al*., and the presence of toxins with molecular weight from 2 to 6 KDa related to the insulin and ω-conotoxin GVIA, a potent inhibitor of neuronal N-type Ca^{2+} channel [193, 194]. Furthermore, the presence of toxins in this species should also be considered as the cyanotoxin microcystin-LR was reported from the low molecular weight fraction from *Z. sociatus* [195]. These evidences clearly support further chemical investigation of *Z.* cf. *sociatus*.

6.1.4 *Antipathozoanthus hickmani* and *Parazoanthus darwini*

The first natural products isolated from *A. hickmani* were the ecdysteroids derivatives ecdysonelactones A-D (**163**-**166**), characterized by the presence of a γ-lactone fused to ring A of the ecdysteroid skeleton. The role of ecdysteroids in zoantharians is not clear and relatively few cases of bioactivity exhibited by these natural products have been reported. An oxytocic activity was reported for 2-deoxyecdysterone (**67**) suggesting possible applications as labour inducer, to control post partum uterine atony and hemorrhage, to produce uterine contraction after cesarean or during uterine surgery or to induce therapeutic abortion [141]. The effects of **67** was compared to those standard agents like oxytocin and $PGF_{2\alpha}$. A potential anti-dengue virus activity was reported from ecdysteroids isolated from *Zoanthus* spp. For example, zoanthone A (**75**) displayed potential antiviral activity against dengue virus type 2 (DENV-2) while ajugasterone C (**73**) showed activity against all dengue virus serotypes. During the study carried out by Cheng *et al*., revealed that modifications of the hydroxyl groups and the side chain influence in the activity of ecdysteroids but most important that the carbonyl group at C-6 and the OH at C-2 are essential for their bioactivities [143]. Lactone containing compounds isolated from different sources have shown different biological activities. In particular, γ-lactones have exhibited bioactivity as antiviral, anticancer, antibacterial, antimalarial, anti-inflammatory among others [253]. The presence of the γ-lactone in the structure of the ecdysteroid could represent an opportunity for finding a different bioactivity from those analogues previously reported. In general, ecdysteroids and its derivatives do not represent a potential source for pharmaceutical applications except for 2-deoxyecdysterone and ajugasterone C described above. Since these natural products seems to be present in all zoantharians, it is necessary to assess their role in these marine invertebrates. Ecdysonelactones A-D (**163**-**166**) were analyzed for their biological activity against Gram-positive and Gram-negative bacteria, antifungal and cance cell lines. These compounds did not display significant activity in the bioassays. Despite the negative results showed by ecdysonelactones A-D, further pharmacological studies with these compounds and their ecological role needs to be assessed.

The second family of natural products isolated from *A. hickmani* are the halogenated dipeptides valdiviamides A-D (**199**-**202**) characterized by the presence of bromine and iodine in the phenol ring. In

addition to this family of halogenated alkaloids, the first chemical study of *Parazoanthus darwini* led us to the isolation and identification of two halogenated tyramine derivatives (**197**-**198**). Therefore, we will also discuss the potential bioactivities of these halogenated alkaloids in this section. An interesting review of bromotyrosine derivatives from marine organisms by Peng *et al.*, revealed the vast range of biological activities including antibacterial, antifungal, anticancer, antiproliferative, antifeedant, antifouling, antimalarial and as Na^+, K^+-ATPase inhibitor [254]. Different classes of natural products from simple halogenated tyrosine derivatives to more complex structures like bastadins have been reported, and the variation of bioactivities is influenced by their different chemical scaffolds and the halogen atom present in the natural product. For example, iodocionin, a iodinated tyramine derivative displayed selective activity against mouse lymphoma (L5178Y) while its brominated analogue did not exhibit activity at all [255]. This result encourages to continue looking further biological activities with the tyramine derivatives (**197**-**198**) from *P. darwini*. In another study, Kim *et al.*, indicated that a potential competitive angiotensin-converting enzyme (ACE) inhibitory peptide required the location of either amino acid residue tryptophan, tyrosine, phenylalanine or proline at the C-terminal and branched-chain aliphatic amino acids at the N-terminal [256]. Interestingly, it has been observed that short-chain peptides showed better ACE inhibitory activity when a hydrophobic amino acid was at the N-terminus such as proline or glycine. Based on these features, valdiviamides A-D represent potential candidates for the ACE inhibitory activity. During our study, valdiviamide B (**200**) was the only dipeptide that exhibited moderate activity against hepatocellular carcinoma (HepG2) with an IC_{50} value of 7.8 µM.

6.1.5 *Palythoa* **cf.** *mutuki*

The bioactivity guided assay of the aqueous/methanolic fraction of *Palythoa* cf. *mutuki* revealed high toxicity in the antibacterial, cytotoxic and antileishmanial assays. The high toxicity exhibited by these fractions could be explained by the presence of palytoxin, one of the most toxic compounds or by the presence of different toxic peptides as reported from other *Palythoa* species. Therefore, it is necessary to determine the chemical content of *P.* cf. *mutuki* and investigate the presence of toxins. There is an important matter to address regarding the presence of palytoxin in zoantharians. The use of different species of *Palythoa* and other zoantharians in home aquariums is becoming a health problem. The bright and fluorescence colors displayed by these sessile invertebrates attracts anyone's attention for decoration of aquariums. However, most of the species being sold are not assess for their toxin content and several cases of palytoxin intoxication through steam inhalation, ocular exposure or skin contact while cleaning aquariums have already been recorded [117]. Deeds *et al.*, reported high concentrations of the toxin in four different zoantharian species sold in aquarium stores clearly demonstrating the high health-related risk of having these organisms at home [119]. In addition, the presence of *Palythoa* and *Zoanthus* species close to

crowded beaches is another potential problem that should be considered. This is the case of *Palythoa* cf. *mutuki*, *Zoanthus* cf. *pulchellus* and *Zoanthus* cf. *sociatus* collected during this study. These invertebrates are found in a large surface area close to Ayangue beach, and this area is also very common for fisheries. Therefore, studies to determine the presence of palytoxin in these species of zoantharians should be carried out to prevent any palytoxin intoxication outbreak. On the other hand, other toxins have been reported from species of the genus *Palythoa* and *Protopalythoa*. For example, Pettit *et al.*, reported the identification of bioactive peptides such as palystatins 1-3 and palystatins A-D from *P. liscia* collected off Mauritius [181, 182]. Later, the toxic peptide characterized by an unusual V-shape α-helical structure with only one disulphide bridge was isolated from the low molecular weight fraction of the Mexican *P. caribaeorum* by Perez *et al* [183], and a similar peptide analogue was identified from *Protopalythoa variabilis* by Liao *et al* [189]. Furthermore, several putative neurotoxic-related peptides and three kunitz-like peptides (PcKuz 1-3) were described from the Brazilian Zoantharians *Protopalythoa variabilis* and *P. caribaeorum* respectively through their transcriptome analysis [184, 186]. Moreover, *Palythoa* species also represent a vast source of enzymes with potential biological and biotechnological applications. A neurotoxic phospholipase A2-PLTX-Pcb1a was reported from the Mexican zoantharian *P. caribaeorum* by Cuevas-Cruz *et al.*, and four bioactive metalloproteases were described from the mucus of the Brazilian *P. caribaeorum* [185, 188]. The transcriptome study of the Brazilian *Protopalythoa variabilis* showed the predictive expression of 13 multifunctional enzymes and 694 enzyme sequences with different activities distributed in 23 sub-subclasses [257]. Most of these enzymes were found with valuable applications in the pharmaceutical, industrial, green organic synthesis and biotechnological industry. The reports of toxic peptides have been limited to two *Palythoa* and one *Protopalythoa* species. Therefore, it is necessary to assess the enzymatic content and determine the presence of bioactive peptides in *Palythoa* cf. *mutuki* and other *Palythoa* species to compare their variability based on their geographical distribution.

In general, if we compare the different biological activities and other applications achieved by natural products isolated from species of zoantharians, the most promising ones with higher toxicity and potential applicability in the pharmaceutical or biotechnological industry are those isolated from species of the suborder Brachycnemina. Some examples include the bioactive alkaloids zoanthamines being the most promising as anti-osteoporotic agents, fluorescent proteins for *in vivo* labelling isolated from *Zoanthus* species, or several mycosporine-like amino acids as components for sunscreen products, to neurotoxins and the most famous non-peptide toxin like palytoxin with potent cytotoxic activity isolated from *Palythoa* species. Interestingly, the presence of several toxins seems to be more common in species of the genus *Palythoa* than in species of the genus *Zoanthus*, and absent from the suborder Macrocnemina. However, the potential of natural products from species of the suborder Macrocnemina should not be discourage since relatively few chemical studies have been carried out on those species in comparison with Brachycnemina

which is the most studied among zoantharians. There is a bright future for discovering new natural products with potential applications and bioactivities from both suborders of zoantharians and the chemical diversity of these interesting invertebrates are still surprising.

6.2 **Chemotaxonomic markers**

6.2.1 Terrazoanthus patagonichus and T. **cf.** *patagonichus*

This is the first study of the chemical diversity of species belonging to the relatively new genus *Terrazoanthus*. Terrazoanthines A-C (**182**-**184**) isolated from *Terrazoanthus patagonichus* and the zoanthoxanthin derivatives zoamides E-F (**185**-**186**) isolated from *Terrazoanthus* cf. *patagonichus* are closely related compounds as they seem to be originated from the same precursor, a C5N3 unit like arginine. The proposed biosynthetic pathway for terrazoanthines involves a [4+2] Diels-Alder cycloaddition while a [6+2] cycloaddition is involved in the synthesis of zoanthoxanthins [230]. It is interesting to highlight the presence in nature of enzymes capable of realize a Diels-Alder reaction and some reports have proven its occurrence [258, 259]. From a chemo taxonomy point of view, a common feature observed in both family of alkaloids isolated from *Terrazoanthus* species is the acylation of the guanidine moiety to form the 2-methyl butyryl unit, a structural part seen in terrazoanthine A (**182**) and zoamide E (**185**). Since, no other compounds with this chemical feature has been reported from zoantharians, we suggest that acylation occurs exclusively in species of the genus *Terrazoanthus*. Even though, zoamides A-D were reported from an unidentified *Parazoanthus* sp., collected from the coast of Philippines, the lack of the taxonomy identification raises the question of the identity of the organism. Therefore, a proper taxonomic identification of *Parazoanthus* sp., from the Philippines is required. In the case that *Parazoanthus* sp., is in fact a species of *Terrazoanthus*, we could propose zoamides as chemical markers for the genus *Terrazoanthus*. Even though, we isolated two zoamides from *T.* cf. *patagonichus* as the major metabolites present in the aqueous/methanolic fraction, the little amount of starting material limited us to obtain enough amount of other metabolites that could have helped to assess other possible chemical markers for this species. It is necessary to analyze the MS profile of the methanolic fraction of *T.* cf. *patagonichus* to deeply investigate the presence of terrazoanthines in this organism. Despite the similar biosynthetic pathway between terrazoanthines and zoanthoxanthin derivatives, and unlike the zoanthoxanthin analogues which are present in other zoantharians, terrazoanthines have only been described in *Terrazoanthus patagonichus*, and this new family of alkaloids could be considered as chemical marker for this species. Furthermore, the sample known as *Terrazonthus* sp., was also analyzed for its chemical composition. Although, no

metabolites were fully characterized due to the low amount of the isolated ones, the absence of terrazoanthines was noticed in the metabolomic study of this organism. This result reinforces the hypothesis to consider these 2-aminoimidazole alkaloids as chemical marker for the species *T. patagonichus*.

6.2.2 *Zoanthus* cf. *pulchellus*

The chemical study of *Zoanthus* cf. *pulchellus* led to the isolation of 3-acetoxynorzoanthamine (**118**) and 3-acetoxyzoanthamine (**119**), two new members of the bioactive zoanthamine family of alkaloids. Within zoantharians, the isolation of zoanthamine alkaloids have only been described in species of the genus *Zoanthus*. However, a structurally similar natural product zooxanthellamine was isolated from the dinoflagellate *Symbiodinium* sp., and lobozoanthamine from the soft coral *Lobophytum* sp. [260, 261]. Recently, Costa-Lotufo reported the presence of zoanthamine alkaloids from *Palythoa caribaeorum* and *P. variabilis* based on MS/MS fragmentation pattern and Global Molecular Networking analysis (GNPS) [180]. This result should be carefully considered as there is no taxonomic identification of these samples and no other publication supports the presence of zoanthamine alkaloids in *Palythoa* species. However, species of the genus *Palythoa* and *Zoanthus* are characterized by their association with symbiotic algae of the genus *Symbiodinium* [262]. Since it has been suggested that dinoflagellates of this genera are responsible for producing zooxanthellamine which is considered a precursor of zoanthamine, it is possible that the MS/MS fragmentation pattern observed in the analysis is originated from species of *Symbiodinium* present is those species of *Palythoa*. In addition, it is important to properly described the species to accurately determine certain compounds or family of compounds as possible chemical markers that will help in the taxonomical identification at species level. For example, the zoanthamine analogues kuroshines have only been described from *Z. Kuroshio*, therefore these alkaloids should be considered specific markers for this species. Considering the difficulty presented to properly identify these group of organisms, the use of complementary tools such as molecular analysis and metabolomics is helping to overcome this issue. In fact, the metabolomic study of the zoantharians from the Tropical Pacific Coast of Ecuador demonstrated the efficiency of this complementary tool in the taxonomical identification of these organisms [65]. During this project, the zoantharian *Zoanthus* cf. *sociatus* collected in the same area as *Zoanthus* cf. *pulchellus* was also studied. Interestingly, no zoanthamine alkaloids were isolated from *Z.* cf. *sociatus* and the metabolomic study confirmed the absence of these alkaloids in the sample. As already mentioned, *Zoanthus* species are characterized by their association with dinoflagellates from the genus *Symbiodinium*. Since Nakamura *et al*., reported the isolation of zooxanthellamine from *Symbiodinium* sp., suggesting zooxanthellamine as a precursor for the biosynthesis of zoanthamines [260]. Therefore, the absenteeism of the associated symbiont responsible to produce the zoanthamine precursor in *Zoanthus* cf. *sociatus* could explain the absence of these alkaloids in the organism or that the species considered as *Zoanthus* cf. *sociatus* is a different one.

Further studies to characterize the associated symbionts of both zoantharians and their chemical diversity should be carried out to confirm our hypothesis and to provide strong evidence of the biosynthesis of zoanthamines. In addition, the synthesis of norzoanthamine was achieved by the group of Miyashita in 41 steps. One of the reactions used in the synthesis was a Diels-Alder reaction for the construction of the ABC ring system. Since the presence of diels alderases in nature has been proven and proposed to be involved in the biosynthesis of terrazoanthines [230], it seems that *Zoanthus* species or its associated symbionts also possesses these enzymes. Therefore, studies on the enzyme content in zoantharias should be carried out to confirm the hypothesis of the presence of diels alderases in zoantharians.

6.2.3 *Antipathozoanthus hickmani* and *Parazoanthus darwini*

Ecdysteroids are the most common metabolites reported from most of zoantharian species. Only species of *Epizoanthus* have not yet been reported to produce these compounds. The relatively few chemical studies on this genus have limited our knowledge of their chemical diversity. Therefore, based on the available data of the chemical diversity of zoantharians, ecdysteroids should be considered as chemical markers of the order Zoantharia. Despite the wide distribution of these natural products among these invertebrates, *A. hickmani* is the producer of a new class of ecdysteroids derivatives named ecdysonelactones A-D (**163**-**166**) characterized by the presence of a γ-lactone ring fused to ring A of the ecdysteroid skeleton. The presence of very reactive secondary alcohols at C-2 and C-3 position of ring A are suitable to acetylation at C-3 and oxidation at C-2 position and the cyclization reaction is suggested to be catalyzed by an enzyme. The presence of the enzyme is important to consider as it could be specific for the genus *Antipathozoathus* or even specific for *A. hickmani*, since ecdysteroids with an acetyl group at C-3 has been reported from *Palythoa*, *Zoanthus* and *Parazoanthus* species. It is necessary to investigate the chemical and enzyme diversity of other species of *Antipathozoanthus* to determine the presence of ecdysonelactones in other members of this genus to conclusively assigned these ecdysteroids derivatives as chemical markers at genus/species level.

On the other hand, bromotyrosine derivatives are very interesting compounds with different chemical scaffolds, which varies from simple bromotyrosine to more structurally complex derivatives isolated mostly from marine sponges of the order Verongida [254]. The first bromotyrosine derivatives described in species of zoantharians are the 3,5 disubstituted hydantoin alkaloids named parazoanthines D-E and G-J isolated from the Mediterranean *Parazoanthus axinellae*. This is the second report of halogenated tyrosine derivatives from a specie of the genus *Parazoanthus* and the first of a specie of the genus *Antipathozoanthus*, both belonging to the family Parazoanthidae. During the metabolomic study of two morphotypes of *P. axinellae,* it was observed that both species differ in their chemical composition [206]. The presence of

parazoanthines which includes some brominated compounds were found only in the slender morphotype while these metabolites were absent in the rocky one. Additionally, no halogenated natural products have been reported from *Savalia savaglia* which also belongs to the same family. Therefore, it is not possible to considered bromotyrosine derivatives as chemical markers for species of the family Parazoanthidae. However, the halogenated tyramine derivatives could be considered as chemical markers for *P. darwini* as these metabolites were also found among the major components in the aqueous/methanolic fraction. Further studies should be carried out to confirm this hypothesis as *Parazoanthus* is considered a polyphiletic genus. On the other hand, Valdiviamides A-D (**199-202**) are the first halogenated tyrosine derivatives reported from species of the genus *Antipathozoanthus*. Valdiviamides A (**199**) and C (**201**) were among the major compounds in the aqueous/methanolic fraction of *A. hickmani*. Since the knowledge of the chemical diversity of species of the genus *Antipathozoanthus* is limited, further chemical studies should be carried out to suggest these halogenated dipeptides as chemical markers for this genus.

7 Conclusions and Perspectives

The Tropical Eastern Pacific ecoregion represent an untapped source for marine biodiscovery, and the Ecuadorian coast was not the exception. This work represents the first chemical investigation of marine invertebrates from the order Zoantharia inhabiting the coast of Ecuador. Additionally, Zoantharians were found to be the second most representative invertebrates in the Marine Protected Area El Pelado and this thesis describes the first chemical investigation of five species from this untapped marine ecosystem. A total of seventeen new and seven known natural products were isolated and identified including a novel family of 2-aminoimidazole alkaloids named terrazoanthines from *T. patagonichus*, two zoanthoxanthin derivatives from *T.* cf. *patagonichus*, two new members of the bioactive family of zoanthamine alkaloids from *Zoanthus* cf. *pulchellus*, four unprecedent ecdysteroids derivatives and four halogenated dipeptides from *Antipathozoanthus hickmani* and two halogenated tyramine derivatives from *Parazoanthus darwini*. Even though, the chemical study of *Terrazoanthus* sp., and *Palythoa* cf. *mutuki* was not completed because of the little amount of the isolated compounds, their chemical characterization should be continued to determine the chemical diversity in both species. There is a lot of interest is species of the genus *Palythoa* as it represents a great source of unique toxic peptides with different pharmacological applications and the identification of these toxins should be considered in all species of the Family Sphenopidae. Further chemical and enzymatic investigations should also be focus on the mucus of *Palythoa* species as represents a good source for discovering bioactive natural products and enzymes with different biotechnological purposes. Considering that more promising bioactivities have been observed from natural products isolated from the suborder Brachycnemina, there is still a lot of potential for uncovering new activities from compounds produced by members of the suborder Macrocnemina. The difference in their biological potential is supported by the limited chemical and biological studies on the suborder Macrocnemina while Brachycnemina is the most studied suborder within Zoantharians.

In total, there are 202 characterized natural products from both suborders and more than ten molecules such as peptides, toxins and fluorescence proteins have been reported only from *Palythoa*, *Protopalythoa* or *Zoanthus* species. This confirms that species of the suborder Brachycnemina is a powerful source of different natural products, toxins and bioactive peptides and just few species of this suborder have been considered for their toxin content besides palytoxin. Thus, from the 399 species of zoantharians observed at the World Register of Marine Database (WORMS), less than 50 species have been chemically studied including some organisms without identification at the species level. Therefore, zoantharians remains as the "golden box" for the search of interesting, bioactive and structurally unique natural products, and

collaboration between chemists, taxonomists and biologist must be encouraged to unveil the treasures hidden in these wonderful group of invertebrates. Additionally, there are some gaps that also needs to be address within the study of zoantharians. First, it is important to properly identify the organisms at the species level that would help to study their worldwide distribution and determine possible chemical markers to help in the systematics of zoantharians and their ecological role in the marine ecosystem. Second, the characterization of the associated symbionts in species of *Palythoa* and *Zoanthus* is another field that requires a lot of work. It is necessary to obtain conclusive evidence of their association in the production of certain metabolites and the ecological roles of these natural products. Furthermore, characterizing the diversity of enzymes would be another potential field for industrial or biotechnological purposes. The presence of enzymes capable of catalyzing reactions such diels alders or halogenation could be useful in chemical synthesis and for industrial applications. Although, the enzymatic characterization should be analyzed in all zoantharian species, those from species of the family Sphenopidae might have higher commercial value because of their wide range of functionalities.

The results from this study highlights the viewpoint of Leal *et al*., who indicated that one of the strategies for the discovery of novel natural products was to explore untapped ecoregions and to study groups of organisms that have been overlooked [11]. Additionally, this work has provided an overview of the great diversity of natural products and the wide range of biological activities and unique chemical archetypes produced by zoantharians. This should encourage natural products chemist to redirect their focus on these beautiful and interesting marine invertebrates.

Other potential source of new natural products are octocorals, which is the most representative group of invertebrates inhabiting the Ecuadorian coast and the TEP. A preliminary bioassay of the methanolic fractions of some octocorals revealed a potent antileishmanial activity, which confirms the potential of continuing studying the chemical diversity from other marine invertebrates inhabiting the Ecuadorian coast. Even though, there is still more investigation on the chemical diversity of zoantharians, octocoral species seems to be the next target to study for their chemical and biological potential.

This project concluded successfully with the first chemical investigation on zoantharians from the Ecuadorian coast and it represents the initial steps in the development of the field of Marine Natural Products in Ecuador.

REFERENCES

1. Snelgrove, P. V., An ocean of discovery: Biodiversity beyond the census of marine life, *Planta Medica*, 2016, **82**, 790-799.
2. WoRMS, World Register Species, http://www.marinespecies.org (accessed 2019-04-25, DOI: 10.14284/170).
3. Montaser, R. and Luesch, H., Marine natural products: a new wave of drugs?, *Future Medicinal Chemistry*, 2011, **3**, 1475-1489.
4. Mora, C., Tittensor, D. P., Adl, S., Simpson, A. G. and Worm, B., How many species are there on earth and in the ocean?, *PLoS Biology*, 2011, **9**, e1001127.
5. Paul, V. J., Arthur, K. E., Ritson-Williams, R., Ross, C. and Sharp, K., Chemical defenses: from compounds to communities, *The Biological Bulletin*, 2007, **213**, 226-251.
6. Núñez-Pons, L. and Avila, C., Natural products mediating ecological interactions in Antarctic benthic communities: a mini-review of the known molecules, *Natural Product Reports*, 2015, **32**, 1114-1130.
7. Hay, M. E. and Fenical, W., Chemical ecology and marine biodiversity: insights and products from the sea, *Oceanography-Washington DC-Oceanography Society-*, 1996, **9**, 10-20.
8. Jaspars, M., De Pascale, D., Andersen, J. H., Reyes, F., Crawford, A. D. and Ianora, A., The marine biodiscovery pipeline and ocean medicines of tomorrow, *Journal of the Marine Biological Association of the United Kingdom*, 2016, **96**, 151-158.
9. Dias, D. A., Urban, S. and Roessner, U., A historical overview of natural products in drug discovery, *Metabolites*, 2012, **2**, 303-336.
10. Gerwick, W. H. and Moore, B. S., Lessons from the past and charting the future of marine natural products drug discovery and chemical biology, *Chemistry & Biology*, 2012, **19**, 85-98.
11. Leal, M. C., Hilário, A., Munro, M. H., Blunt, J. W. and Calado, R., Natural products discovery needs improved taxonomic and geographic information, *Natural Product Reports*, 2016, **33**, 747-750.
12. Moloney, M. F., Irish ethno-botany and the evolution of medicine in Ireland, *MH Gill*, 1919,
13. Leoutsakos, V., A short history of the thyroid gland, *Hormones-Athens-*, 2004, **3**, 268-271.
14. Bergmann, W. and Feeney, R. J., The isolation of a new thymine pentoside from sponges, *Journal of the American Chemical Society*, 1950, **72**, 2809-2810.
15. El-Subbagh, H. I. and Al-Badr, A. A., *Profiles of drug substances, excipients and related methodology*, Elsevier Inc, 2009, vol. 34.
16. Rangel, M. and Falkenberg, M., An overview of the marine natural products in clinical trials and on the market, *Journal of Coastal Life Medicine*, 2015, **3**, 421-428.
17. Altmann, K.-H., Drugs from the oceans: marine natural products as leads for drug discovery, *International Journal for Chemistry*, 2017, **71**, 646-652.
18. PharmaMAr, The U.S. Food and Drug Administration (FDA) has granted Orphan Drug designation to PharmaMar's lurbinectedin, 2018.
19. Hirata, Y. and Uemura, D., Halichondrins-antitumor polyether macrolides from a marine sponge, *Pure and Applied Chemistry*, 1986, **58**, 701-710.
20. Leisch, M., Egle, A. and Greil, R., Plitidepsin: A potential new treatment for relapsed/refractory multiple myeloma, *Future Oncology*, 2018, **15**, 109-120.
21. PharmaMar, PharmaMar announces the approval of Aplidin in Australia for the treatment of multiple myeloma, 2018.
22. Carroll, A. R., Copp, B. R., Davis, R. A., Keyzers, R. A. and Prinsep, M. R., Marine natural products, *Natural Product Reports*, 2019, **36**, 122-173.

23. Blunt, J. and Munro, M., MarinLit, 2003.
24. Shang, J., Hu, B., Wang, J., Zhu, F., Kang, Y., Li, D., Sun, H., Kong, D.-X. and Hou, T., Cheminformatic insight into the differences between terrestrial and marine originated natural products, *Journal of Chemical Information and Modeling*, 2018, **58**, 1182-1193.
25. Oprea, T. I., Property distribution of drug-related chemical databases, *Journal of Computer-Aided Molecular Design*, 2000, **14**, 251-264.
26. Lipinski, C. A., Lombardo, F., Dominy, B. W. and Feeney, P. J., Experimental and computational approaches to estimate solubility and permeability in drug discovery and development settings, *Advanced Drug Delivery Reviews*, 1997, **23**, 3-25.
27. Peng, J., Shen, X., El Sayed, K. A., Dunbar, D. C., Perry, T. L., Wilkins, S. P., Hamann, M. T., Bobzin, S., Huesing, J. and Camp, R., Marine natural products as prototype agrochemical agents, *Journal of Agricultural and Food Chemistry*, 2003, **51**, 2246-2252.
28. Konishi, K., New insecticidally active derivatives of nereistoxin, *Agricultural and Biological Chemistry*, 1968, **32**, 678-679.
29. Cohen, P., Holmes, C. F. and Tsukitani, Y., Okadaic acid: a new probe for the study of cellular regulation, *Trends in Biochemical Sciences*, 1990, **15**, 98-102.
30. Chrapusta, E., Kaminski, A., Duchnik, K., Bober, B., Adamski, M. and Bialczyk, J., Mycosporine-like amino acids: potential health and beauty ingredients, *Marine Drugs*, 2017, **15**, 326.
31. Bhatia, S., Garg, A., Sharma, K., Kumar, S., Sharma, A. and Purohit, A., Mycosporine and mycosporine-like amino acids: A paramount tool against ultra violet irradiation, *Pharmacognosy Reviews*, 2011, **5**, 138.
32. Wada, N., Sakamoto, T. and Matsugo, S., Mycosporine-like amino acids and their derivatives as natural antioxidants, *Antioxidants*, 2015, **4**, 603-646.
33. Shick, J. M. and Dunlap, W. C., Mycosporine-like amino acids and related gadusols: biosynthesis, accumulation, and UV-protective functions in aquatic organisms, *Annual Review of Physiology*, 2002, **64**, 223-262.
34. Bonora, M., Giorgi, C., Bononi, A., Marchi, S., Patergnani, S., Rimessi, A., Rizzuto, R. and Pinton, P., Subcellular calcium measurements in mammalian cells using jellyfish photoprotein aequorin-based probes, *Nature Protocols*, 2013, **8**, 2105.
35. Lohan, D. and Johnston, S., Bioprospecting in Antarctica, United Nations University, 2005, 1-36.
36. Thomas, N. and Kim, S.-K., Beneficial effects of marine algal compounds in cosmeceuticals, *Marine Drugs*, 2013, **11**, 146-164.
37. Spolaore, P., Joannis-Cassan, C., Duran, E. and Isambert, A., Commercial applications of microalgae, *Journal of Bioscience and Bioengineering*, 2006, **101**, 87-96.
38. Mourelle, M. L., Gómez, C. P. and Legido, J. L., The potential use of marine microalgae and cyanobacteria in cosmetics and thalassotherapy, *Cosmetics*, 2017, **4**, 46.
39. Chen, J., Li, J., Dong, W., Zhang, X., Tyagi, R. D., Drogui, P. and Surampalli, R. Y., The potential of microalgae in biodiesel production, *Renewable and Sustainable Energy Reviews*, 2018, **90**, 336-346.
40. Sibi, G., Shetty, V. and Mokashi, K., Enhanced lipid productivity approaches in microalgae as an alternate for fossil fuels–A review, *Journal of the Energy Institute*, 2016, **89**, 330-334.
41. Greenwell, H. C., Laurens, L., Shields, R., Lovitt, R. and Flynn, K., Placing microalgae on the biofuels priority list: a review of the technological challenges, *Journal of the Royal Society Interface*, 2009, **7**, 703-726.
42. Cortés, J., Enochs, I. C., Sibaja-Cordero, J., Hernández, L., Alvarado, J. J., Breedy, O., Cruz-Barraza, J. A., Esquivel-Garrote, O., Fernández-García, C. and Hermosillo, A., *Coral Reefs of the Eastern Tropical Pacific*, Springer, 2017, pp. 203-250.
43. Spalding, M. D., Fox, H. E., Allen, G. R., Davidson, N., Ferdaña, Z. A., Finlayson, M., Halpern, B. S., Jorge, M. A., Lombana, A. and Lourie, S. A., Marine ecoregions of the world: a bioregionalization of coastal and shelf areas, *BioScience*, 2007, **57**, 573-583.

44. Costello, M. J., Tsai, P., Wong, P. S., Cheung, A. K. L., Basher, Z. and Chaudhary, C., Marine biogeographic realms and species endemicity, *Nature Communications*, 2017, **8**, 1057.
45. Glynn, P. W., *Coral Reefs of the Eastern Tropical Pacific*, Springer, 2017, pp. 1-37.
46. Mora, C. and Ross Robertson, D., Factors shaping the range-size frequency distribution of the endemic fish fauna of the Tropical Eastern Pacific, *Journal of Biogeography*, 2005, **32**, 277-286.
47. Katona, S., Polsenberg, J., Lowndes, J., Halpern, B. S., Pacheco, E., Mosher, L., Kilponen, A., Papacostas, K., Guzmán-Mora, A. G. and Farmer, G., Navigating the seascape of ocean management: waypoints on the voyage toward sustainable use, *OpenChannels*, 2017, 1-44.
48. Glynn, P. W., *Elsevier Oceanography Series*, Elsevier, 1990, vol. 52, pp. 55-126.
49. Glynn, P. W., Widespread coral mortality and the 1982–83 El Niño warming event, *Environmental Conservation*, 1984, **11**, 133-146.
50. LaJeunesse, T., Bonilla, H. R., Warner, M., Wills, M., Schmidt, G. and Fitt, W., Specificity and stability in high latitude eastern pacific coral-algal symbioses, *Limnology and Oceanography*, 2008, **53**, 719-727.
51. Durham, J. W., Corals from the gulf of California and the north pacific coast of America, *Geological Society of America*, 1947, **20**, 1-62.
52. Durham, J. and Barnard, J. L., Stony corals of the eastern Pacific collected by the Velero III and Velero IV. Corales pedregosos del Pacífico oriental colectados por el Velero III y el Velero IV, *Allan Hancock Pacific Expeditions.*, 1952, **16**, 1-110.
53. Miloslavich, P., Klein, E., Díaz, J. M., Hernandez, C. E., Bigatti, G., Campos, L., Artigas, F., Castillo, J., Penchaszadeh, P. E. and Neill, P. E., Marine biodiversity in the Atlantic and Pacific coasts of South America: knowledge and gaps, *PloS One*, 2011, **6**, e14631.
54. Baums, I. B., Boulay, J. N., Polato, N. R. and Hellberg, M. E., No gene flow across the Eastern Pacific B arrier in the reef-building coral *Porites lobata*, *Molecular Ecology*, 2012, **21**, 5418-5433.
55. Maté, J. L., Brandt, M., Grassian, B. and Chiriboga, Á., *Coral Reefs of the Eastern Tropical Pacific*, Springer, 2017, pp. 593-637.
56. Sánchez, J. A. and Ballesteros, D., The invasive snowflake coral (Carijoa riisei) in the Tropical Eastern Pacific, Colombia, *Revista de Biología Tropical*, 2014, **62**, 199-207.
57. Galván-Villa, C. M. and Ríos-Jara, E., First detection of the alien snowflake coral Carijoa riisei (Duchassaing and Michelotti, 1860)(Cnidaria: Alcyonacea) in the port of Manzanillo in the Mexican Pacific, *Bioinvasions Records*, 2018, **7**, 1-6.
58. Cruz, M., Gaibor, N., Mora, E., Jiménez, R. and Mair, J., The known and unknown about marine biodiversity in Ecuador (continental and insular), *Gayana*, 2003, **67**, 232-260.
59. Hickman Jr, C. P., Evolutionary responses of marine invertebrates to insular isolation in Galapagos, *Galapagos Research*, 2009, **66**, 32-42.
60. Terán, M., Clark, K., Suárez, C., Campos, F., Denkinger, J., Ruiz, D. and Jiménez, P., High-priority areas identification and conservation gap analysis of the marine biodiversity from continental Ecuador, Ministerio del Ambiente. Quito, Ecuador, 2006, 1-32.
61. Cruz, M., Especies de moluscos submareales e intermareales y macrofauna bentónica de la Bahía de Manta, Ecuador, *Acta Oceanografica del Pacifico*, 2013, **18**, 101-115.
62. Rivera, F. and Martínez, P., Guía fotográfica de corales y octocorales: Parque Nacional Machalilla y Reserva de Producción Faunística Marino Costera Puntilla de Santa Elena, NAZCA and Conservación Internacional, Ecuador, 2011, 1-86.
63. Bo, M., Lavorato, A., Di Camillo, C. G., Poliseno, A., Baquero, A., Bavestrello, G., Irei, Y. and Reimer, J. D., Black coral assemblages from Machalilla National Park (Ecuador), *Pacific Science*, 2012, **66**, 63-82.
64. Soler-Hurtado, M. D. M. and López-González, P. J., Two new gorgonian species (Anthozoa: Octocorallia: Gorgoniidae) from Ecuador (Eastern Pacific), *Marine Biology Research*, 2012, **8**, 380-387.

65.   Jaramillo, K. B., Reverter, M., Guillen, P. O., McCormack, G., Rodriguez, J., Sinniger, F. and Thomas, O. P., Assessing the zoantharian diversity of the Tropical Eastern Pacific through an integrative approach, *Scientific Reports*, 2018, **8**, 7138.

66.   Steiner, S. C., Riegl, B., Lavorato, A. and Rodríguez, J., Community structure of shallow water Alcyonacea (Anthozoa: Octocorallia) from the southern Tropical Eastern Pacific, *Ecological Research*, 2018, **33**, 457-469.

67.   Reimer, J., Sinniger, F. and Hickman, C., Zoanthid diversity (Anthozoa: Hexacorallia) in the Galapagos Islands: a molecular examination, *Coral Reefs*, 2008, **27**, 641-654.

68.   Carreiro-Silva, M., Ocaña, O., Stanković, D., Sampaio, Í., Porteiro, F. M., Fabri, M.-C. and Stefanni, S., Zoantharians (Hexacorallia: Zoantharia) associated with cold-water corals in the azores region: New species and associations in the deep sea, *Frontiers in Marine Science*, 2017, **4**.

69.   Reimer, J. D., Lin, M., Fujii, T., Lane, D. J. and Hoeksema, B. W., The phylogenetic position of the solitary zoanthid genus *Sphenopus* (Cnidaria: Hexacorallia), *Contributions to Zoology*, 2012, **81**, 43-54.

70.   Sinniger, F., Montoya-Burgos, J.-I., Chevaldonné, P. and Pawlowski, J., Phylogeny of the order Zoantharia (Anthozoa, Hexacorallia) based on the mitochondrial ribosomal genes, *Marine Biology*, 2005, **147**, 1121-1128.

71.   Reimer, J. D., Nakachi, S., Hirose, M., Hirose, E. and Hashiguchi, S., Using hydrofluoric acid for morphological investigations of zoanthids (Cnidaria: Anthozoa): a critical assessment of methodology and necessity, *Marine Biotechnology*, 2010, **12**, 605-617.

72.   Reimer, J. D., Nonaka, M., Sinniger, F. and Iwase, F., Morphological and molecular characterization of a new genus and new species of parazoanthid (Anthozoa: Hexacorallia: Zoantharia) associated with Japanese Red Coral, *Coral Reefs*, 2008, **27**, 935-949.

73.   Di Camillo, C., Bo, M., Puce, S. and Bavestrello, G., Association between *Dentitheca habereri* (Cnidaria: Hydrozoa) and two zoanthids, *Italian Journal of Zoology*, 2010, **77**, 81-91.

74.   Behenna, D. C., Stockdill, J. L. and Stoltz, B. M., The biology and chemistry of the zoanthamine alkaloids, *Angewandte Chemie International Edition*, 2008, **47**, 2365-2386.

75.   Reimer, J. D., Poliseno, A. and Hoeksema, B. W., Shallow-water zoantharians (Cnidaria, Hexacorallia) from the Central Indo-Pacific, *ZooKeys*, 2014, 1-57.

76.   Kise, H., Fujii, T., Masucci, G. D., Biondi, P. and Reimer, J. D., Three new species and the molecular phylogeny of *Antipathozoanthus* from the Indo-Pacific Ocean (Anthozoa, Hexacorallia, Zoantharia), *ZooKeys*, 2017, 97.

77.   Reimer, J. and Fujii, T., Four new species and one new genus of zoanthids (Cnidaria, Hexacorallia) from the Galápagos Islands, *ZooKeys*, 2010, **42**, 1-36.

78.   Verrill, A., Review of the corals and polyps of the west coast of America. 6. Transact. Connect, 1869, **1**, 377-567.

79.   Cutress, C. E. and Pequegnat, W. E., Three new species of Zoantharia from California, *Pacific Science*, 1960, **14**, 89-100.

80.   Fautin, D. G., Hickman, C. P., Daly, M. and Molodtsova, T., Shallow-Water Sea Anemones (Cnidaria: Anthozoa: Actiniaria) and Tube Anemones (Cnidaria: Anthozoa: Ceriantharia) of the Galápagos Islands1, 2, *Pacific Science*, 2007, **61**, 549-574.

81.   Reimer, J. D. and Hickman Jr, C. P., Preliminary survey of zooxanthellate zoanthids (Cnidaria: Hexacorallia) of the Galapagos, and associated symbiotic dinoflagellates (Symbiodinium spp.), *Galápagos Research*, 2009, **66**, 14-19.

82.   Bergmann, W., Feeney, R. J. and Swift, A. N., Contributions to the Study of Marine Products. XXXI. Palysterol and other Lipid Components of sea Anemones, *The Journal of Organic Chemistry*, 1951, **16**, 1337-1344.

83.   Gupta, K. C. and Scheuer, P. J., Zoanthid sterols, *Steroids*, 1969, **13**, 343-356.

84.   Quinn, R., Moore, R. E., Kashiwagi, M. and Norton, T. R., Anticancer activity of zoanthids and the associated toxin, palytoxin, against Ehrlich ascites tumor and P-388 lymphocytic leukemia in mice, *Journal of Pharmaceutical Sciences*, 1974, **63**, 257-260.

85. Kanazawa, A., Teshima, S.-I. and Ando, T., Sterols of coelenterates, *Comparative Biochemistry and Physiology Part B: Comparative Biochemistry*, 1977, **57**, 317-323.

86. Kokke, W. C. M. C., Fenical, W., Bohlin, L. and Djerassi, C., Sterol synthesis by cultured zooxanthellae; implications concerning sterol metabolism in the host-symbiont association in caribbean gorgonians, *Comparative Biochemistry and Physiology Part B: Comparative Biochemistry*, 1981, **68**, 281-287.

87. Kelecom, A. and Solé-Cava, A. M., Comparative study of zoanthid sterols the genus *Palythoa* (Hexacorallia, Zoanthidea), *Comparative Biochemistry and Physiology Part B: Comparative Biochemistry*, 1982, **72**, 677-682.

88. Diop, M., Leung-Tack, D., Braekman, J.-C. and Kornprobst, J.-M., Composition en stérols de quatre zoanthaires du genre *Palythoa* de la presqu-île du Cap-Vert, *Biochemical Systematics and Ecology*, 1986, **14**, 151-154.

89. Miralles, J., Diop, M., Ferrer, A. and Kornprobst, J.-M., Sterol composition of the ahermatypic zoantharia: *Palythoa senegambiensis* carter and its commensal, the decapoda *Diogenes ovatus* miers. Inadequacy of sterol content for chemotaxonomy of *Palythoa* genus, *Comparative Biochemistry and Physiology Part B: Comparative Biochemistry*, 1988, **89**, 209-212.

90. Elbagory, A. M., Meyer, M., Ali, A.-H. A., Ameer, F., Parker-Nance, S., Benito, M. T., Doyagüez, E. G., Jimeno, M. L. and Hussein, A. A., New polyhydroxylated sterols from *Palythoa tuberculosa* and their apoptotic activity in cancer cells, *Steroids*, 2015, **101**, 110-115.

91. Pinto, F. C., Almeida, J. G. L., Silveira, E. R., Costa, A. M., Guimarães, L. A., Wilke, D. V., Costa-Lotufo, L. V., Torres, M. d. C. M. and Pessoa, O. D. L., Steroids from the Brazilian Zoanthids *Palythoa caribaeorum* and *Palythoa variabilis*, *Journal of the Brazilian Chemical Society*, 2017, **28**, 485-491.

92. Kelecom, A., Studies of Brazilian marine invertebrates. VIII. Zoanthosterol, a new sterol from the Zoanthid *Zoanthus sociatus* (Hexacorallia, Zoanthidea), *Bulletin des Societes Chimiques Belges*, 1981, **90**, 971-976.

93. Kelecom, A., Studies of Brazilian marine invertebrates. VIII. Zoanthosterol, a new sterol from the zoanthid *Zoanthus sociatus* (hexacorallia, zoanthidea), *Bulletin des Sociétés Chimiques Belges*, 1981, **90**, 971-976.

94. Kelecom, A. and Solé-Cava, A., Studies of Brazilian marine invertebrates. IX. Comparative study of zoanthid sterols 1. The genus *Zoanthus*, *Mem. Inst. Butantan*, 1980, **44/45**, 451-462.

95. Kokke, W., Withers, N. W., Massey, I. J., Fenical, W. and Djerassi, C., Isolation and synthesis of 23-methyl-22-dehydrocholesterol-a marine sterol of biosynthetic significance, *Tetrahedron Letters*, 1979, **20**, 3601-3604.

96. Attaway, D. H., Isolation and partial characterization of Caribbean palytoxin, Ph.D, The University of Oklahoma., 1968.

97. Moore, R. E. and Scheuer, P. J., Palytoxin: a new marine toxin from a coelenterate, *Science*, 1971, **172**, 495-498.

98. Uemura, D., Hirata, Y., Iwashita, T. and Naoki, H., Studies on palytoxins, *Tetrahedron*, 1985, **41**, 1007-1017.

99. Rossi, R., Castellano, V., Scalco, E., Serpe, L., Zingone, A. and Soprano, V., New palytoxin-like molecules in Mediterranean *Ostreopsis* cf. *ovata* (dinoflagellates) and in *Palythoa tuberculosa* detected by liquid chromatography-electrospray ionization time-of-flight mass spectrometry, *Toxicon*, 2010, **56**, 1381-1387.

100. Patocka, J., Nepovimova, E., Wu, Q. and Kuca, K., Palytoxin congeners, *Archives of Toxicology*, 2018, **92**, 143-156.

101. Ramos, V. and Vasconcelos, V., Palytoxin and analogs: biological and ecological effects, *Marine Drugs*, 2010, **8**, 2021-2037.

102. Moore, R. E. and Bartolini, G., Structure of palytoxin, *Journal of the American Chemical Society*, 1981, **103**, 2491-2494.

103. Uemura, D., Ueda, K., Hirata, Y., Naoki, H. and Iwashita, T., Further studies on palytoxin. II. Structure of palytoxin, *Tetrahedron Letters*, 1981, **22**, 2781-2784.
104. Moore, R. E., Woolard, F. X., Sheikh, M. Y. and Scheuer, P. J., Ultraviolet chromophores of palytoxins, *Journal of the American Chemical Society*, 1978, **100**, 7758-7759.
105. Uemura, D., Ueda, K., Hirata, Y., Katayama, C. and Tanaka, J., Structural studies on palytoxin, a potent coelenterate toxin, *Tetrahedron Letters*, 1980, **21**, 4857-4860.
106. Cha, J., Christ, W., Finan, J., Fujioka, H., Kishi, Y., Klein, L., Ko, S., Leder, J., McWhorter, W. and Pfaff, K., Stereochemistry of palytoxin. Part 4. Complete structure, *Journal of the American Chemical Society*, 1982, **104**, 7369-7371.
107. Fujioka, H., Christ, W., Cha, J., Leder, J., Kishi, Y., Uemura, D. and Hirata, Y., Stereochemistry of palytoxin. Part 3. C7-C51 segment, *Journal of the American Chemical Society*, 1982, **104**, 7367-7369.
108. Klein, L., McWhorter, W., Ko, S., Pfaff, K., Kishi, Y., Uemura, D. and Hirata, Y., Stereochemistry of palytoxin. Part 1. C85-C115 segment, *Journal of the American Chemical Society*, 1982, **104**, 7362-7364.
109. Ko, S., Finan, J., Yonaga, M., Kishi, Y., Uemura, D. and Hirata, Y., Stereochemistry of palytoxin. Part 2. C1-C6, C47-C74, and C77-C83 segments, *Journal of the American Chemical Society*, 1982, **104**, 7364-7367.
110. Moore, R. E., Bartolini, G., Barchi, J., Bothner-By, A. A., Dadok, J. and Ford, J., Absolute stereochemistry of palytoxin, *Journal of the American Chemical Society*, 1982, **104**, 3776-3779.
111. Kishi, Y., Natural products synthesis: palytoxin, *Pure and Applied Chemistry*, 1989, **61**, 313-324.
112. Suh, E. M. and Kishi, Y., Synthesis of palytoxin from palytoxin carboxylic acid, *Journal of the American Chemical Society*, 1994, **116**, 11205-11206.
113. Beress, L., Zwick, J., Kolkenbrock, H., Kaul, P. and Wassermann, O., A method for the isolation of the caribbean palytoxin (C-PTX) from the coelenterate (zooanthid) *Palythoa caribaeorum*, *Toxicon*, 1983, **21**, 285-290.
114. Kimura, S. and Hashimoto, Y., Purification of the toxin in a zoanthid *Palythoa tuberculosa*, L. o. M. Biochemistry Report 0037-2870, The University of Tokyo, 1973, 713-718.
115. Hirata, Y., Uemura, D., Ueda, K. and Takano, S., Several compounds from *Palythoa tuberculosa* (Coelenterata), *Pure and Applied Chemistry*, 1979, **51**, 1875-1883.
116. Ciminiello, P., Dell'Aversano, C., Dello Iacovo, E., Fattorusso, E., Forino, M., Grauso, L., Tartaglione, L., Florio, C., Lorenzon, P. and De Bortoli, M., Stereostructure and biological activity of 42-hydroxy-palytoxin: A new palytoxin analogue from Hawaiian *Palythoa* subspecies, *Chemical Research in Toxicology*, 2009, **22**, 1851-1859.
117. Tartaglione, L., Pelin, M., Morpurgo, M., Dell'Aversano, C., Montenegro, J., Sacco, G., Sosa, S., Reimer, J. D., Ciminiello, P. and Tubaro, A., An aquarium hobbyist poisoning: Identification of new palytoxins in *Palythoa* cf. *toxica* and complete detoxification of the aquarium water by activated carbon, *Toxicon*, 2016, **121**, 41-50.
118. Sawelew, L., Gault, F., Nuccio, C., Perez, Y. and Lorquin, J., Characterisation of palytoxin from an undescribed *Palythoa* (Anthozoa: Zoantharia: Sphenopidae) with significant in vitro cytotoxic effects on cancer cells at picomolar doses, *BioRxiv*, 2018, 292219.
119. Deeds, J. R., Handy, S. M., White, K. D. and Reimer, J. D., Palytoxin found in *Palythoa* sp. zoanthids (Anthozoa, Hexacorallia) sold in the home aquarium trade, *PLoS One*, 2011, **6**, e18235.
120. Gleibs, S., Mebs, D. and Werding, B., Studies on the origin and distribution of palytoxin in a Caribbean coral reef, *Toxicon*, 1995, **33**, 1531-1537.
121. Seemann, P., Gernert, C., Schmitt, S., Mebs, D. and Hentschel, U., Detection of hemolytic bacteria from *Palythoa caribaeorum* (Cnidaria, Zoantharia) using a novel palytoxin-screening assay, *Antonie Van Leeuwenhoek*, 2009, **96**, 405-411.
122. Fukui, M., Murata, M., Inoue, A., Gawel, M. and Yasumoto, T., Occurrence of palytoxin in the trigger fish *Melichtys vidua*, *Toxicon*, 1987, **25**, 1121-1124.

123. Biré, R., Trotereau, S., Lemée, R., Delpont, C., Chabot, B., Aumond, Y. and Krys, S., Occurrence of palytoxins in marine organisms from different trophic levels of the French Mediterranean coast harvested in 2009, *Harmful Algae*, 2013, **28**, 10-22.

124. Mahnir, V. M., Kozlovskaya, E. P. and Kalinovsky, A. I., Sea anemone *Radianthus macrodactylus*—a new source of palytoxin, *Toxicon*, 1992, **30**, 1449-1456.

125. Mori, S., Sugahara, K., Maeda, M., Nomoto, K., Iwashita, T. and Yamagaki, T., Insecticidal activity guided isolation of palytoxin from a red alga, *Chondria armata*, *Tetrahedron Letters*, 2016, **57**, 3612-3617.

126. Kerbrat, A. S., Amzil, Z., Pawlowiez, R., Golubic, S., Sibat, M., Darius, H. T., Chinain, M. and Laurent, D., First evidence of palytoxin and 42-hydroxy-palytoxin in the marine cyanobacterium *Trichodesmium*, *Marine Drugs*, 2011, **9**, 543-560.

127. Ciminiello, P., Dell'Aversano, C., Dello Iacovo, E., Forino, M., Tartaglione, L., Pelin, M., Sosa, S., Tubaro, A., Chaloin, O. and Poli, M., Stereoisomers of 42-hydroxy palytoxin from Hawaiian *Palythoa toxica* and *P. tuberculosa*: stereostructure elucidation, detection, and biological activities, *Journal of Natural Products*, 2014, **77**, 351-357.

128. Fraga, M., Vilariño, N., Louzao, M. C., Molina, L. a., López, Y., Poli, M. and Botana, L. M., First identification of palytoxin-like molecules in the atlantic coral species *Palythoa canariensis*, *Analytical Chemistry*, 2017, **89**, 7438-7446.

129. Frelin, C. and Van Renterghem, C., Palytoxin. Recent electrophysiological and pharmacological evidence for several mechanisms of action, *Gen Pharmacol*, 1995, **26**, 33-37.

130. Rossini, G. P. and Bigiani, A., Palytoxin action on the Na^+,K^+-ATPase and the disruption of ion equilibria in biological systems, *Toxicon*, 2011, **57**, 429-439.

131. Oku, N., Sata, N. U., Matsunaga, S., Uchida, H. o. and Fusetani, N., Identification of palytoxin as a principle which causes morphological changes in rat 3Y1 cells in the zoanthid *Palythoa* aff. *margaritae*, *Toxicon*, 2004, **43**, 21-25.

132. Ciminiello, P., Dell'Aversano, C., Dello Iacovo, E., Forino, M., Randazzo, A. and Tartaglione, L., Identification of Palytoxin–Ca^{2+} Complex by NMR and Molecular Modeling Techniques, *Journal of Organic Chemistry*, 2013, **79**, 72-79.

133. Murphy, L. T. and Charlton, N. P., Prevalence and characteristics of inhalational and dermal palytoxin exposures reported to the National Poison Data System in the US, *Environmental Toxicology and Pharmacology*, 2017, **55**, 107-109.

134. Harada, S., Yamamoto, N. and Fujiki, H., Lysis of human immunodeficiency virus infected cells by TPA-type and non-TPA type tumor promoters, *AIDS Research and Human Retroviruses*, 1988, **4**, 99-105.

135. Valverde, I., Lago, J., Vieites, J. and Cabado, A., In vitro approaches to evaluate palytoxin-induced toxicity and cell death in intestinal cells, *Journal of Applied Toxicology*, 2008, **28**, 294-302.

136. Görögh, T., Bèress, L., Quabius, E. S., Ambrosch, P. and Hoffmann, M., Head and neck cancer cells and xenografts are very sensitive to palytoxin: decrease of c-jun n-terminale kinase-3 expression enhances palytoxin toxicity, *Molecular Cancer*, 2013, **12**, 1-12.

137. Fedorov, S., Stonik, V. and Elyakov, G., Identification of ecdysteroids of hexactinic corals, *Chemistry of Natural Compounds*, 1988, **24**, 517-518.

138. Chen, S.-R., Wang, S.-W., Su, C.-J., Hu, H.-C., Yang, Y.-L., Hsieh, C.-T., Peng, C.-C., Chang, F.-R. and Cheng, Y.-B., Anti-Lymphangiogenesis Components from Zoanthid *Palythoa tuberculosa*, *Marine Drugs*, 2018, **16**, 47.

139. Shigemori, H., Sato, Y., Kagata, T. and Kobayashi, J. i., Palythoalones A and B, new ecdysteroids from the marine zoanthid *Palythoa australiae*, *Journal of Natural Products*, 1999, **62**, 372-374.

140. Lee, J.-C., Chang, F.-R., Chen, S.-R., Wu, Y.-H., Hu, H.-C., Wu, Y.-C., Backlund, A. and Cheng, Y.-B., Anti-dengue virus constituents from Formosan zoanthid Palythoa mutuki, *Marine Drugs*, 2016, **14**, 151.

141. Parameswaran, P. s., Naik, C. G., Gonsalves, C. and Achuthankutty, C. T., Isolation of 2-deoxyecdysterone, a novel oxytocic agent, from a marine *Zoanthus* sp., *Journal of the Indian Institute of Science*, 2001, **81**, 169-173.

142. Suksamrarn, A., Jankam, A., Tarnchompoo, B. and Putchakarn, S., Ecdysteroids from a *Zoanthus* sp., *Journal of Natural Products*, 2002, **65**, 1194-1197.

143. Cheng, Y.-B., Lee, J.-C., Lo, I.-W., Chen, S.-R., Hu, H.-C., Wu, Y.-H., Wu, Y.-C. and Chang, F.-R., Ecdysones from *Zoanthus* spp. with inhibitory activity against dengue virus 2, *Bioorganic & Medicinal Chemistry Letters*, 2016, **26**, 2344-2348.

144. Behenna Douglas , C., Stockdill Jennifer , L. and Stoltz Brian , M., The biology and chemistry of the zoanthamine alkaloids, *Angewandte Chemie International Edition*, 2008, **47**, 2365-2386.

145. Rocha, C., Bioactive compounds from Zoanthids (Cnidaria: Anthozoa): A brief review with emphasis on alkaloids, *International Research Journal of Biochemistry and Bioinformatics*, 2013, **3**, 1-6.

146. Rao, C. B., Anjaneyula, A. S. R., Sarma, N. S., Venkatateswarlu, Y., Rosser, R. M., Faulkner, D. J., Chen, M. H. M. and Clardy, J., Zoanthamine; a novel alkaloid from a marine zoanthid, *Journal of the American Chemical Society*, 1984, **106**, 7983-7984.

147. Rao, C. B., Anjaneyulu, A. S. R., Sarma, N. S., Venkateswarlu, Y., Rosser, R. M. and Faulkner, D. J., Alkaloids from a marine Zoanthid, *Journal of Organic Chemistry*, 1985, **50**, 3757-3760.

148. Faulkner, D. J., Rao, C. B., Rao, D. V., S. N. Raju, V. and W. Sullivan, B., Two new alkaloids from an indian species of *Zoanthus*, *Heterocycles*, 1989, **28**, 103-106.

149. Atta ur, R., Ahmed Alvi, K., Ali Abbas, S., Iqbal Choudhary, M. and Clardy, J., Zoanthaminone, a new alkaloid from a marine zoanthid, *Tetrahedron Letters*, 1989, **30**, 6825-6828.

150. Li, F., Chen, A. and Zhang, J., miR-9 stimulation enhances the differentiation of neural stem cells with zoanthamine by regulating Notch signaling, *American Journal of Translational Research*, 2019, **11**, 1780-1788.

151. Fukuzawa, S., Hayashi, Y., Uemura, D., Nagatsu, A., Yamada, K. and Ijuin, Y., The isolation and structures of five new alkaloids, norzoanthamine, oxyzoanth amine, norzoanthaminone, cyclozoanthamine and epinorzoanthamine, *Heterocyclic Communications*, 1995, **1**, 207-214.

152. Kuramoto, M., Yamaguchi, K., Tsuji, T. and Uemura, D., Zoanthamines, antiosteoporotic alkaloids, *Drugs from the Sea*, 2000, 98.

153. Kuramoto, M., Hayashi, K., Yamaguchi, K., Yada, M., Tsuji, T. and Uemura, D., Structure-activity relationship of norzoanthamine exhibiting significant inhibition of osteoporosis, *Bulletin of the Chemical Society of Japan*, 1998, **71**, 771-779.

154. Yamaguchi, K., Yada, M., Tsuji, T., KuRAMoTo, M. and UEMURA, D., Suppressive effect of norzoanthamine hydrochloride on experimental osteroporosis in ovariectomized mice, *Biological and Pharmaceutical Bulletin*, 1999, **22**, 920-924.

155. Farrokhnia, M. and Mahnam, K., Molecular dynamics and docking investigations of several zoanthamine-type marine alkaloids as matrix metaloproteinase-1 inhibitors, *Iranian Journal of Pharmaceutical Research*, 2017, **16**, 173.

156. Kinugawa, M., Fukuzawa, S. and Tachibana, K., Skeletal protein protection: the mode of action of an anti-osteoporotic marine alkaloid, norzoanthamine, *Journal of bone and mineral metabolism*, 2009, **27**, 303-314.

157. Genji, T., Fukuzawa, S. and Tachibana, K., Distribution and Possible Function of the Marine Alkaloid, Norzoanthamine, in the Zoanthid Zoanthus sp. Using MALDI Imaging Mass Spectrometry, *Marine Biotechnology*, 2010, **12**, 81-87.

158. Inoue, H., Hidaka, D., Fukuzawa, S. and Tachibana, K., Truncated norzoanthamine exhibiting similar collagen protection activity, toward a promising anti-osteoporotic drug, *Bioorganic & Medicinal Chemistry Letters*, 2014, **24**, 508-509.

159. Daranas, A. H., Fernández, J., Gavín, J. and Norte, M., Epioxyzoanthamine, a new zoanthamine-type alkaloid and the unusual deuterium exchange in this series, *Tetrahedron*, 1998, **54**, 7891-7896.

160. Daranas, A. H., Fernández, J., Gavín, J. and Norte, M., New alkaloids from a marine zoanthid, *Tetrahedron*, 1999, **55**, 5539-5546.

161. Villar, R. M., Gil-Longo, J., Daranas, A. H., Souto, M. a. L., Fernández, J. J., Peixinho, S., Barral, M. A., Santafé, G., Rodríguez, J. and Jiménez, C., Evaluation of the effects of several zoanthamine-type alkaloids on the aggregation of human platelets, *Bioorganic & Medicinal Chemistry*, 2003, **11**, 2301-2306.

162. Hirai, G., Oguri, H., Hayashi, M., Koyama, K., Koizumi, Y., Moharram, S. M. and Hirama, M., Synthesis and preliminary biological evaluation of truncated zoanthenol analogues, *Bioorganic & Medicinal Chemistry Letters*, 2004, **14**, 2647-2651.

163. Cen-Pacheco, F., Norte, M., Fernández, J. J. and Daranas, A. H., Zoaramine, a Zoanthamine-like Alkaloid with a New Skeleton, *Organic Letters*, 2014, **16**, 2880-2883.

164. Cen-Pacheco, F., Norte Martín, M., Fernández, J. J. and Hernández Daranas, A., New Oxidized Zoanthamines from a Canary Islands *Zoanthus* sp, *Marine Drugs*, 2014, **12**, 5188-5196.

165. Cheng, Y.-B., Lan, C.-C., Liu, W.-C., Lai, W.-C., Tsai, Y.-C., Chiang, M. Y., Wu, Y.-C. and Chang, F.-R., Kuroshines A and B, new alkaloids from *Zoanthus kuroshio*, *Tetrahedron Letters*, 2014, **55**, 5369-5372.

166. Cheng, Y.-B., Lo, I. W., Shyur, L.-F., Yang, C.-C., Hsu, Y.-M., Su, J.-H., Lu, M.-C., Chiou, S.-F., Lan, C.-C., Wu, Y.-C. and Chang, F.-R., New alkaloids from Formosan zoanthid *Zoanthus kuroshio*, *Tetrahedron*, 2015, **71**, 8601-8606.

167. Hsu, Y.-M., Chang, F.-R., Lo, I. W., Lai, K.-H., El-Shazly, M., Wu, T.-Y., Du, Y.-C., Hwang, T.-L., Cheng, Y.-B. and Wu, Y.-C., Zoanthamine-type alkaloids from the zoanthid *Zoanthus kuroshio* collected in taiwan and their effects on inflammation, *Journal of Natural Products*, 2016, **79**, 2674-2680.

168. Guillen, P., Gegunde, S., Jaramillo, K., Alfonso, A., Calabro, K., Alonso, E., Rodriguez, J., Botana, L. and Thomas, O., Zoanthamine alkaloids from the zoantharian *Zoanthus* cf. *pulchellus* and their effects in neuroinflammation, *Marine Drugs*, 2018, **16**, 242.

169. Cariello, L., Crescenzi, S., Zanetti, L. and Prota, G., A survey on the distribution of zoanthoxanthins in some marine invertebrates, *Comparative Biochemistry and Physiology Part B: Comparative Biochemistry*, 1979, **63**, 77-82.

170. Ito, S., Isolation and structure of a mycosporine from the zoanthidian *Palythoa tuberculosa*, *Tetrahedron Letters*, 1977, **18**, 2429-2430.

171. Takano, S., Isolation and structure of a new amino acid, palythine, from the zoanthid *Palythoa tuberculosa*, *Tetrahedron Letters*, 1978, **26**, 2299-2300.

172. Takano, S., Uemura, D. and Hirata, Y., Isolation and structure of two new amino acids, palythinol and palythene, from the zoanthid *Palythoa tubercolosa*, *Tetrahedron Letters*, 1978, **19**, 4909-4912.

173. Uemura, D., Toya, Y., Watanabe, I. and Hirata, Y., Isolation and structures of two new pyrazines, palythazine and isopalythazine from *Palythoa tuberculosa*, *Chemistry Letters*, 1979, **8**, 1481-1482.

174. Pettit, G. R. and Fujii, Y., Antineoplastic agents. 81. the glycerol ethers of *Palythoa liscia*, *Journal of Natural Products*, 1982, **45**, 640-643.

175. Han, C., Qi, J., Shi, X., Sakagami, Y., Shibata, T., Uchida, K. and Ojika, M., Prostaglandins from a Zoanthid: Paclitaxel-like neurite-degenerating and microtubule-stabilizing activities, *Bioscience, Biotechnology and Biochemistry*, 2006, **70**, 706-711.

176. Wilke, D. V., Jimenez, P. C., Pessoa, C., Moraes, M. O. d., Araújo, R. M., Silva, W. M. B. d., Silveira, E. R., Pessoa, O. D. L., Braz-Filho, R. and Lopes, N. P., Cytotoxic lipidic α-amino acids from the zoanthid *Protopalythoa variabilis* from the northeastern coast of Brazil, *Journal of the Brazilian Chemical Society*, 2009, **20**, 1455-1459.

177. Wilke, D. V., Jimenez, P. C., Araújo, R. M., da Silva, W. M. B., Pessoa, O. D. L., Silveira, E. R., Pessoa, C., de Moraes, M. O., Skwarczynski, M. and Simerska, P., Pro-apoptotic activity of lipidic α-amino acids isolated from *Protopalythoa variabilis*, *Bioorganic & Medicinal Chemistry*, 2010, **18**, 7997-8004.

178.	Almeida, J., Maia, A., Wilke, D., Silveira, E., Braz-Filho, R., La Clair, J., Costa-Lotufo, L. and Pessoa, O., Palyosulfonoceramides A and B: unique sulfonylated ceramides from the Brazilian zoanthids *Palythoa caribaeorum* and *Protopalyhtoa variabilis*, *Marine Drugs*, 2012, **10**, 2846-2860.

179.	Alencar, D. B., Melo, A. A., Silva, G. C., Lima, R. L., Pires-Cavalcante, K., Carneiro, R. F., Rabelo, A. S., Sousa, O. V., Vieira, R. H. and Viana, F. A., Antioxidant, hemolytic, antimicrobial, and cytotoxic activities of the tropical Atlantic marine zoanthid *Palythoa caribaeorum*, *Anais da Academia Brasileira de Ciências*, 2015, **87**, 1113-1123.

180.	Costa-Lotufo, L., Carnevale-Neto, F., Trindade-Silva, A., Silva, R., Silva, G., Wilke, D., Pinto, F., Sahm, B., Jimenez, P. and Mendonça, J., Chemical profiling of two congeneric sea mat corals along the Brazilian coast: adaptive and functional patterns, *Chemical Communications*, 2018, **54**, 1952-1955.

181.	Pettit, G. R., Fujii, Y., Hasler, J. A., Schmidt, J. M. and Michel, C., Antineoplastic agents 78. isolation of palystatins 1-3 from the indian ocean *Palythoa liscia*, *Journal of Natural Products*, 1982, **45**, 263-269.

182.	Pettit, G. R., Fujii, Y., Hasler, J. A. and Schmidt, J. M., Isolation and characterization of palystatins AD, *Journal of Natural Products*, 1982, **45**, 272-276.

183.	Lazcano-Pérez, F., Vivas, O., Román-González, S. A., Rodríguez-Bustamante, E., Castro, H., Arenas, I., García, D. E., Sánchez-Puig, N. and Arreguín-Espinosa, R., A purified *Palythoa* venom fraction delays sodium current inactivation in sympathetic neurons, *Toxicon*, 2014, **82**, 112-116.

184.	Huang, C., Morlighem, J.-E. R., Zhou, H., Lima, E. P., Gomes, P. B., Cai, J., Lou, I., Perez, C. D., Lee, S. M. and Radis-Baptista, G., The transcriptome of the zoanthid *Protopalythoa variabilis* (Cnidaria, Anthozoa) predicts a basal repertoire of toxin-like and venom-auxiliary polypeptides, *Genome Biology and Evolution*, 2016, **8**, 3045-3064.

185.	Guarnieri, M. C., de Albuquerque Modesto, J. C., Pérez, C. D., Ottaiano, T. F., da Silva Ferreira, R., Batista, F. P., de Brito, M. V., Campos, I. H. M. P. and Oliva, M. L. V., Zoanthid mucus as new source of useful biologically active proteins, *Toxicon*, 2018, **143**, 96-107.

186.	Liao, Q., Li, S., Siu, S. W. I., Yang, B., Huang, C., Chan, J. Y.-W., Morlighem, J.-E. t. R., Wong, C. T. T., Rádis-Baptista, G. and Lee, S. M.-Y., Novel Kunitz-like peptides discovered in the zoanthid *Palythoa caribaeorum* through transcriptome sequencing, *Journal of Proteome Research*, 2018, **17**, 891-902.

187.	Liao, Q., Gong, G., Siu, S., Wong, C., Yu, H., Tse, Y., Rádis-Baptista, G. and Lee, S., A Novel ShK-like toxic peptide from the transcriptome of the cnidarian *Palythoa caribaeorum* displays neuroprotection and cardioprotection in zebrafish, *Toxins*, 2018, **10**, 238.

188.	Cuevas-Cruz, M., Lazcano-Pérez, F., Hernández-Guzmán, U., Díaz de la Vega-Castañeda, K. H., Román-González, S. A., Valdez-Cruz, N. A., Velasco-Bejarano, B., Colín-González, A. L., Santamaría, A. and Gómez-Manzo, S., A novel phospholipase A2 isolated from *Palythoa caribaeorum* possesses neurotoxic activity, *Toxins*, 2019, **11**, 89.

189.	Liao, Q., Li, S., Siu, S. W. I., Morlighem, J.-É. R., Wong, C. T. T., Wang, X., Rádis-Baptista, G. and Lee, S. M.-Y., Novel neurotoxic peptides from *Protopalythoa variabilis* virtually interact with voltage-gated sodium channel and display anti-epilepsy and neuroprotective activities in zebrafish, *Archives of Toxicology*, 2019, **93**, 189-206.

190.	Kittredge, J. and Hughes, R., The occurrence of α-amino-β-phosphonopropionic acid in the zoanthid, *Zoanthus sociatus*, and the ciliate, *Tetrahymena pyriformis*, *Biochemistry*, 1964, **3**, 991-996.

191.	Babu, U., Bhandari, S. and Garg, H., Hariamide, a novel sulfated sphingolipid from a *Zoanthus* sp. of the Indian coast, *Journal of Natural Products*, 1997, **60**, 1307-1309.

192.	Parameswaran, P. and Achuthankutty, C., Isolation of peridininol, an anti-spasmodic carotenoid pigment from *Zoanthus* sp., *Proceedings of Andra Pradesh Akademi of Sciences*, 2007, **9**, 135-138.

193.	Diaz-Garcia, C. M., Sanchez-Soto, C., Fuentes-Silva, D., Leon-Pinzon, C., Dominguez-Perez, D., Varela, C., Rodriguez-Romero, A., Castañeda, O. and Hiriart, M., Low molecular weight

compounds from *Zoanthus sociatus* impair insulin secretion via Ca^{+2} influx blockade and cause glucose intolerance in vivo, *Toxicon*, 2012, **59**, 306-314.

194. Domínguez-Pérez, D., Diaz-Garcia, C., García-Delgado, N., Sierra-Gómez, Y., Castañeda, O. and Antunes, A., Insights into the toxicological properties of a low molecular weight fraction from *Zoanthus sociatus* (Cnidaria), *Marine Drugs*, 2013, **11**, 2873-2881.

195. Domínguez-Pérez, D., Rodríguez, A., Osorio, H., Azevedo, J., Castañeda, O., Vasconcelos, V. and Antunes, A., Microcystin-LR detected in a low molecular weight fraction from a crude extract of *Zoanthus sociatus*, *Toxins*, 2017, **9**, 89.

196. Matz, M. V., Fradkov, A. F., Labas, Y. A., Savitsky, A. P., Zaraisky, A. G., Markelov, M. L. and Lukyanov, S. A., Fluorescent proteins from nonbioluminescent Anthozoa species, *Nature Biotechnology*, 1999, **17**, 969-973.

197. Labas, Y. A., Gurskaya, N., Yanushevich, Y. G., Fradkov, A., Lukyanov, K., Lukyanov, S. and Matz, M., Diversity and evolution of the green fluorescent protein family, *Proceedings of the National Academy of Sciences*, 2002, **99**, 4256-4261.

198. Yanushevich, Y. G., Bulina, M., Gurskaya, N., Savitskii, A. and Lukyanov, K., Key amino acid residues responsible for the color of green and yellow fluorescent proteins from the coral polyp *Zoanthus* sp., *Russian Journal of Bioorganic Chemistry*, 2002, **28**, 274-277.

199. Zagranichny, V. E., Rudenko, N. V., Gorokhovatsky, A. Y., Zakharov, M. V., Shenkarev, Z. O., Balashova, T. A. and Arseniev, A. S., zFP538, a yellow fluorescent protein from coral, belongs to the DsRed subfamily of GFP-like proteins but possesses the unexpected site of fragmentation, *Biochemistry*, 2004, **43**, 4764-4772.

200. Remington, S. J., Wachter, R. M., Yarbrough, D. K., Branchaud, B., Anderson, D., Kallio, K. and Lukyanov, K. A., zFP538, a yellow-fluorescent protein from *Zoanthus*, contains a novel three-ring chromophore, *Biochemistry*, 2005, **44**, 202-212.

201. Yampolsky, I. V., Balashova, T. A. and Lukyanov, K. A., Synthesis and spectral and chemical properties of the yellow fluorescent protein zFP538 chromophore, *Biochemistry*, 2009, **48**, 8077-8082.

202. Pletneva, N., Pletnev, S., Tikhonova, T., Popov, V., Martynov, V. and Pletnev, V., Structure of a red fluorescent protein from *Zoanthus*, zRFP574, reveals a novel chromophore, *Acta Crystallographica Section D: Biological Crystallography*, 2006, **62**, 527-532.

203. Pletneva, N., Pletnev, V., Tikhonova, T., Pakhomov, A. A., Popov, V., Martynov, V. I., Wlodawer, A., Dauter, Z. and Pletnev, S., Refined crystal structures of red and green fluorescent proteins from the button polyp *Zoanthus*, *Acta Crystallographica Section D: Biological Crystallography*, 2007, **63**, 1082-1093.

204. Searle, P. A. and Molinski, T. F., 4-Dehydroecdysterone, a new ecdysteroid from the zoanthid *Parazoanthus* sp., *Journal of Natural Products*, 1995, **58**, 264-268.

205. Pawlik, J. R., Chanas, B., Toonen, R. J. and Fenical, W., Defenses of Caribbean sponges against predatory reef fish. I. Chemical deterrency, *Marine Ecology Progress Series*, 1995, **127**, 183-194.

206. Cachet, N., Genta-Jouve, G., Ivanisevic, J., Chevaldonné, P., Sinniger, F., Culioli, G., Pérez, T. and Thomas, O. P., Metabolomic profiling reveals deep chemical divergence between two morphotypes of the zoanthid *Parazoanthus axinellae*, *Scientific Reports*, 2015, **5**, 8282.

207. Sturaro, A., Guerriero, A., De Clauser, R. and Pietra, F., A new, unexpected marine source of a molting hormone. Isolation of ecdysterone in large amounts from the zoanthid *Gerardia savaglia*, *Experientia*, 1982, **38**, 1184-1185.

208. Guerriero, A. and Pietra, F., Isolation, in large amounts, of the rare plant ecdysteroid ajugasterone-C from the mediterranean zoanthid *Gerardia savaglia*, *Comparative Biochemistry and Physiology Part B: Comparative Biochemistry*, 1985, **80**, 277-278.

209. Guerriero, A., Traldi, P. and Pietra, F., Gerardiasterone, a new ecdysteroid with a 20, 22, 23, 25-tetrahydroxylated side chain from the mediterranean zoanthid *Gerardia savaglia*, *Journal of the Chemical Society, Chemical Communications*, 1986, 40-41.

210. Honda, T., Takada, H., Miki, S. and Tsubuki, M., Synthesis and structure elucidation of a novel ecdysteroid, gerardiasterone, *Tetrahedron Letters*, 1993, **34**, 8275-8278.
211. Tsubuki, M., Takada, H., Katoh, T., Miki, S. and Honda, T., Synthesis and structural elucidation of a new zooecdysteroid gerardiasterone, *Tetrahedron*, 1996, **52**, 14515-14532.
212. Guillen, P., Calabro, K., Jaramillo, K., Dominguez, C., Genta-Jouve, G., Rodriguez, J. and Thomas, O., Ecdysonelactones, ecdysteroids from the Tropical Eastern Pacific zoantharian *Antipathozoanthus hickmani*, *Marine Drugs*, 2018, **16**, 58.
213. Cariello, L., Crescenzi, S., Prota, G., Giordano, F. and Mazzarella, L., Zoanthoxanthin, a heteroaromatic base from *Parazoanthus* cfr. *axinellae* (zoantharia): structure confirmation by X-ray crystallography, *Journal of the Chemical Society, Chemical Communications*, 1973, 99-100.
214. Cariello, L., Crescenzi, S., Prota, G., Capasso, S., Giordano, F. and Mazzarella, L., Zoanthoxanthin, a natural 1, 3, 5, 7-tetrazacyclopent-azulene from *Parazoanthus axinellae*, *Tetrahedron*, 1974, **30**, 3281-3287.
215. Cariello, L. and Tota, B., Inhibition of succinic oxidase activity of beef heart mitochondria by a new fluorescent metabolite, zoanthoxantin, *Experientia*, 1974, **30**, 244-245.
216. Cariello, L., Crescenzi, S., Prota, G. and Zanetti, L., New zoanthoxanthins from the mediterranean zoanthid *Parazoanthus axinellae*, *Experientia*, 1974, **30**, 849-850.
217. Pašić, L., Sepčić, K., Turk, T., Maček, P. and Poklar, N., Characterization of parazoanthoxanthin A binding to a series of natural and synthetic host DNA duplexes, *Archives of Biochemistry and Biophysics*, 2001, **393**, 132-142.
218. Sepčić, K., Turk, T. and Maček, P., Anticholinesterase activity of the fluorescent zoanthid pigment, parazoanthoxanthin A, *Toxicon*, 1998, **36**, 937-940.
219. Rozman, K. B., Araoz, R., Sepčić, K., Molgo, J. and Šuput, D., Parazoanthoxanthin A blocks Torpedo nicotinic acetylcholine receptors, *Chemico-Biological Interactions*, 2010, **187**, 384-387.
220. Komoda, Y., Shimizu, M., Kaneko, S., Yamamoto, M. and Ishikawa, M., Chemistry of paragracine, a biologically active marine base from *Parazoanthus gracilis* (Lwowsky), *Chemical and Pharmaceutical Bulletin*, 1982, **30**, 502-508.
221. Seyama, I., Wu, C. and Narahashi, T., Current-dependent block of nerve membrane sodium channels by paragracine, *Biophysical Journal*, 1980, **29**, 531-537.
222. Komoda, Y., Shimizu, M. and Ishikawa, M., Structures of biologically active minor bases related to paragracine from *Parazoanthus gracilis* LWOWSKY, *Chemical and Pharmaceutical Bulletin*, 1984, **32**, 3873-3879.
223. Schwartz, R. E., Yunker, M. B., Scheuer, P. J. and Ottersen, T., Constituents of bathyal marine organisms: a new zoanthoxanthin from a coelenterate, *Tetrahedron Letters*, 1978, **19**, 2235-2238.
224. Schwartz, R. E., Yunker, M. B., Scheuer, P. J. and Ottersen, T., Pseudozoanthoxanthins from gold coral, *Canadian Journal Of Chemistry*, 1979, **57**, 1707-1711.
225. Turk, T., Maček, P. and Šuput, D., Inhibition of acetylcholinesterase by a pseudozoanthoxanthin-like compound isolated from the zoanthid *Parazoanthus axinellae* (O. Schmidt), *Toxicon*, 1995, **33**, 133-142.
226. D'Ambrosio, M., Roussis, V. and Fenical, W., Zoamides AD: New marine zoanthoxanthin class alkaloids from an encrusting Philippine *Parazoanthus* sp., *Tetrahedron Letters*, 1997, **38**, 717-720.
227. Cariello, L., Crescenzi, S., Prota, G. and Zanetti, L., Zoanthoxanthins of a new structural type from *Epizoanthus arenaceus* (Zoantharia), *Tetrahedron*, 1974, **30**, 4191-4196.
228. Jiménez, C. and Crews, P., 13C-NMR assignments and cytotoxicity assessment of zoanthoxanthin alkaloids from zoanthid corals, *Journal of Natural Products*, 1993, **56**, 9-14.
229. Matsumura, K., Taniguchi, T., Reimer, J. D., Noguchi, S., Fujita, M. J. and Sakai, R., KB343, a cyclic tris-guanidine alkaloid from Palauan zoantharian *Epizoanthus illoricatus*, *Organic Letters*, 2018, **20**, 3039-3043.
230. Guillen, P. O., Jaramillo, K. B., Genta-Jouve, G., Sinniger, F., Rodriguez, J. and Thomas, O. P., Terrazoanthines, 2-aminoimidazole alkaloids from the Tropical Eastern Pacific zoantharian *Terrazoanthus onoi*, *Organic Letters*, 2017, **19**, 1558-1561.

231. Guillen, P. O., Jaramillo, K. B., Jennings, L., Genta-Jouve, G. g., de la Cruz, M., Cautain, B., Reyes, F., Rodríguez, J. and Thomas, O. P., Halogenated Tyrosine Derivatives from the Tropical Eastern Pacific Zoantharians *Antipathozoanthus hickmani* and *Parazoanthus darwini*, *Journal of Natural Products*, 2019.

232. Cachet, N., Genta-Jouve, G., Regalado, E. L., Mokrini, R., Amade, P., Culioli, G. and Thomas, O. P., Parazoanthines A−E, hydantoin alkaloids from the mediterranean sea anemone *Parazoanthus axinellae*, *Journal of Natural Products*, 2009, **72**, 1612-1615.

233. Wefer, J. and Lindel, T., Total synthesis of the marine natural product parazoanthine F by copper-mediated C–N coupling, *European Journal of Organic Chemistry*, 2015, **2015**, 6370-6381.

234. Audoin, C., Cocandeau, V., Thomas, O., Bruschini, A., Holderith, S. and Genta-Jouve, G., Metabolome consistency: Additional parazoanthines from the mediterranean zoanthid *Parazoanthus axinellae*, *Metabolites*, 2014, **4**, 421-432.

235. Kljajić, Z., Schröder, H. C., Rottmann, M., Cuperlović, M., Movsesian, M., Uhlenbruck, G., Gasić, M., Zahn, R. K. and Müller, W. E., A d-mannose-specific lectin from *Gerardia savaglia* that inhibits nucleocytoplasmic transport of mRNA, *European Journal of Biochemistry*, 1987, **169**, 97-104.

236. Müller, W., Renneisen, K., Kreuter, M. H., Schröder, H. and Winkler, I., The D-mannose-specific lectin from *Gerardia savaglia* blocks binding of human immunodeficiency virus type I to H9 cells and human lymphocytes in vitro, *Journal of Acquired Immune Deficiency Syndromes*, 1988, **1**, 453-458.

237. Li, C.-J., Schmitz, F. J. and Kelly-Borges, M., A New Lysine Derivative and New 3-Bromopyrrole Carboxylic Acid Derivative from Two Marine Sponges, *J. Nat. Prod.*, 1998, **61**, 387-389.

238. Cachet, N., Genta-Jouve, G., Ivanisevic, J., Chevaldonne, P., Sinniger, F., Culioli, G., Perez, T. and Thomas, O. P., Metabolomic profiling reveals deep chemical divergence between two morphotypes of the zoanthid Parazoanthus axinellae, *Sci. Rep.*, 2015, **5**, 8282.

239. Suksamrarn, A., Jankam, A., Tarnchompoo, B. and Putchakarn, S., Ecdysteroids from a Zoanthus sp, *J. Nat. Prod.*, 2002, **65**, 1194-1197.

240. Jizba, J., Herout, V. and Sorm, F., Polypodine B/A novel ecdysone-like substances from plant material, *Tetrahedron Lett.*, 1967, **8**, 5139-5143.

241. Smith, S. G. and Goodman, J. M., Assigning Stereochemistry to Single Diastereoisomers by GIAO NMR Calculation: The DP4 Probability, *J. Am. Chem. Soc.*, 2010, **132**, 12946-12959.

242. Cachet, N., Genta-Jouve, G., Ivanisevic, J., Chevaldonné, P., Sinniger, F., Culioli, G., Pérez, T. and Thomas, O. P., Metabolomic profiling reveals deep chemical divergence between two morphotypes of the zoanthid Parazoanthus axinellae, *Sci. Rep.*, 2015, **5**, 8282.

243. Das, J., Bhandari, M. and Lovely, C. J., *Studies in Natural Products Chemistry*, Elsevier, 2016, vol. 50, pp. 341-371.

244. Liu, J., Li, X.-W. and Guo, Y.-W., Recent advances in the isolation, synthesis and biological activity of marine guanidine alkaloids, *Marine Drugs*, 2017, **15**, 324.

245. Berlinck, R. G., Bertonha, A. F., Takaki, M. and Rodriguez, J. P., The chemistry and biology of guanidine natural products, *Natural Product Reports*, 2017, **34**, 1264-1301.

246. Feichtinger, K., Zapf, C., Sings, H. L. and Goodman, M., Diprotected triflylguanidines: a new class of guanidinylation reagents, *The Journal of Organic Chemistry*, 1998, **63**, 3804-3805.

247. Pandya, A. N., Baraiya, A. B., Jalani, H. B., Pandya, D., Kaila, J. C., Kachler, S., Salmaso, V., Moro, S., Klotz, K.-N. and Vasu, K. K., Discovery of 2-aminoimidazole and 2-amino imidazolyl-thiazoles as non-xanthine human adenosine A 3 receptor antagonists: SAR and molecular modeling studies, *MedChemComm*, 2018, **9**, 676-684.

248. Kumar, R., Khan, S. and MS Chauhan, P., 2-Aminoimidazole, glyciamidine and 2-thiohydantoin-marine alkaloids as molecular inspirations for the development of lead structures, *Current Drug Targets*, 2011, **12**, 1689-1708.

249. Atkinson, A. J., Wang, J., Zhang, Z., Gold, A., Jung, D., Zeng, D., Pollard, A. and Coronell, O., Grafting of bioactive 2-aminoimidazole into active layer makes commercial RO/NF membranes anti-biofouling, *Journal of Membrane Science*, 2018, **556**, 85-97.

250. Rogers, S. A., Huigens, R. W., Cavanagh, J. and Melander, C., Synergistic effects between conventional antibiotics and 2-aminoimidazole-derived antibiofilm agents, *Antimicrobial Agents and Chemotherapy*, 2010, **54**, 2112-2118.

251. Linares, D., Bottzeck, O., Pereira, O., Praud-Tabariès, A. and Blache, Y., Designing 2-aminoimidazole alkaloids analogs with anti-biofilm activities: Structure–activities relationships of polysubstituted triazoles, *Bioorganic & Medicinal Chemistry Letters*, 2011, **21**, 6751-6755.

252. Gao, C.-H., Wang, Y.-F., Li, S., Qian, P.-Y. and Qi, S.-H., Alkaloids and sesquiterpenes from the South China Sea gorgonian *Echinogorgia pseudossapo*, *Marine Drugs*, 2011, **9**, 2479-2487.

253. Agata, K., Ludmila, M., Maria, N. and Stanislaw, L., Gamma-lactones with potential biological activity, *Polish Journal of Natural Sciences*, 2017, **32**, 495-511.

254. Peng, J., Li, J. and Hamann, M. T., *The Alkaloids: Chemistry and Biology*, Elsevier, 2005, vol. 61, pp. 59-262.

255. Aiello, A., Fattorusso, E., Imperatore, C., Menna, M. and Müller, W., Iodocionin, a cytotoxic iodinated metabolite from the Mediterranean ascidian Ciona edwardsii, *Marine Drugs*, 2010, **8**, 285-291.

256. Kim, S.-K., Ngo, D.-H. and Vo, T.-S., *Advances in Food and Nutrition Research*, Elsevier, 2012, vol. 65, pp. 249-260.

257. RL Morlighem, J.-É., Huang, C., Liao, Q., Braga Gomes, P., Daniel Pérez, C., de Brandão Prieto-da-Silva, Á., Ming-Yuen Lee, S. and Radis-Baptista, G., The holo-transcriptome of the Zoantharian *Protopalythoa variabilis* (Cnidaria: Anthozoa): A plentiful source of enzymes for potential application in green chemistry, industrial and pharmaceutical biotechnology, *Marine drugs*, 2018, **16**, 207.

258. Byrne, M. J., Lees, N. R., Han, L.-C., van der Kamp, M. W., Mulholland, A. J., Stach, J. E., Willis, C. L. and Race, P. R., The catalytic mechanism of a natural Diels–Alderase revealed in molecular detail, *Journal of the American Chemical Society*, 2016, **138**, 6095-6098.

259. Klas, K., Tsukamoto, S., Sherman, D. H. and Williams, R. M., Natural Diels–Alderases: elusive and irresistable, *Journal of Organic Chemistry*, 2015, **80**, 11672-11685.

260. Nakamura, H., Kawase, Y., Maruyama, K. and Murai, A., Studies on polyketide metabolites of a symbiotic dinoflagellate, *Symbiodinium* sp.: a new C30 marine alkaloid, zooxanthellamine, a plausible precursor for zoanthid alkaloids, *Bulletin of the Chemical Society of Japan*, 1998, **71**, 781-787.

261. Fattorusso, E., Romano, A., Taglialatela-Scafati, O., Achmad, M. J., Bavestrello, G. and Cerrano, C., Lobozoanthamine, a new zoanthamine-type alkaloid from the Indonesian soft coral *Lobophytum* sp., *Tetrahedron Letters*, 2008, **49**, 2189-2192.

262. Costa, C. F., Sassi, R., Gorlach-Lira, K., LaJeunesse, T. and Fitt, W., Seasonal changes in zooxanthellae harbored by zoanthids (Cnidaria, Zoanthidea) from coastal reefs in northeastern Brazil, *Pan-American Journal of Aquatic Sciences*, 2013, **8**, 253-264.

263. Tubaro, A., Del Favero, G., Beltramo, D., Ardizzone, M., Forino, M., De Bortoli, M., Pelin, M., Poli, M., Bignami, G. and Ciminiello, P., Acute oral toxicity in mice of a new palytoxin analog: 42-hydroxy-palytoxin, *Toxicon*, 2011, **57**, 755-763.

264. Del Favero, G., Sosa, S., Poli, M., Tubaro, A., Sbaizero, O. and Lorenzon, P., In vivo and in vitro effects of 42-hydroxy-palytoxin on mouse skeletal muscle: structural and functional impairment, *Toxicology Letters*, 2014, **225**, 285-293.

265. Fujiki, H., Suganuma, M., Nakayasu, M., Hakii, H., Horiuchi, T., Takayama, S. and Sugimura, T., Palytoxin is a non-12-O-tetradecanoylphorbol-13-acetate type tumor promoter in two-stage mouse skin carcinogenesis, *Carcinogenesis*, 1986, **7**, 707-710.

266. Ishida, Y., Takagi, K., Takahashi, M., Satake, N. and Shibata, S., Palytoxin isolated from marine coelenterates. The inhibitory action on (Na, K)-ATPase, *Journal of Biological Chemistry*, 1983, **258**, 7900-7902.

267. Lazzaro, M., Tashjian Jr, A. H., Fujiki, H. and Levine, L., Palytoxin: An extraordinarily potent stimulator of prostaglandin production and bone resorption in cultured mouse calvariae, *Endocrinology*, 1987, **120**, 1338-1345.

268. Ruiz, Y., Fuchs, J., Beuschel, R., Tschopp, M. and Goldblum, D., Dangerous reef aquaristics: Palytoxin of a brown encrusting anemone causes toxic corneal reactions, *Toxicon*, 2015, **106**, 42-45.

269. Bellocci, M., Ronzitti, G., Milandri, A., Melchiorre, N., Grillo, C., Poletti, R., Yasumoto, T. and Rossini, G. P., A cytolytic assay for the measurement of palytoxin based on a cultured monolayer cell line, *Analytical Biochemistry*, 2008, **374**, 48-55.

270. Kagiava, A., Aligizaki, K., Katikou, P., Nikolaidis, G. and Theophilidis, G., Assessing the neurotoxic effects of palytoxin and ouabain, both Na+/K+-ATPase inhibitors, on the myelinated sciatic nerve fibres of the mouse: An ex vivo electrophysiological study, *Toxicon*, 2012, **59**, 416-426.

271. Pelin, M., Zanette, C., De Bortoli, M., Sosa, S., Della Loggia, R., Tubaro, A. and Florio, C., Effects of the marine toxin palytoxin on human skin keratinocytes: role of ionic imbalance, *Toxicology*, 2011, **282**, 30-38.

272. Souza, D. S., Grossi-de-Sa, M. F., Silva, L. P., Franco, O. L., Gomes-Junior, J. E., Oliveira, G. R., Rocha, T. L., Magalhaes, C. P., Marra, B. M. and Grossi-de-Sa, M., Identification of a novel β-N-acetylhexosaminidase (Pcb-NAHA1) from marine zoanthid *Palythoa caribaeorum* (Cnidaria, Anthozoa, Zoanthidea), *Protein Expression and Purification*, 2008, **58**, 61-69.

273. Lakshmi, V., Saxena, A., Pandey, K., Bajpai, P. and Misra-Bhattacharya, S., Antifilarial activity of *Zoanthus* species (Phylum Coelenterata, Class Anthzoa) against human lymphatic filaria, *Brugia malayi*, *Parasitology Research*, 2004, **93**, 268-273.

274. Konuklugil, B., Heydari, H., Genc, Y. and Ozgen, U., Bioactivity screening of some marine species from Turkey's coasts, *Farmacia*, 2018, **66**, 342-346.

275. Bhakuni, D. S. and Rawat, D. S., Bioactive marine natural products, *Springer Science & Business Media*, 2006,

8 Appendix

Appendix A: Bioactivity tables of Natural Products Isolated from *Palythoa* species

Table 4 Biological activities of palytoxin and its analogues isolated from *Palythoa s*pecies.

Name	Place of Collection	Compound	Bioactivity	LC_{50}	LD_{50}	Reference
P. toxica	Hawai	palytoxin	acute oral toxicity		767 µg/kg	[116]
			toxicity in mice intraperitoneal		15-50 ng/Kg	[97]
			toxicity in mice intravenously		30-150 ng/Kg	[97]
			Ehrlich ascites carcinoma in mice		5-84 ng/kg	[84]
		42-OH-50*R*-palytoxin	acute oral toxicity		652 µg/kg	[116]
		42-OH-palytoxin	skeletal myotubes by increasing Ca concentration	6 nM		[116]

Cont…

Name	Place of Collection	Compound	Bioactivity	LC$_{50}$	EC$_{50}$	LD$_{50}$	Concentration	Reference
P. toxica	Hawai	42-OH-50*R*-palytoxin	Acute oral toxicity	651 μg/Kg				[263]
			Erythrocyte hemolysis		7.6 and 13.2 x10^{-12} M			[263]
			mouse skeletal muscle cells		0.30 nM			[264]
P. caribaeorum	Puerto Rico	Palytoxin	toxicity on shore crab Carcinus maenas			62.5 ng/Kg		[113]
			UKHN-1 (oropharynx)			1.2 ng/mL		[136]
			UKHN-3 (tongue)			3.0 ng/mL		[136]
	Curacao, Netherlands	Methanolic fraction	Hemolysis				20 μl	[121]

Cont…

Name	Place of Collection	Compound	Bioactivity	EC_{50}	LD_{50}	Concentration	Reference
P. tuberculosa	Hawai	42-OH-50S-palytoxin	HaCaT cell (human skin keratinocytes)	9.3×10^{-10} M			[127]
		42-OH-50*R*-palytoxin	HaCaT cell (human skin keratinocytes)	1.0×10^{-10} M			
		palytoxin	HaCaT cell (human skin keratinocytes)	2.7×10^{-11} M			
	Ishigaki Islands, Japan	palytoxin	Tumor promoter in mouse ear		0.02 μg		[265]
			Inhibition of Na, K A-Tpase in guinea pig hearth		3.1×10^{-6} M		[266]
			Inhibition of Na, K A-Tpase in guinea pig hog cerebral cortex		9.0×10^{-7} M		
	Okinawa, Japan	palytoxin	Enhance bone resorption		3×10^{-13} M		[267]
			Inhibit bone resorption			> 10 pg/mL	

Cont…

Name	Place of Collection	Compound	Bioactivity	IC$_{50}$	LC$_{50}$	Reference
P. aff. *clavata/sakurajimensis*	Aquarium (Indonesia)	palytoxin	NHDF (dermal fibroblast)	> 1x 106 pM		[118]
			HBL-100 (mammary epithelial)	0.65 pM		
			A549 (lung carcinoma)	0.67 pM		
			Hs683 (glioma)	0.58 pM		
			U373n (glioma)	0.56 pM		
			9L (gliosarcoma) in rat	0.39 pM		
			B16F10 (melanoma) in mouse	0.44 pM		
P. aff. *margaritae*	Nakanoshima Islands, Japan		3Y1 Cells (rat fibroblast cell)		0.72 pM	[131]

Cont…

Name	Place of Collection	Compound	Bioactivity	IC$_{50}$	EC$_{50}$	Concentration	Reference
Palythoa sp.	Japan	palytoxin	Inhibition of human immunodeficiency virus producing cells (MOLT-4/HIVHTLV-IIIB cells)			2 pg/mL	[134]
			MOLT-4/HIV HTLV-IIIB			2 pg/mL	
Palythoa sp.	(Aquarium)		Irreversible visual impairment			0.4 μg/Kg	[268]
Commercial palytoxin (Wako Chemicals)	-		MCF-7 (breast cancer cell line)		0.53 nM		[269]
Commercial palytoxin (Wako Chemicals)	-		myelinated sciatic nerve fibers (mouse)	0.32 nM			[270]

Cont…

Name	Place of Collection	Compound	Bioactivity	IC_{50}	LC_{50}	Concentration	Reference
Commercial palytoxin (Wako Chemicals)	synthetic	palytoxin	HaCaT cell (human skin keratinocytes)		6.1×10^{-11} M		[271]
			NBT reduccion assay (superoxide anion)		3×10^{-10} M		
			Extracellular Na^+ and Ca^{2+}		1.0×10^{-7} M		
			MCF-7 (breast cancer cell line)			> 0.2 nM	
			CaCo-2 (human intestinal cell line)	0.1 nM			[135]

Table 5 Biological activities of miscellanea natural products and sterols isolated from *Palythoa* species

Name	Place of Collection	Compound	Bioactivity	IC$_{50}$	Concentration	Reference
P. caribaeorum	Brazil	*β-N*-acetylhexosaminidase (Pcb-NAHA1)	*p*-nitrophenyl-2-acetoamide-2-deoxy-*β*-D-*N*-acetylglucosamide substrate (pNP-GlcNAc)		3 mM	[272]
		DCM Fraction	Antioxidant	11.13 µg/mL		[179]
		70% MeOH Fraction	Antioxidant	11.25 µg/mL		
		EtOAc Fraction	Antioxidant	11.74 µg/mL		
		Aquous Fraction	Antioxidant	11.28 µg/mL		
		Metalloproteases 55, 63, 109 and 260 KDa (mucus)	papain inhibition		1 to 5 µg	[185]

Cont…

Name	Place of Collection	Compound	Bioactivity	IC_{50}	LD_{50}	Concentration	Reference
P. caribaeorum	Brazil	Metalloproteases 55, 63, 109 and 260 KDa (mucus)	trypsin inhibition			8 to 32 µg	[185]
			platellet inhibition			2.3 µg	
			pro-coagulant activity			0.75 µg	
			anticoagulant activity			1.5 to 6 µg	
		PcKuz-3	Citotoxicity Zebrafish	10 to 20 µM			[186]
		PcShK3	Citotoxicity Zebrafish		30 to 40 µM		[187]
			cardioprotective activity			< 20 µM	
			neuroprotective activity			30 µM	

Cont…

Name	Place of Collection	Compound	Bioactivity	IC50	LC_{50}	Concentration	Reference
P. caribaeorum	Veracruz, Mexico	A2-PLTX-Pcb1a	neurotoxic activity			3.5 mg/mL via intraventricular injection	[188]
P. caribaeorum/P. variabilis	Brazil	6β-carboxyl-24(*R*)-(8→6)-abeo-ergostan-3β,5β-diol	humna colonrectal tumor cell line (HCT-116)	50 µM after 24 hours and 50 µM after 72 hours			[91]
P. Kochii	Okinawa, Japan	PGA$_2$	nerve growth factor induced PC12 cell neurite (NGF-PC12 cell)	20 µM			[175]
			Stimulate tubulin polimerization			100 µM	
P. liscia	Mauritius, Tombeau bay	Ethanol extract	murine P388 lymphocytic leukemia (PS system)		0.029 µg/mL		[174]

Cont…

Name	Place of Collection	Compound	Bioactivity	LC$_{50}$	EC$_{50}$	Concentration	Reference
P. liscia	Mauritius, Tombeau bay	palystatin 1	murine P388 lymphocytic leukemia (PS in vivo system)			0.3 mg/Kg	[181]
		palystatin A	murine P388 lymphocytic leukemia (PS in vivo system)		0.0023 µg/mL		[182]
		palystatin B			0.020 µg/mL		
		palystatin C			0.0018 µg/mL		
P. mutuki	Vietnam	peridine	DENV 1	7.62 µM			[140]
			DENV 2	4.50 µM			
			DENV 3	5.84 µM			
			DENV 4	6.51 µM			
			inhibition of DENV protease	8.50 µM			

Cont…

Name	Place of Collection	Compound	Bioactivity	IC$_{50}$	Reference
P. tuberculosa	Red Sea	palysterol F	breast adenocarcinoma (MCF-7)	82 µM	[90]
			colon adenocarcinoma (HT-29)	122 µM	
			human cervical carcinoma (HeLa)	126 µM	
			non-cancerous human cell line (KMST-6)	128 µM	
	Taiwan	tuberazine C	anti-lymphangiogeneic activity in human lymphatic endothelial cells (LECs)	33 µg/mL	[138]

Cont…

Name	Place of Collection	Compound	Bioactivity	IC$_{50}$	Reference
Protopalythoa variabilis	Brazil	(2*S*)-2-aminotriacontanoic acid + (2*S*)-2-aminohentriacontanoic acid	human colon cancer (HCT-8)	0.13 µg/mL	[176]
			melanoma (MDA-MB-435)	0.05 µg/mL	
			CNS glioblastoma (SF-295)	0.07 µg/mL	
			Leukemia (HL-60)	0.1 µg/mL	

Cont…

Name	Place of Collection	Compound	Bioactivity	LD_{50}	Concentration	Reference
Protopalythoa variabilis	Brazil	ShK/Aurelin-like peptide	Citotoxicity Zebrafish	15-20 µM		[184]
			Locomotion test Zebrafish		10 µM	
		anthozoan neurotoxin-like peptide	Citotoxicity Zebrafish	3-30 µM		
		Pp V-shape α-helical peptide (PpVα)	disturbed locomotion in Zebrafish		> 5 µM linear/>2.5 µM folded	[189]
		Pp V-shape α-helical peptide (PpVα)	Citotoxicity Zebrafish	10.88 µM folded/21.23 µM linear		
		Pp V-shape α-helical peptide (PpVα)	neuroprotective activity		> 1 µM folded and linear forms	

Appendix B: Bioactivity tables of Natural Products Isolated from
***Zoanthus* species**

Table 6 Biological activities of zoanthamine alkaloids isolated from *Zoanthus* species.

Name	Place of Collection	Compound	Bioactivity	IC$_{50}$	ED$_{50}$	Concentration	Reference
Zoanthus sp	Bay of Bengal, India	28-deoxyzoanthenamine	Antiinflammatory (Inhibiton phorbol myristate cetate (PMA)		9 µg/ear		[148]
			Analgesic activity			50 mg/Kg	
	Amami Islands, Japan	norzoanthamine	P388 murine leukemia cells	24 µg/mL			[151]
		oxyzoanthamine		7.0 µg/mL			
		norzoanthaminone		1.0 µg/mL			
		cyclozoanthamine		24 µg/mL			
		epinorzoanthamine		2.6 µg/mL			
	Canary Islands	zoanthenol	selective collagen-induced aggregation			0.125 to 1 mM	[161]
		norzoanthamine	inhibition of trombin-collagen and arachidonic acid-induced platelet aggregation			0.3 to 1 mM	

Cont…

Name	Place of Collection	Compound	Bioactivity	Concentration	Reference
Zoanthus sp.	Canary Islands	30-hydroxynorzoanthamine	collagen-induced aggregation	0.3 and 1 mM	[161]
		oxyzoanthamine	Pro-aggregan effect	0.125 to 1.5 mM	
	Ayamaru coast, Japan	norzoanthamine	Inhibition of IL-6	13 µg/mL	[153]
		norzoanthamine hydrochloride		4.7 µg/mL	
	Gujarat, India	Chloroform/Methanol (1:1) extract	Atnifilaria activity against Brugia malayi	125 µg/mL	[273]
Z. numphaeus	Brazil	11-hydroxyzoanthamine	inhibition of trombin-collagen and arachidonic acid-induced platelet aggregation	0.3, 0.5 and 1mM	[161]
		3-hydroxynorzoanthamine	collagen-induced aggregation	0.3 and 1 mM	
		zoanthaminone	Pro-aggregan effect	1 mM	

Cont…

Name	Place of Collection	Compound	Bioactivity	IC$_{50}$	Concentration	Reference
Z. kuroshio	Kaohsiung city, Taiwan.	kuroshine E	Melanoma cell line B16	120 µM		[166]
		5α-iodozoanthenamine	anti-inflammatory activity		10 µM	[167]
Zoanthus cf. *pulchellus*	San Pedro, Ecuador	3-acetoxynorzoanthamine	neuro-inflammatory activity in microglia BV-2 cells (ROS and NO)		0.001 to 10 µM (dose depended)	[168]
		norzoanthamine			0.001 to 10 µM (dose depended)	
		3-acetoxyzoanthamine			0.001 to 10 µM	
		zoanthamine			0.001 to 10 µM	
		3-hydroxynorzoanthamine			0.001 to 10 µM	

Table 7 Biological activities of ecdysteroids isolated from *Zoanthus* species.

Name	Place of Collection	Compound	Bioactivity	EC$_{50}$	Concentration	Reference
Zoanthus sp.	Goa coast, India	2-deoxyecdysterone	Oxytoxic acitivty (oxytoxin and PGF2α)		50, 100, 200 μg/mL	[141]
	Taiwan	zoanthone A	DENV-2	19.61 μM		[143]
		ajugasterone C	DENV-1	15.7 μM		
			DENV-2	10.05 μM		
			DENV-3	9.48 μM		
			DENV-4	12.15 μM		

Table 8 Biological activities of diverse natural products isolated from *Zoanthus* species.

Name	Place of Collection	Compound	Bioactivity	LD$_{50}$	Concentration	Reference
Zoanthus sp.	Veraval, Gujarat, India	DCM:MeOH extract (1:1)	human lymphatic filaria Brugia malayi		125 μg/mL	[273]
Zoanthus sociatus	La Habana, Cuba	Low molecular weight fraction	reduced glucose stimulated insulin secretion > 60%		50 μg/mL	[193]
			reduced calcium elevation in isolated β-cells		50 μg/mL	
			elevation of plasma glucose in rats		300 μg/Kg intraperitoneal	
			toxic effect	792 μg/Kg in mice		[194]

Appendix C: Bioactivity tables of Natural Products Isolated from species belonging to the suborder Macrocnemina

Table 9 Biological activity of natural products isolated from *Parazoanthus* species.

Name	Place of Collection	Compound	Bioactivity	IC$_{50}$	EC$_{50}$	Reference
P*arazoanthus* cf. *axinellae*		zoanthoxanthin	Inhibition of succinic oxidase	5.7×10^{-4} M		[214]
Parazoanthus axinellae	Marsseille coast, France	parazoanthine C	Microtox assay		1.64 µM	[232]
	Turkey	methanolic extract	Human larynx epidermoid carcinoma cell lineHep-2	230.1 µg/mL		[274]
		methanolic extract	Inhibition of tyrosinase	97.72 µg/mL		

Cont…

Name	Place of Collection	Compound	Bioactivity	LD50	Ki	Reference
Parazoanthus sp.	Northern Adriatic Sea	pseudozoanthoxanthin	AChE inhibitory activity		4 µM	[225]
Parazoanthus spp.	India	extract	Hypoglycaemic and spasmolytic activity	> 1000 mg/kg in mice		[275]

Table 10 Biological activities of natural products isolated from *Epizoanthus* species.

Name	Place of Collection	Compound	Bioactivity	IC_{50}	LD_{50}	Reference
Epizoanthus spp.	India	extract	Hypoglycaemic		0.38 mg/kg in mice	[275]
Epizoanthus sp.	Fiji Islands	2-*N*-demethyl-zoanthoxanthin	Human colon adenocarcinoma (HCT8)	1.61 µg/mL		[228]
			Human lung carcinoma (A549)	2.38 µg/mL		
Epizoanthus illoricatus	Republic of Palau	KB343	human tumor cell line (HeLa)	4.93 µM		[229]
			neuronal cell line (SH-SY5Y)	3.40 µM		

Table 11 Biological activities of natural products isolated from *Savalia* and *Antipathozanthus* species

Name	Place of Collection	Compound	Bioactivity	IC$_{50}$	Association constant (Ka)	Concentration	Reference
Savalia savaglia	Kator bay, Yugoslavia	D-mannose-specific lectin	hemagglutination inhibition		2.8 x 10-8 M		[235]
			anti-HIV activity in H9 cells			0.2 µM	[236]
			anti-HIV-1 strain D 34/human lymphocite system			0.67 µM	
Antipathozonthus hickmani	El Pelado Islet, Ecuador	valdiviamide B	hepatocellular carcinoma cell line (HepG2)	7.8 µM			[231]

Appendix D: Supplementary Information

Terrazoanthines, 2-aminoimidazole alkaloids from the Eastern Pacific zoantharian *Terrazoanthus onoi*

Supplementary Information for

Terrazoanthines, 2-aminoimidazole alkaloids from the Eastern Pacific zoantharian *Terrazoanthus onoi*

Paul O. Guillen,[†,‡] Karla B. Jaramillo,[†,‡] Gregory Genta-Jouve,[§] Frederic Sinniger,[⊥] Jenny Rodriguez,*[,†] Olivier P. Thomas*[,§]

† Escuela Superior Politécnica del Litoral, Centro Nacional de Acuacultura e Investigaciones Marinas, km 30.5 *via* Perimetral, Guayaquil, Ecuador.

‡ National University of Ireland Galway, School of Chemistry, Marine Biodiscovery, University Road, Galway, Ireland.

§ Université Paris Descartes, équipe C-TAC, COMETE UMR 8638 CNRS, 4 avenue de l'observatoire, 75006 Paris, France

⊥ University of the Ryukyus, Tropical Biosphere Research Center, 3422 Sesoko, 905-0227 Okinawa, Japan

Biological Material. *Terrazoanthus onoi* Reimer & Fujii, 2010 is a macrocnemic zoantharian of the family of Hydrozoanthidae (Cnidaria, Anthozoa, Hexacorallia, Zoantharia). This species is present in the Pacific Ocean and it can be recognized by its external appearance, ecology and by DNA analyses. Most specimens observed in situ were encountered on rocky substrates with some of them growing on the octocoral *Muricea* spp. and the black corals *Antipathes galapagensis* (Deichmann, 1941) and *Myriopathes* sp.

Sampling. The zoantharian colony selected to isolate the chemical compounds was growing on rocky substrate to avoid potential contamination from the invertebrates used as substrates in cases of colonies growing on octocorals or black corals. The specimen was collected by SCUBA diving in August 2015 at the Marine Protected Area "El Pelado", Ecuador, at 15 m depth (1°56'6.00"S, 80°47'22.08"W). Fragments of the colony were fixed in: a) 4% formalin for detailed morphological analyses, b) 95% Ethanol for phylogenetic analyses and c) the remaining material was kept at -80 °C for chemical studies. Voucher sample are kept at CENAIM under the number 150807EP07-08

Taxonomic Identification. Morphological information was obtained from the formalin fixed sample and in situ observations. Observations included: polyp measurements (oral disk diameter, polyp height), number of tentacles, colors of column, oral disk, tentacles and coenenchyme, relative amount of sand encrustation and host species or substrate. Cnidome data were obtained from the pharynx, mesenterial filaments and tentacles; in addition, column samples were also processed but mineral inclusions impeded objective quality observations. To observe the cnidae, a little piece of tissue from formalin preserved sample was used for the smashed preparations which were analyzed, photographed, and measured using a light microscope (40x), we followed the nomenclature by England (1991)

DNA extraction and sequencing. DNA data were obtained from the fragment fixed in ethanol 95%. DNA extraction, PCR and sequencing were made as described in Sinniger et al. (2010). Specimens were amplified for mitochondrial cytochrome oxidase subunit I (COI), mitochondrial small ribosomal subunit (16S), nuclear internal transcribed spacer region (ITS-2) and nuclear small ribosomal subunit (18S). PCR primers and conditions were based on Sinniger et al. 2013 (and references therein). Amplified products were visualized by 1.5% agarose gel electrophoresis and sequenced at a commercial sequencing company (MacroGen Inc., Korea).

DNA taxonomy. Chromatograms were checked for quality and the resulting sequences were manually assembled using BioEdit software version 7.2.0. Sequences were compared with publicly available zoantharian using the National Center for Biotechnology Information's Basic Local Alignment Search Tool (NCBI BLAST). New zoantharian sequences acquired in this study were deposited in GenBank (accession numbers KY694963-KY694966) and compared by BLAST with original sequences of *Terrazoanthus onoi* and other zoantharians. It must be noted that according to the accession numbers

listed in the original description, most *T. onoi* sequences are listed in GenBank as *T. sinnigeri* and here we compared sequences using the accession numbers listed in the original publication (Table I in Reimer and Fujii 2010).

Morphological analyzes. Contracted polyps measured 2.0–5.0 mm diameter and 3.0–6.0 mm height (measured starting from the coenenchyme). Oral discs of the polyps were surrounded by an average of 36 tentacles. Color of the coenenchyme and the polyps column was a brownish dark yellow, while the oral disk and tentacles were dark red. Tips of the tentacles were white. The coenenchyme and the polyp column were relatively heavily incrusted by mineral particles. The colony sampled for this study had approximately 210 polyps and was collected from a rocky substrate colonized by red and brown thread algae and some cirripeds crustaceans (family Balanidae). Cnidae in the pharynx were composed mainly of b-mastigophores with occasional p-mastigophores and spirocysts; holotrichs were uncommonly observed. In the mesenterial filaments, p-mastigophores were common with only few holotrichs. The tentacles had the highest cnidae diversity with common spirocysts, occasional p-mastigophores and few holotrichs and b-mastigophores.

Figure S1. In situ photographs of *Terrazoanthus onoi* at the MPA El Pelado, August 25, 2015.

DNA sequences of *Terrazoanthus onoi*. Unfortunately no DNA sequences are published from either the holotype or paratypes from *T. onoi,* however, when comparing with non-type specimens sequences (from different islands in the Galapagos) published together with the original description, the 840 bp mitochondrial COI sequence obtained from our sample was identical to the 280 bp sequences from the original description (GU357560.1-GU357567.1, GU357557.1, EU333791.1-EU333794.1 but it was slightly different from two additional longer sequences (JN582016.1 and JN582017.1) of *T. onoi* from Bo et al. 2012 (1 and 2 bp difference out of 595 and 593 bp respectively). The sequence GU357558 is listed as *T. onoi* in the original description and in GenBank but appears to correspond to a completely different zoantharian (*Antipathozoanthus hickmani*) and we removed it from our comparisons.

Unfortunately, based on the sequences currently published, COI does not allow distinguishing between *T. onoi* and *T. sinnigeri*. However, 16S shows differences between the single *T. sinnigeri* sequence published and *T. onoi*. Our 920 bp 16S sequence overlap fully and is identical to the original 16S sequences of *T. onoi* (EU333758.1-EU333763.1, EU333766.1, EU333767.1, 561-573 bp) and displays the 1 bp difference with EU333764.1 also assigned to *T. onoi* and 2 bp with EU333765.1 assigned to *T. sinnigeri*. EU333768.1 assigned also to *T. onoi* according to Reimer and Fujii 2010 is largely different from any zoantharian known and we ignored this sequence in our comparisons, as it may be artefactual. The nuclear ITS region is more variable and may be more adapted to distinguish between *T. onoi* and *T. sinnigeri* although significant intraspecific variability can be observed with this marker in some instances. ITS region sequence of the specimen studied here (774 bp) matched perfectly with most *T. onoi* sequences (625 bp, EU333804.1-EU333806.1, EU333808.1 and EU333809.1) and with *T. onoi* from mainland Ecuador (826 bp, JN582022.1). Three *T. onoi* sequences (EU333803.1, EU333807.1 and JN582023.1) differed by a single bp. The ITS region of *T. sinnigeri* is different from *T. onoi* through a small indel at the beginning of the sequences obtained with the primers used and corresponding to the 5' end region of the nuclear small ribosomal subunit (18S), in addition the first site of the ITS2 is different between *T. onoi* and *T. sinnigeri* in most cases. The 1756 bp sequenced from the nuclear small ribosomal subunit (18S) were congruent with our sample belonging to *Terrazoanthus* based on phylogenetic comparisons with other zoantharians, although currently no reference sequences from *T. onoi* or *T. sinnigeri* are available.

Rationale for species identification.

The other closely related species, *T. sinnigeri*, is clearly different in color, habitat and DNA (with distinct ITS sequences). One or two bp differences in the COI marker may suggest significant difference in zoantharians, however, in our case, the differences occurred near a poly G and near a poly T at the end of the sequence and may therefore be due to PCR artefacts although in our chromatograms the divergent sites were clearly unambiguous. Overall, based on our experience and current knowledge in *Terrazoanthus*, the differences from the previous works observed here in DNA, morphology or cnidae are not significant enough to justify considering that our sample may belong to a distinct species. While DNA may prove problematic to distinguish reliably between *T. onoi* and *T. sinnigeri*, based on the combination of the morphological observations, in particular the characteristic red coloration, the habitat (on rocks and black corals) and the dimensions of the polyps, as well as based on DNA comparisons we are confident to assign the sample analysed here to the species *T. onoi*.

References.

Reimer JD, Fujii T (2010) four new species and one new genus of zoanthids (Cnidaria, Hexacorallia) from the Galápagos Islands. ZooKeys 42: 1–36.

Sinniger F, Reimer JD, Pawlowski J (2010) The Parazoanthidae DNA taxonomy: Description of two new genera. Marine Biodiversity 40: 57–70.

Bo, M., Lavorato, A., Di Camillo, C. G., Poliseno, A., Baquero, A., Bavestrello, G. & Reimer, J. D. (2012). Black coral assemblages from Machalilla National Park (Ecuador). Pacific Science, *66*(1), 63-81

England, K. W., & Robson, E. A. (1991). Nematocysts of sea anemones (Actiniaria, Ceriantharia and Corallimorpharia: Cnidaria): nomenclature. In *Coelenterate biology: Recent research on Cnidaria and Ctenophora* (pp. 691-697). Springer Netherlands.

General Experimental Procedures. Optical rotations were measured at the sodium D line (589.3 nm), at 20 °C on a Unipol L1000 Schmidt + Haensch polarimeter with a 10 cm cell. UV spectra were acquired in spectroscopic grade MeOH on a Varian, Cary 100 UV-Vis spectrophotometer. Electronic Circular Dichroism spectra were obtained on a Jasco J-810 spectropolarimeter system. NMR spectra were obtained on an Agilent 600 MHz spectrometer equipped with cryoprobe with pulsed field gradient and signals were referenced in ppm to the residual solvent signals (CHD$_2$OD, at δ_H 3.31 and δ_C 49.0). HRESIMS data were measured with a UHR-qTOF Agilent 6540 mass spectrometer. HPLC purification was carried out on a Waters 600 system equipped with a Waters 717 Plus autosampler, a Waters 998 photodiode array detector, and a Sedex 75 evaporative light-scattering detector.

Extraction and Isolation. The freeze-dried sample (29.9 g) was extracted with a mixture DCM/MeOH (1:1), three times using 500 mL each time under ultrasound at room temperature and the solvents removed under pressure obtaining an extract (2.4 g). The extract was fractionnated by C$_{18}$ reversed phase vacuum liquid chromatography (LiChroprep® RP-18, 40-63μm) using a mixture of solvents of decreasing polarity 1). H$_2$O, 2). H$_2$O/MeOH (1:1), 3). H$_2$O/MeOH (1:3), 4). MeOH, 5). MeOH/DCM (3:1), 6). MeOH/DCM (1:1), and 7). DCM (using 500 mL of each solvent). The fractions 3 and 4 were pooled and pre-purified by preparative RP-HPLC using a Phenyl Hexyl column (Symmetry, 19 x 250 mm, 5 μm), using an isocratic method CH$_3$CN: H$_2$O:acetic acid (15:85:0.1) as a mobile phase at a flow rate of 12 mL/min with detection at λ 254 nm for 50 min, obtaining 12 fractions. These fractions were finally purified by semi-preparative RP-HPLC using a Phenyl Hexyl column (Symmetry, 10 x 250 mm, 5 μm), using CH$_3$CN:H$_2$O:acetic acid 18:82:0.1 as mobile phase at 3.5 mL/min leading to pure compounds Terrazoanthine A (**1**) (5.41 mg), Terrazoanthine B (**2**) (3.15 mg) and Terrazoanthine C (**3**) (1.6 mg).

Terrazoanthine A (1). Yellowish oil; $[\alpha]_{20}{}^D$ + 10.0 (*c* 0.48, MeOH); UV (CH$_3$OH) λ_{max} (log ε) 262 (3.29) nm; ECD (*c* 4.9 × 10^{-5} M, CH$_3$OH) λ_{max} ($\Delta\varepsilon$) 234 (-0.47), 269 (+3.7) nm; ^{1}H NMR data see table 1 and ^{13}C NMR data see Table 2; HRESIMS *m/z* 407.2187 [M+H]$^+$ (calcd for C$_{22}$H$_{27}$N$_6$O$_2$, 407.2190 Δ -0.7 ppm).

Terrazoanthine B (2). Yellowish oil; $[\alpha]_{20}{}^D$ + 4.4 (*c* 0.31, MeOH); UV (CH$_3$OH) λ_{max} (log ε) 264 (3.17) nm; ^{1}H NMR data see table 1 and ^{13}C NMR data see Table 2; HRESIMS *m/z* 393.2043 [M+H]$^+$ (calcd for C$_{21}$H$_{25}$N$_6$O$_2$, 393.2034 Δ +2.3 ppm).

Terrazoanthine C (3). Yellowish oil; $[\alpha]_{20}^D$ + 7.5 (*c* 0.16, MeOH); UV (CH$_3$OH) λ_{max} (log ε) 277 (3.03) nm; ECD (*c* 5.6 × 10^{-5} M, CH$_3$OH) λ_{max} ($\Delta\varepsilon$) 287 (+3.3) nm; ^{1}H NMR data see table 1 and ^{13}C NMR data see Table 2; HRESIMS *m/z* 360.1556 [M+H]$^+$ (calcd for C$_{18}$H$_{22}$N$_3$O$_5$, 360.1554 $\varDelta$ +0.2 ppm).

UHPLC-qToF analysis of 1 in (+)-ESI
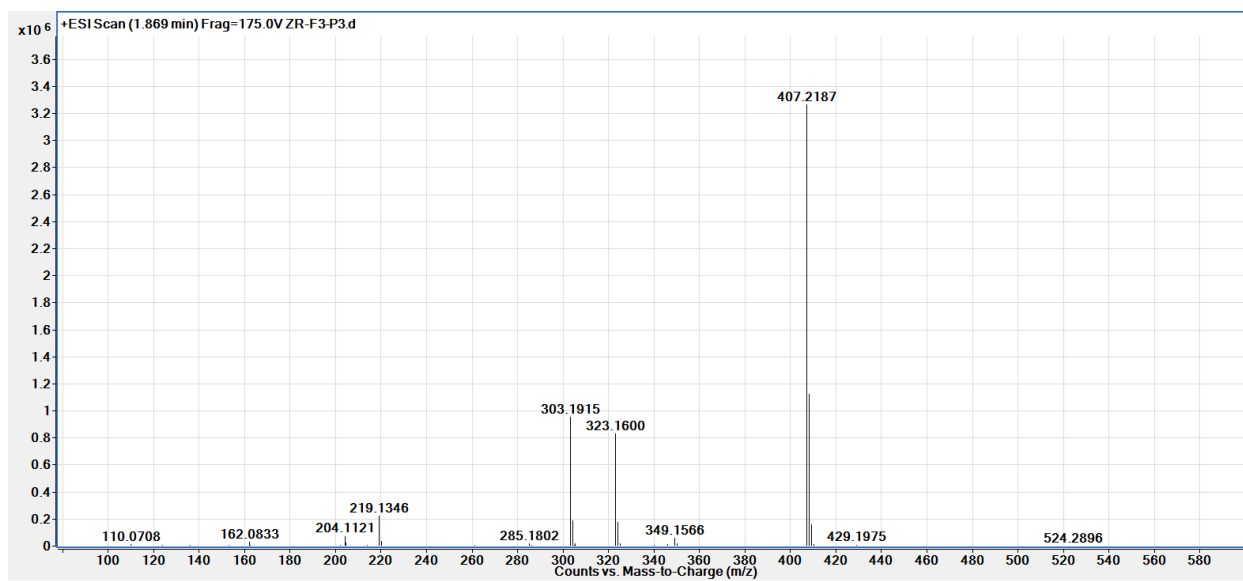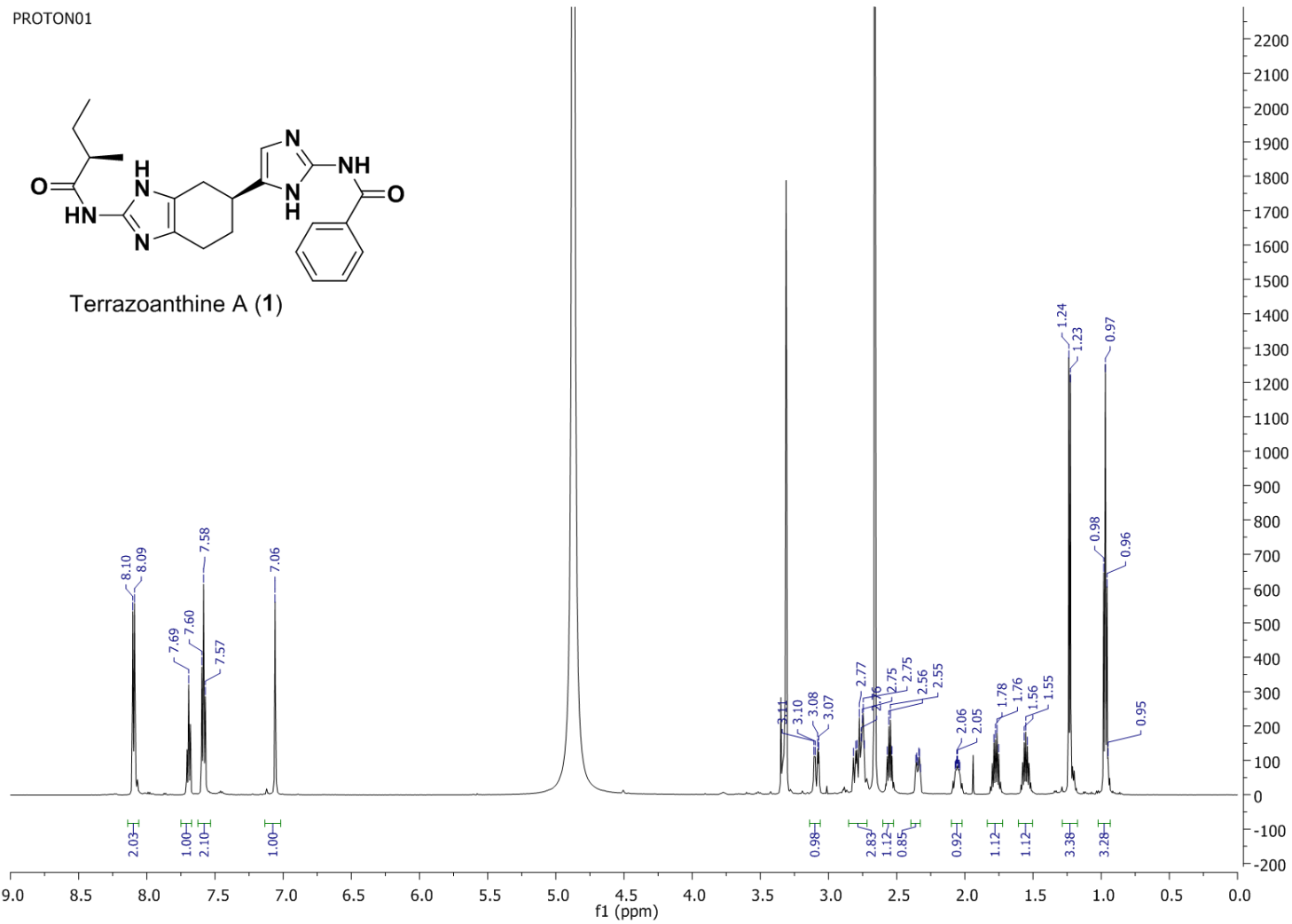
PROTON01

Terrazoanthine A (**1**)

^{1}H NMR spectrum of **1** at 600 MHz in CD$_3$OD
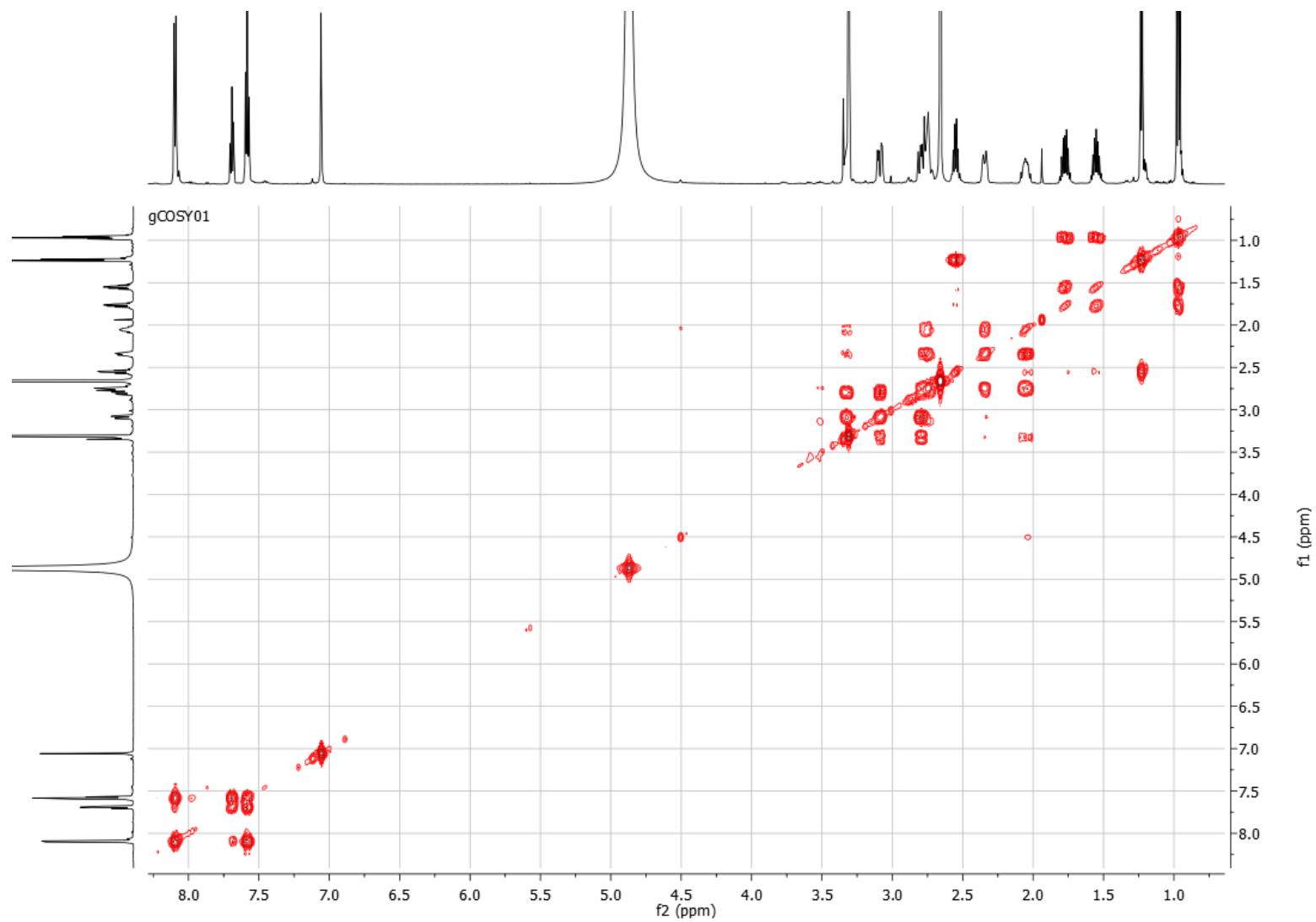
COSY NMR spectrum of **1** at 600 MHz in CD$_3$OD

CARBON01
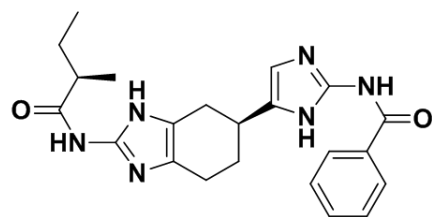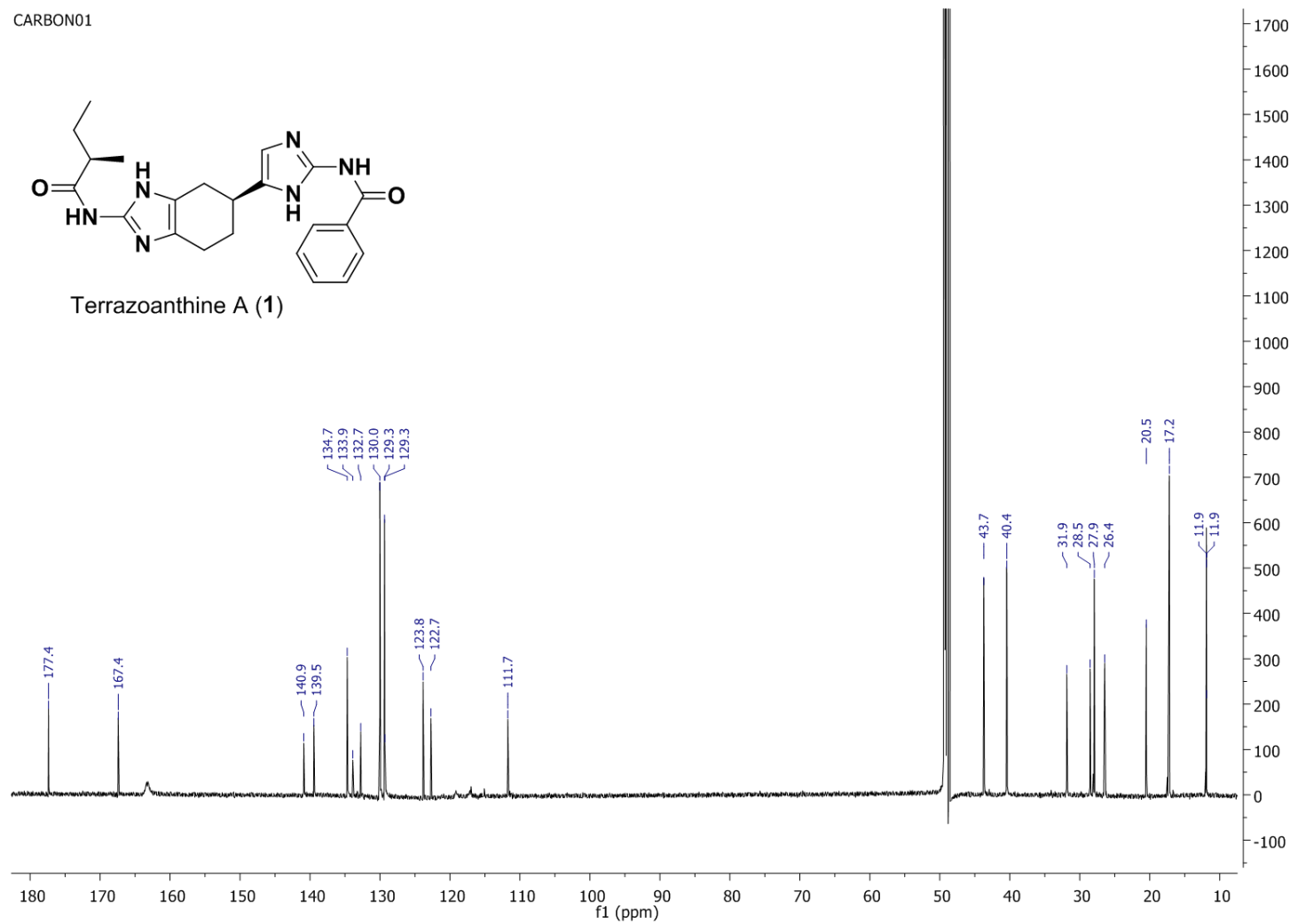
Terrazoanthine A (**1**)

^{13}C NMR spectrum of **1** at 125 MHz in CD$_3$OD
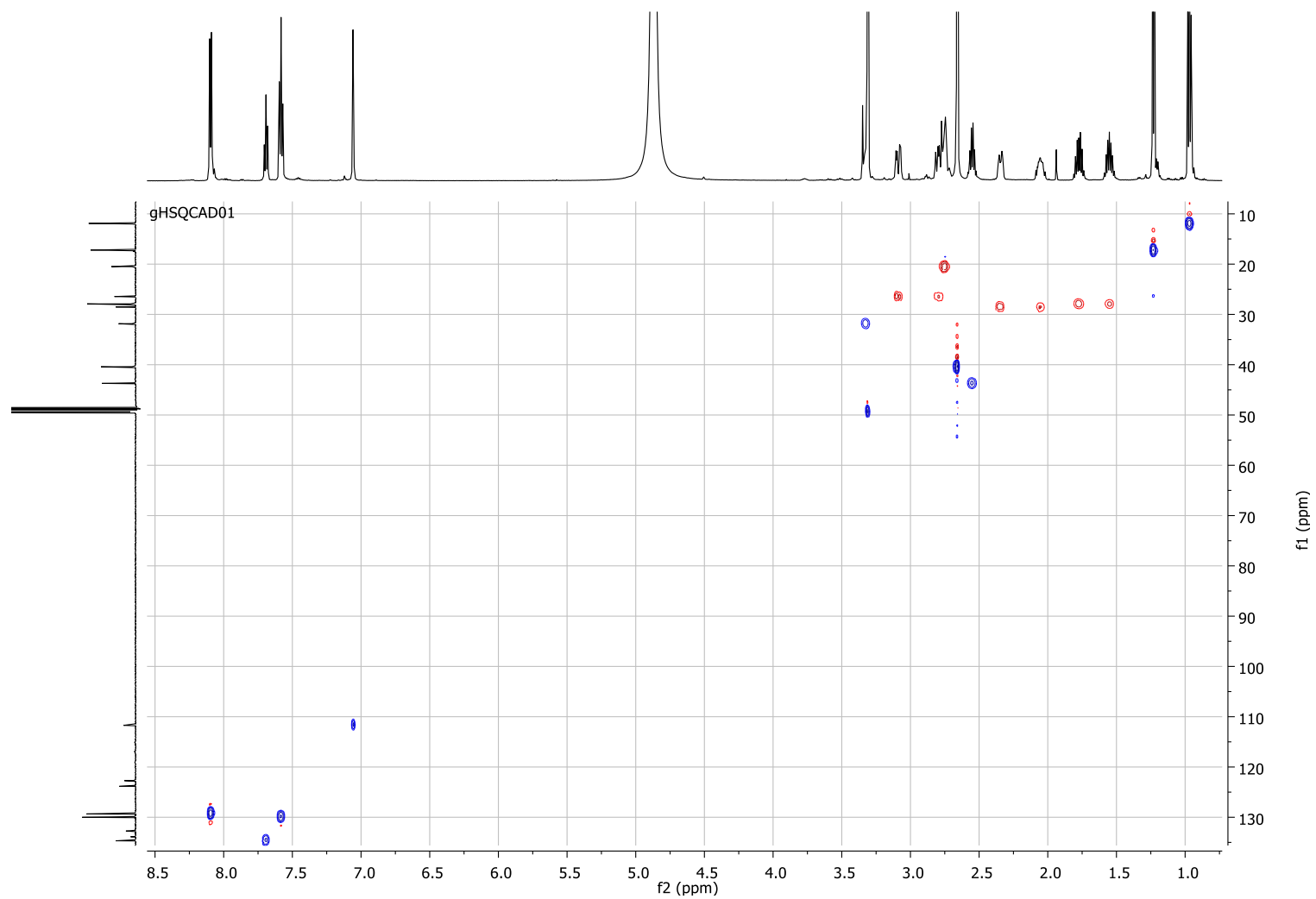
HSQC NMR spectrum of **1** at 600 MHz in CD₃OD
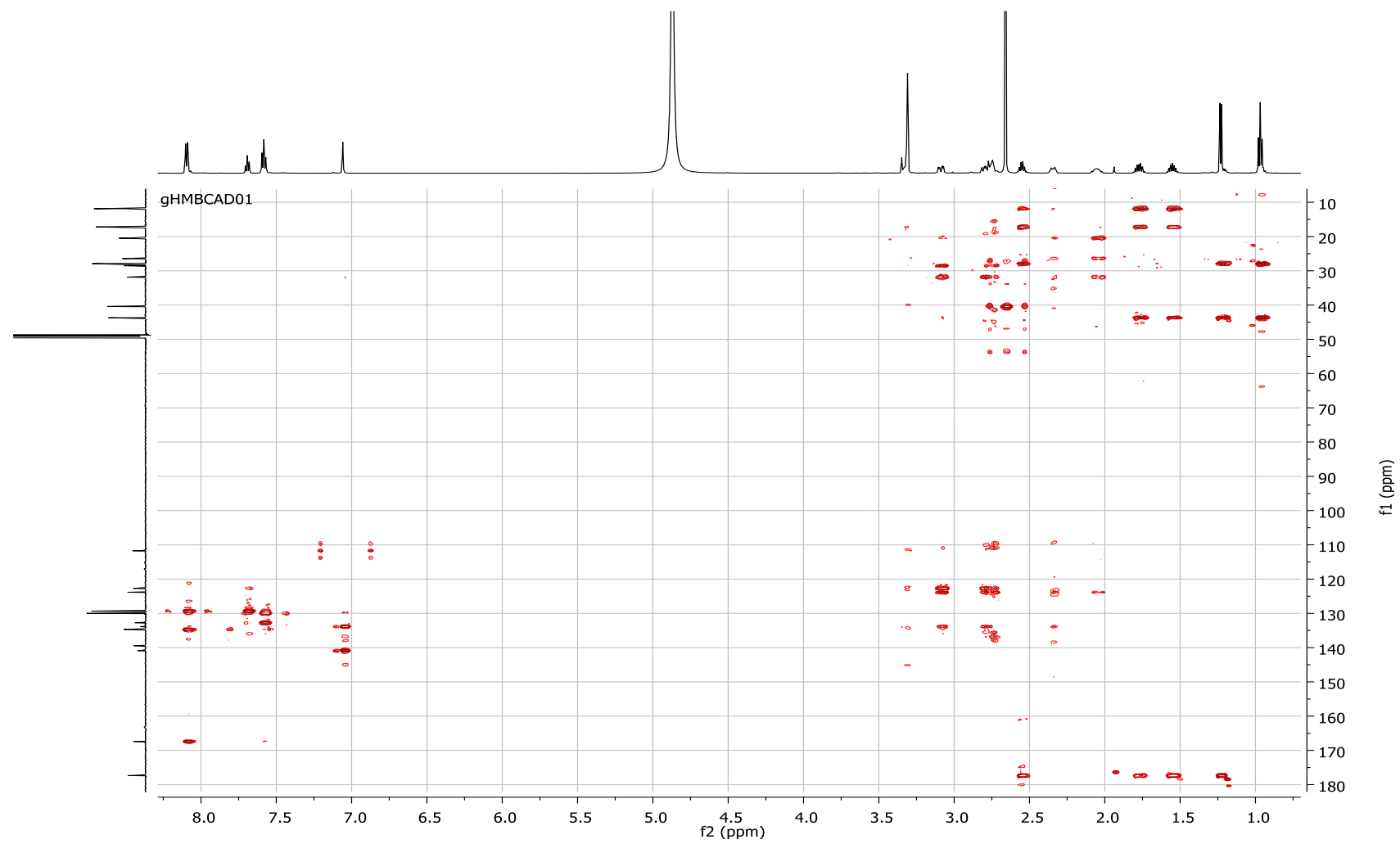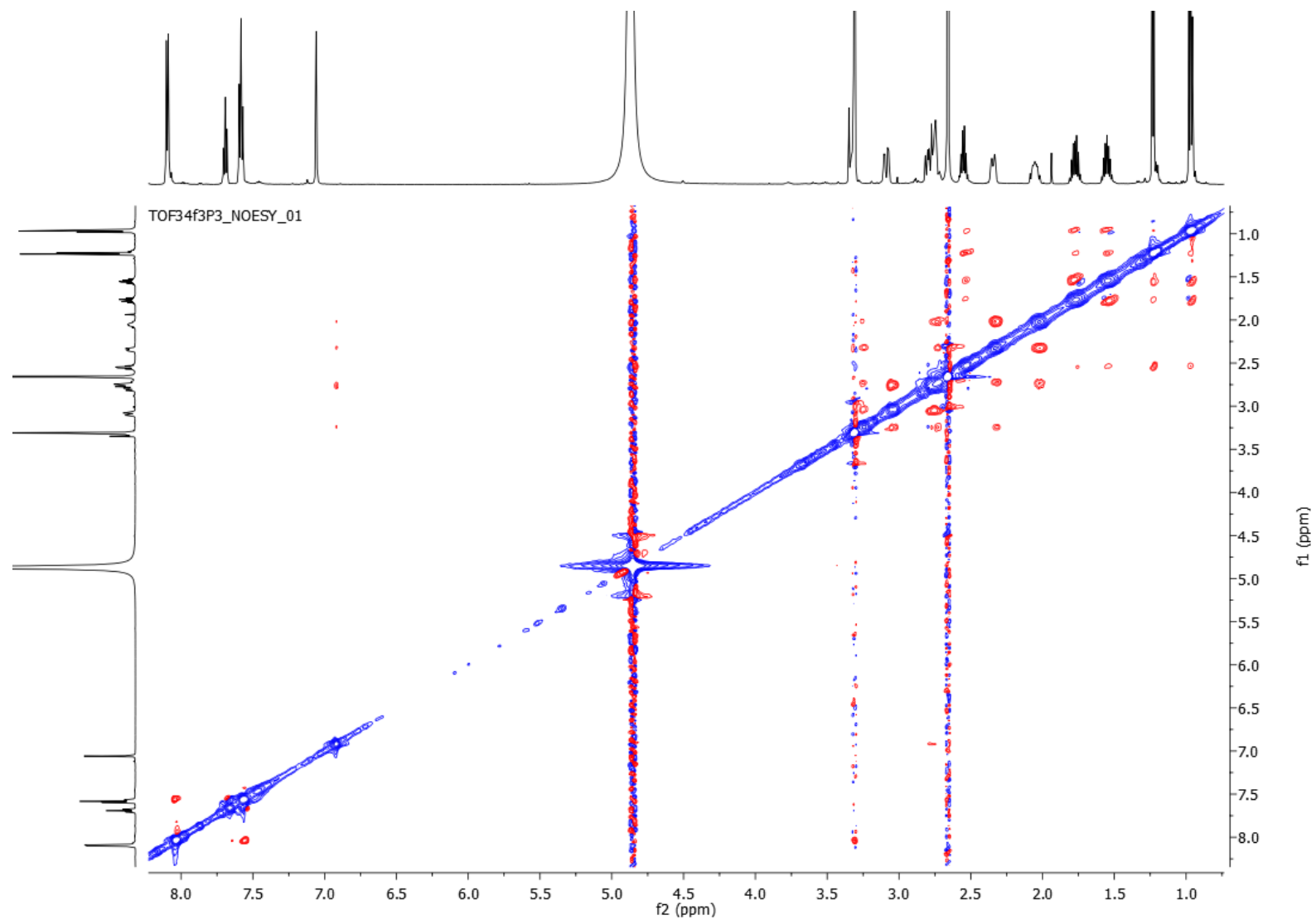
HMBC NMR spectrum of **1** at 600 MHz in CD$_3$OD

TOF34f3P3_NOESY_01

NOESY NMR spectrum of **1** at 600 MHz in CD₃OD

PROTON01

13.26

12.11

11.58

8.40

6.80
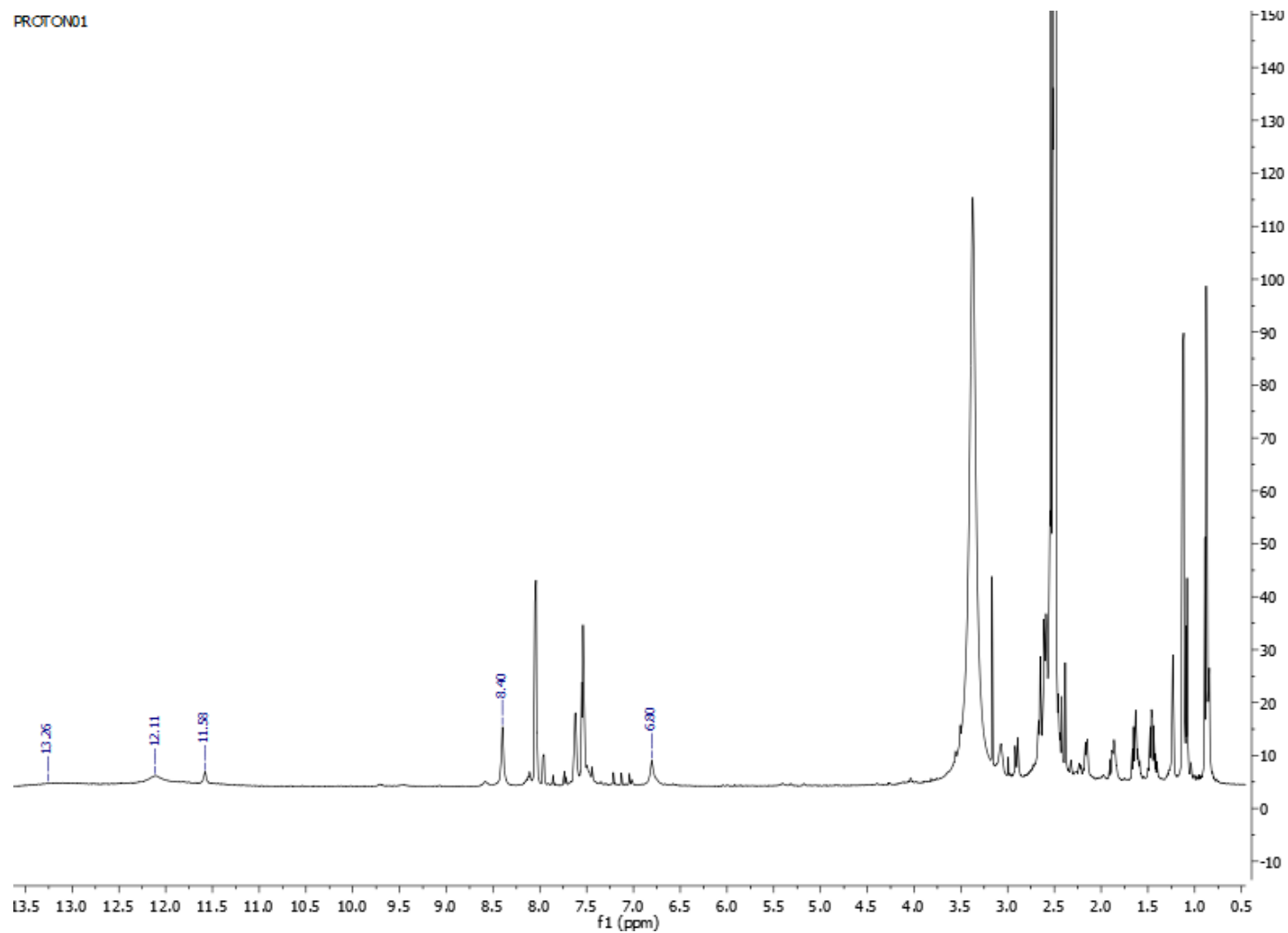
¹H NMR spectrum of **1** at 600 MHz in DMSO-d_6

ROESY01

f1 (ppm)

f2 (ppm)
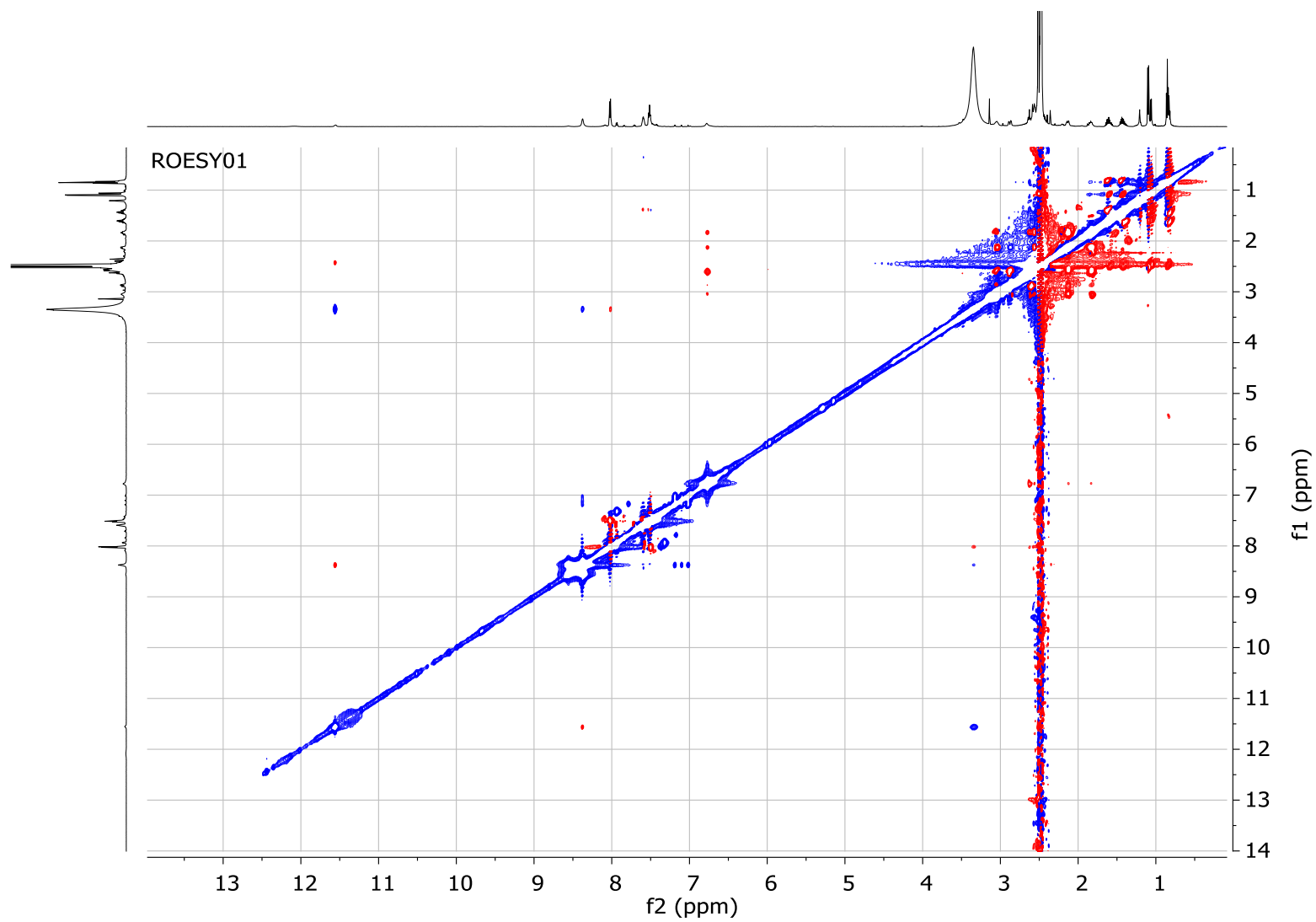
ROESY NMR spectrum of **1** at 600 MHz in DMSO-d_6

UHPLC-qToF analysis of 2 in (+)-ESI
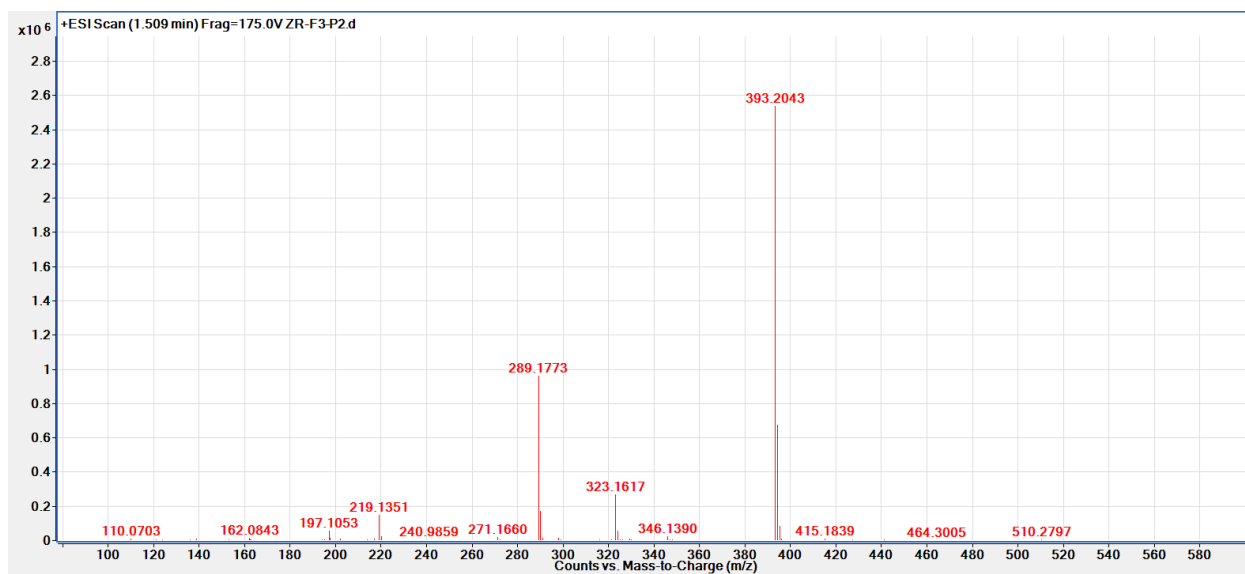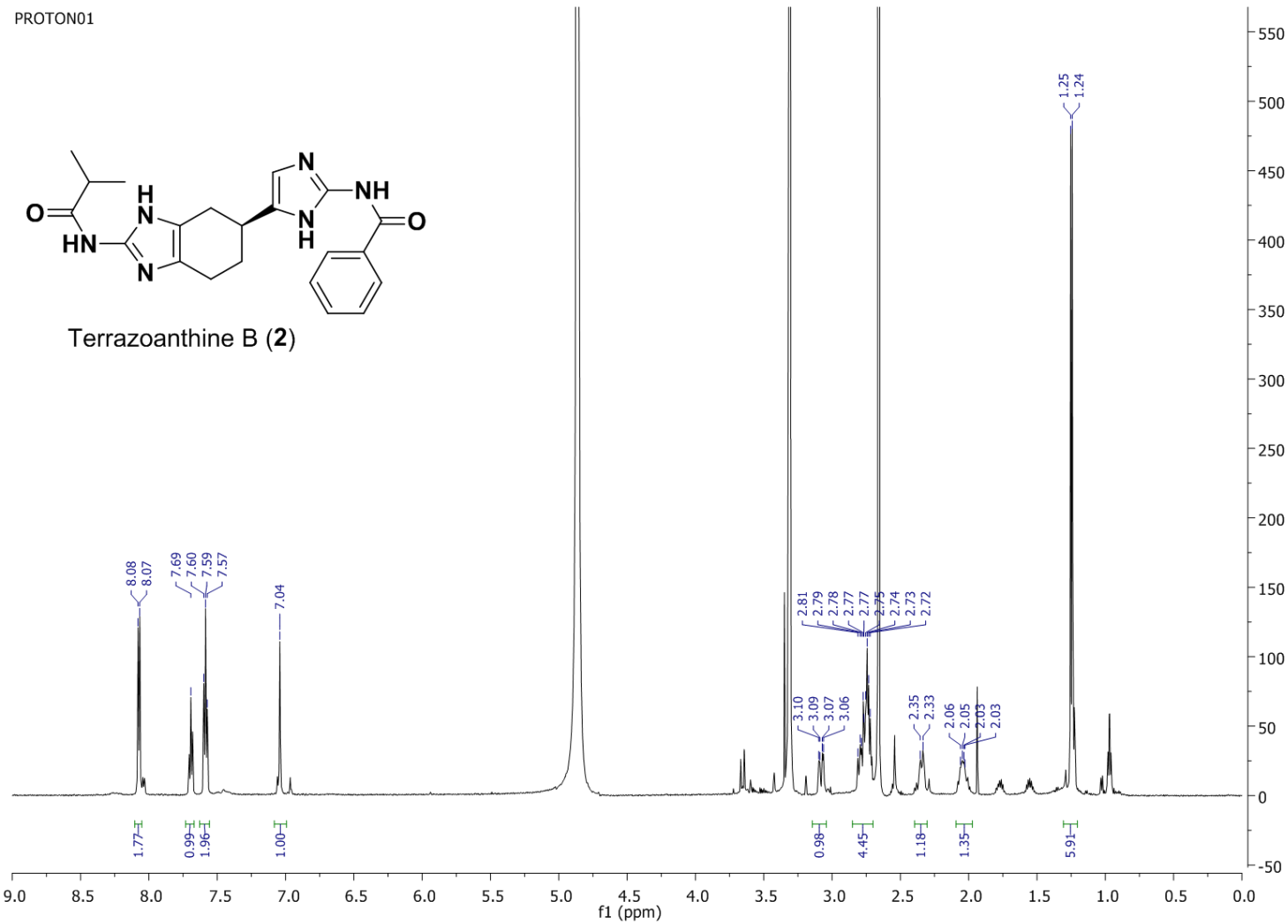
PROTON01

Terrazoanthine B (**2**)

^{1}H NMR spectrum of **2** at 600 MHz in CD$_3$OD

COSY NMR spectrum of **2** at 600 MHz in CD₃OD

CARBON01

Terrazoanthine B (**2**)
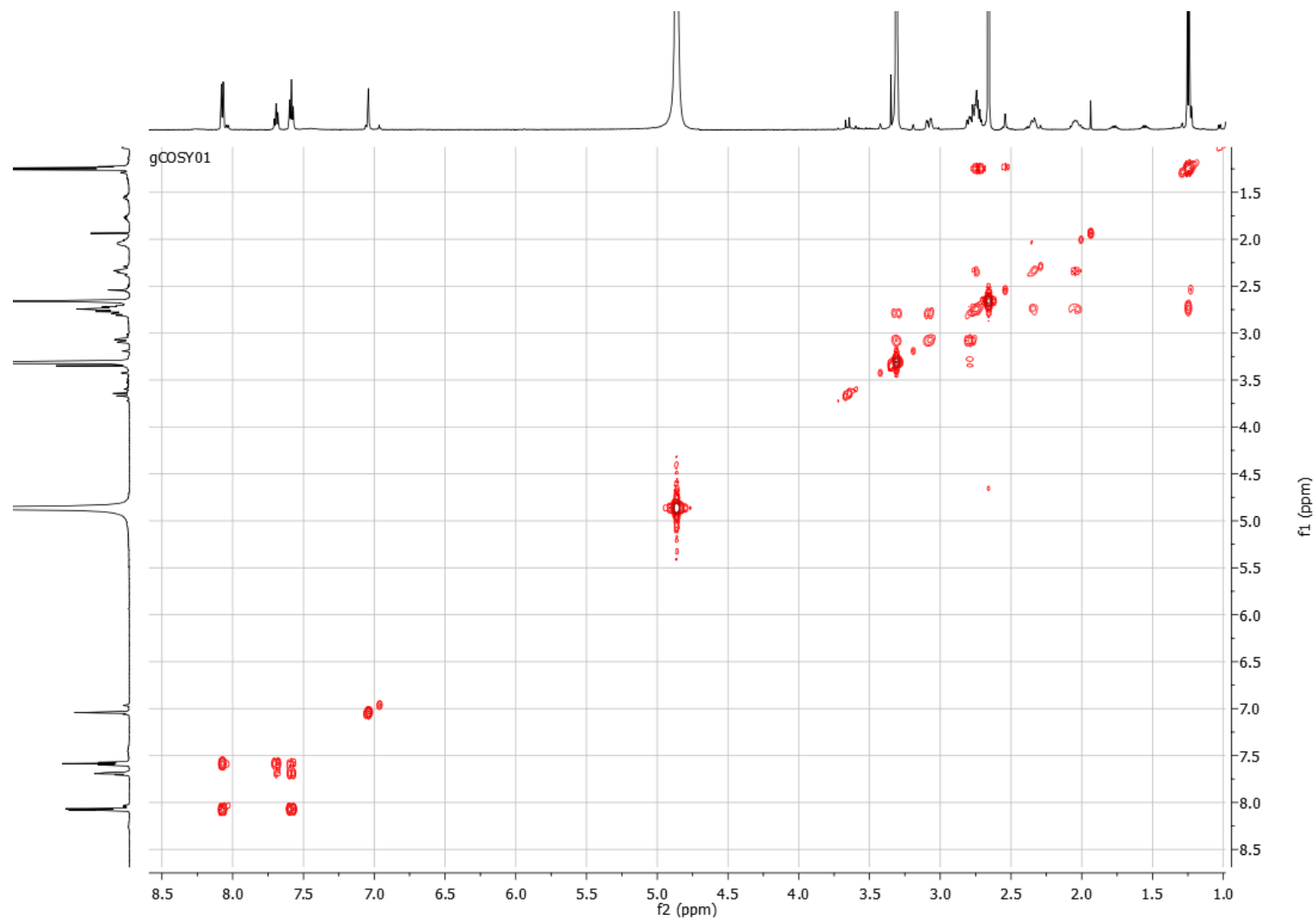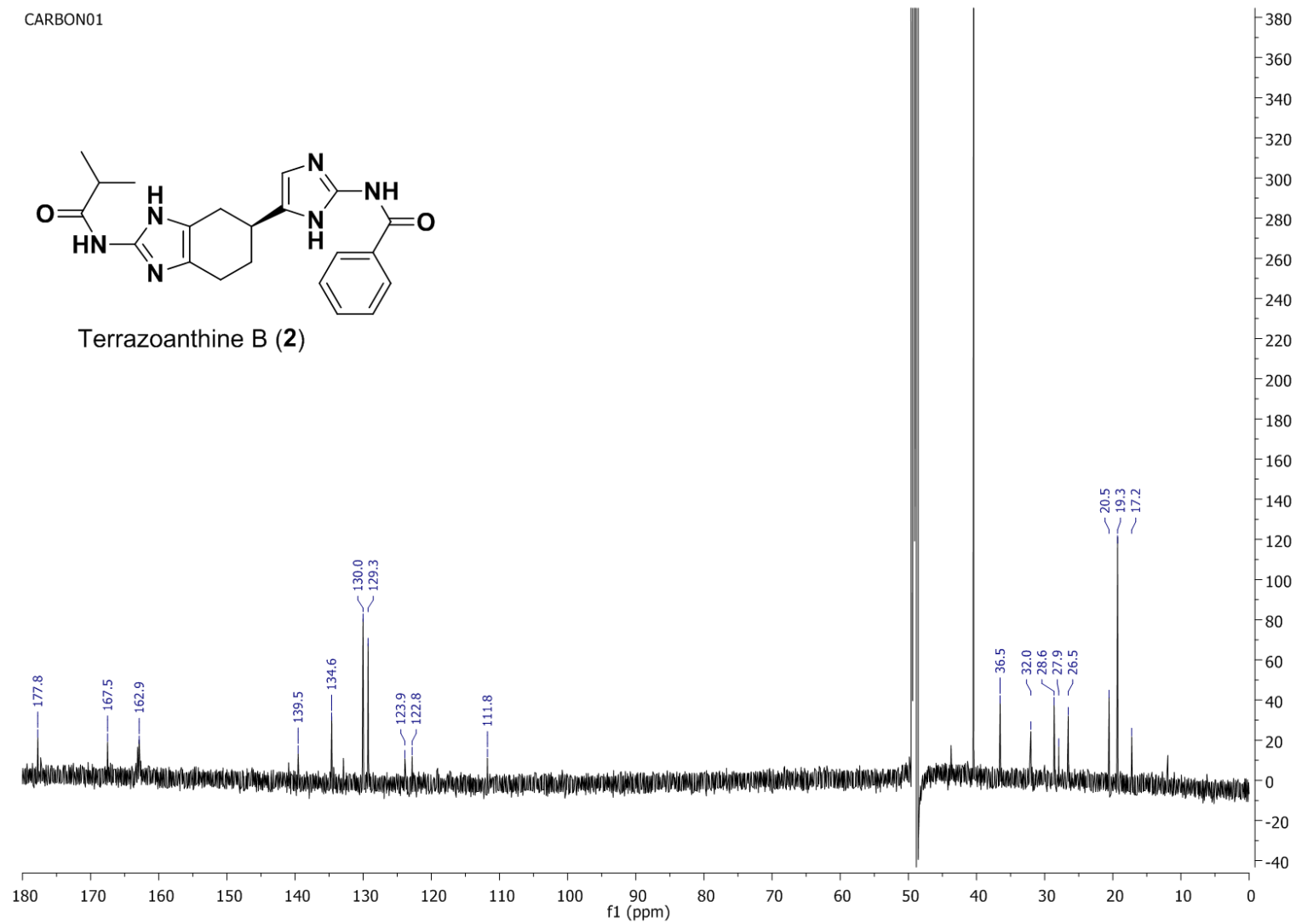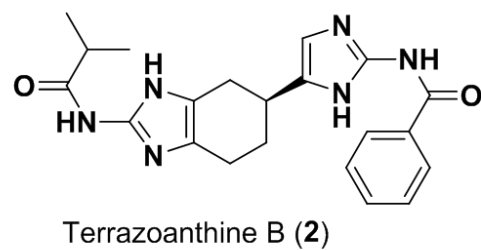
^{13}C NMR spectrum of **2** at 125 MHz in CD$_3$OD

gHSQCAD01
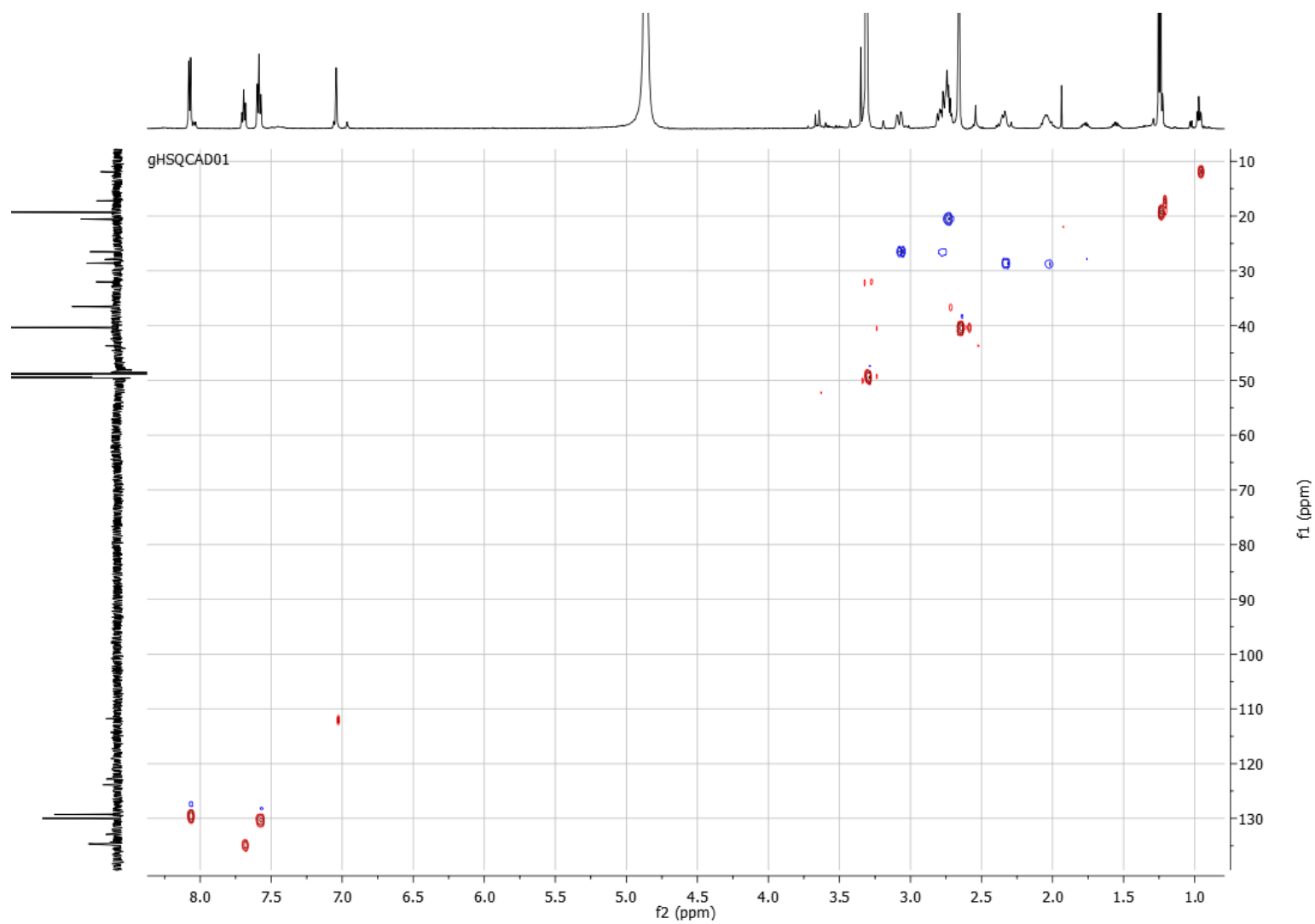
HSQC NMR spectrum of **2** at 600 MHz in CD₃OD

HMBC NMR spectrum of **2** at 600 MHz in CD₃OD

UHPLC-qToF analysis of 3 in (+)-ESI

+ESI Scan (3.304 min) Frag=175.0V ZR-F6-P1.d

360.1556

361.1574

362.1430

Counts vs. Mass-to-Charge (m/z)

PROTON01
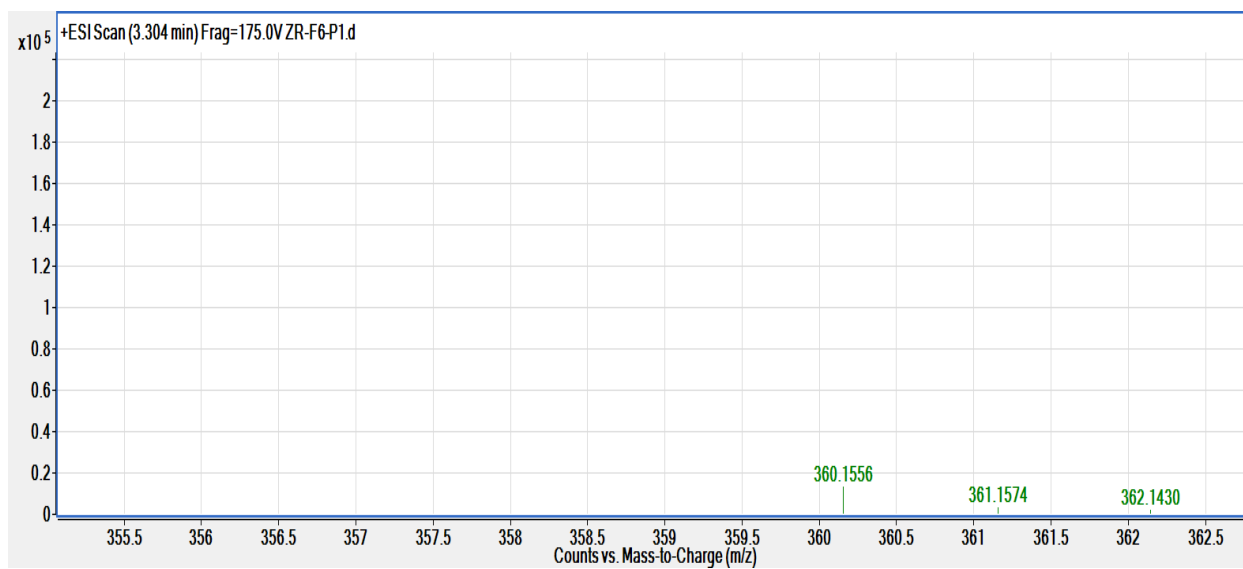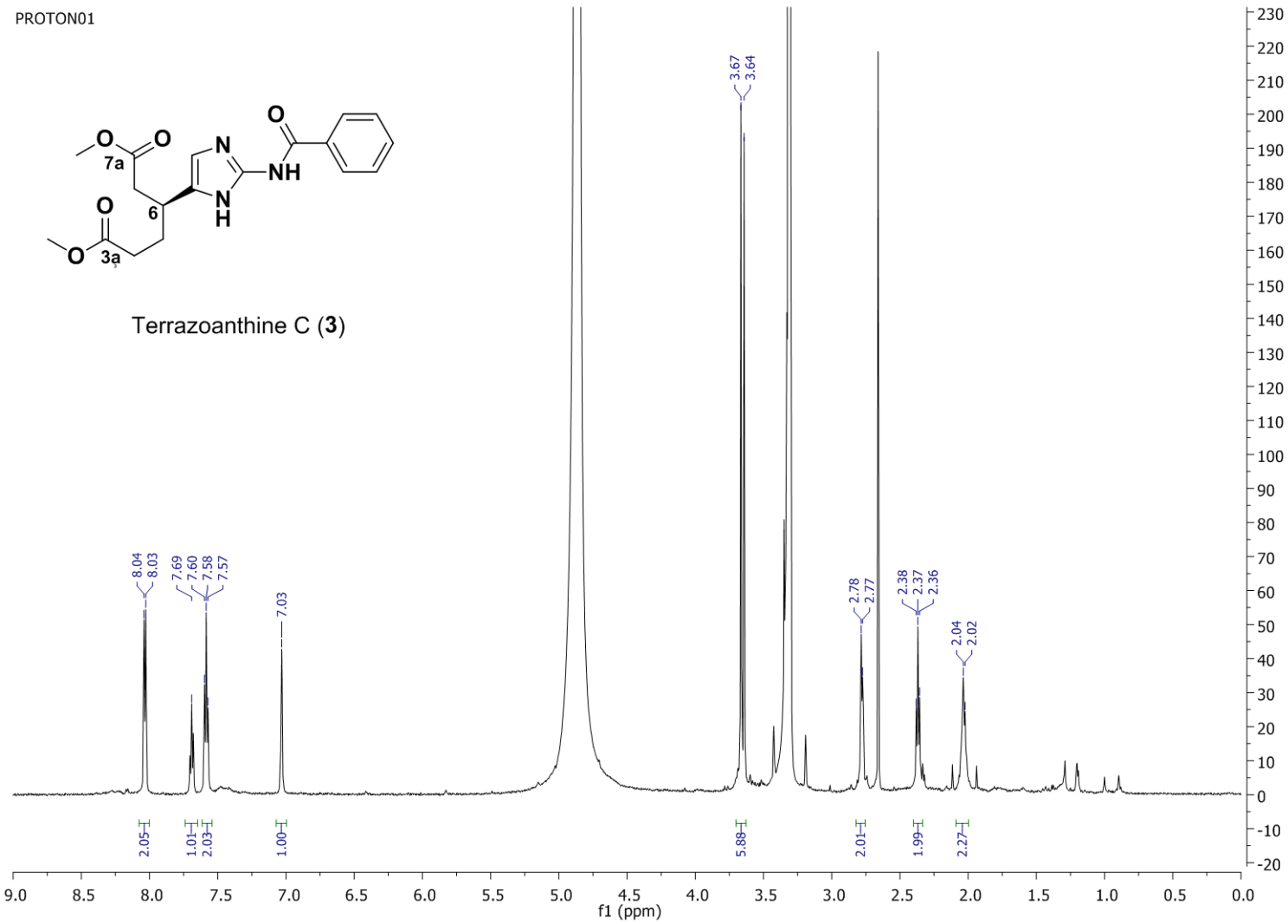
^{1}H NMR spectrum of **3** at 600 MHz in CD$_3$OD
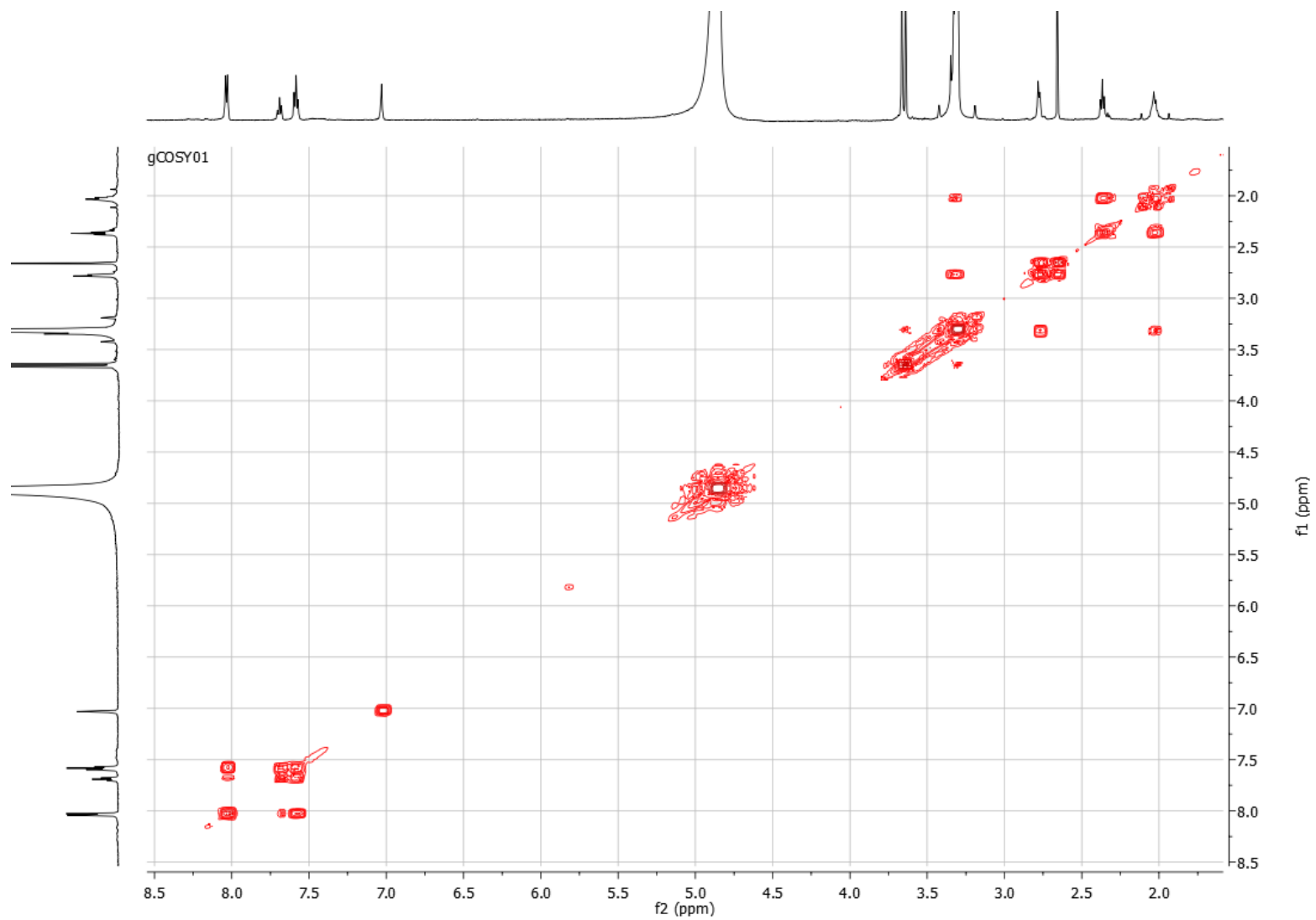
COSY NMR spectrum of **3** at 600 MHz in CD₃OD

CARBON02

^{13}C NMR spectrum of **3** at 125 MHz in CD$_3$OD

gHSQCAD01
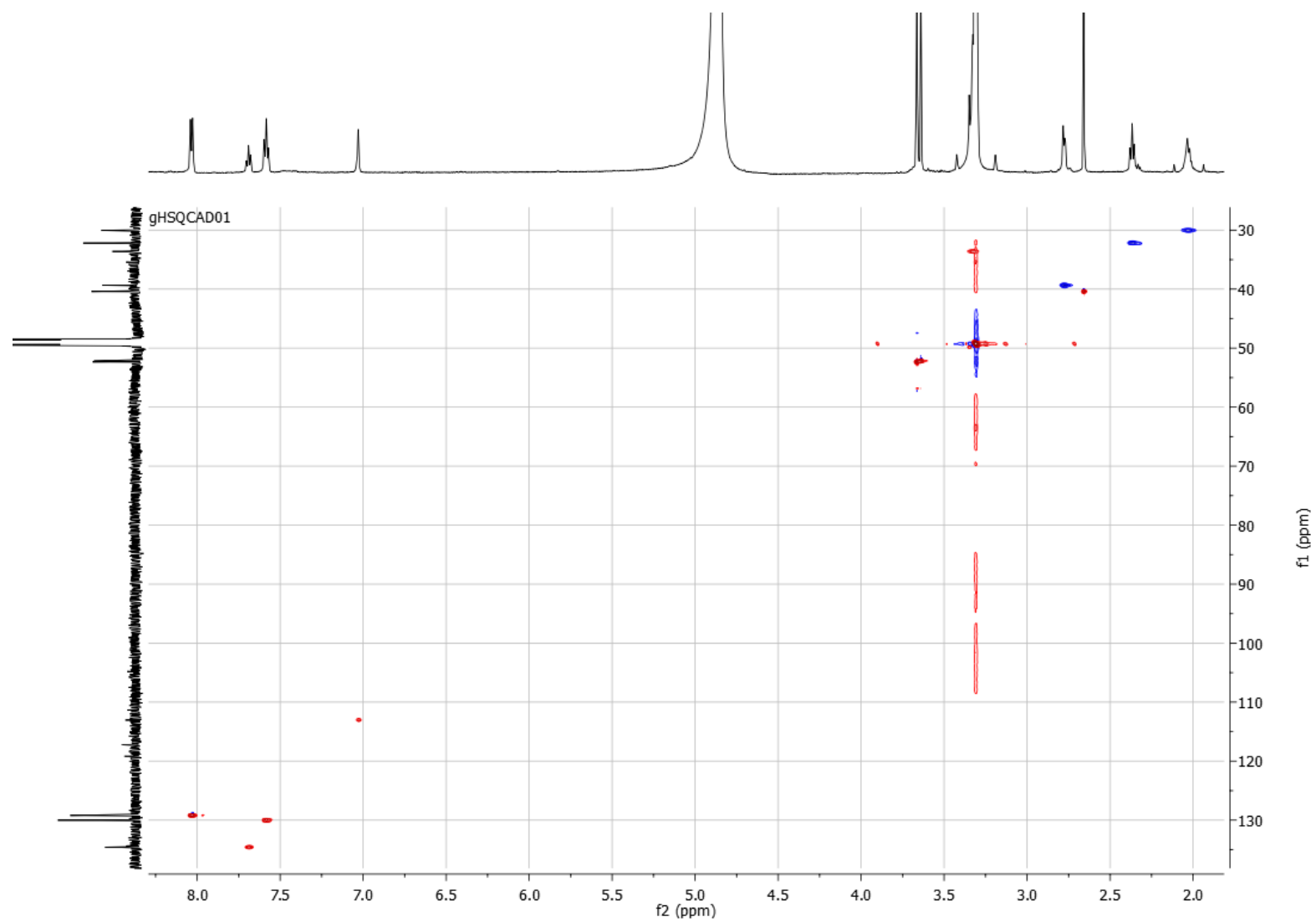
HSQC NMR spectrum of **3** at 600 MHz in CD₃OD

HMBC NMR spectrum of **3** at 600 MHz in CD$_3$OD

ECD spectrum of 1

See Figure 4 in the article

ECD spectrum of 3

Terrazoanthine C (3)
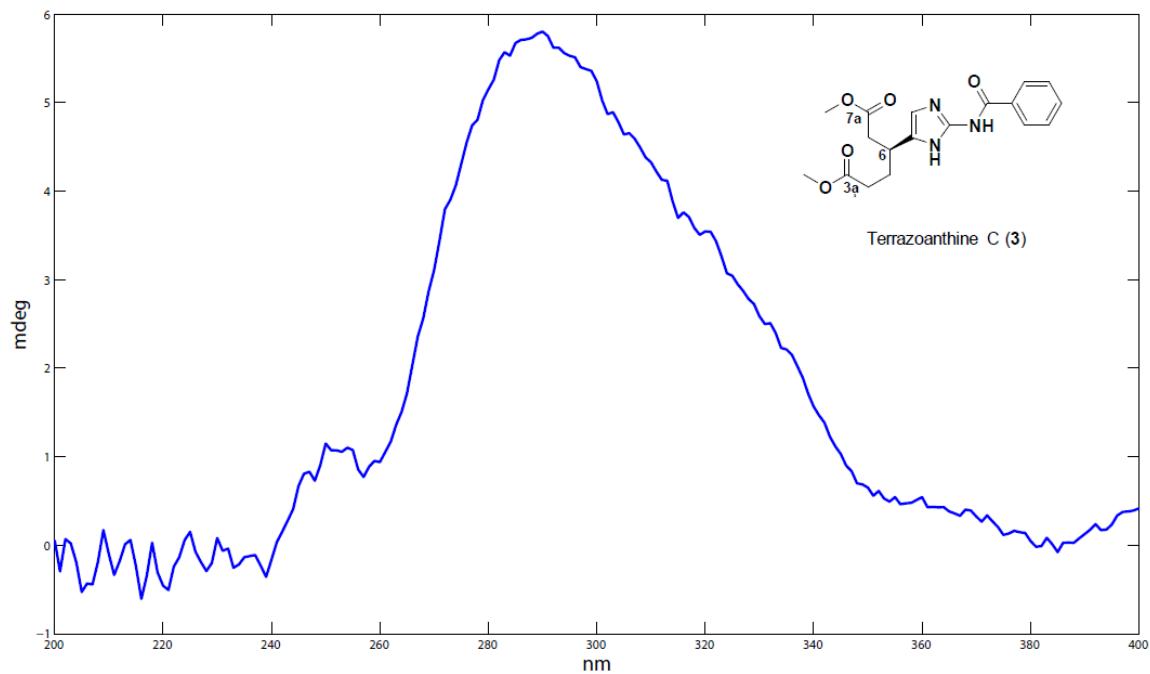
Computational Methods

All calculations have been realized using the Gaussian 09W package.[1] After geometry optimization of all structures (B3LYP/6-31g(d)), the absence of imaginary modes was checked by a frequency calculation at the same level of theory.

Determination of the substitution pattern.

The ^{13}C NMR chemical shifts have been calculated using the GIAO method on the most stable conformer for each regioisomer (see table below) and the DP4 probability was calculated.[2]
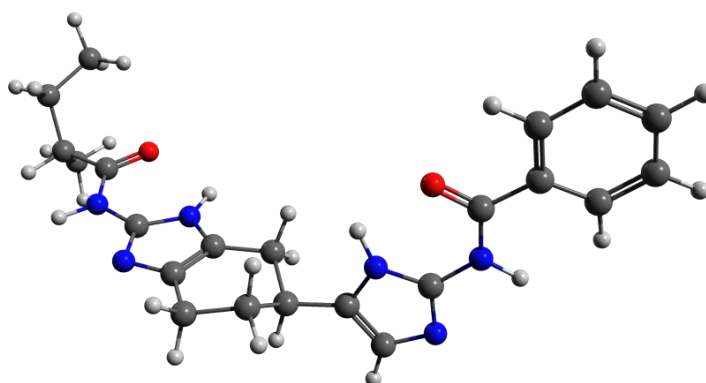
Most stable conformer of **1** (>99%)

---

[1] Gaussian 09, Revision D.01, M. J. Frisch, G. W. Trucks, H. B. Schlegel, G. E. Scuseria, M. A. Robb, J. R. Cheeseman, G. Scalmani, V. Barone, B. Mennucci, G. A. Petersson, H. Nakatsuji, M. Caricato, X. Li, H. P. Hratchian, A. F. Izmaylov, J. Bloino, G. Zheng, J. L. Sonnenberg, M. Hada, M. Ehara, K. Toyota, R. Fukuda, J. Hasegawa, M. Ishida, T. Nakajima, Y. Honda, O. Kitao, H. Nakai, T. Vreven, J. A. Montgomery, Jr., J. E. Peralta, F. Ogliaro, M. Bearpark, J. J. Heyd, E. Brothers, K. N. Kudin, V. N. Staroverov, T. Keith, R. Kobayashi, J. Normand, K. Raghavachari, A. Rendell, J. C. Burant, S. S. Iyengar, J. Tomasi, M. Cossi, N. Rega, J. M. Millam, M. Klene, J. E. Knox, J. B. Cross, V. Bakken, C. Adamo, J. Jaramillo, R. Gomperts, R. E. Stratmann, O. Yazyev, A. J. Austin, R. Cammi, C. Pomelli, J. W. Ochterski,
R. L. Martin, K. Morokuma, V. G. Zakrzewski, G. A. Voth, P. Salvador, J. J. Dannenberg, S. Dapprich, A. D. Daniels,
O. Farkas, J. B. Foresman, J. V. Ortiz, J. Cioslowski, and D. J. Fox, Gaussian, Inc., Wallingford CT, 2013.
[2] Assigning Stereochemistry to Single Diastereoisomers by GIAO NMR Calculation: The DP4 Probability Steven G. Smith and Jonathan M. Goodman J. Am. Chem. Soc., 2010, 132 (37), pp 12946–12959
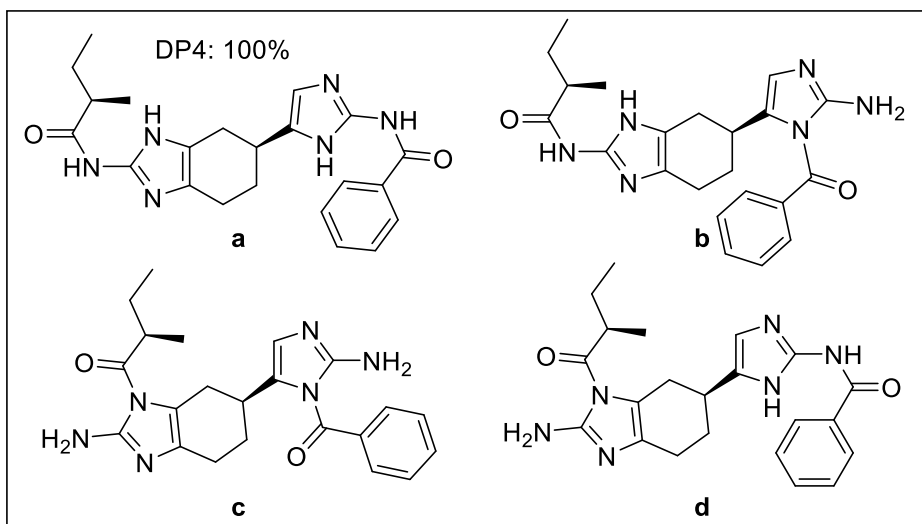
arbitrary					
			δ_C in ppm (125 MHz)		
number	exp	a	b	c	d
10-C	139.4	132.4861	132.0343	144.0272	136.7626
14-C	140.9	131.6191	142.0585	143.9996	130.4488
17-C	177.3	163.4843	163.1815	171.1219	169.0887
18-C	43.7	46.0339	43.6484	42.1054	48.9422
1-C	124	128.3676	128.1894	134.563	131.9957
20-C	24.2	20.3019	14.0268	17.9499	13.7102
21-C	27.9	31.0563	30.1038	27.5143	25.996
22-C	11.9	13.6578	14.1858	12.5998	14.4599
23-C	167.5	154.102	164.4856	164.5182	154.6197
24-C	133	127.0707	129.7194	127.6877	127.1068
26-C	129.3	124.1945	125.0993	125.3261	123.8536
27-C	130	122.2997	122.1131	122.3038	122.2687
28-C	134.6	124.4529	125.8711	126.5609	124.757
29-C	130	121.0934	121.0489	121.0751	121.3602
2-C	122.9	113.7316	113.9202	109.3499	120.903
30-C	129.3	117.4324	123.4459	125.1708	117.5929
3-C	20.6	22.955	23.0519	26.3511	22.8383
4-C	28.6	32.3846	29.3485	27.3781	31.8097
5-C	32	32.2866	31.0661	34.5895	31.8196
6-C	26.5	28.5054	31.2568	34.6947	30.3352
7-C	134.4	123.2348	122.687	122.5776	123.9158
8-C	117	117.1828	123.0865	121.395	117.431

WARNING: One or more of the carbon shifts have large errors (largest error 14,1 ppm).
DP4 calculation has been attempted anyway, but you may wish to check the input data.
To check the assignments, click Show Assignments.

This calculation will use the DP4-database2 version of the database and the t distribution.
(To change these options select the desired database and distribution from the menus at the
top of the applet and then click Calculate).

Results of DP4 using the carbon data only:
 Isomer 1: 100,0%
 Isomer 2: 0,0%
 Isomer 3: 0,0%
 Isomer 4: 0,0%

(c) Jonathan M Goodman and Steven G Smith

Accessed via : http://www-jmg.ch.cam.ac.uk/tools/nmr/DP4/
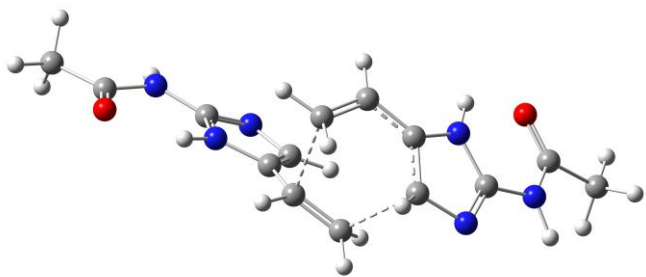
Determination of the absolute configuration of 1

Rotational strengths have been calculated for 20 excited states and the ECD spectrum was plotted using the SpecDis 1.61 software available at https://specdis-software.jimdo.com/.[3]

Transition state for the Diels-Alder reaction leading to 1

Conformations of reactants, products and transition states were fully optimized without constraint using Hartree-Fock method with STO-3G basis set as implemented in Gaussian 09 software package. Vibrational analysis within the harmonic approximation was performed at the same level of theory upon geometrical optimization convergence. Local minima and first-order saddle points were characterized by their respective numbers of imaginary frequencies.

Table 1: Calculated transition state at the RHF level.

	TS
	E(RHF) = -1004.11701694
	Lowest frequency = -1005.18i cm^{-1}

Symbol	X	Y	Z
C	-0.32315	2.41743	1.5234
C	0.48953	1.2705	1.79422
C	-0.51359	3.58107	2.4141
C	-0.00611	3.84947	3.64248
N	-1.32194	4.68723	2.10778
C	-1.22595	5.54506	3.17965
N	-0.443	5.08864	4.14586
N	-1.93191	6.77512	3.20583

[3] SpecDis: Quantifying the Comparison of Calculated and Experimental Electronic Circular Dichroism Spectra, T. Bruhn, A. Schaumlöffel, Y. Hemberger, G. Bringmann, Chirality 2013, 25, 243–249

H	-1.2865	2.29706	1.04064
H	0.83217	1.01839	2.78773
H	0.23178	0.29327	1.41197
H	0.66098	3.22512	4.2179
H	-1.84999	4.91943	1.2629
C	-2.59782	7.31538	2.07083
H	-1.72623	7.38191	3.99804
C	-3.13044	8.74264	2.2997
H	-3.81195	8.75459	3.14576
H	-3.65524	9.07705	1.41123
H	-2.30711	9.42113	2.5059
O	-2.74243	6.67783	1.0379
C	0.72262	2.71839	-0.86094
C	0.33884	3.63506	-0.00066
C	1.54686	1.52997	-0.55771
C	2.09131	1.10297	0.60837
N	1.935	0.57338	-1.50909
C	2.67778	-0.36654	-0.83172
N	2.8108	-0.09688	0.45844
N	3.23978	-1.48442	-1.5
H	0.43276	2.79693	-1.90276
H	1.00786	4.39002	0.38723
H	-0.54003	4.23896	-0.17508
H	2.91385	1.5547	1.14251
H	1.70286	0.48051	-2.50109

C	2.90786	-1.8407	-2.83657
H	3.69422	-2.17104	-0.89989
C	3.50434	-3.19255	-3.27228
H	4.58601	-3.17186	-3.17232
H	3.24308	-3.38356	-4.30759
H	3.11224	-3.99281	-2.65054
O	2.23648	-1.11439	-3.55494
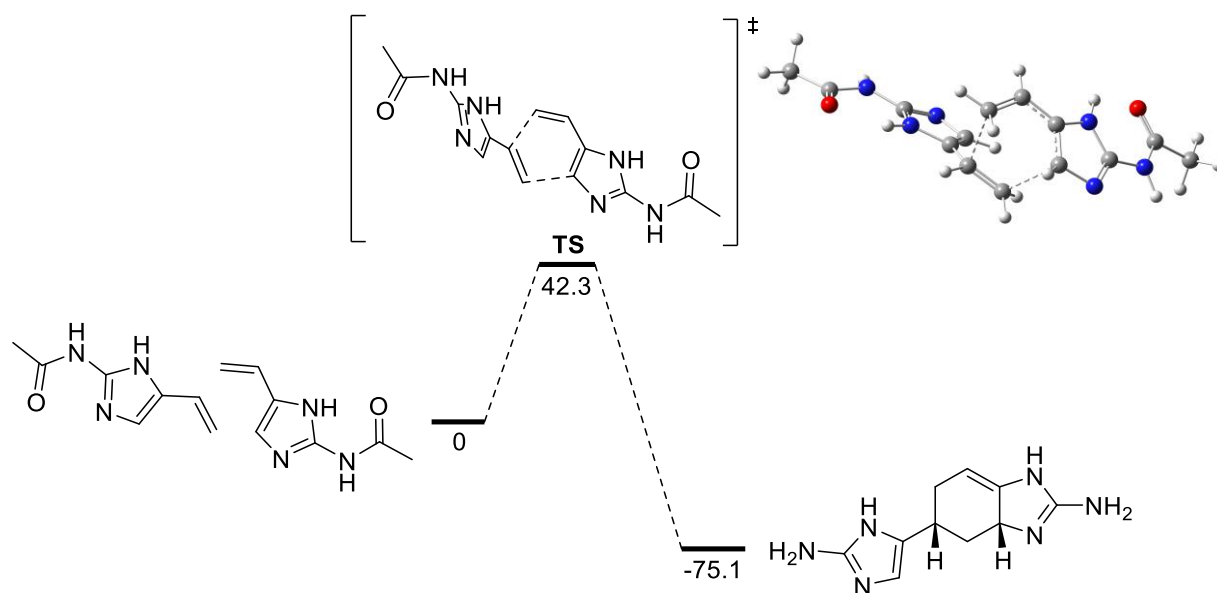
Biological Assays

Compounds **1**−**3** were tested in a wide panel of biological assays, including antibacterial activity against Gram-positive (methicillin resistant *Staphylococcus aureus*, MRSA and MSSA) and Gram-negative (*Acinetobacter baumannii*, *Escherichia coli*, *Klebsiella pneumoniae* and *Pseudomonas aeruginosa*) bacteria, antifungal activity against *Aspergillus fumigatus*, and cell growth inhibition of the human liver tumor cell line (HepG2), following a methodology previously described.[4] None of the compound showed activity at a concentration of 96 µg.mL^{-1} or below for antimicrobial and cytotoxicity.

---

[4] Audoin, C.; Bonhomme, D.; Ivanisevic, J.; de la Cruz, M.; Cautain, B.; Monteiro, M. C.; Reyes, F.; Rios, L.; Perez, T.; Thomas, O. P., Balibalosides, an original family of glucosylated sesterterpenes produced by the Mediterranean sponge Oscarella balibaloi. *Mar. Drugs* **2013,** 11, 1477-1489.

Zoanthamine alkaloids from the Zoantharian *Zoanthus* cf. *pulchellus* and their effect in neuroinflammation

Supplementary Information
for

Zoanthamine alkaloids from the Zoantharian *Zoanthus* cf. *pulchellus* and their effect in neuroinflammation

Paul O. Guillen [1,2], Sandra Gegunde [3], Karla B. Jaramillo [1,4], Amparo Alfonso [3], Kevin Calabro [2], Eva Alonso [3], Jenny Rodriguez [1], Luis M. Botana [3,*], and Olivier P. Thomas [2,*]

[1] ESPOL Escuela Superior Politécnica del Litoral, ESPOL, Centro Nacional de Acuacultura e Investigaciones Marinas, Campus Gustavo Galindo km. 30.5 vía Perimetral, P.O.Box 09-01-5863, Guayaquil, Ecuador.; P.GUILLENMENA1@nuigalway.ie, K.JARAMILLOAGUILAR1@nuigalway.ie, jenrodri@espol.edu.ec

[2] Marine Biodiscovery, School of Chemistry and Ryan Institute, National University of Ireland Galway (NUI Galway), University Road, H91 TK33 Galway, Ireland; kevin.calabro@nuigalway.ie, olivier.thomas@nuigalway.ie

[3] Departamento de Farmacología, Facultad de Veterinaria, Universidade de Santiago de Compostela, 27002 Lugo, Spain; sandra.gegunde@rai.usc.es, amparo.alfonso@usc.es, eva.alonso@usc.es, luis.botana@usc.es

[4] Zoology, School of Natural Sciences and Ryan Institute, National University of Ireland Galway (NUI Galway), University Road, H91 TK33 Galway, Ireland

* Correspondence: luis.botana@usc.es and olivier.thomas@nuigalway.ie; Tel.: +353-91-493563

P   **Figure S1**. (+)-HRESIMS analysis of **1**

P   **Figure S2**. ^{1}H NMR spectrum of **1** at 500 MHz in CDCl$_3$

P   **Figure S3**. COSY NMR spectrum of **1** at 500 MHz in CDCl$_3$

P   **Figure S4**. ^{13}C NMR spectrum of **1** at 125 MHz in CDCl$_3$

P   **Figure S5**. HSQC NMR spectrum of **1** at 500MHz in CDCl$_3$

P   **Figure S6**. HMBC NMR spectrum of **1** at 500MHz in CDCl$_3$

P   **Figure S7**. HMBC NMR spectrum of **1** at 500MHz in CDCl$_3$

P   **Figure S8**. (+)-HRESIMS analysis of **2**

P   **Figure S9**. ^{1}H NMR spectrum of **2** at 500 MHz in CDCl$_3$

P   **Figure S10**. COSY NMR spectrum of **2** at 500 MHz in CDCl$_3$

P   **Figure S11**. ^{13}C NMR spectrum of **2** at 125 MHz in CDCl$_3$

P   **Figure S12**. HSQC NMR spectrum of **2** at 500 MHz in CDCl$_3$

P   **Figure S13**. HMBC NMR spectrum of **2** at 500 MHz in CDCl$_3$

min) Frag=175.0V ZVSPF3P5.d

540.2956

6.2925   519.2884   526.2840   538.2761   548.2883   552.2570

516   518   520   522   524   526   528   530   532   534   536   538   540   542   544   546   548   550   552
Counts vs. Mass-to-Charge (m/z)
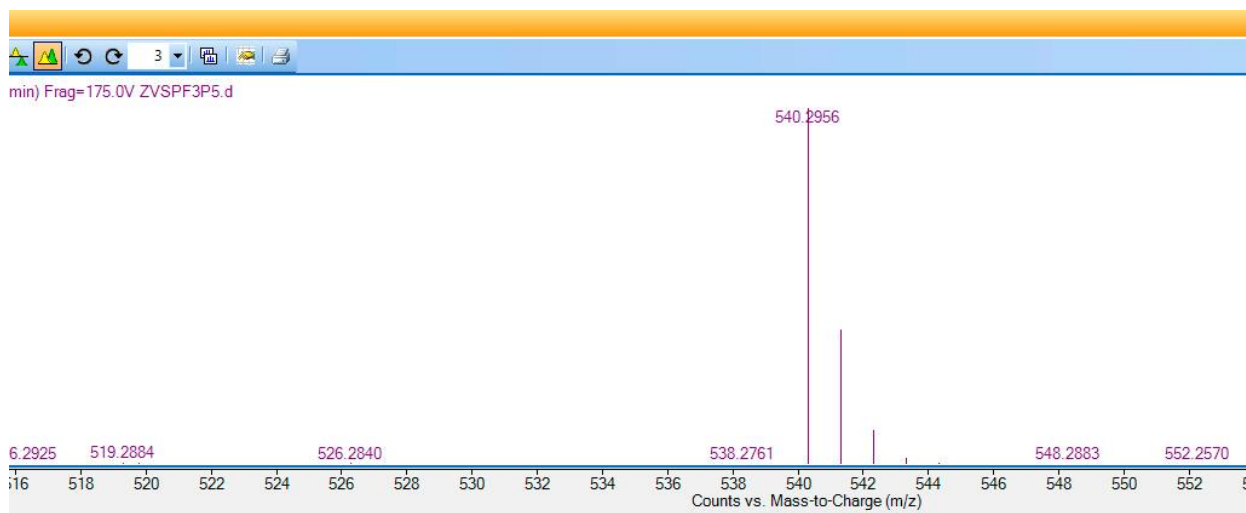
Figure S1. (+)-HRESIMS analysis of **1**.
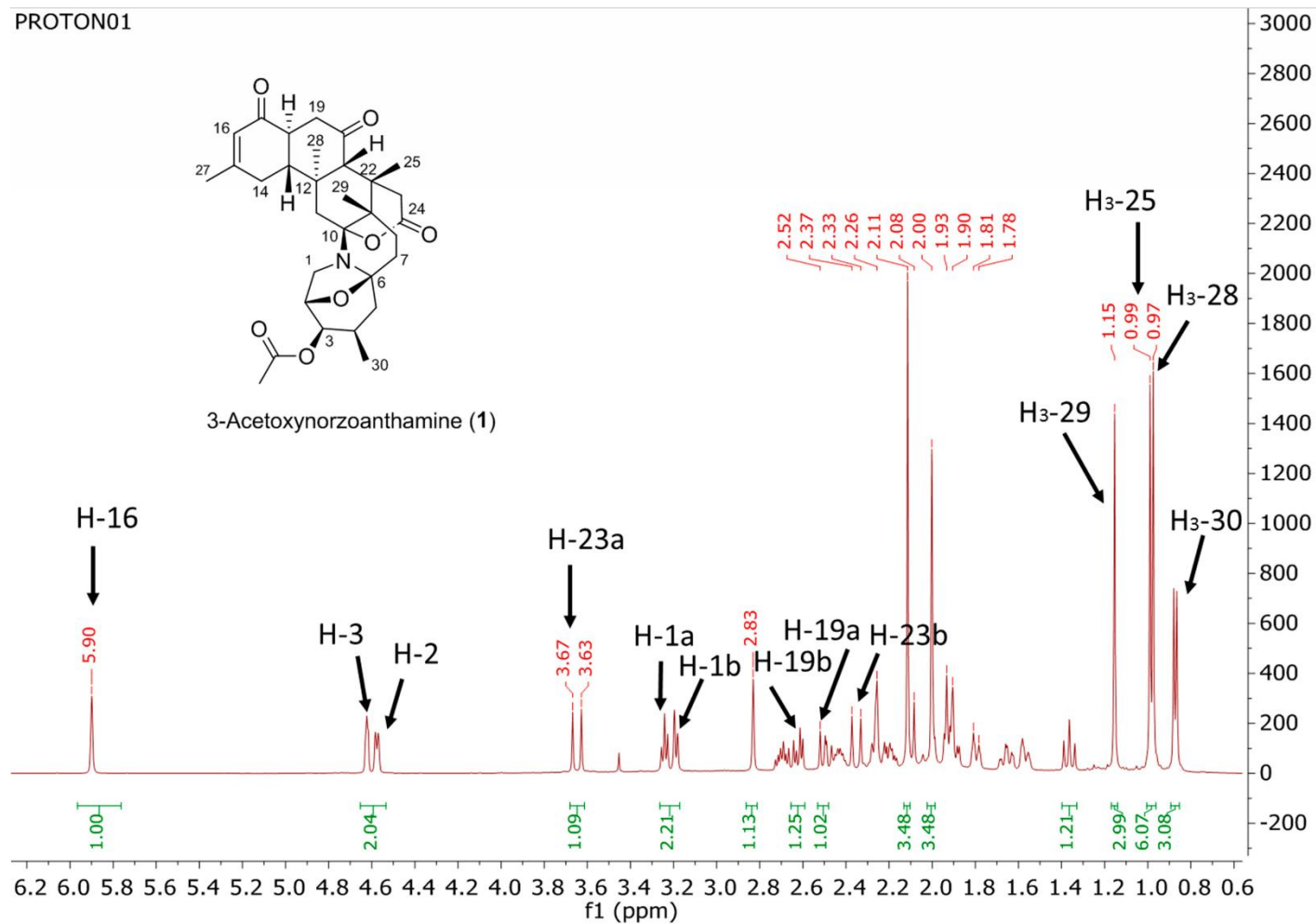
Figure S2. ^{1}H NMR spectrum of **1** at 500 MHz in CDCl$_3$
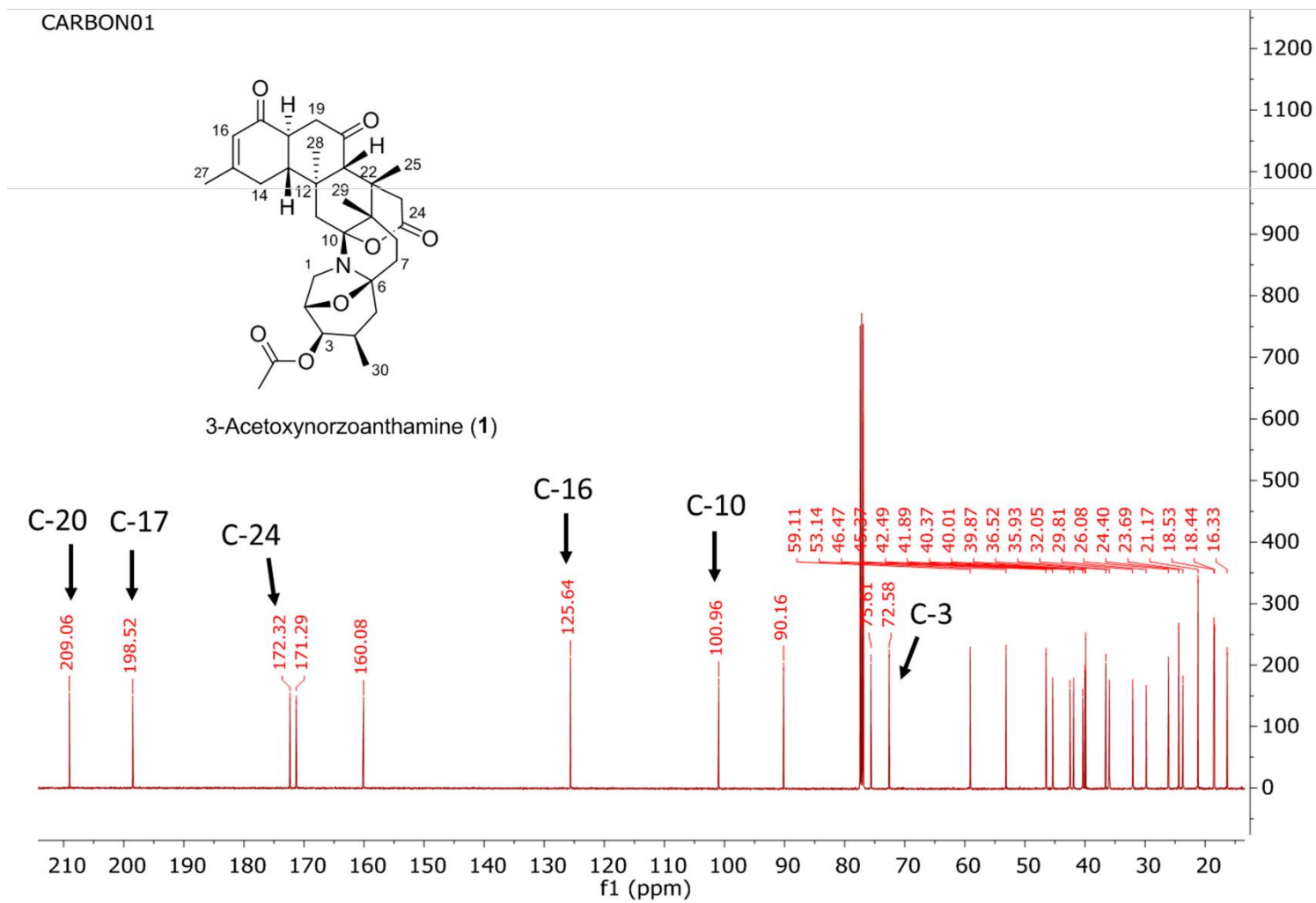
Figure S3. ^{13}C NMR spectrum of 1 at 125 MHz in CDCl$_3$
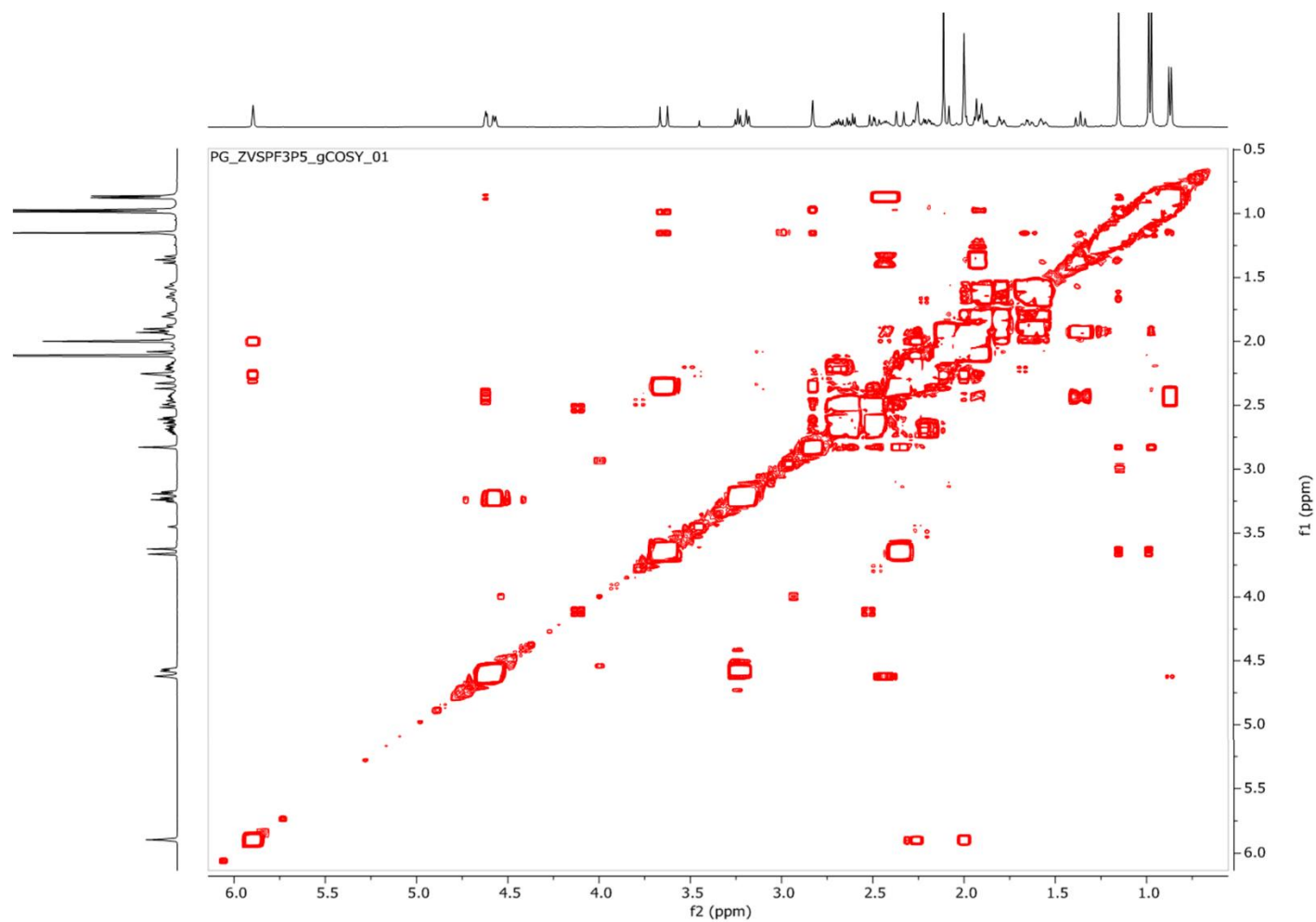
Figure S4. COSY NMR spectrum of **1** at 500 MHz in CDCl₃

gHSQCAD01
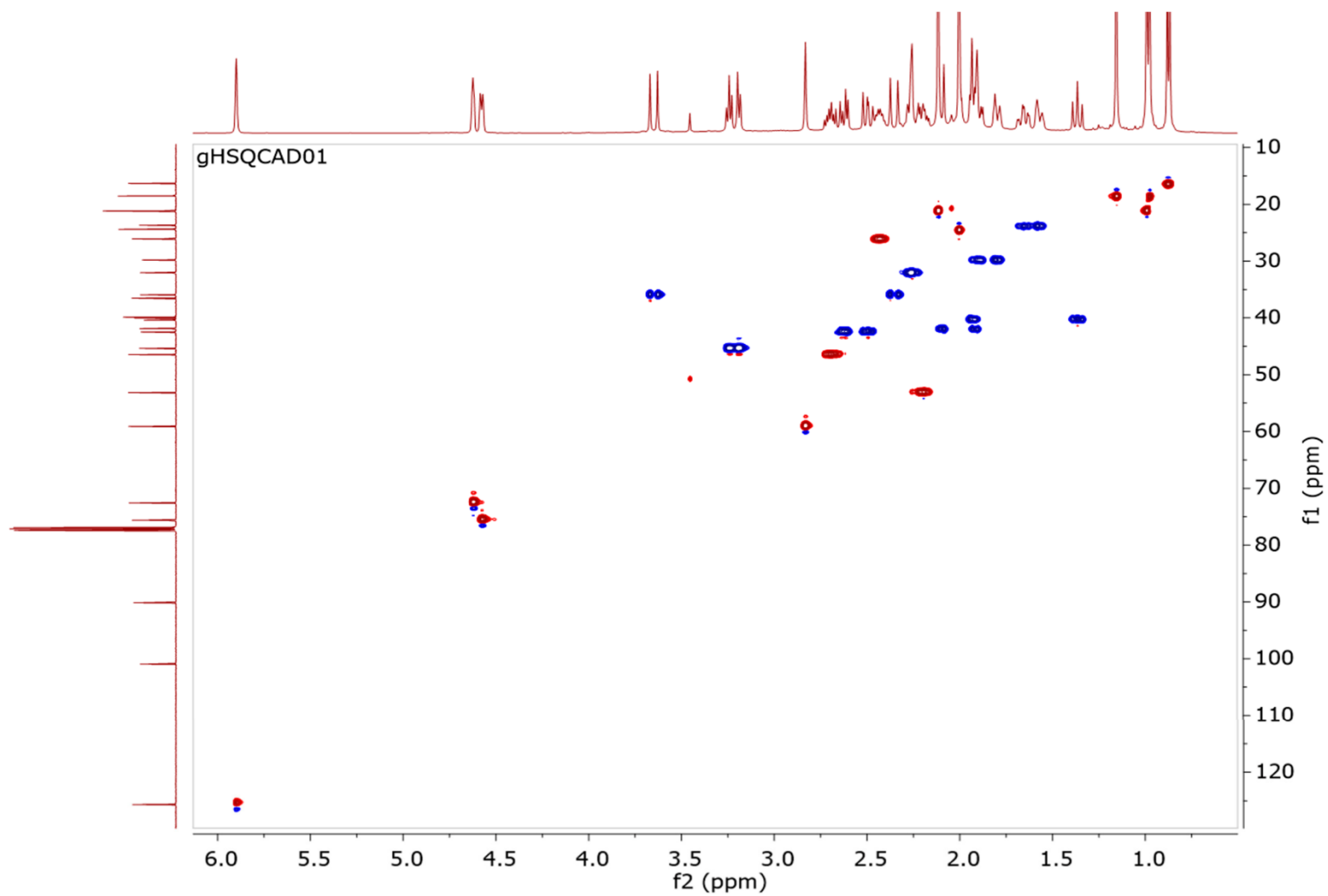
Figure S3. HSQC NMR spectrum of **1** at 500MHz in CDCl₃
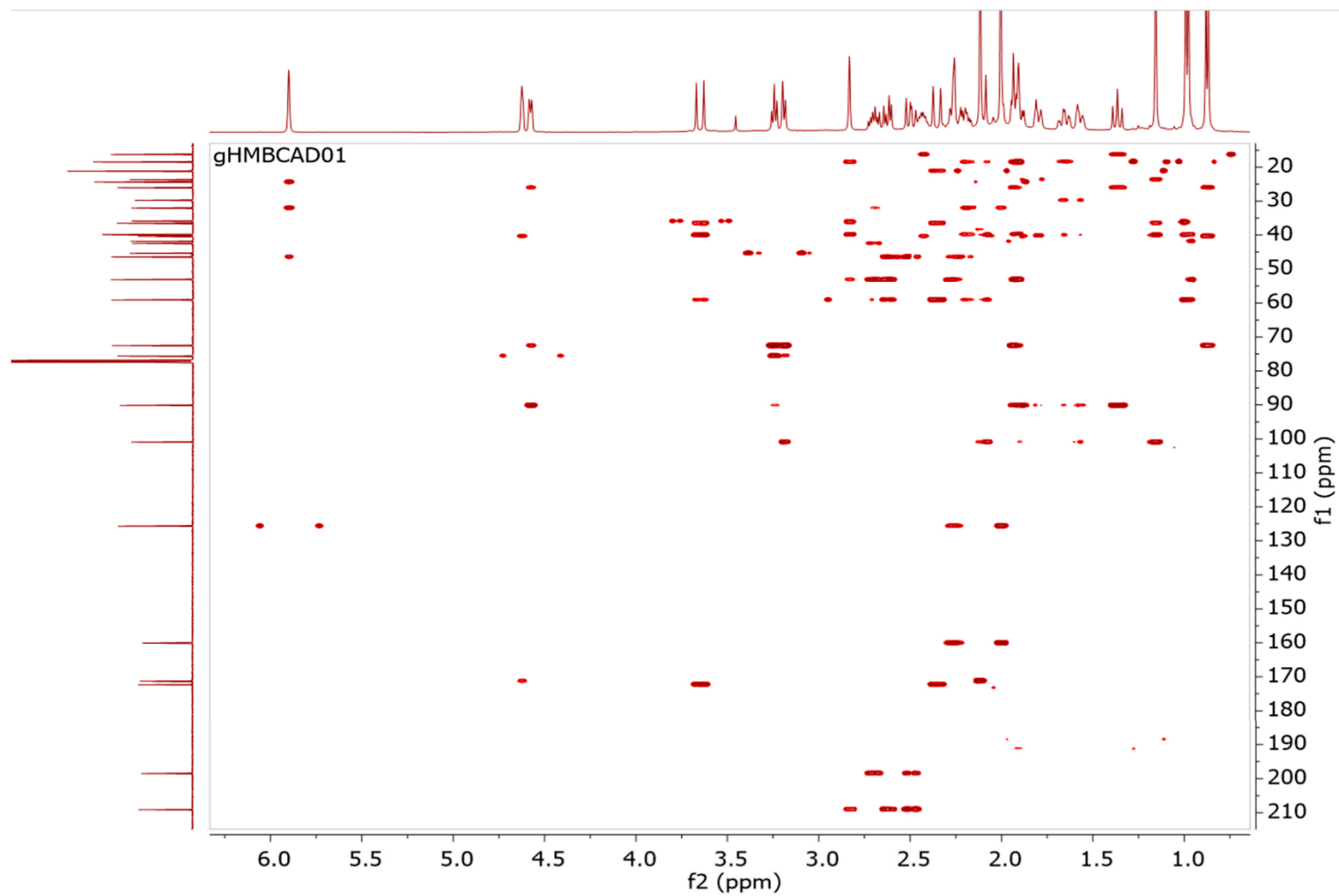
Figure S4. HMBC NMR spectrum of **1** at 500MHz in CDCl₃
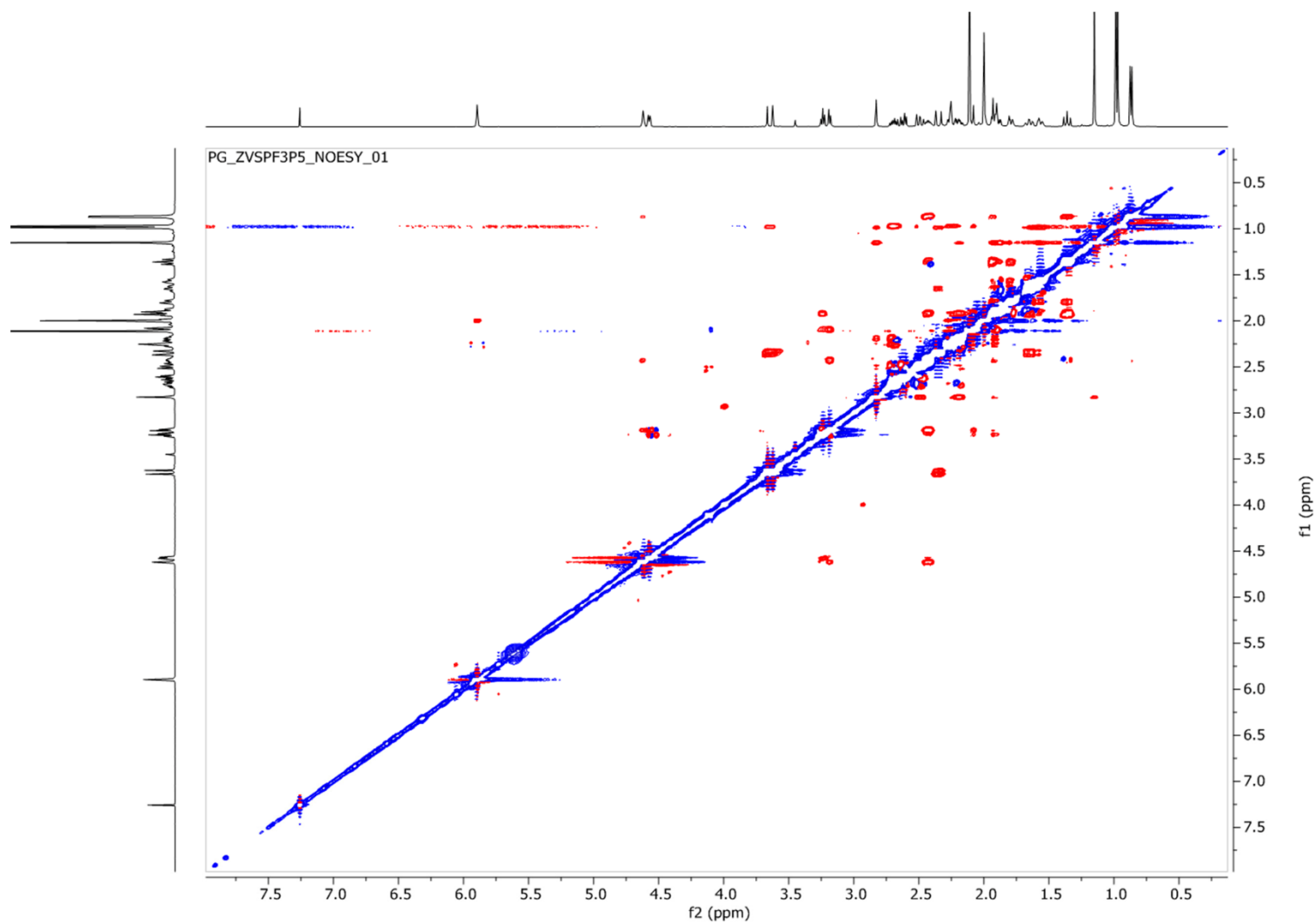
Figure S7. NOESY NMR spectrum of **1** at 500 MHz in CDCl₃
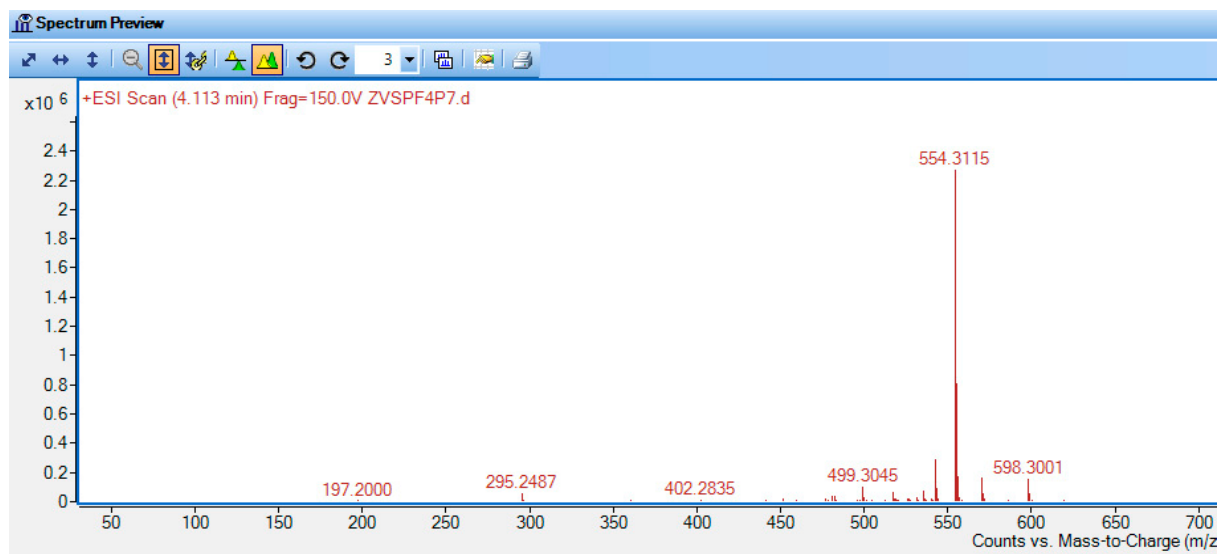
Figure S8. UHPLC-qToF analysis of **2** in (+)-ESI
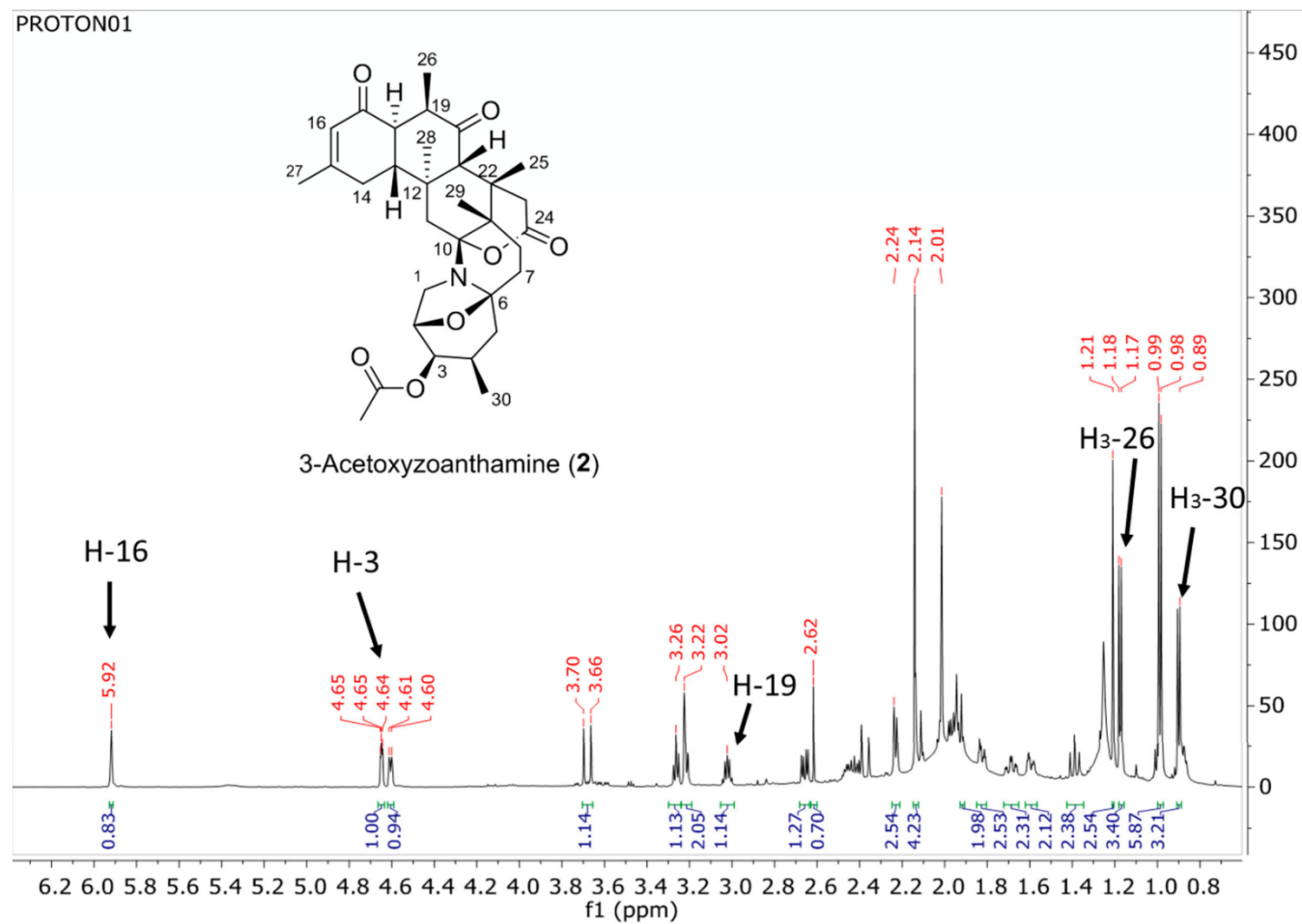
Figure S5. ¹H NMR spectrum of **2** at 500 MHz in CDCl₃

CARBON01

3-Acetoxyzoanthamine (**2**)
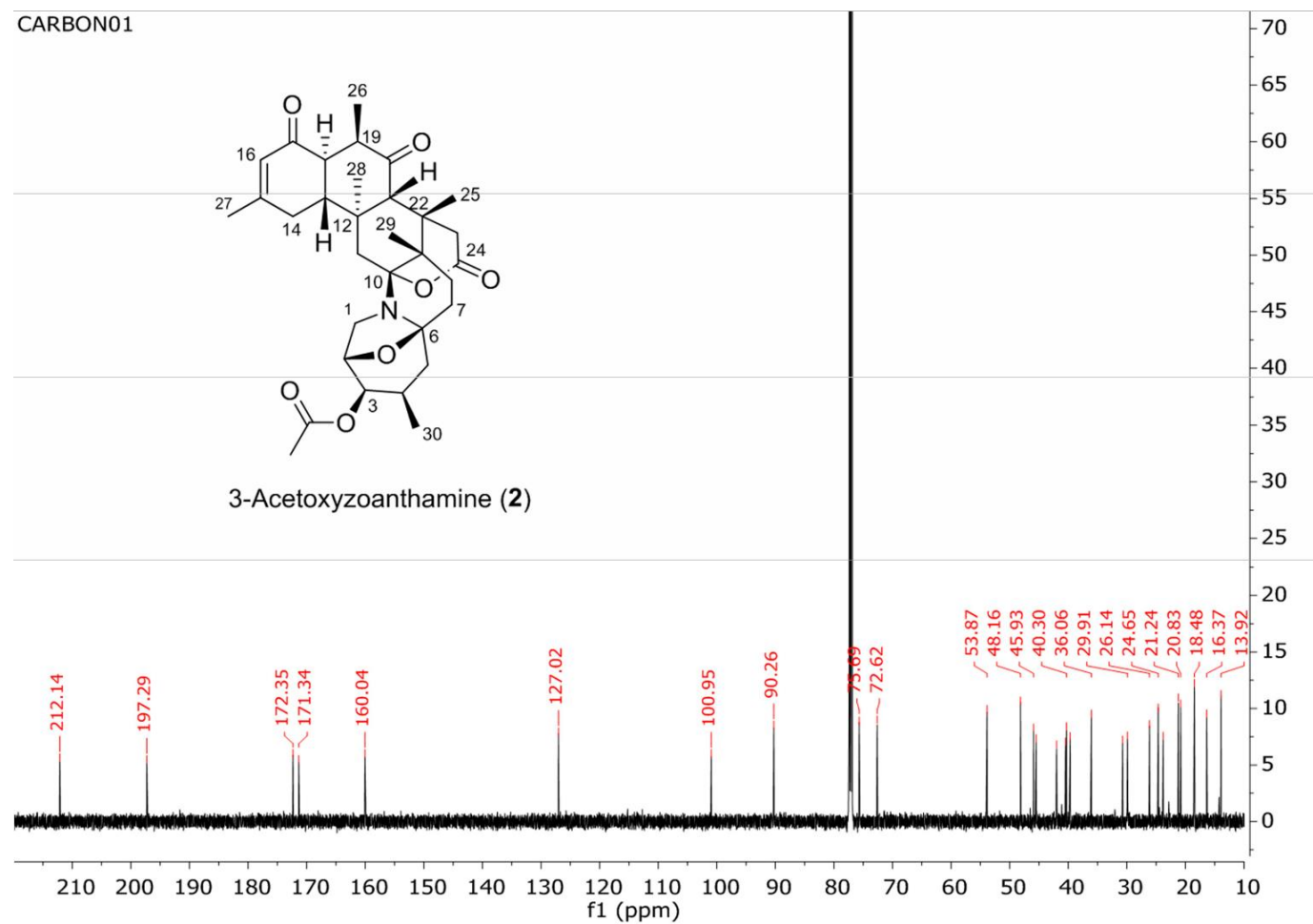
Figure S9. ^{13}C NMR spectrum of **2** at 125 MHz in CDCl$_3$
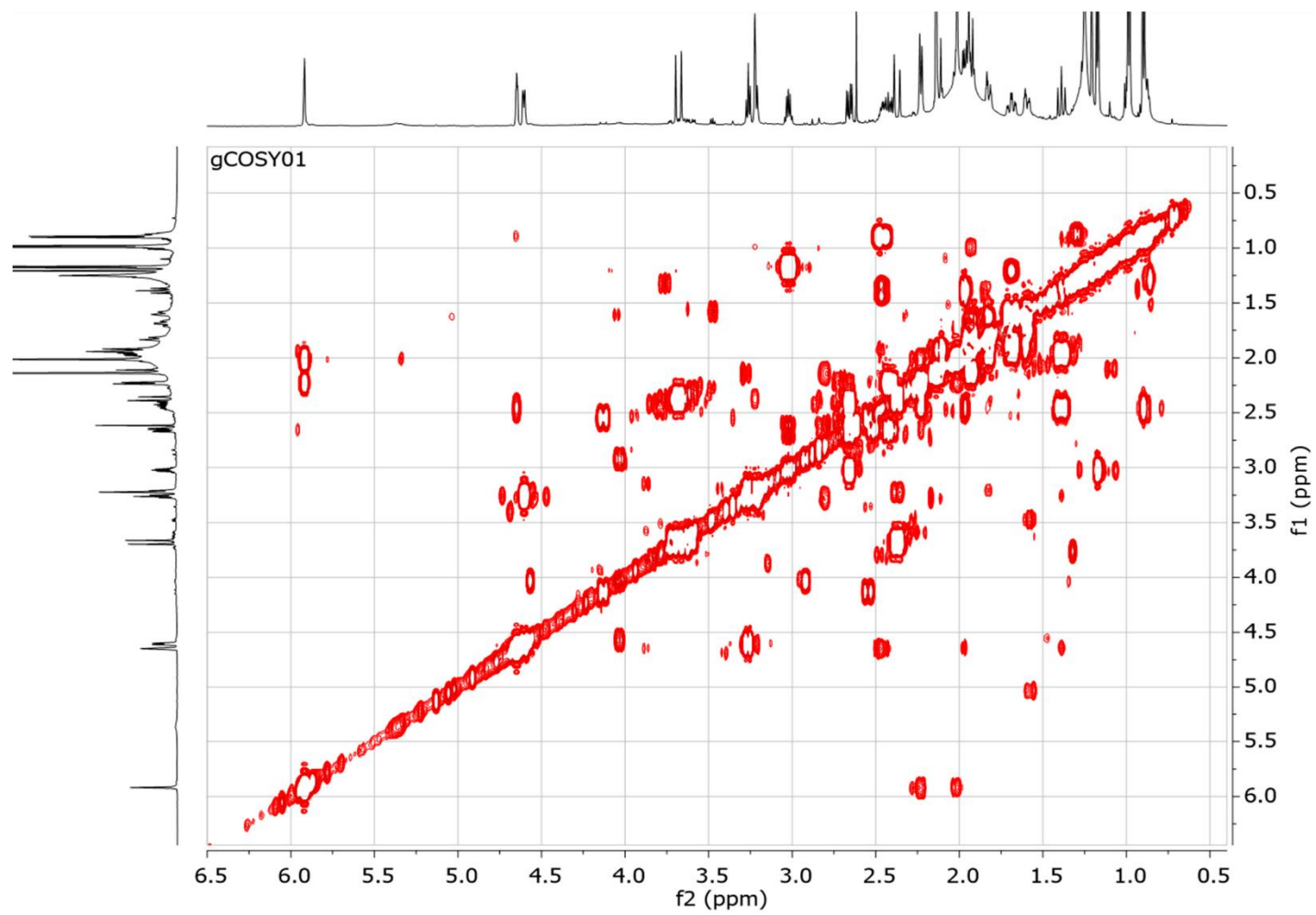
Figure S10. COSY NMR spectrum of **2** at 500 MHz in CDCl₃
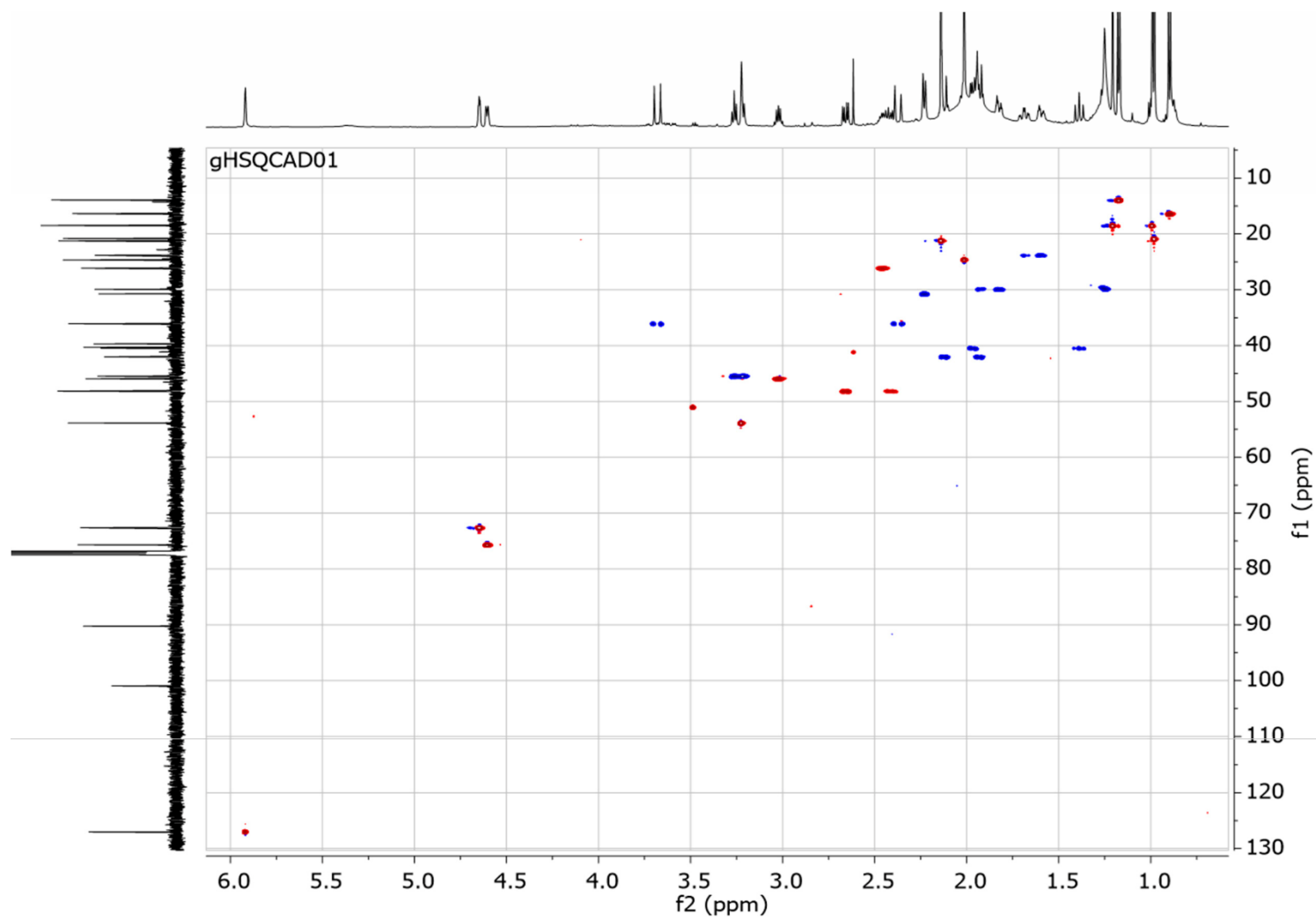
Figure S6. HSQC NMR spectrum of **2** at 500 MHz in CDCl₃
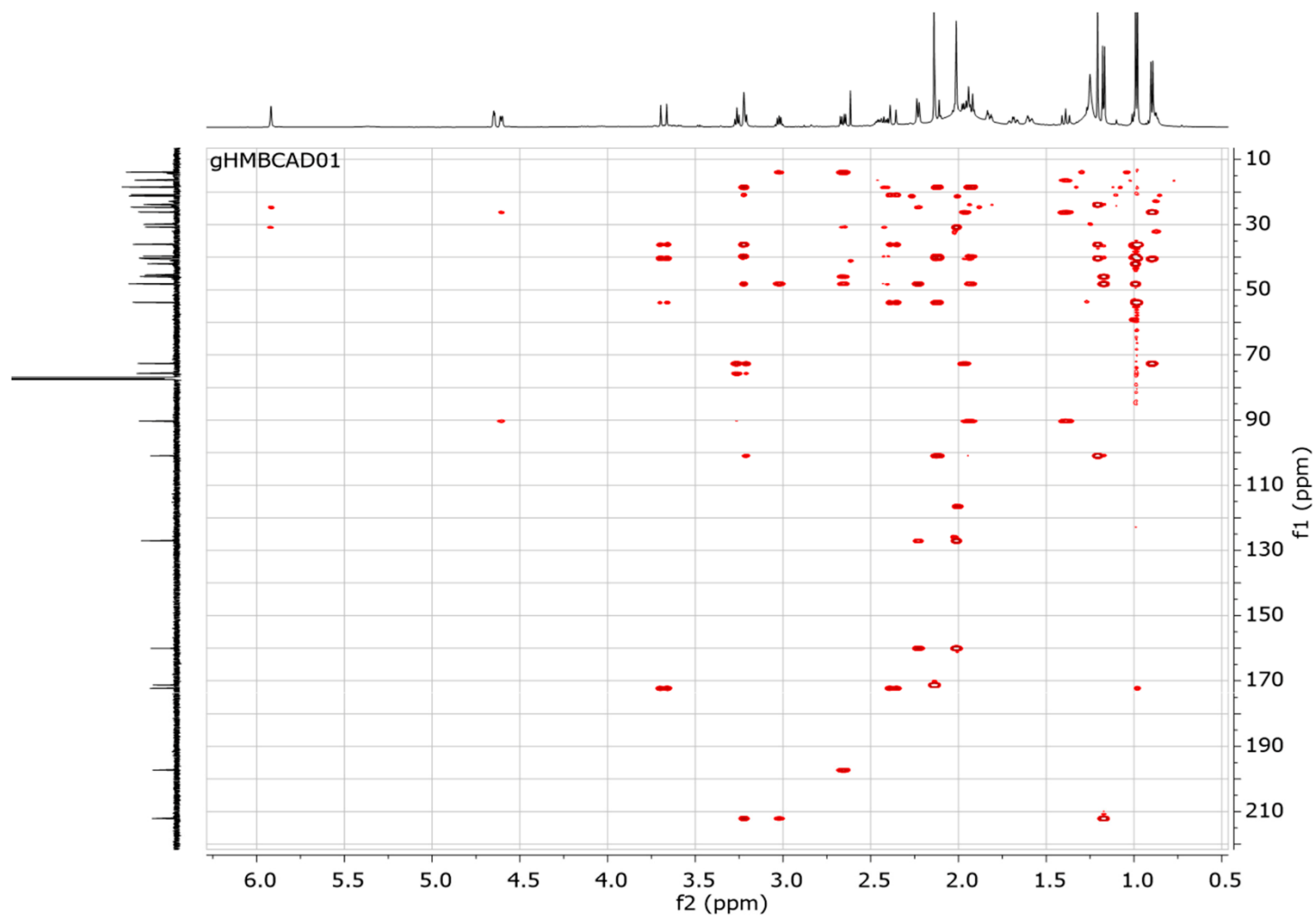
Figure S7. HMBC NMR spectrum of **2** at 500 MHz in CDCl$_3$

Ecdysonelactones, ecdysteroids from the Tropical Eastern Pacific Zoantharian *Antipathozoanthus hickmani*

Supplementary Information for

Ecdysonelactones, ecdysteroids from the Tropical Eastern Pacific Zoantharian *Antipathozoanthus hickmani*

Paul O. Guillen [1, 2]**, Kevin Calabro** [2]**, Karla B. Jaramillo** [1, 3]**, Cristobal Dominguez** [1]**, Grégory Genta-Jouve** [4]**, Jenny Rodriguez** [1]**,* and Olivier P. Thomas** [2]**,***

[1] Escuela Superior Politécnica del Litoral, ESPOL, Centro Nacional de Acuacultura e Investigaciones Marinas, CENAIM, Campus Gustavo Galindo km. 30.5 vía Perimetral, P.O.Box 09-01-5863, Guayaquil, Ecuador.

[2] National University of Ireland Galway, School of Chemistry, Marine Biodiscovery, University Road, H91 TK33 Galway, Ireland.

[3] National University of Ireland Galway, School of Zoology, Ryan Institute, University Road, H91 TK33 Galway, Ireland.

[4] Équipe C-TAC, COMETE UMR 8638 CNRS, Université Paris Descartes, 4 avenue de l'observatoire, 75006 Paris, France.

* Correspondence: jenrodri@espol.edu.ec; olivier.thomas@nuigalway.ie. Tel.: +33(0)674802384

Taxonomic identification of the specimen

Biological material. Antipathozoanthus hickmani is a Macrocnemic zoantharian of the family of Parazoanthidae (Cnidaria, Anthozoa, Hexacorallia, Zoantharia, Macrocnemina).[5] It was identified for the first time in the Pacific Ocean at the Galapagos Islands and then it was reported in the northern coast of mainland Ecuador.[6] The colony sampled had approximately 124 polyps, they were collected at 24 m depth from the branches of the black coral *Myriopathes panamensis* at the Marine Protected Area "El Pelado" Ecuador (See Figure below). Most of them have been found growing on the branches of two black corals *Antipathes galapagensis* and *Myriopathes* spp.

Sampling. The specimen was collected by SCUBA diving in September 2015 at 24 m depth from the site named "La Pared" (1°55′58.24′′S/ 80°47′32.83′′W) at the rocky reefs of the Marine Protected Area El Pelado. (Site type: vertical cliff of 31 m depth), East coast of mainland Ecuador. Interestingly, the specimens observed of *A. hickmani* always were found in the deepest locations from the MPA (2 of 13 different sites). The separation from the branches of the black corals was performed cautiously to avoid any contamination from the host tissues. The specimen was fixed partly in 4% formaldehyde and 95% ethanol for systematic analyses and the remaining material was kept in -80 °C freezer for chemical compound analyses. A voucher sample is kept at CENAIM-ESPOL under the number 150924EP01-02.

Systematic analysis

Morphological characterization. The morphological characters were analysed from the formalin sample, in situ annotations and *in situ* pictures to determine the polyp size (height, width, and oral disk diameter), number of mesenteries, number of tentacles, type of sphincter, colours (tentacles, oral disk, column and coenenchyme), sand encrustations and related/substrate type.

---

[5] Reimer, J. D. & Fujii, T. Four new species and one new genus of zoanthids (Cnidaria, Hexacorallia) from the Galápagos Islands. ZooKeys 42, 1, (2010).

[6] Bo, M. et al. Black coral assemblages from Machalilla National Park (Ecuador). Pacific Science 66, 63-81, (2012).

DNA extraction and sequencing. The DNA data were extracted from ethanol 95% fixed samples. DNA extraction was obtained according to the guanidine extraction protocol as previously described.[7] Samples were them amplified for mitochondrial 16S rDNA using the primers 16Sant0a,16SbmoH based in the thermal cycle conditions mentioned.[8] For the nuclear internal transcribed spacer region (ITS-2) rDNA using the primers Zoan-f, Zoan-r and the protocol described with standard Taq polymerase.[9] The amplified DNA products were sent to the sequencing company (MacroGen Inc, Korea). The *A. hickmani* sequences obtained of were deposited in GenBank, with the accessions numbers XXXXXXXX and XXXXXXX.

Phylogenetic analysis. The resulting sequences were manually assembled, and the chromatograms were checked for quality using Geneious 10.2.2. The *A. hickmani* sequences were compared with publicly available sequences from the original *A. hickmani* and other zoantharians using the National Centre for Biotechnology Information's Basic Local Alignment Search Tool (NCBI BLAST).

RESULTS

Systematics.

Antipathozoanthus hickmani **(Reimer & Fujii, 2010)**

Material examined. Specimen number: 150924EP01-02. Type locality: East coast of mainland Ecuador, Santa Elena province, and Marine Protected Area "El Pelado" site "Bajo La Pared", geographical coordinates: 1°55'58.24''S/ 80°47'32.83''W.

---

[7] Sinniger, F., Reimer, J. D. & Pawlowski, J. The Parazoanthidae (Hexacorallia: Zoantharia) DNA taxonomy: description of two new genera. Marine Biodiversity 40, 57-70, (2010).

[8] Sinniger, F., Montoya-Burgos, J.-I., Chevaldonné, P. & Pawlowski, J. Phylogeny of the order Zoantharia (Anthozoa, Hexacorallia) based on the mitochondrial ribosomal genes. Marine Biology 147, 1121-1128, (2005).

[9] Reimer, J. D., Sinniger, F., Fujiwara, Y., Hirano, S. & Maruyama, T. Morphological and molecular characterization of Abyssoanthus nankaiensis,, a new family, new genus and new species of deep-sea zoanthid (Anthozoa : Hexacorallia : Zoantharia) from a north-west Pacific methane cold seep. Invertebrate Systematics 21, 255-262, (2007).
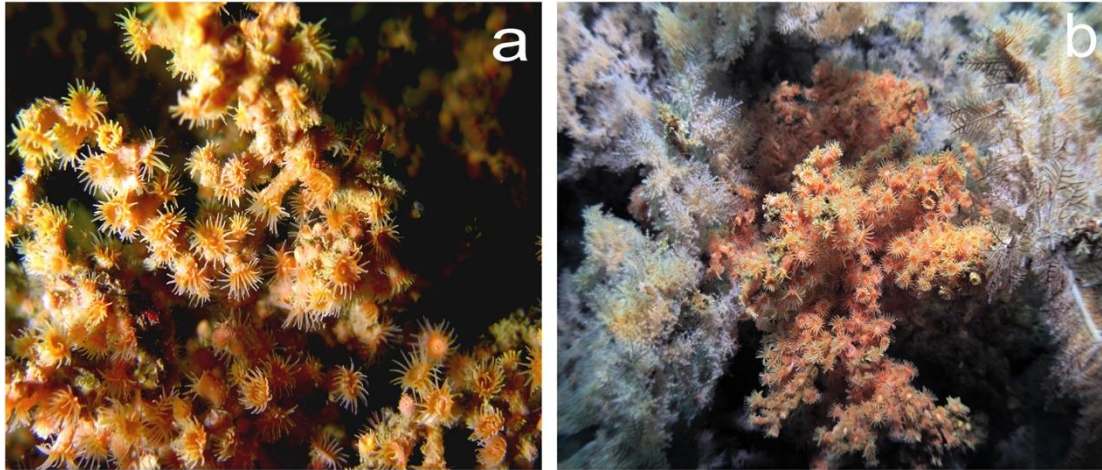
Figure. *In situ* pictures of *A. hickmani* at the MPA El Pelado, September 24, 2015. a) A closer view of the polyps of *A. hickmani*; b) The colony of *A. hickmani* on the branches of the black coral *M. panamensis*.

Morphological data: Alive/contracted polyps measured 6.0-12.0 / 2.0-4.0mm diameter and 2-6 mm height (measured starting from the coenenchyme). Number of tentacles and mesenteries number approximately 36-40. Colours of the tentacles were yellow or orange, while the oral disk were yellow-cream and the column-coenenchyme were orange-cream. *A. hickmani* presented a Cteniform endodermal type of sphincter muscle.[10] A relative amount of sand encrusted was visualized on the polyp's column and coenenchyme.

Molecular phylogeny. The results of molecular data were consistent with the literature data available. The mt 16S rDNA marker was successful sequenced for the sample 150924EP01-02 of *A. hickmani* (1061bp) this sequence was equal to the sequences from the original descriptions of *A. hickmani*. (EU333755, EU333756, both 582 bp) Only 1 bp was different from the *A. hickmani* EU333757 (582 bp). The Internal Transcribed Spacer region (ITS1, 5.8S and ITS2) was successful sequenced for *A. hickmani*, only one SNP and a polyA stretch of 9 successive bp instead of 7 bp in ITS1 remarkable the sequence of 150924EP01-02 *A. hickmani* (849 bp) from the original descriptions of *A. hickmani* (EU333797, EU333798, 703 bp).

---

[10] Swain, T. D., Schellinger, J. L., Strimaitis, A. M. & Reuter, K. E. Evolution of anthozoan polyp retraction mechanisms: convergent functional morphology and evolutionary allometry of the marginal musculature in order Zoanthidea (Cnidaria: Anthozoa: Hexacorallia). BMC Evol. Biol. 15, 123, (2015).
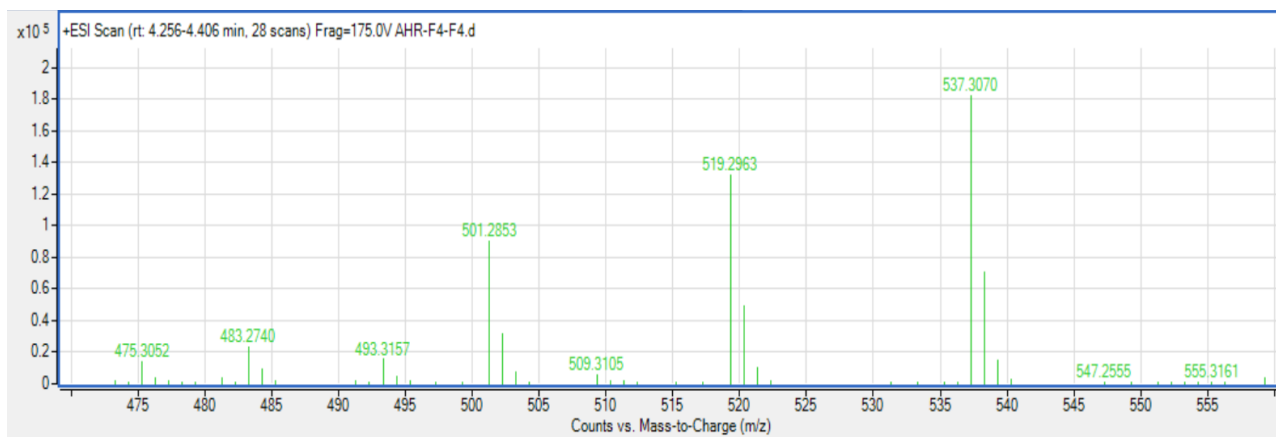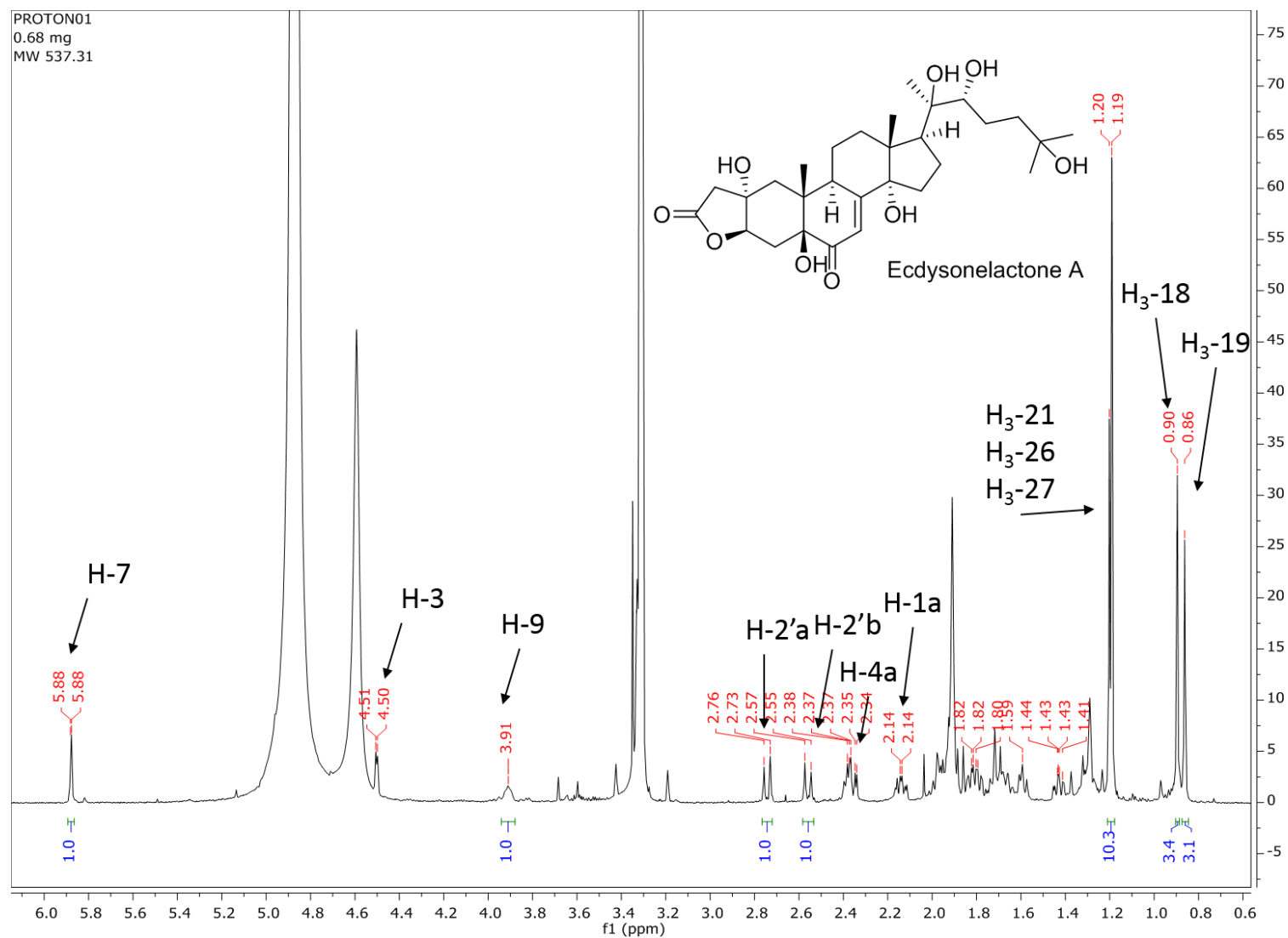
Figure S1. UHPLC-qToF analysis of **1** in (+)-ESI

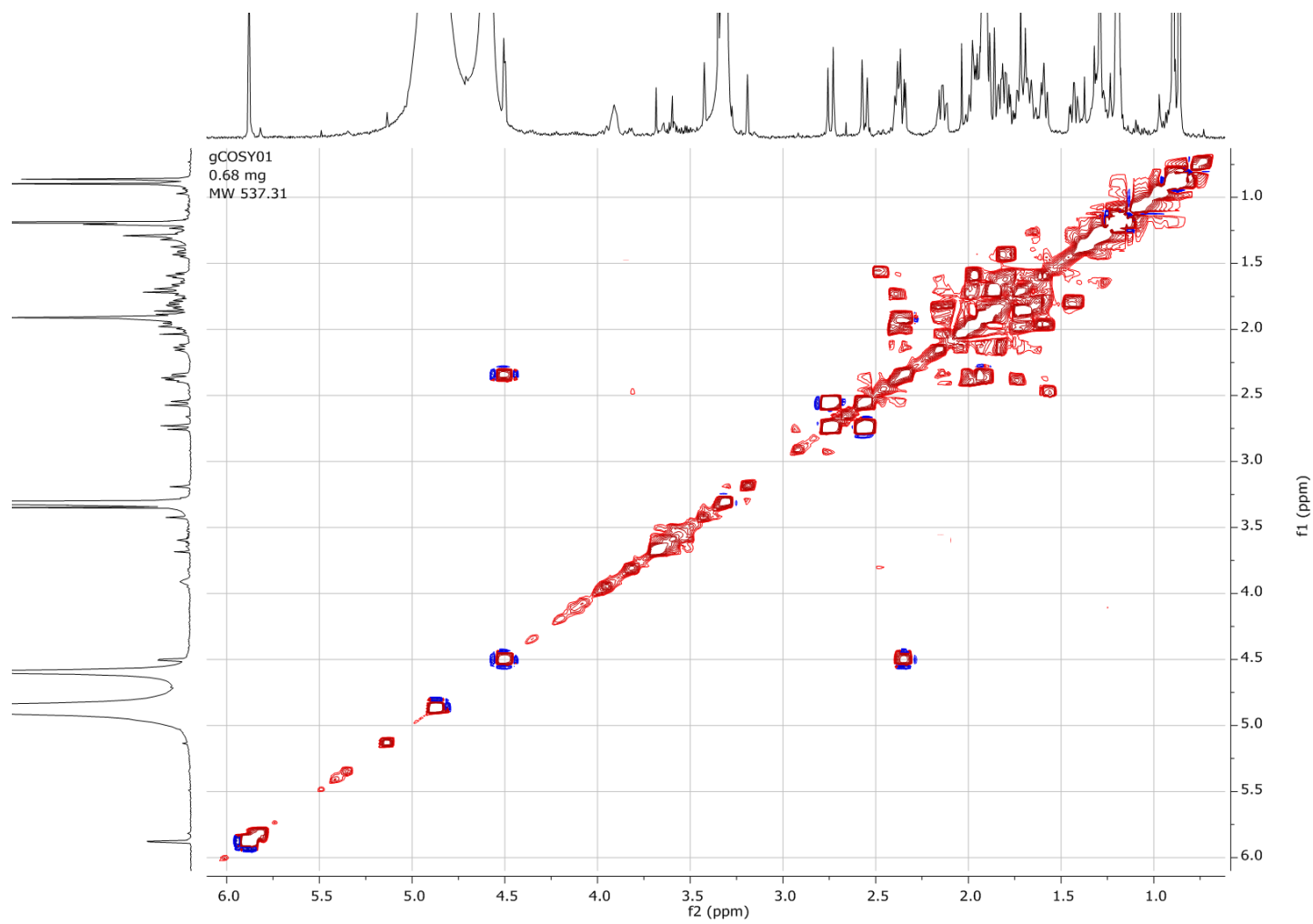**Figure S2**. ¹H NMR spectrum of **1** at 600 MHz in CD₃OD

gCOSY01
0.68 mg
MW 537.31

Figure S3. COSY NMR spectrum of **1** at 600 MHz in CD₃OD

CARBON01
0.68 mg
MW 537.31

Ecdysonelactone A

C-6 203.9

C-1' 176.3

C-8 169.2

C-7 120.1

84.9
82.5
78.4
77.9
77.8
74.2
71.3

50.4
47.5
42.4
42.1
39.2
38.4
32.6
31.9
31.9
29.7
28.9

22.3
21.5
21.0
18.1
16.7

f1 (ppm)
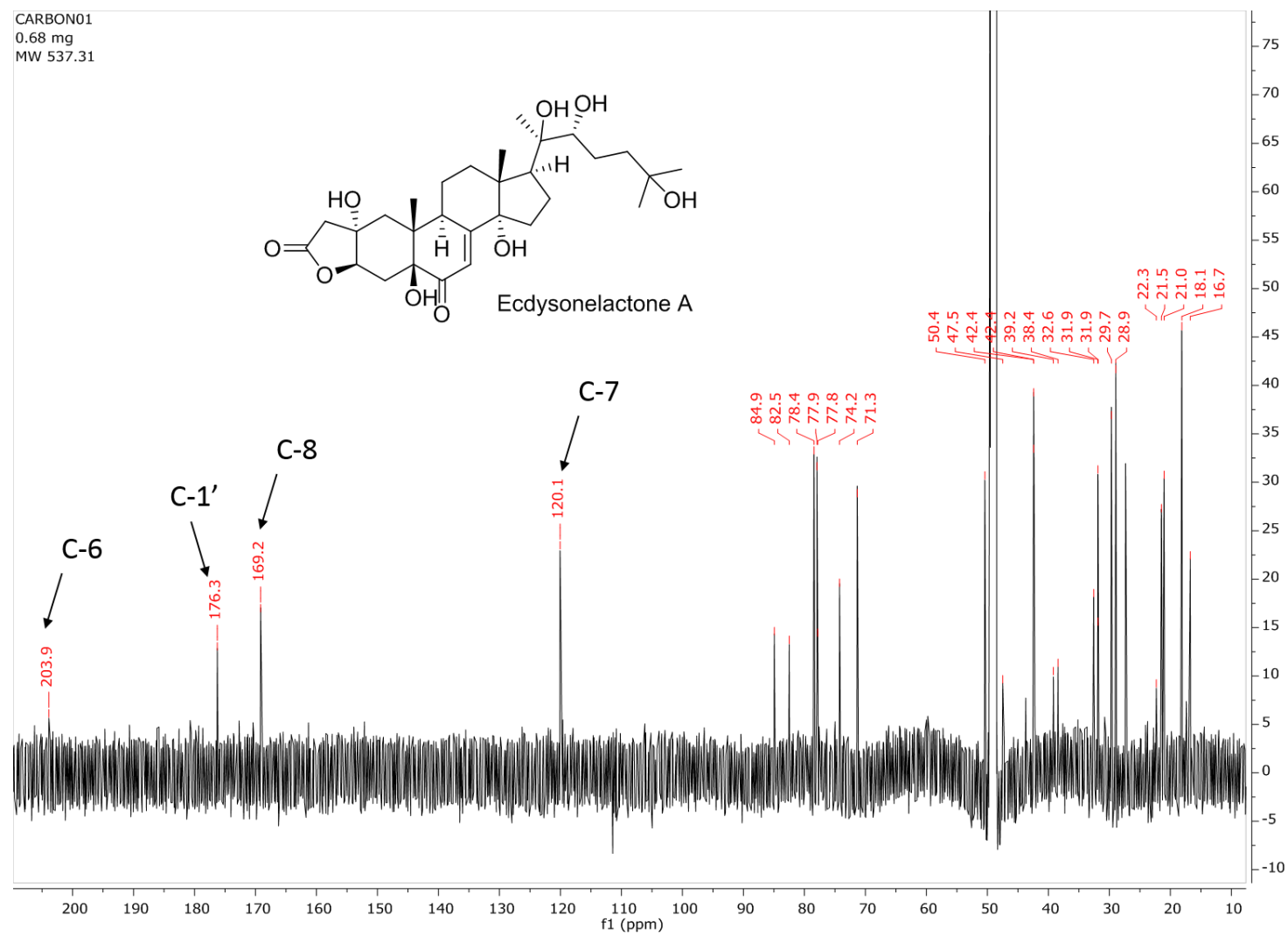
Figure S4. ¹³C NMR spectrum of **1** at 150 MHz in CD₃OD

220
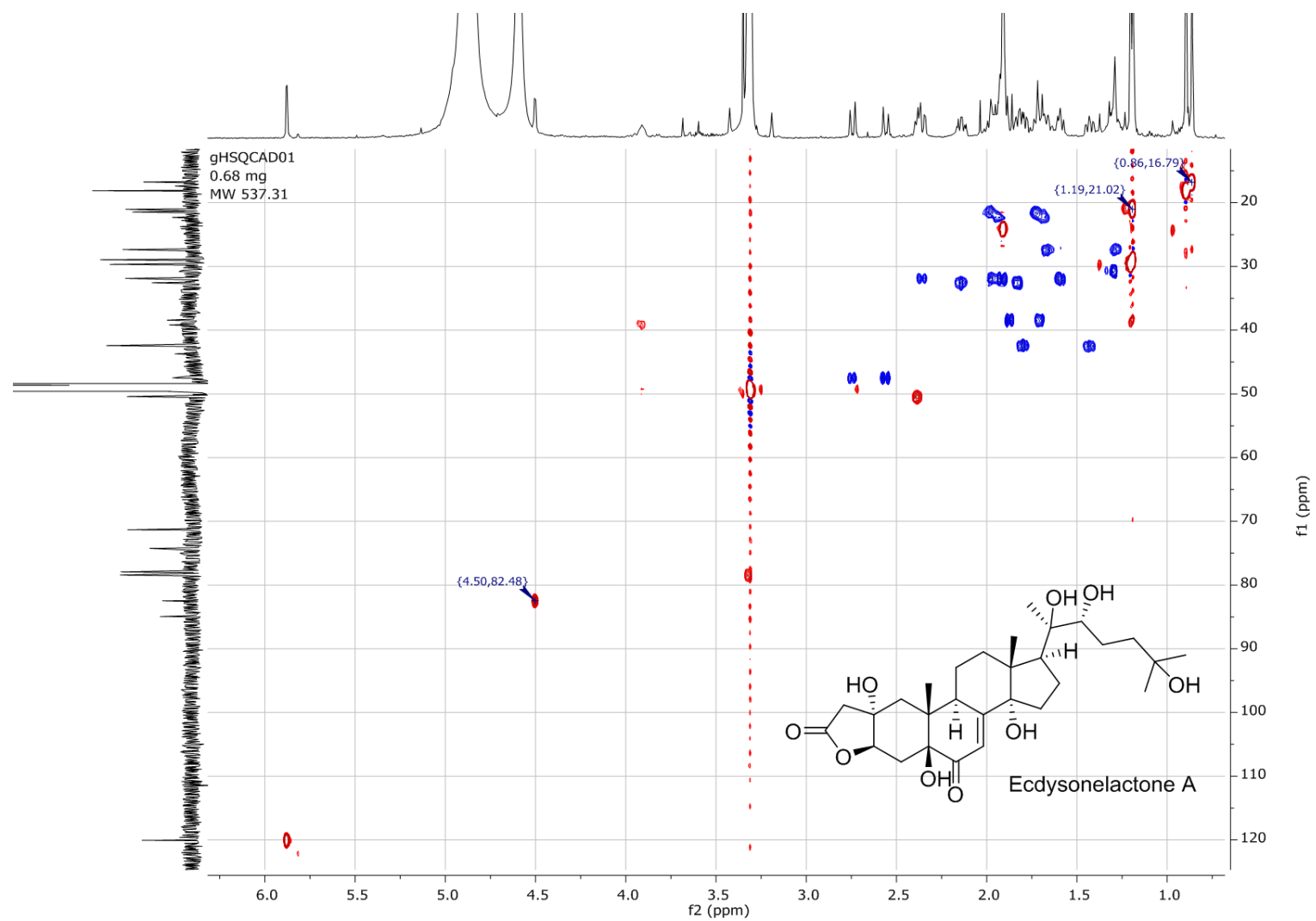
Figure S5. HSQC NMR spectrum of **1** at 600 MHz in CD₃OD
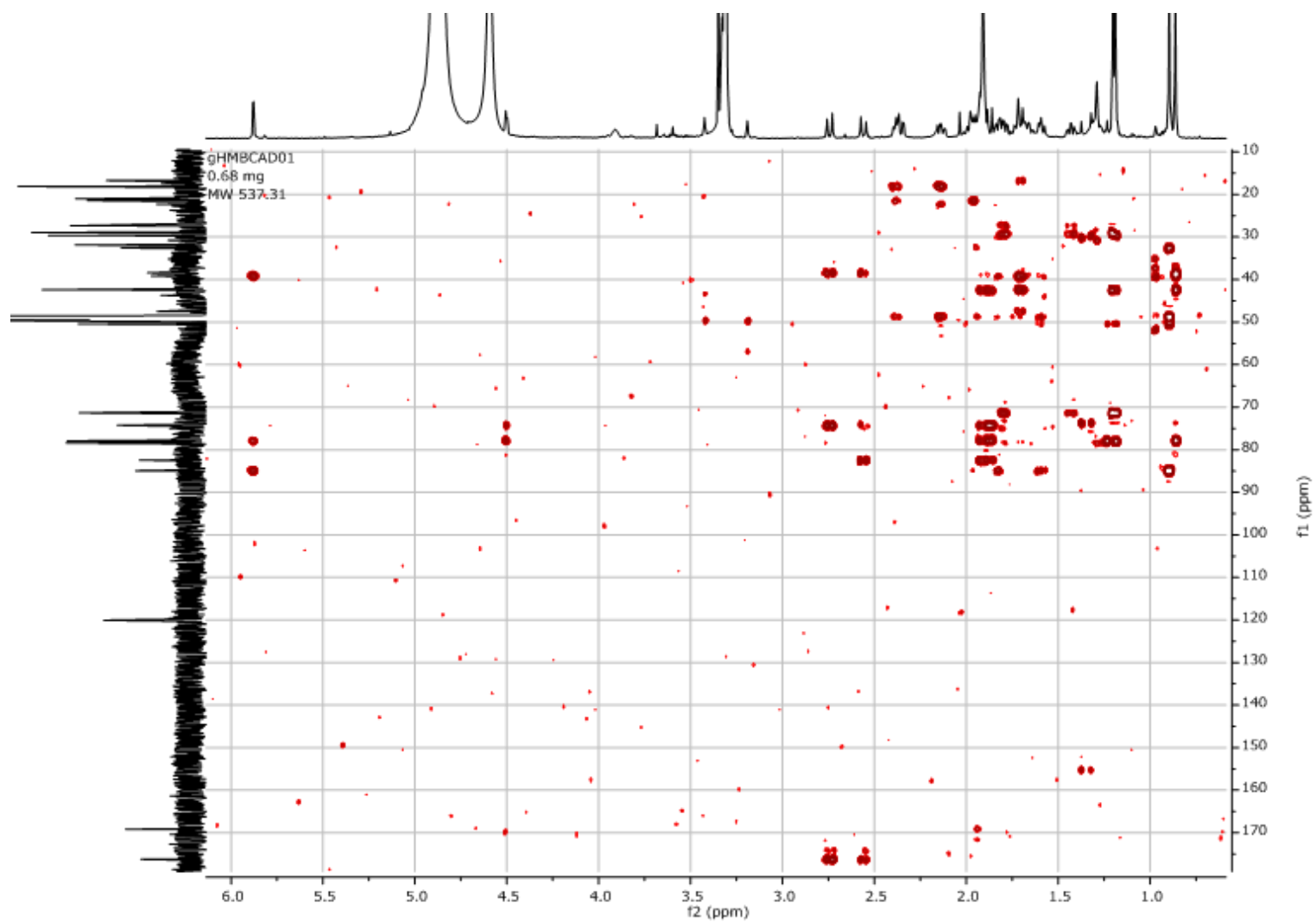
Figure S6. HMBC NMR spectrum of **1** at 600 MHz in CD₃OD
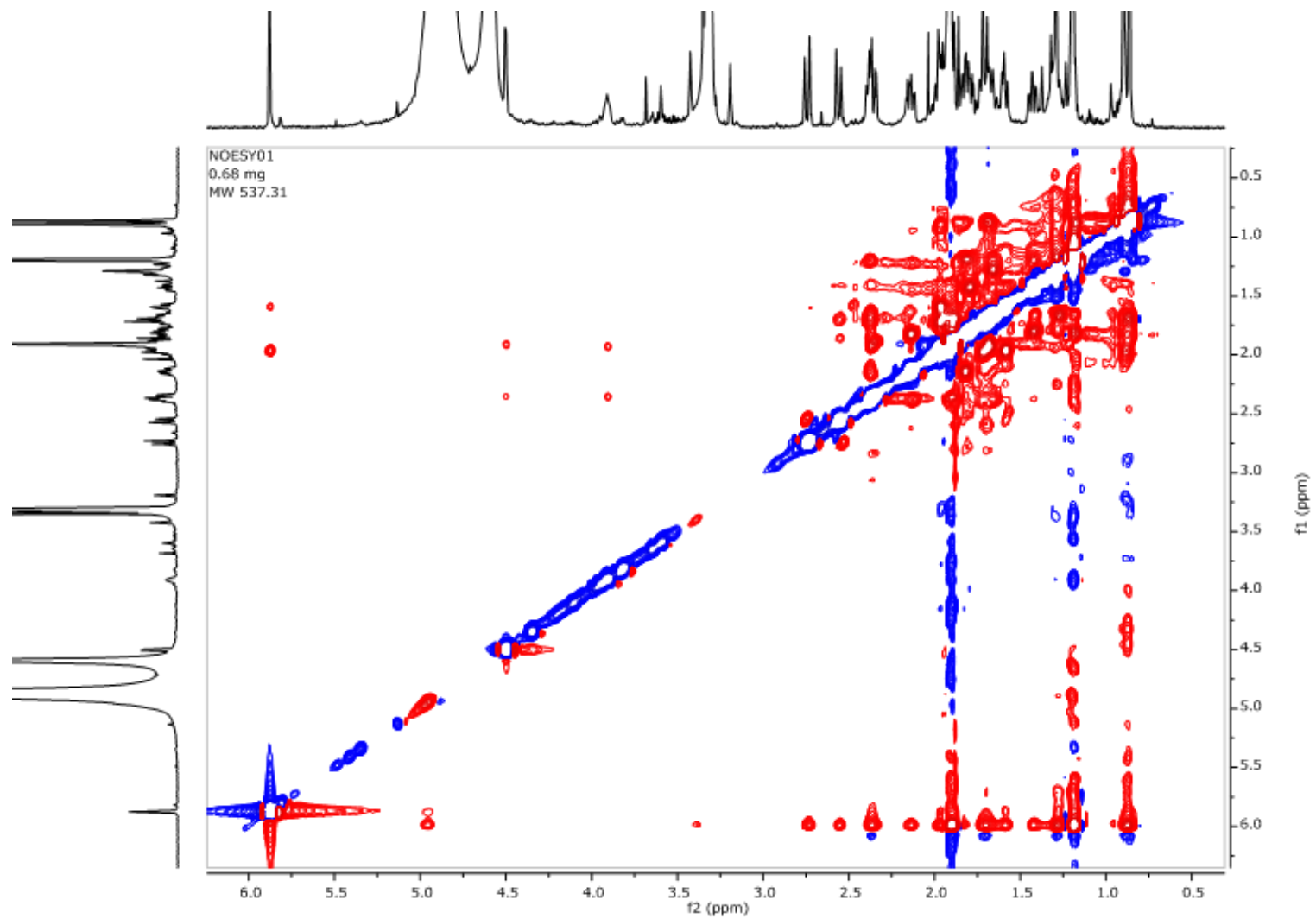
Figure S7. NOESY NMR spectrum of **1** at 600 MHz in CD₃OD
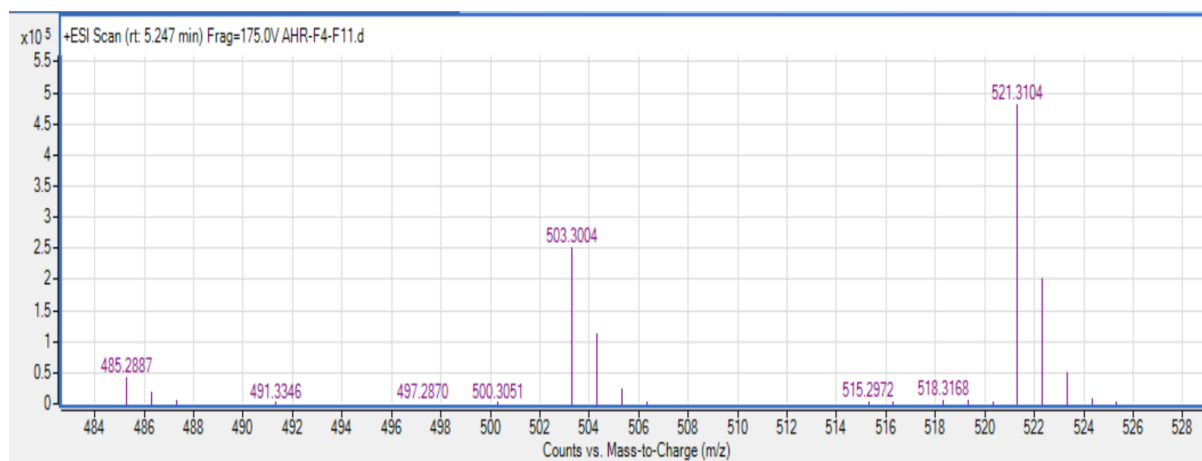
Figure S8. UHPLC-qToF analysis of **2** in (+)-ESI
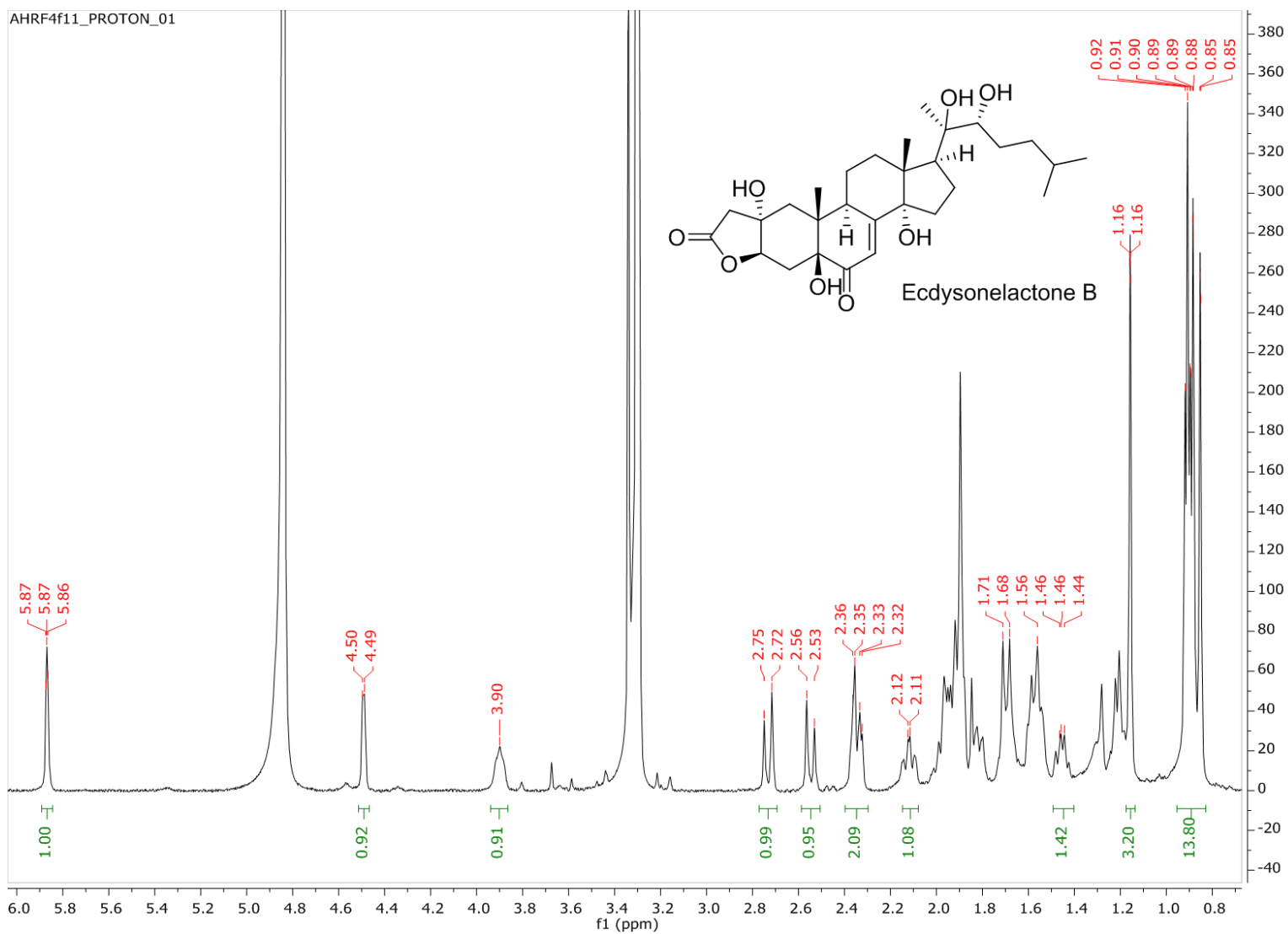
Figure S9. ^{1}H NMR spectrum of **2** at 600 MHz in CD₃OD

Figure S10. COSY NMR spectrum of **2** at 600 MHz in CD₃OD

AHRF4f11_CARBON_01
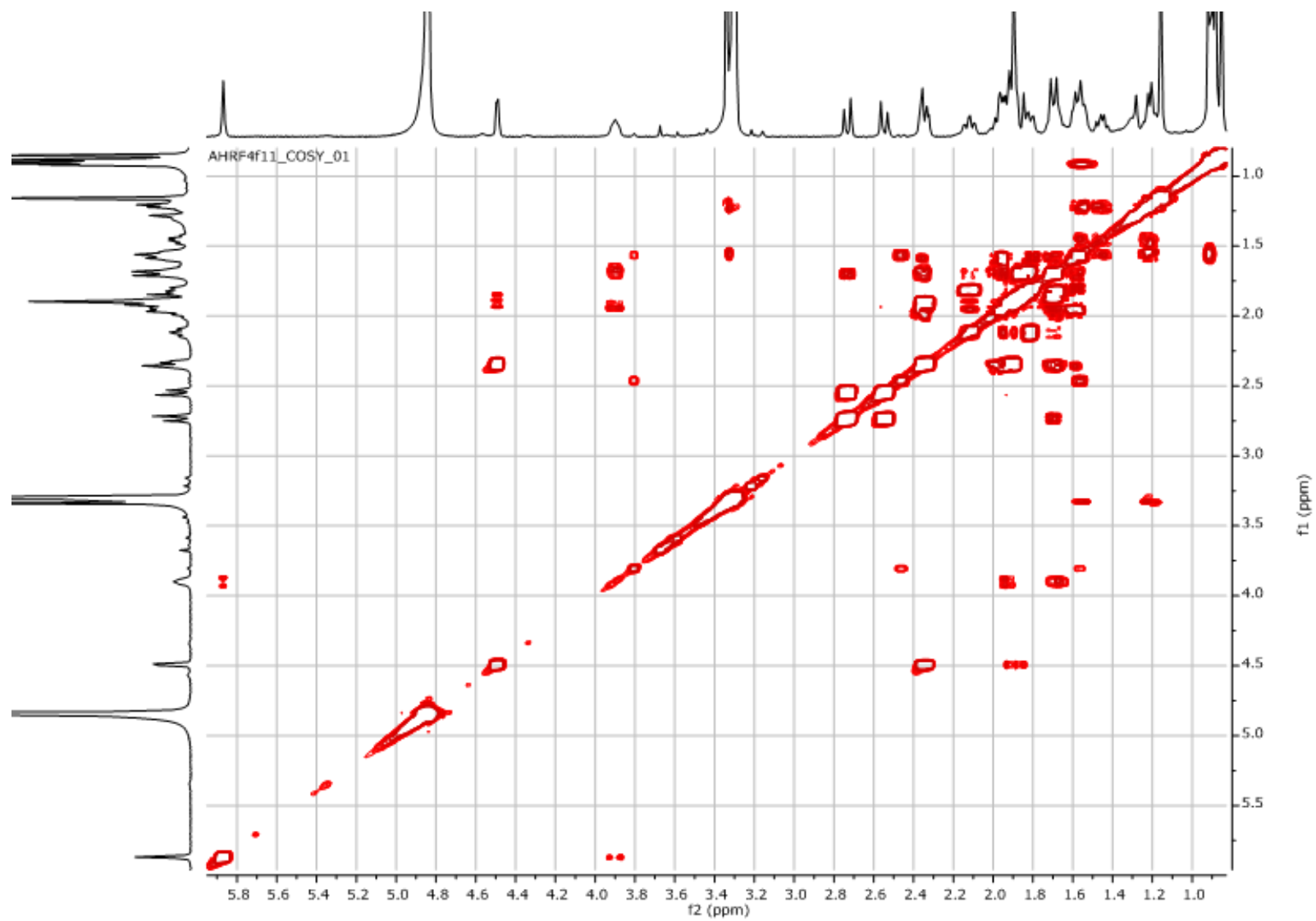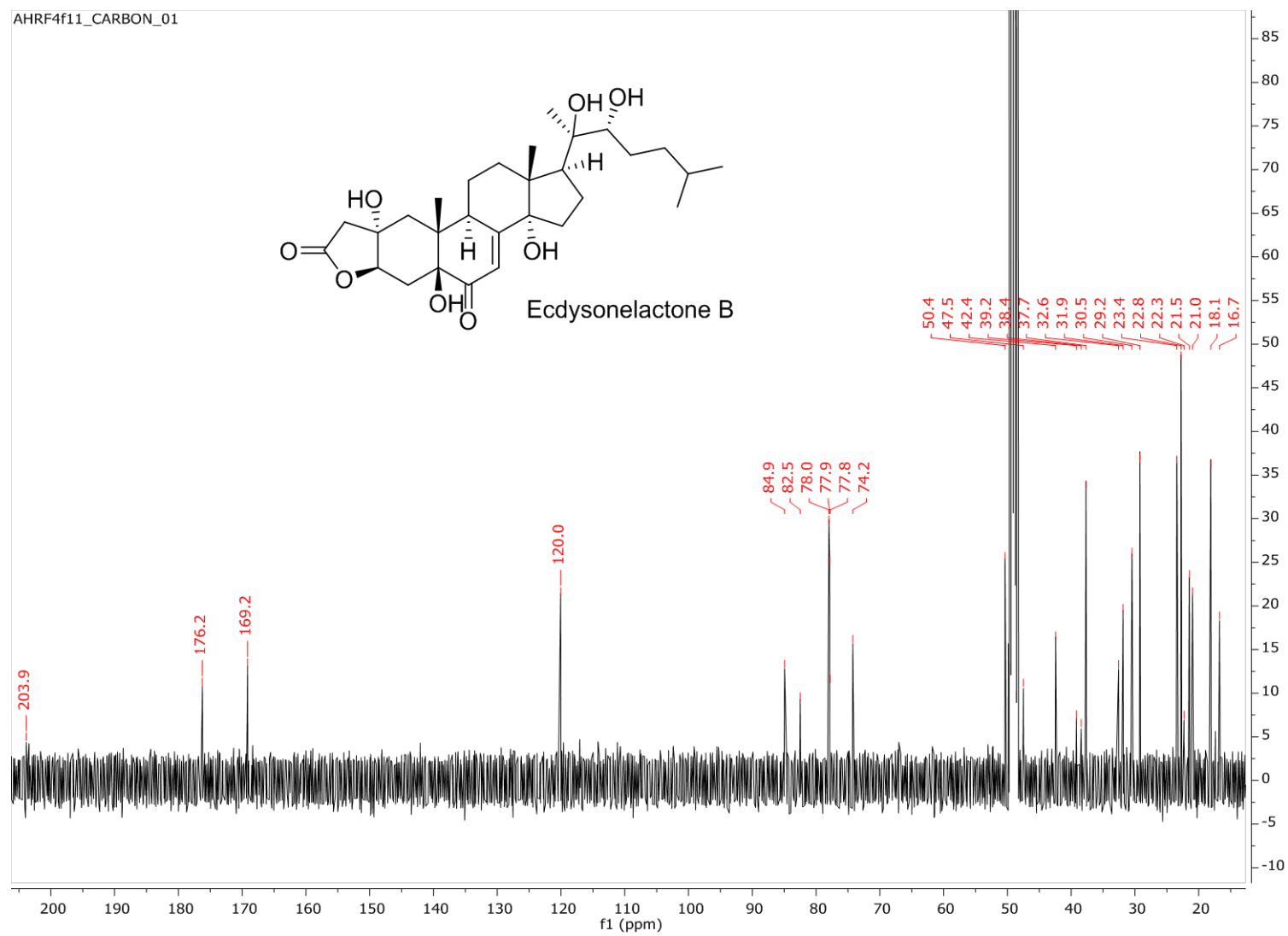
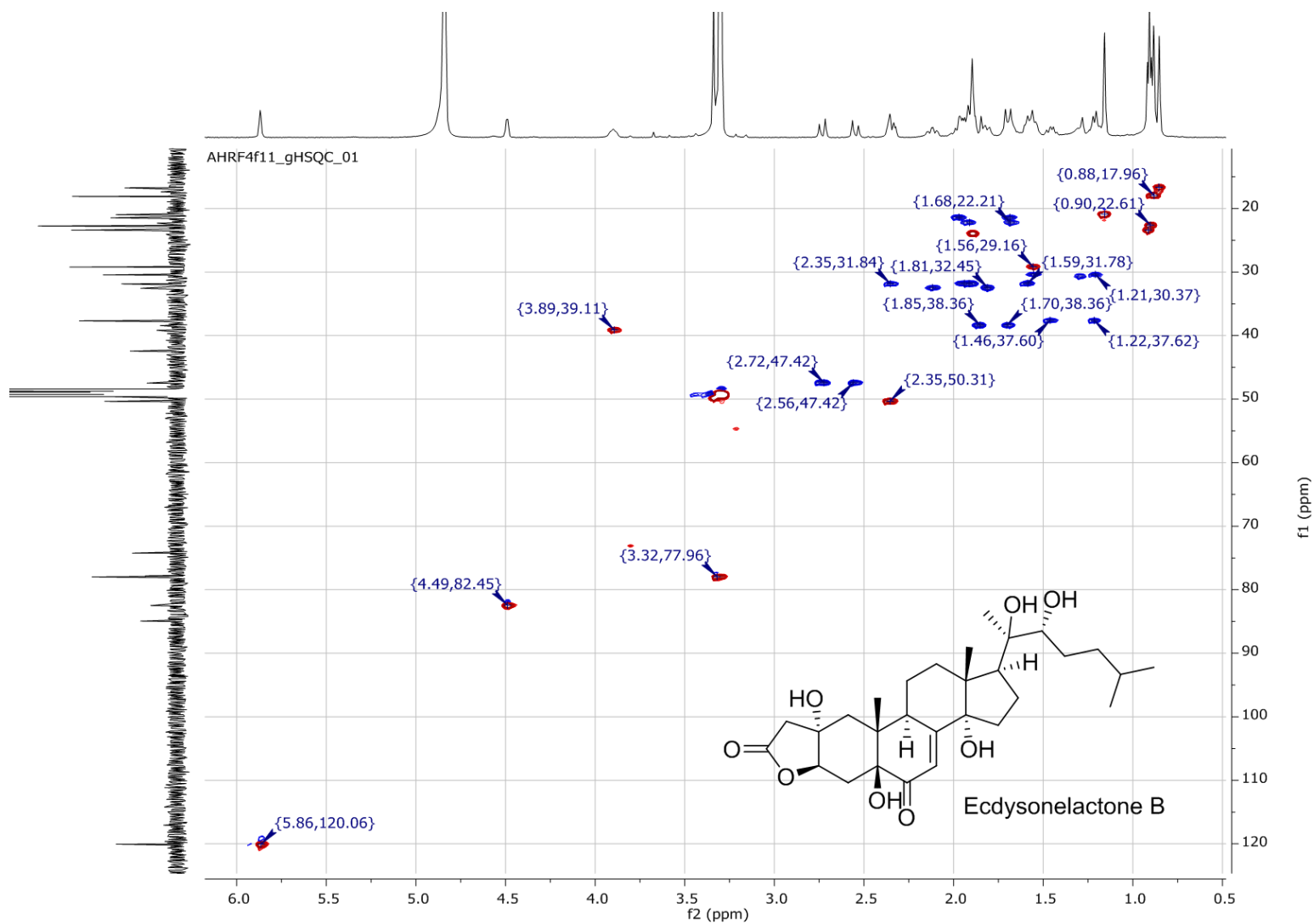**Figure S11**. ^{13}C NMR spectrum of **2** at 150 MHz in CD₃OD

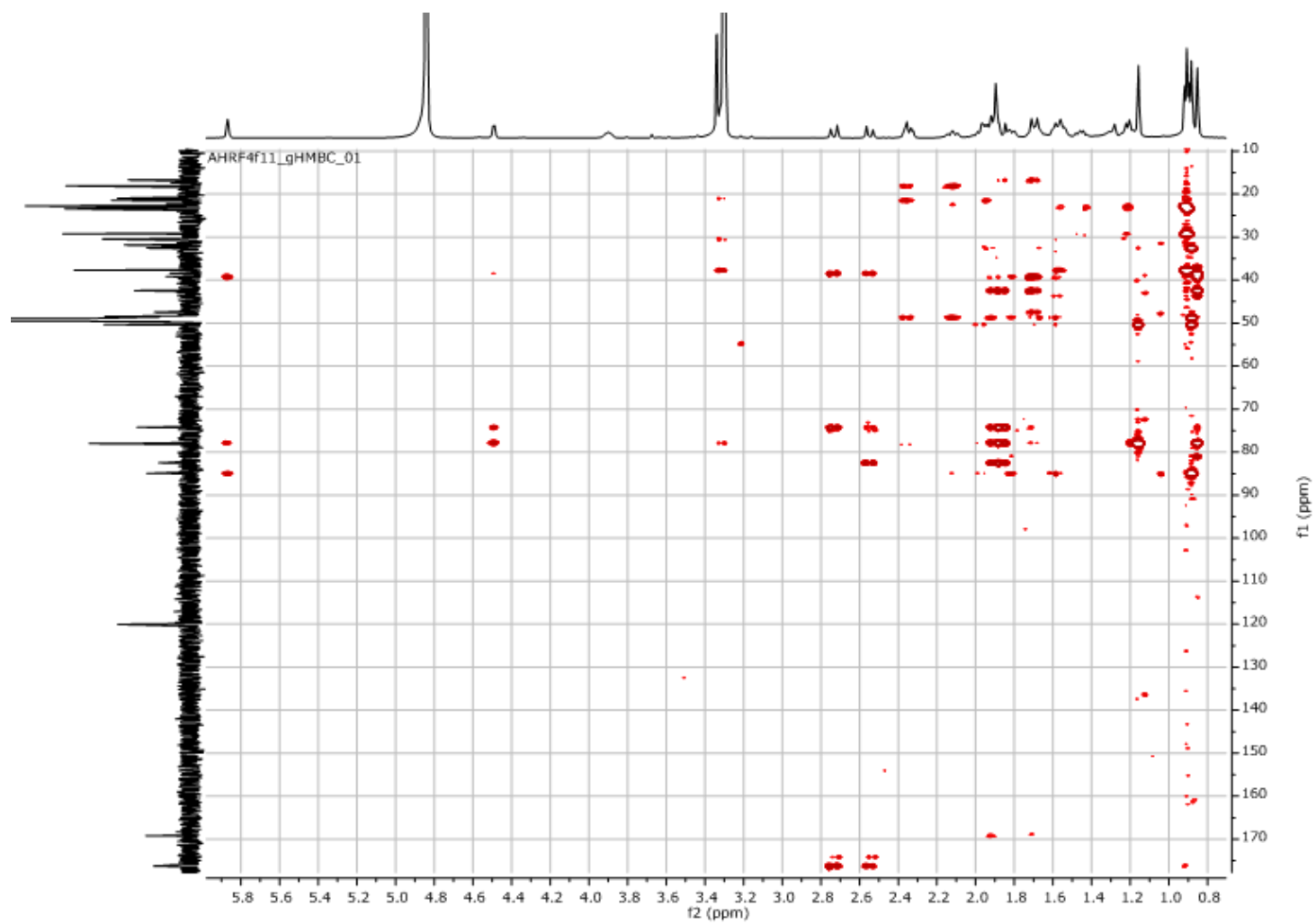**Figure S12**. HSQC NMR spectrum of **2** at 600 MHz in CD₃OD

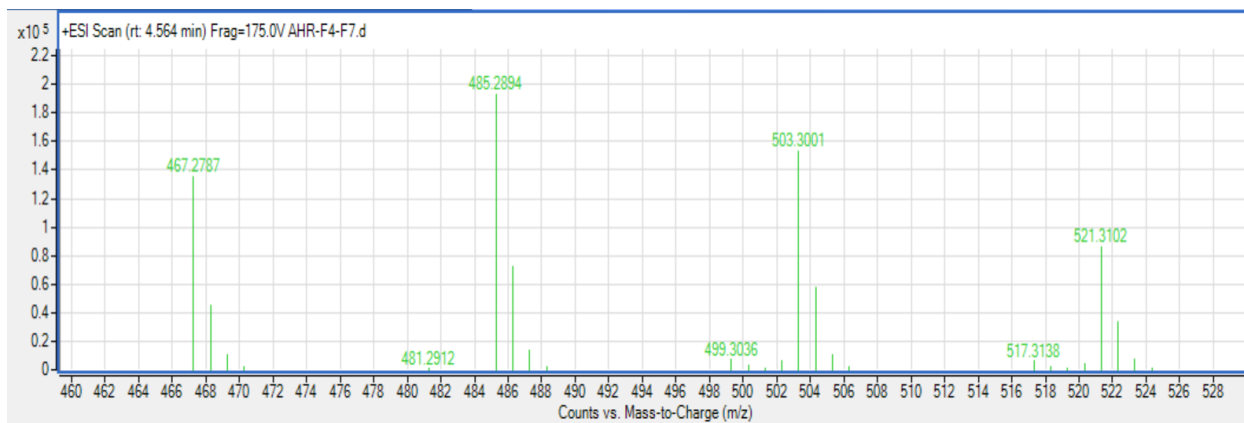**Figure S13.** HMBC NMR spectrum of **2** at 600 MHz in CD₃OD

Figure S20. UHPLC-qToF analysis of **3** in (+)-ESI
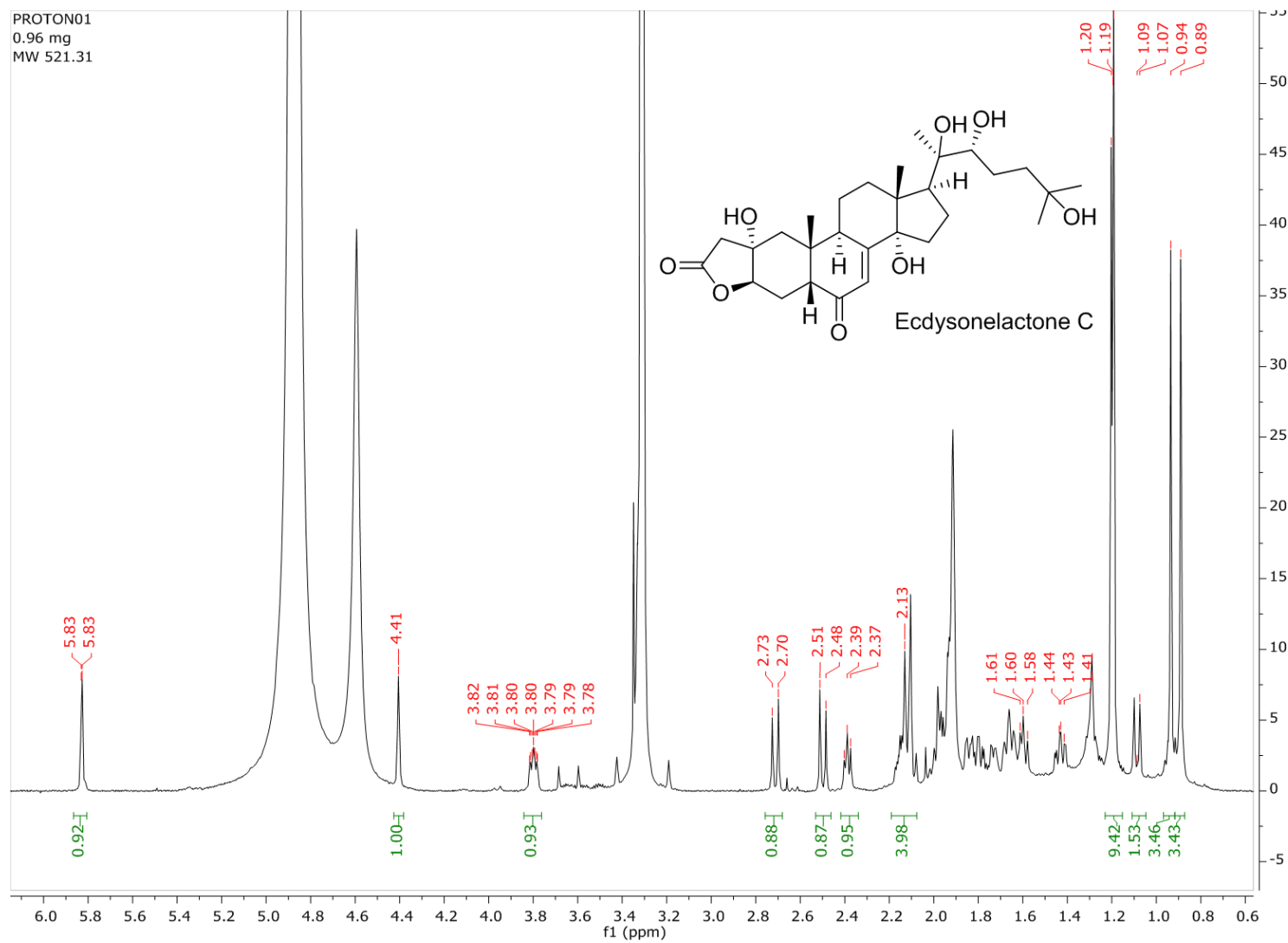
Figure S215. ¹H NMR spectrum of **3** at 600 MHz in CD₃OD

gCOSY01
0.96 mg
MW 521.31
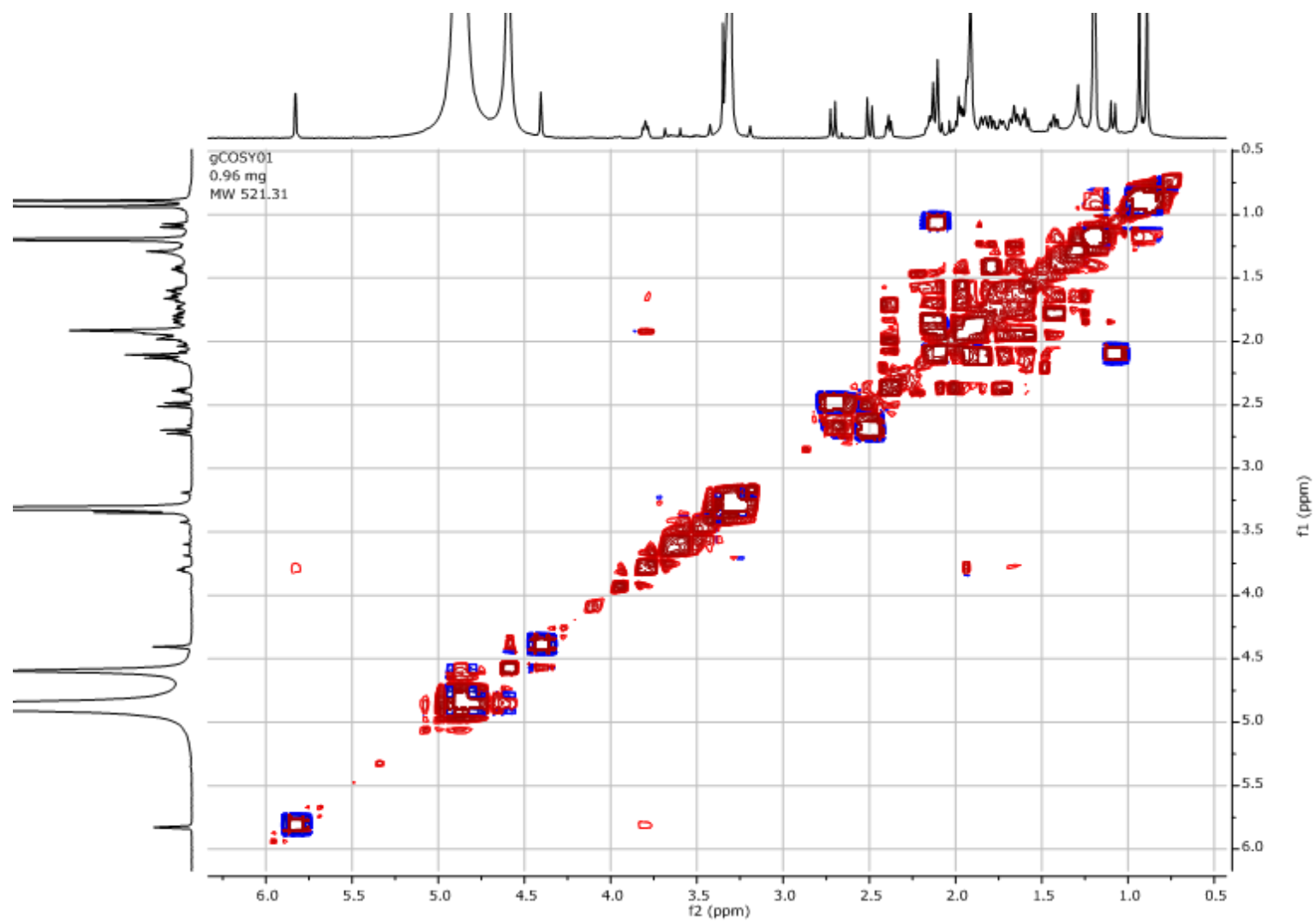
Figure S16. COSY NMR spectrum of **3** at 600 MHz in CD₃OD
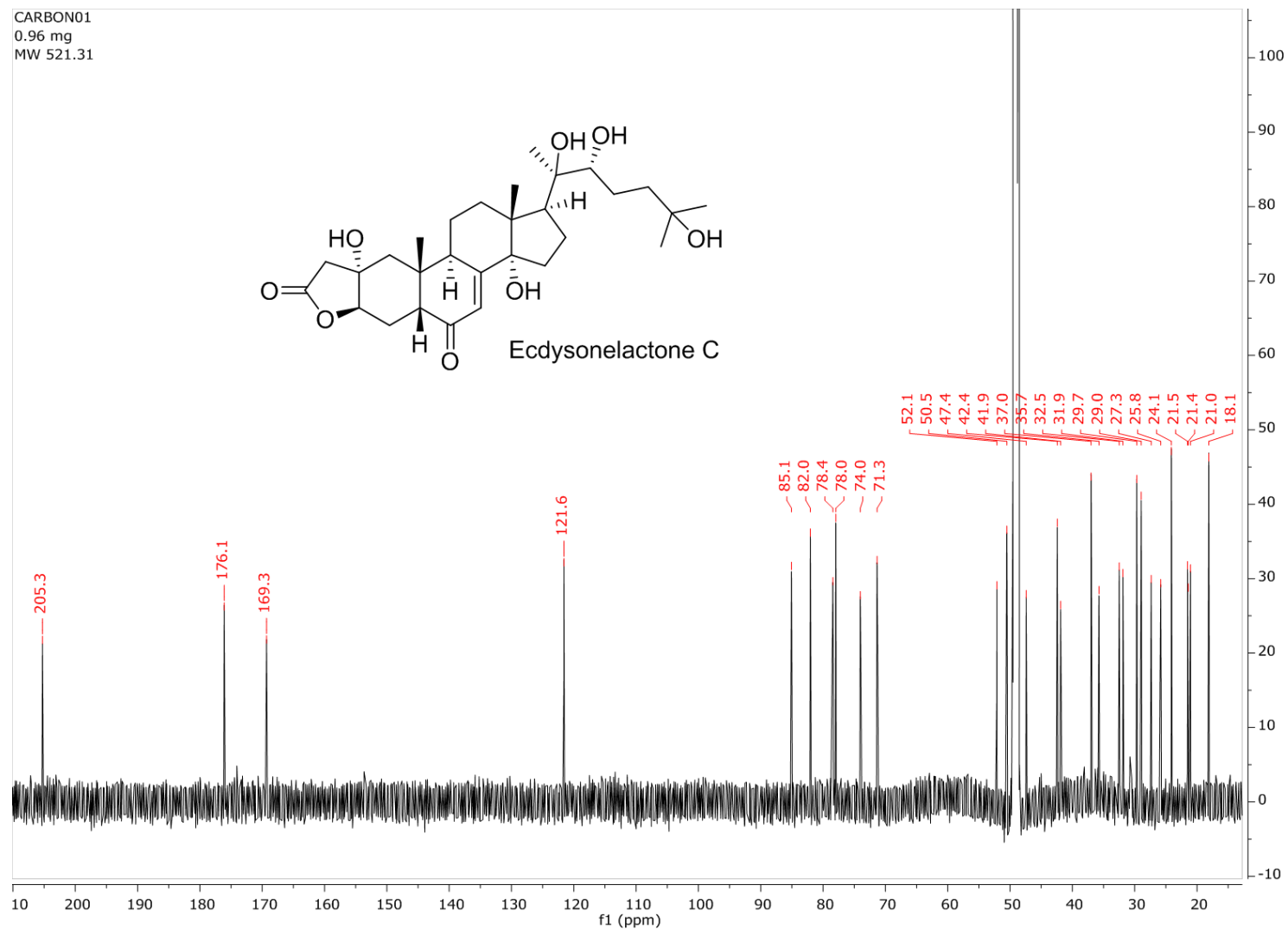
Figure S22. ^{13}C NMR spectrum of **3** at 150 MHz in CD$_3$OD
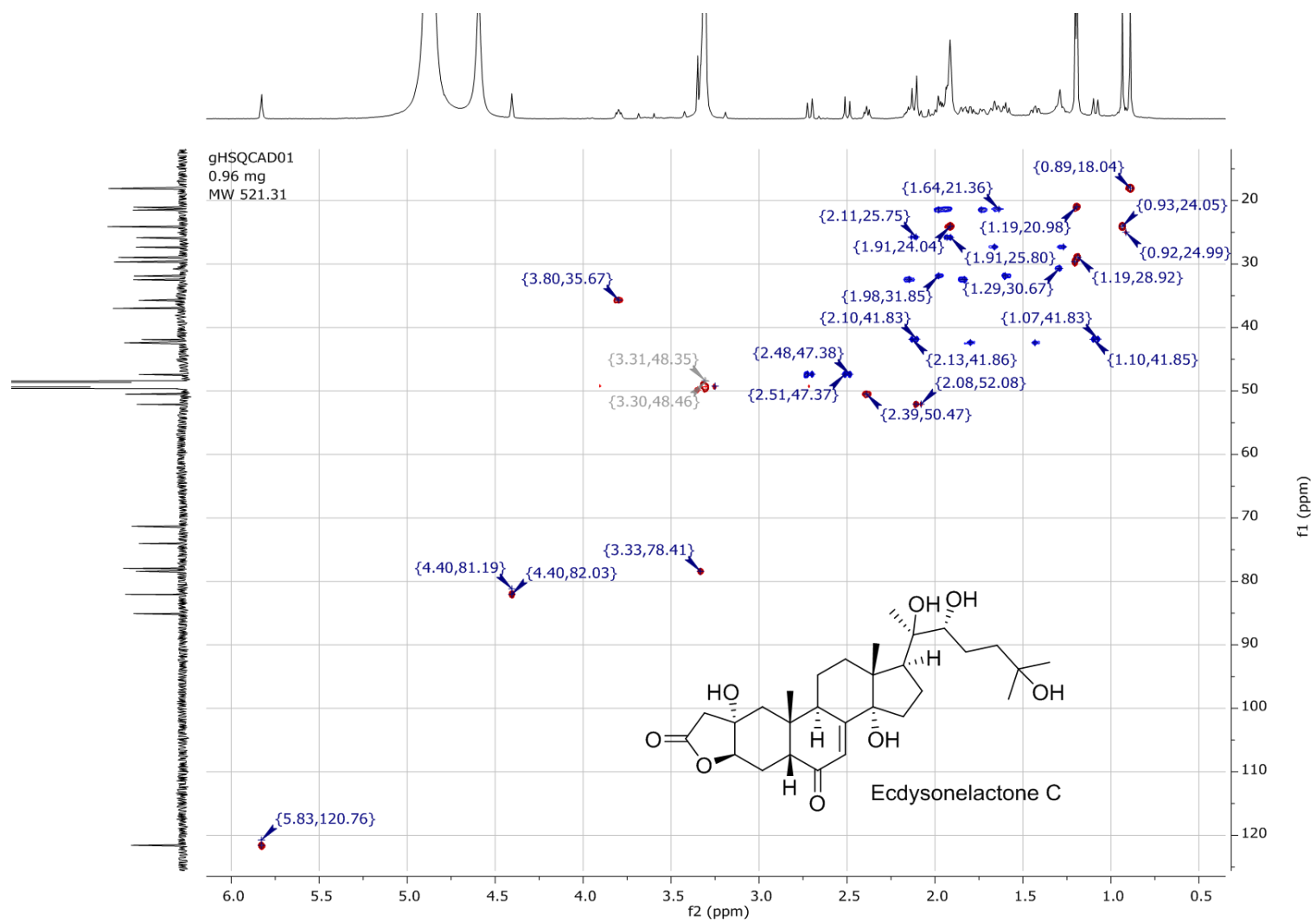
Figure S18. HSQC NMR spectrum of **3** at 600 MHz in CD₃OD

gHMBCAD01
0.96 mg
MW 521.31
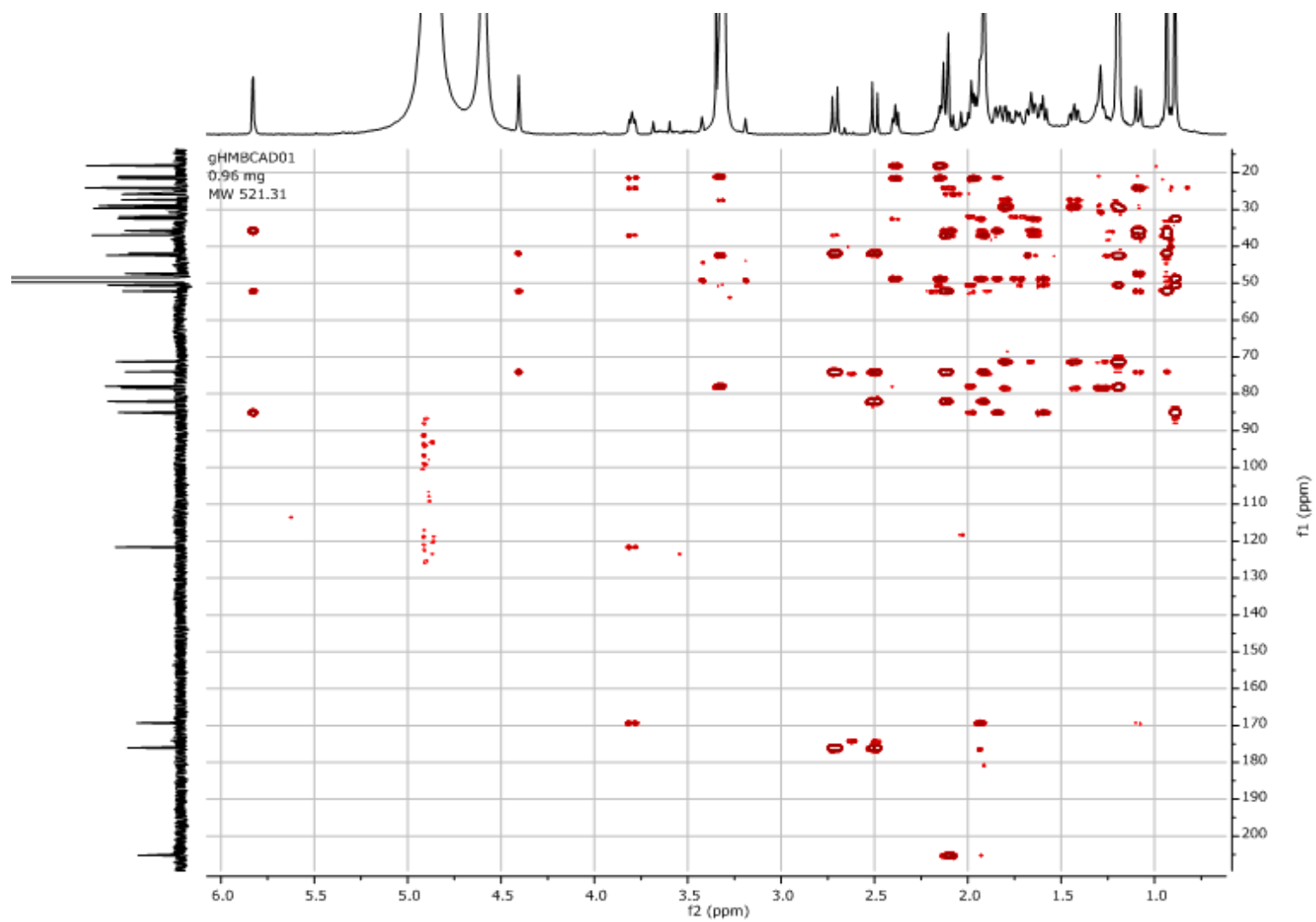
Figure S23. HMBC NMR spectrum of **3** at 600 MHz in CD₃OD
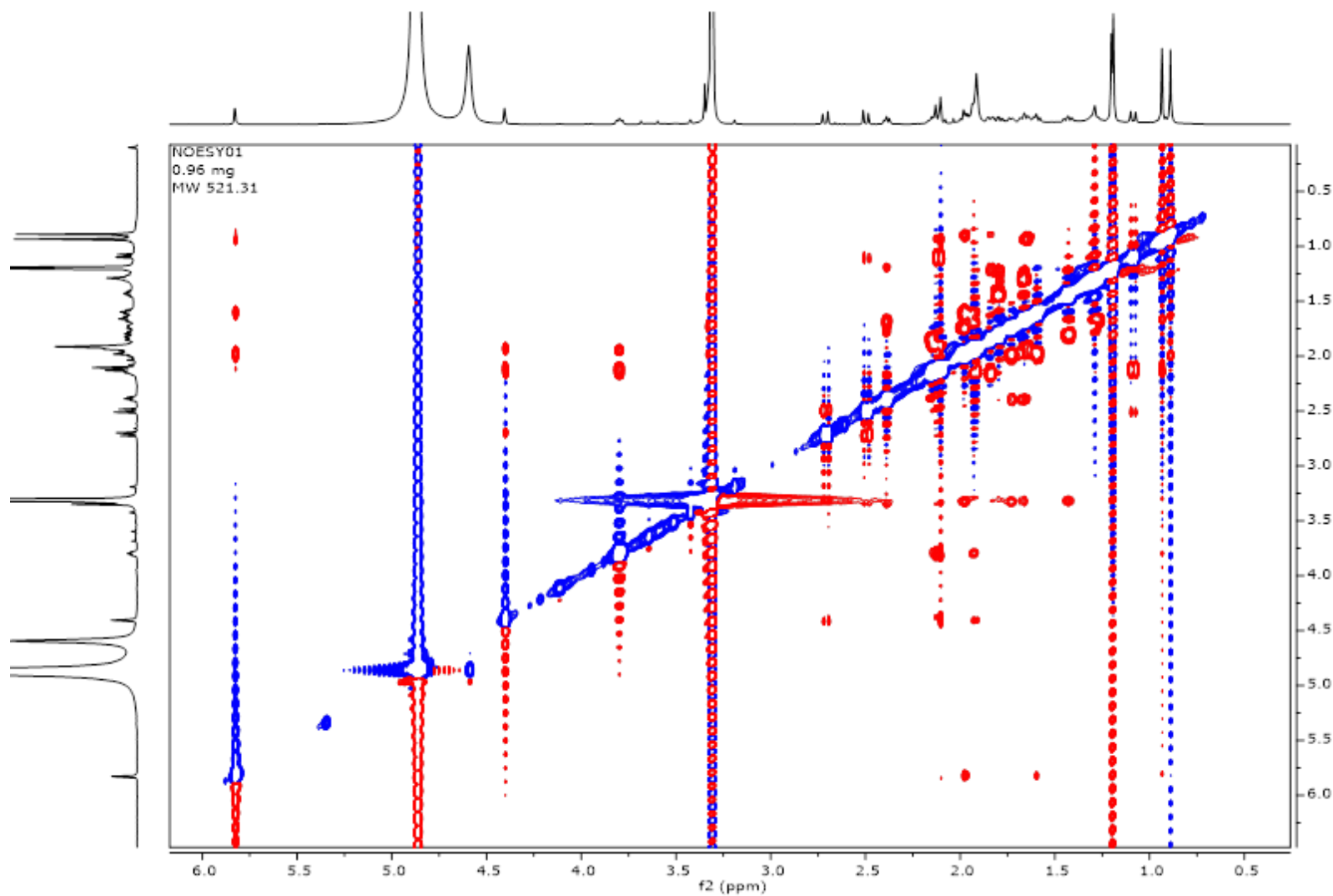
Figure S20. NOESY NMR spectrum of **3** at 600 MHz in CD₃OD

x10 4 +ESI Scan (rt: 4.524 min) Frag=175.0V AH-F3-P8.d

521.3104

503.2991

467.2847   477.2851   481.3133   485.2885   489.3127   496.3012   501.2826   511.3270   519.3047

Counts vs. Mass-to-Charge (m/z)

Figure S21. (+)-HRESIMS analysis of **4**.

Figure S242 ¹H NMR spectrum of **4** at 600 MHz in CD₃OD
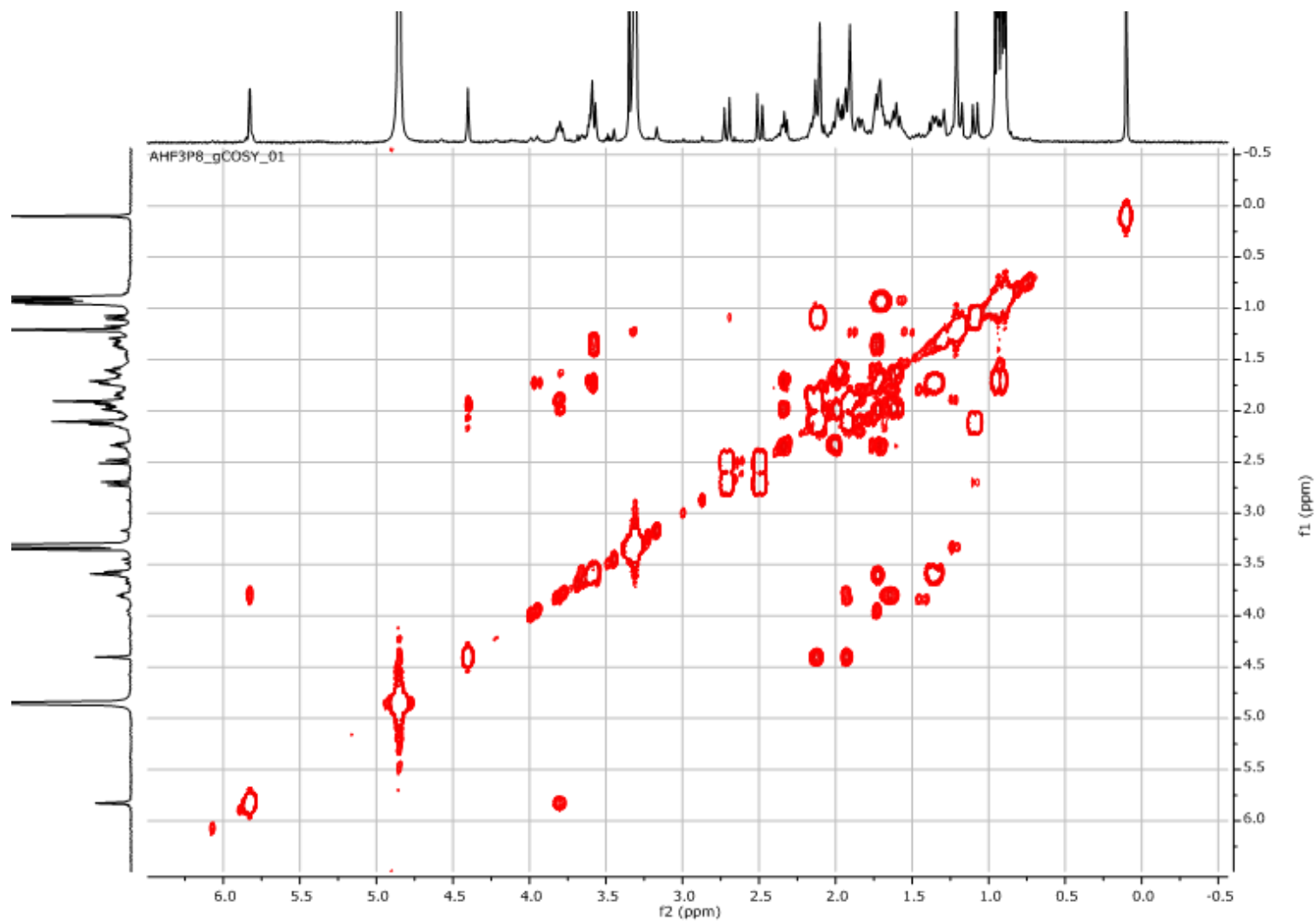
Figure S225. COSY NMR spectrum of **4** at 600 MHz in CD₃OD
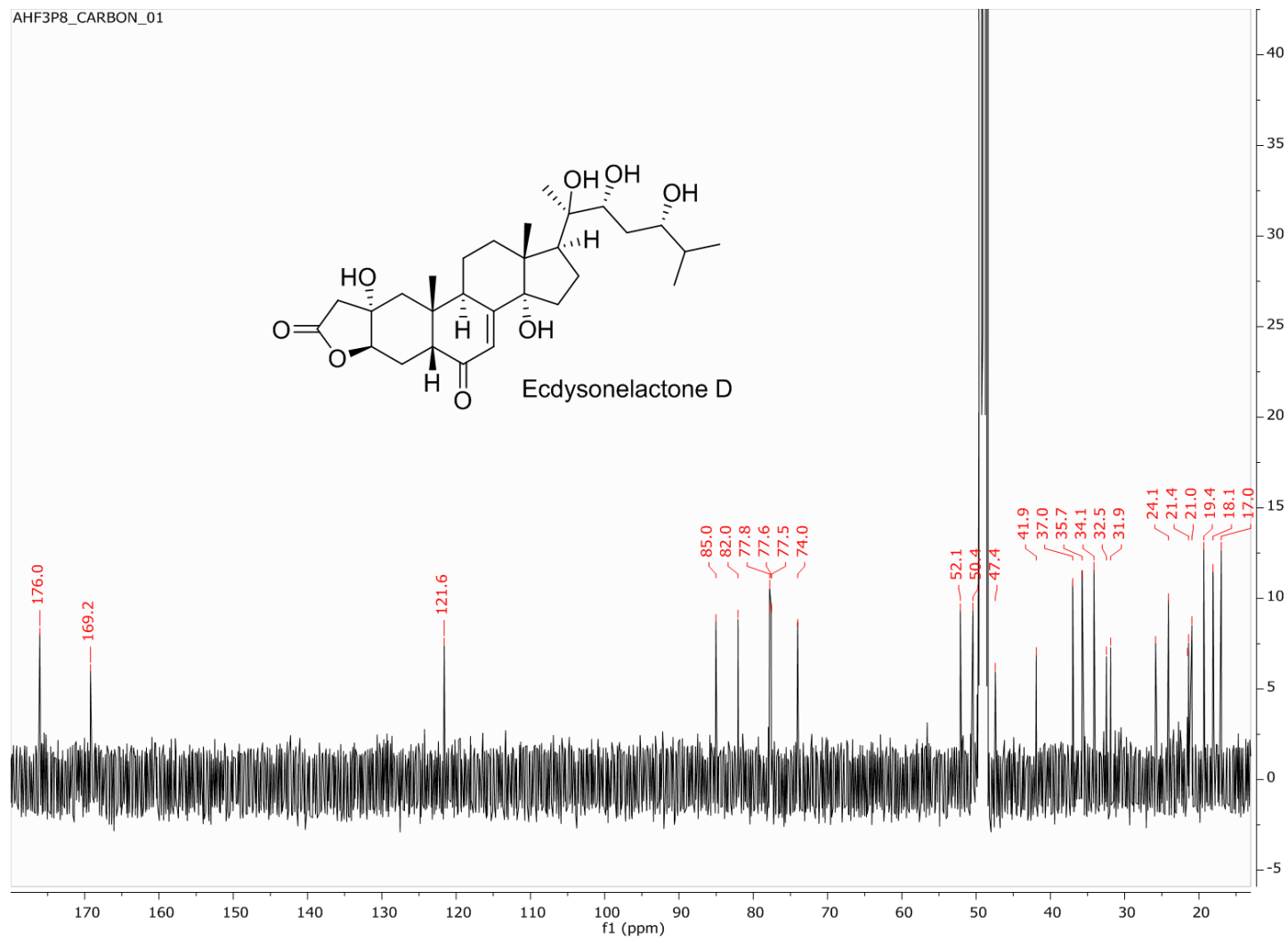
Figure S226. ^{13}C NMR spectrum of **4** at 150 MHz in CD$_3$OD
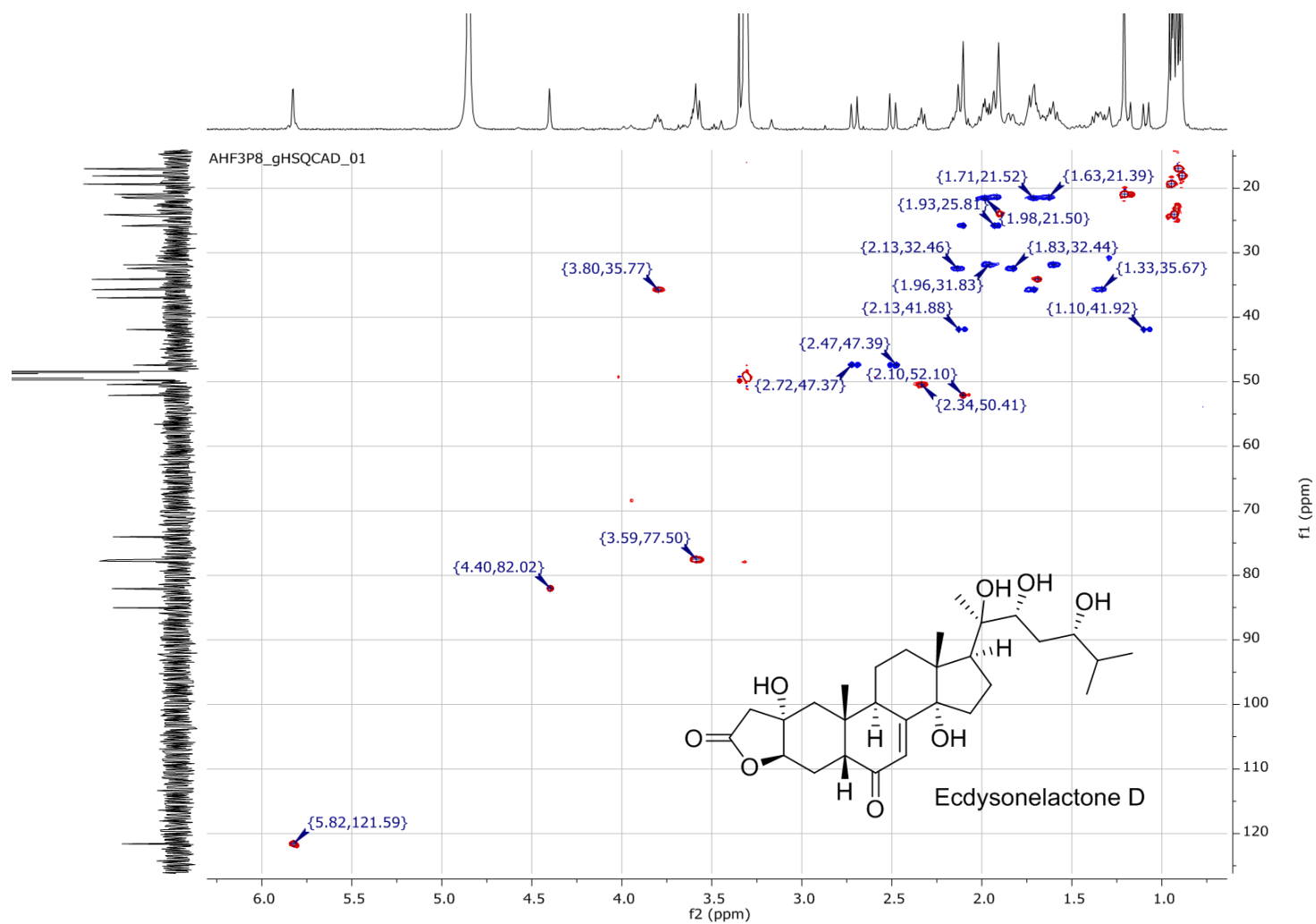
Figure S25. HSQC NMR spectrum of **4** at 600 MHz in CD₃OD

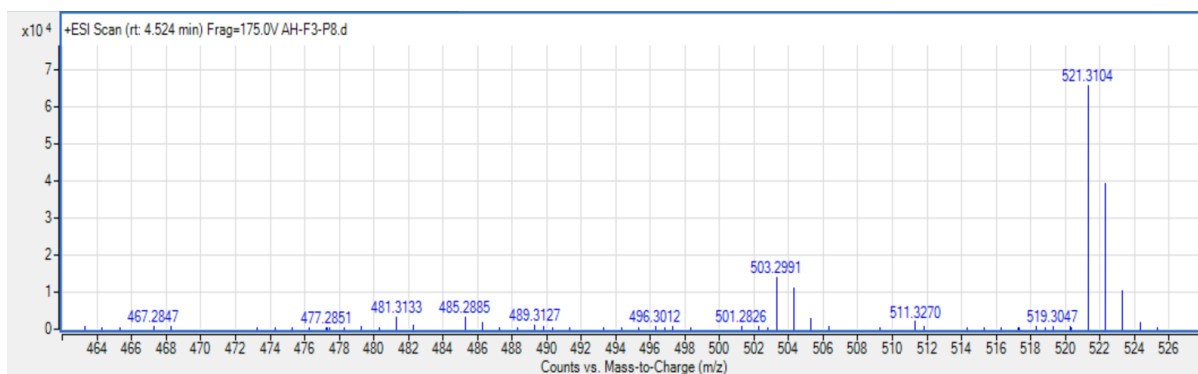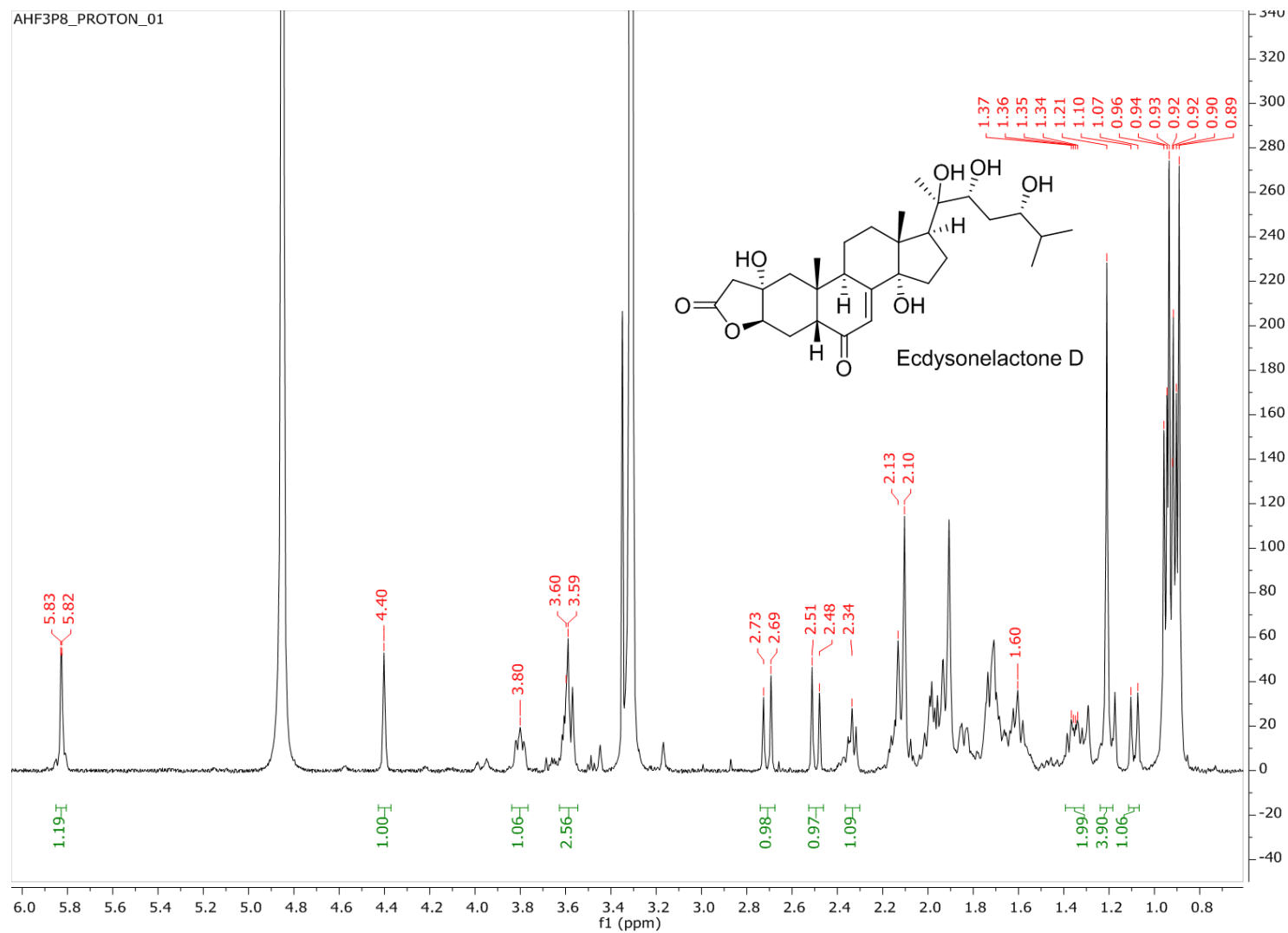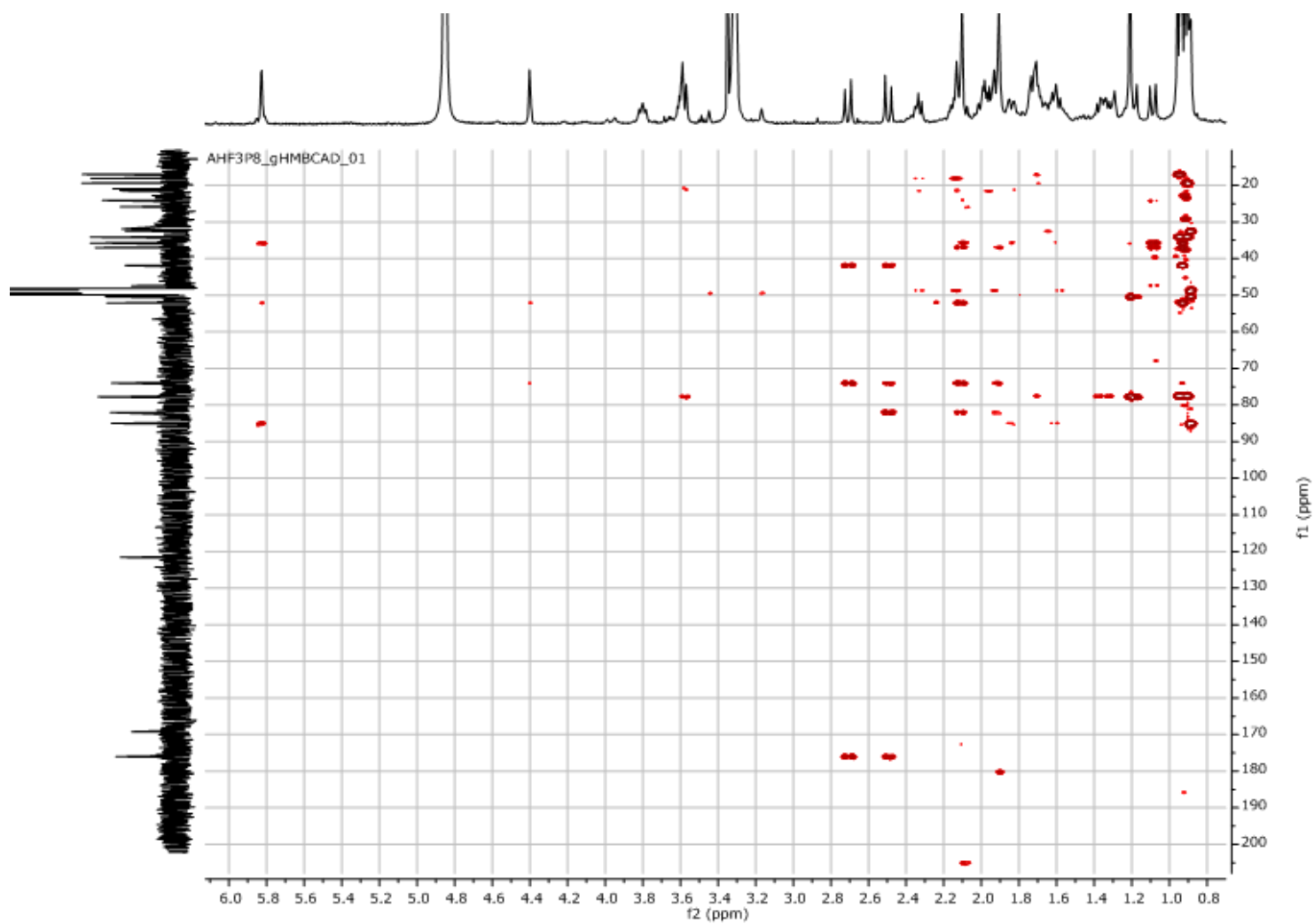**Figure S26**. HMBC NMR spectrum of **4** at 600 MHz in CD₃OD

Computational details.

The most stable conformer was generated using the MMFF94 force field (MarvinView (version 6.2.2), calculation module developed by ChemAxon) and the geometry described in Ohta *et al.*[11] as initial input. The ^{3J}H,H couplings were predicted using MSpin[12] for each diasteroisomers.
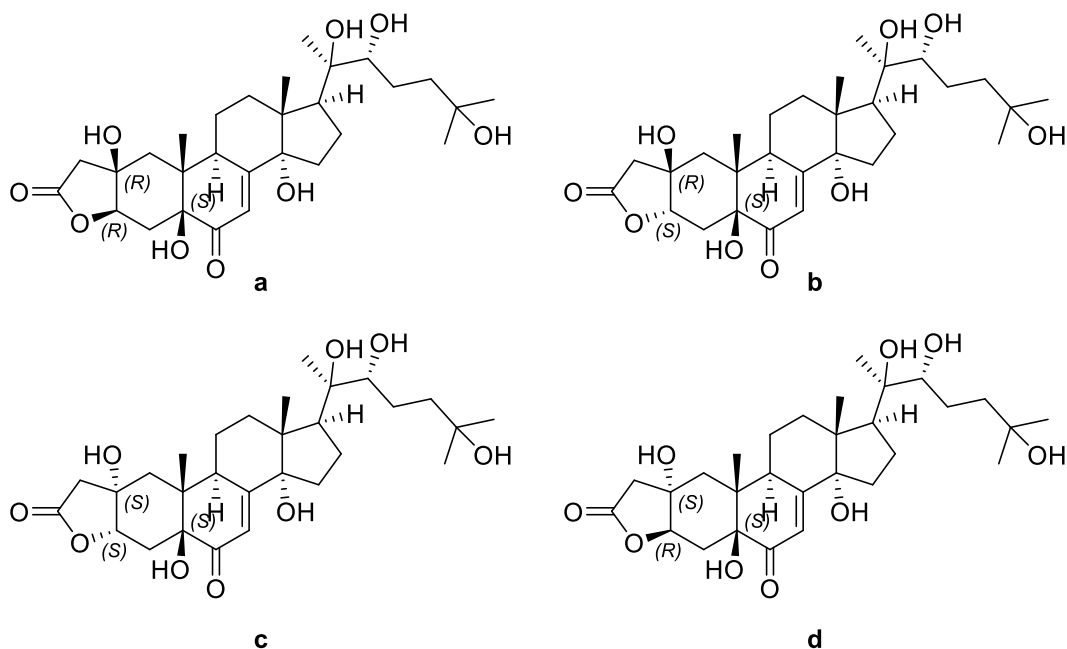
Cartesian coordinates of the most stable conformers of each diastereoisomer of 1.
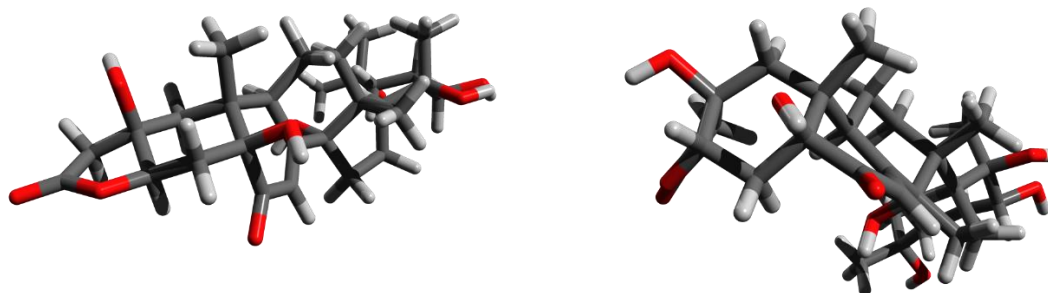
| C | -3.41240 | 2.21550 | 10.18410 | C | -1.54260 | 4.37680 | 10.00810 |
| C | -2.21870 | 2.55190 | 11.05650 | C | -2.35740 | 3.17150 | 9.55550 |

[11] Shinji Ohta, Jian-Ru Guo, Yoshikazu Hiraga, Takayuki Suga 24-Epi-pterosterone: A novel phytoecdyson from the roots of Athyrium yokoscense Phytochemistry 1996, 41(3), 745-747. DOI: 10.1016/0031-9422(95)00688-5
[12] A. Navarro-Vázquez MSpin-RDC. A program for the use of Residual Dipolar Couplings for Structure Elucidation of Small Molecules. Magn. Reson. Chem. 2012, 50, S73-S79. DOI: 10.1002/mrc.3905

C	-1.15700	3.32170	10.28750	C	-1.58570	2.12250	8.75870
C	-0.64380	2.45930	9.09710	C	-0.29340	1.72110	9.47640
C	-1.80120	1.97080	8.15020	C	0.66340	2.93200	9.66170
C	-2.96200	1.32250	9.02490	C	-0.09770	4.06100	10.43160
C	-4.34470	1.67220	11.24170	C	-1.70480	5.37730	8.87780
C	-4.01300	2.61690	12.38280	C	-2.98920	4.93990	8.24100
O	-2.79050	3.21590	12.17430	O	-3.38320	3.72330	8.71630
C	0.15910	1.26700	9.65720	C	0.40350	0.60020	8.69690
C	0.43640	0.11610	8.78300	C	1.25570	0.96580	7.54740
C	-0.18450	-0.04420	7.60790	C	1.58000	2.24790	7.31090
C	-1.30550	0.87060	7.10410	C	1.19770	3.40600	8.24940
C	0.21830	-1.12400	6.62570	C	2.25790	2.68510	6.03270
C	0.68260	-0.50930	5.26370	C	3.49570	3.59550	6.28620
C	-0.49260	0.30970	4.69670	C	3.00090	4.85110	7.03520
C	-0.96000	1.39820	5.68400	C	2.31070	4.48780	8.35930
C	1.34910	-2.11020	6.93600	C	2.79150	1.66450	5.02520
C	1.75150	-2.67580	5.56260	C	3.72790	2.48290	4.12050
C	1.03910	-1.81860	4.47470	C	3.96220	3.86080	4.81140
O	-4.70800	2.79690	13.36940	O	-3.60400	5.56970	7.39590
O	-4.03920	3.38880	9.65900	O	-2.16800	4.97850	11.16290
C	-2.37180	3.19370	7.37180	C	1.85360	2.50710	10.57610
C	1.91290	0.42350	5.42600	C	4.58180	2.87350	7.12400
O	-0.96500	-1.92300	6.43720	O	1.23860	3.43580	5.33980
C	1.82410	-1.77690	3.12760	C	5.36990	4.45420	4.50320
C	2.20740	-3.19790	2.57120	C	5.63570	4.64550	2.96460

C	1.12750	-4.04100	1.87140	C	5.07520	5.89780	2.26810
C	-0.02780	-4.49700	2.76460	C	3.54950	6.01060	2.23240
C	-0.88220	-5.64120	2.18420	C	3.01350	7.02980	1.20500
C	-1.96080	-6.03510	3.19930	C	1.48160	7.03310	1.23160
C	-1.52730	-5.26160	0.85050	C	3.54640	8.44210	1.45490
O	3.26430	-2.98290	1.59850	O	7.07800	4.69270	2.80390
C	1.09890	-0.95660	2.05330	C	5.65720	5.75270	5.26520
O	3.08450	-1.11390	3.35680	O	6.35980	3.50350	4.95130
O	0.65370	1.26100	10.78440	O	0.22760	-0.58510	8.97850
O	0.29060	3.24380	8.34400	O	-0.68510	1.20160	10.75500
H	0.08340	-2.30360	4.26120	H	3.22950	4.55290	4.38700
H	-2.17620	0.21650	6.94340	H	0.37000	3.89140	7.72710
O	-0.03550	-6.77310	1.97830	O	3.43080	6.60980	-0.09590
H	-1.76340	1.63570	11.45750	H	-2.85960	2.69980	10.40860
H	-0.33370	3.58900	10.96330	H	-1.39930	2.46950	7.73530
H	-1.53500	4.29160	9.94390	H	-2.23790	1.24600	8.63770
H	-2.62140	0.35830	9.42370	H	0.48820	4.98800	10.44450
H	-3.81980	1.10980	8.37380	H	-0.13820	3.76520	11.49150
H	-5.39930	1.77350	10.97180	H	-1.81730	6.40200	9.24570
H	-4.10650	0.64890	11.54460	H	-0.92260	5.34020	8.12310
H	1.21810	-0.54420	9.14030	H	1.52190	0.14430	6.89270
H	-1.34030	-0.34460	4.45760	H	2.30300	5.42670	6.41450
H	-0.21770	0.80480	3.76160	H	3.82870	5.52840	7.26230
H	-1.84660	1.86030	5.23390	H	1.88490	5.40700	8.77770
H	-0.19420	2.17940	5.74880	H	3.09290	4.17510	9.05670

H	1.03710	-2.92030	7.60430	H	2.00130	1.19710	4.42710
H	2.21850	-1.61990	7.38750	H	3.35980	0.86390	5.51200
H	1.44660	-3.72430	5.48170	H	3.26920	2.63450	3.13660
H	2.84240	-2.64570	5.46600	H	4.65640	1.92420	3.96150
H	-4.82120	3.12930	9.13940	H	-3.13730	4.93230	11.06670
H	-3.26780	2.91580	6.80630	H	1.50890	2.00870	11.48910
H	-1.64450	3.61720	6.67230	H	2.53790	1.81900	10.06950
H	-2.63250	4.03400	8.01630	H	2.43440	3.37390	10.90990
H	2.12600	0.95210	4.49040	H	5.38680	3.56070	7.40270
H	2.81820	-0.11930	5.71370	H	5.03470	2.03390	6.58770
H	1.76150	1.19150	6.19040	H	4.18500	2.46130	8.05660
H	-1.13830	-2.37790	7.27900	H	0.57680	2.80000	5.01710
H	2.67810	-3.78890	3.36400	H	5.32020	3.75000	2.41880
H	1.62650	-4.92280	1.44810	H	5.46250	5.89900	1.24050
H	0.74070	-3.49790	1.00100	H	5.50650	6.79680	2.72470
H	-0.68890	-3.64810	2.96080	H	3.18430	6.29440	3.22510
H	0.39230	-4.83320	3.71990	H	3.13910	5.02260	1.98860
H	-2.56100	-6.87420	2.82990	H	1.07780	7.71360	0.47310
H	-2.63280	-5.19870	3.41810	H	1.09610	7.33790	2.21010
H	-1.50710	-6.37090	4.13910	H	1.08500	6.03900	0.99530
H	-2.16850	-6.07190	0.48470	H	3.11330	9.15250	0.74110
H	-2.13690	-4.35690	0.94290	H	3.31180	8.78650	2.46720
H	-0.77260	-5.10010	0.07360	H	4.63040	8.49240	1.30770
H	3.61880	-3.86160	1.37030	H	7.25420	4.71620	1.84550
H	1.59620	-1.04880	1.08050	H	6.59890	6.20460	4.93250

H	0.05840	-1.27340	1.93240	H	4.86020	6.48960	5.13060
H	1.12560	0.11240	2.28030	H	5.79710	5.56980	6.33410
H	3.63160	-1.35440	2.57830	H	7.16700	3.73520	4.44230
H	0.96950	3.56850	8.96510	H	-0.73960	0.22670	10.65500
H	-0.58510	-7.49960	1.63570	H	3.07020	7.24000	-0.74420
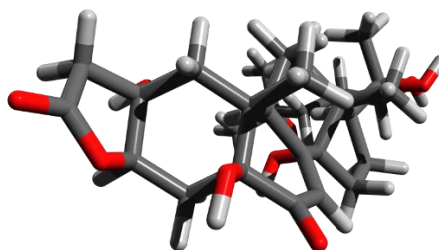
C	-1.38120	4.43350	9.71710	C	-4.56730	1.31610	8.76210
C	-2.27250	3.21250	9.63710	C	-3.92690	0.98320	10.13620
C	-1.65920	2.13380	8.75670	C	-2.38970	0.87690	10.12650
C	-0.32630	1.69500	9.40560	C	-1.71840	2.12990	9.49750
C	0.69060	2.87110	9.60470	C	-2.23680	2.32120	8.03280
C	-0.03430	4.07040	10.34130	C	-3.78880	2.49550	8.08420
C	-2.30150	5.37170	10.46760	C	-5.97290	1.81950	9.16990
C	-3.63350	4.96190	9.86880	C	-5.61110	2.40310	10.49280
O	-3.50960	3.75810	9.20220	O	-4.42050	1.97860	10.94870
C	0.29250	0.54190	8.61320	C	-0.20830	1.95740	9.43540
C	1.24150	0.84260	7.52600	C	0.37930	1.05080	8.43390
C	1.67260	2.09410	7.30190	C	-0.35400	0.59700	7.39410
C	1.29200	3.28960	8.19180	C	-1.79390	1.07740	7.13180
C	2.47020	2.45420	6.06830	C	0.16860	-0.49260	6.46270

C	3.72350	3.32270	6.38280	C	0.05720	-0.03710	4.97630
C	3.22250	4.62740	7.03600	C	-1.46470	0.21200	4.69830
C	2.42650	4.34910	8.32020	C	-2.02390	1.33210	5.60520
C	3.03650	1.36960	5.14850	C	1.62780	-0.94340	6.54910
C	4.07560	2.10860	4.28930	C	1.85930	-1.68760	5.21880
C	4.31570	3.50410	4.94120	C	0.69330	-1.27910	4.26010
O	-4.67090	5.59890	9.93680	O	-6.37530	3.06400	11.17680
O	-1.13560	5.01660	8.43110	O	-4.63470	0.21990	7.88580
C	1.83030	2.40550	10.56070	C	-1.63920	3.65300	7.47540
C	4.70830	2.59540	7.33330	C	0.88230	1.25560	4.66040
O	1.54740	3.21070	5.25670	O	-0.64200	-1.63350	6.67400
C	5.76740	4.02540	4.72120	C	1.11770	-1.26780	2.73740
C	6.15450	4.14410	3.20110	C	1.68060	-2.66270	2.24930
C	5.69810	5.38730	2.41720	C	0.69340	-3.83530	1.96910
C	4.18490	5.56380	2.27370	C	-0.15390	-4.35660	3.14280
C	3.76190	6.55610	1.17080	C	-0.88920	-5.69710	2.84680
C	2.23290	6.62900	1.10400	C	-1.67340	-6.13660	4.10000
C	4.34550	7.95360	1.38860	C	-1.88500	-5.54370	1.68240
O	7.60550	4.12990	3.14770	O	2.37450	-2.44780	1.04150
C	6.05520	5.34060	5.45370	C	-0.05320	-0.84170	1.82110
O	6.67880	3.05340	5.27820	O	2.16580	-0.32630	2.62630
O	-0.01710	-0.62870	8.84160	O	0.52130	2.54310	10.22130
O	-0.68180	1.15530	10.69770	O	-2.03740	3.26330	10.28050
H	3.64920	4.20600	4.43330	H	-0.07780	-2.04390	4.39860
H	0.50680	3.77790	7.60970	H	-2.38520	0.18090	7.37590

O	4.23480	6.05570	-0.08190	O	0.03620	-6.70070	2.50080
H	-2.46080	2.78670	10.63360	H	-4.34400	0.02550	10.52550
H	-1.52770	2.47950	7.72540	H	-2.02940	0.72550	11.16740
H	-2.35890	1.29000	8.69830	H	-2.10850	-0.03770	9.56630
H	0.61890	4.94940	10.35960	H	-4.21230	2.68630	7.07480
H	-0.20050	3.79150	11.39080	H	-3.97740	3.42300	8.67050
H	-2.32240	5.18430	11.54480	H	-6.38910	2.53250	8.42540
H	-2.10220	6.42330	10.24580	H	-6.69440	0.99780	9.36950
H	1.49730	-0.00210	6.89700	H	1.40150	0.72150	8.58210
H	2.59270	5.19670	6.34130	H	-2.04760	-0.71520	4.88690
H	4.05620	5.28710	7.29250	H	-1.65860	0.49980	3.65110
H	1.99770	5.29960	8.65880	H	-3.10780	1.46090	5.40270
H	3.14920	4.05820	9.08660	H	-1.52870	2.25980	5.27650
H	2.27500	0.91040	4.50830	H	1.91810	-1.52070	7.45280
H	3.52930	0.56880	5.71150	H	2.26500	-0.03550	6.54970
H	3.70200	2.23610	3.26670	H	1.82390	-2.79090	5.35190
H	4.98790	1.50610	4.22690	H	2.87220	-1.40760	4.85610
H	-1.95530	4.99170	7.90120	H	-5.10830	-0.51490	8.35550
H	1.43550	1.97430	11.48710	H	-1.87320	4.51000	8.14170
H	2.47310	1.65090	10.09710	H	-0.53590	3.59730	7.36620
H	2.46280	3.24180	10.87510	H	-2.07670	3.92560	6.49440
H	5.51760	3.26150	7.64830	H	0.70590	1.57710	3.61410
H	5.16630	1.71690	6.86850	H	1.97500	1.11600	4.76680
H	4.22220	2.23920	8.24640	H	0.61880	2.10300	5.32200
H	0.82370	2.61180	5.00620	H	-0.49250	-1.94520	7.60600

H	5.84440	3.23930	2.66760	H	2.41790	-3.00300	3.01210
H	6.15180	5.32730	1.41920	H	1.33020	-4.67970	1.62570
H	6.13870	6.28610	2.86540	H	0.02810	-3.55790	1.12590
H	3.76980	5.90870	3.22660	H	-0.93170	-3.61330	3.39590
H	3.74650	4.58410	2.04520	H	0.51970	-4.51540	4.01320
H	1.90620	7.28520	0.28910	H	-0.98620	-6.27720	4.96180
H	1.80600	7.00210	2.04070	H	-2.43100	-5.37260	4.37950
H	1.80420	5.64210	0.89520	H	-2.19470	-7.10030	3.91440
H	3.98840	8.64800	0.61920	H	-1.36470	-5.28600	0.73750
H	4.06960	8.35590	2.36860	H	-2.63520	-4.75470	1.90570
H	5.43730	7.94850	1.30450	H	-2.42170	-6.50100	1.50710
H	7.85260	4.10930	2.20520	H	3.15440	-3.06300	1.02590
H	7.04060	5.73590	5.18040	H	0.24910	-0.88640	0.75300
H	5.30720	6.10630	5.22850	H	-0.93460	-1.50120	1.96420
H	6.10200	5.19580	6.53650	H	-0.34170	0.20720	2.00710
H	7.53070	3.23250	4.82430	H	2.28540	-0.06930	1.67450
H	-0.85820	0.19960	10.55720	H	-1.75760	3.08790	11.21760
H	3.94260	6.66900	-0.77870	H	0.67030	-6.80870	3.25770

*Predicted couplings for each diastereoisomers of **1**.*

Appendix F: Supplementary Information Paper IV

Halogenated tyrosine derivatives from the Tropical Eastern Pacific
Zoantharians *Antipathozoanthus hickmani* and *Parazoanthus darwini*.

Supplementary Information for

Halogenated tyrosine derivatives from the Tropical Eastern Pacific Zoantharians *Antipathozoanthus hickmani* and *Parazoanthus darwini*.

Paul O. Guillen, [†,‡] Karla B. Jaramillo, [†,§] Laurence Jennings, [‡] Grégory Genta-Jouve, [⊥,‖] Mercedes de la Cruz, [∇] Bastien Cautain, [∇] Fernando Reyes, [∇] Jenny Rodríguez, [†] Olivier P. Thomas [,‡]*

Biological material.

Antipathozanthus hickmani is already described in a previous article by Guillen et al. *Mar. Drugs* **2018**, *16*(2), 58. We worked on the same sample and therefore have the same voucher.

Parazoanthus darwini (J. Reimer & Fujii, 2010 is a zoantharian that belongs to the suborder Macrocnemina of the family of Parazoanthidae (Cnidaria, Anthozoa, Hexacorallia, Zoantharia, Macrocnemina). It was described as a new species by (J. Reimer & Fujii, 2010) at the Galapagos Islands in the Tropical Eastern Pacific ecoregion and also it was reported in the Equatorial Front at the Marine Protected Area El Pelado (MPA) (known in Spanish as REMAPE) at the southeast mainland off Ecuador (Jaramillo et al., 2018). The colony sampled had around 200 small polyps, and it was covering a big area on a rocky substrate in the dive spot named "La Pared" at the MPA El Pelado in Ecuador.

Terrazoanthus **cf.** *patagonichus* (Carlgren, 1899) is a Macrocnemic zoantharian of the family Hydrozoanthidae (Cnidaria, Anthozoa, Hexacorallia, Zoantharia). This species has been reported in different sites from the Easter Pacific, including cold and warm ocean currents as Chile (Carlgren, 1899) and in the Tropical Eastern Pacific (TEP) (J. Reimer & Fujii, 2010) (Bo et al., 2012) (Jaramillo et al., 2018). The colony collected had approximately 68 small polyps, and it was found close to another red colony of *T. patagonichus* of widely spread on a rocky substrate in the dive spot called "Acuario" at the MPA El Pelado in Ecuador.

Sampling. Specimens collection was performed by SCUBA diving in two different sites at the MPA El Pelado, East coast of mainland Ecuador, Santa Elena province. The first colony of *P. darwini* was collected in August 2015 at 25 m of depth from a rocky substrate in the dive spot named "La Pared" 1°55'58.24''S/ 80°47'32.83''W, site type: vertical cliff of 31 m of depth, collected by O. P. Thomas. (Figure S1. a-b). The second colony of *T.* **cf.** *patagonichus* was sampled in April 2017 at 12m of depth from rocky substrate in the dive spot "Acuario" 1°56'10.20''S/ 80°47'20.12''W, site type: a mixed habitat formed by sandy areas and large rocks covered by high diversity of octocorals, collected by K. B. Jaramillo (Figure S2. a-b). The specimens were divided partly in 4% formaldehyde and 95% ethanol for systematic analyses and the remaining material was kept in a -80 °C freezer for chemical analyses. The voucher samples are kept at the National Center of Aquaculture and Marine Research (CENAIM) under the numbers 150820EP01-05 (*P.darwini*) and 170416EP02-01 (*T.cf. patagonichus*).

Morphological characterization. The morphological features were examined from the formalin samples, *in situ* remarks and pictures to assess the polyp's external measurements (height, width, and oral disk diameter), number of mesenteries, number of tentacles, type of sphincter, colours (tentacles, oral disk, column and coenenchyme), sand encrustations and related/substrate type. Additional *in situ* pictures were obtain with digital camera Canon G16 model to corroborate the identification of this reported species.

DNA extraction and sequencing. DNA were obtained from ethanol 95% fixed samples following the Guanidine extraction protocol as described in (Frederic Sinniger, Reimer, & Pawlowski, 2010). Two molecular markers were therefore amplified to confirm the species identification, the mitochondrial 16S-rRNA and the nuclear internal transcribed spacer region (ITS-2 rDNA), primers and PCR amplification protocols are described in (Frédéric Sinniger, Montoya-Burgos, Chevaldonné, & Pawlowski, 2005) (J. D. Reimer, Sinniger, Fujiwara, Hirano, & Maruyama, 2007) (J. Reimer & Fujii, 2010). The amplified DNA products were sent to the sequencing company (MacroGen Inc, Korea). The **P. darwini** sequences acquired were placed in GenBank (NCBI), with the accessions numbers MH003894 (16SrRNA) and MH029324 (ITS-2 rDNA). Unfortunately, the sample of **T. cf. patagonichus**, has not been sequenced yet because it was found later in another expedition. The respective molecular analyses will be performed soon, and it will be included in our next integrative taxonomy research with more zoantharian species from the Pacific. (Jaramillo et al. in prep).

Phylogenetic analysis. The chromatograms acquired from sequences results were checked for quality using BioEdit software version 7.2.5.0. (Hall, 1999) or Geneious 10.2.2. (Kearse et al., 2012) and trimmed appropriately. The *P. darwini* sequences obtained in our previous study (Jaramillo et al., 2018) were compare by BLAST with public data available from the original sequences of *P. darwini* and other zoantharians using the National Centre for Biotechnology Information's Basic Local Alignment Search Tool (NCBI BLAST). A Bayesian tree were obtained with Mr. Bayes 3.1.2 implemented in Geneious. Bayesian analyses were performed on the complete alignments, with gaps treated as missing data. The Bayesian tree were made with other zoantharian sequences from Ecuador and data available in NCBI.

*Morphological data***. P. darwini:** Zoantharian colony covers some cm² on rocky substrates in small or large areas and some of them near small caves. Alive/contracted polyps measured 3.0-6.0 / 1.0-3.0mm diameter and 2- 4 mm height (measured starting from the coenenchyme).

Number of tentacles and mesenteries number approximately 24-28. Colours of the tentacles were orange or cream, while the oral disk were pale orange and the column-coenenchyme were light pink or cream. *P. darwini* presented a Cteniform endodermal type of sphincter muscle[*]. A heavily number of mineral particles incrusted was visualized on the polyp's column and coenenchyme.

* *According to* (Swain, Schellinger, Strimaitis, & Reuter, 2015).
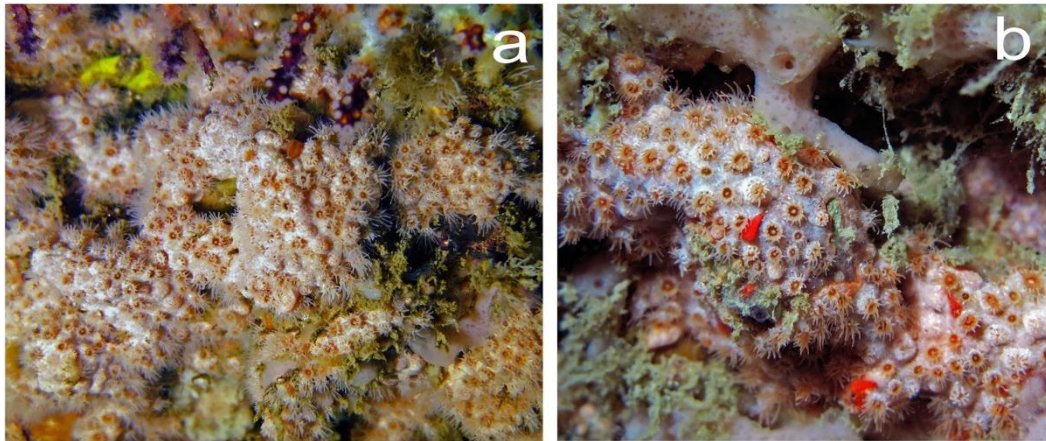
Figure S1. *In situ* pictures of *P. darwini* at the MPA El Pelado, August 20, 2015. a) Large colony *of P. darwini* over the rocky substrate; b)*. A closer view of the polyps of *P. darwini*.

Terrazoanthus* cf. *patagonichus. Zoantharian colony covering rocky substrates in areas exposed with strong currents. Alive/contracted polyps measured 4.0-12.0 / 2.0-4.0mm diameter and 5- 10 mm height (measured starting from the coenenchyme). Number of tentacles and mesenteries approximately 32-40 at the oral disc. Pale brown/purple color at the coenenchyme and contracted polyps, while the open oral disk and tentacles has a red/brown dark color. Polyp's column and coenenchyme is heavily incrusted by mineral particles. Few small colonies were found covering rocky substrates and only in one dive spot "Acuario" of the whole study area.

Molecular phylogeny. The results of molecular data are available in our recent study published (Jaramillo et al., 2018).
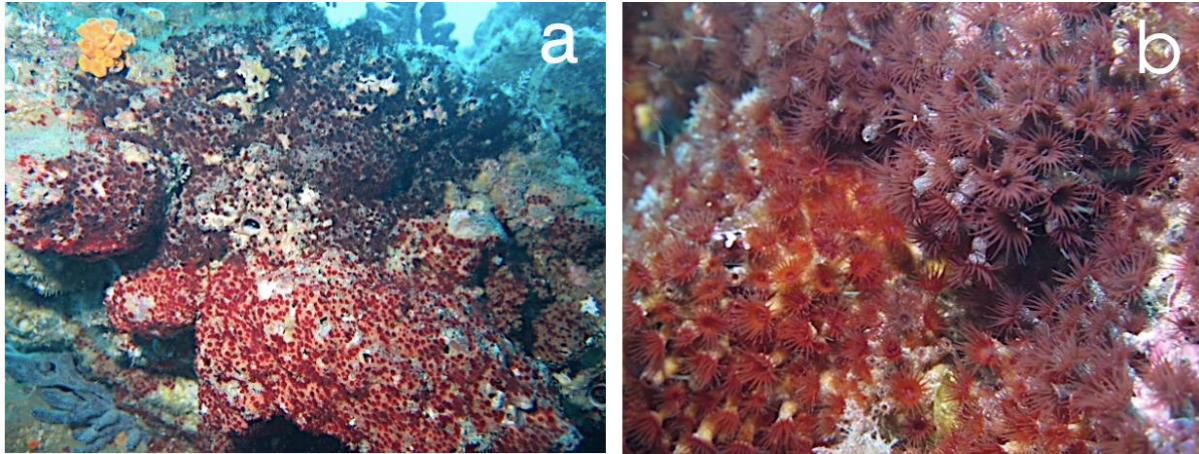
Figure S2. *In situ* pictures of *T.*cf. *patagonichus* at the MPA El Pelado, April 16, 2017. a) Large colony *of T.*cf. *patagonichus* close to the red zoantharian colony of *T. patagonichus* covering some rocks; b). A closer view of the polyps of *T.*cf. *patagonichus* (brown) and *T. patagonichus* (red).

References

Bo, M., Lavorato, A., Di Camillo, C. G., Poliseno, A., Baquero, A., Bavestrello, G., et al. (2012) Black coral assemblages from Machalilla National Park (Ecuador). Pacific Science, 66, 63-81.

Carlgren, O. (1899) Zoantharien.

Hall, T. (1999) BioEdit software, version 5.0. 9. North Carolina State University, Raleigh, NC.

Jaramillo, K. B., Reverter, M., Guillen, P. O., McCormack, G., Rodriguez, J., Sinniger, F., et al. (2018) Assessing the Zoantharian Diversity of the Tropical Eastern Pacific through an Integrative Approach. Scientific Reports, 8, 7138.

Kearse, M., Moir, R., Wilson, A., Stones-Havas, S., Cheung, M., Sturrock, S., et al. (2012) Geneious Basic: an integrated and extendable desktop software platform for the organization and analysis of sequence data. Bioinformatics, 28, 1647-1649.

Reimer, J. & Fujii, T. (2010) Four new species and one new genus of zoanthids (Cnidaria, Hexacorallia) from the Galápagos Islands. Zookeys, 42, 1.

Reimer, J. D., Sinniger, F., Fujiwara, Y., Hirano, S. & Maruyama, T. (2007) Morphological and molecular characterization of Abyssoanthus nankaiensis,, a new family, new genus and new

species of deep-sea zoanthid (Anthozoa : Hexacorallia : Zoantharia) from a north-west Pacific methane cold seep. Invertebr. Syst., 21, 255-262.

Sinniger, F., Montoya-Burgos, J.-I., Chevaldonné, P. & Pawlowski, J. (2005) Phylogeny of the order Zoantharia (Anthozoa, Hexacorallia) based on the mitochondrial ribosomal genes. Marine Biology, 147, 1121-1128.

Sinniger, F., Reimer, J. D. & Pawlowski, J. (2010) The Parazoanthidae (Hexacorallia: Zoantharia) DNA taxonomy: description of two new genera. Marine Biodiversity, 40, 57-70.

Swain, T. D., Schellinger, J. L., Strimaitis, A. M. & Reuter, K. E. (2015) Evolution of anthozoan polyp retraction mechanisms: convergent functional morphology and evolutionary allometry of the marginal musculature in order Zoanthidea (Cnidaria: Anthozoa: Hexacorallia). BMC Evolutionary Biology, 15, 123.
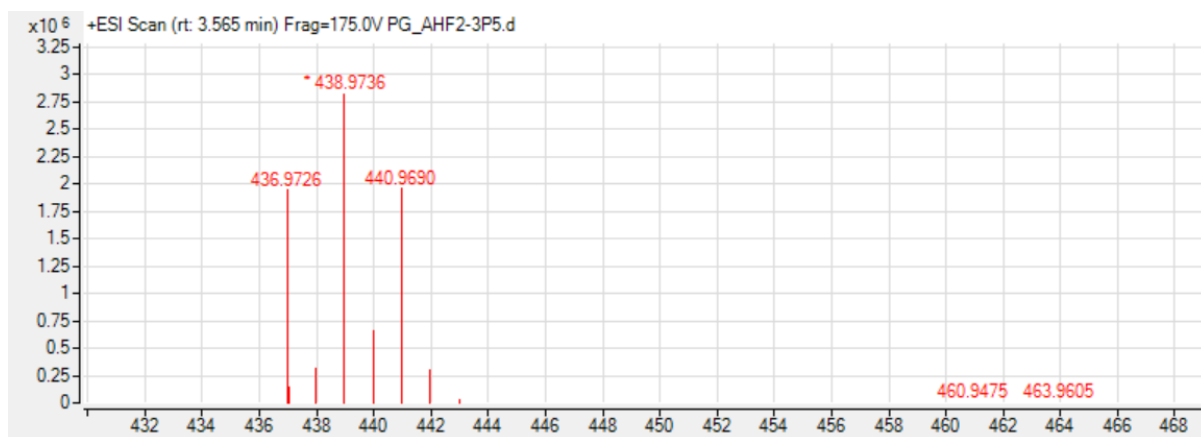
Figure S3. (+)-HRESIMS analysis of **1**.
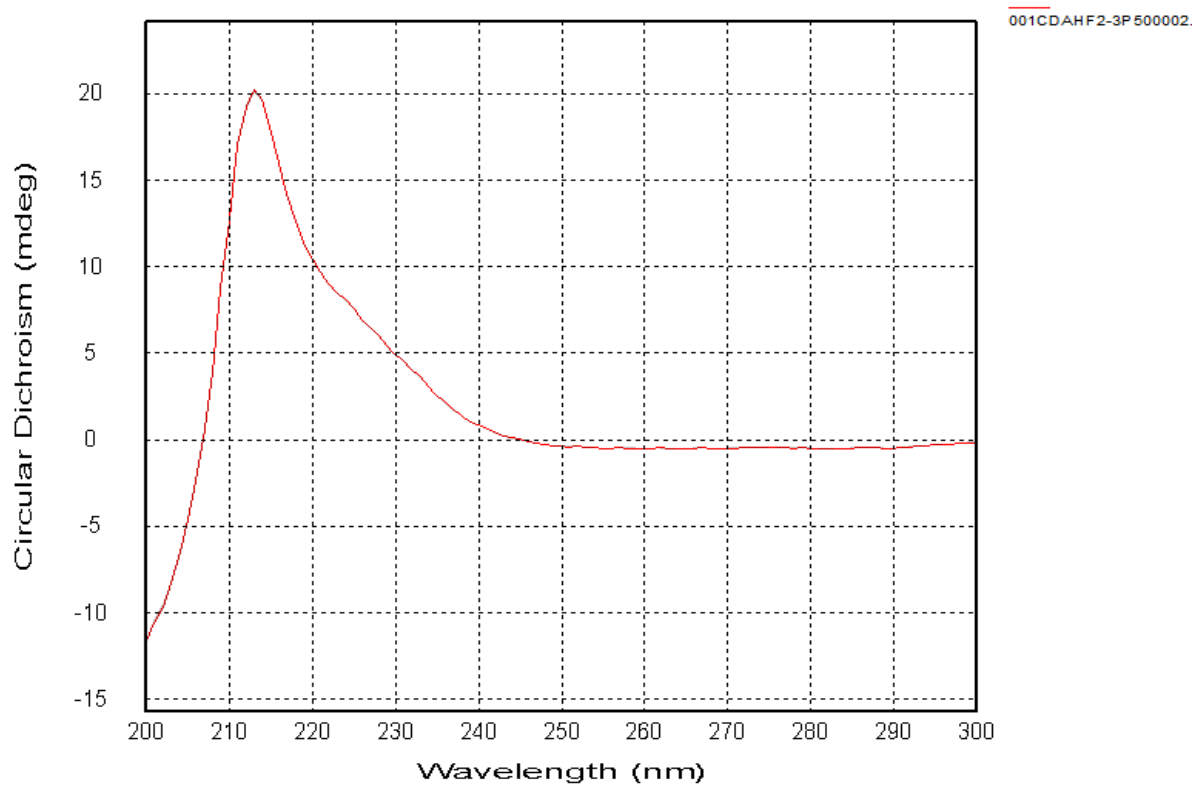
Figure S4. ECD spectrum of **1**.
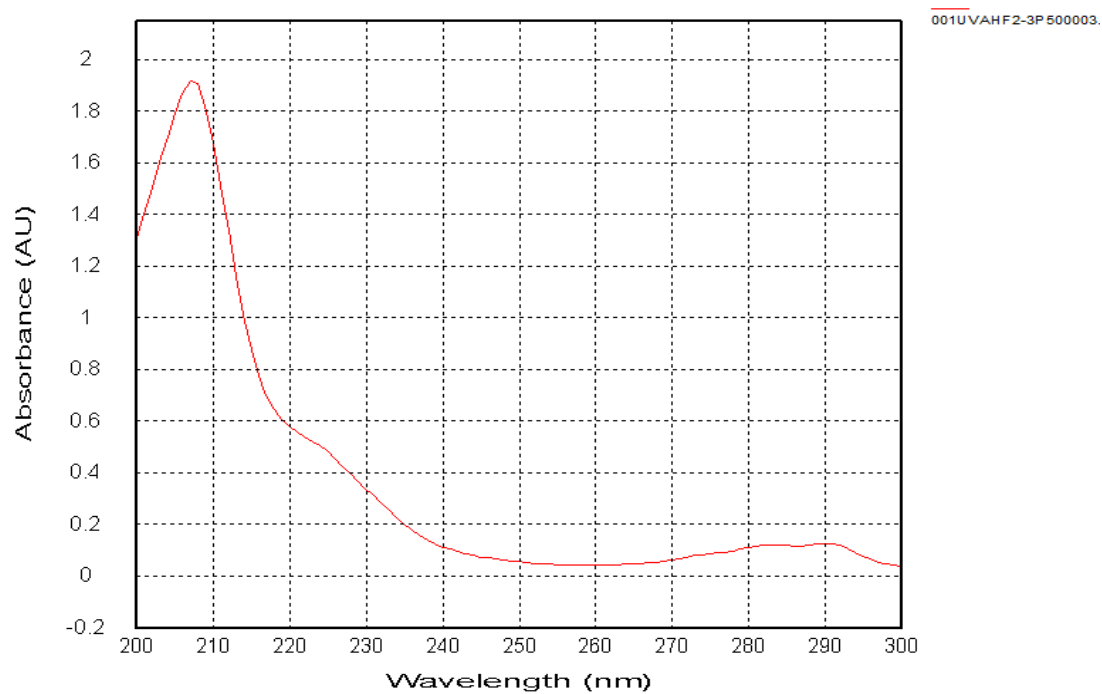
Figure S5. UV spectrum of **1**.
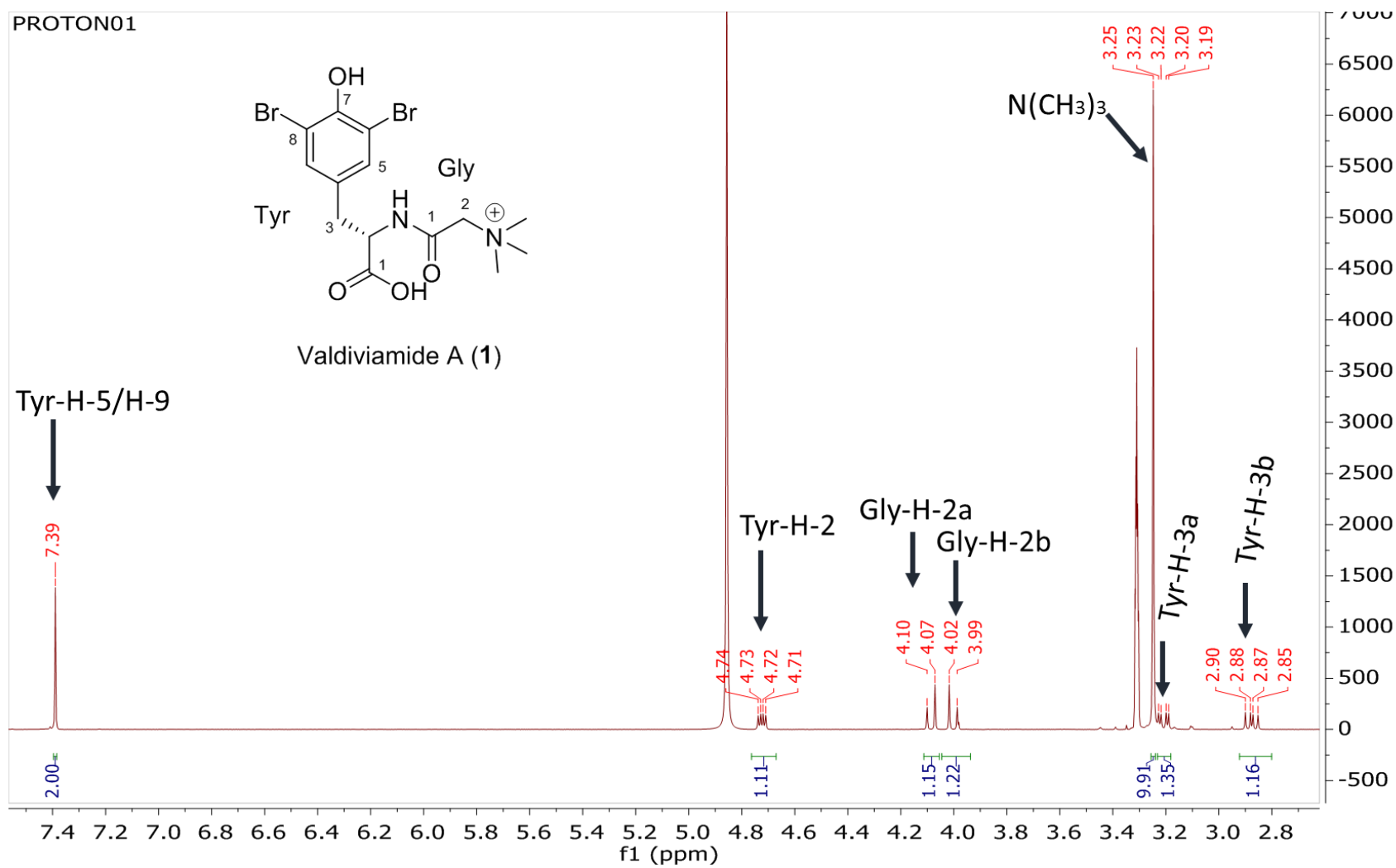
Figure S6 ¹H NMR spectrum of **1** at 500 MHz in CD₃OD

Figure S7. COSY NMR spectrum of **1** at 500 MHz in CD₃OD
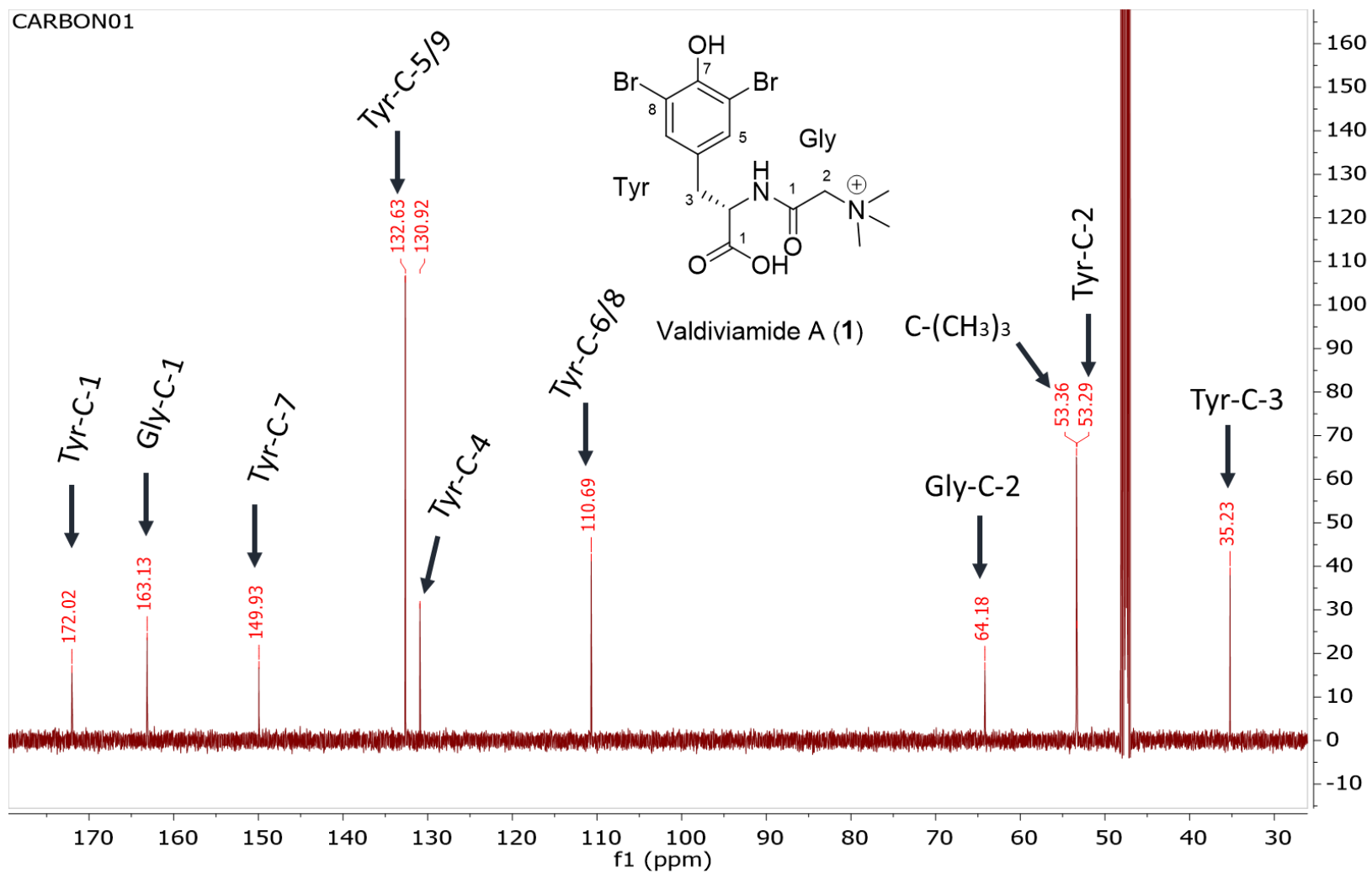
Figure S8. ^{13}C NMR spectrum of **1** at 125 MHz in CD$_3$OD
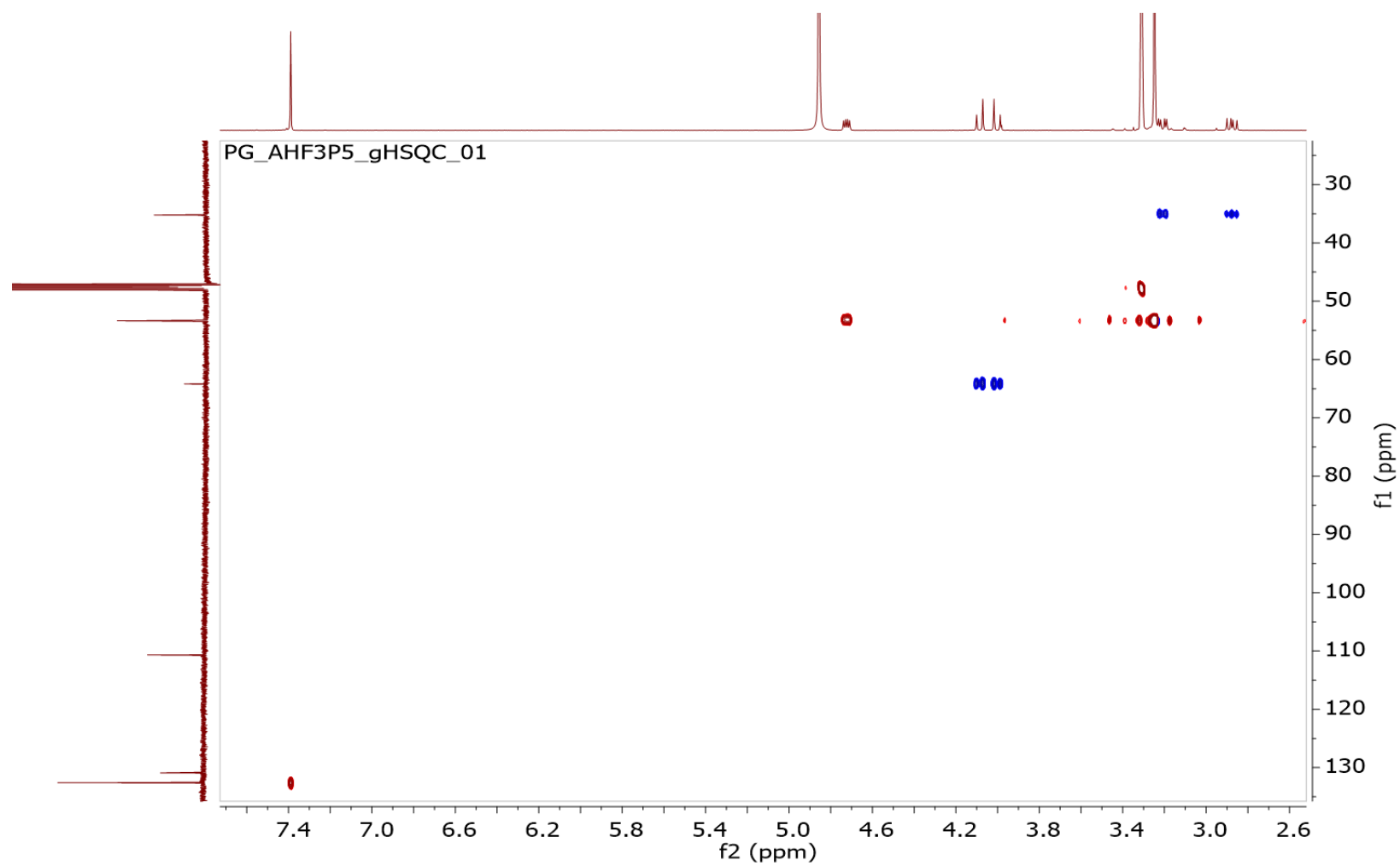
Figure S9. HSQC NMR spectrum of **1** at 500MHz in CD₃OD

PG_AHF3P5_gHMBCAD_01
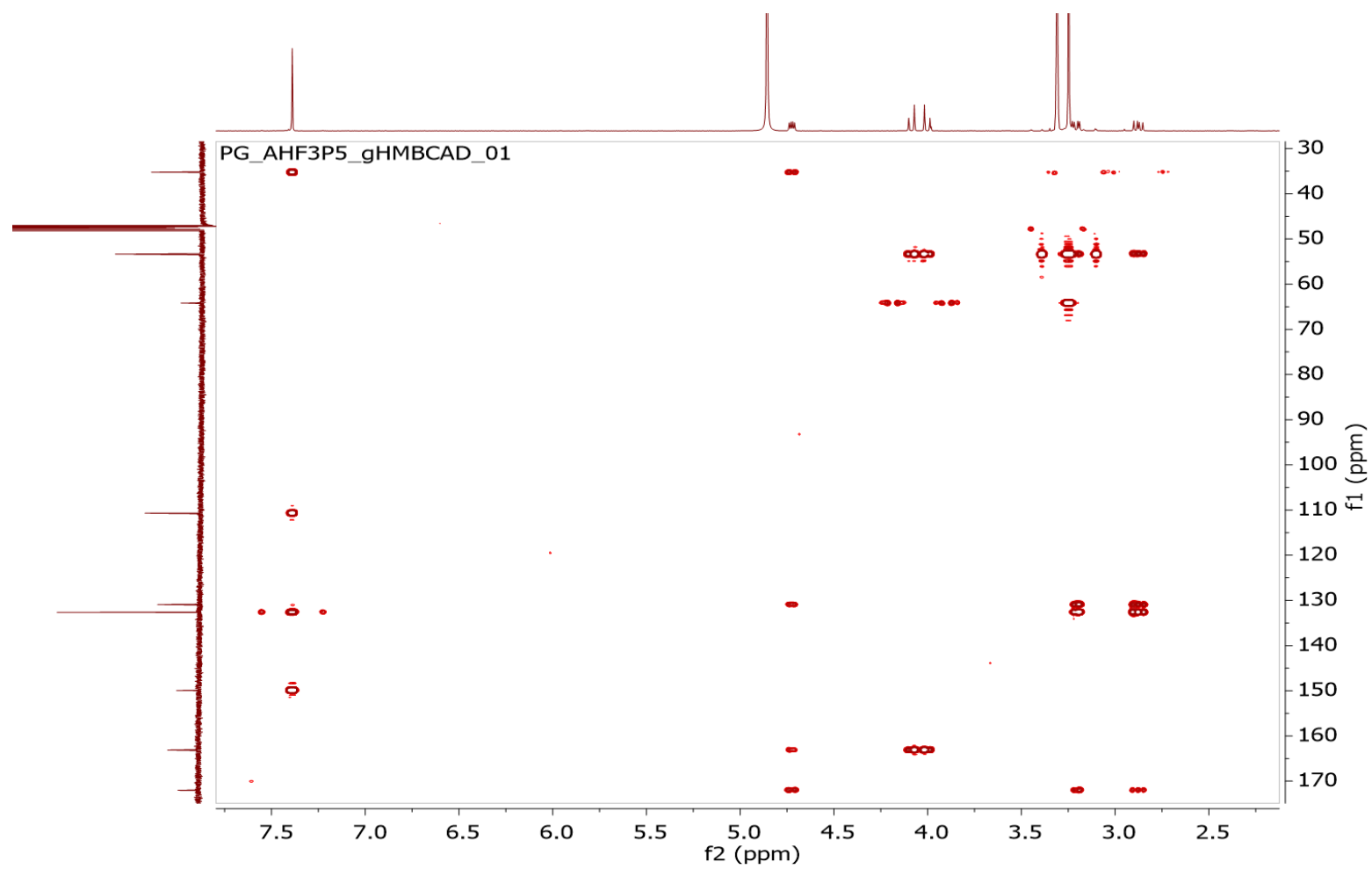
Figure S10. HMBC NMR spectrum of **1** at 500MHz in CD₃OD
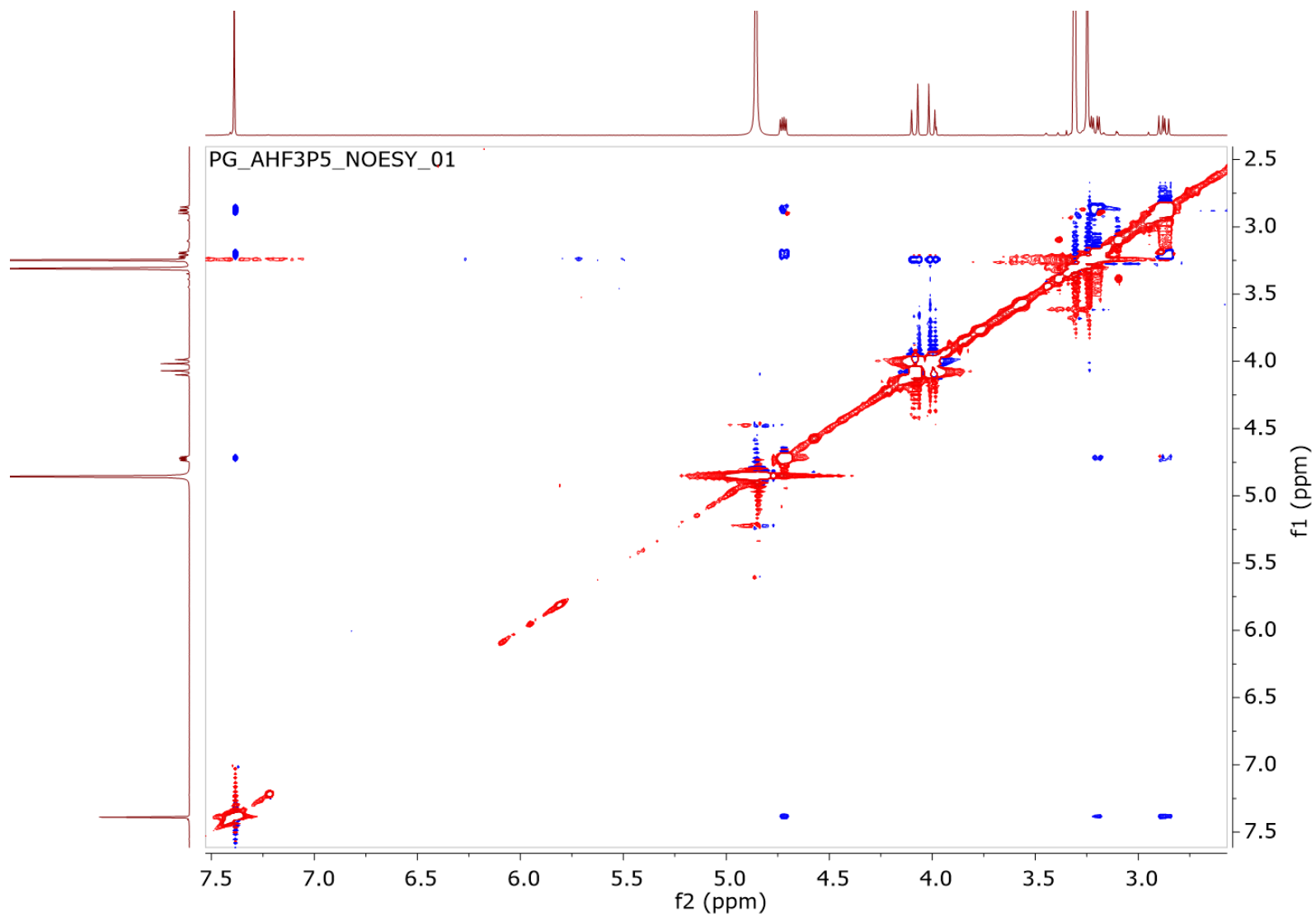
Figure S11. NOESY NMR spectrum of **1** at 500 MHz in CD₃OD
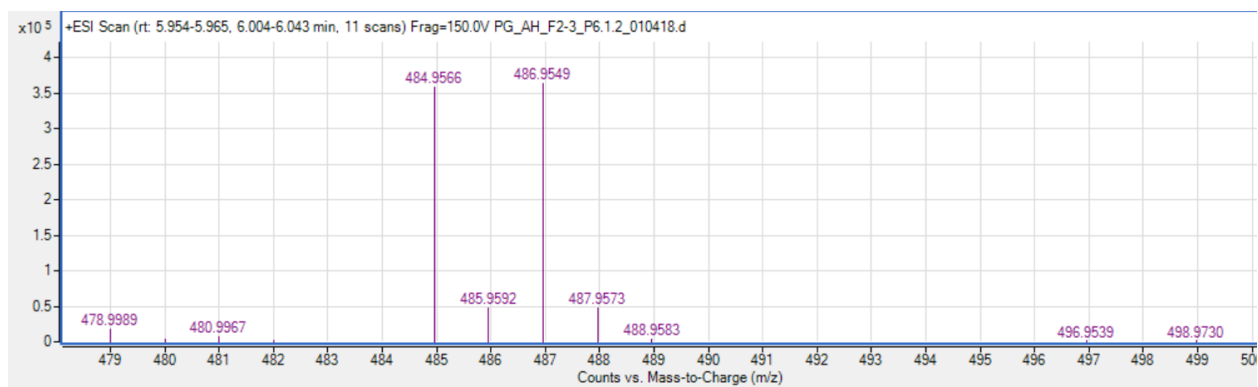
Figure S12. (+)-HRESIMS analysis of **2** in (+)-ESI

001CDAHF23P61200009
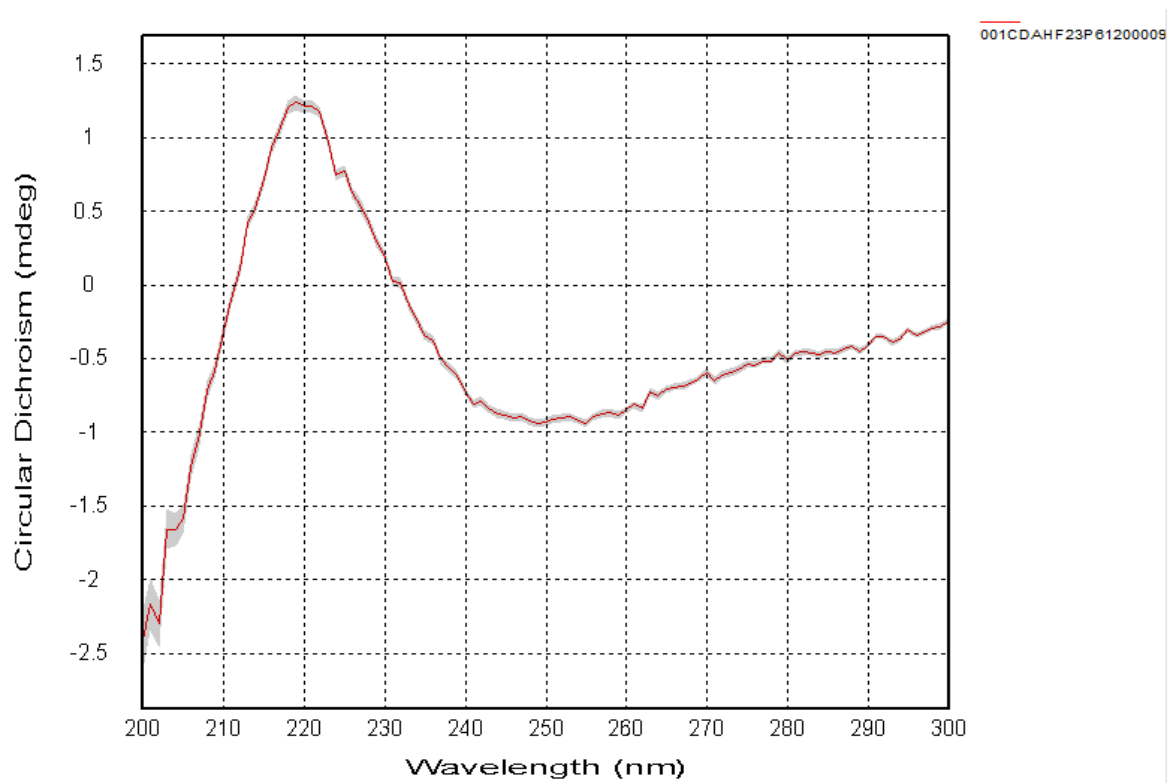
Figure S13. ECD spectrum of **2**

001UVAHF23P61200008
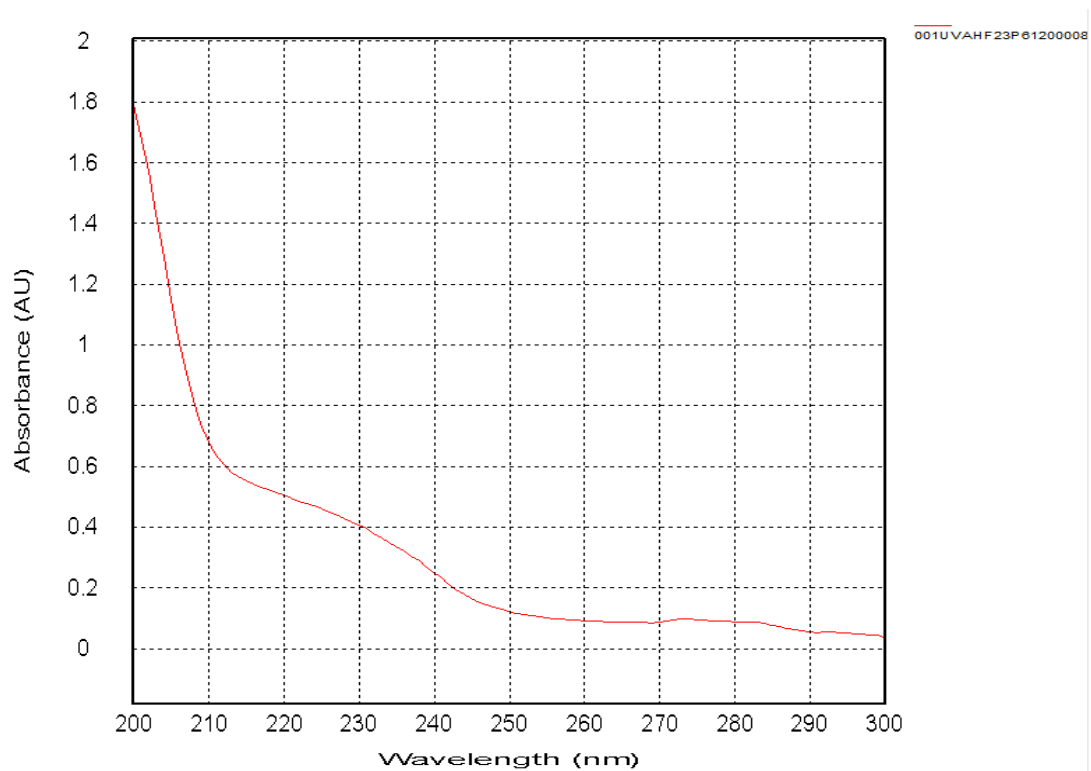
Figure S14. UV spectrum of **2**
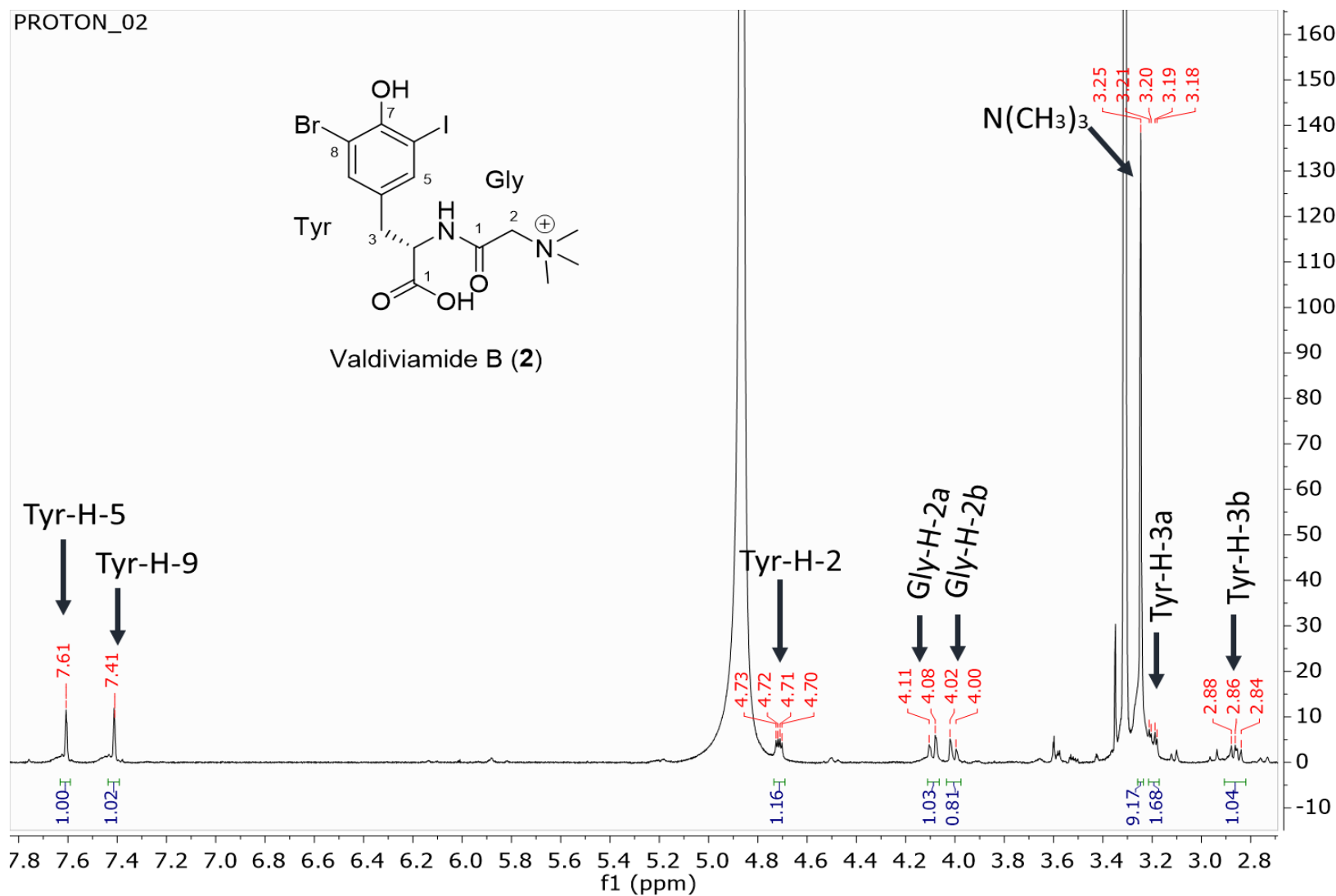
Figure S15. ^{1}H NMR spectrum of **2** at 500 MHz in CD$_3$OD
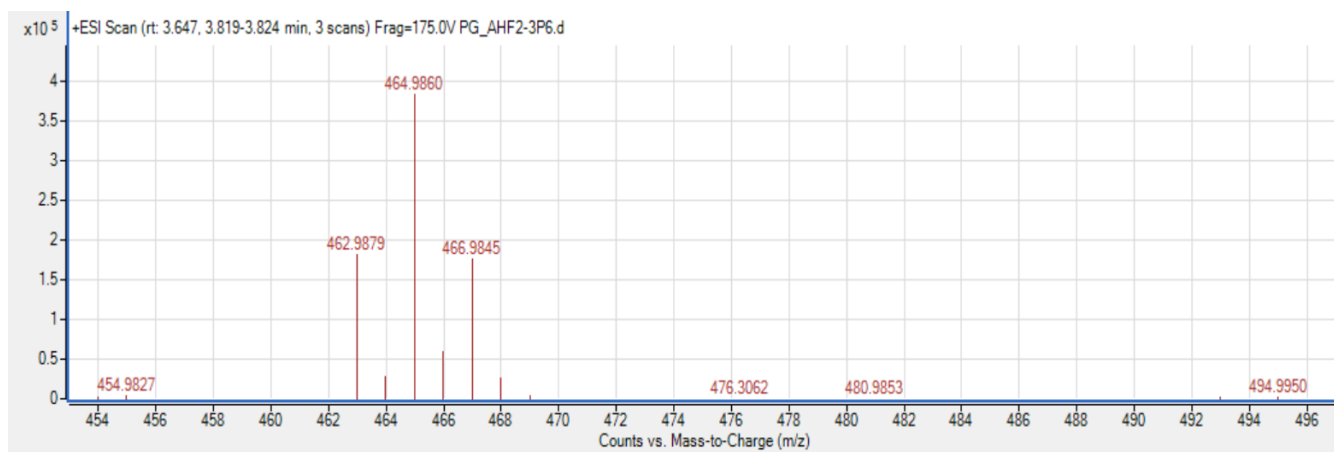
Figure S16. (+)-HRESIMS analysis of **3** in (+)-ESI
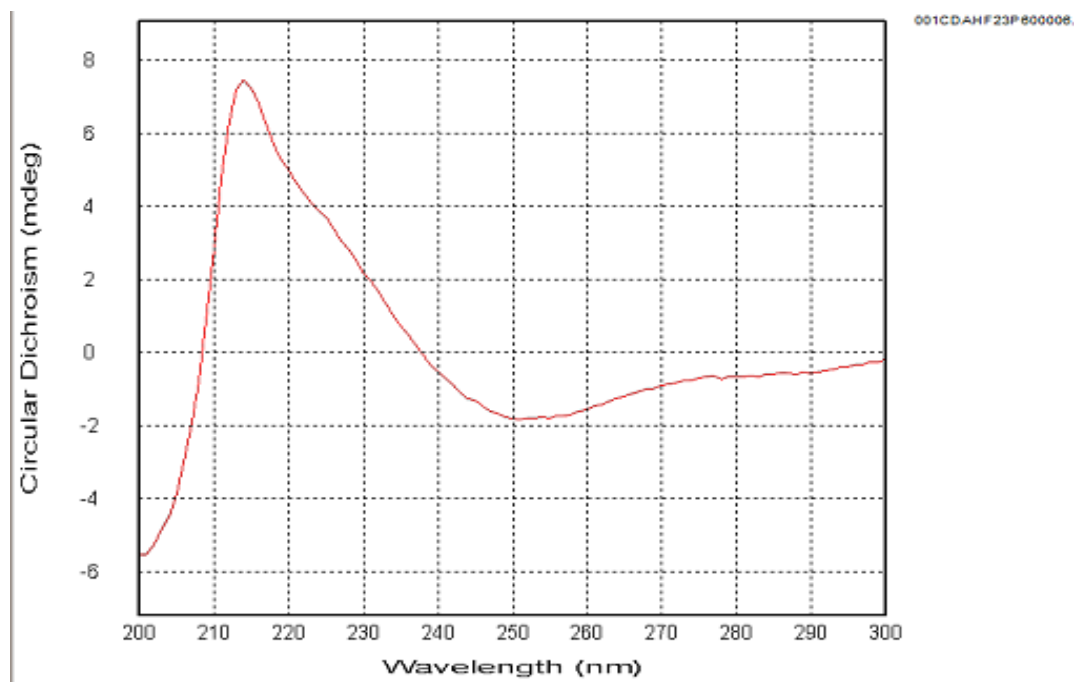
Figure S17. ECD spectrum of **3**.
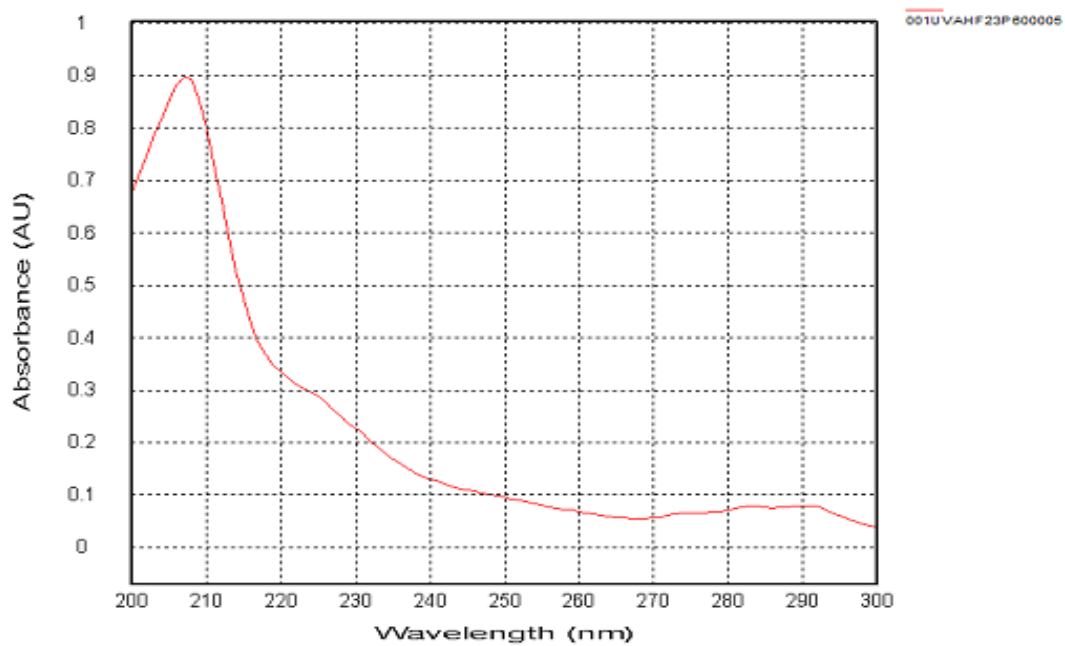
Figure S18. UV spectrum of **3**.
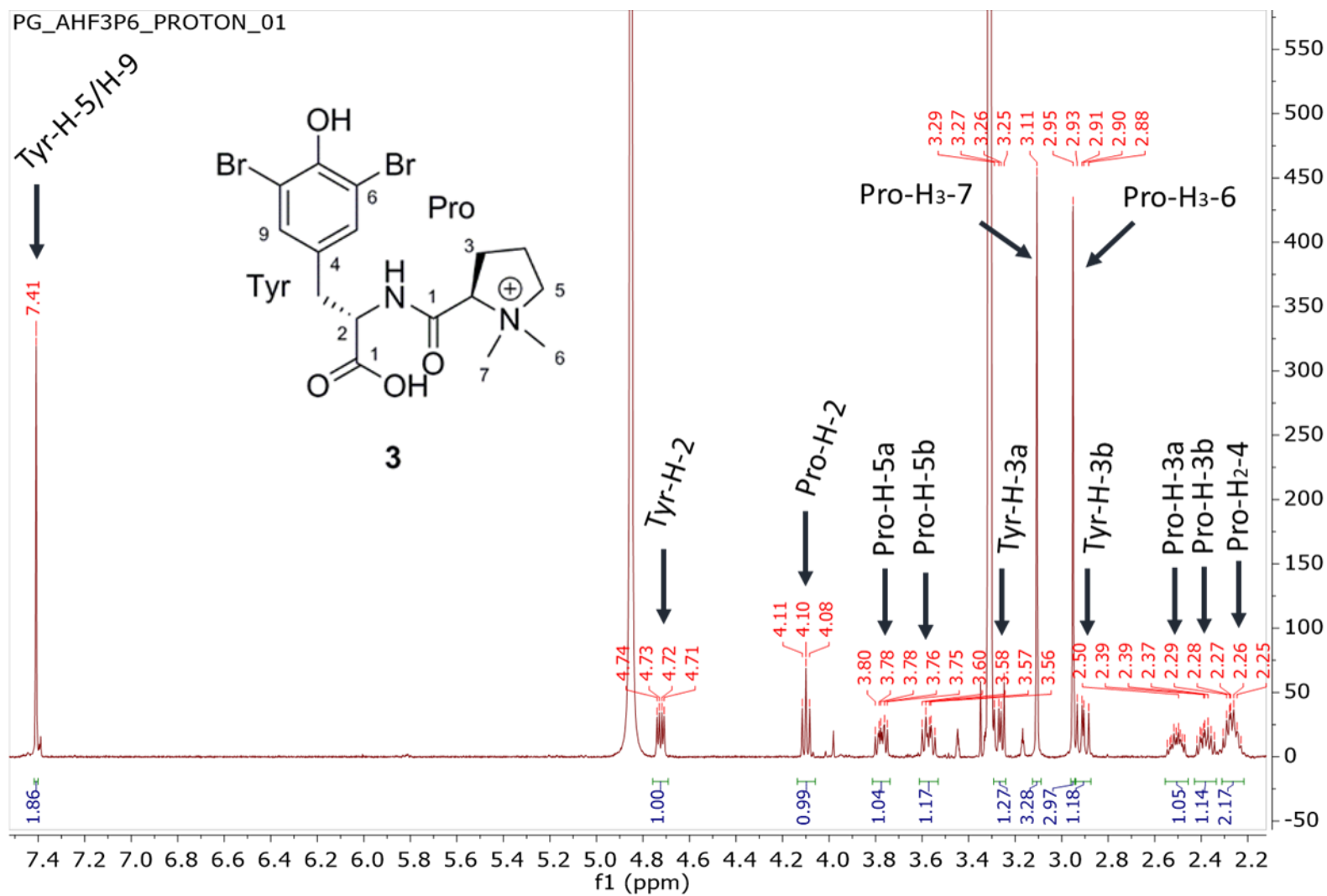
Figure S19. ¹H NMR spectrum of **3** at 500 MHz in CD₃OD
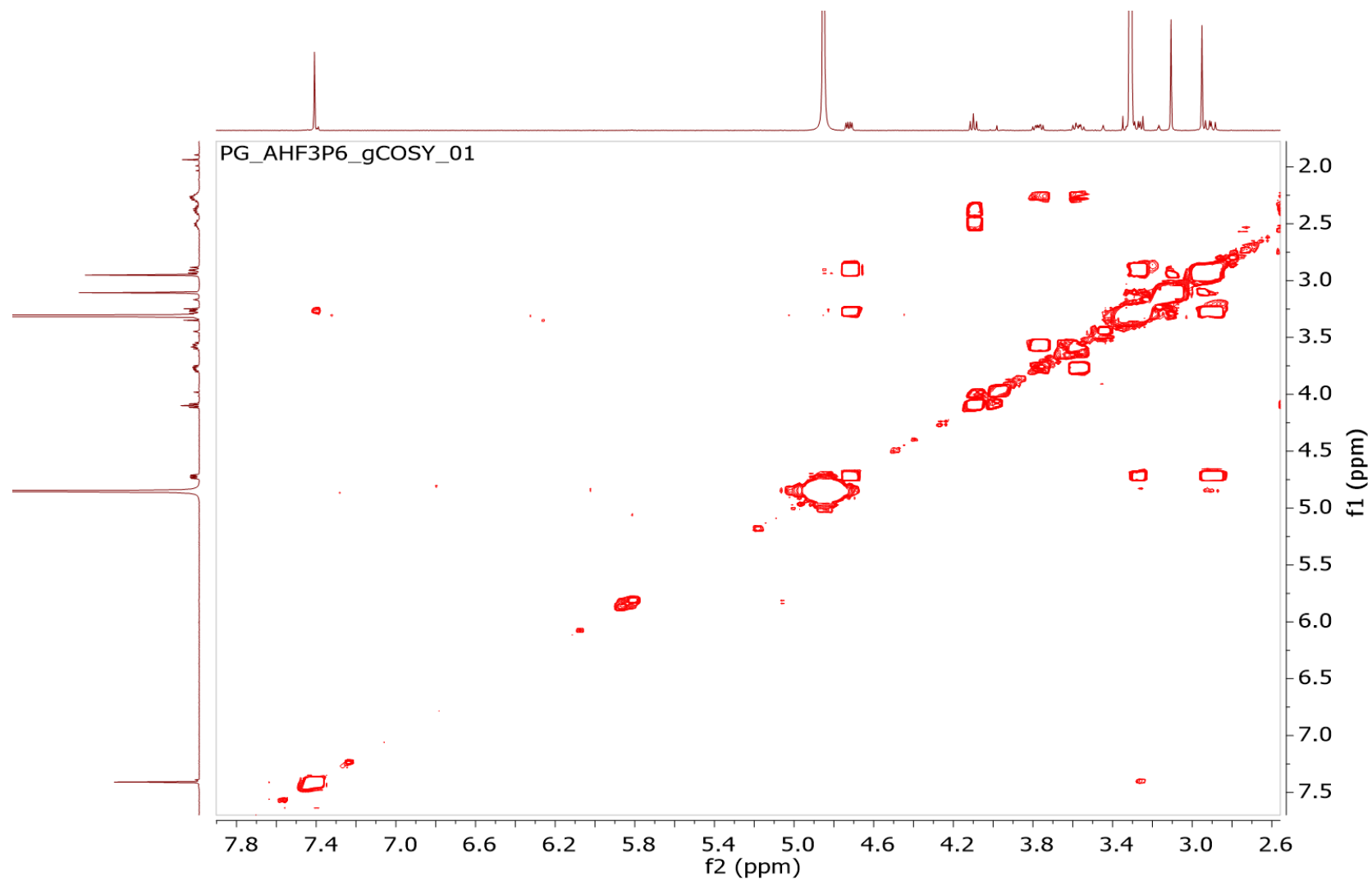
Figure S20. COSY NMR spectrum of **3** at 500 MHz in CD₃OD
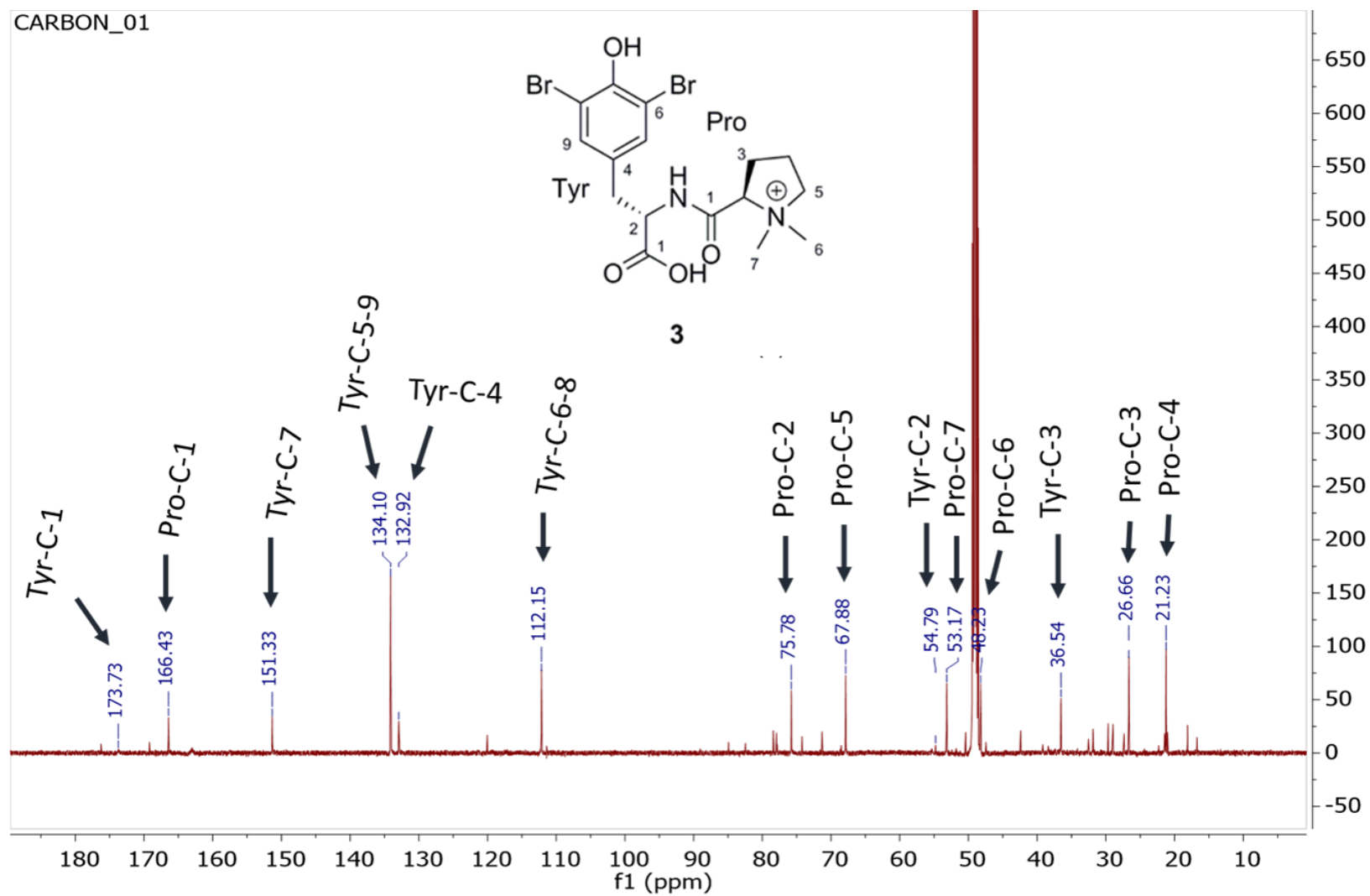
Figure S21. ^{13}C NMR spectrum of **3** at 125 MHz in CD₃OD
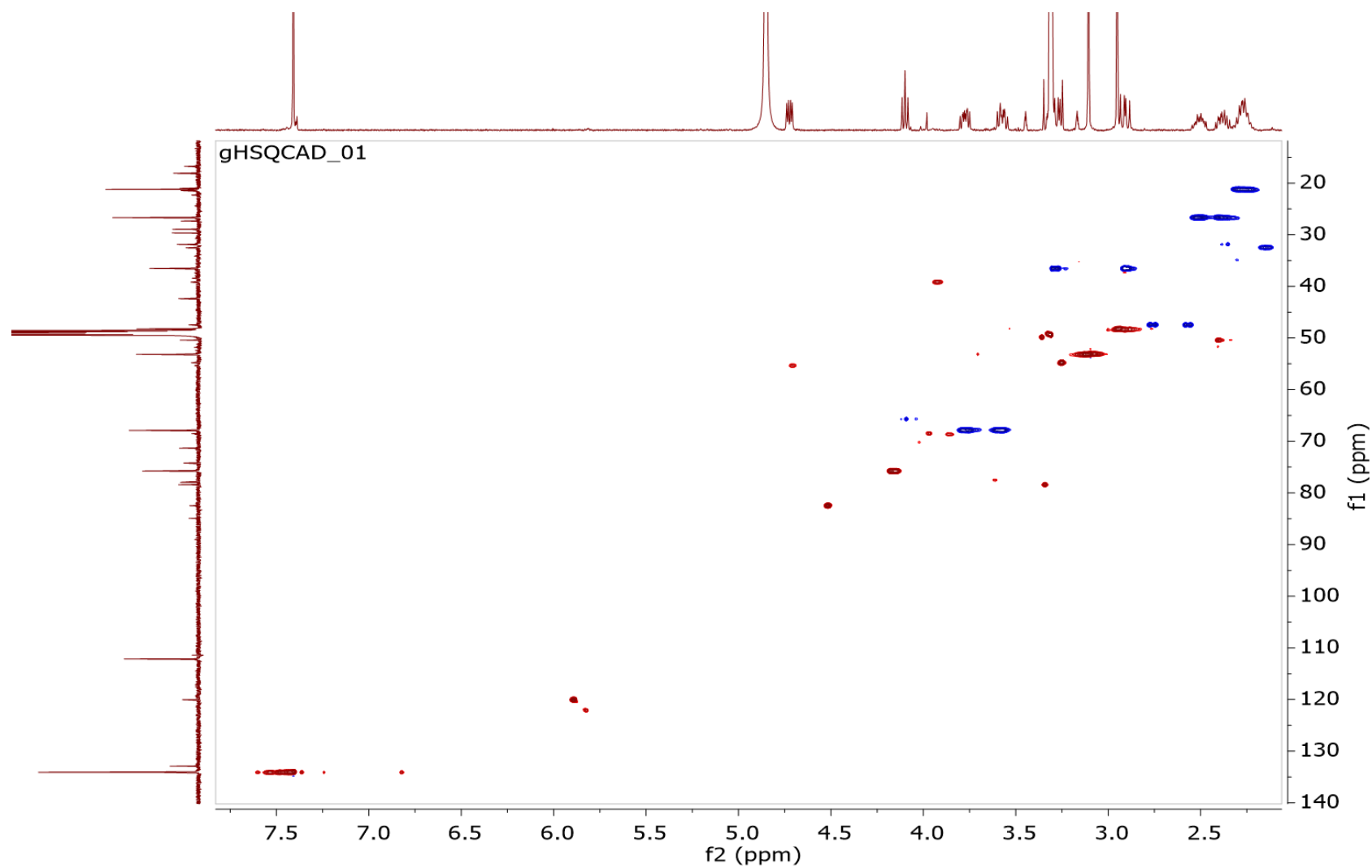
Figure S22. HSQC NMR spectrum of **3** at 500 MHz in CD₃OD
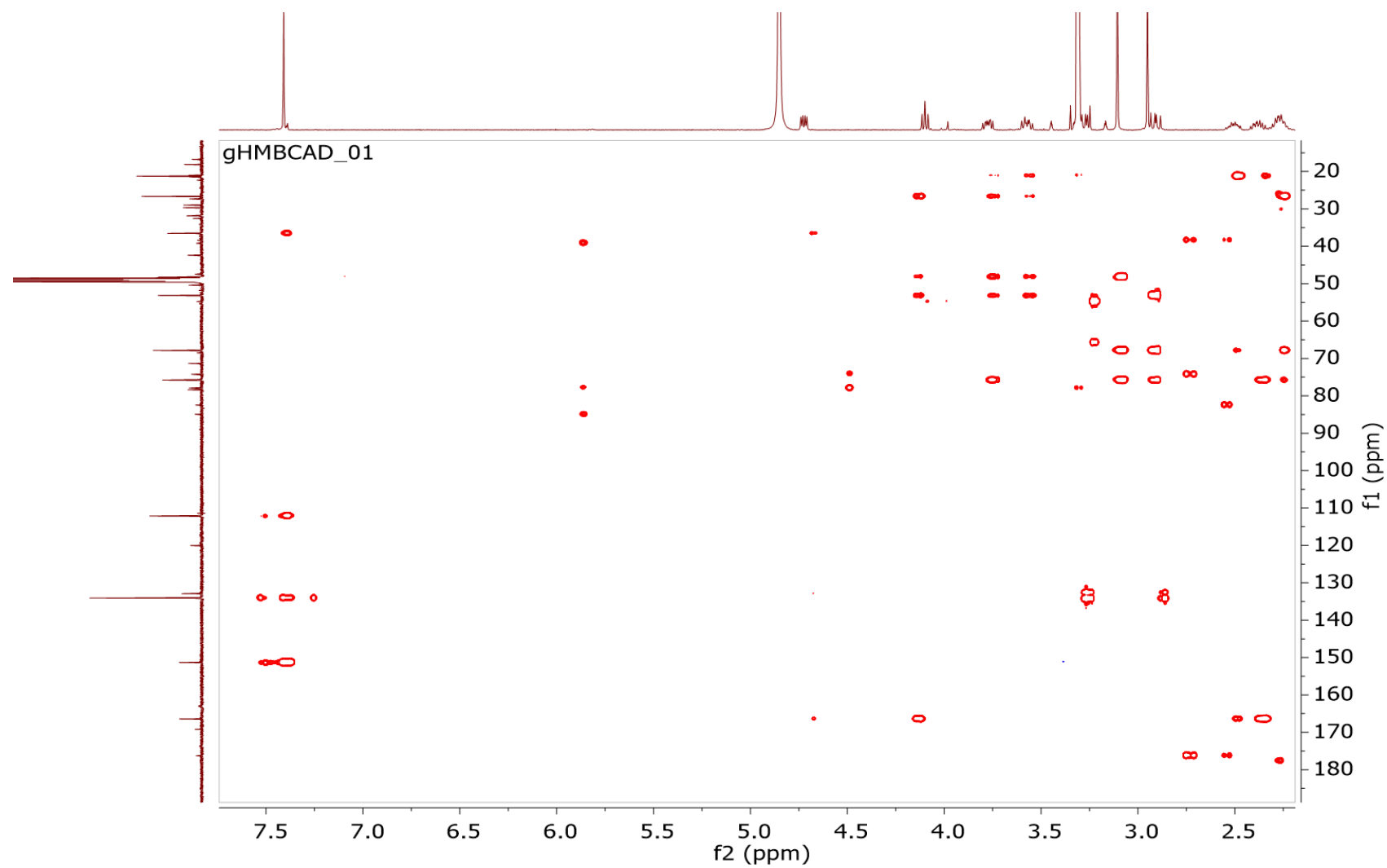
Figure S23. HMBC NMR spectrum of **3** at 500 MHz in CD₃OD
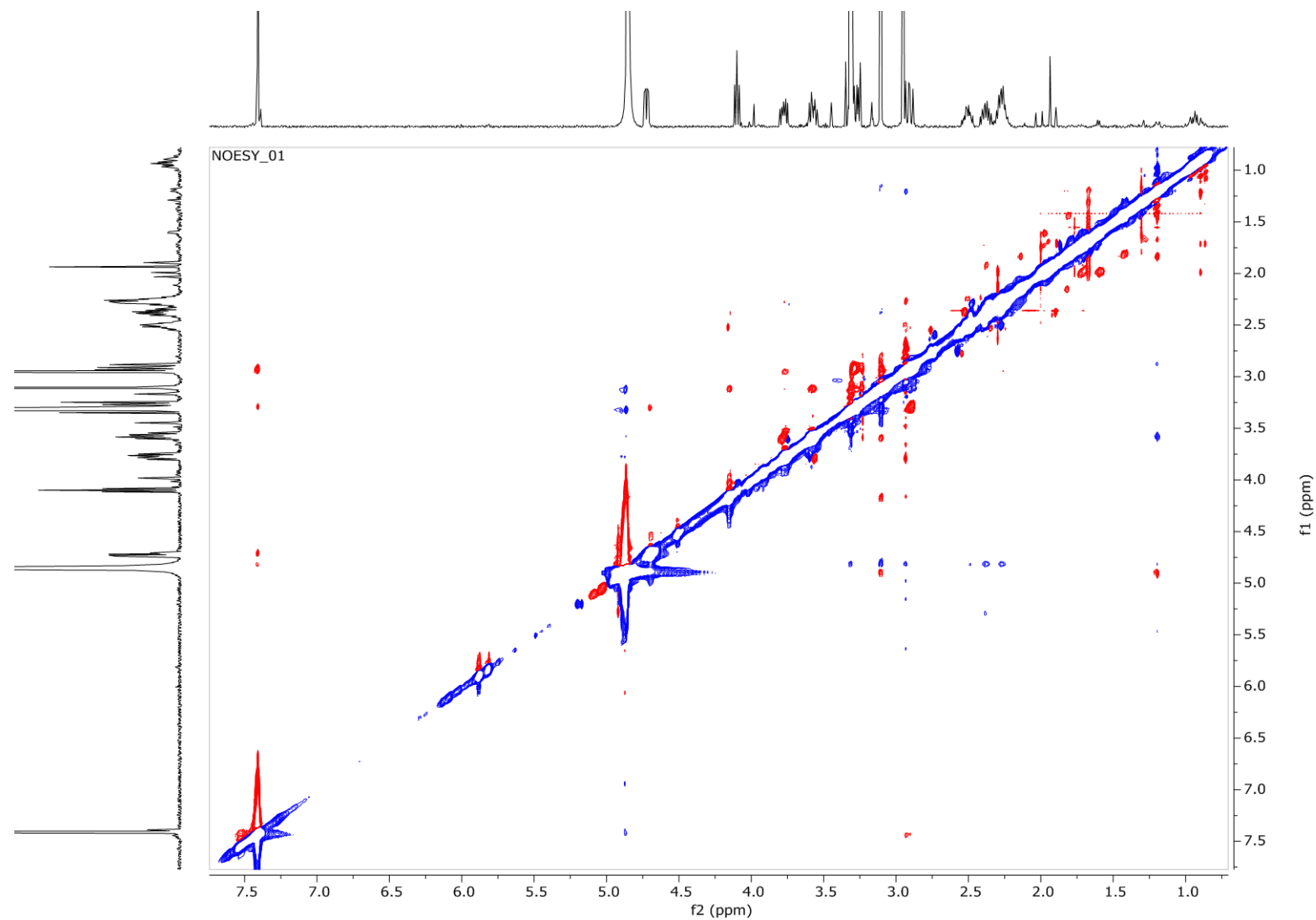
Figure S24. NOESY NMR spectrum of **3** at 500 MHz in CD₃OD
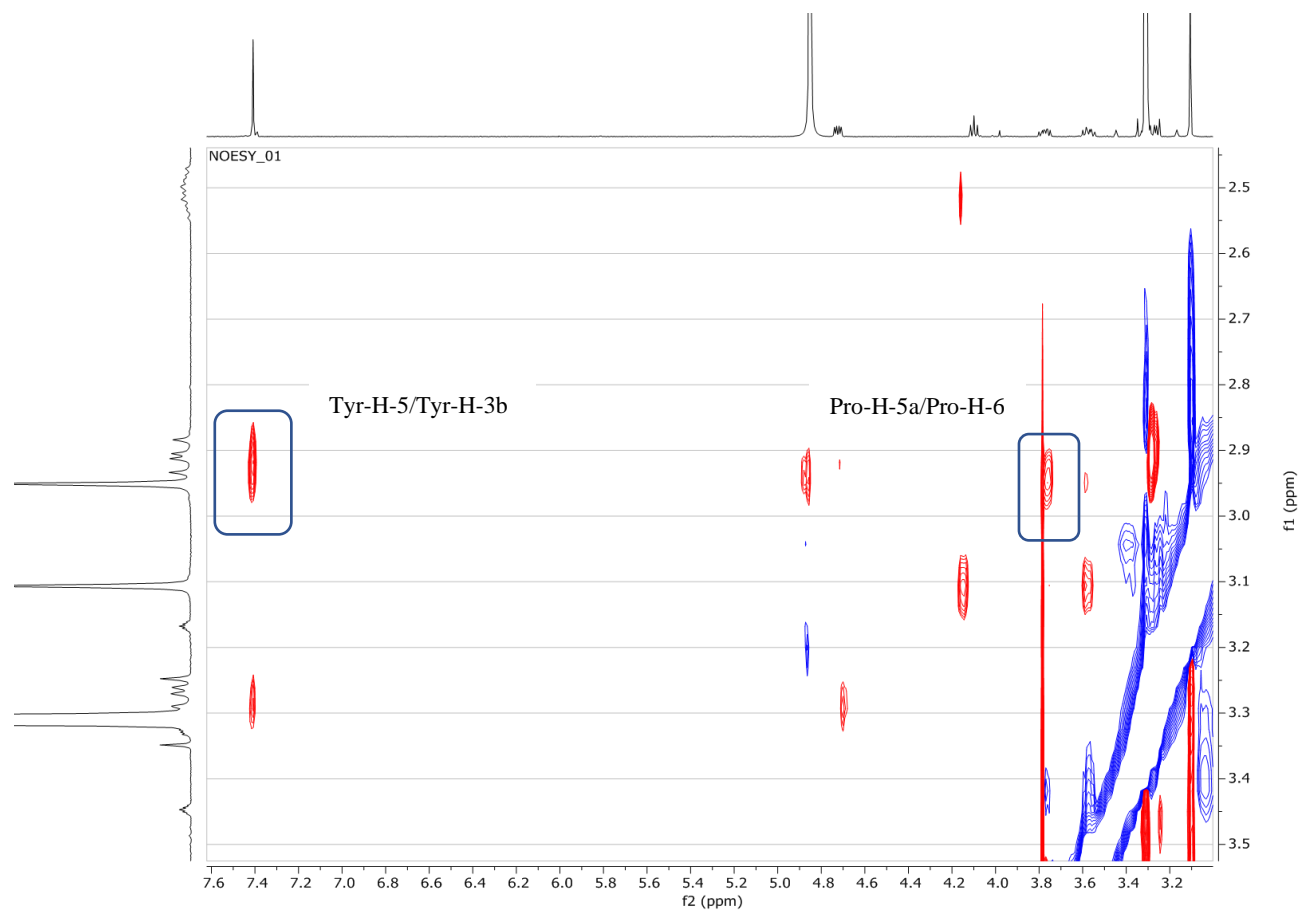
Figure S25. Zoom of the NOESY NMR spectrum of **3** showing an absence of nOe between Tyr-H-5 and Pro-H-6 and H-7
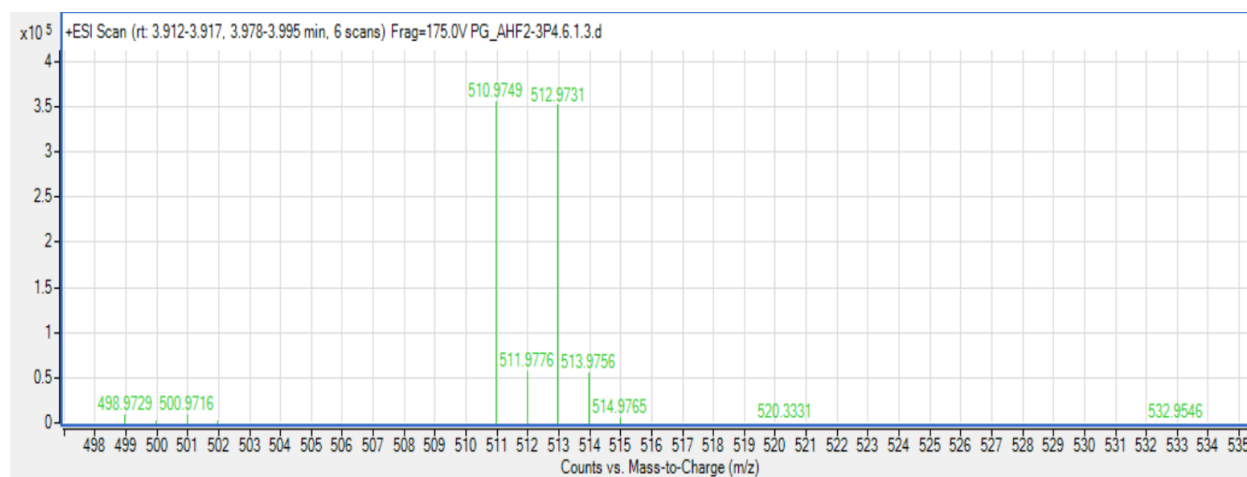
Figure S26. (+)-HRESIMS analysis of **4** in (+)-ESI

01CDAHF23P61300011.
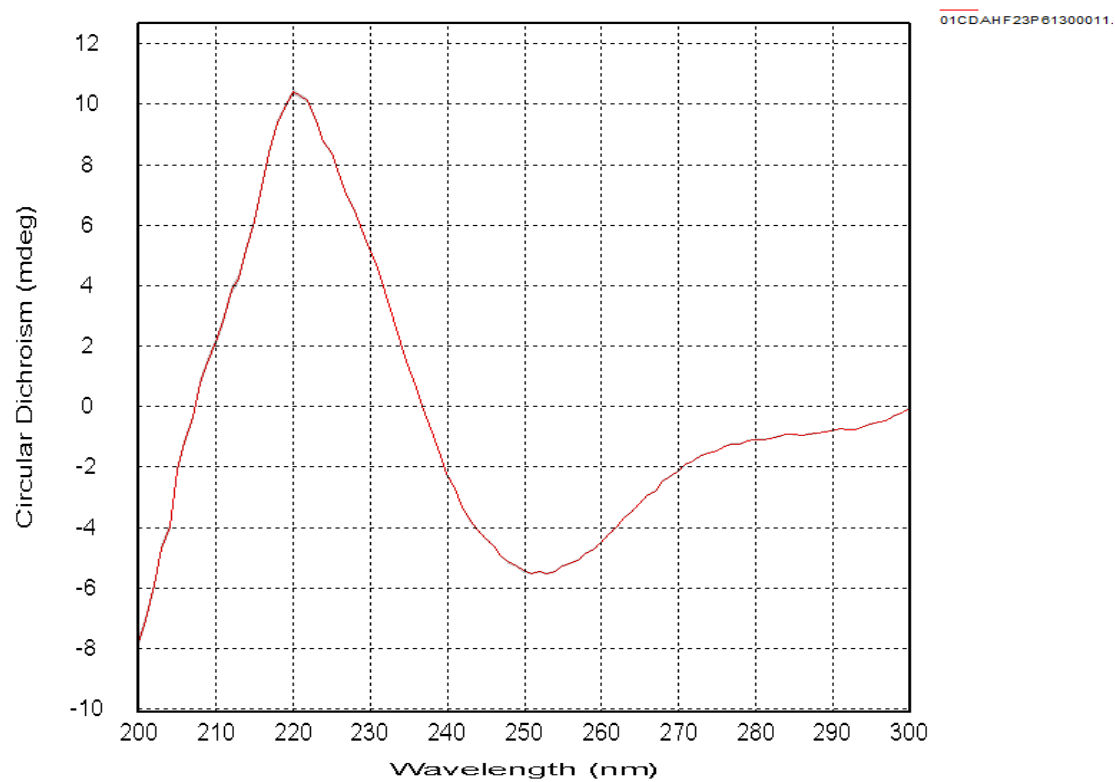
Figure S27. ECD spectrum of **4**

01UVAHF23P61300010.
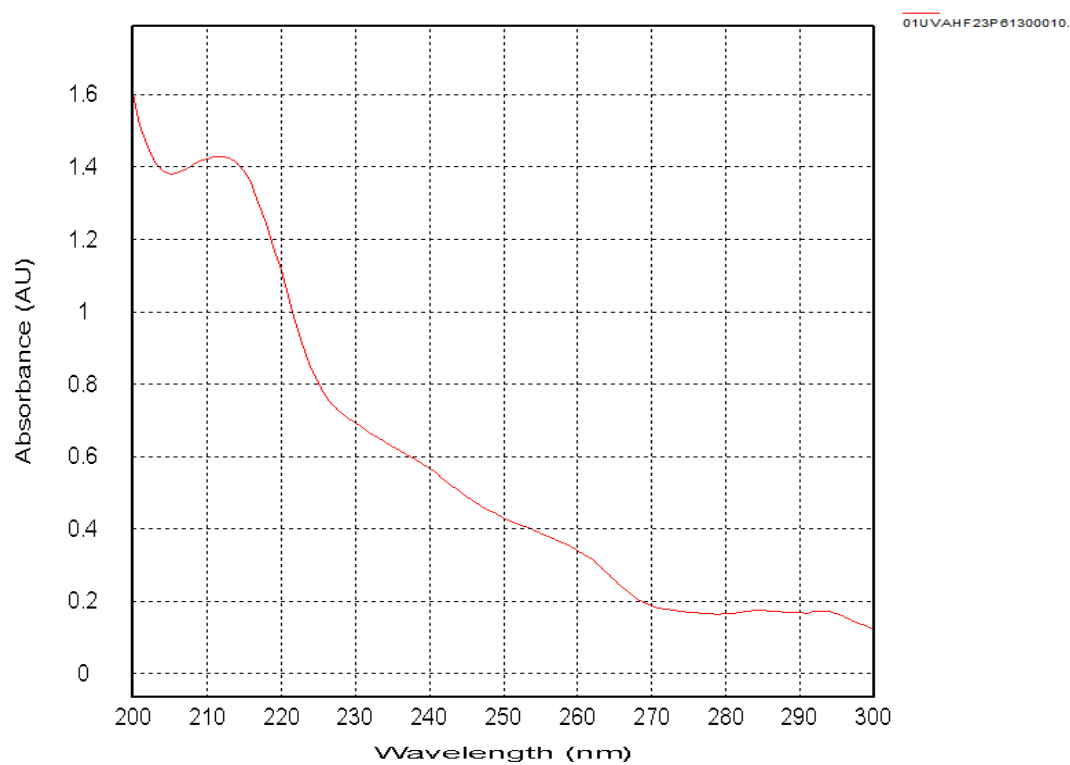
Figure S28. UV spectrum of **4**
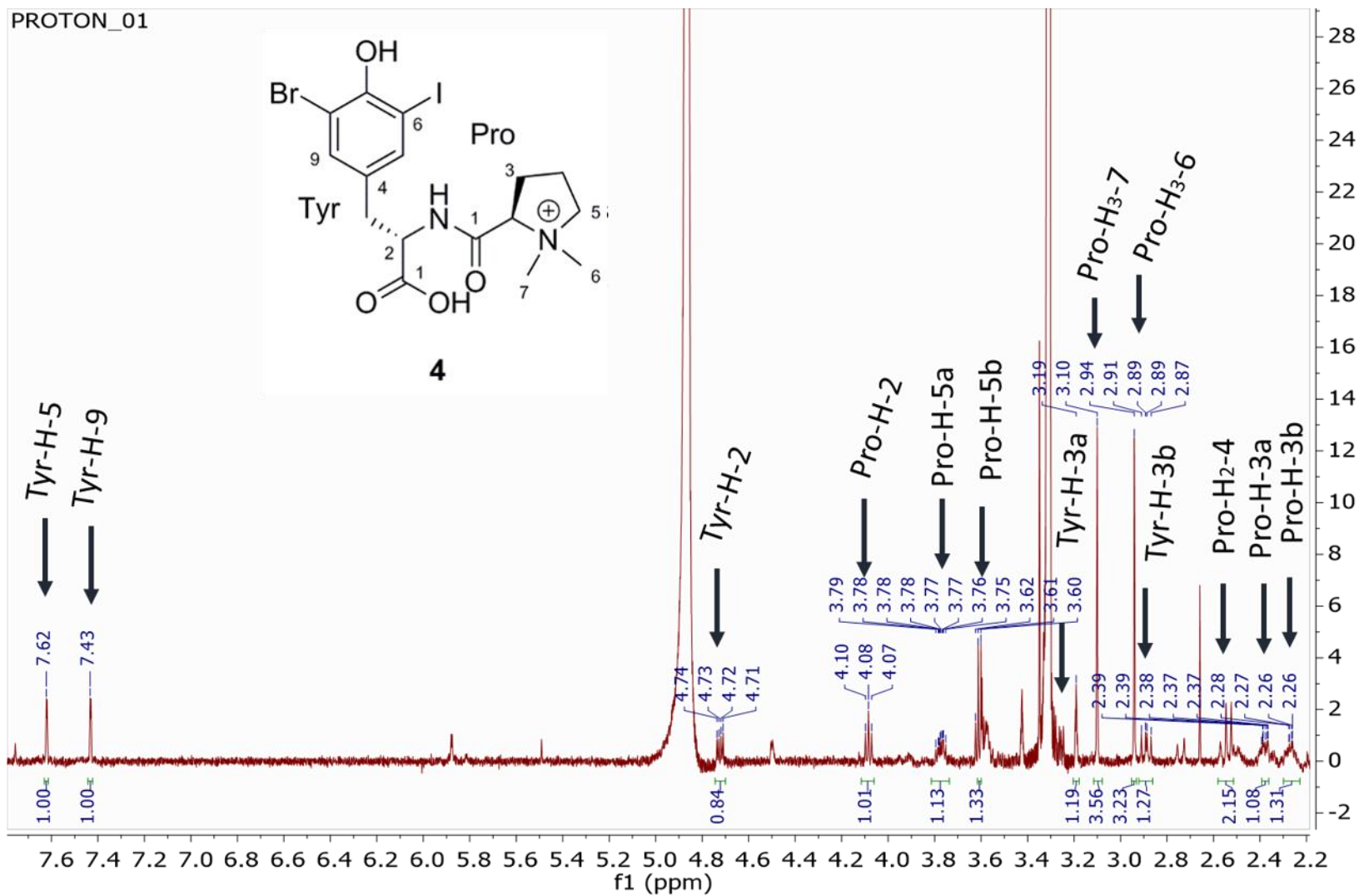
Figure S29. ¹H NMR spectrum of 4 at 500 MHz in CD₃OD
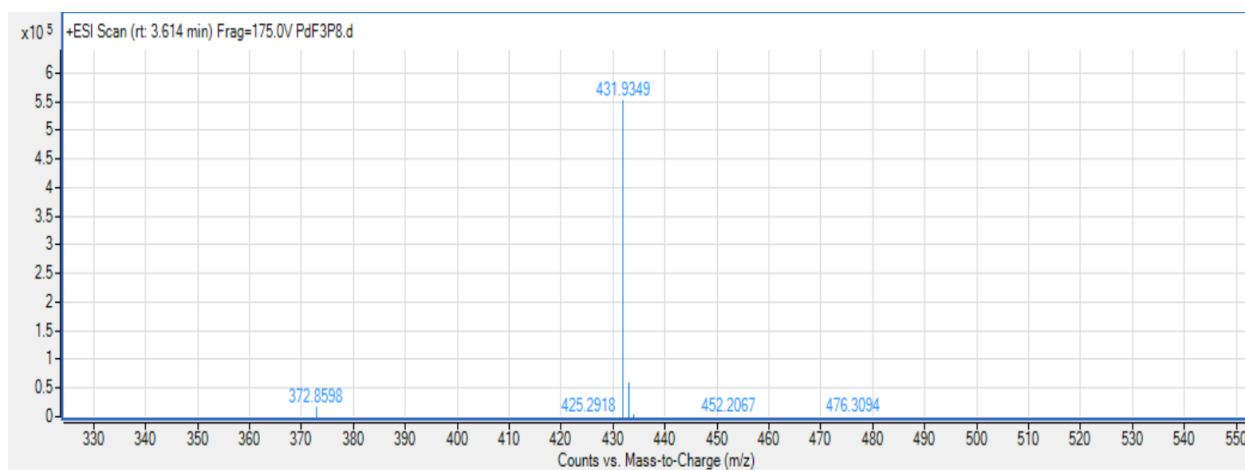
Figure S30. (+)-HRESIMS analysis of **5** in (+)-ESI
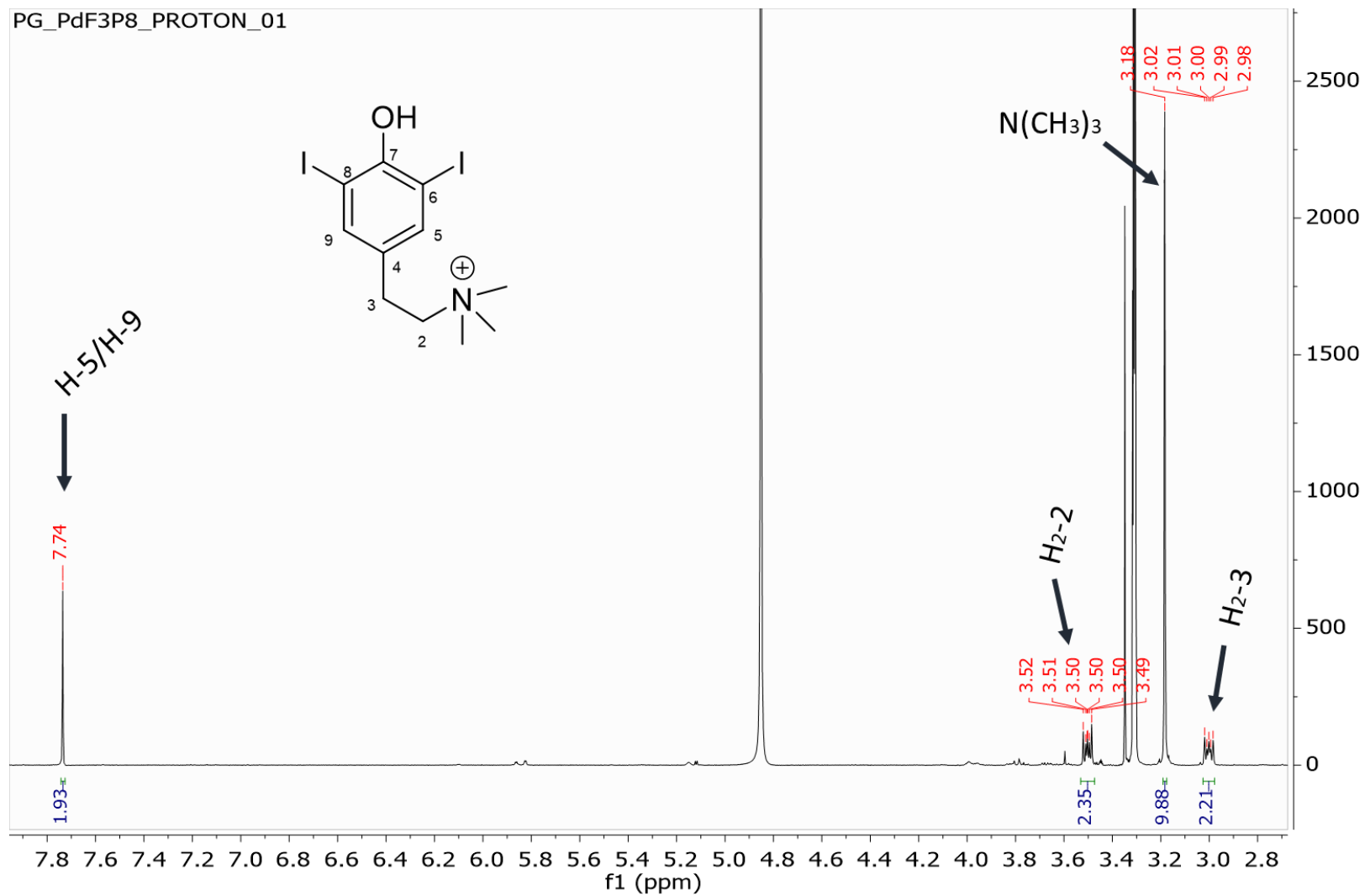
Figure S31. ¹H NMR spectrum of **5** at 500 MHz in CD₃OD
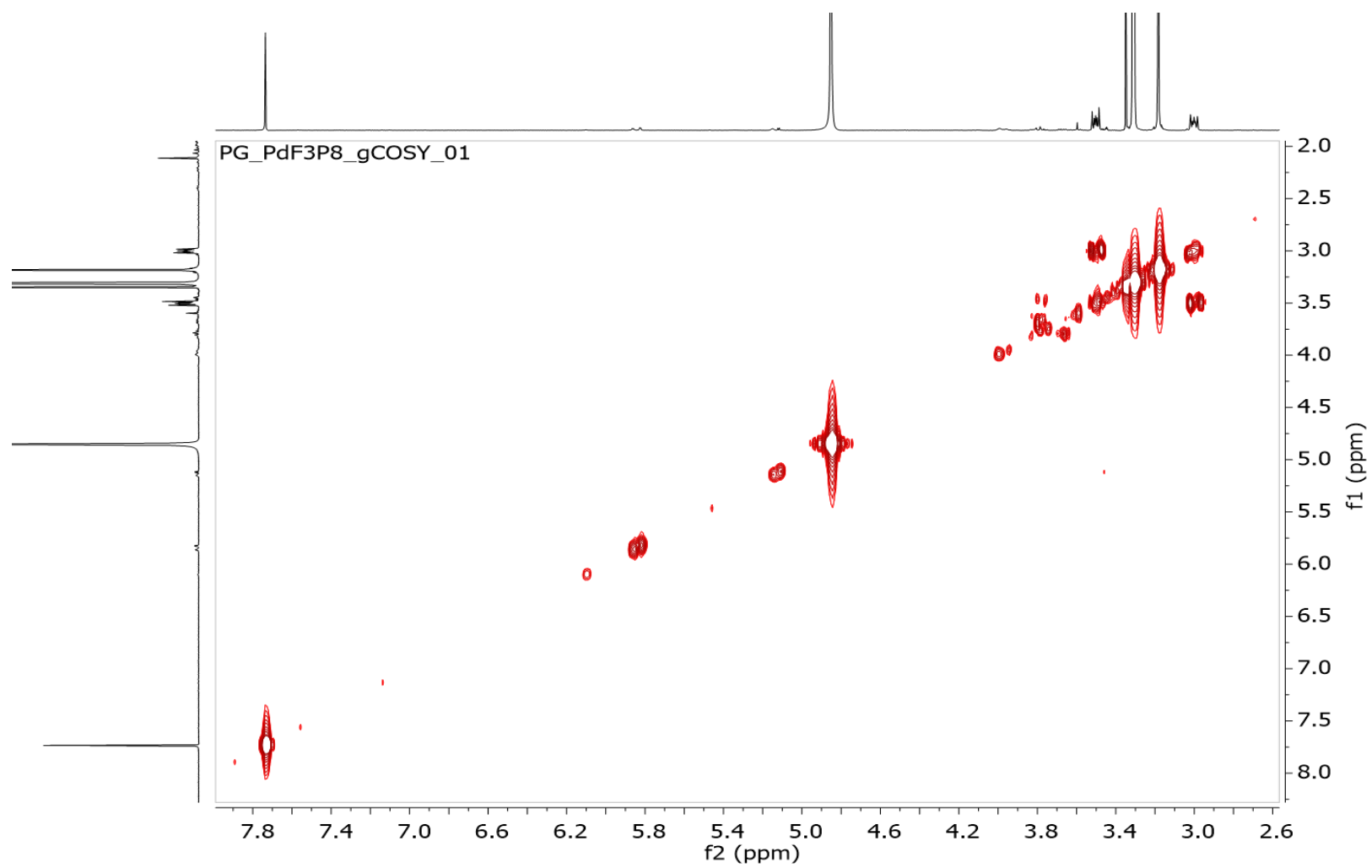
Figure S32. COSY NMR spectrum of **5** at 500 MHz in CD₃OD
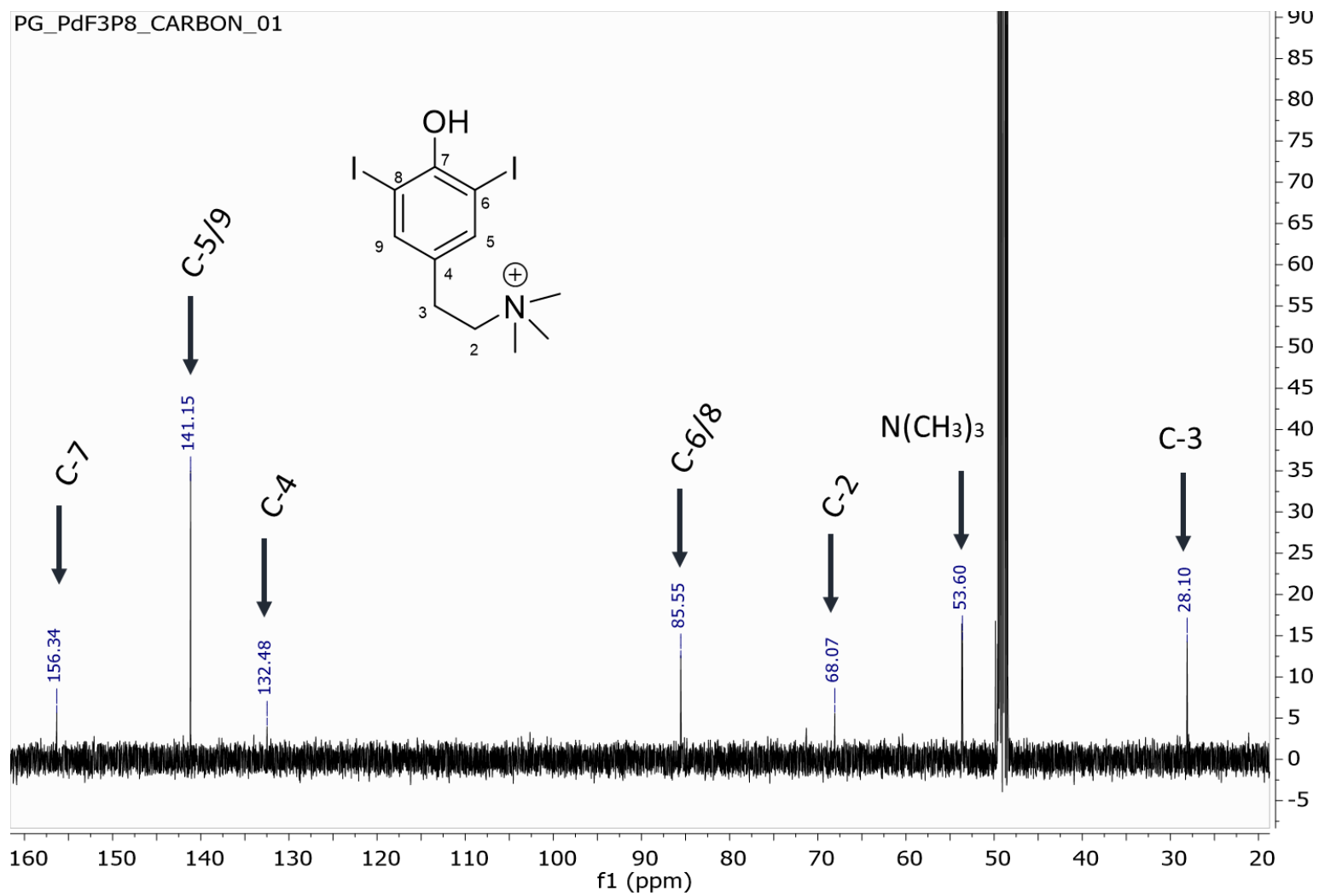
Figure S33. ^{13}C NMR spectrum of **5** at 125 MHz in CD$_3$OD
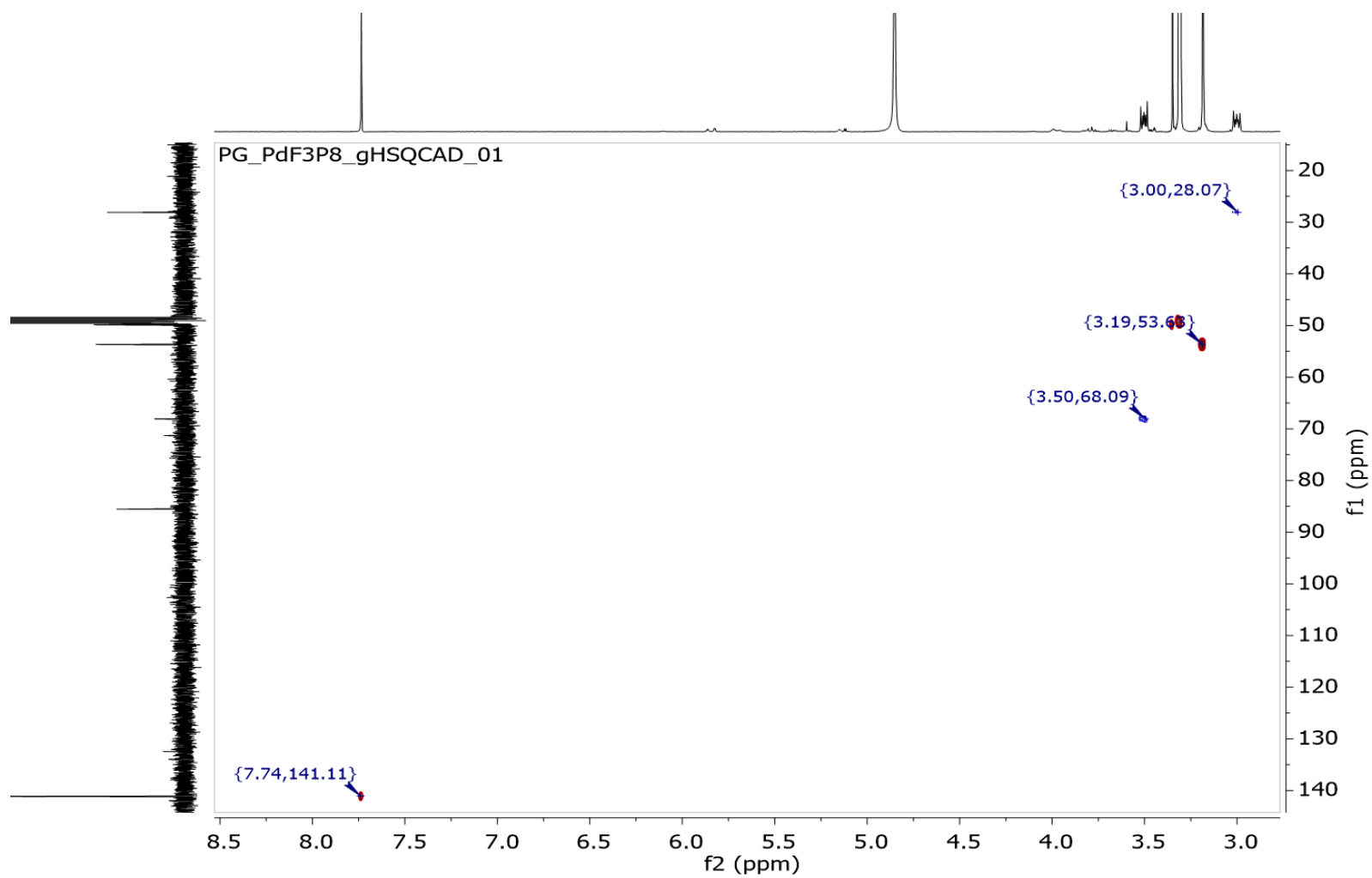
Figure S34. HSQC NMR spectrum of **5** at 500 MHz in CD₃OD
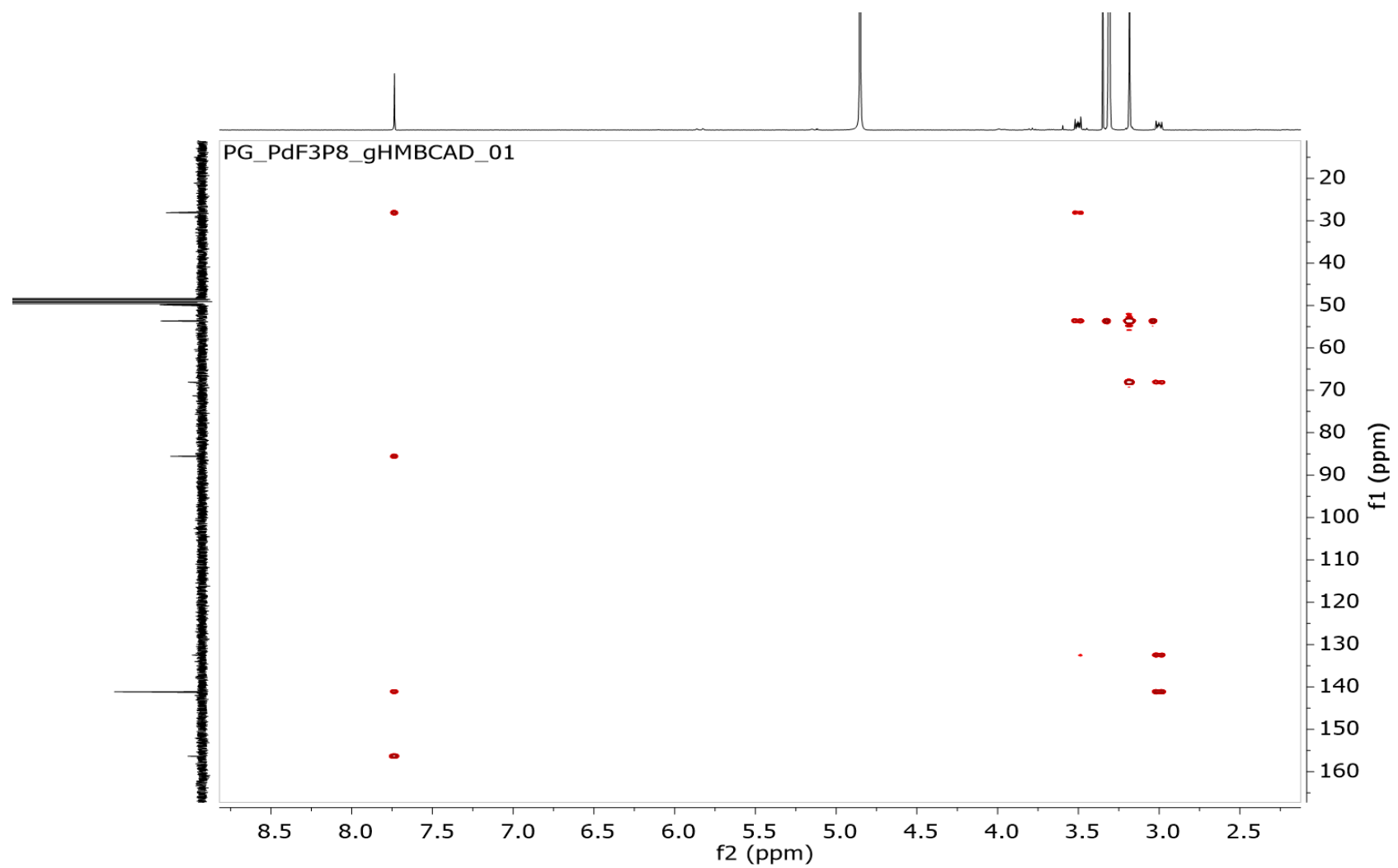
Figure S35. HMBC NMR spectrum of **5** at 500 MHz in CD₃OD
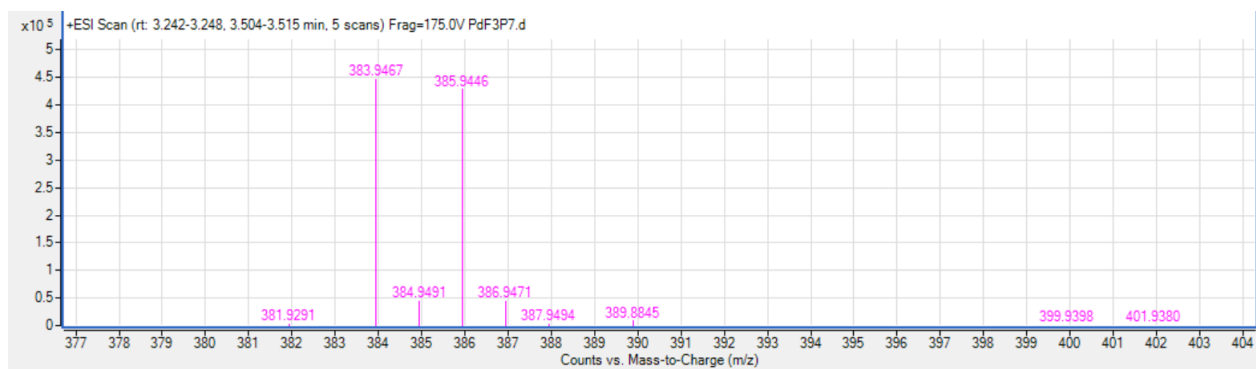
Figure S36. (+)-HRESIMS analysis of **6** in (+)-ESI
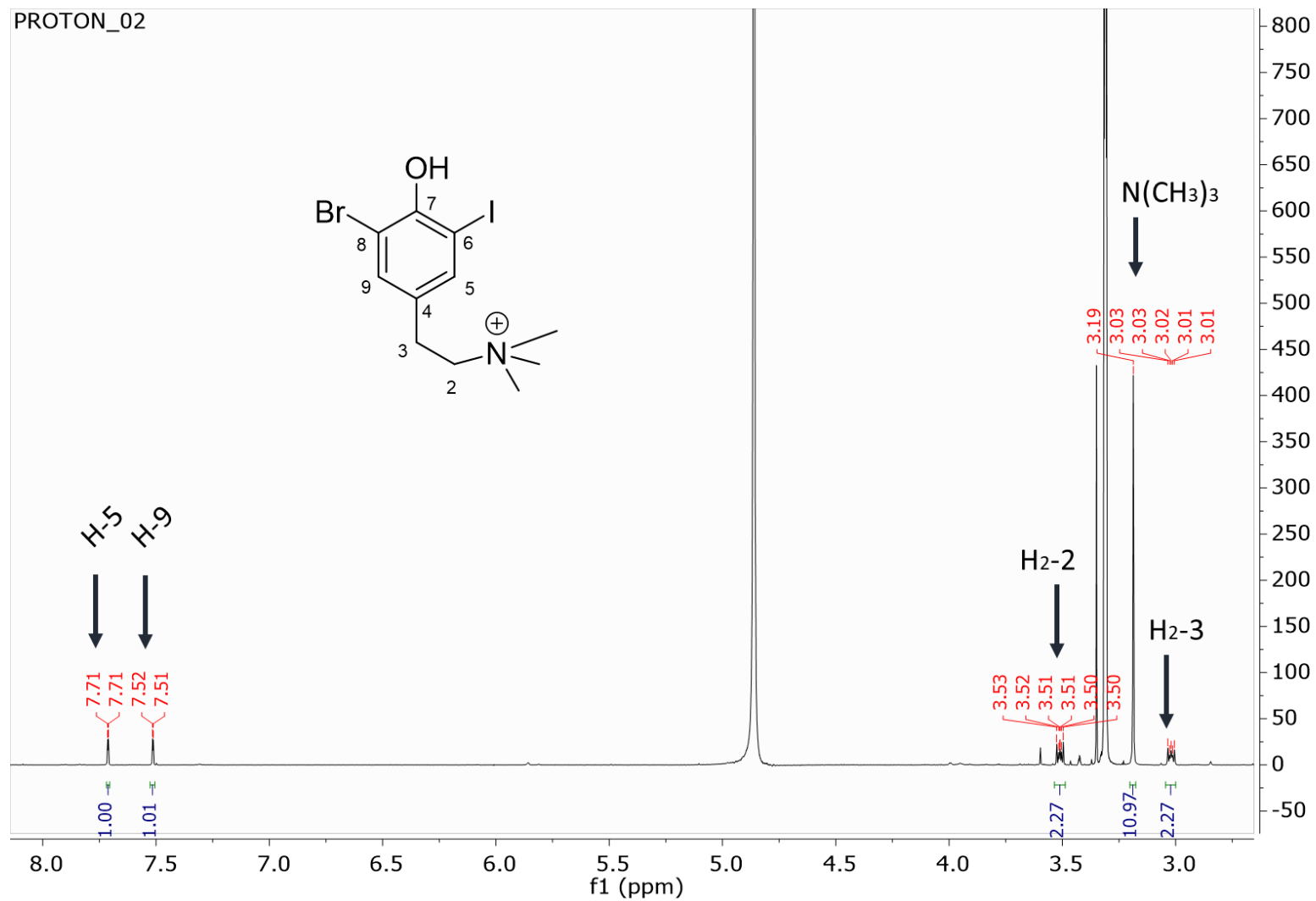
Figure S37. ¹H NMR spectrum of **6** at 500 MHz in CD₃OD

gCOSY_01
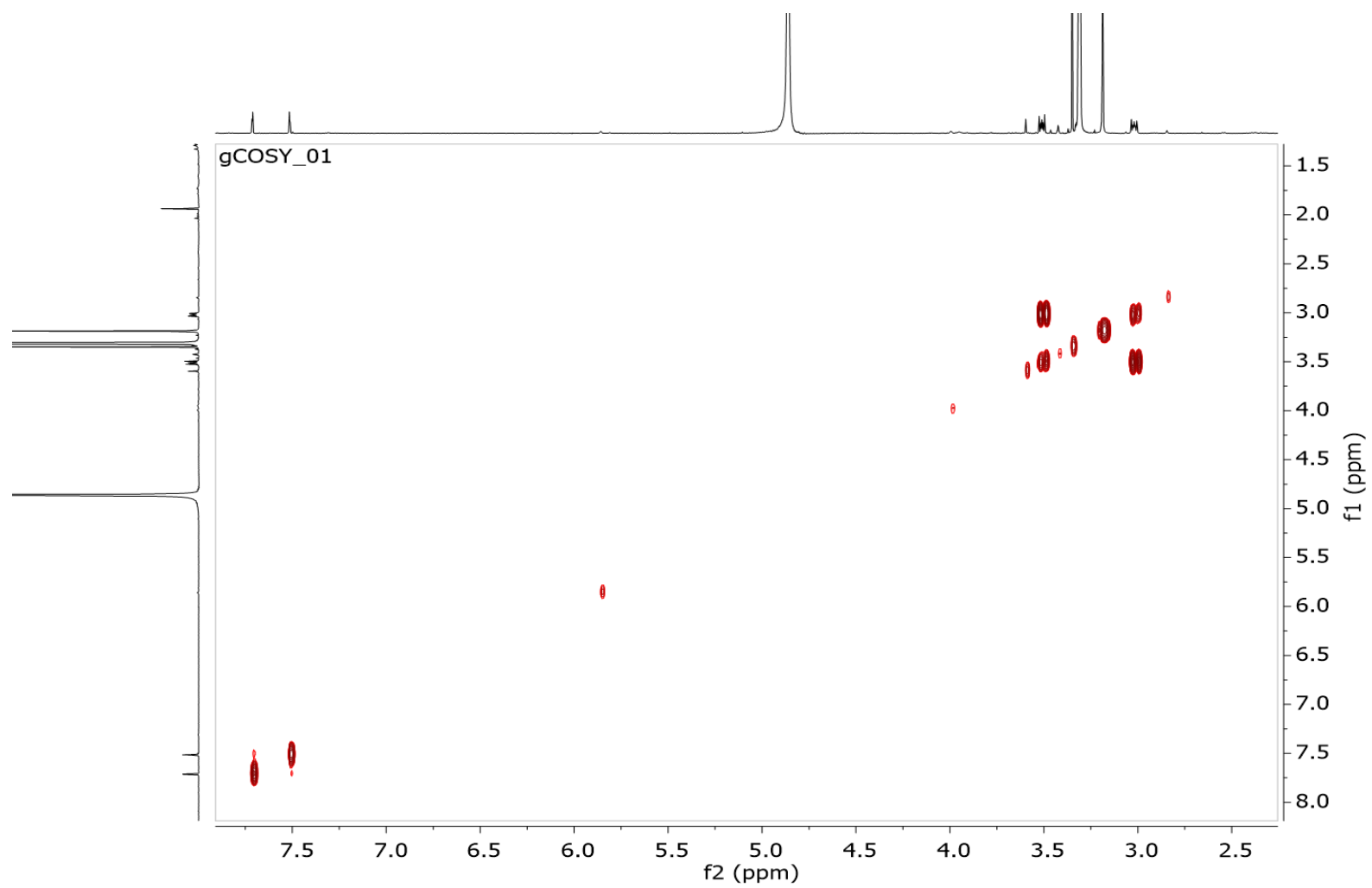
Figure S38. COSY spectrum of **6** at 500 MHz in CD₃OD
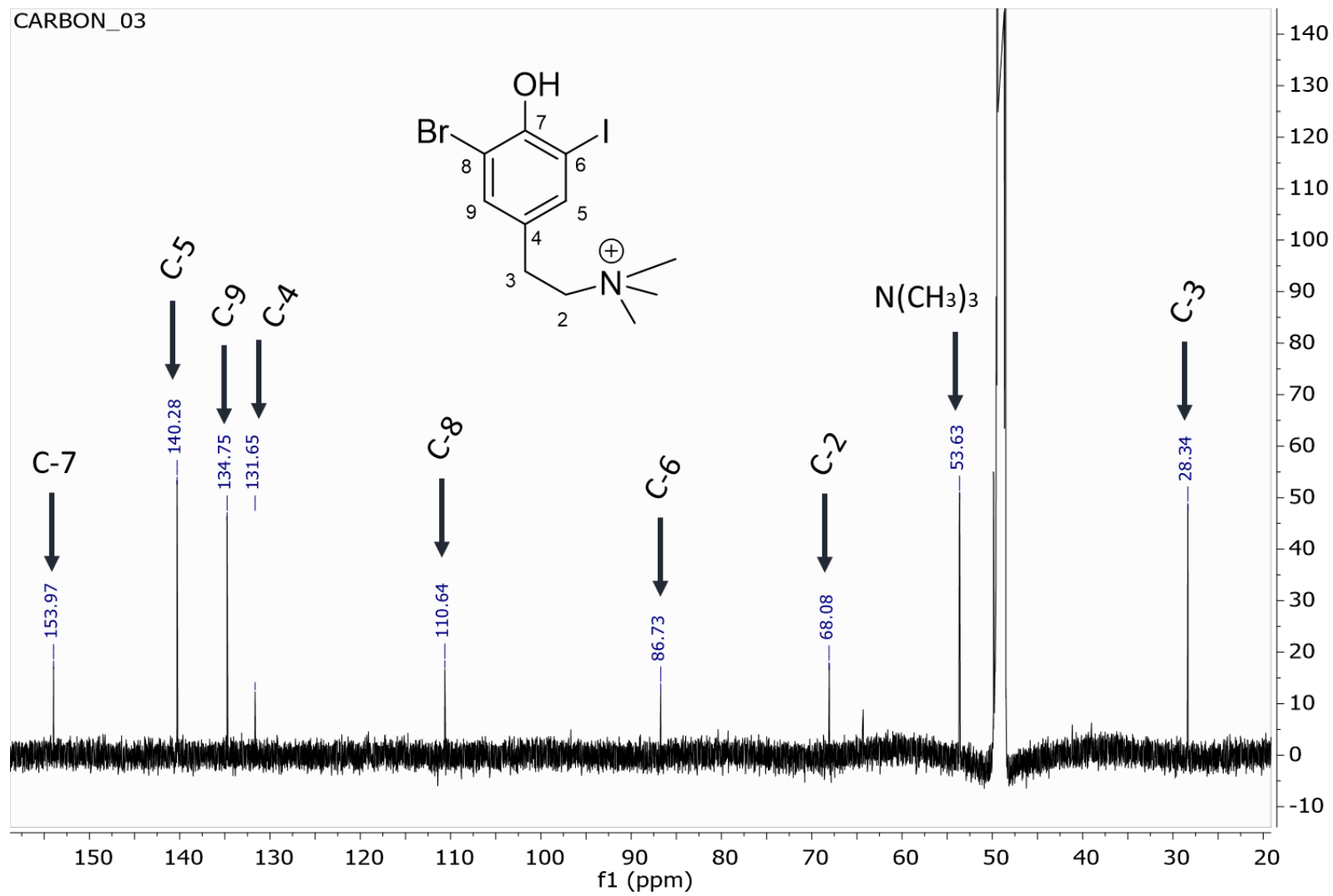
Figure S39. ¹³C NMR spectrum of **6** at 125 MHz in CD₃OD

gHSQCAD_01

{3.02,28.35}

{3.19,53.62}

{3.51,68.06}

{7.51,134.73}

{7.71,140.26}

f1 (ppm)

f2 (ppm)
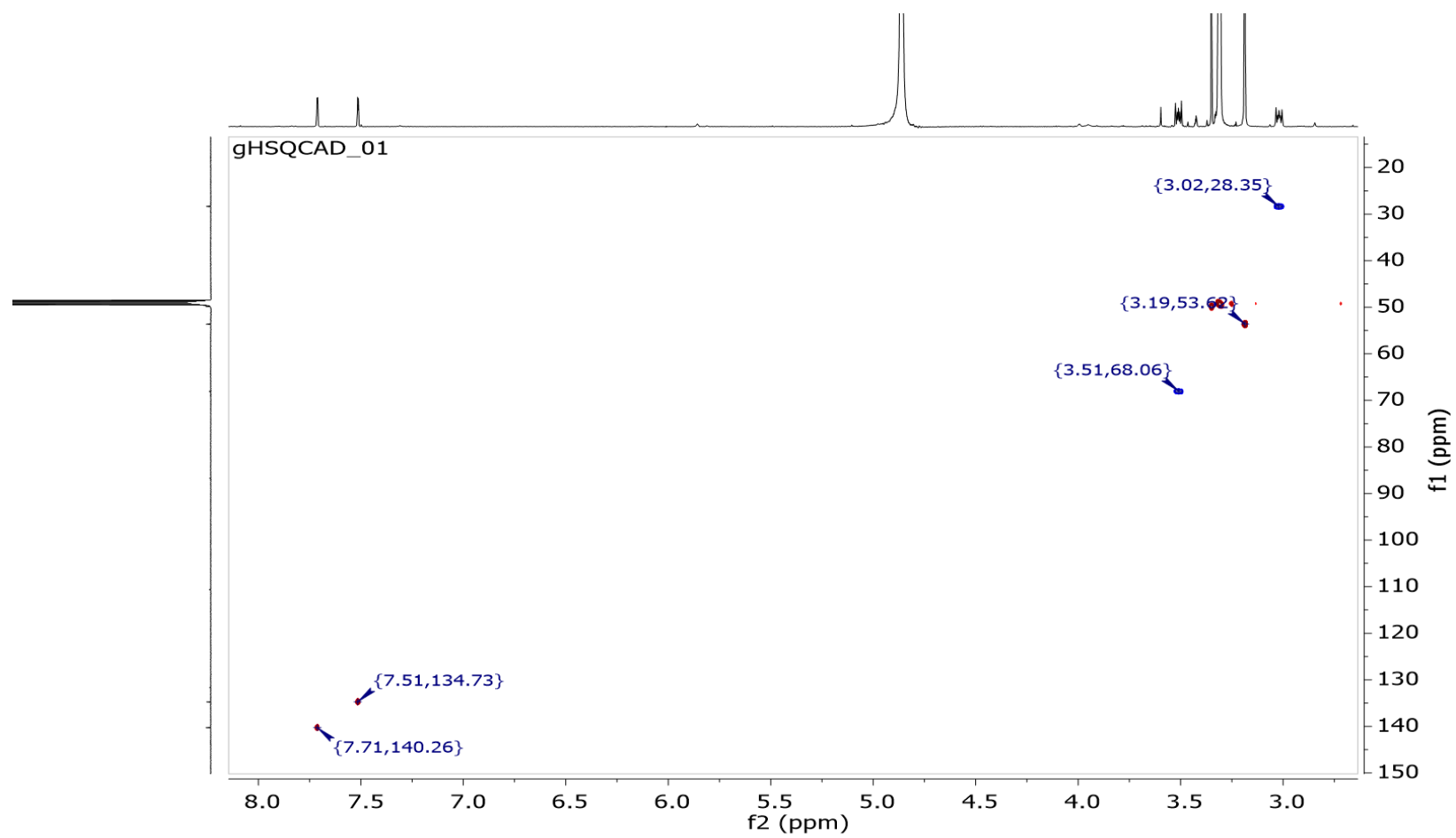
Figure S40. HSQC spectrum of **6** at 500 MHz in CD₃OD
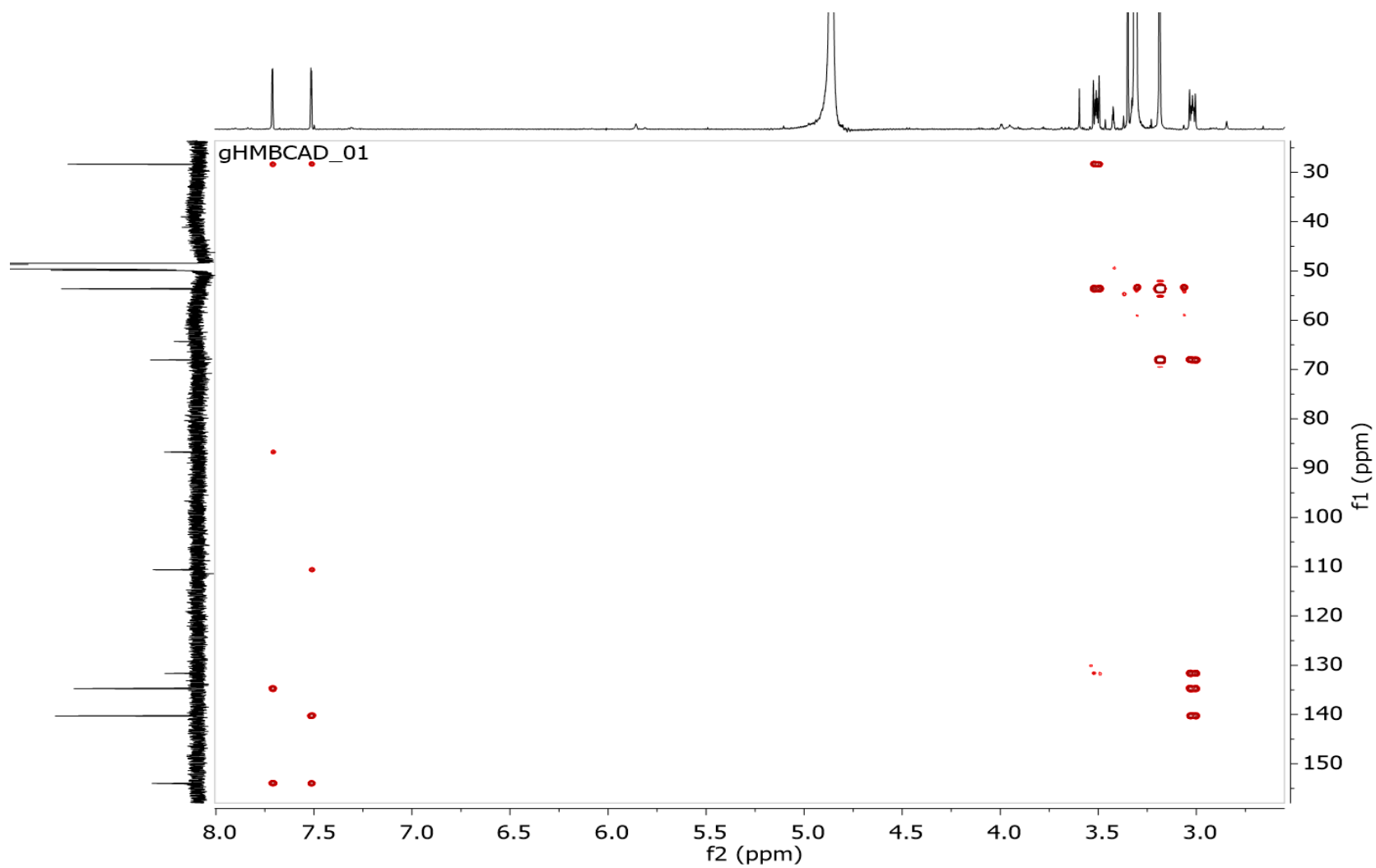
Figure S41. HMBC spectrum of **6** at 500 MHz in CD₃OD
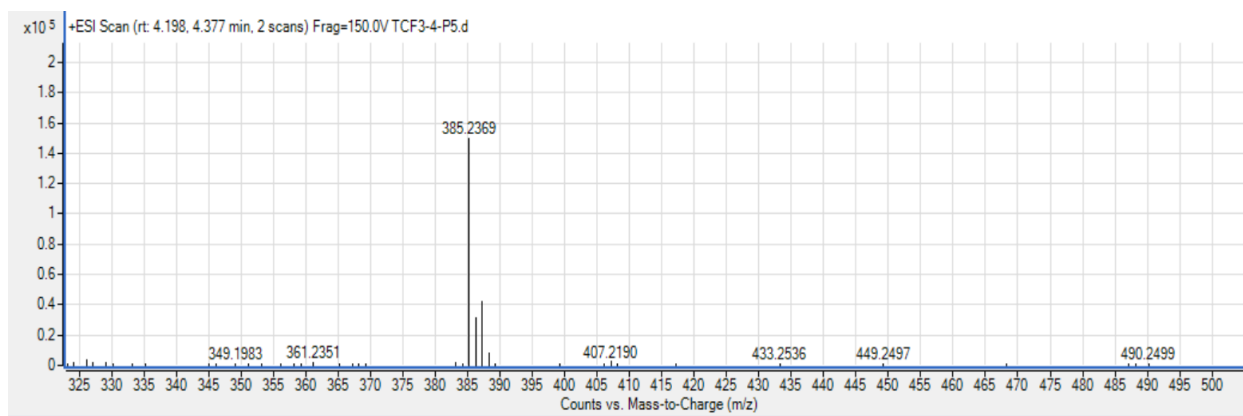
Figure S42. (+)-HRESIMS analysis of **zoamide E (7)** in (+)-ESI
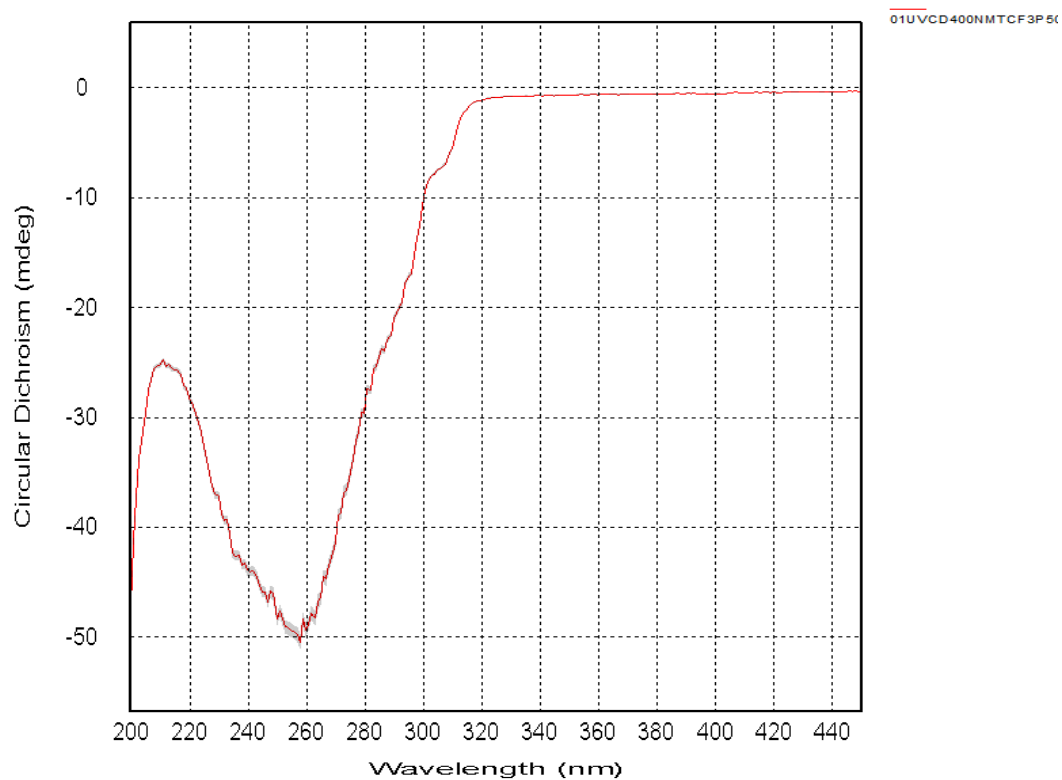
Figure S43. ECD spectrum of **zoamide E (7)**
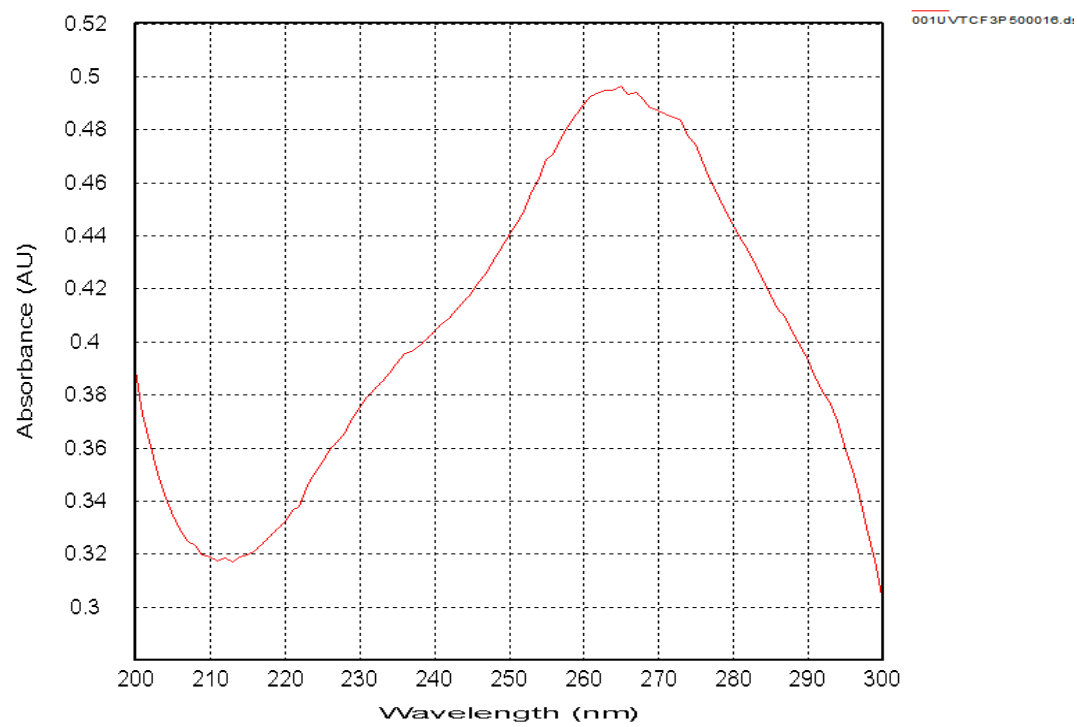
Figure S44. UV spectrum of **zoamide E (7)**
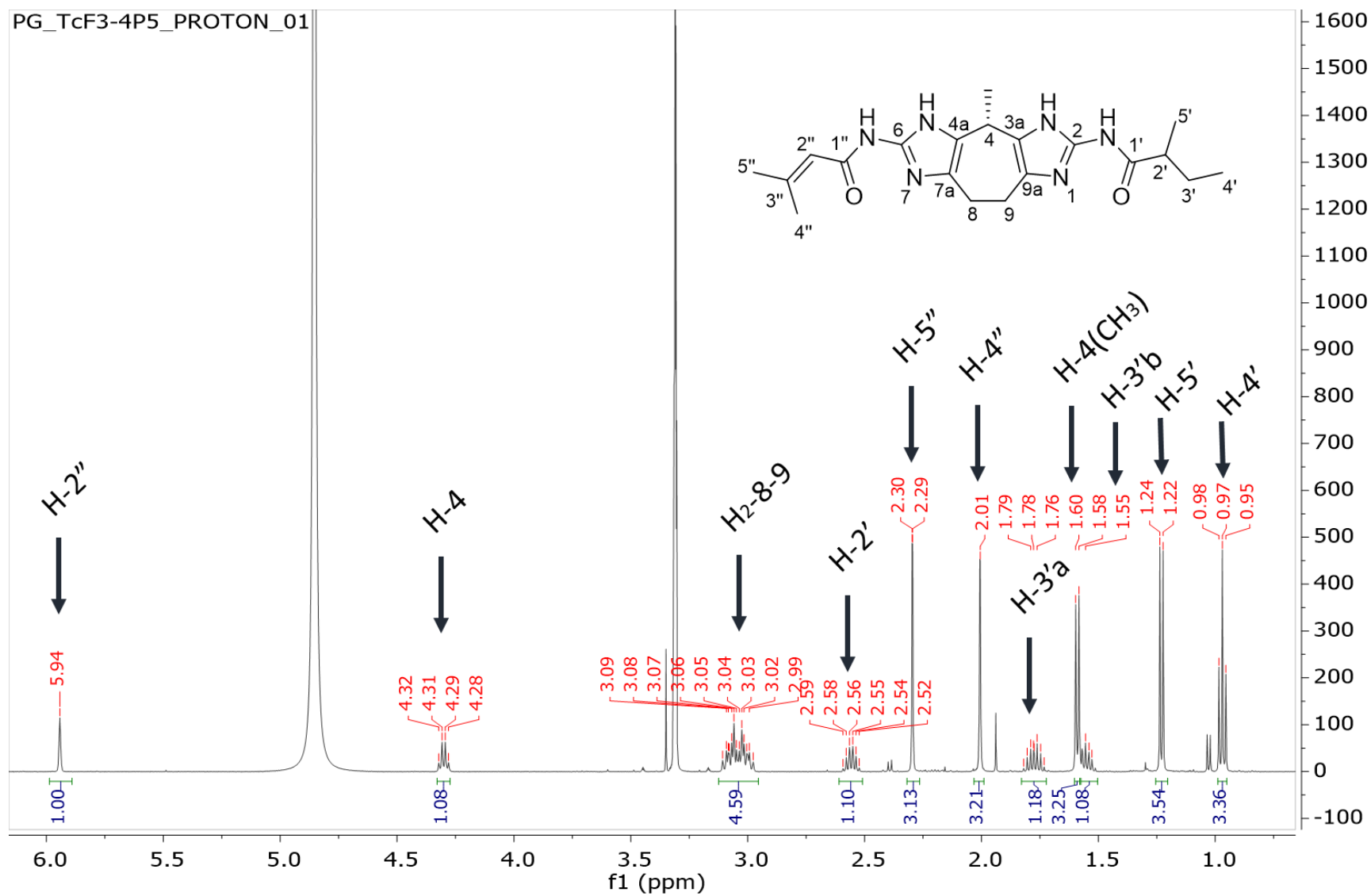
Figure S45. ^{1}H NMR spectrum of **zoamide E (7)** at 500 MHz in CD$_3$OD
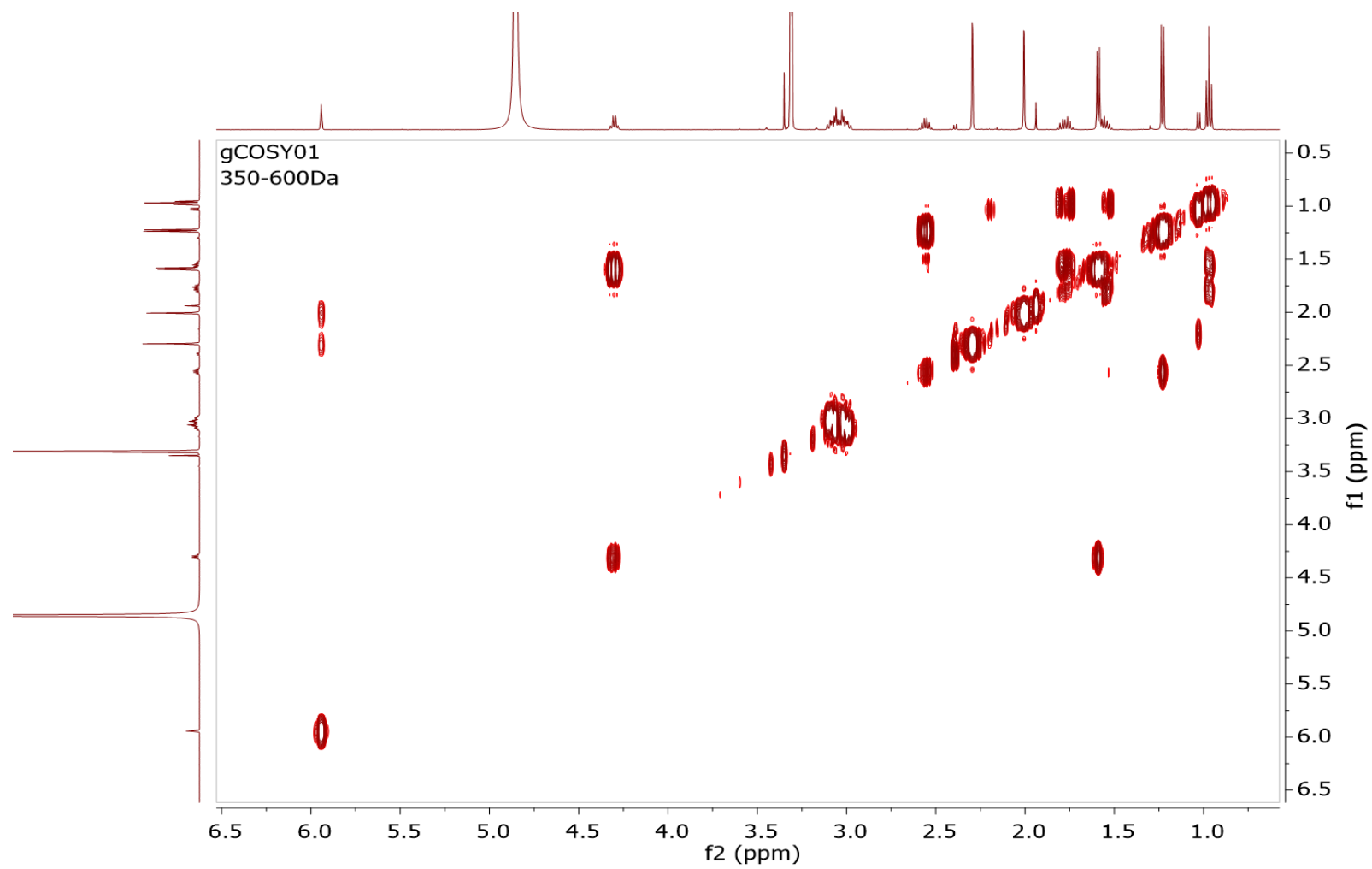
Figure S46. COSY NMR spectrum of **zoamide E (7)** at 500 MHz in CD₃OD
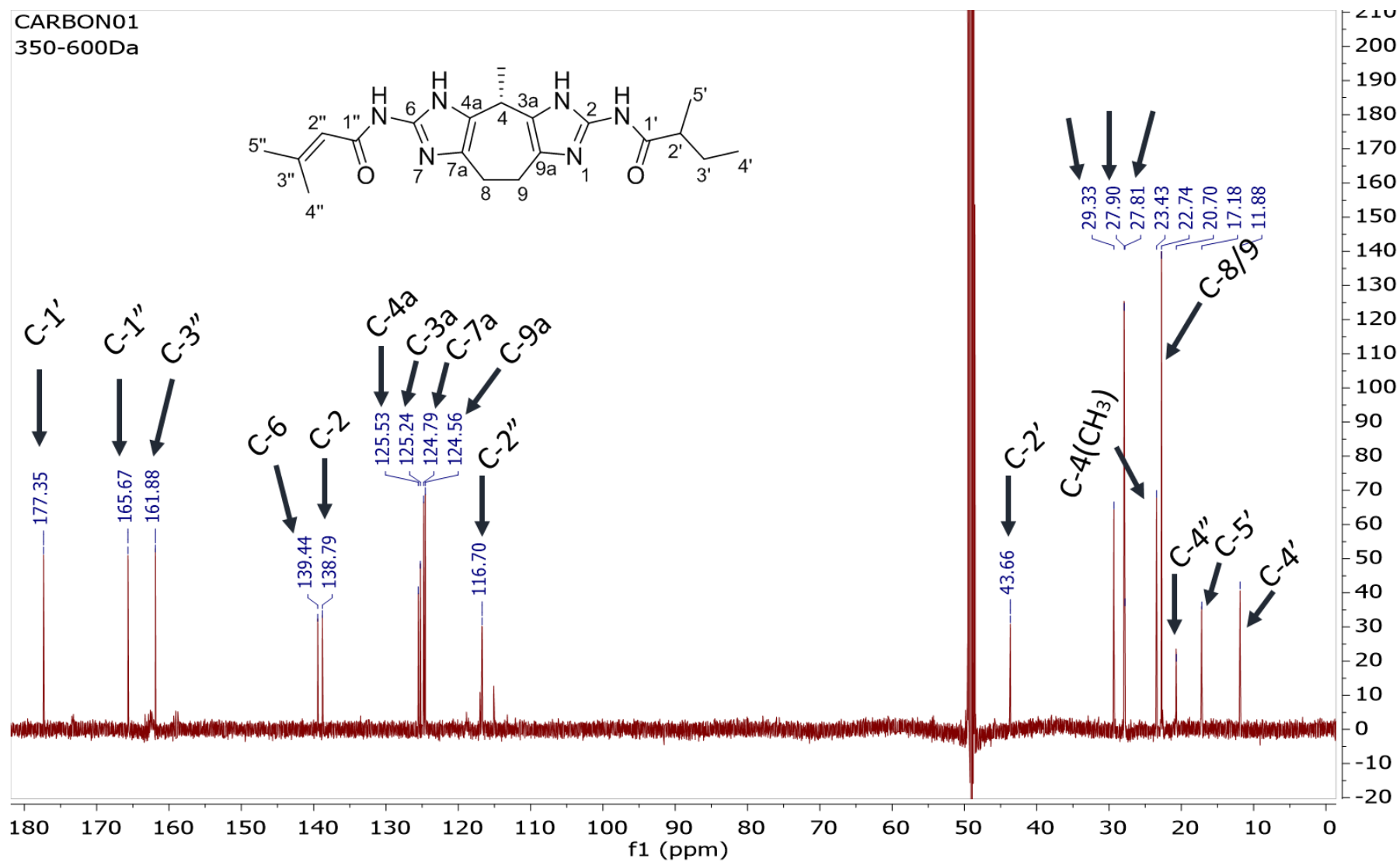
Figure S47. ^{13}C NMR spectrum of **zoamide E (7)** at 125 MHz in CD$_3$OD
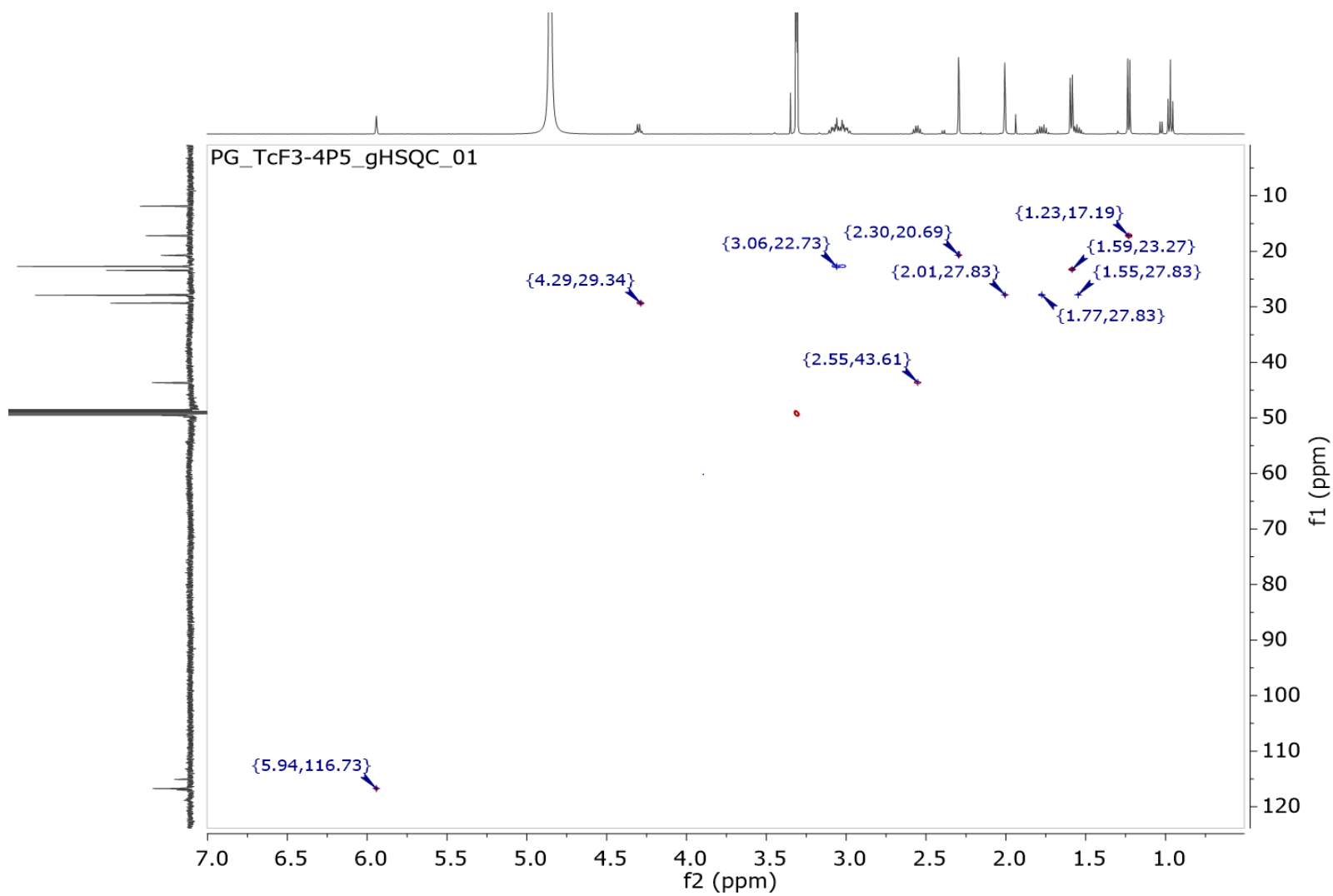
Figure S48. HSQC NMR spectrum of **zoamide E (7)** at 500 MHz in CD₃OD

PG_TcF3-4P5_gHMBC_01
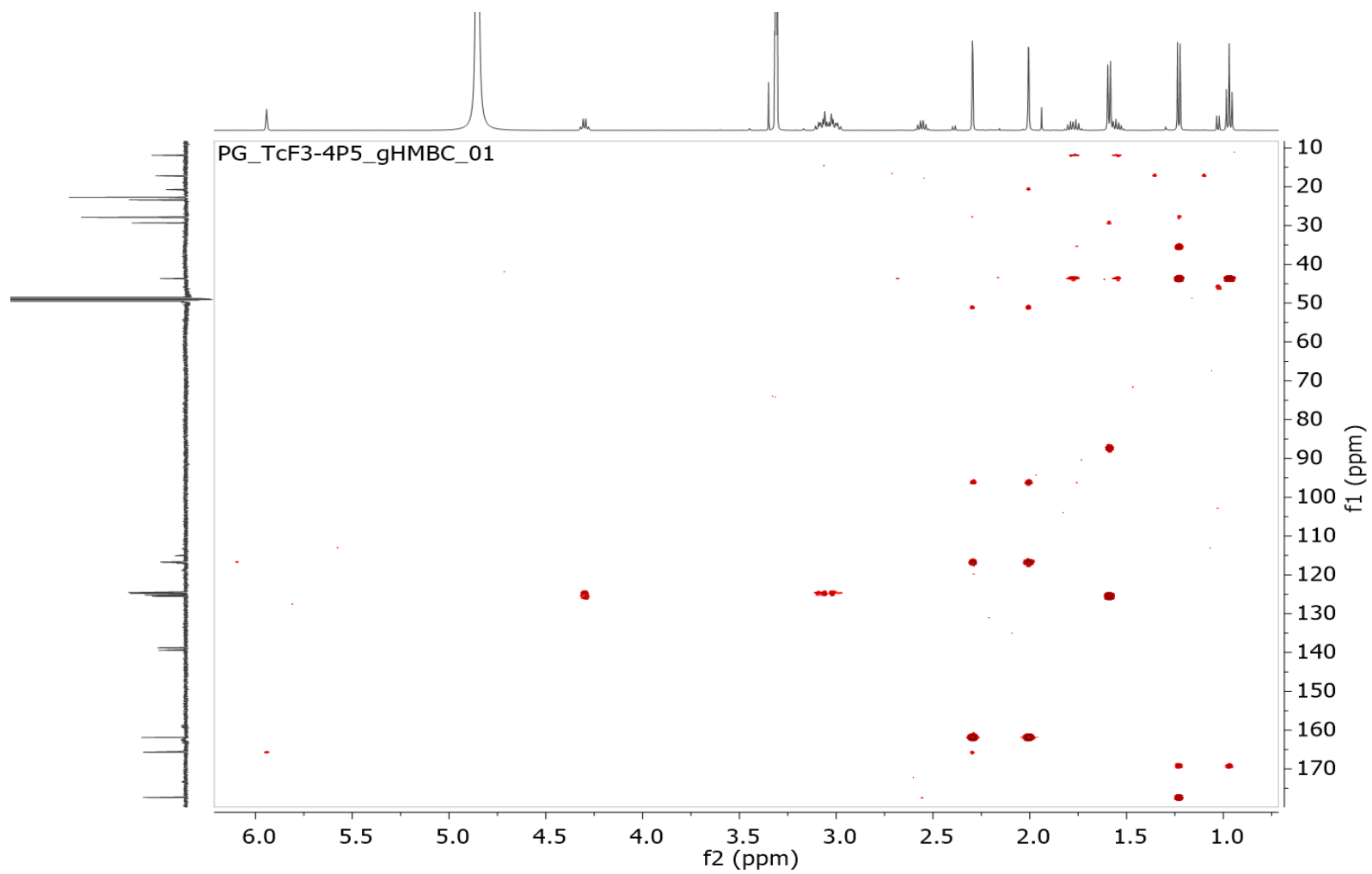
Figure S49. HMBC NMR spectrum of **zoamide E (7)** at 500 MHz in CD₃OD
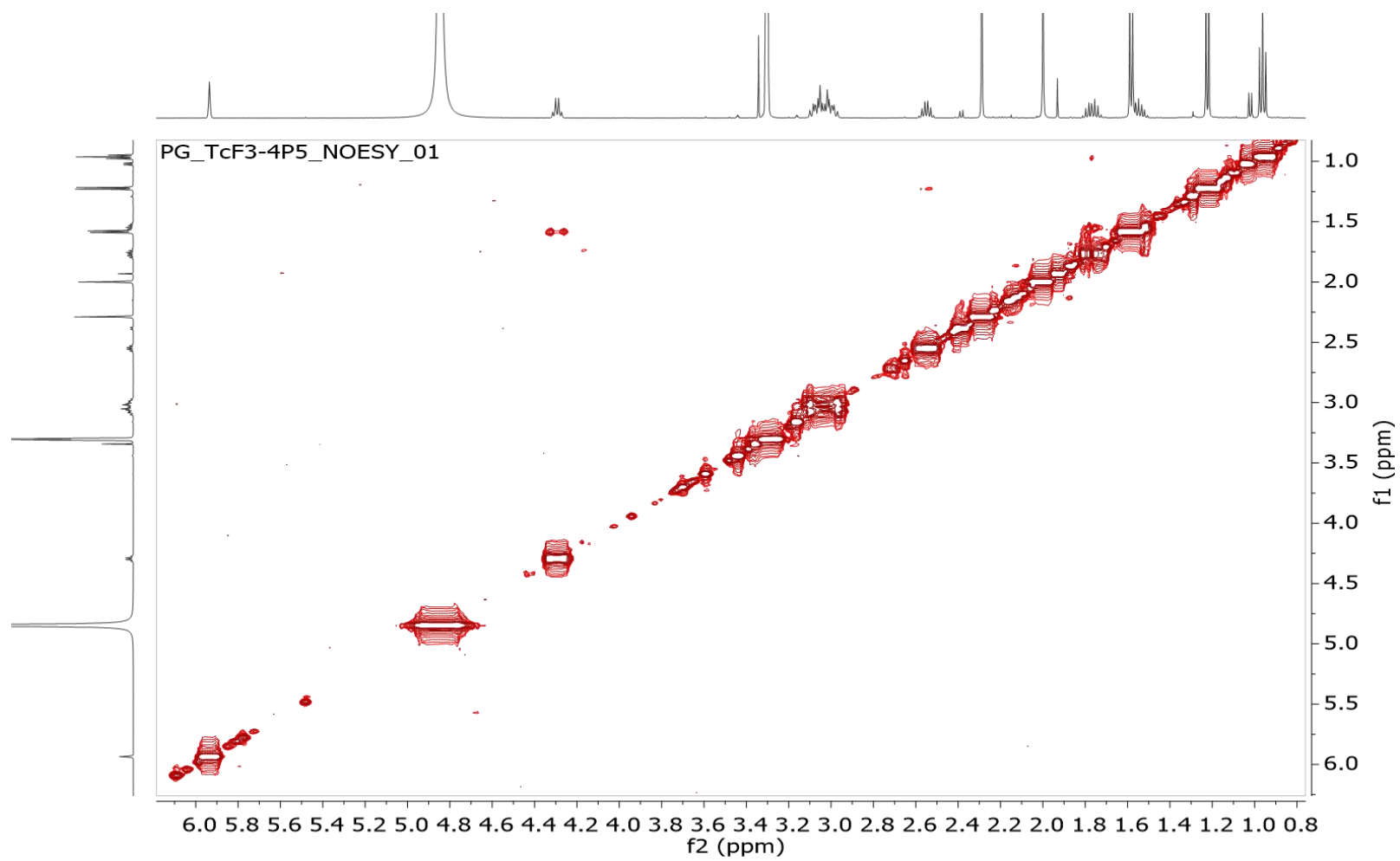
Figure S50. NOESY NMR spectrum of **zoamide E (7)** at 500 MHz in CD₃OD
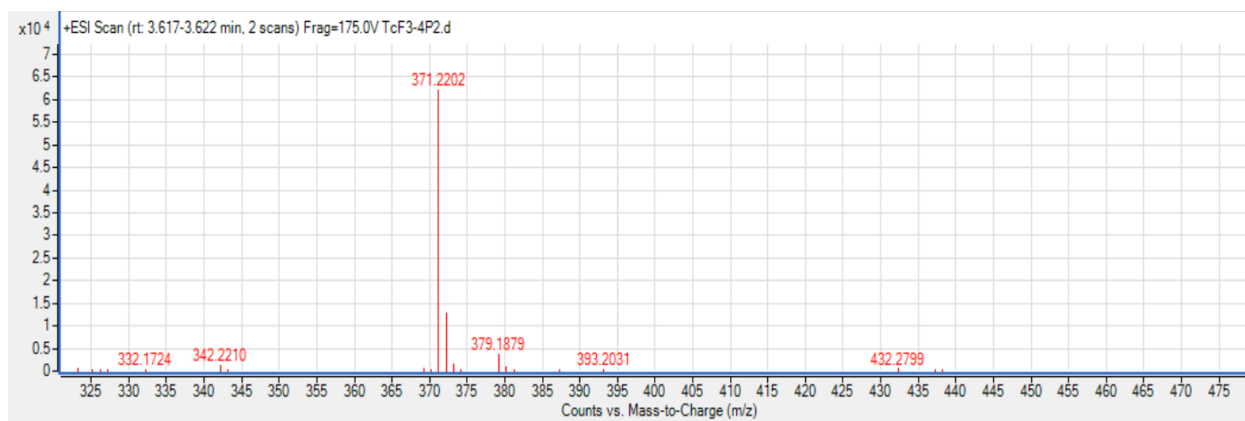
Figure S51. (+)-HRESIMS analysis of **zoamide F (8)** in (+)-ESI
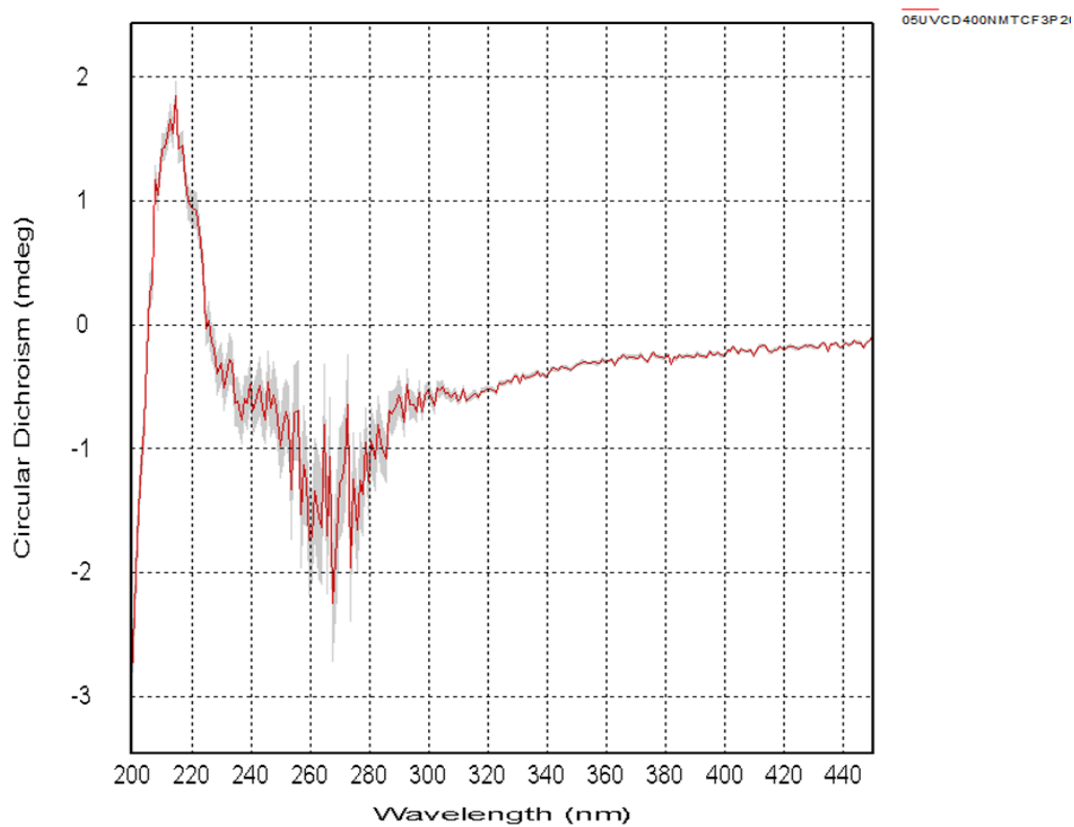
Figure S52. ECD spectrum of **zoamide F (8)**
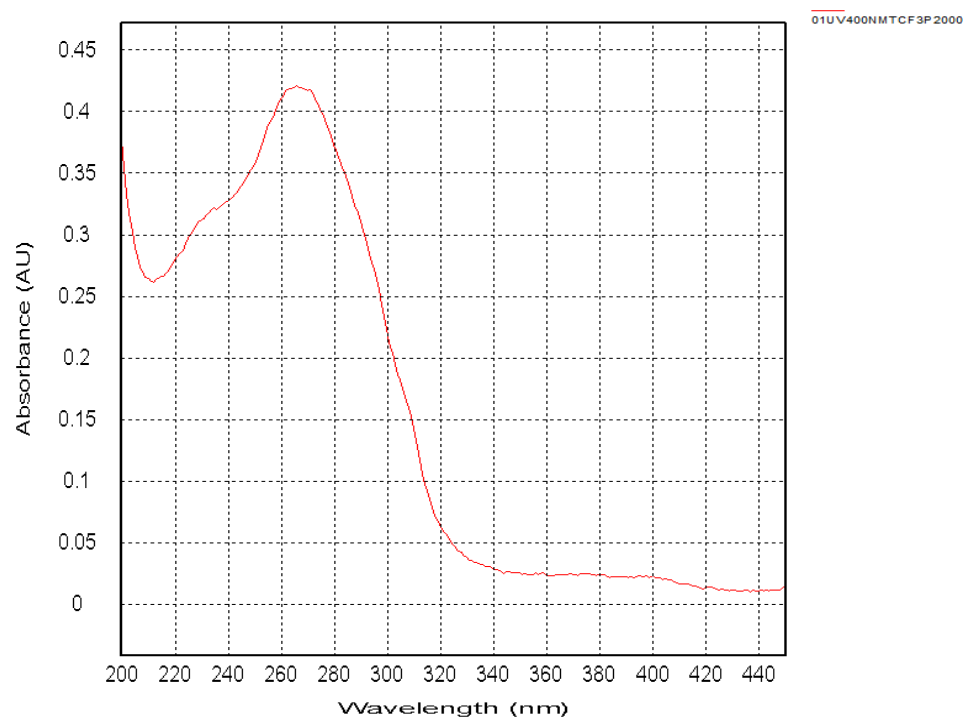
Figure S53. UV spectrum of **zoamide F (8)**
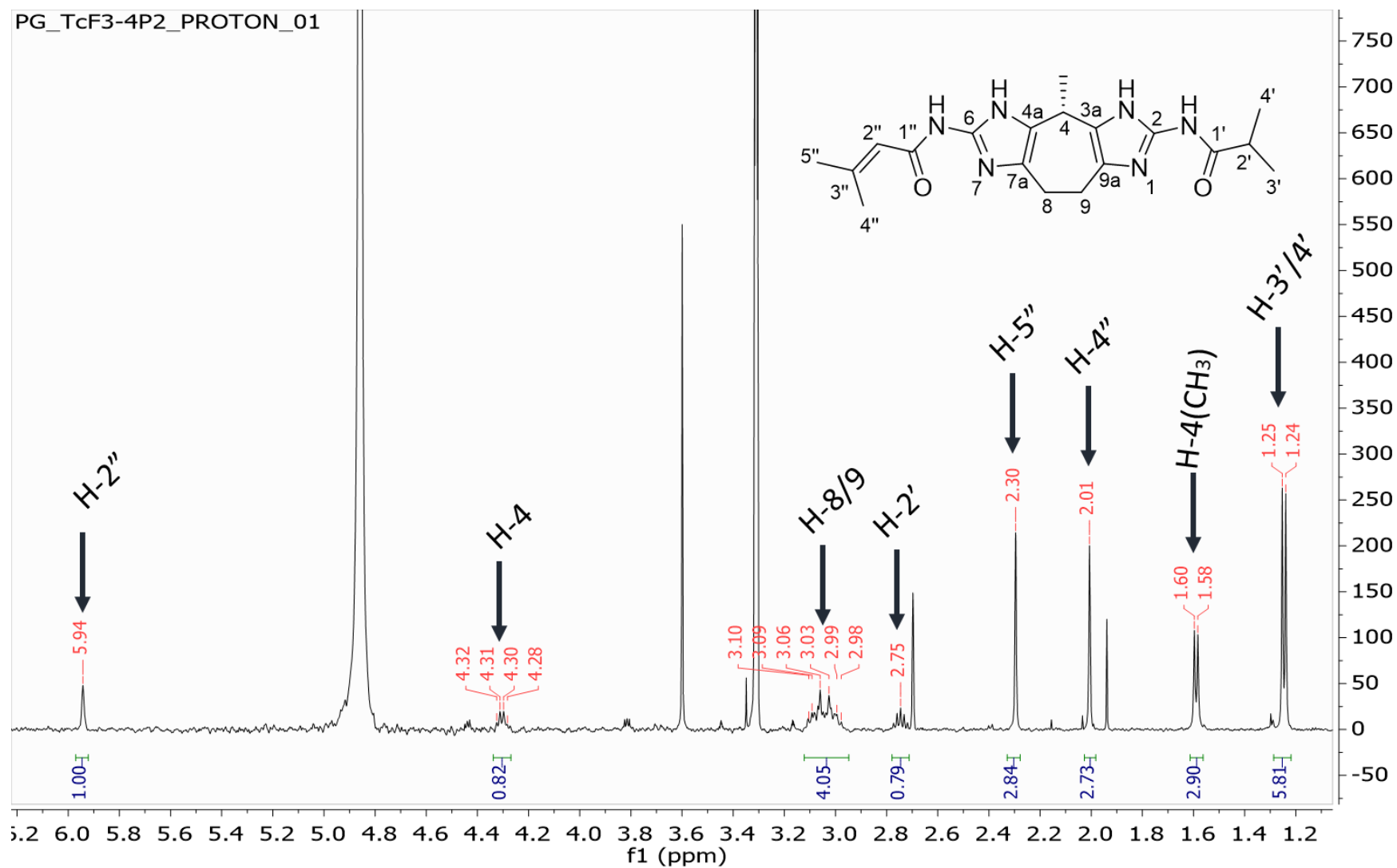
Figure S54. ¹H NMR spectrum of **zoamide F (8)** at 500 MHz in CD₃OD
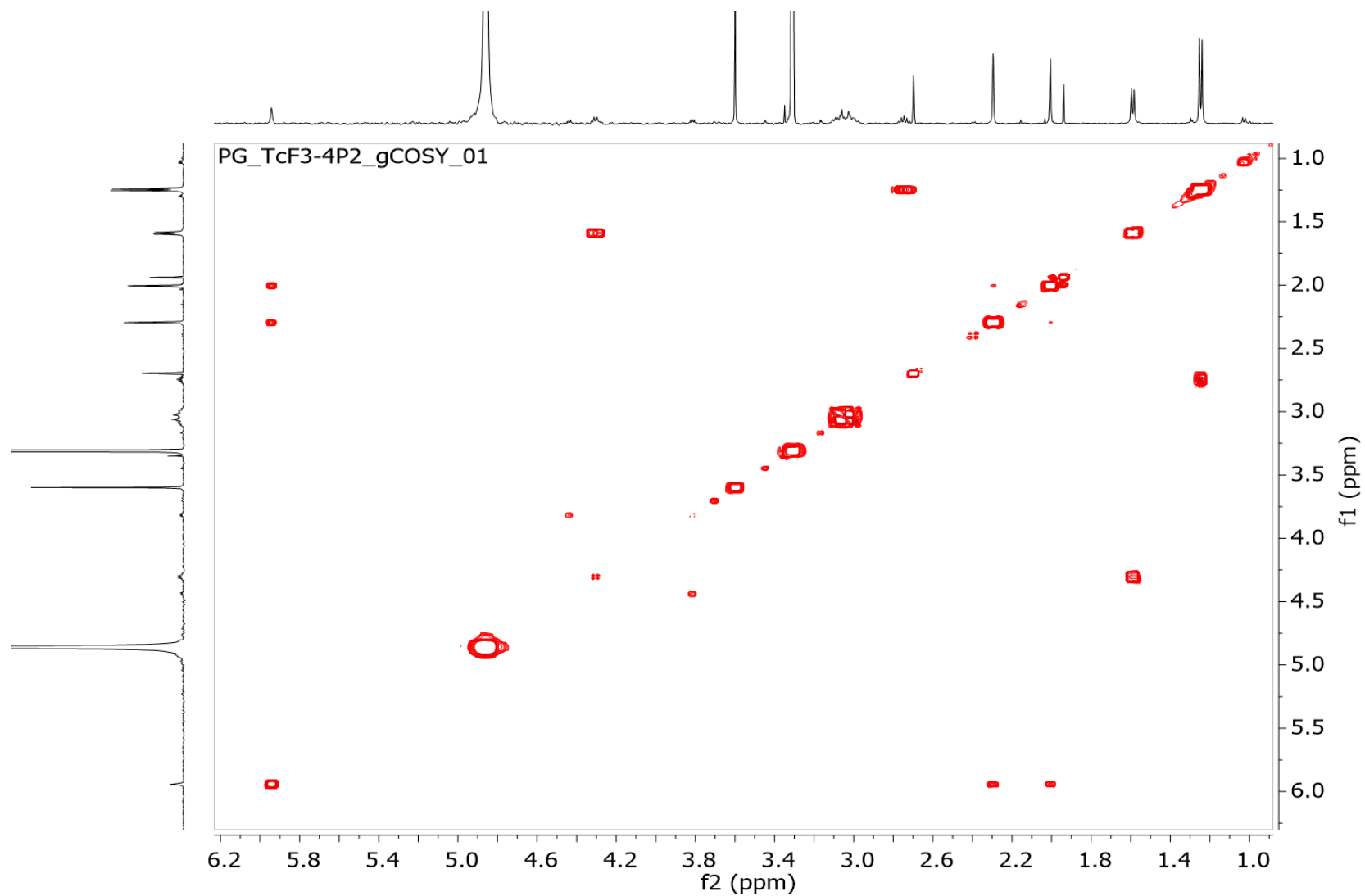
Figure S55. COSY NMR spectrum of **zoamide F (8)** at 500 MHz in CD₃OD
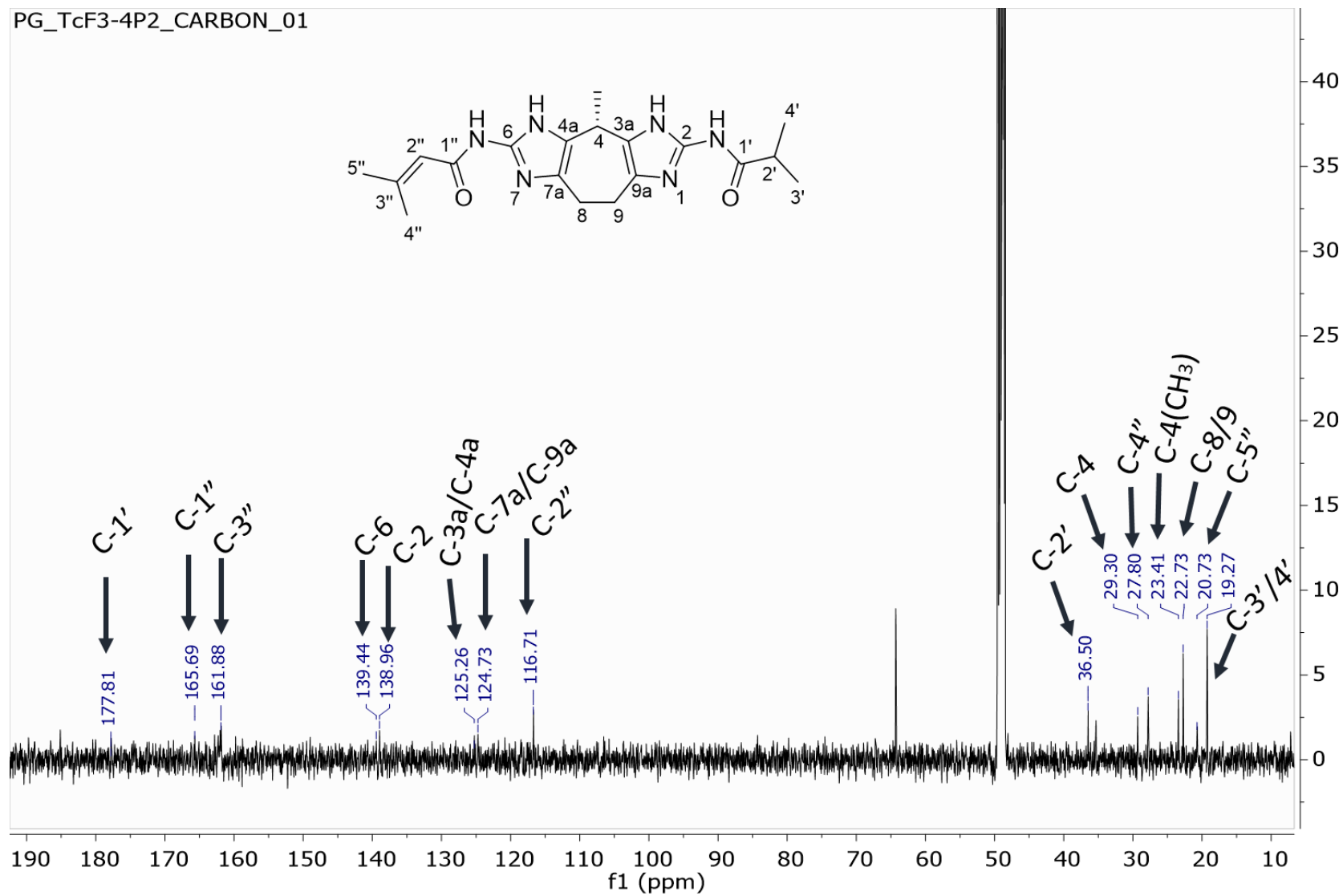
Figure S56. ¹³C NMR spectrum of **zoamide F (8)** at 125 MHz in CD₃OD
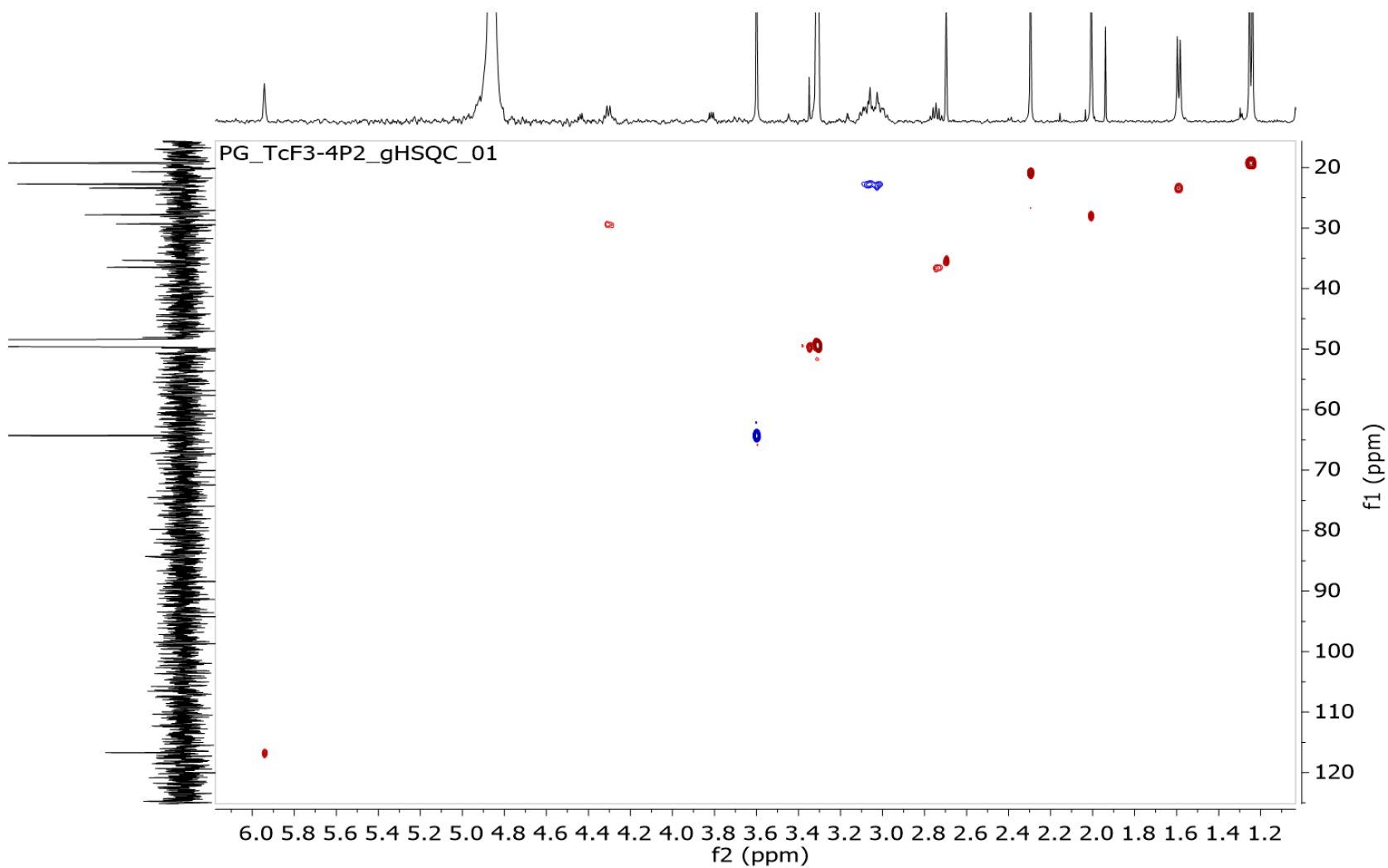
Figure S57. HSQC NMR spectrum of **zoamide F** at 500 MHz in CD₃OD
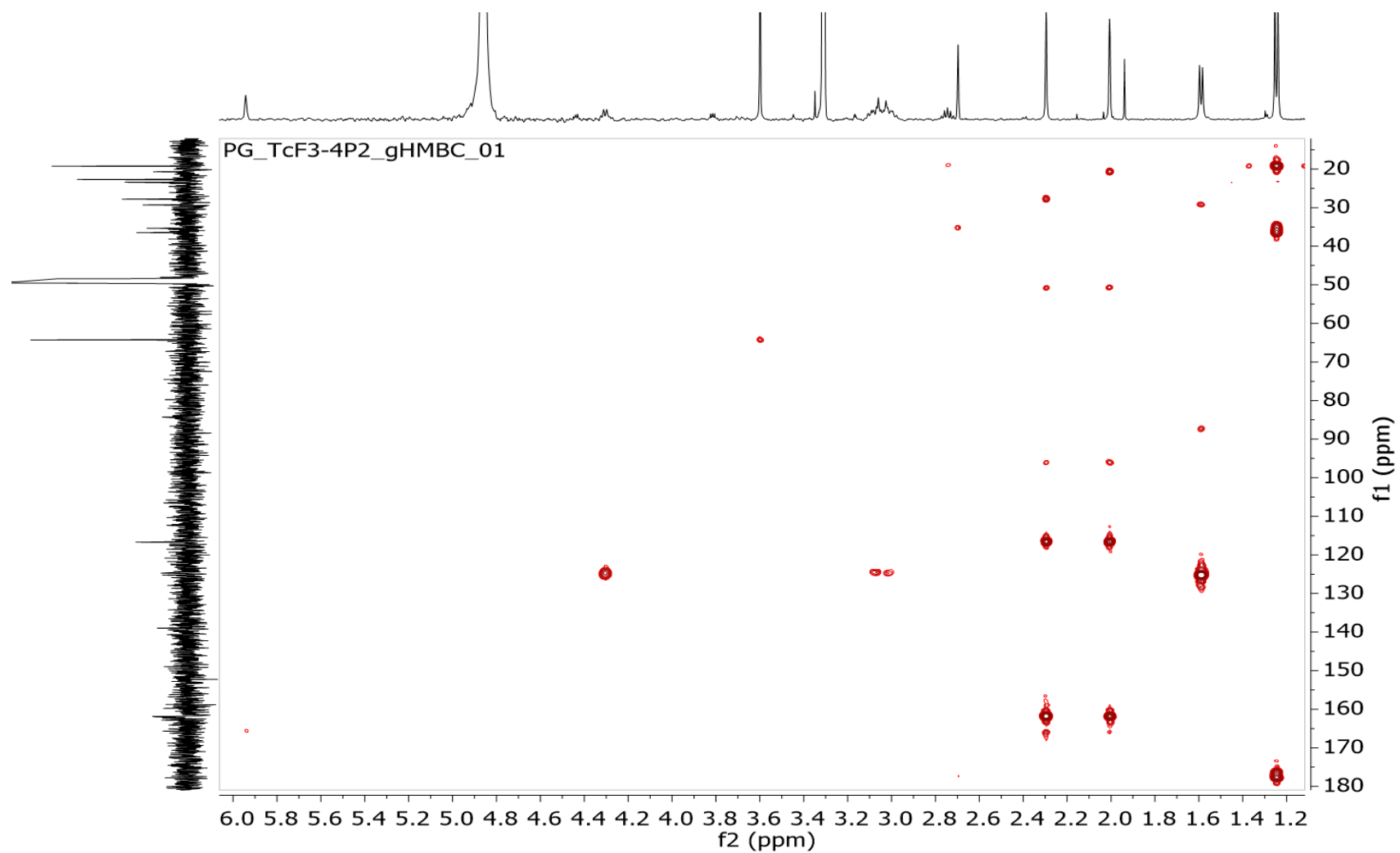
Figure S58. HMBC NMR spectrum of **zoamide F** at 500 MHz in CD₃OD
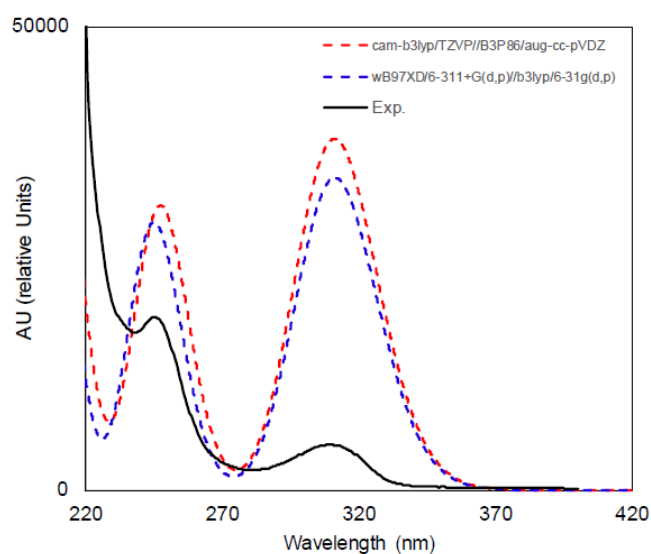
Figure S59: Predicted UV spectra of Zoamide F (**8**) with the ωB97X-D/6-311+G(d,p)// B3LYP/6-31G(d, p) and cam-B3LYP/def2-TZVP//B3P86/aug-cc-pVDZ functional/basis set combinations and the matching experimental UV spectrum of **8**.
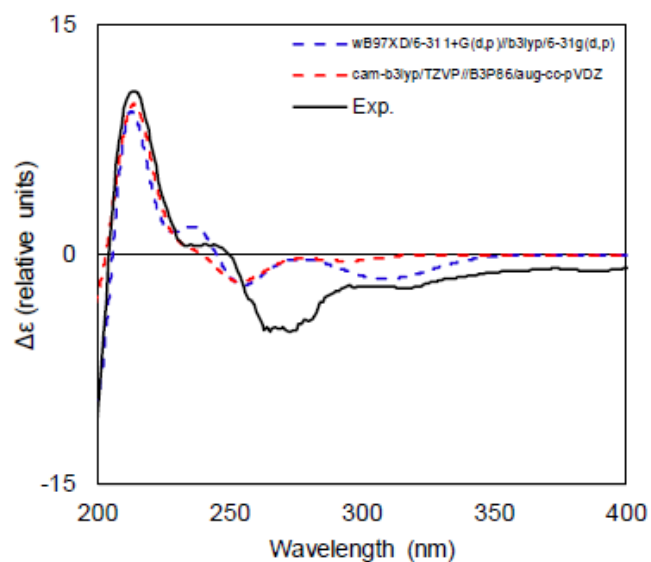
Figure S60: The predicted ECD of the R configuration of the C-4 chiral center of Zoamide F (**8**) with the matching experimental spectrum of **8**.

Table S1: The Cartesian coordinates of conformer 1 of Valdiviamide A (**1**)

Atom	Coordinates		
	X	Y	Z
C	-0.83603	-0.63325	1.114471
C	-2.04457	-1.18298	0.677686
C	-3.00992	-0.37635	0.088486
C	-2.82495	1.002856	-0.08879
C	-1.60984	1.53571	0.365228
C	-0.63632	0.741764	0.955827
C	0.234291	-1.49951	1.740682
Br	-1.29418	3.415228	0.174181
O	-3.73032	1.829119	-0.65069
Br	-4.66149	-1.16564	-0.49346
C	1.25099	-2.11152	0.735999
N	1.979013	-1.10426	-0.02332
C	0.581366	-3.15406	-0.15934
C	3.251943	-0.76727	0.26813
C	3.810969	0.306841	-0.68107
N	5.272571	0.64567	-0.49748
O	3.901628	-1.24714	1.189192
C	5.628969	1.670075	-1.54783
C	5.531374	1.248168	0.864502
C	6.148188	-0.56949	-0.69835
O	-0.03315	-4.09177	0.292655
O	0.74059	-2.92346	-1.46677
H	-2.24182	-2.24146	0.803317
H	0.281426	1.201821	1.304437
H	-0.22028	-2.32854	2.286763
H	0.81204	-0.91338	2.459095
H	-4.53053	1.340747	-0.91655
H	1.993277	-2.65993	1.322817
H	1.514504	-0.67912	-0.8226
H	3.247919	1.234253	-0.54803
H	3.686538	-0.01929	-1.71658
H	6.677409	1.936584	-1.42405
H	5.465454	1.237034	-2.53366
H	4.999771	2.548637	-1.41223
H	6.580981	1.534973	0.910285
H	4.899	2.12839	0.975982
H	5.298156	0.507013	1.621815
H	7.187034	-0.24706	-0.64602
H	5.928095	-1.29021	0.082448
H	5.936524	-0.98733	-1.68214
H	0.282931	-3.62838	-1.97368

Table S2: The Cartesian coordinates of conformer 2 of Valdiviamide A (**1**)

Atom	Coordinates		
	X	Y	Z
C	-0.79659	0.671099	-1.06898
C	-0.52522	-0.68977	-0.8944
C	-1.47482	-1.53542	-0.33782
C	-2.73594	-1.0717	0.064259
C	-2.99325	0.293494	-0.13144
C	-2.05182	1.151552	-0.68588
C	0.24636	1.59737	-1.65375
Br	-4.71015	0.992369	0.373141
O	-3.61262	-1.94735	0.596569
Br	-1.05969	-3.39269	-0.12108
C	1.195114	2.255165	-0.61074
N	1.96114	1.281144	0.155687
C	0.434315	3.236335	0.279833
C	3.236952	0.974088	-0.15396
C	3.881629	0.014779	0.859651
N	5.159492	-0.65318	0.401801
O	3.842033	1.426626	-1.11855
C	5.559527	-1.63822	1.473384
C	4.950431	-1.40724	-0.88981
C	6.277606	0.351389	0.236244
O	-0.20148	4.15815	-0.17494
O	0.53633	2.968552	1.585971
H	0.430442	-1.098	-1.20322
H	-2.30405	2.196473	-0.82617
H	-0.23345	2.40562	-2.20942
H	0.879183	1.04965	-2.35579
H	-4.44834	-1.50451	0.831849
H	1.916742	2.857994	-1.16916
H	1.518469	0.851592	0.964698
H	3.181519	-0.7817	1.121082
H	4.119078	0.57119	1.770489
H	6.4963	-2.10658	1.175499
H	5.689612	-1.10329	2.413141
H	4.778231	-2.39053	1.572151
H	5.86745	-1.9493	-1.11589
H	4.12786	-2.10831	-0.75139
H	4.722933	-0.69564	-1.6774
H	7.17844	-0.19342	-0.04265
H	5.994311	1.059709	-0.53517
H	6.426959	0.857264	1.189559
H	0.018523	3.631883	2.091215

Table S3: The Cartesian coordinates of conformer 3 of Valdiviamide A (**1**)

Atom	Coordinates		
	X	Y	Z
C	-0.66913	-1.24024	-1.06396
C	-0.97301	0.004015	-1.62052
C	-1.97893	0.794543	-1.08011
C	-2.7244	0.383703	0.033181
C	-2.40636	-0.87188	0.573668
C	-1.40393	-1.67251	0.043151
C	0.43474	-2.09828	-1.63949
Br	-3.406	-1.49558	2.090777
O	-3.68805	1.197142	0.511103
Br	-2.36432	2.492322	-1.87889
C	1.75041	-2.02938	-0.82373
N	2.30409	-0.68538	-0.80733
C	2.735308	-3.09063	-1.33041
C	2.73224	-0.08962	0.32445
C	3.349505	1.294973	0.066438
N	3.654635	2.114042	1.300083
O	2.653397	-0.58621	1.441275
C	2.410433	2.348363	2.124618
C	4.719124	1.4564	2.14878
C	4.177483	3.450598	0.831793
O	2.440927	-4.26084	-1.40781
O	3.930262	-2.59528	-1.66713
H	-0.42791	0.360613	-2.4874
H	-1.20058	-2.63829	0.493587
H	0.639791	-1.7966	-2.67155
H	0.126167	-3.14506	-1.66617
H	-4.13388	0.79605	1.278561
H	1.540164	-2.29803	0.215165
H	2.448206	-0.22241	-1.7031
H	2.676176	1.890666	-0.55419
H	4.29044	1.170291	-0.47639
H	2.670784	3.017949	2.943016
H	1.657683	2.812557	1.488181
H	2.059767	1.394271	2.504808
H	4.941289	2.121419	2.982099
H	4.340697	0.502866	2.501753
H	5.608586	1.316754	1.535231
H	4.421325	4.048831	1.708288
H	5.069234	3.288762	0.227829
H	3.406694	3.945081	0.242317
H	4.502033	-3.33133	-1.97416

Table S4: The Cartesian coordinates of conformer 4 of Valdiviamide A (**1**)

Atom	Coordinates		
	X	Y	Z
C	-0.83763	-0.6207	1.103299
C	-2.04362	-1.19146	0.68137
C	-3.03081	-0.40885	0.099086
C	-2.86898	0.972168	-0.08676
C	-1.65724	1.525697	0.350692
C	-0.66059	0.754879	0.936346
C	0.248873	-1.47126	1.723258
Br	-1.38038	3.414564	0.13939
O	-3.86816	1.675849	-0.65618
Br	-4.66872	-1.23081	-0.4568
C	1.272537	-2.06653	0.71527
N	2.01105	-1.04674	-0.01705
C	0.608048	-3.09014	-0.20495
C	3.285082	-0.72843	0.291001
C	3.852729	0.385898	-0.60454
N	5.337405	0.637751	-0.46949
O	3.92861	-1.24727	1.19521
C	5.704784	1.699016	-1.47851
C	5.687114	1.149906	0.909519
C	6.134595	-0.60914	-0.77351
O	0.003741	-4.04499	0.224374
O	0.757152	-2.82173	-1.50623
H	-2.22052	-2.25245	0.815364
H	0.2526	1.233326	1.272009
H	-0.19282	-2.30852	2.267414
H	0.820255	-0.87997	2.442599
H	-3.63557	2.619775	-0.72417
H	2.008188	-2.62745	1.298215
H	1.554224	-0.59694	-0.80718
H	3.345535	1.325776	-0.37102
H	3.663103	0.150066	-1.65435
H	6.769051	1.908243	-1.38296
H	5.483183	1.328376	-2.47834
H	5.125518	2.597882	-1.272
H	6.753125	1.372331	0.923556
H	5.113871	2.058066	1.09309
H	5.439403	0.383935	1.636751
H	7.191014	-0.34534	-0.75718
H	5.913513	-1.35705	-0.0188
H	5.854225	-0.96422	-1.76478
H	0.30147	-3.51552	-2.03005

Table S5: The Cartesian coordinates of conformer 5 of Valdiviamide A (**1**)

Atom	Coordinates		
	X	Y	Z
C	0.782281	-0.68851	-0.99952
C	2.062812	-1.14617	-0.6784
C	3.013293	-0.27314	-0.16412
C	2.740396	1.085902	0.049585
C	1.452299	1.526784	-0.28778
C	0.493338	0.665598	-0.80251
C	-0.26556	-1.6334	-1.54362
Br	1.012677	3.37461	-0.04
O	3.626498	1.975976	0.540874
Br	4.764017	-0.94077	0.259144
C	-1.19059	-2.28034	-0.46996
N	-1.99619	-1.30995	0.257704
C	-0.40806	-3.10531	0.544814
C	-3.17464	-0.86433	-0.21635
C	-3.86466	0.123394	0.740479
N	-5.25143	0.566822	0.334487
O	-3.64851	-1.19159	-1.29838
C	-5.76467	1.480609	1.421244
C	-5.224	1.338431	-0.96505
C	-6.19169	-0.61007	0.215681
O	-0.3492	-2.85863	1.727138
O	0.214607	-4.12986	-0.04388
H	2.328719	-2.18519	-0.83735
H	-0.48345	1.057315	-1.06245
H	0.210226	-2.44559	-2.09704
H	-0.91956	-1.10689	-2.24215
H	4.479049	1.546716	0.73744
H	-1.86785	-2.96021	-0.99609
H	-1.67851	-1.05138	1.190556
H	-3.25321	1.024999	0.829645
H	-3.95089	-0.32642	1.732554
H	-6.75987	1.821442	1.140189
H	-5.80808	0.926374	2.357757
H	-5.08976	2.330077	1.516254
H	-6.2349	1.688891	-1.16825
H	-4.55176	2.187472	-0.84554
H	-4.87617	0.678468	-1.75289
H	-7.18971	-0.22378	0.014133
H	-5.85284	-1.24582	-0.59587
H	-6.18552	-1.15216	1.160864
H	0.722632	-4.63058	0.630015

Table S6: The Cartesian coordinates of conformer 6 of Valdiviamide A (**1**)

Atom	Coordinates		
	X	Y	Z
C	0.837877	-0.62084	-1.10363
C	2.04375	-1.19157	-0.68127
C	3.030753	-0.40891	-0.09879
C	2.868939	0.972173	0.086786
C	1.657343	1.525631	-0.35109
C	0.660817	0.754754	-0.93689
C	-0.24851	-1.47137	-1.72384
Br	1.380349	3.414493	-0.13998
O	3.868146	1.676009	0.655969
Br	4.668463	-1.23083	0.457784
C	-1.27253	-2.06634	-0.71611
N	-2.01075	-1.04636	0.016189
C	-0.60849	-3.09032	0.20411
C	-3.28498	-0.72821	-0.29121
C	-3.85234	0.385928	0.60473
N	-5.33708	0.637843	0.470198
O	-3.92883	-1.24698	-1.19523
C	-5.68715	1.150618	-0.90851
C	-6.13422	-0.60912	0.773823
C	-5.70414	1.698678	1.479789
O	-0.00459	-4.04536	-0.22534
O	-0.75734	-2.82188	1.50537
H	2.220624	-2.2526	-0.81504
H	-0.25228	1.233189	-1.27281
H	0.193247	-2.30876	-2.26774
H	-0.81956	-0.88007	-2.44344
H	3.634444	2.619498	0.726249
H	-2.00829	-2.62699	-1.2992
H	-1.55385	-0.5968	0.806406
H	-3.34524	1.32589	0.371376
H	-3.66244	0.149791	1.654432
H	-6.75322	1.372813	-0.92223
H	-5.11413	2.058988	-1.09171
H	-5.43942	0.385008	-1.63611
H	-7.19062	-0.3452	0.758012
H	-5.9135	-1.35667	0.018648
H	-5.85354	-0.96479	1.76479
H	-6.76838	1.908177	1.38447
H	-5.4825	1.327475	2.479399
H	-5.12473	2.597549	1.273694
H	-0.302	-3.51587	2.029189

Table S7: The Cartesian coordinates of conformer 7 of Valdiviamide A (**1**)

Atom	Coordinates		
	X	Y	Z
C	-0.66917	-1.24005	-1.06406
C	-0.97285	0.004337	-1.62042
C	-1.97877	0.794859	-1.07998
C	-2.72441	0.383893	0.03315
C	-2.40656	-0.87183	0.573442
C	-1.40415	-1.67245	0.04289
C	0.434676	-2.09813	-1.63957
Br	-3.40641	-1.49574	2.090313
O	-3.68802	1.197348	0.511138
Br	-2.36388	2.492828	-1.87848
C	1.750282	-2.02946	-0.8237
N	2.304221	-0.68556	-0.8073
C	2.735018	-3.09093	-1.33026
C	2.732406	-0.08983	0.324483
C	3.350127	1.294552	0.066447
N	3.65481	2.113833	1.300067
O	2.653294	-0.58631	1.441337
C	4.178114	3.450204	0.831753
C	2.410259	2.348539	2.12397
C	4.71879	1.456179	2.149403
O	2.440367	-4.26106	-1.40773
O	3.930142	-2.59587	-1.66678
H	-0.42763	0.36106	-2.48717
H	-1.20094	-2.63834	0.493162
H	0.639857	-1.79636	-2.67159
H	0.125976	-3.14486	-1.66642
H	-4.13409	0.796069	1.278364
H	1.539916	-2.29803	0.215191
H	2.448569	-0.22269	-1.70308
H	2.677275	1.890273	-0.55466
H	4.291322	1.169504	-0.47585
H	4.421731	4.048537	1.708241
H	5.070072	3.288084	0.228171
H	3.407658	3.944739	0.241886
H	2.670324	3.018302	2.942312
H	1.657861	2.81267	1.487068
H	2.059272	1.394595	2.50424
H	4.940635	2.121307	2.98272
H	4.340053	0.502754	2.502337
H	5.608533	1.316309	1.536313
H	4.501784	-3.33206	-1.97372

Table S8: The Cartesian coordinates of conformer 8 of Valdiviamide A (**1**)

Atom	Coordinates		
	X	Y	Z
C	-0.78699	-0.70387	1.002213
C	-2.07427	-1.14337	0.675623
C	-3.01464	-0.26087	0.161109
C	-2.72217	1.094645	-0.05006
C	-1.42951	1.516372	0.293282
C	-0.47992	0.645121	0.81062
C	0.24961	-1.66224	1.544043
Br	-0.9653	3.363194	0.047973
O	-3.68042	1.900952	-0.55107
Br	-4.7673	-0.90554	-0.2638
C	1.174513	-2.3071	0.468631
N	1.97743	-1.33472	-0.25944
C	0.39114	-3.13159	-0.54597
C	3.157373	-0.88804	0.210129
C	3.84344	0.097929	-0.75183
N	5.217034	0.571239	-0.33532
O	3.635823	-1.21401	1.290449
C	5.721951	1.488857	-1.42277
C	5.161918	1.349301	0.959318
C	6.179829	-0.58563	-0.20069
O	0.329322	-2.88276	-1.72771
O	-0.22848	-4.15814	0.042257
H	-2.35264	-2.17967	0.831432
H	0.500165	1.025584	1.07467
H	-0.2352	-2.4751	2.088542
H	0.904607	-1.14662	2.249752
H	-3.34929	2.811184	-0.65754
H	1.853181	-2.98679	0.993139
H	1.655975	-1.07506	-1.19071
H	3.218233	0.987536	-0.86275
H	3.950001	-0.36538	-1.73575
H	6.708699	1.848991	-1.13604
H	5.782413	0.93094	-2.35614
H	5.032615	2.32556	-1.52709
H	6.162952	1.723704	1.1685
H	4.471709	2.182339	0.829786
H	4.822979	0.686228	1.74846
H	7.167144	-0.17791	0.011185
H	5.844154	-1.22508	0.609254
H	6.196118	-1.13115	-1.14374
H	-0.73759	-4.65835	-0.63117

Table S9: The Cartesian coordinates of conformer 9 of Valdiviamide A (**1**)

Atom	Coordinates		
	X	Y	Z
C	-0.51363	-1.30721	-1.03322
C	-0.67737	-0.03356	-1.58272
C	-1.67814	0.81191	-1.12088
C	-2.55933	0.428194	-0.10058
C	-2.38289	-0.85927	0.429756
C	-1.38573	-1.71334	-0.02026
C	0.587356	-2.22578	-1.51017
Br	-3.57094	-1.45276	1.816936
O	-3.51052	1.295112	0.302732
Br	-1.86762	2.550459	-1.90255
C	1.854506	-2.18205	-0.60808
N	2.489445	-0.87458	-0.60938
C	2.861561	-3.23516	-1.07028
C	2.554703	-0.08966	0.485498
C	3.399887	1.174693	0.253817
N	3.279152	2.243535	1.316742
O	2.02324	-0.34563	1.558536
C	4.099888	3.424718	0.858843
C	1.845703	2.689507	1.483472
C	3.82832	1.768237	2.642903
O	3.910196	-2.98845	-1.61798
O	2.416229	-4.46991	-0.81424
H	-0.02557	0.30328	-2.38101
H	-1.29172	-2.70018	0.420262
H	0.876955	-1.96407	-2.53234
H	0.230004	-3.25771	-1.52726
H	-4.05939	0.906731	1.008355
H	1.57037	-2.41024	0.42125
H	2.997664	-0.60982	-1.45177
H	3.126596	1.637758	-0.69691
H	4.454616	0.89087	0.202817
H	4.04555	4.197039	1.62446
H	5.131805	3.10486	0.720918
H	3.691503	3.797068	-0.07964
H	1.831924	3.523666	2.183387
H	1.468796	3.010949	0.513037
H	1.263947	1.85748	1.867394
H	3.767437	2.597143	3.346643
H	3.235669	0.924628	2.980457
H	4.868175	1.476964	2.498076
H	3.062959	-5.12473	-1.15405

Table S10: The Cartesian coordinates of conformer 10 of Valdiviamide A (**1**)

Atom	Coordinates		
	X	Y	Z
C	-0.79341	-0.26363	-0.60453
C	-1.12462	1.06416	-0.31617
C	-2.44236	1.42695	-0.07937
C	-3.48801	0.491402	-0.12032
C	-3.1329	-0.83286	-0.41213
C	-1.8174	-1.20967	-0.65367
C	0.642627	-0.66086	-0.85752
Br	-4.51417	-2.16499	-0.48024
O	-4.74851	0.91071	0.113445
Br	-2.8544	3.257835	0.303433
C	1.524403	-0.79526	0.421818
N	2.910242	-1.06976	0.060597
C	1.040821	-1.93525	1.31227
C	3.820632	-0.09159	-0.10241
C	5.185072	-0.61861	-0.57682
N	6.356626	0.305835	-0.32475
O	3.593867	1.10017	0.073157
C	6.265458	1.557319	-1.16876
C	6.450482	0.676827	1.135656
C	7.610107	-0.43926	-0.71433
O	1.431311	-3.07628	1.209546
O	0.122513	-1.52812	2.18902
H	-0.35153	1.824297	-0.28095
H	-1.59475	-2.24619	-0.88235
H	1.129743	0.091955	-1.48294
H	0.681454	-1.60852	-1.40166
H	-5.37951	0.17081	0.047992
H	1.495773	0.138799	0.984268
H	3.165374	-2.04691	-0.07492
H	5.139589	-0.79303	-1.65529
H	5.416681	-1.56676	-0.08737
H	7.155524	2.155113	-0.97748
H	6.232193	1.261172	-2.21669
H	5.36464	2.095091	-0.89264
H	7.363506	1.252347	1.280409
H	5.58042	1.268872	1.40302
H	6.490616	-0.23979	1.723542
H	8.461525	0.224241	-0.57118
H	7.709629	-1.32019	-0.0817
H	7.534583	-0.73245	-1.76055
H	-0.20241	-2.30099	2.70014

Table S11: The Cartesian coordinates of conformer 11 of Valdiviamide A (**1**)

Atom	Coordinates		
	X	**Y**	**Z**
C	-0.76719	-1.10606	-1.1189
C	-1.15247	0.140907	-1.61075
C	-2.16807	0.857096	-0.9874
C	-2.83862	0.371215	0.142582
C	-2.43668	-0.88655	0.619155
C	-1.42701	-1.61297	0.005685
C	0.337853	-1.89735	-1.78194
Br	-3.31845	-1.6198	2.152889
O	-3.82937	1.026125	0.781595
Br	-2.68132	2.567736	-1.69231
C	1.665385	-1.88229	-0.98437
N	2.212744	-0.53956	-0.87975
C	2.644286	-2.90118	-1.58248
C	2.732511	-0.05825	0.267801
C	3.207544	1.398314	0.139199
N	4.035416	1.917746	1.2932
O	2.79632	-0.68919	1.315685
C	3.223909	1.986856	2.567193
C	5.264736	1.06759	1.511378
C	4.476895	3.315933	0.934028
O	2.361732	-4.0705	-1.70523
O	3.816829	-2.37185	-1.94452
H	-0.6684	0.557479	-2.4871
H	-1.15683	-2.58468	0.405447
H	0.521444	-1.50833	-2.78851
H	0.040109	-2.9421	-1.89145
H	-4.01595	1.880329	0.352773
H	1.474058	-2.22952	0.034641
H	2.275969	0.015424	-1.73135
H	2.33516	2.051148	0.050945
H	3.811261	1.514478	-0.76394
H	3.853695	2.421866	3.341927
H	2.35869	2.624251	2.387803
H	2.913592	0.982317	2.834638
H	5.869361	1.541665	2.283092
H	4.952719	0.076051	1.823751
H	5.822566	1.021493	0.576506
H	5.055702	3.716259	1.76489
H	5.090251	3.273412	0.035077
H	3.594775	3.930723	0.760615
H	4.384178	-3.08347	-2.31149

Table S12: The Cartesian coordinates of conformer 12 of Valdiviamide A (**1**)

Atom	Coordinates		
	X	**Y**	**Z**
C	-0.78284	-0.29099	-0.57935
C	-1.09626	1.038982	-0.28886
C	-2.41369	1.415208	-0.06658
C	-3.4731	0.49644	-0.1249
C	-3.13636	-0.83033	-0.4274
C	-1.82269	-1.22057	-0.65145
C	0.650758	-0.70922	-0.81164
Br	-4.53162	-2.13778	-0.53787
O	-4.76803	0.81086	0.083348
Br	-2.81044	3.254312	0.320769
C	1.519196	-0.82818	0.478699
N	2.909331	-1.1059	0.137141
C	1.027232	-1.95692	1.378323
C	3.809999	-0.12609	-0.06386
C	5.186573	-0.66144	-0.49266
N	6.330974	0.320064	-0.36832
O	3.566671	1.06975	0.052045
C	6.177305	1.473241	-1.33459
C	6.448229	0.844488	1.04293
C	7.599152	-0.42315	-0.71213
O	1.435752	-3.09419	1.309537
O	0.08013	-1.54526	2.221577
H	-0.31369	1.788518	-0.23902
H	-1.61092	-2.25809	-0.88573
H	1.152126	0.026643	-1.44585
H	0.68408	-1.66694	-1.33813
H	-4.86852	1.758641	0.286189
H	1.482409	0.112787	1.029424
H	3.174254	-2.08573	0.046606
H	5.136898	-0.96522	-1.54182
H	5.451584	-1.53753	0.103042
H	7.053187	2.112637	-1.23414
H	6.124067	1.068445	-2.3447
H	5.268779	2.012132	-1.08743
H	7.343085	1.462378	1.100136
H	5.563606	1.430368	1.272536
H	6.537406	-0.00417	1.720577
H	8.431841	0.276234	-0.65606
H	7.739734	-1.23277	0.002615
H	7.511175	-0.82185	-1.72183
H	-0.24834	-2.31229	2.73914

Table S13: The Cartesian coordinates of conformer 13 of Valdiviamide A (**1**)

Atom	Coordinates		
	X	**Y**	**Z**
C	-0.71597	-1.20357	-1.07237
C	-1.09735	0.015345	-1.63217
C	-2.11039	0.769007	-1.05111
C	-2.7847	0.349264	0.103278
C	-2.38666	-0.88184	0.648582
C	-1.37825	-1.64502	0.077996
C	0.390468	-2.02699	-1.69224
Br	-3.27209	-1.52603	2.219892
O	-3.77466	1.041688	0.704351
Br	-2.60728	2.43916	-1.85628
C	1.724209	-1.95009	-0.90813
N	2.24009	-0.59188	-0.85885
C	2.720443	-2.96701	-1.47951
C	2.75478	-0.05512	0.266285
C	3.267738	1.379424	0.056444
N	3.807268	2.067336	1.289516
O	2.808715	-0.63213	1.345258
C	5.012238	1.341015	1.841831
C	4.234442	3.455225	0.876964
C	2.746136	2.192628	2.358388
O	2.467679	-4.14741	-1.54973
O	3.871539	-2.4218	-1.88487
H	-0.6113	0.381248	-2.52975
H	-1.11142	-2.59351	0.532084
H	0.562585	-1.6992	-2.72239
H	0.102191	-3.07923	-1.73458
H	-3.95553	1.87292	0.229778
H	1.549298	-2.26232	0.124889
H	2.289695	-0.07068	-1.73252
H	2.458346	2.003661	-0.32987
H	4.072267	1.371083	-0.6836
H	5.400318	1.922152	2.677062
H	4.703394	0.353175	2.167349
H	5.762345	1.272638	1.054522
H	4.632316	3.96534	1.75278
H	5.00185	3.37508	0.108323
H	3.368452	3.991502	0.491465
H	3.166338	2.767405	3.182418
H	1.891524	2.718833	1.934249
H	2.463161	1.19756	2.685639
H	4.451517	-3.13193	-2.2345

Table S14: The Cartesian coordinates of conformer 14 of Valdiviamide A (**1**)

Atom	Coordinates		
	X	**Y**	**Z**
C	-0.82816	-0.24833	-0.66063
C	-1.83682	-1.21479	-0.65625
C	-3.15187	-0.86307	-0.38042
C	-3.52032	0.459876	-0.10003
C	-2.49258	1.415686	-0.11795
C	-1.17425	1.078276	-0.39058
C	0.608668	-0.62708	-0.94267
Br	-2.93862	3.249407	0.236783
O	-4.81397	0.737277	0.15987
Br	-4.50358	-2.21937	-0.38824
C	1.50334	-0.69268	0.32649
N	2.886745	-1.00158	-0.02907
C	0.978556	-1.71732	1.332916
C	3.873176	-0.08223	0.022703
C	5.231281	-0.65624	-0.41813
N	6.405447	0.290015	-0.31518
O	3.722004	1.081057	0.377242
C	7.631883	-0.47079	-0.75834
C	6.230349	1.485407	-1.22358
C	6.618086	0.751073	1.108346
O	0.371984	-1.42872	2.356342
O	1.240075	-2.97523	0.935759
H	-1.60007	-2.25056	-0.87355
H	-0.41694	1.854914	-0.39745
H	1.067653	0.109031	-1.60855
H	0.648091	-1.59438	-1.45023
H	-4.9373	1.686368	0.343274
H	1.504024	0.274138	0.828039
H	3.089059	-1.94549	-0.35386
H	5.167827	-0.97533	-1.46164
H	5.471933	-1.5316	0.190105
H	8.488811	0.198599	-0.70183
H	7.777283	-1.32339	-0.09648
H	7.486685	-0.80894	-1.78339
H	7.134153	2.089674	-1.16059
H	6.092675	1.125043	-2.24255
H	5.363921	2.048696	-0.89287
H	7.527066	1.350219	1.134715
H	5.758953	1.338015	1.416134
H	6.732818	-0.12859	1.741019
H	0.885856	-3.60874	1.59529

Table S15: The Cartesian coordinates of conformer 15 of Valdiviamide A (**1**)

Atom	Coordinates		
	X	**Y**	**Z**
C	-0.87909	-0.26544	-0.72007
C	-1.8754	-1.24027	-0.66172
C	-3.18354	-0.88787	-0.34858
C	-3.55477	0.436662	-0.08113
C	-2.53696	1.401322	-0.14933
C	-1.22925	1.064402	-0.46274
C	0.551249	-0.63106	-1.05059
Br	-2.97528	3.233787	0.192012
O	-4.80602	0.83202	0.22772
Br	-4.53393	-2.25213	-0.28575
C	1.505752	-0.59078	0.171826
N	2.874596	-0.88958	-0.24089
C	1.052471	-1.54966	1.275144
C	3.898296	-0.03054	-0.04912
C	5.216971	-0.54563	-0.65016
N	6.456546	0.229767	-0.26423
O	3.802144	1.051861	0.514473
C	7.638031	-0.48224	-0.87783
C	6.416865	1.640782	-0.80622
C	6.639492	0.259808	1.234896
O	0.539256	-1.19736	2.309731
O	1.270122	-2.82957	0.940602
H	-1.63829	-2.27859	-0.86592
H	-0.47854	1.845968	-0.51104
H	0.95696	0.069974	-1.78569
H	0.588198	-1.62831	-1.497
H	-5.42051	0.075456	0.230009
H	1.511734	0.407379	0.607475
H	3.044	-1.78531	-0.69572
H	5.146871	-0.51559	-1.74078
H	5.382709	-1.58264	-0.34907
H	8.53998	0.074831	-0.62924
H	7.694752	-1.49032	-0.4696
H	7.505477	-0.51903	-1.95821
H	7.358293	2.124455	-0.54968
H	6.306623	1.588955	-1.88892
H	5.576691	2.160459	-0.35783
H	7.592316	0.742035	1.448109
H	5.8197	0.818285	1.675501
H	6.650574	-0.76617	1.601701
H	0.962068	-3.41375	1.665866

Table S16: The Cartesian coordinates of conformer 16 of Valdiviamide A (**1**)

Atom	Coordinates		
	X	**Y**	**Z**
C	-0.76852	-1.14901	-1.08798
C	-1.52108	-1.62766	-0.01041
C	-2.51696	-0.84608	0.557515
C	-2.81124	0.441818	0.082489
C	-2.04426	0.900627	-0.99704
C	-1.04489	0.127809	-1.57628
C	0.322817	-1.9949	-1.70375
Br	-2.39031	2.653911	-1.69878
O	-3.79603	1.148332	0.67538
Br	-3.53097	-1.54355	2.024983
C	1.643732	-1.97535	-0.89389
N	2.217605	-0.641	-0.83139
C	2.608875	-3.03226	-1.44636
C	2.699618	-0.11362	0.312564
C	3.21768	1.322412	0.130866
N	3.996404	1.887331	1.29743
O	2.70201	-0.69027	1.393111
C	4.487406	3.254781	0.887743
C	3.122006	2.042429	2.521218
C	5.193197	1.026089	1.625419
O	2.301632	-4.19752	-1.54601
O	3.800657	-2.53955	-1.79742
H	-1.33592	-2.62008	0.386778
H	-0.48713	0.524872	-2.41712
H	0.526054	-1.65435	-2.72409
H	0.001549	-3.03598	-1.7707
H	-3.9107	2.014579	0.244124
H	1.435551	-2.28093	0.135135
H	2.331372	-0.13196	-1.70612
H	2.368243	1.988894	-0.04026
H	3.870961	1.37405	-0.74335
H	5.032707	3.687722	1.724886
H	5.143984	3.151333	0.024995
H	3.629461	3.877016	0.636879
H	3.720375	2.507661	3.303265
H	2.281311	2.685199	2.262128
H	2.776368	1.060399	2.826378
H	5.76738	1.529242	2.401946
H	4.842919	0.059284	1.972702
H	5.797749	0.918662	0.72526
H	4.358159	-3.27297	-2.13537

Table S17: The Cartesian coordinates of conformer 17 of Valdiviamide A (**1**)

Atom	Coordinates		
	X	Y	Z
C	-0.70588	-1.20481	-1.07014
C	-1.48342	-1.65359	0.002447
C	-2.47787	-0.84876	0.538891
C	-2.74621	0.433942	0.035685
C	-1.95445	0.863492	-1.03807
C	-0.95567	0.066901	-1.58581
C	0.383576	-2.07885	-1.64856
Br	-2.2659	2.609309	-1.77606
O	-3.73178	1.162759	0.59902
Br	-3.52685	-1.50576	2.000531
C	1.694708	-2.04793	-0.82356
N	2.291319	-0.72241	-0.81013
C	2.650255	-3.14256	-1.31598
C	2.725346	-0.13142	0.322037
C	3.374755	1.238043	0.060486
N	3.774366	2.01868	1.291607
O	2.622642	-0.61833	1.441031
C	2.580158	2.303593	2.172516
C	4.838004	1.292469	2.08326
C	4.345998	3.334394	0.821167
O	2.316622	-4.30159	-1.40143
O	3.868241	-2.68919	-1.62852
H	-1.31888	-2.64111	0.420361
H	-0.37779	0.440969	-2.42356
H	0.60297	-1.77097	-2.67588
H	0.05159	-3.1179	-1.68844
H	-3.82947	2.022263	0.149963
H	1.468402	-2.30422	0.215218
H	2.463833	-0.27314	-1.7079
H	2.687043	1.86812	-0.50853
H	4.279378	1.097461	-0.53716
H	2.911575	2.939412	2.992173
H	1.829958	2.823347	1.577371
H	2.191569	1.36222	2.547236
H	5.134683	1.933224	2.91235
H	4.423657	0.357025	2.444355
H	5.689557	1.111574	1.428084
H	4.64983	3.907704	1.69556
H	5.206855	3.137643	0.183676
H	3.580355	3.874222	0.265758
H	4.41993	-3.44471	-1.92475

Table S18: The Cartesian coordinates of conformer 18 of Valdiviamide A (**1**)

Atom	Coordinates		
	X	Y	Z
C	-0.66915	-1.24015	-1.06403
C	-0.97314	0.004097	-1.62055
C	-1.97909	0.794542	-1.08007
C	-2.72446	0.383632	0.033268
C	-2.40629	-0.87194	0.573715
C	-1.40385	-1.67249	0.043116
C	0.434744	-2.09812	-1.63963
Br	-3.40578	-1.49572	2.090878
O	-3.68812	1.197	0.511293
Br	-2.36465	2.492307	-1.87879
C	1.750411	-2.02926	-0.82387
N	2.304089	-0.68526	-0.80742
C	2.735321	-3.09049	-1.33057
C	2.732363	-0.08959	0.324354
C	3.349646	1.295001	0.066391
N	3.654709	2.114055	1.300059
O	2.653617	-0.58627	1.441148
C	2.410455	2.348356	2.124524
C	4.719156	1.456413	2.148806
C	4.177575	3.450619	0.831816
O	2.440919	-4.26069	-1.40805
O	3.93032	-2.59517	-1.66715
H	-0.42812	0.360749	-2.48746
H	-1.2004	-2.63826	0.493519
H	0.63978	-1.79636	-2.67168
H	0.126194	-3.1449	-1.6664
H	-4.13398	0.795788	1.278674
H	1.540155	-2.29795	0.215009
H	2.448123	-0.22222	-1.70318
H	2.676355	1.890708	-0.55426
H	4.290611	1.170324	-0.47639
H	2.670758	3.017913	2.94296
H	1.657745	2.812574	1.488056
H	2.059759	1.394255	2.504665
H	4.94127	2.121431	2.982141
H	4.340715	0.502874	2.501752
H	5.608651	1.316779	1.535303
H	4.421373	4.04884	1.70833
H	5.069355	3.288795	0.227891
H	3.406813	3.945108	0.242309
H	4.502097	-3.33122	-1.97415

Table S19: The Cartesian coordinates of conformer 19 of Valdiviamide A (**1**)

Atom	Coordinates		
	X	Y	Z
C	0.557167	1.274722	-1.04925
C	1.356431	1.692428	0.019988
C	2.36124	0.873559	0.512207
C	2.620166	-0.39262	-0.03571
C	1.810592	-0.78947	-1.1086
C	0.798785	0.021048	-1.61138
C	-0.5458	2.165946	-1.57238
Br	2.120223	-2.5087	-1.90881
O	3.614723	-1.13754	0.488299
Br	3.436542	1.48564	1.974152
C	-1.83603	2.114751	-0.70585
N	-2.44887	0.797374	-0.70984
C	-2.8446	3.150694	-1.20346
C	-2.57714	0.043614	0.401252
C	-3.34294	-1.26447	0.135637
N	-3.43488	-2.21798	1.304803
O	-2.14323	0.349349	1.504577
C	-4.20078	-1.60685	2.456055
C	-4.18497	-3.43815	0.827871
C	-2.0639	-2.65034	1.769892
O	-3.87898	2.887105	-1.76981
O	-2.41755	4.39324	-0.95237
H	1.197925	2.665886	0.471774
H	0.20421	-0.32715	-2.44853
H	-0.80101	1.883286	-2.59811
H	-0.20506	3.203447	-1.59687
H	3.704068	-1.98391	0.013325
H	-1.58468	2.357299	0.328702
H	-2.89103	0.496396	-1.57697
H	-2.86738	-1.80819	-0.68404
H	-4.36687	-1.02633	-0.16429
H	-4.29664	-2.3632	3.233687
H	-3.65178	-0.74413	2.818583
H	-5.18674	-1.31506	2.095656
H	-4.2699	-4.13482	1.660356
H	-5.17482	-3.13452	0.489994
H	-3.63099	-3.8965	0.009873
H	-2.19447	-3.39922	2.549688
H	-1.53375	-3.0833	0.922207
H	-1.53673	-1.78252	2.152693
H	-3.06399	5.037275	-1.31259

Table S20: The Cartesian coordinates of conformer 20 of Valdiviamide A (**1**)

Atom	Coordinates		
	X	Y	Z
C	-0.79405	-0.26543	-0.6011
C	-1.12599	1.062401	-0.31366
C	-2.44419	1.425056	-0.07958
C	-3.48977	0.489463	-0.12269
C	-3.13387	-0.83474	-0.41376
C	-1.81782	-1.21144	-0.65241
C	0.642358	-0.66282	-0.85208
Br	-4.51475	-2.16707	-0.48545
O	-4.7507	0.908987	0.108185
Br	-2.8573	3.255951	0.302068
C	1.524875	-0.78974	0.427586
N	2.910047	-1.0672	0.066458
C	1.040648	-1.92379	1.325361
C	3.823615	-0.09143	-0.09361
C	5.185775	-0.62294	-0.56976
N	6.359379	0.302676	-0.33264
O	3.600766	1.10076	0.083732
C	7.609566	-0.44692	-0.72432
C	6.263228	1.54718	-1.18654
C	6.463598	0.685851	1.123984
O	1.425601	-3.06694	1.226011
O	0.127549	-1.50902	2.20404
H	-0.35308	1.82268	-0.2771
H	-1.59456	-2.24791	-0.88072
H	1.128827	0.086697	-1.48205
H	0.681539	-1.61342	-1.39106
H	-5.38179	0.169331	0.040367
H	1.497964	0.147951	0.983929
H	3.16298	-2.04486	-0.06971
H	5.134789	-0.80695	-1.6464
H	5.419052	-1.56712	-0.07334
H	8.462493	0.21689	-0.59203
H	7.712287	-1.32276	-0.08518
H	7.527052	-0.74854	-1.76763
H	7.154877	2.145999	-1.00616
H	6.222733	1.242323	-2.2317
H	5.364731	2.087884	-0.90859
H	7.37814	1.261695	1.257467
H	5.595865	1.280784	1.39233
H	6.507066	-0.22589	1.719158
H	-0.19853	-2.27836	2.719778

Table S21: The Cartesian coordinates of conformer 21 of Valdiviamide A (**1**)

Atom	Coordinates		
	X	**Y**	**Z**
C	-0.7606	-0.30153	-0.52718
C	-1.07537	1.02766	-0.23431
C	-2.39709	1.4103	-0.05165
C	-3.45979	0.499086	-0.15546
C	-3.12106	-0.82708	-0.45807
C	-1.80303	-1.22383	-0.64121
C	0.676529	-0.72703	-0.7211
Br	-4.51965	-2.12476	-0.62729
O	-4.75962	0.819385	0.009885
Br	-2.79325	3.248092	0.34437
C	1.517388	-0.83398	0.588363
N	2.912083	-1.12434	0.277526
C	1.000702	-1.94736	1.493156
C	3.820636	-0.15245	0.074259
C	5.221882	-0.70927	-0.23279
N	6.299918	0.324575	-0.46432
O	3.571679	1.046526	0.12715
C	7.581395	-0.42146	-0.74786
C	5.980778	1.195882	-1.65724
C	6.508229	1.184367	0.761032
O	1.415382	-3.08404	1.460199
O	0.025135	-1.52346	2.297036
H	-0.29046	1.771799	-0.15155
H	-1.58981	-2.26066	-0.87715
H	1.194847	-0.00066	-1.35257
H	0.71788	-1.69092	-1.23557
H	-4.8618	1.765692	0.218589
H	1.474328	0.114494	1.125958
H	3.175131	-2.10718	0.21812
H	5.176578	-1.33088	-1.13054
H	5.554078	-1.33703	0.597765
H	8.372051	0.308054	-0.91601
H	7.823718	-1.04651	0.110475
H	7.443007	-1.03667	-1.63582
H	6.826573	1.861782	-1.8221
H	5.838354	0.551986	-2.52458
H	5.079303	1.760671	-1.44371
H	7.346131	1.851659	0.564556
H	5.600111	1.74806	0.948218
H	6.739986	0.532381	1.602693
H	-0.31664	-2.28156	2.819041

Table S22: The Cartesian coordinates of conformer 22 of Valdiviamide A (**1**)

Atom	Coordinates		
	X	**Y**	**Z**
C	0.745586	0.841517	-0.90325
C	0.780059	-0.54636	-1.05397
C	1.865355	-1.28292	-0.59376
C	2.958398	-0.67561	0.038619
C	2.900621	0.719146	0.184345
C	1.827356	1.467489	-0.27785
C	-0.42874	1.652051	-1.40667
Br	4.361714	1.615174	1.049704
O	3.984061	-1.44448	0.460767
Br	1.873449	-3.18386	-0.83191
C	-1.29182	2.238657	-0.27026
N	-1.88533	1.22193	0.596721
C	-2.33673	3.228425	-0.80655
C	-2.91976	0.454939	0.206753
C	-3.41906	-0.48777	1.313339
N	-4.46053	-1.49731	0.887486
O	-3.43016	0.517954	-0.90581
C	-5.7384	-0.81824	0.449189
C	-3.94245	-2.38497	-0.21981
C	-4.76734	-2.35894	2.088387
O	-2.28014	3.743211	-1.89753
O	-3.27072	3.517987	0.108171
H	-0.04035	-1.06069	-1.5419
H	1.840785	2.54501	-0.15171
H	-1.05902	1.039751	-2.05324
H	-0.07316	2.490885	-2.00904
H	4.681034	-0.90063	0.870332
H	-0.65154	2.841483	0.384692
H	-1.51248	1.133676	1.539027
H	-3.85992	0.108283	2.116842
H	-2.5791	-1.04937	1.728902
H	-6.46818	-1.59353	0.220382
H	-6.0966	-0.19902	1.270985
H	-5.52685	-0.21262	-0.42576
H	-4.69442	-3.14689	-0.41968
H	-3.76807	-1.7767	-1.10154
H	-3.01817	-2.85282	0.117701
H	-5.53026	-3.08215	1.804626
H	-3.85814	-2.87347	2.396195
H	-5.13323	-1.72397	2.894056
H	-3.88487	4.182515	-0.26896

Table S23: The Cartesian coordinates of conformer 23 of Valdiviamide A (**1**)

Atom	Coordinates		
	X	Y	Z
C	-0.71605	-1.20348	-1.0724
C	-1.0975	0.015443	-1.63215
C	-2.11055	0.76905	-1.05105
C	-2.7848	0.349236	0.103351
C	-2.38671	-0.88187	0.648604
C	-1.37829	-1.645	0.07796
C	0.390392	-2.02682	-1.69235
Br	-3.27207	-1.52613	2.219924
O	-3.77478	1.041595	0.704474
Br	-2.60755	2.439212	-1.85612
C	1.724168	-1.94997	-0.90828
N	2.240092	-0.59178	-0.85894
C	2.720409	-2.96687	-1.47972
C	2.754996	-0.05514	0.266144
C	3.267975	1.379412	0.056361
N	3.807493	2.067256	1.289489
O	2.809165	-0.63228	1.34504
C	2.746448	2.192306	2.358461
C	5.012601	1.340989	1.841619
C	4.234485	3.455246	0.877058
O	2.467527	-4.14723	-1.55023
O	3.871723	-2.42173	-1.88453
H	-0.61148	0.381389	-2.52973
H	-1.11142	-2.59349	0.532023
H	0.562477	-1.69896	-2.72247
H	0.102172	-3.07908	-1.73473
H	-3.95567	1.872859	0.229953
H	1.549309	-2.26226	0.124736
H	2.289165	-0.07032	-1.73249
H	2.458627	2.003697	-0.32996
H	4.072543	1.371052	-0.68364
H	3.166615	2.767151	3.182462
H	1.891687	2.718358	1.934428
H	2.463679	1.197183	2.685717
H	5.400679	1.922062	2.676895
H	4.703871	0.353075	2.16702
H	5.762646	1.272798	1.054237
H	4.632448	3.965277	1.75288
H	5.001779	3.375276	0.108285
H	3.368383	3.99149	0.491767
H	4.451737	-3.13189	-2.23406

**Table S24:** The Cartesian coordinates of conformer 24 of Valdiviamide A (**1**)

Atom	Coordinates		
	X	Y	Z
C	0.764574	-0.70256	-0.98026
C	2.059151	-1.13626	-0.68325
C	3.001414	-0.24641	-0.18357
C	2.706683	1.106312	0.039616
C	1.404695	1.523493	-0.27389
C	0.453265	0.645473	-0.77444
C	-0.27233	-1.66859	-1.50831
Br	0.934348	3.361932	-0.01287
O	3.585408	2.010135	0.518708
Br	4.772144	-0.8791	0.205302
C	-1.17105	-2.33092	-0.42153
N	-1.99934	-1.37534	0.299894
C	-0.35672	-3.12256	0.595095
C	-3.21329	-1.00579	-0.14991
C	-3.97464	-0.11482	0.845591
N	-5.18711	0.59607	0.286405
O	-3.68242	-1.35546	-1.2271
C	-6.2729	-0.38439	-0.09619
C	-5.72053	1.496194	1.374323
C	-4.82085	1.448477	-0.90534
O	-0.28743	-2.85728	1.772713
O	0.282134	-4.14078	0.012463
H	2.341969	-2.16962	-0.84973
H	-0.53535	1.018785	-1.01575
H	0.212897	-2.47288	-2.06513
H	-0.94558	-1.15751	-2.19996
H	4.44885	1.595483	0.698094
H	-1.83286	-3.03415	-0.93618
H	-1.67226	-1.07885	1.218073
H	-3.30885	0.653746	1.244254
H	-4.32077	-0.73082	1.680002
H	-7.13452	0.187026	-0.4385
H	-5.89453	-1.02959	-0.88206
H	-6.53667	-0.96479	0.787334
H	-6.61251	1.995374	0.999065
H	-5.96794	0.889455	2.244296
H	-4.95873	2.231021	1.630907
H	-5.70455	2.012221	-1.20056
H	-4.02491	2.131382	-0.60978
H	-4.49366	0.799717	-1.71174
H	0.811454	-4.61901	0.686295

**Table S25:** The Cartesian coordinates of conformer 25 of Valdiviamide A (**1**)

Atom	Coordinates		
	X	Y	Z
C	-0.83562	-0.63363	1.114122
C	-0.63514	0.741253	0.955371
C	-1.60835	1.535757	0.36503
C	-2.82393	1.003621	-0.08865
C	-3.00967	-0.37549	0.088779
C	-2.04462	-1.18265	0.677726
C	0.234393	-1.50056	1.739954
Br	-4.66186	-1.16399	-0.49257
O	-3.72891	1.830447	-0.65037
Br	-1.2916	3.415079	0.173812
C	1.250409	-2.11306	0.734847
N	1.978721	-1.10617	-0.02471
C	0.579864	-3.15498	-0.16044
C	3.250319	-0.76652	0.269319
C	3.808862	0.309323	-0.67819
N	5.271632	0.644715	-0.49736
O	3.899038	-1.2449	1.191846
C	5.628254	1.669087	-1.54766
C	5.534606	1.245685	0.86453
C	6.144004	-0.57231	-0.70077
O	-0.03483	-4.09255	0.291593
O	0.738419	-2.92394	-1.46787
H	0.282968	1.200787	1.303745
H	-2.24247	-2.241	0.803429
H	-0.22048	-2.32937	2.28611
H	0.812713	-0.91482	2.458233
H	-4.5293	1.342506	-0.91647
H	1.992546	-2.66204	1.321351
H	1.514957	-0.68225	-0.82506
H	3.247954	1.237358	-0.54041
H	3.681004	-0.01303	-1.71444
H	6.677282	1.933872	-1.42515
H	5.46272	1.236836	-2.5335
H	5.000628	2.548565	-1.41072
H	6.58519	1.529158	0.908663
H	4.905187	2.12783	0.977502
H	5.300256	0.504848	1.621799
H	7.183717	-0.25227	-0.65107
H	5.924432	-1.29272	0.080471
H	5.92888	-0.98952	-1.68409
H	0.28017	-3.62845	-1.97481

Diasteroisomer *S, S* of compound 3
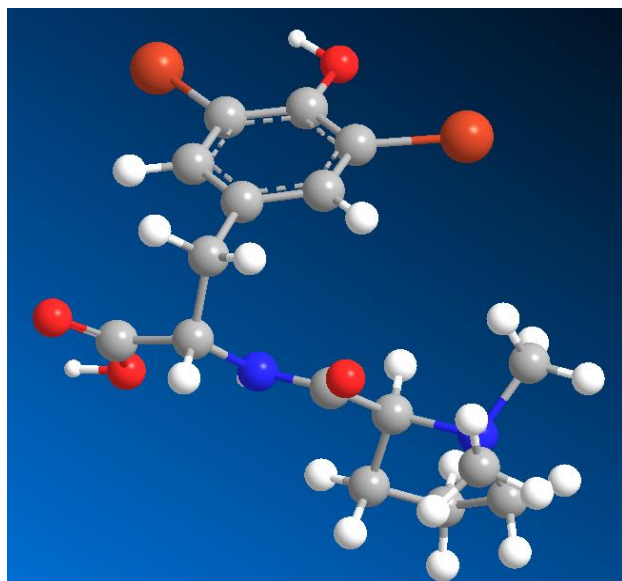
Conformer 1   Conformer 2
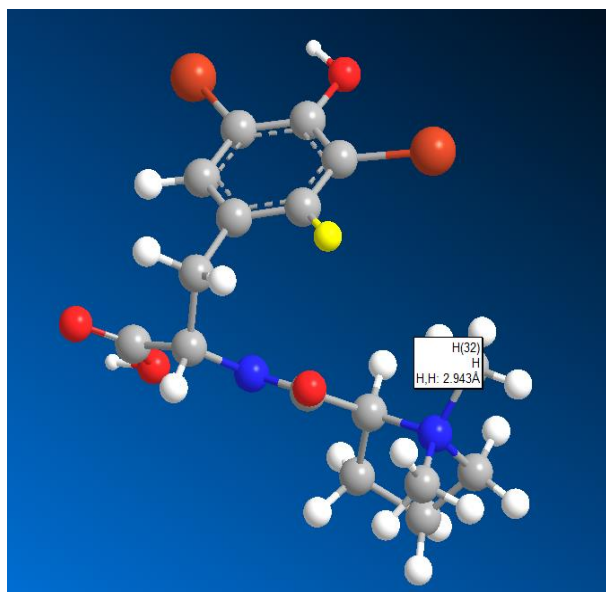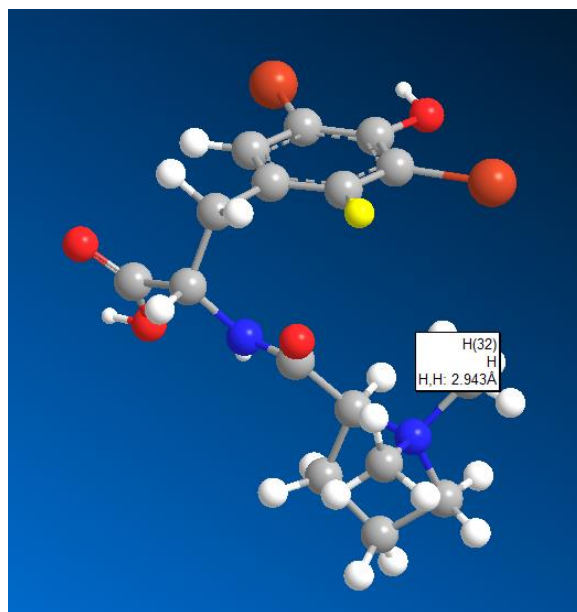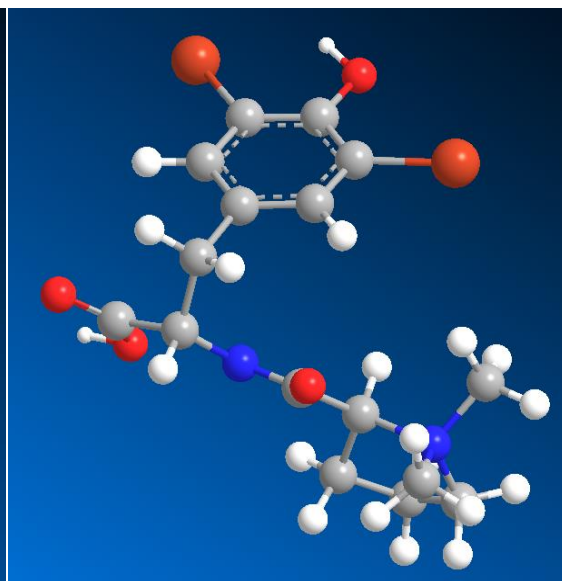

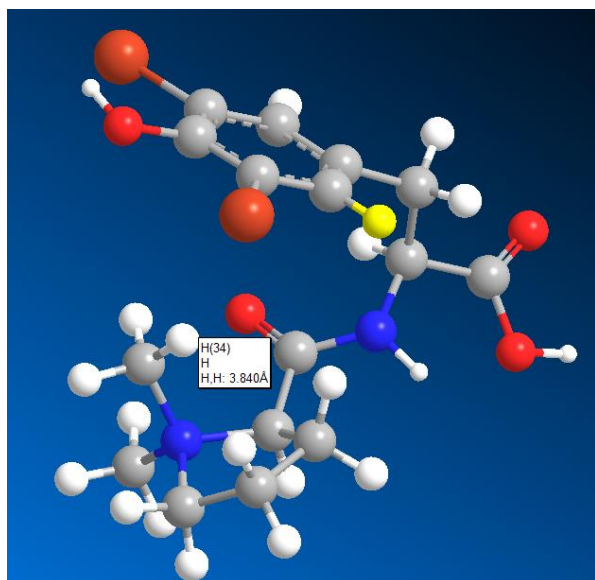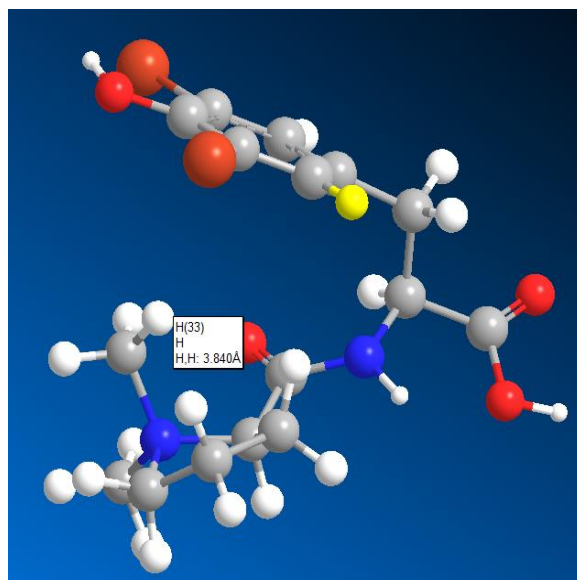Conformer 3   Conformer 4
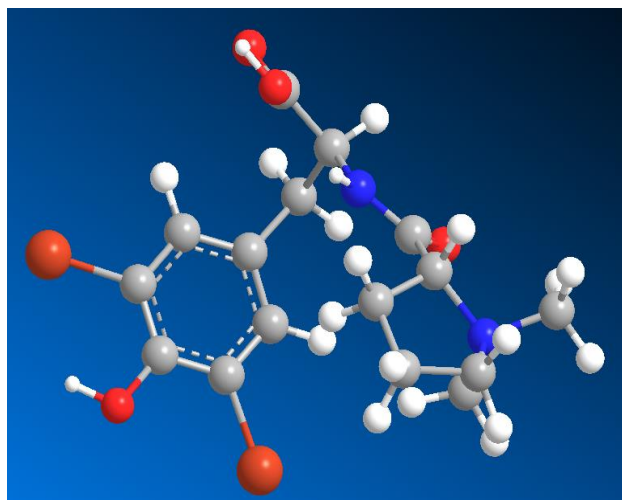
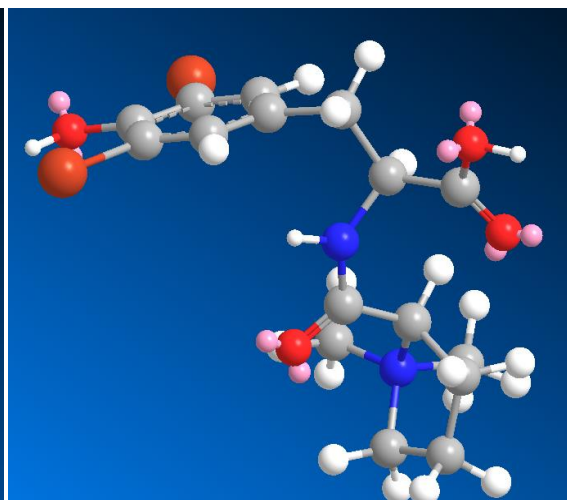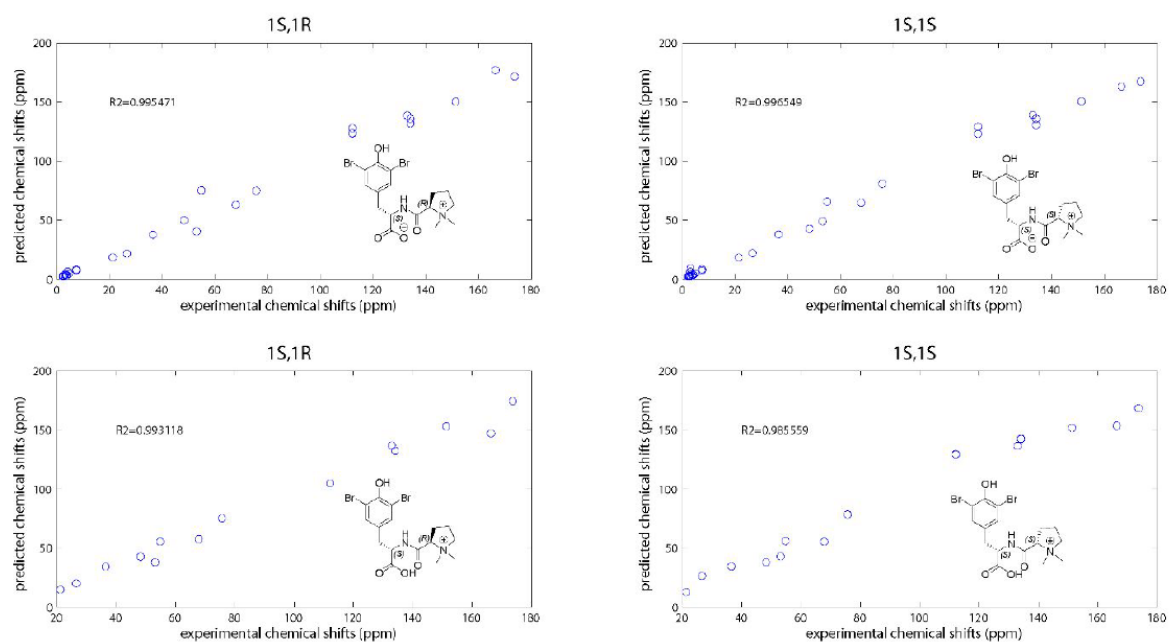Diasteroisomer *S*, *R* of compound 3

Conformer 1

Conformer 2

Conformer 3

Conformer 4

Figure S61: Comparison between predicted and experimental 13C NMR data for the two possible

diastereoisomers of compound **3** and two possible acido/basic forms.